

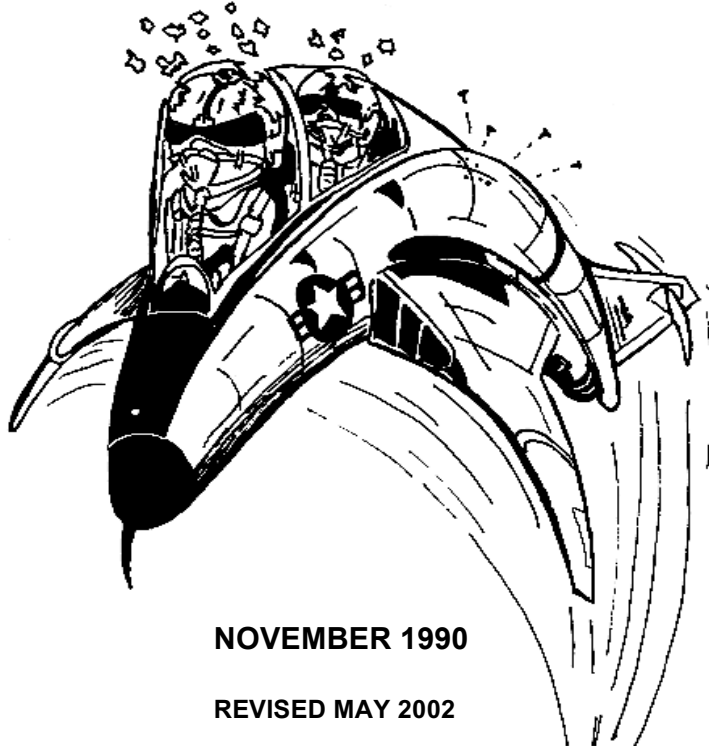
AFFTC-TIH-98-02



STRUCTURES FLIGHT TEST HANDBOOK

WILLIAM J. NORTON
Major, USAF
Flight Test Engineer

A
F
F
T
C



NOVEMBER 1990

REVISED MAY 2002

TECHNICAL INFORMATION HANDBOOK
2nd Edition

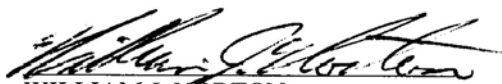
Approved for public release; distribution unlimited.

AIR FORCE FLIGHT TEST CENTER
EDWARDS AIR FORCE BASE, CALIFORNIA
AIR FORCE MATERIEL COMMAND
UNITED STATES AIR FORCE

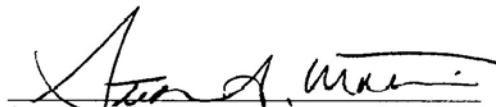
This technical information handbook (AFFTC-TIH-98-02, *Structures Flight Test Handbook*) was prepared as an aid to engineers at the Air Force Flight Test Center, Edwards Air Force Base, California 93523-6843.

Prepared by:

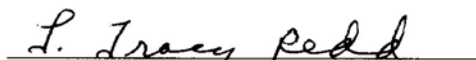
This handbook has been reviewed and is approved for publication: May 20, 2002



WILLIAM J. NORTON
Major, USAF
Flight Test Engineer



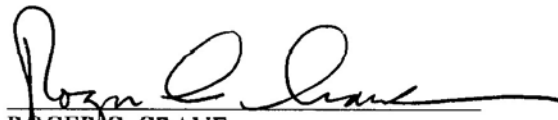
STEPHEN A. MATHIS
Chief, Structures Branch



L. TRACY REDD
Chief, Flight Systems Integration Division



ROBERT G. KENNINGTON
Director, Engineering Directorate, 412th Test Wing



ROGER C. CRANE
Senior Technical Advisor, 412th Test Wing

REPORT DOCUMENTATION PAGE

Form Approved
OMB No. 0704-0188

Public reporting burden for this collection of information is estimated to average 1 hour per response, including the time for reviewing instructions, searching existing data sources, gathering and maintaining the data needed, and completing and reviewing this collection of information. Send comments regarding this burden estimate or any other aspect of this collection of information, including suggestions for reducing this burden to Department of Defense, Washington Headquarters Services, Directorate for Information Operations and Reports (0704-0188), 1215 Jefferson Davis Highway, Suite 1204, Arlington, VA 22202-4302. Respondents should be aware that notwithstanding any other provision of law, no person shall be subject to any penalty for failing to comply with a collection of information if it does not display a currently valid OMB control number. **PLEASE DO NOT RETURN YOUR FORM TO THE ABOVE ADDRESS.**

1. REPORT DATE (<i>DD-MM-YYYY</i>) 20-05-2002		2. REPORT TYPE N/A		3. DATES COVERED (<i>From - To</i>) N/A	
4. TITLE AND SUBTITLE Structures Flight Test Handbook (2nd Edition)				5a. CONTRACT NUMBER	
				5b. GRANT NUMBER	
				5c. PROGRAM ELEMENT NUMBER	
6. AUTHOR(S) William J. Norton, Maior, USAF				5d. PROJECT NUMBER	
				5e. TASK NUMBER	
				5f. WORK UNIT NUMBER	
7. PERFORMING ORGANIZATION NAME(S) AND ADDRESS(ES) AFFTC 412 TW/TSFS 195 East Popson Ave Edwards AFB CA 93524-6844				8. PERFORMING ORGANIZATION REPORT NUMBER AFFTC-TIH-98-02	
9. SPONSORING / MONITORING AGENCY NAME(S) AND ADDRESS(ES) N/A				10. SPONSOR/MONITOR'S ACRONYM(S) N/A	
				11. SPONSOR/MONITOR'S REPORT NUMBER(S) N/A	
12. DISTRIBUTION / AVAILABILITY STATEMENT Approved for public release; distribution unlimited					
13. SUPPLEMENTARY NOTES					
14. ABSTRACT The Structures Flight Test Handbook (2nd Edition) provides a 'broad-brush' overview of the many disciplines encompassed by the structures flight test field. It provides the basic knowledge and introduction required for the new engineer to become productive in the briefest time possible. Experienced flight test engineers may also find the handbook useful as a reference and resource guide. This handbook assumes knowledge of at least undergraduate engineering concepts. Underlying assumptions, applicable standards and regulations, common testing approaches, rules of thumb, and examples are provided in each area. This edition provides updated information derived from lessons learned since the first edition was published.					
15. SUBJECT TERMS vibroacoustics materials ground vibrations instrumentation aerodynamics structural dynamics aeroservoelasticity frequency response flight mechanics loads flutter					
16. SECURITY CLASSIFICATION OF:			17. LIMITATION OF ABSTRACT	18. NUMBER OF PAGES	19a. NAME OF RESPONSIBLE PERSON
a. REPORT UNCLASSIFIED	b. ABSTRACT UNCLASSIFIED	c. THIS PAGE UNCLASSIFIED			19b. TELEPHONE NUMBER (<i>include area code</i>)

This page intentionally left blank.

PREFACE

This handbook was written as a training aid for new engineers assigned to the Air Force Flight Test Center (AFFTC), Edwards AFB, California. Experienced structural flight test engineers may find this handbook useful as a reference and resource guide.

This handbook fills a long-suffered gap in one crucial area of flight test engineering. It will be updated or revised as the structures personnel at the AFFTC see a need or as readers suggest. If the reader finds any omission or errors, this may be corrected in later editions by recommending the changes to the author or the staff of the AFFTC Structures Branch.

The original edition of this handbook has proven very popular, with hundreds of copies distributed within the U.S. Military, Government, aerospace industry, and academic institutions as well as individuals outside the U.S. This handbook has been used as a textbook at the USAF Test Pilot School and the civilian National Test Pilot School. All of this exposure has been gratifying, and has also generated reader remarks and revealed clear deficiencies or errors in the text. Since the writing of the original handbook, the author has considerably expanded his experience in structures flight testing as well as written many other reports and papers on the subject. The author wished to capture that experience in the handbook for the benefit of others. The chapter dealing with airloads flight testing has been given special attention. Thus, was the 2nd Edition born.

A great many people are to thank for making this handbook possible. Those who helped, either directly or indirectly, are too numerous to list here. However, a few are due special mention. The personnel of the Air Force Flight Test Center (AFFTC) Structures Branch, of whom the author has proudly counted himself a part, are to be thanked for the many tedious readings and rereadings of the manuscript and their very helpful comments. Most of all, a great deal is owed to Mr. Tracy Redd, former Branch Chief, who taught the author so much, not all of it about engineering, and tolerated his atypical behavior. Many of the other engineers at the AFFTC also contributed comments on drafts of this handbook, most notably Messrs. Jim Ford, Al Webb, Russ Lenz, Wayne Olsen, and Tom Twisdale. In other USAF organizations thanks are due Ms. Mary Marshall of the 3246th Test Wing, Major Dan Gleason of the USAF Test Pilot School, and Mr. Dave Denner of the Aeronautical Systems Division. Among this nation's outstanding aerospace companies thanks are extended to Messrs. Carl Johnson and Bob Pearson of McDonnell Douglas Corporation and the remarkable Mr. Alex Mackenzie of North American Rockwell. A special thanks to Mr. Mike Kehoe of the NASA Ames/Dryden Flight Research Center. I am especially grateful to Ms. Mary Bradley and Mr. Joe Strofance who caught many grammatical errors and who helped to make this publication look so professional. Much would have been impossible without the kind assistance of Ms. Pat Juenemann.

Additional copies of this handbook can be obtained by contacting the Structures Branch team at the AFFTC.

This page intentionally left blank.

EXECUTIVE SUMMARY

This handbook is intended to provide a 'broad-brush' overview of the many disciplines encompassed by the structures flight test field, and will provide the basic knowledge and introduction required for a new engineer to become productive in the briefest time possible. The reader should have knowledge of at least undergraduate engineering concepts and associated skills. Each chapter provides underlying assumptions, applicable standards and regulations, common testing approaches, rules of thumb, and examples. Development of equations is minimized while specific references to readily available texts or handbooks are provided for those who need to develop a more complete understanding of the supporting mathematics. This handbook is not intended as a textbook, so supplemental reading should become a normal practice for the structures engineer. A comprehensive index and a list of nomenclature are provided for quick reference. An attempt has been made to make this handbook more readable than a textbook.

The primary goal of the handbook is to provide engineers that are new to the field of structures testing with the basic information that they need in order to understand the discipline processes. The information has been gleaned from over 50 years of structures flight testing at AFFTC and elsewhere.

The handbook is organized into 13 different sections. These include such subjects as basic aircraft vibration testing, instrumentation, data reduction techniques and information about the specifics of flight testing at the AFFTC. A set of references is included at the end of each section for those individuals who wish to gain more details on each specific subject.

This page intentionally left blank.

TABLE OF CONTENTS

	<u>Page No.</u>
PREFACE	III
EXECUTIVE SUMMARY	V
TABLE OF CONTENTS	VII
LIST OF ILLUSTRATIONS.....	XIII
LIST OF TABLES	XVIII
1.0 BASICS OF AIRCRAFT	1
1.1 Introduction	1
1.2 Geometry.....	1
1.2.1 Wing Group.....	1
1.2.2 Tail Group	4
1.2.3 Fuselage Group	5
1.2.4 Landing Gear Group.....	5
1.2.5 Miscellaneous.....	7
1.3 Systems	7
1.3.1 Propulsion	8
1.3.2 Hydraulics	11
1.3.3 Electrical	11
1.3.4 Environmental Control System	11
1.3.5 Fuel.....	13
1.3.6 Flight Controls	13
1.3.7 Cockpit Group.....	15
1.3.8 Weapons.....	15
2.0 AERODYNAMICS AND FLIGHT MECHANICS.....	19
2.1 Introduction	19
2.2 Basic Aerodynamics.....	19
2.2.1 The Atmosphere.....	19
2.2.2 Altitude and Airspeed Measurement.....	21
2.2.3 Airflow Visualization.....	22
2.2.4 Supersonic Flight	22
2.2.5 Generation of Lift.....	25
2.2.6 Generation of Drag.....	27
2.2.7 Aerodynamic Modeling.....	28
2.3 Basic Flight Mechanics	29
2.3.1 Reference System.....	29
2.3.2 Weight and Balance	30
2.3.3 Static Stability	30
2.3.4 Dynamic Stability.....	32
2.3.5 Aeroelastic Effects on Stability and Control	33
3.0 MATERIALS	35
3.1 Introduction	35
3.2 Characteristics	35
3.2.1 Stress	35
3.2.2 Strain	35
3.2.3 Stress Analysis	38
3.2.4 Thermal Effects.....	39
3.3 Composites.....	40
3.4 Failure Modes.....	40

TABLE OF CONTENTS (Continued)

	<u>Page No.</u>
3.4.1 Creep	41
3.4.2 Work-Hardening.....	41
3.4.3 Delamination	41
3.4.4 Cracking	41
3.4.5 Fatigue.....	41
3.4.6 Corrosion.....	42
3.5 Inspections.....	42
3.5.1 Stress Visualization	42
3.5.2 Dye Penetration	42
3.5.3 Magnetic Particles	42
3.5.4 X-Ray	43
3.5.5 Ultrasonics.....	43
3.5.6 Eddy Current	43
3.6 Definitions.....	43
4.0 BASIC STRUCTURAL DYNAMICS	45
4.1 Introduction	45
4.2 Basic System Elements.....	45
4.3 Simple System Models	47
4.3.1 Free Response Case.....	48
4.3.2 Forced Response Case.....	52
4.4 Supplemental Concepts	55
4.4.1 Response Relationships	55
4.4.2 Complex Modes	57
4.4.3 Beating	57
4.4.4 Harmonics	57
4.4.5 Jump Phenomenon	57
4.5 Modal Analysis.....	58
4.5.1 Multidegree of Freedom Systems.....	58
4.5.2 Coordinate Transformation and Solution	60
5.0 LOADS.....	65
5.1 Introduction	65
5.2 Types of Loads	65
5.2.1 Maneuver Loads	66
5.3 Loads Ground Testing	72
5.4 Airloads Flight Testing.....	72
5.4.1 Maneuvers	75
5.4.1.1 Symmetric Maneuvers	75
5.4.1.2 Asymmetric Maneuvers.....	76
5.4.1.3 Ground Maneuvers	77
5.4.2 Instrumentation.....	77
5.4.2.1 Strain Gages.....	77
5.4.2.2 Pressure Sensors	79
5.4.3 Inspections.....	80
5.4.4 Avoiding Overloads	80
5.4.4.1 Flight to 80-Percent Airloads	80
5.4.4.2 Flight to 100-Percent Airloads.....	80
5.4.4.3 Testing Tolerances.....	81
5.4.4.4 Concurrent Testing	85
5.4.5 Regression Testing	86
5.4.5.1 Following Structural Changes	86

TABLE OF CONTENTS (Continued)

	<u>Page No.</u>
5.4.5.2 Following Software Changes	87
5.4.6 Gust Loads	87
5.4.6.1 Gust Loads Flight Tests.....	88
5.4.7 Load Alleviation Systems	89
5.5 Landing Gear.....	90
5.5.1 Landing Gear Loads.....	90
5.5.1.1 Landing Gear Loads Testing	91
5.5.2 Landing Gear Shimmy	93
5.5.2.1 Landing Gear Shimmy Testing	93
6.0 FLUTTER	97
6.1 Introduction	97
6.2 Description	97
6.2.1 Flutter Examples	99
6.2.2 Flutter Suppression.....	102
6.3 Flutter Prediction.....	102
6.3.1 K-Method	104
6.3.2 PK-Method.....	107
6.3.3 P-Method.....	108
6.3.4 Other Methods.....	109
6.4 Other Aeroelastic Phenomena	109
6.4.1 Panel Flutter	109
6.4.2 Buzz	109
6.4.3 Stall Flutter.....	110
6.4.4 Divergence	110
6.4.5 Control Reversal.....	110
6.4.6 Limit Cycle Oscillation	111
6.4.7 Buffet	111
6.4.8 Mechanical Vibration.....	111
6.4.9 Dynamic Response.....	112
6.4.10 Aerothermoelasticity	112
6.5 Preliminary Ground Tests	112
6.5.1 Wind Tunnel Tests	113
6.5.2 Ground Vibration Tests.....	113
6.6 Flutter Flight Tests	114
6.6.1 Excitation	114
6.6.1.1 Pulse	114
6.6.1.2 Sweep	115
6.6.1.3 Burst-and-Decay Data	118
6.6.1.4 Pyrotechnic.....	118
6.6.1.5 Air Turbulence	118
6.6.2 Procedures	119
6.7 Data Reduction	121
6.8 Store Flutter Testing.....	122
6.9 Rules of Thumb	123
7.0 GROUND VIBRATION TESTS	125
7.1 Introduction	125
7.2 Overview	125
7.3 Underlying Assumptions.....	126
7.4 Preparation	126
7.4.1 Aircraft Configuration.....	126

TABLE OF CONTENTS (Continued)

	<u>Page No.</u>
7.4.2 Reducing Nonlinearities	127
7.4.2.1 Preloads	127
7.5 Aircraft Suspension	128
7.6 Electrodynamic Shakers	128
7.6.1 Characteristics	128
7.6.1.1 Physical Features	129
7.6.1.2 Selection	129
7.6.2 Suspension	130
7.6.3 Attachment to the Structure	130
7.6.4 Impedance Mismatch	133
7.7 Transducer Installation	134
7.8 Excitation Techniques	134
7.8.1 Operating Inputs	134
7.8.2 Transient	135
7.8.2.1 Impact	135
7.8.2.2 Step Relaxation	138
7.8.3 Sine Waveforms	138
7.8.3.1 Sine Sweep	138
7.8.3.2 Sine Dwell	139
7.8.3.3 Chirp	140
7.8.4 Random	140
7.8.4.1 Pure Random	140
7.8.4.2 Pseudorandom	140
7.8.4.3 Periodic Random	141
7.8.4.4 Burst Random	141
7.9 Linearity Check	141
7.10 Surveys	142
7.11 Modal Results	143
7.11.1 Multipoint Data	143
7.11.2 Mode Visualization	144
7.11.3 Orthogonality Check	144
8.0 AEROSERVOELASTICITY	149
8.1 Introduction	149
8.1.1 Pilot-In-The-Loop Oscillations	150
8.2 Control Theory	152
8.2.1 Basic Concepts	152
8.2.2 Compensation	154
8.2.3 Representations	155
8.2.3.1 Root-Locus	155
8.2.3.2 Bode	157
8.2.3.3 Nyquist and Polar	159
8.3 Analysis	159
8.4 Ground Tests	160
8.5 Flight Tests	162
8.5.1 Notch Filter	163
9.0 VIBRO-ACOUSTICS	167
9.1 Introduction	167
9.2 General Vibration	168
9.3 Fundamentals of Sound	168
9.4 Measurement of Sound	169

TABLE OF CONTENTS (Continued)

	<u>Page No.</u>
9.5 Flight Tests	174
9.5.1 Preliminary Ground Tests	174
9.5.2 Test Concepts	174
9.5.3 Data Analysis	176
10.0 INSTRUMENTATION	181
10.1 Introduction	181
10.2 Strain Gages	181
10.2.1 Selection	182
10.2.2 Measurement	183
10.2.3 Calibration	185
10.2.4 Installation	186
10.3 Accelerometers	187
10.3.1 Selection	188
10.3.2 Measurement	189
10.3.3 Calibration	189
10.3.4 Installation	190
10.4 Force Transducers	191
10.5 Pressure Sensors	191
10.6 Microphones	193
10.7 Other Common Transducers	194
10.7.1 Temperature Sensors	194
10.7.2 Displacement Transducers	194
10.7.3 Time Code Generators	194
10.7.4 Discretets	195
10.8 Instrumentation Systems	195
10.8.1 Frequency Division Multiplex Systems	197
10.8.2 Pulse Code Modulation Systems	198
11.0 FREQUENCY RESPONSE DATA ANALYSIS	201
11.1 Introduction	201
11.2 Time Domain	201
11.2.1 Logarithmic Decrement Method	202
11.2.2 Logarithmic (Peak) Amplitude Method	202
11.2.3 Multiple Degrees-of-Freedom Responses	202
11.2.4 Random Decrement Method	204
11.2.5 Correlation Functions	205
11.2.6 Lissajous Figures	206
11.3 Frequency Domain	208
11.3.1 Fourier Transformations	209
11.3.2 Autospectrums	211
11.3.3 Power Spectral Density	212
11.3.4 Half-Power Method	213
11.3.5 Other Common Presentations	215
11.3.6 Transfer Functions	219
11.3.7 Coherence Function	220
11.3.8 CO/QUAD Method	221
11.3.9 Nyquist Plots and Circle Fit	222
11.3.10 Laplace (S-Plane) Transformation	224
11.3.11 Bode Plots	226
11.3.12 Z-Plane Transformation	227

TABLE OF CONTENTS (Concluded)

	<u>Page No.</u>
12.0 SIGNAL PROCESSING	229
12.1 Introduction	229
12.2 Resolution.....	229
12.2.1 Frequency Resolution.....	229
12.2.2 Damping Resolution.....	230
12.2.3 Amplitude Resolution.....	231
12.3 Error	231
12.3.1 Quantization	231
12.3.2 Aliasing	232
12.3.3 Leakage	233
12.3.4 Ranging	234
12.3.5 Other Sources of Error	234
12.4 Processing Techniques	235
12.4.1 Windowing	235
12.4.1.1 Hanning Window.....	235
12.4.1.2 Flat Top Window.....	236
12.4.1.3 Uniform Window.....	237
12.4.1.4 Force Window	237
12.4.1.5 Exponential Window	238
12.4.2 Ensemble Averaging	238
12.4.2.1 Root Mean Squared Averaging	239
12.4.2.2 Linear Averaging	239
12.4.2.3 Overlap Averaging	239
12.4.3 Adding and Subtracting Spectra.....	239
12.4.4 Zoom Transform.....	240
12.4.5 Zero Insertion	240
12.4.6 Decimation	241
12.4.7 Cutoff	241
12.4.8 Filtering.....	241
13.0 FLIGHT TESTING AT THE AIR FORCE FLIGHT TEST CENTER.....	245
13.1 Introduction	245
13.2 Responsible Organizations	245
13.3 Aircraft Modifications	246
13.3.1 Analysis.....	246
13.3.2 Flight Tests.....	246
13.4 Test Planning.....	247
13.4.1 Preliminary Planning.....	247
13.4.2 The Test Plan.....	247
13.4.3 The Review Cycle	248
13.4.4 Final Preparations.....	249
13.5 Conduct of the Test	249
13.5.1 Preflight Briefing.....	249
13.5.2 Control Room Operations.....	249
13.6 Test Reports.....	250
LIST OF ABBREVIATIONS, ACRONYMS, AND SYMBOLS.....	253
INDEX.....	263

LIST OF ILLUSTRATIONS

<u>Figure</u>	<u>Title</u>	<u>Page No.</u>
1	Wing Planform Definitions.....	1
2	Wing Incidence.....	2
3	Anhedral and Dihedral Definition	2
4	Wing Control Surfaces	3
5	Tail Group and Control.....	4
6	The Canard and Delta Wing	5
7	Fuselage Group.....	6
8	Fuselage Station and Butt Line Definition.....	7
9	Typical Landing Gear	7
10	Typical Turbine Engine	11
11	Typical Supersonic Inlet	12
12	Typical Engine Exhaust Nozzle.....	12
13	Aerial Refueling Boom and Receptacle System.....	13
14	Aerial Refueling Probe and Drogue System.....	14
15	Typical Mechanical Control System.....	14
16	Typical Fighter/Trainer Cockpit.....	16
17	Example Weapon Pylon and Store Ejector Rack.....	17
18	Relationships of Airspeed Forms with Altitude.....	23
19	Streamlines Around an Airfoil.....	24
20	Pressure Distribution on an Airfoil.....	24
21	Shocks.....	25
22	Airfoil Geometry Terminology.....	25
23	Lift Generation on an Airfoil	25
24	Example of Circulation.....	26
25	Wingtip Vortices.....	26
26	Example Vortex Generator Installation	27
27	Example of Aerodynamic Paneling of an Aircraft.....	29
28	Basic Aircraft Reference System.....	30
29	Statically Stable Airplane cg and a.c. Relationship and Tail Load.....	31
30	Basic Loading and Stresses.....	36
31	Material Deformation Under Load	37
32	Shear Strain Illustration	37
33	Example Stress-Strain Curve.....	38
34	Example Finite Element Model - X-29A Wing Structure.....	39

LIST OF ILLUSTRATIONS (Continued)

<u>Figure</u>	<u>Title</u>	<u>Page No.</u>
35	Examples of Composites.....	40
36	Example S-N Diagram.....	41
37	Basic Spring Element.....	45
38	Basic Damper Element.....	46
39	Basic Mass Element.....	46
40	Example of Combined Basic Elements.....	47
41	Example Structural Model.....	48
42	Free-Body Diagram of Figure 41.....	48
43	Example of an Over-Damped Displacement Response.....	50
44	Example of an Under-Damped Displacement Response.....	50
45	Example of a Undamped Displacement Response.....	51
46	Example of a Divergent Displacement Response.....	51
47	Typical Magnitude Response Showing Effect of Resonance and Damping.....	53
48	Definition of Phase Angle.....	54
49	Typical Phase Angle Response Showing Effect of Resonance and Damping.....	54
50	Relationship of Displacement, Velocity, and Acceleration.....	55
51	Vibration Nomograph for Sinusoidal Motion.....	56
52	The Beating Phenomena.....	57
53	The Jump Phenomena.....	58
54	Example of a Multidegree of Freedom System.....	58
55	Beam Bending Problem with Mode Shape.....	62
56	Forces Acting on an Aircraft in a Level Turn.....	66
57	Forces Acting in a 90-Degree Roll Attitude.....	67
58	Significance of the V-n Diagram.....	68
59	Example Maximum Loads Related to V-n Plot (Fighter-Bomber).....	69
60	Example V-g Diagrams - T-38A Aircraft (Symmetric).....	70
61	Example Load Factor Limits Chart - T-38A Aircraft.....	71
62	Example Loads Cross-Plot.....	74
63	Example Loads Strain Gage Installation - F-15 Wing.....	78
64	Illustration of Airloads Envelope Safety Margins.....	81
65	Definitions of Airloads Flight Test Measurement Limits.....	82
66	Comparison of Design Limit Load and Gust Load Factor with Weight.....	88
67	Maneuver Load Control Results for L-1011 (71 Percent of Semispan).....	90
68	Typical Runway Repair Landing Gear Testing Profiles.....	92

LIST OF ILLUSTRATIONS (Continued)

<u>Figure</u>	<u>Title</u>	<u>Page No.</u>
69	Collar's Aeroelastic Triangle of Forces	97
70	Example Wing Flutter Model and Deformed Shape - F/A-18 Wing	103
71	Example Aircraft Flutter Model - F-15 STOL	103
72a	Example V-G Diagram	106
72b	Example V-f Diagram	106
73	Example Flutter Boundary Analysis Result	107
74	Stagnation Temperatures	112
75	Diagram of Flutter Investigation During Development	113
76	Wand Flutter Exciter System	116
77	Electrodynamic Exciter	116
78	Vane or Flutteron Exciter	117
79	Flutter Expansion Example	119
80	Example Store Flutter Instrumentation Installation	123
81	Schematic of Typical Ground Vibration Test Equipment Arrangement	129
82	Characteristics of a Driving Point Measurement	132
83	Characteristics of a Cross-Point Measurement	133
84	Influence of Impact Hammer Tips	136
85	Influence of Impact Hammer Weight and Force (Hammer b with More Weight than Hammer a)	137
86	Effect of Sine Sweep Rate on Data	139
87	Characteristics of Various Random Signal Types	141
88	Example of a Ground Vibration Test Survey Grid	142
89	Example Wing Second Bending Mode Shape Presentations	145
90	Example Sensor Placement Considerations	150
91	Example Determination of Sensor Locations	150
92	Example Fuselage First Vertical Bending Mode Shape	151
93	Aeroservoelastic System Diagram	152
94	Open-Loop System Diagram	153
95	Closed-Loop System Diagram	153
96	Example Multiple Input/Multiple Output System - Aircraft Lateral-Directional Control System	153
97	Block Diagram Algebra	154
98	Typical Pole-Zero Plot	156
99	Root-Locus Plot of Figure 98	156
100	Bode Plot for Equation 113	158

LIST OF ILLUSTRATIONS (Continued)

<u>Figure</u>	<u>Title</u>	<u>Page No.</u>
101	Determining Phase and Gain Margin from a Bode Plot.....	158
102	Determining Phase and Gain Margin from a Polar Plot.....	160
103	Aeroservoelastic Analysis Flow Diagram.....	160
104	Example Notch Filter.....	164
105	Effects of Notch Filter	165
106	Wavelength Versus Frequency of Sound in Air.....	168
107	Sound Fields	171
108	Sound Attenuation in Air.....	171
109	Summing Sound Pressure Levels.....	172
110	Subtracting Sound Pressure Levels.....	172
111	Effect of Measurement Time on Sound Pressure Level Results	173
112	Example Sound Contour Pattern (B-1B Underbelly with Missile Shapes Installed) (for illustrative purposes only).....	175
113	Illustration of Octave and Third-Octave Segmentation of Frequency Spectrum	176
114	Illustration of Octave and Third-Octave Sound Pressure Level Versus a Fourier Transform Presentation	176
115	Example of Sound Pressure Level Test Data Versus Specification Level.....	178
116	Typical Uniaxial Strain Gage Configuration	182
117	Other Common Strain Gage Configurations.....	183
118	Typical Wheatstone Bridge Circuit.....	184
119	Example Strain Gage Installation Loads Measurements - X-29 Wing and Canard ..	185
120	Example Strain Gage Installation	187
121	Common Piezoelectric Accelerometer Components.....	188
122	Three Common Accelerometer Configurations	189
123	Example of Shim-Mounted Accelerometer	190
124	Force Transducer Components	191
125	Common Force Transducer Configurations.....	192
126	Pressure Transducer Components.....	192
127	Typical Small Piezoelectric Pressure Transducer	193
128	Common Measurement Microphones and Components	193
129	Example Strip Chart Recorder Slow Code Trace.....	195
130	Typical Instrumentation System Configuration	196
131	Basic Frequency Division Multiplex System Components.....	197
132	Basic Pulse Code Modulation System Components	198
133	Example of Pulse Code Modulation Encoding	198

LIST OF ILLUSTRATIONS (Continued)

<u>Figure</u>	<u>Title</u>	<u>Page No.</u>
134	Illustration of Commutator Function	199
135	Damped Impulse Response Time History	202
136	Log Amplitude Plot	203
137	Multiple Degrees of Freedom Impulse Response Function	203
138	Random Excitation Response Time History	204
139	(a) Original Random Response Time History (Single Degree of Freedom) (b) Associated Auto-correlation Function.....	206
140	Sample Lissajous Construction.....	207
141	Lissajous Displays for Sinusoidal Inputs at Various Frequency Ratios.....	208
142	Important Lissajous Figures (Same Frequency and Amplitude for Both Signals)....	208
143	Typical Fourier Transformation Results	210
144	Half-Power Damping from a Nonsquared Frequency Response Function	214
145	Half-Power Method from a Squared Frequency Response Function.....	214
146	Half Power Applied to Decibel Scale (Nonsquared Frequency Response Function)	215
147	Half-Power Method Using an Inverse Fourier Transformation for Smoothing	216
148	Common Data Presentations.....	217
149	Modal Parameters from Simple Response Plots	218
150	Diagram of Transfer Function Operation.....	219
151	Example of Ordinary Coherence Function	220
152	CO/QUAD Elements	221
153	Determining Damping from Real or Imaginary Response.....	222
154	Three-Axis Frequency Response Plot.....	223
155	Single Degree of Freedom Nyquist Plot	223
156	Nyquist Plot Analysis	224
157	S-Plane Representations (Single Degree of Freedom).....	225
158	Example S-Plane (Root-Locus) Analysis (Single Degree of Freedom).....	225
159	Magnitude and Phase Diagrams.....	226
160	Single Degree of Freedom Bode Plot	227
161	Example Z-Plane	227
162	Points Required to Define a Mode.....	230
163	Illustration of Minimum Damping Resolution.....	230
164	Illustration of Worst-Case Amplitude Error	231
165	Examples of Aliasing Error	232
166	Aliasing Fold-Down Chart.....	232

LIST OF ILLUSTRATIONS (Concluded)

<u>Figure</u>	<u>Title</u>	<u>Page No.</u>
167	Distorted Waveform Producing Leakage.....	233
168	Illustration of Leakage Error.....	234
169	Application of Hanning Window.....	236
170	Comparison of Hanning and Flat Top Windows	236
171	Flat Top Window.....	237
172	Uniform Window.....	237
173	Application of Force Window.....	238
174	Application of Exponential Window	239
175	Illustration of Overlap Averaging and Result.....	240
176	Example of Zoom Transform Application.....	241
177	Filter Characteristics.....	242
178	A Bank of Hanning Passbands.....	242

LIST OF TABLES

<u>Table</u>	<u>Title</u>	<u>Page No.</u>
1	THE STANDARD ATMOSPHERE	20
2	COMPARISON OF GROUND VIBRATION TEST EXCITATION FORMS	135
3	EXAMPLE C-17A MODES.....	145
4	EXAMPLE AFTI F-111 MODES	146
5	EXAMPLE T-46 MODES.....	146
6	GAIN AND PHASE MARGIN REQUIREMENTS	162
7	OCTAVE AND THIRD-OCTAVE PASSBANDS	170

1.0 BASICS OF AIRCRAFT

1.1 Introduction

Because many of the engineers undertaking structures flight testing have no experience with aircraft, a basic introductory chapter to the subject is felt to be necessary. The objective of this chapter is to introduce you to the basic nomenclature of modern aircraft. Many books have been written encompassing all of the variations in aircraft design, but such is not the purpose here. Instead, only common design features will be presented. Special purpose aircraft like flying boats and helicopters are not covered. If you are uncertain of the function of some aspect of the aircraft you are working with, you are encouraged to ask others. Additional reading in this area is recommended and several fine publications are listed in the reference section at the end this chapter. Aeronautical engineers or experienced flight test engineers may find this chapter rudimentary and may wish to skip it altogether.

1.2 Geometry

Every part and feature of an aircraft serves some function, which may not be obvious even to knowledgeable aeronautical engineers. This section will address some of the more typical design features without detailed explanation of the reasons why things are done one way or another. The intent is only to make the structures engineer conversant in the language associated with aviation.

1.2.1 Wing Group

A top view of an aircraft wing is called the **planform**. There are a number of common terms applied to the planform. The **sweep** refers to the angle between a line perpendicular to the fuselage centerline and a line half way between the leading and trailing edges of the wing (the **mean chord line**). Leading and trailing edge sweep may also be referenced and may change along the span. The **wing span (b)** is measured from wingtip to wingtip perpendicularly to the fuselage centerline (Figure 1). Some wings have pivoting mechanisms that permit the sweep to be changed (variable geometry).

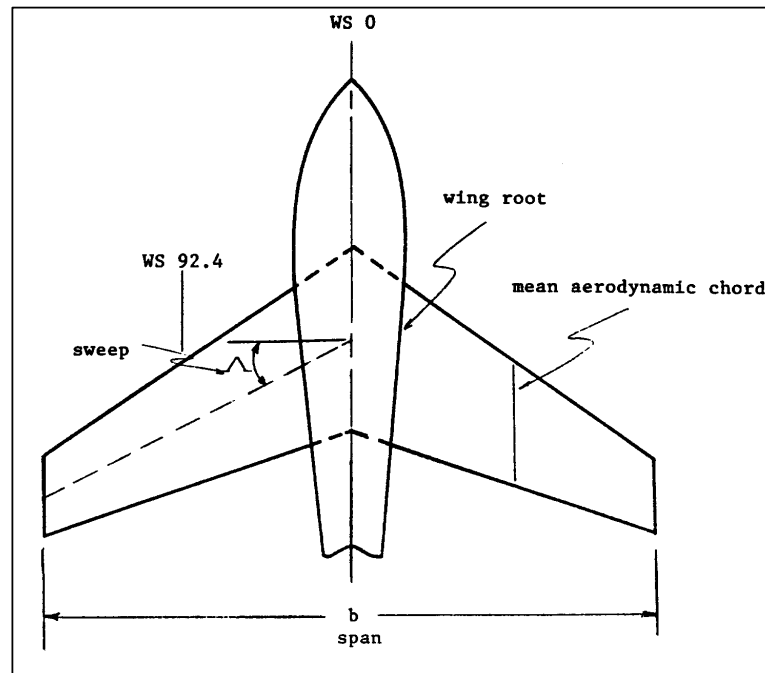


Figure 1 Wing Planform Definitions

Positions along the wing are measured in inches from the fuselage centerline and are referred to as **wing stations (WS)** (Figure 1). For example, a pylon located on one wing may be at WS 34.5, or 34.5 inches from the fuselage centerline.

Wings may be **tapered**, having a larger chord at the root or base than at the tip, and also have tapered thickness. Planform taper is often referred to as the **taper ratio**; the ratio between the root and the tip chord. **Aspect ratio (A)** is defined as:

$$A = b^2 / S \tag{1}$$

where:

S = the planform area.

Incidence refers to the angle between the centerline of the aircraft and a line between the leading and trailing edges of a section of the wing (Figure 2). A wing may be twisted along the span with the incidence increasing (**washin**) or decreasing (**washout**) toward the tip. A wing may be mounted low on the fuselage, mid fuselage, or on top of the fuselage depending upon ground clearance or aerodynamic requirements. The two sides of the wing may be canted upward (**dihedral**) or downward (**anhedral**, Figure 3). Some wings may have vertical surfaces at the tips, which are called **winglets**.

A wing will have a number of movable control surfaces (Figure 4). One or more trailing edge surfaces near the tip of the wing are **ailerons** and move differentially between sides to cause the airplane to roll about its longitudinal axis. A similar device near the root is called a **flap** and will deploy symmetrically downward. This

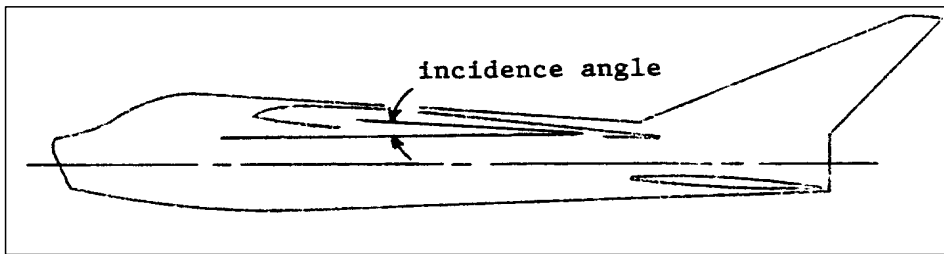


Figure 2 Wing Incidence

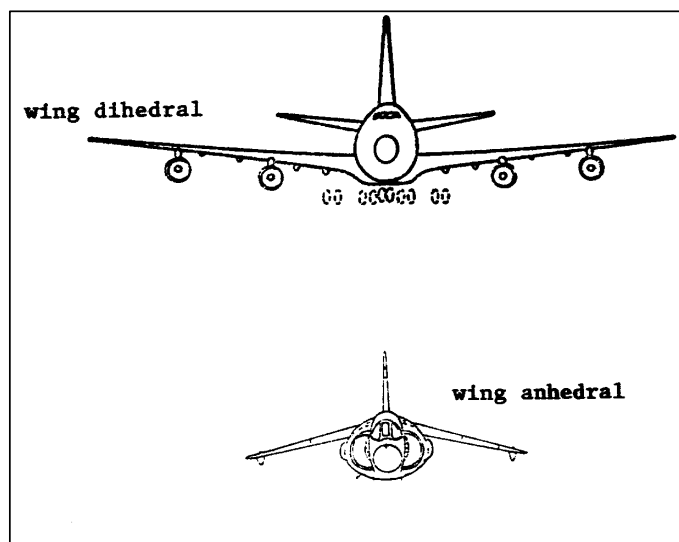


Figure 3 Anhedral and Dihedral Definition

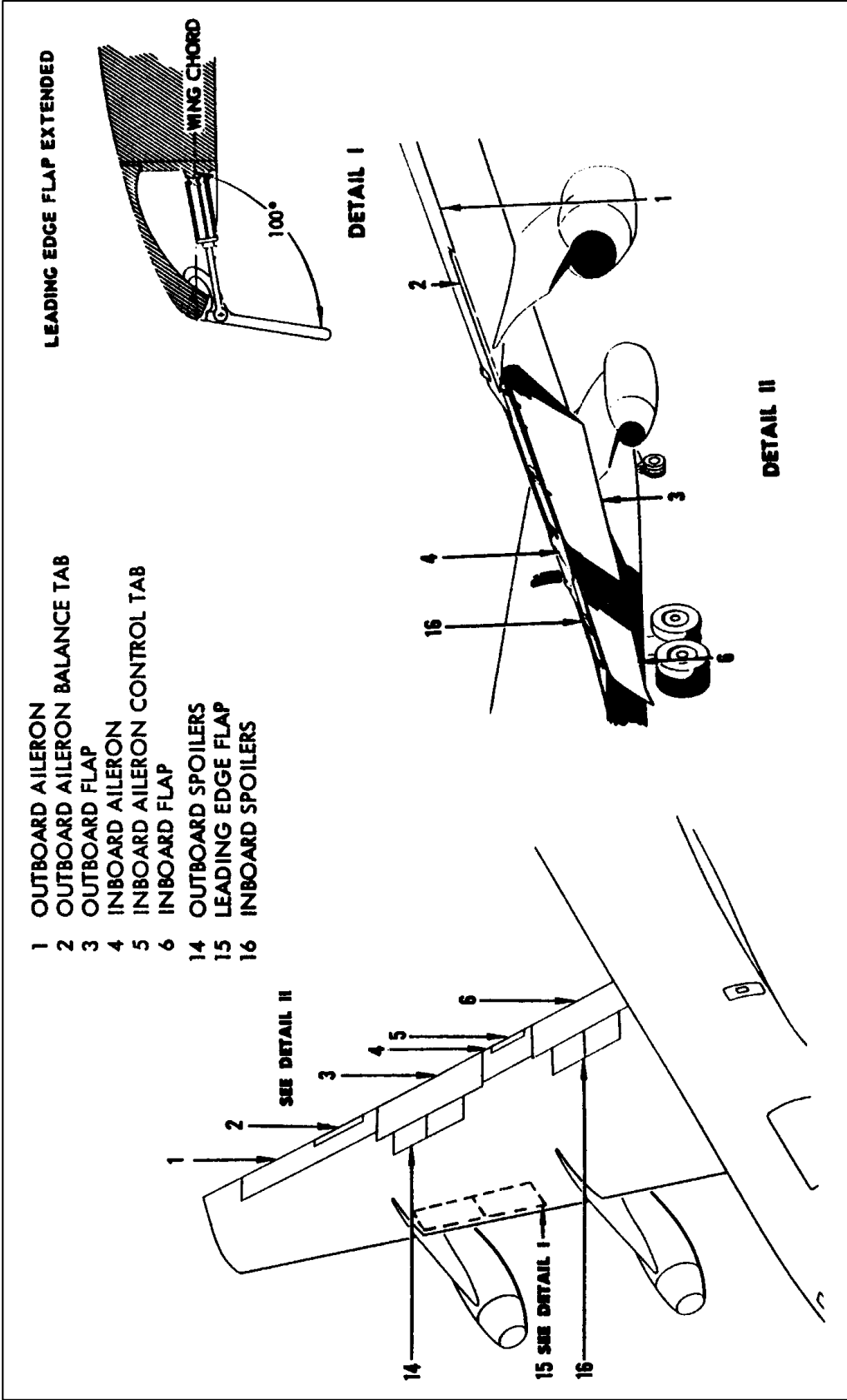


Figure 4 Wing Control Surfaces

allows the plane to fly slower without stalling (Section 2.2.5). Flaps may have multiple parts with slots in between and may slide out on rails. Fighter-type aircraft may have flaps (referred to as flaperons) that move asymmetrically like ailerons for roll control. Surfaces similar to flaps may be placed at the leading edge of the wing (leading edge flaps or slats). Large panels may be designed to rotate from the top or bottom of the wing (spoilers) to slow the aircraft or to produce rolling moments (the B-1B is an example of the latter). Many control surfaces may have much smaller movable surfaces near their trailing edges. These are trim tabs and may assist in moving the surface or to keep it deflected with less mechanical effort.

1.2.2 Tail Group

An aircraft tail unit, or **empennage**, normally consists of a **vertical stabilizer** or fin (one or more) and two **horizontal stabilizers** (Figure 5). A vertical surface usually includes a trailing edge control device called a **rudder**. The rudder causes the nose of the aircraft to yaw in the same direction as the side the trailing edge of the rudder moves (some roll will also most likely occur). The horizontal surfaces may contain trailing edge control devices called **elevators**. Elevators cause the nose of the aircraft to rise or fall in a sense coincident with the elevator motion (nose goes up for trailing edge up elevator). Fighter-type aircraft may have all-moving horizontal stabilizers called **stabilators**, or **stabs**, which can move together for elevator action or differentially for rolling motion. Other aircraft with elevators may have horizontal stabilizers that rotate through a small arc for trimming action. Rudders and elevators may also have trim tabs. The anhedral and dihedral explained earlier also applies to horizontal stabilizers.

Tail arrangements may vary markedly but there are some common designs worth mentioning. The **‘T’ tail** has a single horizontal stabilizer at the top of the vertical stabilizer. Mid-fin designs have been used but the horizontal surface placed at the base of the fin or on the bottom of the tail is most common. If the aircraft has two vertical surfaces they may be perpendicular to the fuselage or canted in or out some amount. A few aircraft have used a **‘V’ tail** arrangement, which uses just two surfaces to perform the functions of the vertical and horizontal stabilizers. Such an arrangement may have control surfaces, which perform the functions of rudders and elevators and are appropriately called **ruddervators**.

Things attached to the top of the fuselage are typically referred to as **dorsal** (e.g., dorsal fairing) and on the bottom as **ventral** (e.g., ventral antennas). One or more small vertical surfaces may project below the tail and are called **ventral fins**. Some airplanes may not have any horizontal surfaces at all (tailless). Such aircraft will usually have a large wing extending far back on the fuselage or have horizontal surfaces forward of the wings called **canards** (Figure 6). For the later case, the wing trailing edge control surfaces have to perform both elevator

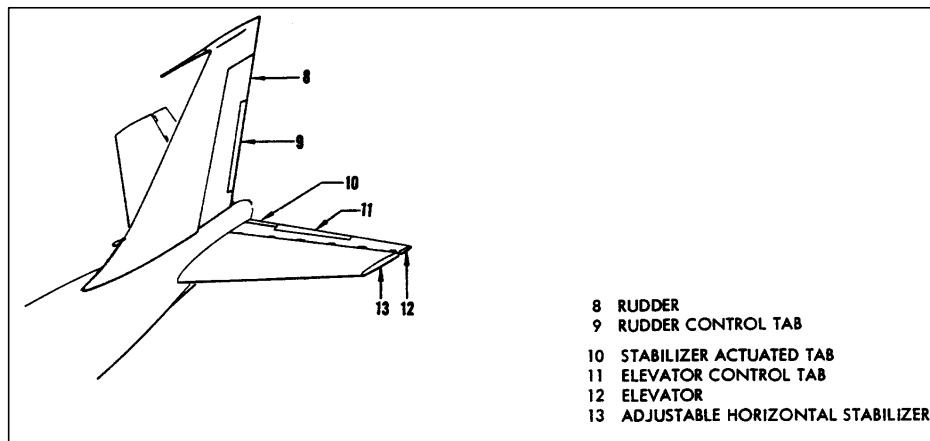


Figure 5 Tail Group and Control

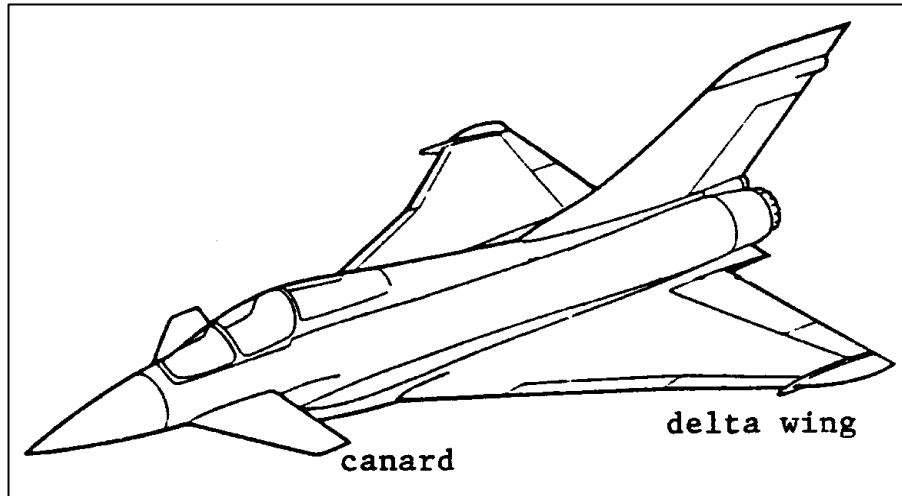


Figure 6 The Canard and Delta Wing

and aileron or flap actions. They are referred to as **elevons**. The canards may be fixed, all-moving, or have trailing edge control devices. Canards serve a similar purpose to that of the aft-mounted horizontal stabilizer and have been mounted in many positions on the forward fuselage.

1.2.3 Fuselage Group

The fuselage is the central structure to which the wing and tail are attached and contains the cockpit, perhaps the engine(s) and landing gear, and most of the aircraft systems (Figure 7).

The nose of the fuselage will usually consist of the **radome** behind which lies the radar (Section 1.3.7). The radome is an aerodynamic fairing made of material through which radar waves will easily propagate. The cockpit, which contains the aircrew, is next in line toward the rear and will have a canopy or windscreen and perhaps some escape hatches. The wings and tail are attached as shown in the figures. If the engine(s) is within the fuselage then the air inlet(s) (Section 1.3.1) will be on the fuselage.

A surface that protrudes into the airstream on command to create drag (Section 2.2.6) and slow the aircraft, a **speedbrake** or **airbrake**, may be included in the fuselage structure (although split aileron speedbrakes are also used). Many access and inspection panels will be found on the fuselage to get at the avionics and other systems. The tail of fighter aircraft may include a **tailhook**, which rotates down on command. By design, in the case of a carrier landing or an emergency (for example, in the event of a wheel brake failure), the tailhook snags an arresting cable across the runway to slow the airplane. Braking parachutes may also be housed in the tail area and are deployed on landing to assist in slowing the aircraft.

Positions on the fuselage are referenced both vertically and longitudinally in inches (Figure 8). The vertical positions are from a **water line (WL)** which is generally some major longitudinal structural member. Water line numbers will be positive above and negative below the WL. For example, the main gear axle may be at WL -67.3, or 67.3 inches below the water line datum. Longitudinal positions are called **fuselage stations (FS)** or **butt (buttock) line (BL)**, and are measured from some convenient datum in inches, generally ahead of the nose of the airplane, and positive aft. The main gear axle, for example, may also be at FS 133.4.

1.2.4 Landing Gear Group

The aircraft will usually have wheels attached to struts, which extend from the fuselage, wings, or engine pods (**nacelles**) by means of hydraulics. This is the landing gear and must absorb most of the shock of the landing impact (hydraulically or pneumatically), as well as provide a means of stopping the plane (Figure 9). The wheel brakes typically consist of multiple disc brake assemblies, which are hydraulically actuated. The gear will most often be

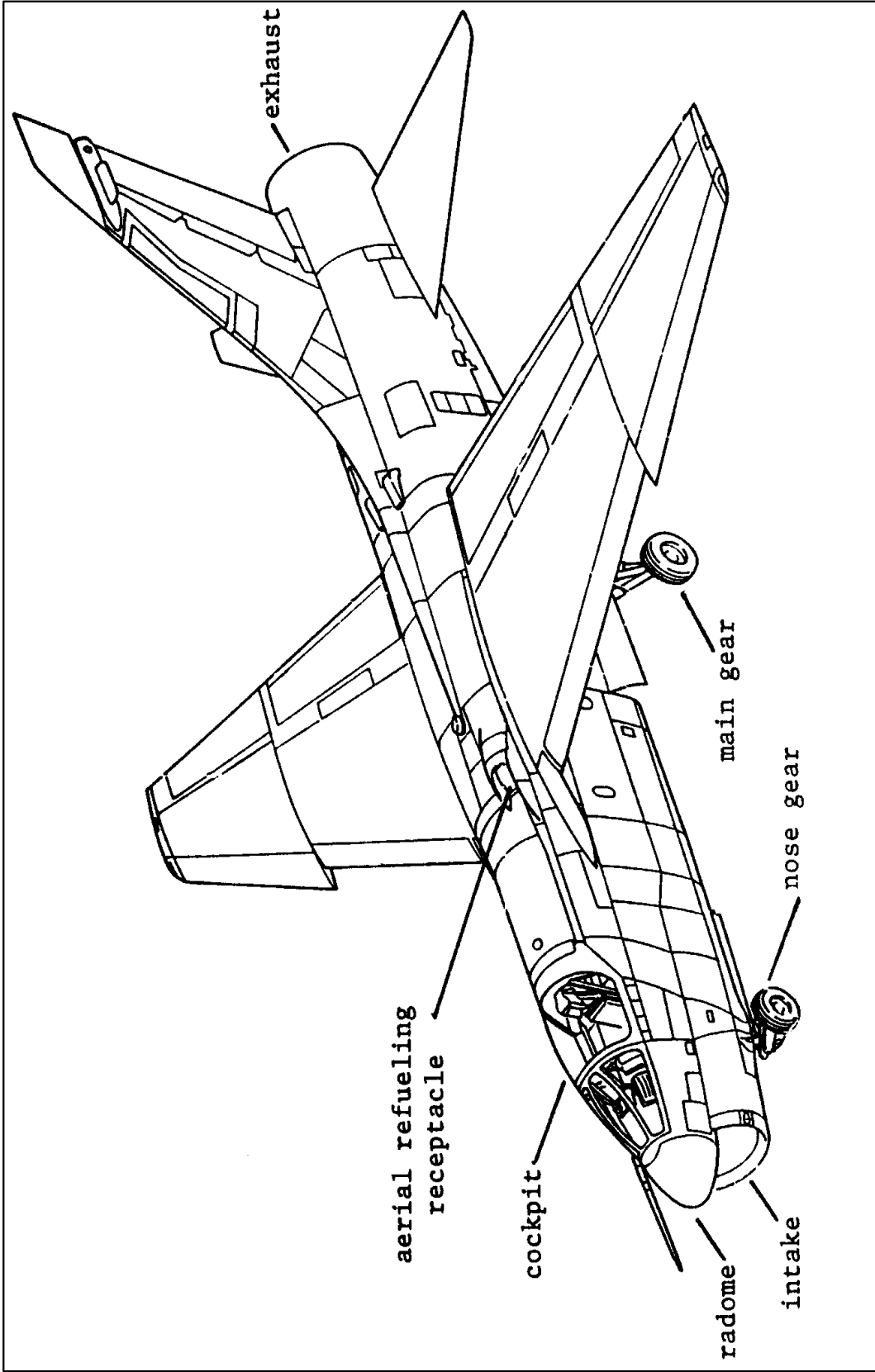


Figure 7 Fuselage Group

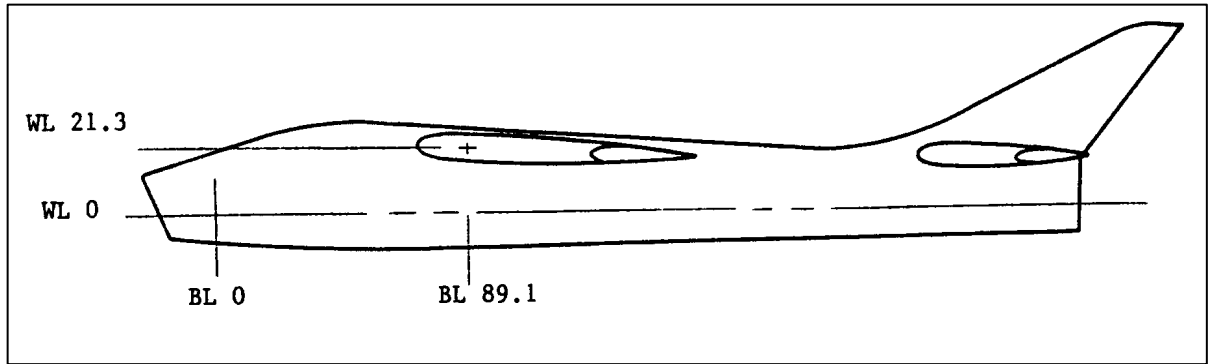


Figure 8 Fuselage Station and Butt Line Definition

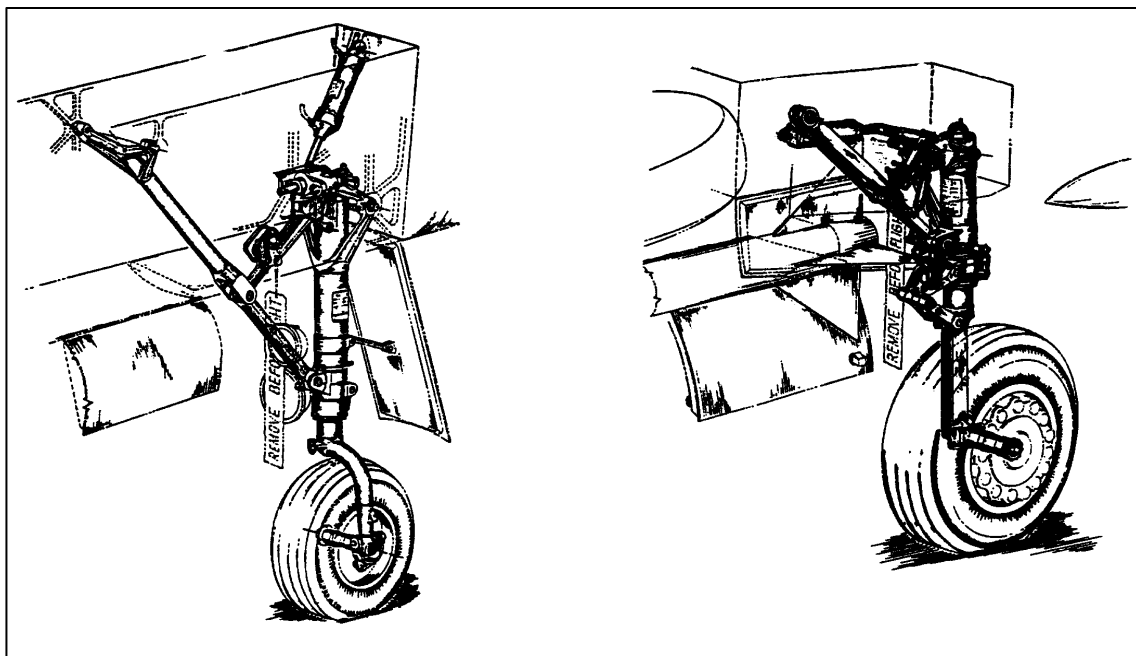


Figure 9 Typical Landing Gear

designed to retract out of the airstream to reduce drag. The tricycle gear arrangement is most popular, with a nose gear and twin main gear assemblies.

1.2.5 Miscellaneous

Fillets are fairings that smoothly transition one surface to another at a junction, such as at the root of the wing or where an engine nacelle joins the wing. **Strakes** may be small surfaces that extend ahead of a leading edge, such as at the root of the vertical stabilizer. Other strakes may be very small surfaces protruding from a larger surface to straighten airflow.

1.3 Systems

Modern military aircraft have become exceedingly complex machines with a myriad of different systems that must work together at the command of the aircrew and onboard computers. Some of the more common systems will be covered in a simple manner. You may need to study the individual systems of the aircraft you're working with in various levels of detail as required for the specific test program. At least a broad familiarization

with the major systems are recommended for even the most superficial flight tests. Do not hesitate to ask for manuals and question the aircrew, maintenance personnel, and other engineers if you are uncertain of particular aspects of a system.

Most of the aircraft systems are controlled through electronic ‘boxes’ scattered throughout the aircraft. Such boxes are collectively called **avionics** and are connected through miles of wires and cable bundles. Computers will control systems with like functions and may be called **flight computers** or **mission computers**. Signals from these myriad systems may come together at a central point called a **data bus** where they may be sent to displays, computers, or monitored during flight testing. Many avionic systems will also have associated external antennas, both flush (conformal) and blade type. Electronic equipment can generate considerable heat, which can be self-damaging. To avoid this damage, the equipment is cooled by conditioned air or liquid provided by an **environmental control system (ECS)** described in Section 1.3.4.

1.3.1 Propulsion

There are only a few types of power plants that are typically used in high performance military aircraft. These are the **turbojet**, **turbofan**, and **turboprop** engines, which share many similar features. The reciprocating engine, such as is in your automobile, will not be covered. Figure 10 shows the principal features of the turbine aircraft engine, the individual sections often being referred to by station numbers, as shown. Each engine has specific performance characteristics in terms of fuel demand and rated thrust. These characteristics will determine the choice of engine for the specific aircraft and mission.

The most forward element of the turbofan engine is the **fan** section. This section consists of one or more rows of rotating, radially-mounted airfoil blades (Section 2.2.5) which increase the velocity and pressure of the air downstream to create thrust. A forward row of blades may be fixed and serve only to pass the airflow at the proper angle into the engine. Some of this air will be exhausted directly out of the engine nacelle (or into the primary exhaust stream for fighter-type turbofan engines) while the rest is channeled into the core of the engine. The amount of air ducted out versus that ducted into the core is defined as the **bypass ratio**. A high bypass ratio engine will tend to be fat, with a very large fan section, and are common on transport-type aircraft. In this case the fan provides most of the thrust. The low bypass engine can be found in fighter applications with the core providing most of the thrust. In a turbojet engine there is no fan section at all.

The turboprop uses propeller blades to do the same job as a fan section but none of the downstream flow is ducted into the core. In fact, the propeller may be connected to the core of the engine only by a gear case, which reduces the rotational speed of the core shaft to a speed compatible with propeller aerodynamics (to avoid supersonic tip speeds). The core exhaust typically produces less than 15 percent of a turboprop’s thrust.

The engine **inlet**, or **intake**, plays a very important role in the engine performance (Figure 11). In all cases, the inlet attempts to produce an ideal pressure distribution at the face of the compressor or fan section. Many engine installations will have very simple, fixed geometry inlets because the airplane is restricted to subsonic speeds. In the case of supersonic flight, the inlet will slow the incoming air to subsonic conditions before the flow encounters fan or compressor blades. This is done by positioning one or more shock waves (Section 2.2.4) and may involve movable ramps or a movable cone within the inlet.

The engine core begins with the **compressor** section, which consists of many rows or stages of alternating fixed (**stator**) and rotating blades, which greatly increase the pressure of the air. The air then enters the **combustion section**, which mixes fuel with the air and burns the mixture to raise the temperature and velocity of the flow. The **turbine** section, several rows of stators and rotary turbine blades, extracts energy from the flow to drive the compressor and fan through the drive shaft, which runs through the center of the engine. Turbofan engines have two compressors (the first being the fan) and two turbines, called the high- and low-pressure components. The fan is tied to the aft, low-pressure turbine by a separate, nested shaft, which turns at a slower speed than the core components. The second compressor and initial turbine are the high-pressure core components and operate on its own, higher speed shaft.

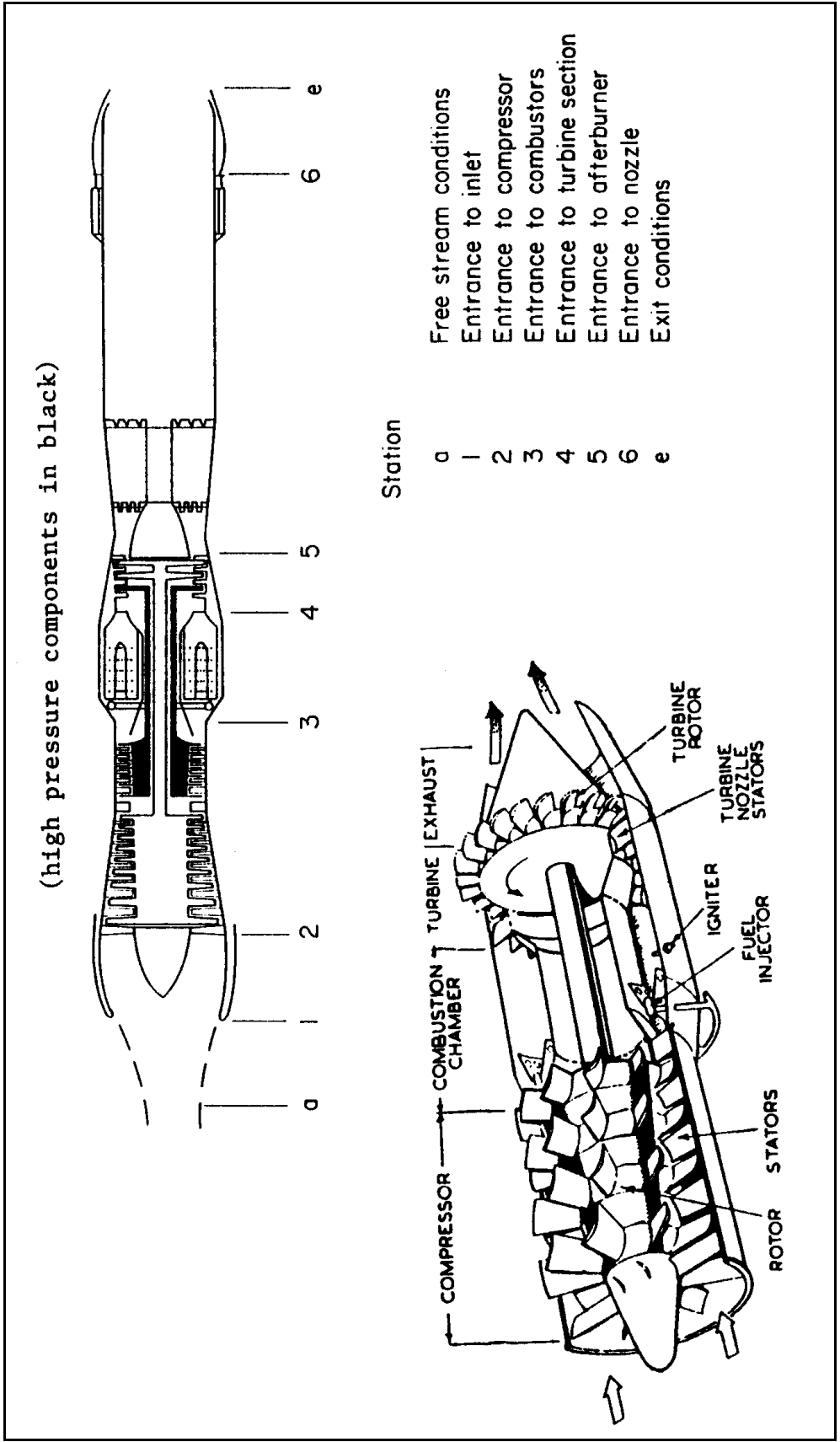


Figure 10 Typical Turbine Engine

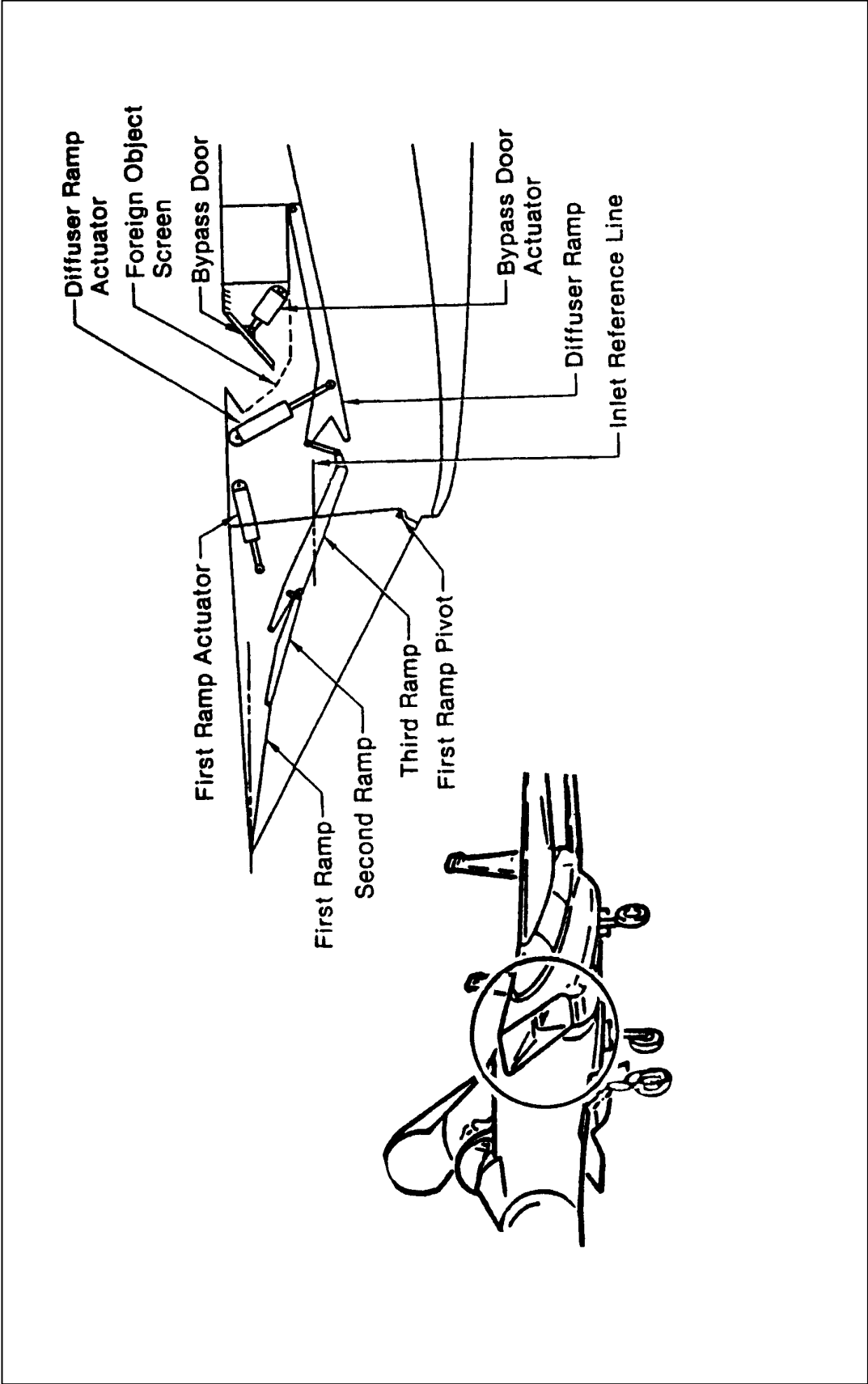


Figure 11 Typical Supersonic Inlet

Bleed air is extracted from the high-pressure compressor for use by the ECS (Section 1.3.4) and for other auxiliary functions. The high-pressure compressor/initial turbine section may also be connected to an **accessory gearbox**, which, through reduction gearing, drives hydraulic pumps and the aircraft electrical generators.

The **nozzle**, or **diffuser**, at the aft end of the engine is also very important (Figure 12). The exhaust nozzle provides the final acceleration of the air through a venturi as it exits the engine. Some fuel may be added as the flow leaves the turbine and ignited (the **afterburner** or **augmentor**) to greatly increase the thrust (and also the fuel flow). The nozzle will likely be able to change its exit area so that the exit pressure approaches the ambient conditions - a critical parameter for efficient production of thrust. Nozzles may incorporate some form of **thrust reverser** to serve as a deceleration mechanism and **thrust vectoring** for additional flight control.

1.3.2 Hydraulics

Hydraulics are used to move heavy appendages against gravity and air pressure. The hydraulic fluid, which is typically highly inflammable, is contained in **reservoirs** and **accumulators** and moved by engine-driven or electric motor-driven pumps through valves and hydraulic pressure lines throughout the aircraft. Hydraulics typically move control surfaces, airbrakes, and the landing gear through rams or actuators. Because of the criticality of these systems, the failure of a hydraulic system is often an emergency situation and will require the plane to return to base immediately. During ground checks or maintenance, during which the engines are not operating, an external hydraulic pump cart is used.

1.3.3 Electrical

Many of the aircraft systems are electrically powered. This power is typically derived from **generators** driven by the engine(s) as an accessory. When the engines are not operating, batteries will supply power briefly for a few essential systems. On the ground, a motor in a ground generator cart will supply power through a ground power receptacle until the engine(s) have been started. Some aircraft have their own onboard independent generator for power before engine start and to power the engine starters themselves. These are called **auxiliary power units (APUs)**. In the event of a failure of all the engines in flight, a small **ram air turbine (RAT)** may be deployed. This is a propeller generator driven by the outside airflow.

The power is distributed to the various aircraft systems through one or more **electrical buses**. Separate buses for ac and dc power are typical. Some systems are dedicated to particular buses or generators so that partial electrical failures may effect only selective systems. Power to individual systems can be cut by pulling **circuit breakers**, the most important of which are generally within easy reach of the aircrew.

1.3.4 Environmental Control System

Most modern military aircraft are equipped with an ECS. It serves the following functions:

- a. Distribution of engine compressor bleed air to components and subsystems such as pressurization of inflatable seals, air-conditioning and pressurization of the cockpit or cabin, equipment compartments, and the avionics.
- b. Anti-icing or de-icing of flight surfaces, engine inlets and ram air scoops; removal of rain, snow, ice, frost, condensation, dust and insect residue from transparent surfaces and sensor windows.
- c. Pressurization of hydraulic system fluid reservoirs and miscellaneous equipment; and purging of gun gas and vapor or fuel from air refueling manifolds (Section 1.3.5).

Environmental control system air-conditioning for the avionics circulates cooled air or fluid. Air is originally obtained through ram air scoops on the skin of the plane and is carried throughout the aircraft through ducting to the avionics. On the ground, before taxi or during check-outs, this cooling air is provided by ground carts through hoses connected to special ports in the aircraft.

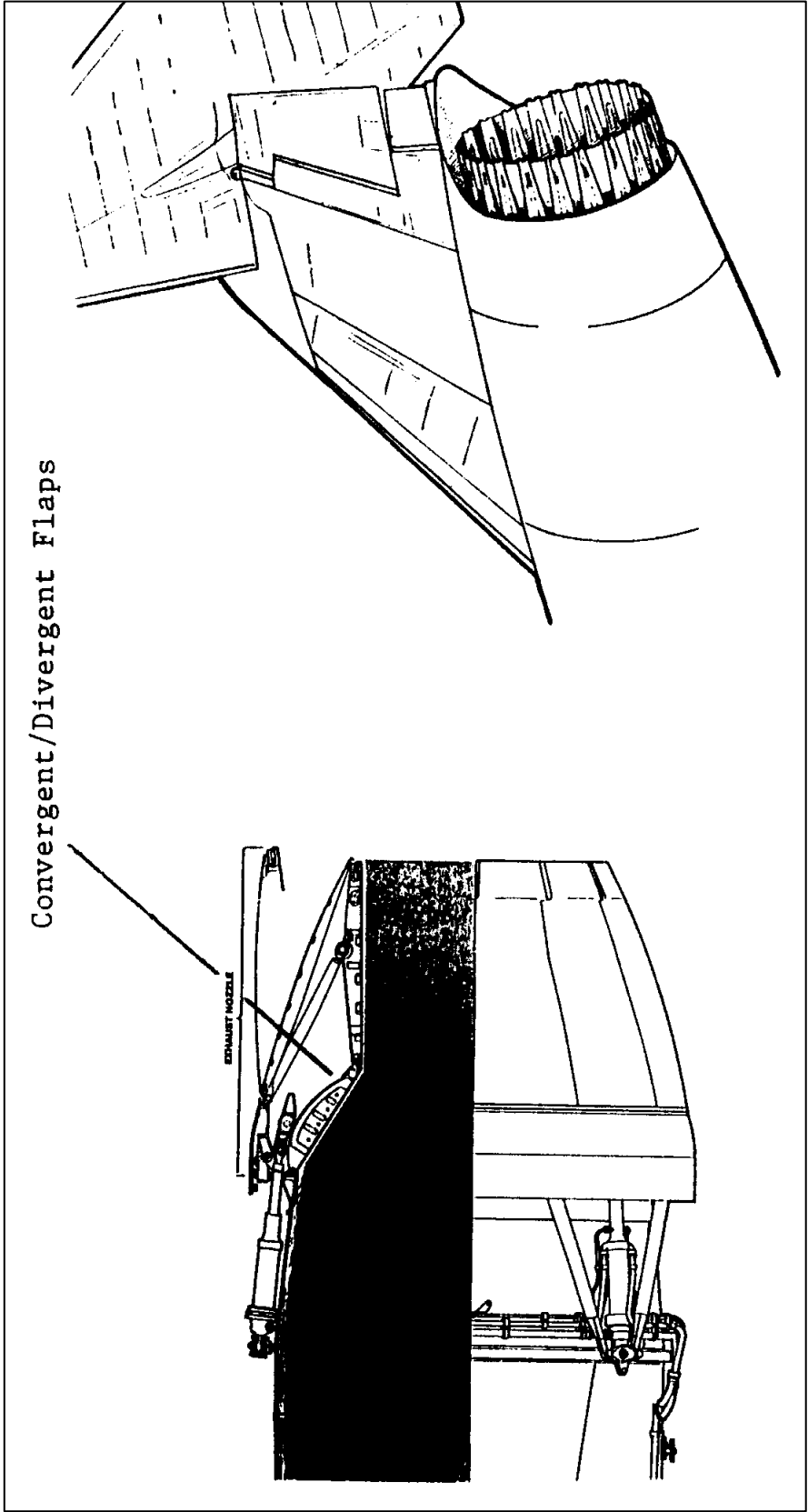


Figure 12 Typical Engine Exhaust Nozzle

1.3.5 Fuel

Fuel to run the engine(s) is typically contained in a number of flexible bladders or metal cells within the structure of the wings and fuselage, or within **external** or '**drop**' tanks attached to pylons beneath the wings or the fuselage. The tanks are usually interconnected to allow the transfer of fuel to the engines and between tanks for weight and balance considerations (Section 2.3.2). The fuel is transferred through fuel lines by fuel pumps, frequently located in the tanks themselves. Major junctions of fuel lines are called **manifolds**.

Aircraft are refueled or defueled on the ground through one or more refueling points and fuel is pumped on board under pressure. Many aircraft can be refueled in flight from a tanker (**aerial refueling [AR]**). The USAF method is '**boom**' **refueling** by which the tanker connects a steerable, telescoping boom with a fuel tube and refueling nozzle into a receptacle on the 'receiver' aircraft (Figure 13). Other services and countries use the '**probe and drogue**' system in which the receiver flies a probe with a nozzle attached to the plane into a 'basket,' or drogue, trailing from the tanker on a retractable hose (Figure 14).

1.3.6 Flight Controls

Pilot commands to the control surfaces which change the aircraft's attitude and flight path are carried from the control column (stick) or yoke for vertical and lateral control and the rudder pedals for directional inputs by push rods, cables, pulleys and bellcranks (Figure 15). Weights and springs within the system will give the pilot the correct 'feel' or feedback needed to properly judge the amount of input required. In most cases the pilot does not directly move the surface, but rather opens and closes hydraulic valves which ports the correct amount of hydraulic fluid under pressure to move the surface via an actuator. The flight control system will often mix motions of several control surfaces in different axes to achieve the desired aircraft response.

Many newer aircraft have electric flight controls that interpret the pilot's commands and generate signals to move the control surfaces (or hydraulic valves) as appropriate. In this case there is no mechanical connection between the stick and rudder pedals and the control surfaces themselves. This is the so-called '**fly-by-wire**' concept. Almost all aircraft have **autopilots** that perform basic functions like keeping the wings level and maintaining the assigned heading with the pilot making no control input. They can also automatically guide the airplane on approach-to-landing paths by tying into navigation radio signals. More sophisticated systems can be programmed to fly pre-selected routes and even perform an entire mission, including weapons release, without pilot intervention.

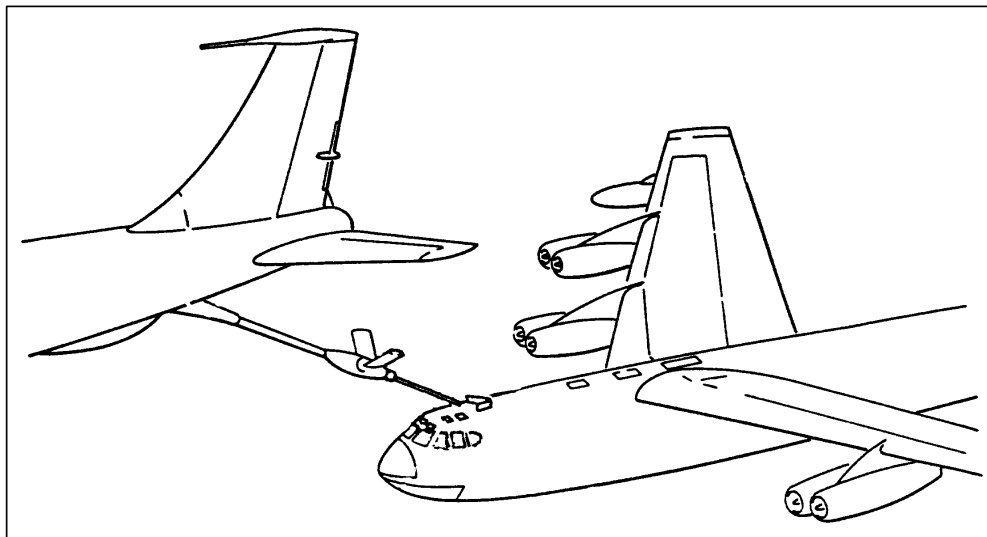


Figure 13 Aerial Refueling Boom and Receptacle System

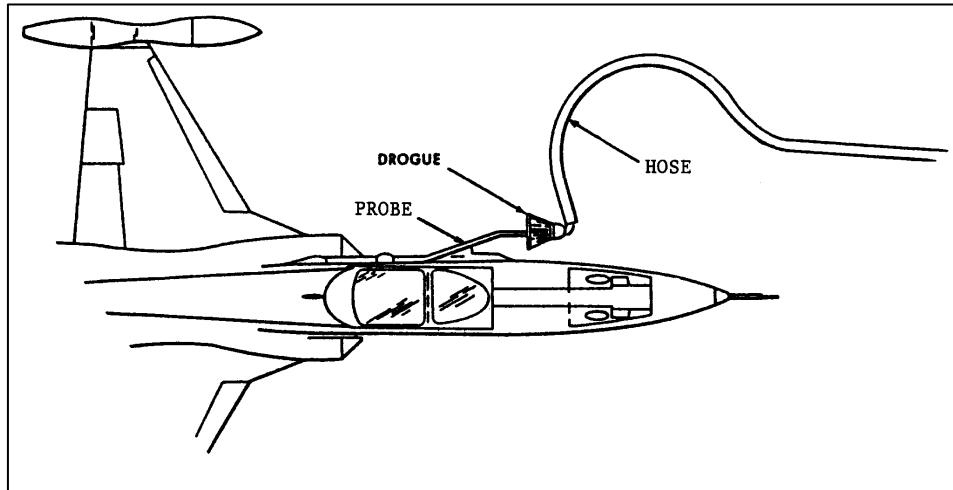


Figure 14 Aerial Refueling Probe and Drogue System

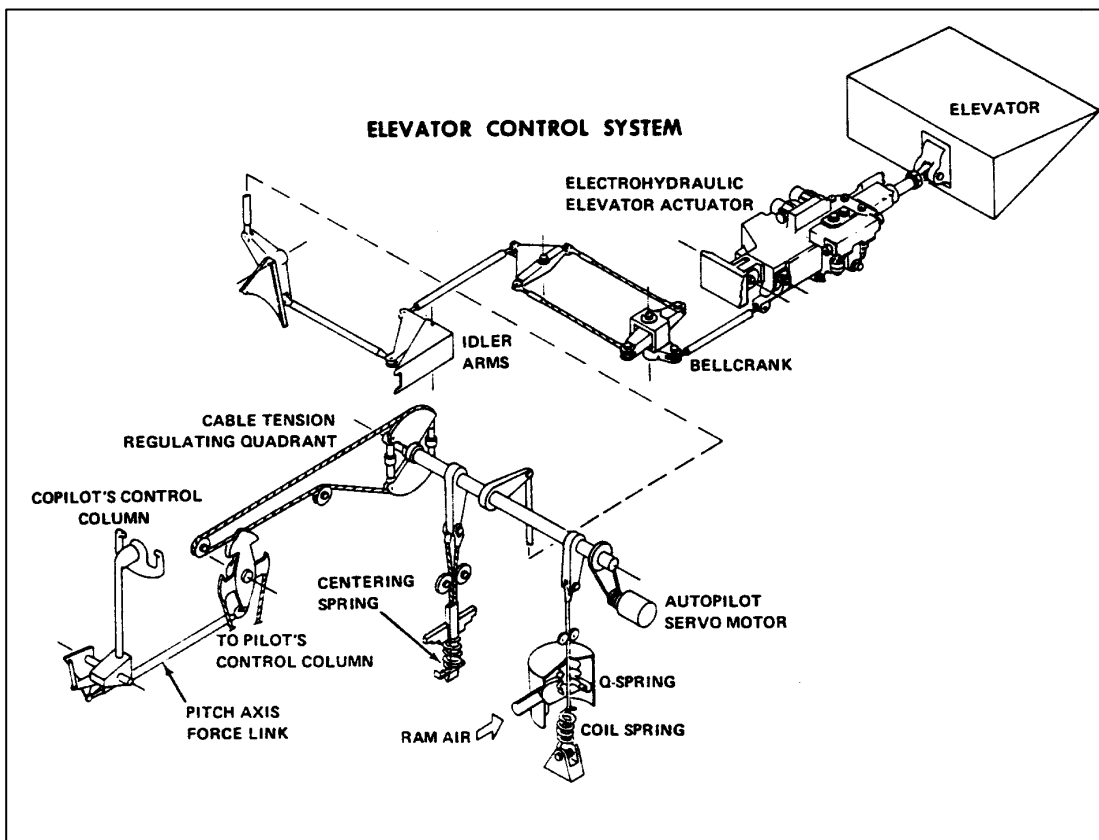


Figure 15 Typical Mechanical Control System

1.3.7 Cockpit Group

An onboard oxygen system provides breathing air to the crew under pressure at high altitude. A separate pressurized air system is available in fighter-type aircraft to inflate the **g-suit** which the crew wear on their lower extremities to increase their tolerance to withstand high g forces (Section 5.2.1). Except for transport aircraft, the crew will be seated in **ejection seats**. These are seats that can be propelled by a rocket motor out of the aircraft on command if the occupant is endangered.

The cockpit contains life support equipment for the pilot plus the controls and instruments needed to operate the aircraft and perform its mission. A typical cockpit arrangement is shown in Figure 16.

The primary flight instrument is the **altimeter**, which displays the aircraft's height as a function of barometric pressure. Many aircraft also have a radar altimeter, which uses radar reflections off the ground to determine altitude. The **airspeed indicator** shows the plane's speed relative to the surrounding air, the **rate-of-climb indicator** displays the rate of ascent or descent as a function of changing ambient pressure, and the **attitude indicator** shows the plane's orientation relative to the earth's gravity center by use of gyros. The principal engine indicators can include the **engine pressure ratio** ([EPR], the ratio of turbine discharge to inlet pressure), the **core rotational speed** (in a turbofan, **N1** for the low-pressure components and **N2** for the high pressure), an **inter-turbine temperature** ([ITT] or [FITT], between the low- and high-pressure turbines in a turbofan engine), **nozzle pressure ratio** ([NPR], the ratio of the pressure at the exit of the turbine to the pressure at the throat of the venturi), **exhaust gas temperature** ([EGT], at the exit of the turbine section) and the **fuel flow**. The primary engine control is the throttle to adjust the engine rotational speed and select afterburner operation. Many of the most recent aircraft have all of these displays integrated on one or more **multifunction displays (MFDs)**—a TV or other type screen—with only a few separate backup instruments.

The aircraft will have many radios at the disposal of the crew. One or more transceivers of the UHF, VHF and HF types are common. Special purpose nonverbal radios will include a **transponder** that shows ground radar controllers the altitude and identity of the aircraft, and the **identification friend-or-foe (IFF)** which transmits an encoded signal. An **intercom**, or **interphone**, permits conversation between the crewmembers and carries the cockpit audio tones and warnings. There may be a couple of navigation radios with associated displays to show the plane's distance, bearing or relative location from a ground transmitter station. Most military aircraft also have a gyroscopic or laser **inertial navigation system (INS)** with its associated display. Much of this navigation data is displayed on a **horizontal situation indicator (HSI)**.

The cockpit will include many other displays to show system status, fault warnings, offensive and defensive systems status, and mission information. Many aircraft also have a **head-up display (HUD)** which reflects the most fundamental data on a glass plate in front of the pilot within the field of view when looking out the forward windscreen. A radar display is also included in the cockpit. The radar may be designed to track other aircraft or to show the weather or terrain on the display in the cockpit.

1.3.8 Weapons

Military aircraft typically carry some form of weaponry, many times external to the structure. Guns are usually internal and fire through a gun port. Large drums of ammunition will be stored within the aircraft. Many weapons that are released from the machine are carried either internally in a bay (bomb or weapons bay) or externally. External weapons may be attached directly to the structure or on pylons fixed to the underside of the wing or fuselage that stand them away from the structure for aerodynamic reasons (Figure 17).

Bombs and missiles may be attached to racks that in turn attach to pylons. The racks will have an attachment and release mechanism and perhaps a wire harness through which power and commands are transmitted. Missiles may be guided or unguided (rockets) and be an air-to-ground or air-to-air weapon. **Chaff** (small strips of metal) and flares are often also carried as defensive measures. Many forms of radio transmitters and receivers are also carried as an offensive or defensive form of electronic warfare (**EW**).

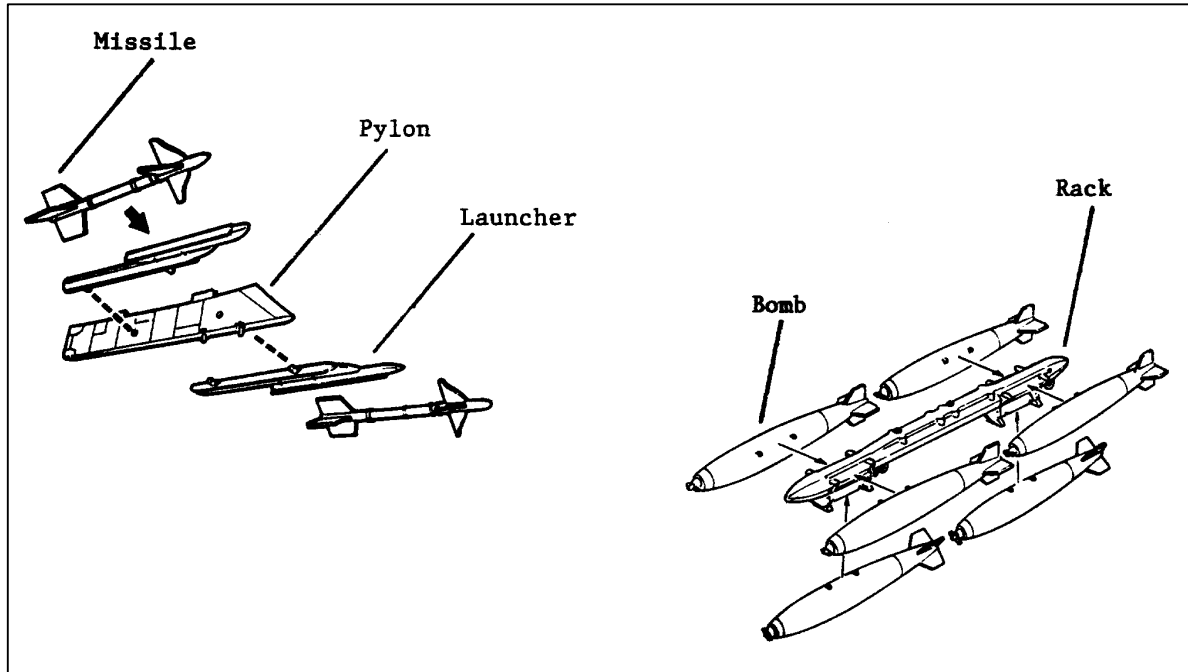


Figure 17 Example Weapon Pylon and Store Ejector Rack

SECTION 1 REFERENCES

1. Hurt, H.H., Jr., *Aerodynamics for Naval Aviators*, NAVWEPS 00-80T-80, U.S. Navy, January 1965.
2. Gunston, Bill and Spick, Mike, *Modern Air Combat*, Crescent Books, New York, New York, 1983.
3. Stinton, Darrol, *The Anatomy of the Aeroplane*, Granada Publishing Limited, London, England, 1980.
4. Stinton, Darrol, *The Design of the Airplane*, Van Nostrand Reinhold Company, New York, New York, 1983.
5. Whitford, Ray, *Design for Air Combat*, Jane's Publishing Company, London, England, 1987.

2.0 AERODYNAMICS AND FLIGHT MECHANICS

2.1 Introduction

Many engineers who first begin working in aircraft structures flight testing have only a rudimentary understanding of aerodynamics and aircraft control. Because in flight the aerodynamic forces are the predominant structural forcing function, it is important that the structures flight test engineer become versed in aerodynamic theory. Aircraft dynamics can also play an important role in structural dynamics. Understanding these details of aircraft operation and the environment in which aircraft function is essential to effective flight test planning. During flight testing, the engineer will be exposed to many terms and concepts for which this chapter will serve as an introduction.

This chapter will provide an extremely broad and simplistic introduction to aerodynamics and aircraft control. The reader is strongly encouraged to pursue the subject further by reviewing the suggested references, particularly Reference 2, which provides a thorough but easily understood overview.

2.2 Basic Aerodynamics

2.2.1 The Atmosphere

The aerodynamic forces and moments acting upon an aircraft in flight are due in large part to the properties of the air in which it flies. Of primary importance is the static pressure at the point in the sky where the aircraft is flying. Pressure (P) is dependent upon the temperature and the density of the fluid (the air). Recall the **Perfect Gas Law**

$$P = \rho R t \quad (2)$$

where:

- ρ = the density,
- t = is the absolute temperature, and
- R = is the gas constant.

Since density and temperature, in general, decrease with altitude and is influenced by humidity and other weather phenomena, it is clear that the pressure distribution within the atmosphere is far from homogeneous.

Air pressure is often defined in inches of mercury (in. Hg) as in a barometer reading (**barometric pressure**). A useful conversion is:

$$\text{in. Hg} = 0.49 \text{ psi} \quad (3)$$

Another useful concept is the standard lapse rates, or the variation of temperature and pressure with altitude. In the lower atmosphere, where most 'airbreathing' flight occurs, these are:

$$(1 \text{ in. Hg})/(1,000 \text{ ft}) \quad (4)$$

$$(2^\circ\text{C})/(1,000 \text{ ft}) \quad (5)$$

In order to provide a predictable change of atmospheric properties with altitude, a **standard atmosphere** (or **standard day** conditions) has been defined (Table 1). By correcting information such as aircraft performance data to this standard, a justified comparison can be made to other data with the effects of atmospheric variations removed.

Table 1
THE STANDARD ATMOSPHERE

Altitude (Z^* , ft)	Temperature (T , °R)	Pressure P (lb/ft ²)	Density ρ (lb sec ² /ft ⁴)	Speed of sound (ft/sec)
0	518.69	2116.20	2.3769 ⁻³	1116.40
1,000	515.12	2040.90	2.3081	1112.60
2,000	511.56	1967.70	2.2409	1108.70
3,000	507.99	1896.70	2.1752	1104.90
4,000	504.43	1827.70	2.1110	1101.00
5,000	500.86	1760.90	2.0482	1097.10
6,000	497.30	1696.00	1.9869 ⁻³	1093.20
7,000	493.73	1633.10	1.9270	1089.30
8,000	490.17	1572.10	1.8685	1085.30
9,000	486.61	1512.90	1.8113	1081.40
10,000	483.04	1455.60	1.7556	1077.40
11,000	479.48	1400.00	1.7011 ⁻³	1073.40
12,000	475.92	1346.20	1.6480	1069.40
13,000	472.36	1294.10	1.5961	1065.40
14,000	468.80	1243.60	1.5455	1061.40
15,000	465.23	1194.80	1.4962	1057.40
16,000	461.67	1147.50	1.4480 ⁻³	1053.30
17,000	458.11	1101.70	1.4011	1049.20
18,000	454.55	1057.50	1.3553	1045.10
19,000	450.99	1014.70	1.3107	1041.00
20,000	447.43	973.27	1.2673	1036.90
21,000	443.87	933.26	1.2249 ⁻³	1032.80
22,000	440.32	894.59	1.1836	1028.60
23,000	436.76	857.24	1.1435	1024.50
24,000	433.20	821.16	1.1043	1020.30
25,000	429.64	786.33	1.0663	1016.10
26,000	426.08	752.71	1.0292 ⁻³	1011.90
27,000	422.53	720.26	9.9311 ⁻⁴	1007.70
28,000	418.97	688.96	9.5801	1003.40
29,000	415.41	658.77	9.2387	1000.13
30,000	411.86	629.66	8.9068	994.85
31,000	408.30	601.61	8.5841 ⁻⁴	990.54
32,000	404.75	574.58	8.2704	986.22
33,000	401.19	548.54	7.9656	981.88
34,000	397.64	523.47	7.6696	977.52
35,000	394.08	499.34	7.3820	973.14
36,000	390.53	476.12	7.1028 ⁻⁴	968.75
37,000	389.99	453.86	6.7800	968.08
38,000	389.99	432.63	6.4629	968.08
39,000	389.99	412.41	6.1608	968.08
40,000	389.99	393.12	5.8727	968.08
41,000	389.99	374.75	5.5982 ⁻⁴	968.08
42,000	389.99	357.23	5.3365	968.08
43,000	389.99	340.53	5.0871	968.08
44,000	389.99	324.62	4.8493	968.08
45,000	389.99	309.45	4.6227	968.08

Table 1 (Concluded)
THE STANDARD ATMOSPHERE

Altitude (Z^* , ft)	Temperature (T , °R)	Pressure P (lb/ft ²)	Density ρ (lb sec ² /ft ⁴)	Speed of sound (ft/sec)
46,000	389.99	294.99	4.4067 ⁻⁴	968.08
47,000	389.99	281.20	4.2008	968.08
48,000	389.99	268.07	4.0045	968.08
49,000	389.99	255.54	3.8175	968.08
50,000	389.99	243.61	3.6391	968.08
51,000	389.99	232.23	3.4692 ⁻⁴	968.08
52,000	389.99	221.38	3.3072	968.08
53,000	389.99	211.05	3.1527	968.08
54,000	389.99	201.19	3.0055	968.08
55,000	389.99	191.80	2.8652	968.08
56,000	389.99	182.84	2.7314 ⁻⁴	968.08
57,000	389.99	174.31	2.6039	968.08
58,000	389.99	166.17	2.4824	968.08
59,000	389.99	158.42	2.3665	968.08
60,000	389.99	151.03	2.2561	968.08

The following variations are often defined as the ratios:

$$\delta = P/P_s \quad (6)$$

$$\sigma = \rho/\rho_s \quad (7)$$

$$\theta = t/t_s \quad (8)$$

where:

_s = denotes standard day sea level conditions.

2.2.2 Altitude and Airspeed Measurement

Aircraft altimeters are calibrated for the standard atmosphere and are essentially sensitive barometers which indicate altitude in the standard atmosphere. However, they normally have the means of correcting the readings for the local pressure conditions. Setting the instrument to the local barometric pressure will allow it to display **density altitude**. If the sea level standard day pressure of 29.92 in. Hg is used then a **pressure altitude** will be read. To reduce the level of standardization corrections required for test data, the pressure altitude is normally used in flight test by setting the aircraft altimeter to 29.92 prior to flight.

The measurement of airspeed is done with the difference of total and static pressures. The **total pressure** (P_T) is the sum of the static and dynamic pressures, as defined by the **Bernoulli Equation** (assuming incompressible air):

$$P_T = P + \rho V^2 / 2 \quad (9)$$

which is constant, and where the **dynamic pressure** term (q) is:

$$q = \rho V_t^2 / 2 = \rho_s V_e^2 / 2 \quad q = \rho V_t^2 / 2 = \rho_s V_e^2 / 2 \quad (10)$$

where:

V_t = true airspeed, and
 V_e = equivalent airspeed, both defined later.

The dynamic pressure is an important measure of the aerodynamic force acting on a flight vehicle. Measurement of the static pressure is normally done on the aircraft skin where the pressure field is corrupted by the presence of the aircraft itself. This produces what are called **position errors**. When the **indicated airspeed** ([IAS] or [KIAS] when given in nautical air miles per hour or **knots**) is corrected for instrument and position errors it is called **calibrated airspeed** ([CAS] or [KCAS]). The error may be additive or subtractive, so CAS could be higher or lower than IAS. The position error can be significantly reduced by sensing the Pitot-static pressures at the tip of a boom (**Pitot-static boom**) extending ahead of the aircraft or on a tube stabilized with a cone which trails behind the aircraft (**trailing cone**). The errors are determined with an **airspeed calibration** test (Reference 1). **Equivalent airspeed** (EAS) is the correction of CAS for compressibility effects. This correction is necessary during flight near and beyond the speed of sound (Section 2.2.4). These corrections are negative, so EAS is always less than CAS above sea level (Figure 18). A final correction will produce **true airspeed** (TAS). This is a correction for air density changes with altitude, defined as:

$$V_t = V_e / \sqrt{\sigma} \quad (11)$$

which makes TAS greater than EAS above sea level.

2.2.3 Airflow Visualization

In an effort to more fully understand the airflow about and pressure distribution on an object in flight, a system of flow visualizations has been developed.

The **streamline** is the most basic element of the visualization system. It shows the direction of travel and path of air molecules in the presence of a body (Figure 19). Closely spaced streamlines imply high velocity and widely spaced streamlines imply a lower velocity. Where the streamline ends on the surface the velocity is zero. This is called a **stagnation point**. During flight testing, it is possible to see the direction of the flow adjacent to a surface by taping an array of **tufts** (short strips of cord, perhaps with a tiny cone attached) to the area of interest on the aircraft. A turbulent flow would be seen as violently disturbed tufts.

The pressure distribution on the body can be shown by a series of arrows (Figure 20). Long arrows indicate a large pressure and small short arrows a lower pressure. Arrows pointing toward the body imply a positive pressure (greater than the surrounding static pressure) and those pointing away from the body imply a negative pressure (lower than static). A change in pressure across a portion of the body is called a **pressure gradient**.

More recently, computer-generated images show colored or shaded zones, each representing different ranges of pressure, velocity, or surface temperature. Shock waves (next section) can be seen and photographed during wind tunnel tests using a system of polarized light and lenses called **Schlieren**. The shocks appear as shadows or 'fringes' in the photograph.

2.2.4 Supersonic Flight

Pressure (or density) waves in the atmosphere (or any fluid), generated by the motion of a body, travel at the speed of sound for the fluid. An object traveling at, or greater than, the speed of sound will be displacing the air molecules faster than they can propagate ahead of the object. The air will pile up into a wave of highly compressed air called a **shock wave**. This phenomena results in a fundamental change in aircraft aerodynamics and requires a separate review.

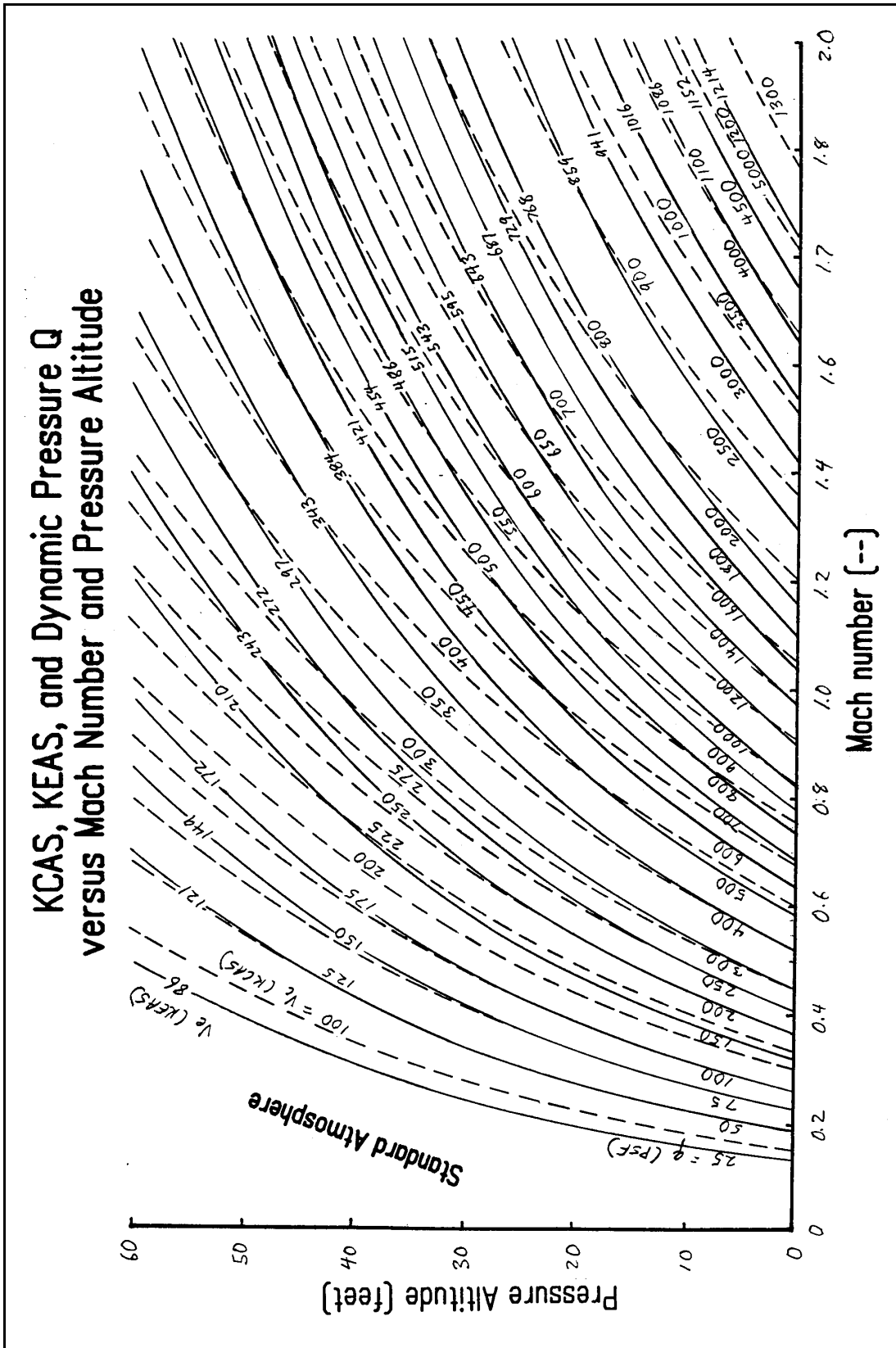


Figure 18 Relationships of Airspeed Forms with Altitude

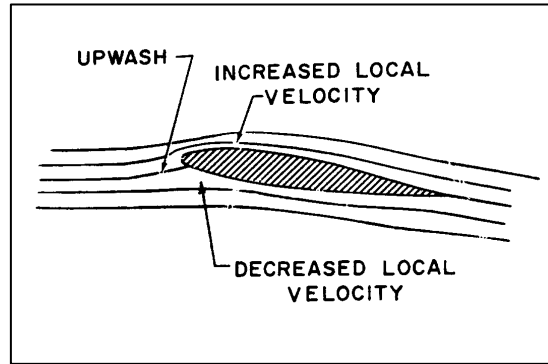


Figure 19 Streamlines Around an Airfoil

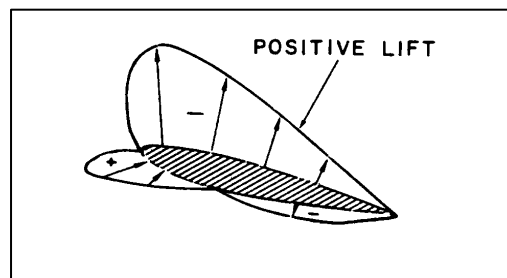


Figure 20 Pressure Distribution on an Airfoil

Flight above the speed of sound is called supersonic flight. Airspeeds can be related to the speed of sound through **Mach numbers (M)** defined as:

$$M = V_t / a = V_c / (a\sqrt{\sigma}) \quad (12)$$

where:

a = the speed of sound.

Since the speed of sound decreases with altitude, at least up to 36,000 feet (see Table 1 and Figure 18), an aircraft would have to travel much faster (relative to the earth) and be subjected to much higher dynamic pressures to fly at Mach 1.0 (**supersonic**) at sea level than at 30,000 foot altitude. Because of the fundamental difference between supersonic and **subsonic** flight (less than the speed of sound) it is convenient to use Mach numbers to refer to the velocity of aircraft capable of supersonic flight.

It has been found convenient to make further definitions of airspeed relative to the speed of sound. Supersonic velocities will typically begin to appear at some points on the surface of the aircraft (called the **critical Mach number**) at about 0.85 M and above. From here to about 1.2 M some subsonic flow will still be present on the aircraft and this is called the **transonic** speed range. There are important performance and control impacts on an aircraft as it enters the transonic region and this is the most challenging flight regime to analyze with any precision. The **hypersonic** range is considered to begin at about 3.0 M.

There are different types of shock waves, dependent upon the geometry of the body in the flow (Figure 21). The **normal shock** occurs ahead of a blunt body. The flow is decelerated aft of the shock to subsonic flow with a great increase in static pressure and density. The **oblique shock** is formed at an acute corner of the body. The flow turns to follow the body and is decelerated with a rise in pressure and density. At an oblique corner an expansion wave will occur to turn the flow, giving an increase in Mach number but a

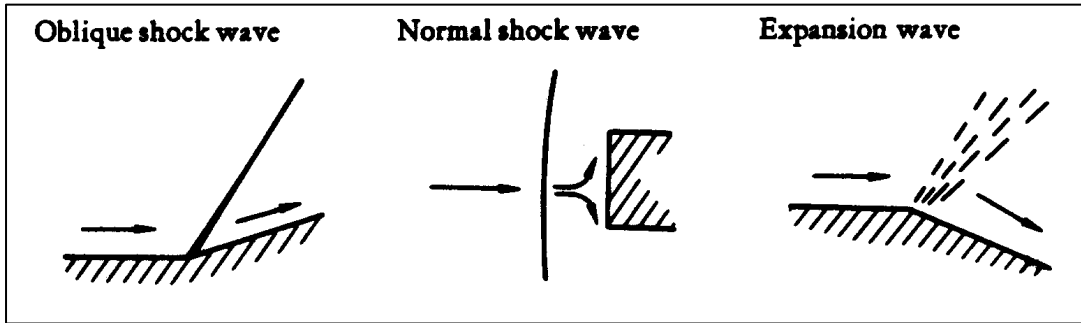


Figure 21 Shocks

decrease in pressure and density. The position and geometry of the shock wave is dependent upon the geometry of the body and the Mach number. Shocks are often unsteady and their movement can effect flight control and aeroelasticity (Section 6.0).

2.2.5 Generation of Lift

The primary lifting surface of an aircraft is the wing. The wing section (cross-section), called an **airfoil**, is the most critical aspect of the wing determining its lift characteristics. Some of the airfoil geometry is defined in Figure 22. Other definitions relative to lift generation are defined in Figure 23.

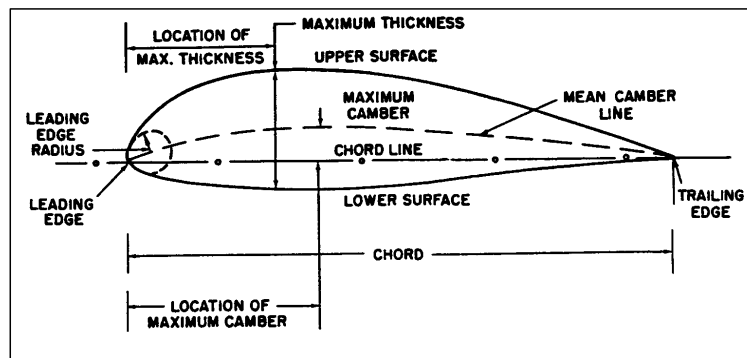


Figure 22 Airfoil Geometry Terminology

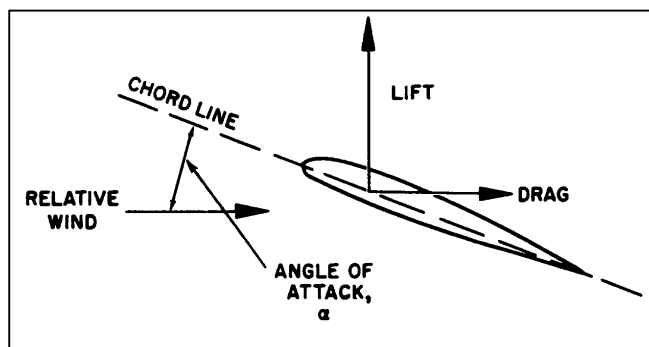


Figure 23 Lift Generation on an Airfoil

The simplest explanation of how an airfoil generates lift is the velocity increase of the air as it flows over the **cambered** upper surface. As the airfoil is propelled through the air (seen from the perspective of the airfoil

as air flowing past the surface) the air molecules immediately adjacent to the surface are displaced against molecules further removed from the surface which resist the displacement by virtue of their inertia and friction with surrounding molecules. The result is an increase in velocity over the airfoil by venturi effect, with the cambered airfoil and surrounding air acting as the constricting walls of a venturi. This velocity increase results in a drop of static pressure on the top of the wing for the total pressure to remain constant (the Bernoulli equation again). However, more complex events must also occur. The presence of the airfoil and the aircraft in general produces an **upwash** effect ahead of the surface and then a **downwash** aft of it. The consequence of this is the production of **circulation** in the flow, essential for lift (Figure 24). The flow of high pressure air around the wingtip to the low pressure region on top of the wing contributes to this circulation by producing a helical flow pattern called a **tip vortex** (Figure 25).

Some of the flow immediately adjacent to the surface (the **boundary layer**) will be smooth (**laminar**) but eventually trips to a **turbulent layer** further aft on the body. The lift on a wing will increase with angle of attack (AOA, see Figure 23) until the pressure gradient on the top of the wing becomes so great that it overcomes the surface viscous forces which hold the boundary layer attached to the surface, and it separates with chaotic flow resulting aft of this point. The **separated flow** over the wing generally results in a sudden loss of lift called **stall**. Up to this point the lift to AOA relationship is linear. Near and at stall this relationship is nonlinear. To achieve stall AOA in level flight generally requires a comparatively slow speed, or a maneuver in which the nose of the plane has been pulled up sharply with respect to the incident air flow. But, stall can occur at any airspeed provided the stall AOA has been exceeded. The lift of the wing can be defined in a nondimensional coefficient form (the **lift coefficient C_L**) as:

$$C_L = L / (qS) \tag{13}$$

where:

- L = lift
- S = the projected area of the wing.

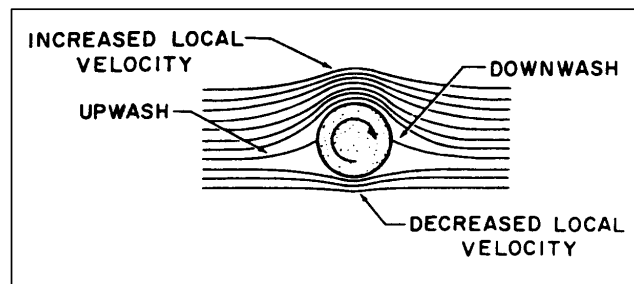


Figure 24 Example of Circulation

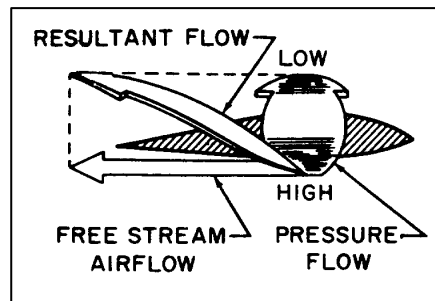


Figure 25 Wingtip Vortices

All of the lift generated by the wing effectively acts at one point called the **center of pressure (c.p.)**. Changes in lift produced by wind gusts or changes in AOA effectively act at the point called the **aerodynamic center (a.c.)**. The importance of these concepts will be discussed further in Section 2.3.2.

It may occasionally be useful to induce flow disturbances in an effort to energize the flow and thus delay separation. This can be done with strips on the leading edge of the wing or, more commonly on high performance aircraft, **vortex generators (VGs)**. Vortex generators are small metal tabs attached vertically to the surface and angled to the flow. They are generally arranged in a line or some other pattern (Figure 26). A **flow straightener** does exactly what the name implies in an effort to induce the flow into a certain pattern. As an example, the F-101 fighter was encountering a bothersome buffeting at cruise which was isolated to adverse flow on the aft fuselage interacting with the engine efflux. The solution was a small sheet metal tab attached at the periphery of each engine nozzle at the location necessary to divert the flow into a more suitable pattern.

The boundary layer, the separation and reattachment of the flow (perhaps induced by structural motion), and the shedding of vortices has a frequency content associated with it. This **unsteady flow** is a critical aspect of aeroelasticity (Section 6.0) but is still not entirely understood.

2.2.6 Generation of Drag

Drag is the sum of the components of aerodynamic force vectors acting on the aircraft that are opposite to the relative wind. This force must be overcome by thrust to achieve flight. The initial introduction to drag, shown in Figure 23, is the portion of the wing normal lift force on the airfoil parallel to the relative wind. This is known as **induced drag**, or drag produced as a result of generating lift.

Because air is viscous, the boundary layer (Section 2.2.5) will produce a resistance to the passage of the air vehicle. This resistance is termed **skin friction drag** and can be minimized by reducing the surface area of the aircraft and by making the surface smoother. A laminar boundary layer has an even velocity profile above a surface and is desirable because of its low skin friction drag. As the flow extends downstream on a body, skin friction will eventually cause the flow to trip to a turbulent state which is thicker and has higher friction, thus, more drag. The separation of this flow usually occurs on aft portions of the aircraft and produces a low pressure zone which acts in the drag direction. This is called **form drag**, and together with skin friction drag makes up the **profile drag**.

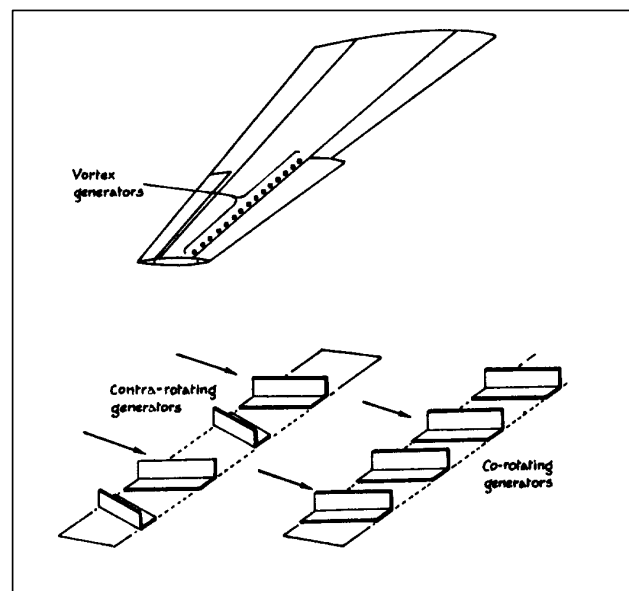


Figure 26 Example Vortex Generator Installation

The characteristics of flow in the vicinity of two surfaces joined at acute angles can produce a drag called **interference drag**. A fairing at this junction can sometimes reduce this drag. This drag combined with profile drag produces a drag termed **parasite drag**. The pressure distribution associated with shocks (Section 2.2.4) can also act opposite to the direction of flight and produce what is called **wave drag**. **Total drag** (D) would be the sum of the parasite, wave and induced drag. The total drag can also be expressed in nondimensional **drag coefficient** (C_D) form as:

$$C_D = D/(qS) \quad (14)$$

2.2.7 Aerodynamic Modeling

The design of high performance aircraft has become so complex, time consuming and expensive that considerable effort must be expended in computer analysis of design options long before wind tunnel models or test aircraft are constructed. A critical element of this analysis is the mathematical modeling of the aerodynamics of a proposed configuration. This modeling must represent the pressure distribution, lift, drag, pressure gradients, etc., faithfully enough that control derivatives (Section 2.3.3) may be derived and aeroelastic forcing functions confidently applied to the structural model.

The field of mathematical aerodynamic modeling is collectively known as **Computational Fluid Dynamics (CFD)**. This field is so complex as to generally require graduate and sometimes doctorate level studies to understand and expand. Only a general introduction to the techniques used will be presented so that the engineer will understand the level of effort and principles involved.

The basis of the modeling methods are mathematically contrived fluid flow elements. These may include a **source** (flow from an infinitesimal singularity), a **sink** (flow into a singularity), a **doublet** (flow into and out of a singularity simultaneously), vortices and circulation. A series of these elements at different strengths are distributed on the surface of the numerical model of the surface or a part of the vehicle. The objective is to have these elements interact in such a way as to force the modeled airstream to flow tangent to the modeled surface, as streamlines would, while faithfully replicating necessary flow characteristics like downwash. The pressure distribution and thus lift and drag forces can then be determined. Unsteady aerodynamics require the introduction of a periodic formulation. Large matrix operations and numerical integrations are involved in CFD which makes the computer operations very costly. There are a number of well-known modeling techniques that an engineer should understand at least in a broad sense. Only the most common methods will be presented.

Lifting line theory is generally restricted to lifting surfaces only. It involves dividing the surface into chordwise strips or panels and superimposing vortices on the panels, normally at the quarter chord. A series of vortices may be used at a number of points along the chord of each panel, thus creating a lattice pattern on the surface. The influence of each vortex upon all others is a fundamental aspect of this method. The distribution may be restricted to just the mean camber line of a wing, or be distributed over an entire enclosed representation of the wing. The distribution of the flow elements on complex surface curvatures can also be done in ways for which analysis techniques are known, such as elliptical, parabolic and hyperbolic distributions. Minor variations on this technique are also known as **strip theory**, **vortex sheets**, and **doublet lattice**.

A similar approach can be extended to the entire aircraft but with many more of the flow model elements employed. An example of such modeling is shown in Figure 27. Compressibility effects can be accounted for to some extent but shocks cannot be modeled by these methods. This restricts these methods to no higher than transonic velocities. Supersonic flow can be accounted for in several ways, the most popular being the **Mach Box** method in which the influence of a conical shock is accounted for in each of many boxes superimposed on the surface. **Piston theory** is principally used for oscillating airfoils. It entails analyzing individual 'slabs' of air distributed across the surface. The translation of the airfoils displaces the gas in the 'slab,' seen as the displacement of a piston at one end of a container of gas, producing compression and expansion waves along the slab.

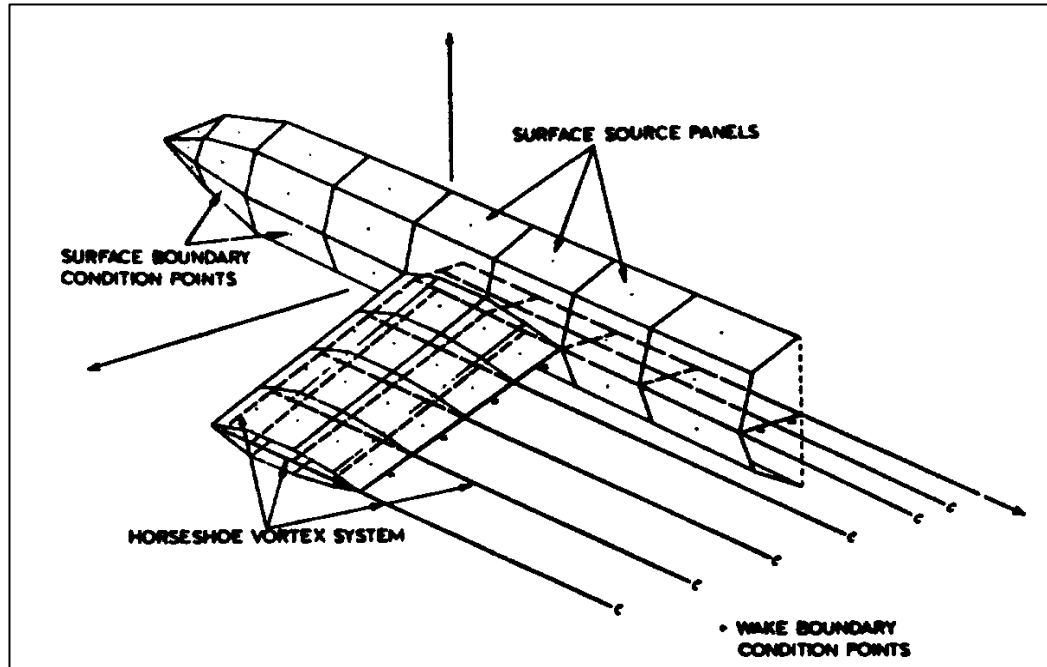


Figure 27 Example of Aerodynamic Paneling of an Aircraft

2.3 Basic Flight Mechanics

Flight mechanics is a broad field that encompasses the basic aerodynamic properties that allow an aircraft to fly, stability considerations, and control techniques. This section is presented to give the uninitiated reader a foundation for the understanding of aerodynamic flight and some of the principles of stability and control that have become so important in the development of advanced combat aircraft and which can impact structural stability. This background will prove important in communicating with controls engineers and test pilots in dealing with aeroservoelastic problems (discussed in Section 8.0), and in-flight test planning.

2.3.1 Reference System

In order to systematically study the dynamics of an aircraft, a reference system has been devised to separate motions into three mutually perpendicular axes or a coordinate system that conforms to the right-hand rule. These axes are shown in Figure 28 and are the **longitudinal**, **lateral**, and **yaw** or **directional axes** along which the aircraft can translate or rotate. Rotation about the longitudinal axis is termed **roll (L)**, the lateral axis **pitch (M)**, and the vertical axis **yaw (N)**. Including translation along these three axes, there are then 6 degrees of freedom for an aircraft in flight. It is often necessary to rotate this axes to a new orientation other than that coincident with the geometric symmetry of the aircraft, such as aligning the longitudinal axes with the incident airflow (the **relative wind**) to account for an angle of attack (α , the angle between the longitudinal axis of the plane and the relative wind in the vertical plane) and **sideslip angle** or β (yawed attitude, or the angle between the longitudinal axis and the relative wind in the lateral plane). This new axes is called the **stability axes** and is just one of a number of possible transformation of axes done to simplify mathematical models or more clearly define aircraft motion.

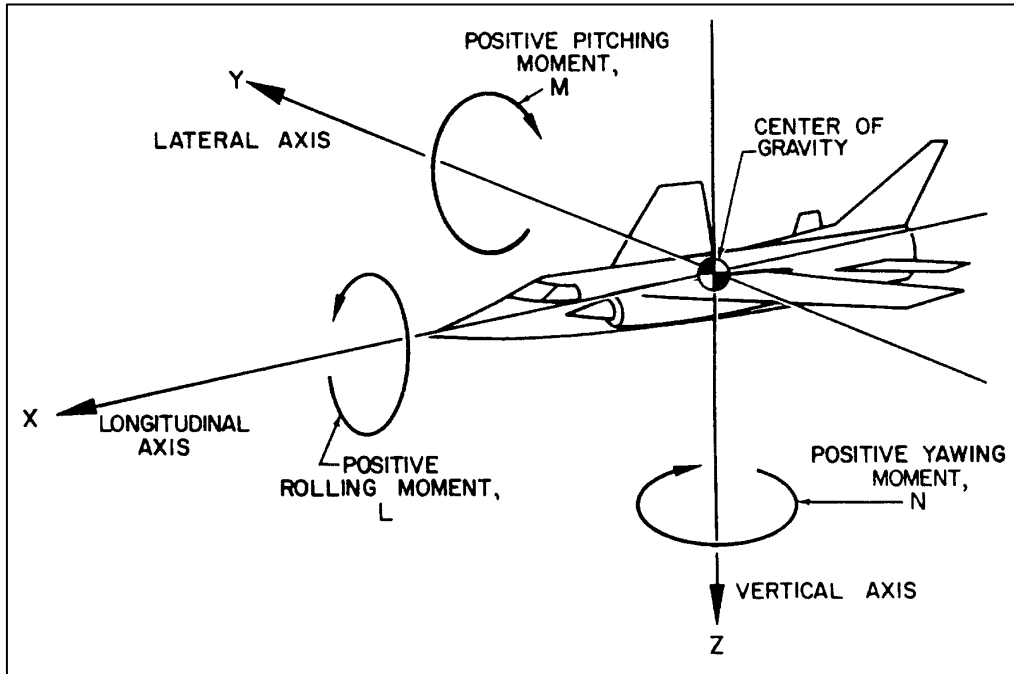


Figure 28 Basic Aircraft Reference System

2.3.2 Weight and Balance

All axes are usually fixed (called **body fixed** axes) to the **center of gravity (cg)** of the aircraft. This is the point about which the mass of the plane is equally distributed in any direction and is typically referred to in terms of percent **mean aerodynamic chord** (percent **MAC**) of the wing airfoil section representing a mean of all the chords across the half-span (see Figure 1). In other words, if suspended from this point the plane would be perfectly balanced and so all aircraft moments act about this point in flight. This point can be determined mathematically by keeping track of every item on the airplane in terms of mass and its distance from some common reference point or datum. Prior to flight testing, the cg is usually checked directly by weighing the plane on scales at an **empty weight** (lacking fuel, payload and aircrew) and determining the cg position using the weight at each landing gear and the distance between them. The **gross weight** would include fuel, payload and aircrew.

This issue of cg position is termed **weight and balance** and is important from the point of view of maximum takeoff gross weight and pitch control authority (explained later). The cg will move about as fuel is transferred or burned, stores are added or dropped, equipment is added or removed, or as wings are swept forward or aft (e.g., as on the B-1 bomber). This empty weight cg is necessary as a constant reference. Weight will also change and is referenced to the fixed empty weight. Naturally, the thrust and lifting capability of an airplane (and thus, the takeoff distance) limits the maximum weight at which an aircraft can operate.

2.3.3 Static Stability

The **longitudinal stability** of an aircraft is related to the position of the plane's aerodynamic center and the cg. The a.c. is the point at which all changes in lift of the entire aircraft take place, as explained earlier for the airfoil alone. Thus, the distance between the cg and a.c. constitute a moment arm. The relationship between the cg and a.c. is illustrated in Figure 29. The lift must overcome the weight or gravity vector concentrated at the cg. For a statically stable aircraft in flight but undisturbed, the cg is ahead of the a.c. and thus, a lift vector at the a.c. produces a nosedown pitching moment about the cg for a level flight attitude if the change in lift is up. To achieve level flight, this moment must be countered by an equal but opposite moment produced by the tail of the aircraft. This means that the overall lift vector of the tail must be down to bring the nose up since it is behind

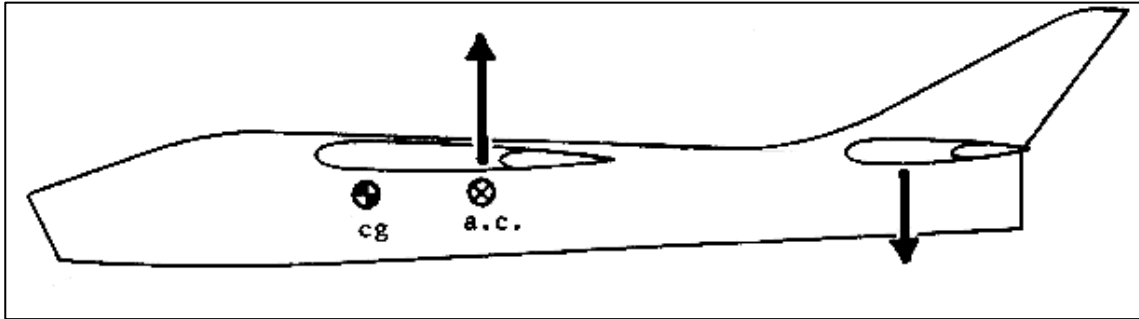


Figure 29 Statically Stable Airplane cg and a.c. Relationship and Tail Load

the cg. This download is produced by a trailing edge-up deflection of the elevator or a trailing edge-up rotation of a stabilator. These effects are shown in Figure 29. If a canard is used (see Section 1.2.2) then it can be uploaded to bring the nose up since it is ahead of the cg and thus, contribute to the overall lift of the plane.

If the cg is far aft and very close to the a.c. because of weight distribution then the moment arm is reduced and a larger change in restoring moment is necessary from the tail load to level the aircraft. This has implications for a takeoff roll where the tail has to produce a very large download at low speeds to raise the nose to a lift-off attitude. Therefore, there are practical limits to the travel of the cg dictated by the size and pitching moments the tail can produce. Also, as explained later, the position of the cg relative to the a.c. has important implications for aircraft stability as well. These same principles apply to the control power in the lateral and directional axes. It should be apparent at this point that an aircraft with the cg aft of the a.c. will be inherently unstable and uncontrollable in the conventional sense (although it is still possible to fly such a plane, as explained later).

Roll is usually commanded by deflection of ailerons. For airplanes with stabilators (see Section 1.2.2), differential rotation of the stabs will also produce a rolling moment. For example, a right roll input by the pilot would produce a right aileron trailing edge-up deflection and an opposite deflection of the left aileron. This produces higher lift on the left wing than the right wing or a rolling moment about the cg that makes the right wing drop and the left wing rise. The plane will continue to roll until the pilot checks the rolling moment with a slight left roll input and then neutral aileron command. The aircraft will remain in a wing-low attitude until corrected by the pilot. The roll attitude reorients the lift vector away from the vertical and tends to pull the plane into a turn toward the low wing. As the plane rolls, the down-going wing will experience a higher AOA than the up-going wing. This produces a change in the orientation of each wing's lift vector that produces a yaw tending to pull the nose toward the outside of the turn. This motion is termed **adverse yaw** and must be countered with rudder for a coordinated, efficient turn. At very high speeds, rolls may be executed by using differential stabilator or flap deflection.

Yaw motion is produced directly by use of the rudder. Deflection of the rudder is analogous to deflecting a wing trailing edge control device. For example, moving the rudder trailing edge right will produce a low pressure on the left face of the vertical tail and will produce a nose-right moment about the cg in the vertical axis. Intentional yaw is used to compensate for crosswinds on landing, and the rudder is used to counter undesirable yaw motion such as adverse yaw. A yaw will change the apparent AOA on the wings (even when wings level) and produce a rolling moment which must be countered with aileron if a constant heading is to be maintained. This yawed, wing-low attitude is called a **steady-heading sideslip** and is used to increase the drag of the airplane for decelerating, pointing the nose for gun firing, or producing sideloads during flight tests (Section 5.0).

By the use of trim tabs or other **trim** systems that bias the entire primary surface or hold the control surface at a deflected angle without pilot effort, it is possible for the pilot to produce just the right balance of forces and moments to maintain flight in either a straight-and-level attitude or some other orientation (within the limits of control effectiveness at the flight speed). When the aircraft is disturbed by a wind gust or a pilot input from this trimmed condition, its geometry and inherent aerodynamics tend to return it to its initial state. For example, a

sudden yaw will produce an AOA on the vertical tail which will create a countering yawing moment. An unintended roll will produce a yawing motion (adverse yaw) which will raise the low wing and return the ship to wings level. A sudden pitch up will increase the AOA on the wing and horizontal tail. The increased upload on the tail and the drop in airspeed (due to reorientation of the thrust vector and increase in drag) will tend to cause the plane to pitch back down. These effects are examples of **static stability** of an airplane.

The preceding four paragraphs have described very simplistically how an airplane flies and how it is controlled in flight. The ease with which the pilot controls the airplane is directly related to its stability and is termed **handling** or **flying qualities**. Many of the most modern aircraft designs are only marginally stable or unstable in one or more axes, and the cg may be coincident or aft of the a.c. Such an airplane is made controllable by computers which automatically monitor the airplane dynamics and compensate for undesirable motion through control surface action uncommanded by the pilot. This is called '**artificial**' **stability** and increases the implications of aeroservoelastic effects (Section 8.0). The advantages of this approach is that the flight characteristics of such a machine can be 'programmed' into the flight control computer. Also, smaller aerodynamic surfaces, meaning less control effort and drag, are typical of this type of design.

2.3.4 Dynamic Stability

Dynamic stability refers to the oscillatory motion of the aircraft after being disturbed from its trimmed state. The static stability will tend to return the aircraft to the trimmed condition but inertia and other factors may cause the ship to overshoot this trimmed attitude. An oscillation may be set up in one or more axes of the aircraft which will eventually **damp** out (decreasing amplitude of the oscillations over time or **positively damped**) until the steady trimmed condition is regained. The amount of damping in the system (the aircraft and its aerodynamics) are important from a handling qualities and mission capability aspect. An **undamped** or **neutrally damped** oscillation (neither increasing nor decreasing in amplitude with time) is undesirable. A **negatively damped** or **divergent** response (increasing in amplitude) is unacceptable as it may lead to dangerous flight attitudes and structural loads which can cause the loss of the ship and crew. **Stick fixed** (held by the pilot) and **stick free** (released by the pilot) dynamics may vary because of the dynamics of the stick or the pilot's body when coupled with the aircraft motion.

Airplanes have certain dynamics that are common to all aircraft by the nature of their basic design. They are called **rigid body modes** because they are aerodynamic in nature and are not dependent upon structural dynamics (fuselage bending, wing torsion, etc.). The most fundamental of these are aircraft pitch, roll and yaw rates motion independent of control surface command. When disturbed in one of these axes by an outside influence (e.g., a wind gust) the plane will oscillate at the characteristic rigid body frequency for that aircraft.

There are more complex rigid body dynamics of which the structures flight test engineer should be aware. In the longitudinal axes these are the phugoid and the short period modes. The **phugoid** is a long period (20 to 100 cycle seconds per cycle) mode in which the pitch attitude changes very slowly with an attendant slow and small change in altitude and airspeed. Because the phugoid period is so long, it is likely that the pilot or autopilot will make some corrective input in the time it takes the mode to diverge significantly and so the mode seldom has time to develop. Thus, some instability in this mode is often tolerated. The **short period** mode has a much higher frequency than the phugoid, a 0.5- to 5.0-seconds period, but is a constant velocity pitching motion with a varying AOA. A poorly damped short period is seldom tolerated because, in attempting to control it manually, the pilot may inadvertently exacerbate the motion due to the time lag between when the input is made and when its effect is apparent. This inadvertent feeding of the rigid body motion has been called **pilot induced oscillation (PIO)**. The result of a PIO can be dangerous aircraft attitudes and airloads. The frequency of the short period mode can also cause it to couple with structural modes and create an aeroservoelastic problem (Section 8.0).

Directional axes modes include the **spin**. This is a low-speed condition in which one wing is stalled, and thus, a combination roll and yaw spinning motion is set up. An asymmetrical power situation (for a multi-engine aircraft) or a sideslip condition are usually associated with spin initiation. Airframe loads created by a spin are often of interest in a loads test (Section 5.0).

There are two lateral modes that are important; the Dutch Roll and the Spiral. The **Dutch Roll** is a combination of roll and yaw (thus, often referred to as a lateral-directional mode) in which the wingtip of the plane will describe an ellipse or circle in the air. The Dutch Roll is usually on the order of less than two cycles per second. The **Spiral mode** involves a very slow rolling and gradual nose drop that eventually leads to a spiraling dive. This mode usually has a frequency of less than one Hertz (cycles per second).

Many aircraft have a feature of the autopilot, flight computer, or a dedicated system that damps out undesired dynamics which can otherwise lead to one of these modes developing. A **yaw damper** is a typical example of this. For this feature, a system applies corrective rudder automatically in response to any yawing moment sensed through an accelerometer or gyro.

All of the aircraft's motions can be modeled mathematically in equations of motion. These equations are the basis of autopilots and other automatic flight control systems. The coefficients in these equations can become very cumbersome so that they are replaced with quantities known as **stability derivatives** (they typically involve partial derivatives). An example of this is $C_{l\beta}$ which is the change in rolling moment coefficient with sideslip angle (β), or:

$$C_{l\beta} = \partial C_l / \partial \beta \quad (15)$$

By themselves the stability derivatives give easily visualized insight into the airplane's dynamic stability.

2.3.5 Aeroelastic Effects on Stability and Control

The interaction of the aerodynamic forces on the aircraft with the elastic behavior of the aircraft structure and the inertia of the airframe is termed **aeroelasticity**. The elastic behavior of an air vehicle can affect its stability and control by deforming the fuselage and lifting surfaces, and altering surface incidences. The principal results are a change in trim requirements which may result in maximum trim authority being reached earlier than predicted, change in lift distribution and pitching moment, and reduction in control surface effectiveness. One example of the latter effect is control reversal, discussed in Section 6.4.5. Other examples of such disturbances are wing torsion producing a **washout** or reduction in AOA at the outboard portion of the wing, fuselage bending altering tailplane incidence, and elevator distortion (sometimes called **rollup**) altering control effectiveness. Wing, fuselage and aileron distortion tends to be destabilizing while tailplane, elevator and general control surface distortion is usually stabilizing. The aeroelasticians may be able to assist stability and controls engineers in identifying such effects when unexpected difficulties arise.

SECTION 2 REFERENCES

1. Herrington, Russel M., Major, USAF, et al, Flight Test Engineering Handbook, AF Technical Report No. 6273, AFFTC, Edwards AFB, California, January 1966.
2. Hurt, H.H., Jr., Aerodynamics for Naval Aviators, NAVWEPS 00-80T-80, U.S. Navy, January 1965.
3. Kuethe, A.M. and Chow, C., *Foundation of Aerodynamics: Bases of Aerodynamic Design*, John Wiley & Sons, New York, New York, 1976.
4. Hess, Johnson and Rubbert, *Panel Methods*, AIAA Professional Study Series, AIAA, Washington D.C.
5. Roskam, Jan, *Airplane Flight Dynamics and Automatic Flight Controls*, Roskam Aviation and Engineering Corp., Lawrence, Kansas, 1979.
6. Etkin, Bernard, *Dynamics of Flight, Stability and Control* John Wiley and Sons, New York, New York, 1965.
7. Ground School Notes Book "C", *Stability and Control* Empire Test Pilot School, Farnborough, 1961.

3.0 MATERIALS

3.1 Introduction

The load bearing capability and dynamics of a structure are closely tied to the materials that compose the item. Because of this, it is important that the structures flight test engineer have a sound understanding of materials and their behavior. Composites and plastics are now firmly established as aircraft materials and can not be ignored. This chapter will attempt to provide a basic foundation upon which the engineer can build with additional reading.

3.2 Characteristics

3.2.1 Stress

A material may be subjected to a variety of external loads including **tension** (pulling), **compression** (pressing), **shear** (slicing), **torsion** (twisting), **bending** and combinations of these (Figure 30). The resistance of the material to the applied load is termed **stress** (σ) and is expressed for the simple **axial** case as:

$$\sigma = P/A \quad (16)$$

or load over the area in units such as pounds per square inch (psi). There can therefore, be **tension stress**, **compression stress**, and **shear stress**. The nature of the force application and the shape of the article may produce a combination of lesser stresses throughout the body, or component stresses. Sharp changes in geometry can create **stress concentrations** under load. Solving for the magnitudes and orientations of these stresses can become very complex.

The maximum stress and its orientation defines the **principal stress** for a plane. Three mutually perpendicular principal stresses are defined by establishment off of the most significant principle stresses that can be resolved in the infinite orientations within an article. For example, the maximum axial stress in a landing gear strut is the most significant of all stress directions that can be defined for that component and serves as the basis for the two other axes, the associated stresses of which now become the principal stresses in those axes.

Not all stresses are from external sources. Another source is the **residual stresses** from fabrication and assembly, rubbing of mated surfaces, weld joints, etc. There are many maintenance practices that are intended to avoid producing additional internal stresses.

3.2.2 Strain

Strain (e) is deformation in the article, caused by the stress, divided by the original dimension, or

$$e = \Delta L/L \quad (17)$$

where:

ΔL = change in length

L = original length.

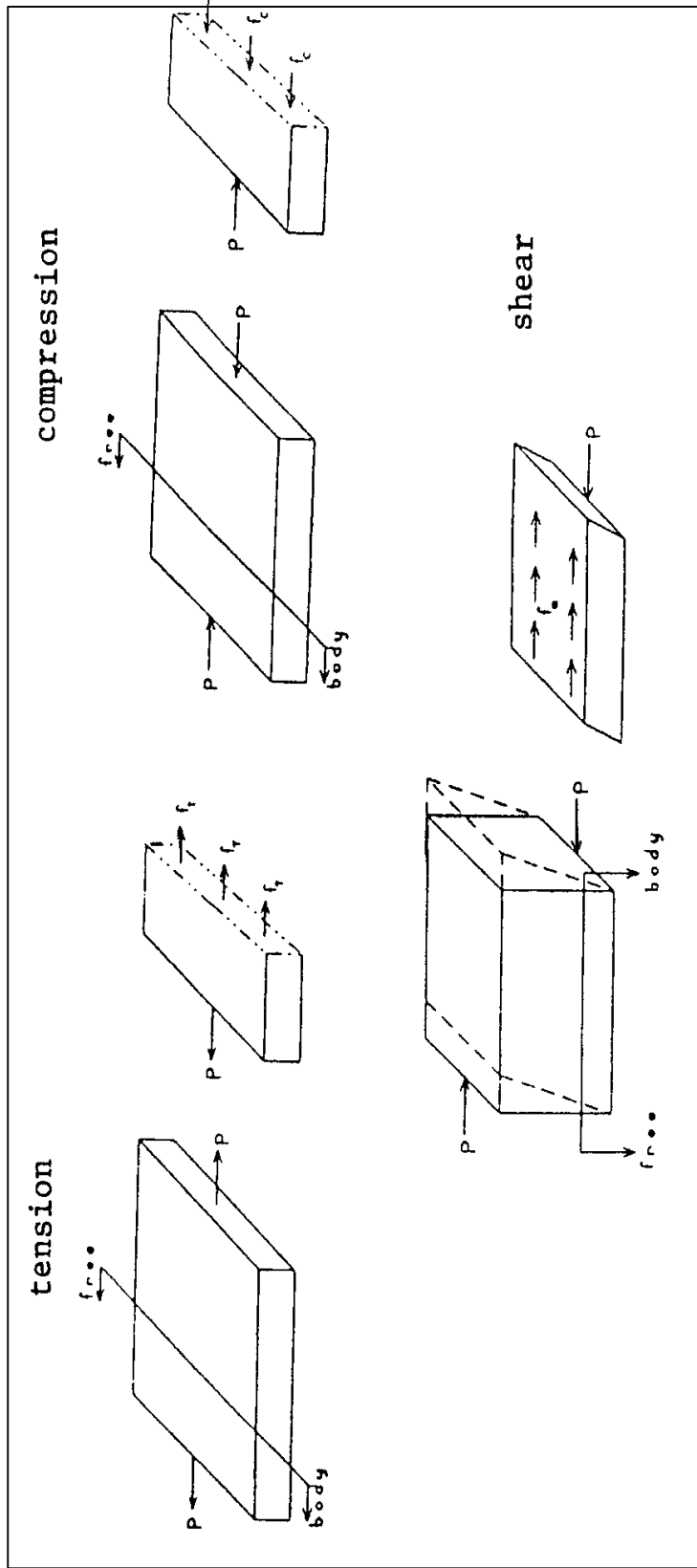


Figure 30 Basic Loading and Stresses

A tension load will produce some material stretching in the axis of the load (Figure 31). The deformations should be measured in this axis. Conversely, compression will squeeze the material to a shorter length and the deformations should be measured in the axis of this force. Note that a tension load produces a reduction in the width of the sample as shown in Figure 31. A relationship between the two strains is termed **Poisson's Ratio** (μ) and is expressed as:

$$\mu = |e_w / e_l| \quad (18)$$

where the subscripts:

W = widthwise
L = lengthwise.

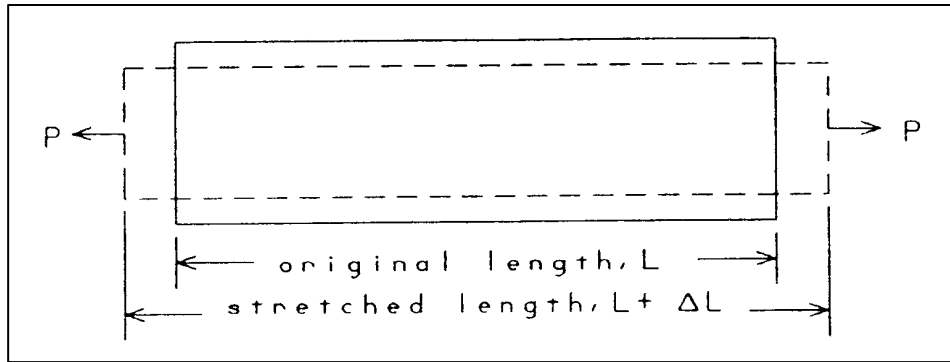


Figure 31 Material Deformation Under Load

Shear strain is measured as shown in Figure 32 and is expressed as:

$$\gamma = \Delta L / L \quad (19)$$

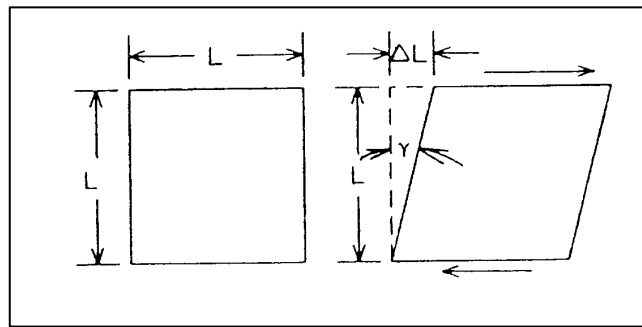


Figure 32 Shear Strain Illustration

The principal stresses have associated **principal strains**. The stress-strain properties of a material are linear for a large percentage of the load that can be applied before the material fails. This is expressed by **Hooke's Law** and defines the **modulus of elasticity (Young's Modulus [E])**:

$$E = \sigma / e \quad (20)$$

Typical values of E are 30,000,000 psi for steel and 10,000,000 psi for aluminum. For shear loads the modulus of elasticity is known as the **Shear Modulus (G)** or:

$$G = \sigma / \gamma \quad (21)$$

Multiple loads in multiple axes applied to a complex shape can produce deformations that require rigorous analysis to predict.

All of this behavior can be expressed in a stress-strain curve like that shown in Figure 33. The linear portion of the curve up to the **limit stress** corresponds to Hooke's Law. At or slightly beyond this point is the **yield** or **elastic limit**. Beyond this stress the material will not return to its initial shape even after the load is removed. In most applications this is considered to be a material failure but, in some situations, only a fracture is defined as failure. Considerable deformation under load will continue beyond this load up to the **ultimate stress** without loss of load-bearing capability. Beyond ultimate, the load cannot be sustained and cracking or actual breakage will quickly occur.

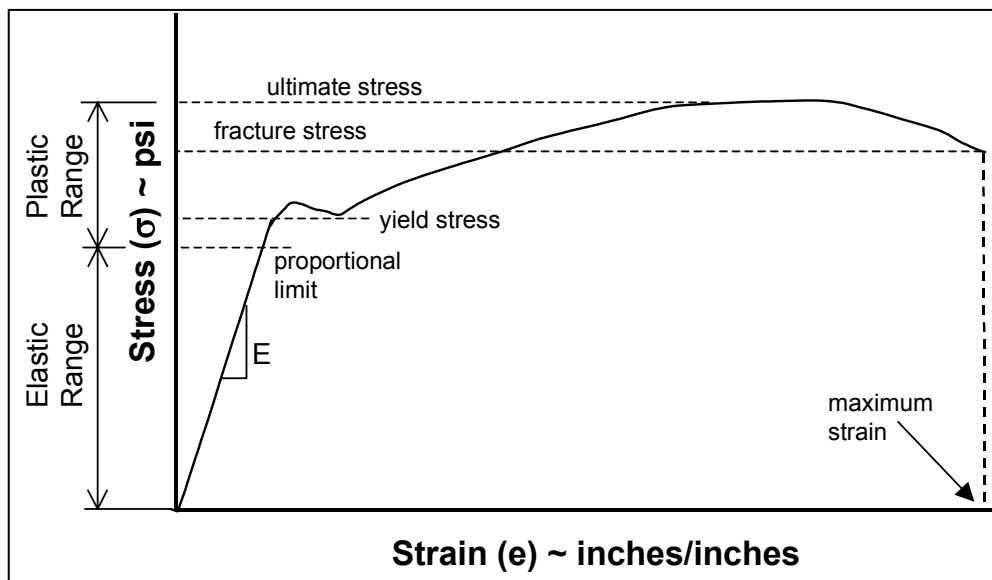


Figure 33 Example Stress-Strain Curve

3.2.3 Stress Analysis

The prediction of the stresses and strains produced by different loading configurations is the field of stress analysis. The principal objective of stress analysis is to ensure that the structure has a reasonable **factor of safety** on the actual failure stress. For aircraft applications, the failure stress of a component must be greater than 1.5 times the stress produced at the maximum load expected to be experienced in normal operation (the **design limit load** or **DLL**). This, then, includes a 50-percent factor of safety. The value of 1.5 DLL is referred to as the **ultimate load**. It is important to notice that permanent deformation may occur within the factor of safety. In most cases this is considered acceptable as it provides a 'get home' capability after which overstressed components can be replaced once the airplane is safely back on the ground. A load bearing capability beyond the ultimate load is defined as the **margin of safety**. This is expressed as:

$$\frac{\text{failure load as factor of DLL}}{1.5 \text{ DLL}} - 1 \quad (22)$$

A structure that completely fails at 1.76 DLL would have a margin of safety of 17 percent.

Stress analysis of the entire aircraft to verify the factor of safety involves complex modeling of the structure's components, their elastic behavior, and **load paths** between the components (the redistribution of loads throughout the structure as the load condition changes). The analysis may be refined using laboratory and flight test loads data. This analysis is essential before aircraft components are actually subjected to flight loads and is extensively referenced during loads flight tests (Section 5.0).

Most stress analyses today is done using **finite element modeling** (FEM). This is a computer technique in which a structure is represented mathematically as a collection of interconnected beams, plates, solid members, etc., with the dimensions of the overall array identical to the real article. The behavior of these simple elements can be easily represented by low order, linear equations. The material properties of the actual structure are modeled by assigning such quantities as Young's moduli to each element. It is important that applicable boundary conditions be defined. Since aircraft are already truss-like structures, the elements may represent actual physical structural members (Figure 34), but this is not mandatory. Distributed loads applied to the structure must be concentrated at the **nodes** of the model (junction of the elements). For aerodynamic loads, the aero model discussed in Section 2.2.7 may become part of the program. The equations defining the stress, strains and dynamic motion of each element can be combined in matrix form with all the elements. The solution of the matrix equations with an applied load or loads (static or dynamic) allows the resulting stresses, deformations and dynamic response at each node to be resolved. The model can be refined to reflect ground and flight test data as it becomes available to improve the faithfulness of the resulting predictions. The original and still widely used FEM computer code is NASTRAN.

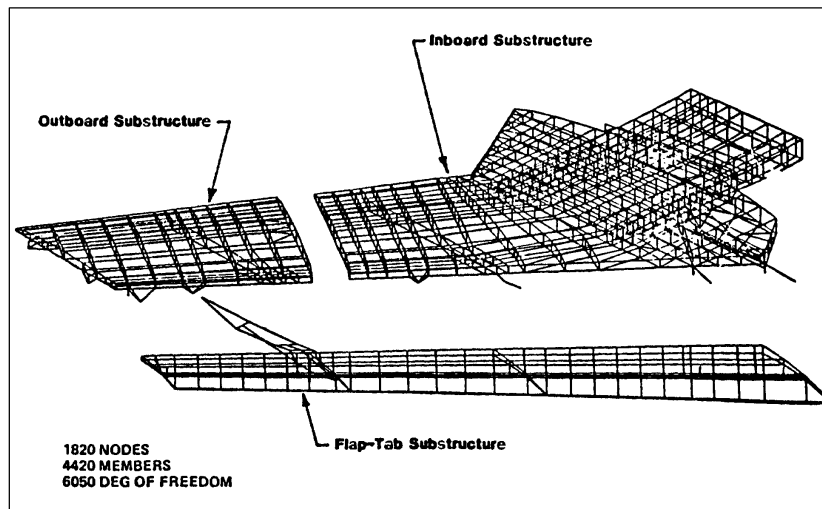


Figure 34 Example Finite Element Model - X-29A Wing Structure

3.2.4 Thermal Effects

Flight through the atmosphere involves a certain amount of **kinetic heating** due to friction between the air molecules and the surface of the aircraft (Section 6.4.10). The heating from internal sources, such as engines, must also be considered. Up to a certain point, convective cooling from the heat conductivity of the air will play a significant role in cooling the surface, but at high Mach numbers the kinetic heating will become dominant. The heating will be greatest at stagnation points of the air flow on the surface (see Section 2.2.3). This heating results in both a **thermal expansion** of the material (strain), resulting **thermal stresses** particularly at interfaces and fasteners, and a drop in E. The latter effect tends to reduce the load bearing capability of the structure. These effects are considered during the design and material selection process to allow thermal expansion without detrimental stresses. The aircraft skin is directly heated by the friction and the internal structure is heated in turn by conduction. The rate of temperature rise of the internal structure is a function of the material

and the duration of the heat soak. For example, the surface of the space shuttle orbiter will already have been significantly cooled by convection and radiation upon landing while the temperature of the internal structure is still rising. Active cooling of the airframe may be necessary in extreme conditions.

3.3 Composites

Metals are typically **isotropic**; the material properties are the same in any direction within the material. Modern composite materials are **orthotropic** with the properties different in three mutually perpendicular planes of symmetry and a function of the orientation at a point in the body. Man-made composite materials offer the opportunity to tailor the material properties in any axis to meet the expected loading configuration as economically as possible.

Instead of being composed of one homogenous substance, composites are **in-homogeneous**, or a combination of two or more substances. The type of composites most often used as structural components in aircraft are those made of long, thin glass or carbon fibers suspended in an epoxy matrix. These fibers by themselves have remarkably high tensile stress capabilities but very little compression capabilities, such as for a rope. A component made from such composites which load the fibers strictly in tension could be significantly lighter than a metal component designed to sustain the same load, while at the same time reducing radar reflectivity in a combat scenario. The use of composites generally means fewer parts and fasteners used in the aircraft's construction, which in turn means fewer points for crack origination and less attention required for maintenance (allowing reduced costs).

Composites are most often produced as layered laminates, each layer consisting of a sheet of unidirectional fibers. The orientation of each layer may be varied to give the desired properties in each axis (Figure 35). Some composites (particularly the glass fiber variety) come in weaves for ease of handling or to produce a particular material property.

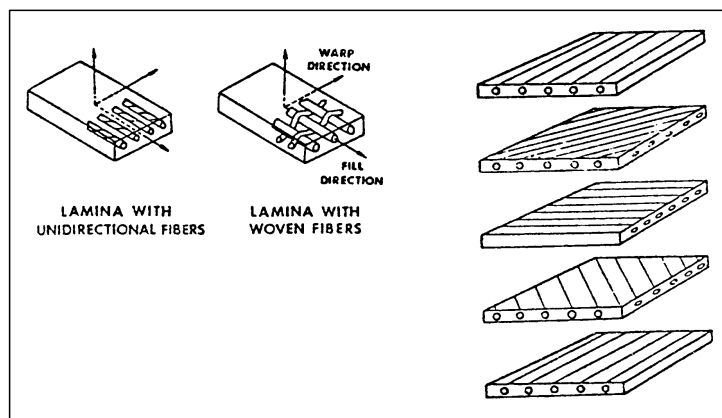


Figure 35 Examples of Composites

3.4 Failure Modes

This section will touch on the various mechanisms that can produce a loss of structural strength or a material failure in an aircraft structure. Most aircraft are designed for a 'life' of several thousand flight hours at a typical load spectrum mission profile. Analysis and laboratory testing are necessary to ensure that none of these failure modes will result in problems before the expiration of this life time. Reskinning of the lower wing skin on the KC-135 and replacement of the C-5A and A-6 wings are just a few examples of costly rework during service when structural problems needed correction.

3.4.1 Creep

A material subjected to a constant load over a long period will begin to deform beyond its initial loaded shape. This is known as creep and will continue slowly until failure occurs if the load is not relieved. Repeated thermal expansion and contraction can also produce creep. Elevated temperatures can accelerate the creep process. Creep is a critical consideration in the service life prediction of a component, particularly with the tight tolerances to which engine and airframe components are being manufactured today.

3.4.2 Work-Hardening

Also known as **strain hardening** and **cold working**, work-hardening refers to the loading of a material beyond its yield stress but less than its ultimate stress producing a permanent set or deformation. The stress-strain characteristics of the specimen are changed with the principal result that ductility is reduced (Section 3.6).

3.4.3 Delamination

Materials that are bonded together or composed of laminates bonded together may experience a failure of this bond, called delamination. Common causes of delamination are the expansion of air or frozen water trapped between the laminates, the presence of a void or material defect, component over stress, loading in an undesirable direction (compression leading to buckling in composites), or improper manufacturing. Delamination is most common in plastics and composites (see Section 3.3). For example, the F-111 aircraft suffered numerous stabilator delaminations above Mach 2.0 resulting in large sections of the outer surface and inner honeycomb material separating from the aircraft in flight.

3.4.4 Cracking

A metal component will usually display cracks as the first evidence of overstress. These cracks will typically originate at areas of stress concentrations such as rivet holes and may not be visible to the naked eye. Once found, a common technique is to '**stop drill**' the crack by drilling a small hole at the end of the crack (if it can be found). A patch riveted or welded over the damaged area may be necessary.

3.4.5 Fatigue

Many materials will eventually fail in one manner or another if subjected to repeated loads less than the ultimate sustainable load. This effect is presented in an **S-N diagram** (Figure 36) where S is the stress and N is the number of loading cycles to which the item is subjected. Cyclical thermal stresses can also lead to fatigue. The plot shows the number of cycles the component can withstand at a given stress before failure is likely. Predicting the fatigue life of a component as a function of operational loading cycles is an essential part of establishing the service life of an aircraft.

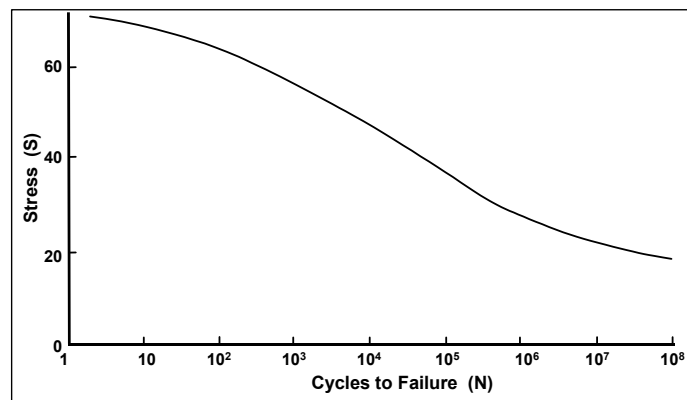


Figure 36 Example S-N Diagram

3.4.6 Corrosion

Corrosion is the disintegration of a metal through interaction with the environment and may be influenced by factors such as stress, fatigue, water and temperature. Corrosion transforms the metal into a substance that has little of the strength of the original material. The two basic types of corrosion are chemical and electrochemical corrosion.

Corrosion may be localized or uniform over the surface. Apart from the **rust** and **oxidation** with which we are most familiar, there are many other types of corrosion modes. Pale, **flaking** type corrosion is common. **Exfoliation** corrosion can be identified by the lifting away of the metal in thin layers. Abrasion by rubbing (**fretting**) of two butted surfaces or some external source can remove protective films and thus allow corrosion to begin. The placement of two dissimilar metals together will promote **electrochemical corrosion**. Corrosion may be accompanied by **pitting** which may penetrate deeply and provide an origin for cracks.

Certain electrochemical treatments and coatings (apart from simple primer or paint) help to prevent corrosion. Periodic inspections are mandated to search for corrosion. Many types of corrosion can be removed by simply sanding and polishing, provided that too much of the material is not removed (typically less than 15 percent of the original thickness). A patch riveted over an effected area or complete replacement of the component area may be necessary if the strength of the item is in doubt.

3.5 Inspections

Many methods of **nondestructive inspection (NDI)** exist. The engineer should be familiar with these as they are commonly used to determine the presence or extent of damage that may have been caused in development flight testing. Additionally, the aircraft repair depot maintains a database of stresses measured at a few specific locations on each aircraft in the fleet and correlated with events (cruise, landing, etc.). These data are recorded automatically by a **flight data recorder** on a tape which is routinely downloaded every few flights. The database permits the tracking of load cycles according to how the aircraft is being utilized and early prediction of life expectancy and failures.

3.5.1 Stress Visualization

Components may be coated with a resin-like paint that becomes brittle when dry. Under load this coating will crack in a pattern which can be interpreted to indicate principal stress directions and stress concentrations. A photo-elastic technique uses a clear plastic model of the component. By viewing the loaded model through polarized light, lines or '**fringes**' become visible that also indicate the direction of the stresses and stress concentrations. Certain coatings will discolor in a manner that will later allow a determination of the maximum temperature to which the surface has been subjected if detrimentally high temperatures are suspected.

3.5.2 Dye Penetration

A cleaned surface (paint must be removed) is treated with a fluorescent liquid which will penetrate cracks or discontinuities and make them visible under a black light. The whole process requires some skill and the time to do it properly, and only surface flaws will be displayed. However, the results are immediate and the technique is highly portable.

3.5.3 Magnetic Particles

Also known by the brand name Magnaflux, this technique requires the cleaned part to be treated with magnetic particles while it is magnetized. After further treatment, the flaws will be visible either under normal light or black light depending upon the particles used. Surface or near-surface flaws can be seen by this technique but requires some equipment that can become bulky depending upon the size of the component to be inspected.

3.5.4 X-Ray

Deep voids and flaws can be found in virtually any material through this process. Considerable skill and expensive equipment is required to produce and interpret the 'shadow' photograph.

3.5.5 Ultrasonics

By passing a high frequency sound wave through a component, the thickness of the material can be measured by the return time of the sound wave after it bounces off of the far side of the part. Any flaw present within the part will also reflect the waves and produce a shorter return time. A flaw at any depth can be found very quickly but requires expensive equipment and a skilled operator.

3.5.6 Eddy Current

This method is restricted to metals and involves inducing an electrical current in the material. A flaw will disturb the current and this can be detected on a meter. Any part of the aircraft can be inspected if accessible, but only a small area at a time. This method is highly portable and the equipment is inexpensive, but some skill is required to perform the inspection properly.

3.6 Definitions

Brittleness — measure of a material's lack of ductility, by one definition breakage at 5 percent or less strain implies brittleness

Ductility — ability of a material to deform without breaking

Durability — ability to resist cracking, corrosion, thermal degradation, delamination, wear, and the effects of foreign object damage over time

Elasticity — ability of a material to return to its undeformed shape after all loads have been removed

Hardness — resistance to plastic deformation resulting from impact loads

Plasticity — deformation characteristics of a material beyond its elastic limit

Resilience — a measure of the amount of energy a material can absorb elastically in a unit volume of the material

Strength — ability to withstand external loads without failure

Toughness — total energy absorbed before failure occurs (area under the stress-strain curve)

SECTION 3 REFERENCES

1. Dole, Charles E., *Fundamentals of Aircraft Material Factors*, University of Southern California, Los Angeles, California, 1987.
2. Military Specification Airplane Strength and Rigidity Reliability Requirements, Repeated Loads and Fatigue, MIL-A- 008866B.
3. Military Specification Airplane Damage Tolerance Requirements, MIL-A-83444.
4. Military Specification Airplane Strength and Rigidity, Sonic Fatigue, MIL-A-008893.
5. *Aeroelasticity*, Chapter 12, Flying Qualities Theory and Flight Test Techniques, USAF Test Pilot School, Edwards AFB, California.

4.0 BASIC STRUCTURAL DYNAMICS

4.1 Introduction

A real mechanical system, such as an aircraft structure, can deform in practically infinite directions (called **degrees of freedom**), is constructed of nonhomogeneous materials, nonuniform in mass and material properties, and acted upon (forced) by a wide spectrum of inputs of which many are random. To study the most dominant of the structure's dynamic properties and responses it is necessary to reduce the numerous uncertainties by neglecting the less significant of them and modeling the remainder in some empirical and tractable manner.

This chapter will provide the basic knowledge to examine a structure's problem in its most elemental form and yet still permit some useful engineering conclusions to be drawn without man-months of costly and time-consuming computer analysis. It emphasizes concepts routinely used in structures flight testing and assumes an understanding of undergraduate dynamics.

4.2 Basic System Elements

Any structural material will have some elastic properties. Among these is **stiffness**, or resistance to deformation. This resistance does not mean that the material will not deform, although perhaps not visibly. The resistance can be thought of as a restoring force countering the applied force and seeking to return the structure to its original undeformed configuration. Such a force (F_s) can be modeled as that produced by a stretched spring. This is shown in Figure 37 and can be expressed as:

$$F_s = k(x_2 - x_1) \quad (23)$$

where:

k = the **spring constant**, and
 x = the displacements shown.

This equation is valid only for a material deforming within its linear **elastic range**, that is the range at which the material will return to its undeformed shape after the load is discontinued (see Section 3.2.2).

The modeling element relating forces (F_d) to velocities is the viscous damper like that shown in Figure 38 and expressed in the equation:

$$F_d = c(\dot{x}_2 - \dot{x}_1) \quad (24)$$

where:

c = the **coefficient of viscous damping**.

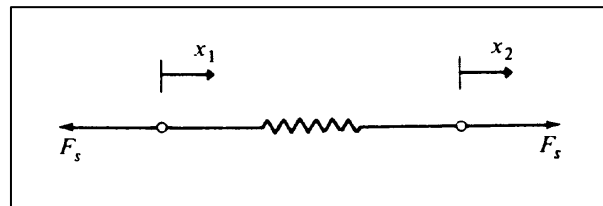


Figure 37 Basic Spring Element

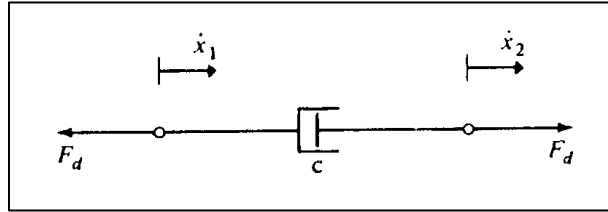


Figure 38 Basic Damper Element

This equation is also only valid for a linear relationship. The damper can be thought of as a property that extracts energy from the system. It resists an increase in displacement velocity and actually reduces it, eventually, completely to zero in the unforced case. As the equation suggests, this **viscous damping** is proportional to velocity. Another type of damping, termed **proportional damping**, is a function of the mass and stiffness of the system. **Structural damping** (sometimes called **hysteretic damping**) is the result of internal friction and strain and is proportional to the displacement amplitude squared. Finally, **coulomb damping** is simply the friction that resists the motion of two bodies moving against each other, such as internal components of a structure. Only the viscous damping component is modeled linearly and dealt with in this chapter.

Finally, elements of the structure can be modeled with ‘**lump**’ or **point masses** (Figure 39). **Newton’s Second Law of Motion** provides an expression for the inertial properties of this discrete mass, relating forces to accelerations.

$$F_m = m\ddot{x} \quad (25)$$

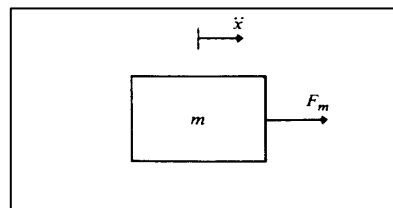


Figure 39 Basic Mass Element

For a simple bending case, the stiffness can be expressed as:

$$EI = \text{constant} \quad (26)$$

where:

- E = **Young’s modulus** (Section 3.2.2), and
- I = the cross-sectional area moment of inertia.

The equivalent spring constant (k_{eq}) can be derived in terms of these properties by starting from the basic relationship:

$$k_{eq} = P/\delta \quad (27)$$

where:

- P = the transverse applied load, and
- δ = the deflection of the object at the point of load application.

For a simple torsion case, the stiffness (GJ) can be expressed as:

$$GJ = \text{constant} \quad (28)$$

where:

G = the **shear modulus**, and
 J = the polar moment of inertia of the cross-section.

An equivalent spring constant can be derived using these terms from the relationship:

$$k_{eq} = M/\theta \quad (29)$$

where:

M = the applied torque, and
 θ = is the angular displacement.

These relationships are introduced because they reoccur repeatedly in structural analysis.

All of these discrete elements, except the point mass, are considered massless, and linear for small displacements. They can be combined in parallel and series, such as those shown in Figure 40, with associated reduced equation forms. These then are our most basic building blocks for modeling a structure.

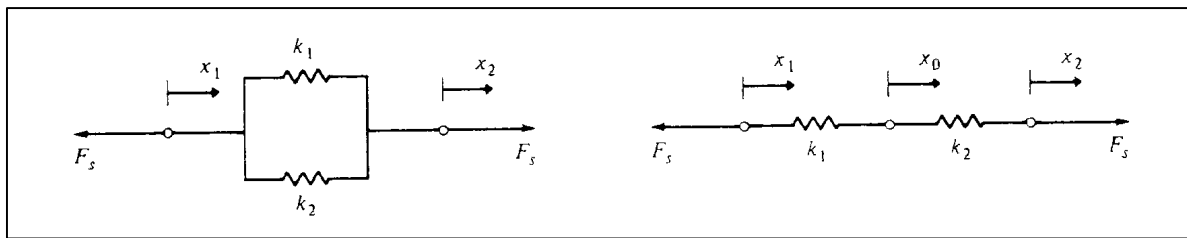


Figure 40 Example of Combined Basic Elements

4.3 Simple System Models

Consider the case of a mass free to move in one direction (a **single degree of freedom [SDOF]**) but with some stiffness and damping. Such a system can be modeled as shown in Figure 41 with a force applied as shown as well as gravity acting on the mass. A free body diagram of this problem (Figure 42) shows that a sum of forces written in their equivalent elemental model form would be:

$$F(t) = m\ddot{y}(t) + c\dot{y}(t) + ky(t) + mg \quad (30)$$

where:

g = the acceleration of gravity.

However, if the coordinates originate at the equilibrium point, then:

$$\begin{aligned} y(t) &= x(t) - x_{st} \\ \dot{y}(t) &= \dot{x}(t) \\ \ddot{y}(t) &= \ddot{y}(t) \end{aligned}$$

and Equation 30 becomes:

$$F(t) = m\ddot{x}(t) + c\dot{x}(t) + kx(t) - kx_{st} + mg$$

Since at equilibrium the static force $-kx_{st}$ exactly cancels out the mg force (Figure 41), the system equation becomes:

$$F(t) = m\ddot{x}(t) + c\dot{x}(t) + kx(t) \quad (31)$$

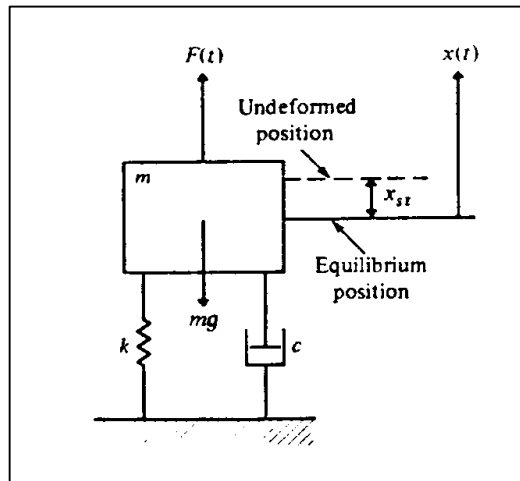


Figure 41 Example Structural Model

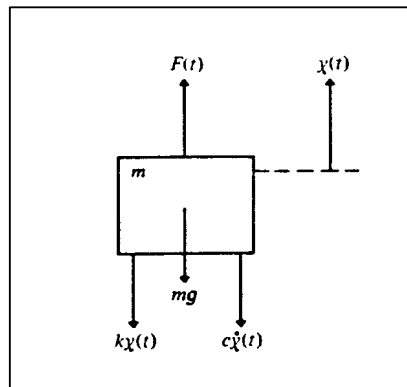


Figure 42 Free-Body Diagram of Figure 41

4.3.1 Free Response Case

For the unforced case, and after dividing equation 31 through by m ,

$$0 = \ddot{x} + a\dot{x} + bx \quad (32)$$

This is a second order, linear, homogeneous differential equation of motion of the mass, called a **spring-mass-damper system**. It can easily be seen that if the mass is disturbed and then allowed to respond freely, it will oscillate about its equilibrium position due to the action of the spring. The oscillation will be at one frequency typical of that system, which is called the **damped natural frequency** (ω_d). This motion will eventually reduce to zero as a result of the damper action.

It can be observed that the amplitude of the motion damps out exponentially. Therefore, for small displacements, the displacement can be assumed to be of the form:

$$x(t) = Ae^{st} \quad (33)$$

where:

A = some amplitude, and
s = the Laplace variable.

Substituting this term into the general equation (32), the characteristic equation for the system is derived, or:

$$0 = s^2 + as + b \quad (34)$$

and s now represents the roots of this equation. It is convenient to define some useful parameters:

$$\omega_n^2 = k / m \quad (35)$$

called the **undamped natural frequency**, or the oscillatory frequency for the same system without damping. The damped natural frequency is related to this by:

$$\omega_d = \omega_n \sqrt{1 - \zeta^2} \quad (36)$$

where:

$$\zeta = c / (2m\omega_n) \quad (37)$$

and is called the **viscous damping factor**. This can also be expressed as the **damping ratio**:

$$\zeta = c / c_r \quad (38)$$

where:

c = the damping present in the system, and
c_r = the **critical damping coefficient**, or the highest damping that will still produce oscillatory motion.

Also,

$$\tau = c / k \quad (39)$$

is termed the **time constant** (τ) and defines the speed of return of the system to equilibrium.

Applying equations 35 and 37 to equation 34, it now becomes:

$$0 = s^2 + 2\zeta\omega_n s + \omega_n^2 \quad (40)$$

This equation has two roots:

$$s_1, s_2 = \omega_n (-\zeta \pm \sqrt{\zeta^2 - 1}) \quad (41)$$

If the damping factor (ζ) is greater than 1, the roots will be real and the system is termed **overdamped**. This means that once disturbed and allowed to respond freely, the system will return to equilibrium quickly without

overshoots or oscillation, as shown in Figure 43. This is also called a **deadbeat** response. If the damping factor is between 0 and 1 then the roots will be imaginary and the system will be **underdamped**. This means that the system will oscillate about the equilibrium condition with the motion slowly decaying to zero (Figure 44). For $\zeta = 0$, we obtain the **undamped** or neutrally damped case in which the system will continue to oscillate indefinitely at the same amplitude without decaying (Figure 45). For ζ less than 0, we have an **unstable system** with oscillations increasing in amplitude with time. This is called **divergence** (Figure 46). Naturally, the amplitude will quickly reach magnitudes that exceed the elastic restoring ability of the structure's material and structural failure will result.

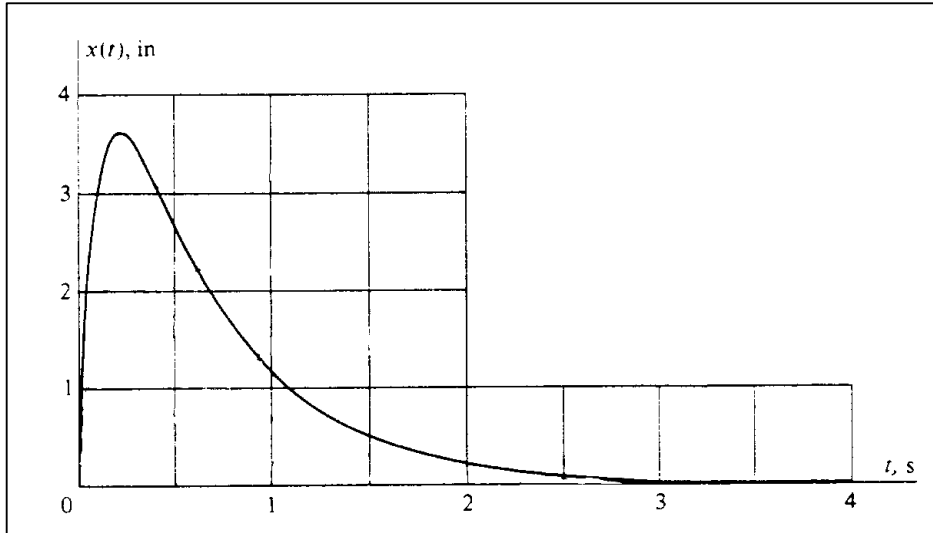


Figure 43 Example of an Over-Damped Displacement Response

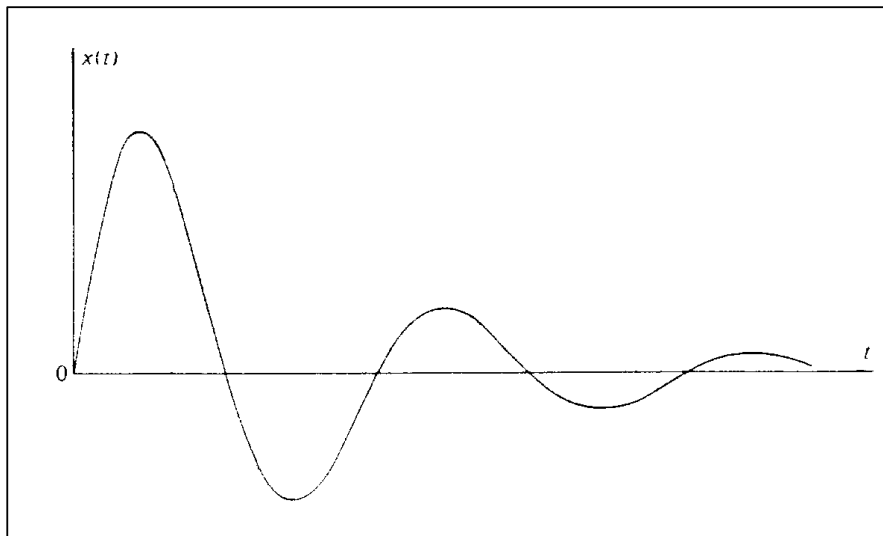


Figure 44 Example of an Under-Damped Displacement Response

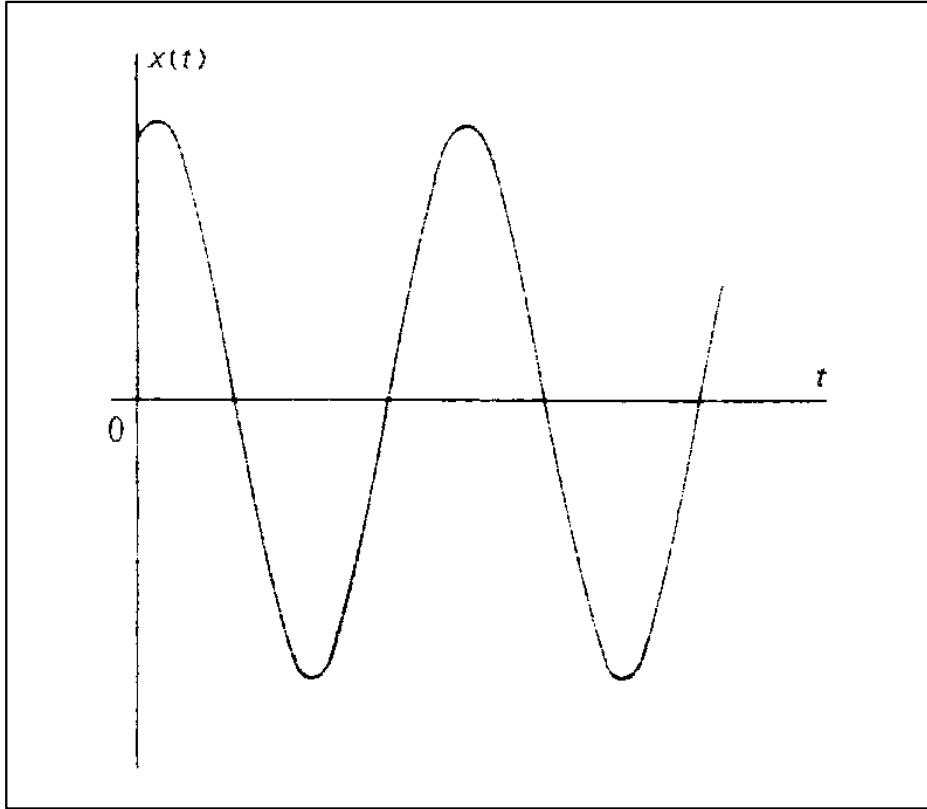


Figure 45 Example of a Undamped Displacement Response

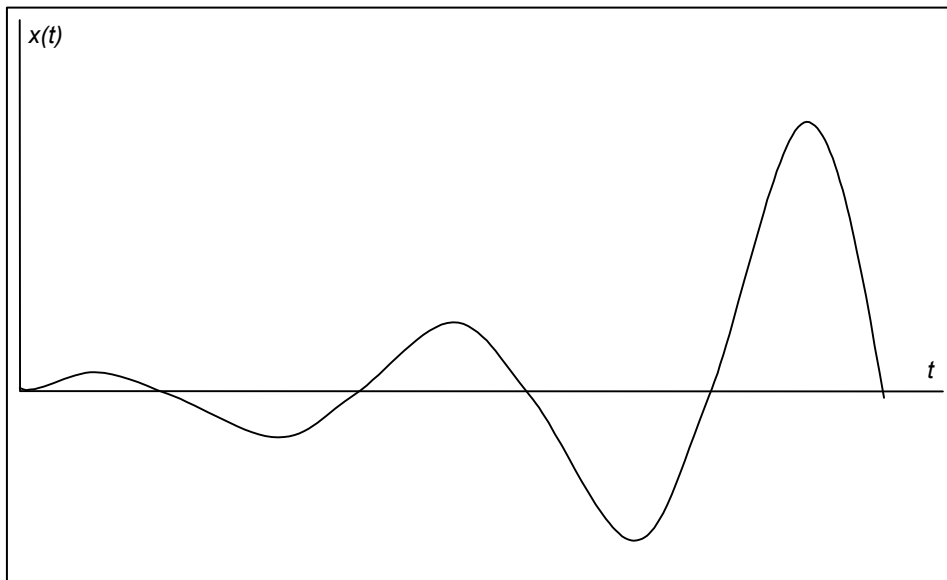


Figure 46 Example of a Divergent Displacement Response

4.3.2 Forced Response Case

A forced system is a system disturbed by some external excitation. The disturbance can be in the form of some initial displacement or velocity, or as an applied force. Since idealized linear systems modeled as differential equations have been assumed, the response to initial conditions (**transient response** or the homogenous solution) and the forced response (steady-state case or the particular solution) can be solved separately and combined through superposition for an expression of the total motion.

For the forced motion case we must return to equation 31 and make the substitutions made for equation 40. At the same time, a **harmonic excitation** can be assumed of the form:

$$F(t) = \omega_n^2 mA \cos(\omega t) \quad (42)$$

where:

ω = the frequency of the input.

The reason that the **harmonic forcing function** is of importance is the possibility of this oscillatory input occurring at the natural frequency of the system. The importance of this will be explained shortly. The nonhomogeneous equation has now been developed of the form:

$$\omega_n^2 A \cos(\omega t) = \ddot{X}(t) + 2\zeta\omega_n \dot{X}(t) + \omega_n^2 X(t) \quad (43)$$

If one also assumes that the **steady-state** or harmonic response solution will have the form:

$$x(t) = C_1 \sin(\omega t) + C_2 \cos(\omega t) \quad (44)$$

or, after substitution and manipulation (Reference 3)

$$x(t) = X(\omega) \cos(\omega t - \phi) \quad (45)$$

where:

$$X(\omega) = \frac{A}{\{[1 - (\omega/\omega_n)^2]^2 + (2\zeta\omega/\omega_n)^2\}^{1/2}} \quad (46)$$

and the **phase angle** is:

$$\phi = \tan^{-1} \left\{ \frac{2\zeta\omega/\omega_n}{1 - (\omega/\omega_n)^2} \right\} \quad (47)$$

The steady-state response can also be expressed in the complex exponential form as:

$$x(t) = X(i\omega)e^{i\omega t} \quad (48)$$

However, the formulation in equation 45 will be retained.

All the tools needed to examine the important system responses to a harmonic excitation are now in hand. Figure 47 shows how the system amplitude (expressed as $X(\omega)/A$ or **transmissibility**) will react as the excitation frequency approaches the natural frequency of the system. It can be seen that the amplitude of the

response increases as the two frequencies approach each other. When they are identical the amplitude is the greatest and, with no damping present, the motion will sustain itself indefinitely.

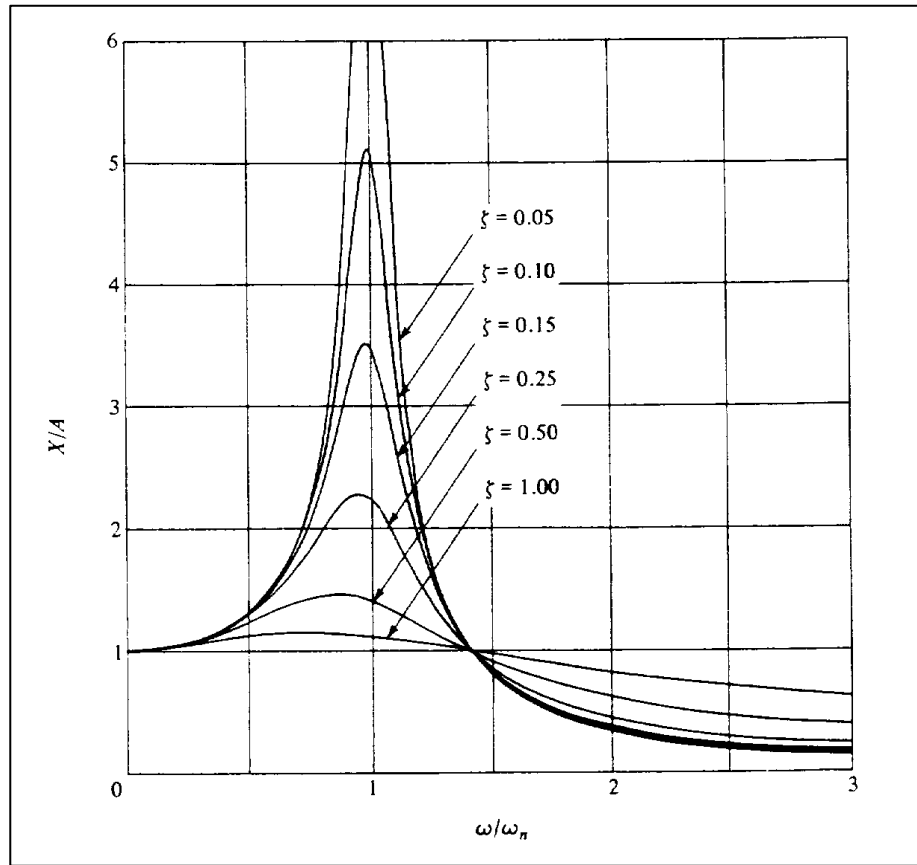


Figure 47 Typical Magnitude Response Showing Effect of Resonance and Damping

This is the undamped case discussed in the previous section. The coalescence of the natural frequency and the excitation frequency is called the **resonance** case. A structure will have an infinite number of such resonant frequencies or **modes**, although only the first few in ascending order of frequency are usually of importance as they contain the most energy. The equation of motion is no longer valid at resonance, but this is seldom of interest in real applications. Suffice it to say that the magnitude of the response will grow without bound. The peak responses at all other conditions will occur at:

$$\omega = \omega_n \sqrt{1 - 2\zeta^2} \quad (49)$$

At frequencies less than the resonance the response is governed by stiffness or restoring forces. At resonance, all of the restoring forces result from damping only. At frequencies above the resonance the motion is dominated by the inertia or mass. The phase angle is an expression of the difference between the peaks of the force and the response, as shown in Figure 48 where both have the same frequency ($\tau =$ time constant). The **period** of the oscillation (T) is defined as:

$$T = 2\pi / \omega_n \quad (50)$$

(ω_n in rad/sec) and is the time to complete one cycle of the motion, such as positive peak to positive peak. The reciprocal of equation 50 is just the natural frequency in cycles per second (Hertz or Hz) rather than radians per second. Figure 49 shows that at resonance the phase angle is always 90 degrees (said to be out of phase 90

degrees, or $\pi/2$). At 0 phase angle the two waveforms are exactly in phase and are moving in the same direction. At 180 degrees, they are exactly out of phase and are moving in different directions, that is, the maximum positive peak of one wave occurs at the same time as the maximum negative peak of the other.

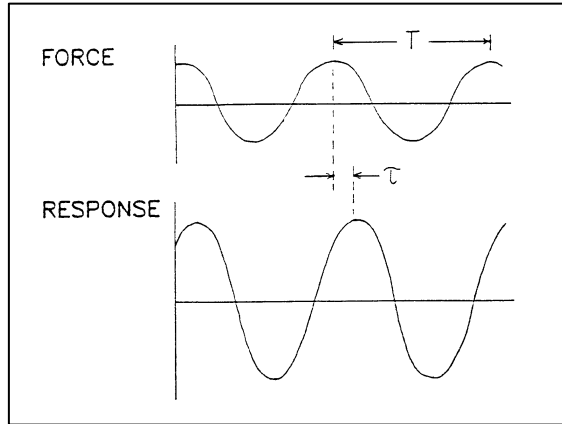


Figure 48 Definition of Phase Angle

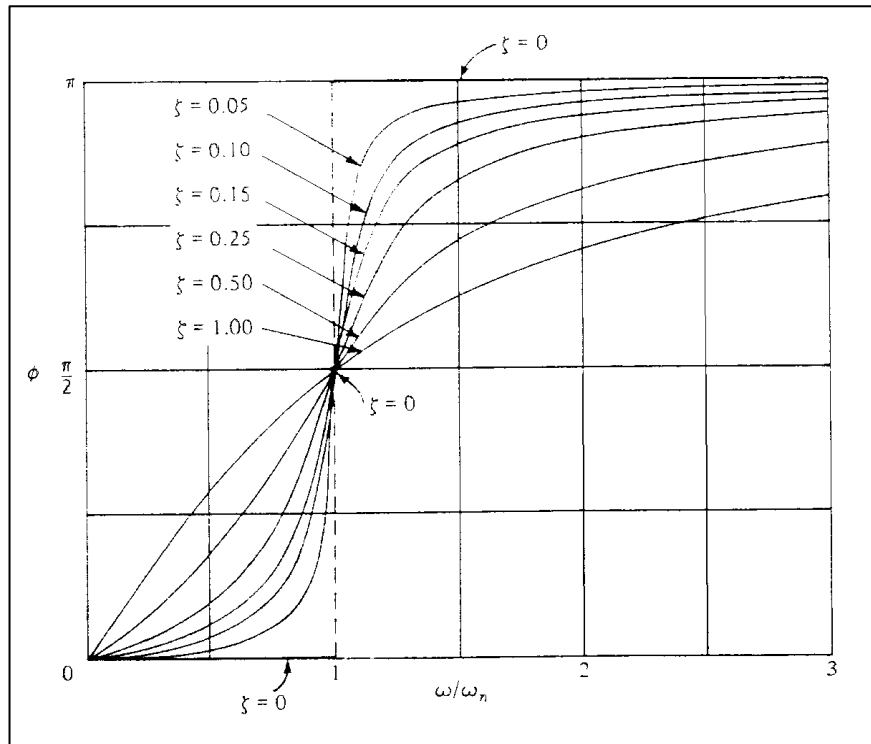


Figure 49 Typical Phase Angle Response Showing Effect of Resonance and Damping

This section has focused on a SDOF system only and used only one analysis method with one type of forcing function so that basic concepts could be easily illustrated. In fact, **multiple degree of freedom system (MDOF)** is the norm and will be dealt with later in this chapter. There are certain energy approaches to mechanical systems analysis, particularly using Hamilton's Principle and the Lagrangian. The Fourier Series and Laplace methods are also popular ways of analyzing these structures. The response to a unit step function or a random input (analyzed with a convolution integral) is also very useful. Readers are encouraged to follow-up on these areas to round out their understanding of structural dynamics.

4.4 Supplemental Concepts

4.4.1 Response Relationships

It is important to understand the relationship between the different system responses. So far only displacement has been discussed, but velocity and acceleration can be addressed as well.

Recall that velocity is just the time derivative of displacement, and acceleration is the time derivative of velocity. In the last section, an expression for the displacement of the spring-mass-damper system that was a function of cosine (equation 45) was developed. Differentiating this once will produce a sine function with the amplitude increased because of the product of the original amplitude and the frequency of the input function. This velocity expression can be differentiated again with similar results, but with the function once again becoming a cosine with a sign change. The result of these operations is illustrated in Figure 50.

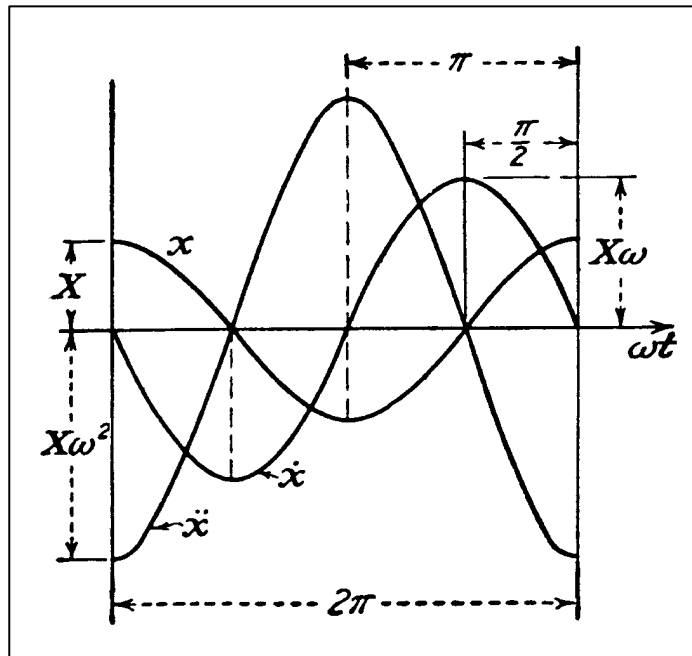


Figure 50 Relationship of Displacement, Velocity, and Acceleration

If the first peak of each of the waveforms in Figure 50 is examined, it can be seen that from displacement to velocity there was a 90-degree phase shift, and from velocity to acceleration yet another 90-degree shift as well as the sign change (or 180 degrees from displacement). In the case of the resonance condition discussed at the end of the last section, the displacement is 90 degrees out of phase with the forcing function, but the velocity is exactly in phase (phase angle of 0). This is the condition of maximum response of the oscillating system.

Several specific force/response relationships have been established and may be encountered on occasion.

$$\text{Accelerance or Inertance} = \text{Acceleration/Force} \quad (51)$$

$$\text{Effective or Apparent Mass} = 1/\text{Accelerance} \quad (52)$$

$$\text{Mobility} = \text{Velocity/Force} \quad (53)$$

$$\text{Impedance} = 1/\text{Mobility} \quad (54)$$

$$\text{Dynamic Compliance} = \text{Displacement/Force} \quad (55)$$

$$\text{Dynamic or Apparent Stiffness} = 1/\text{Dynamic Compliance} \quad (56)$$

For a pure, undamped, sinusoidal motion it is possible to derive peak (versus peak-to-peak) velocity and displacement from acceleration and frequency alone without an equation of motion. This is really just a unit conversion and can be shown graphically in Figure 51, or stated mathematically:

$$x_p(\text{inches}) = 9.78 \ddot{x} / \omega^2 \quad (57)$$

$$\dot{x}_p(\text{inches/sec}) = 61.42 \ddot{x} / \omega \quad (58)$$

where:

- \ddot{x} is in g's,
- ω is in Hz, and
- p indicates peak response.

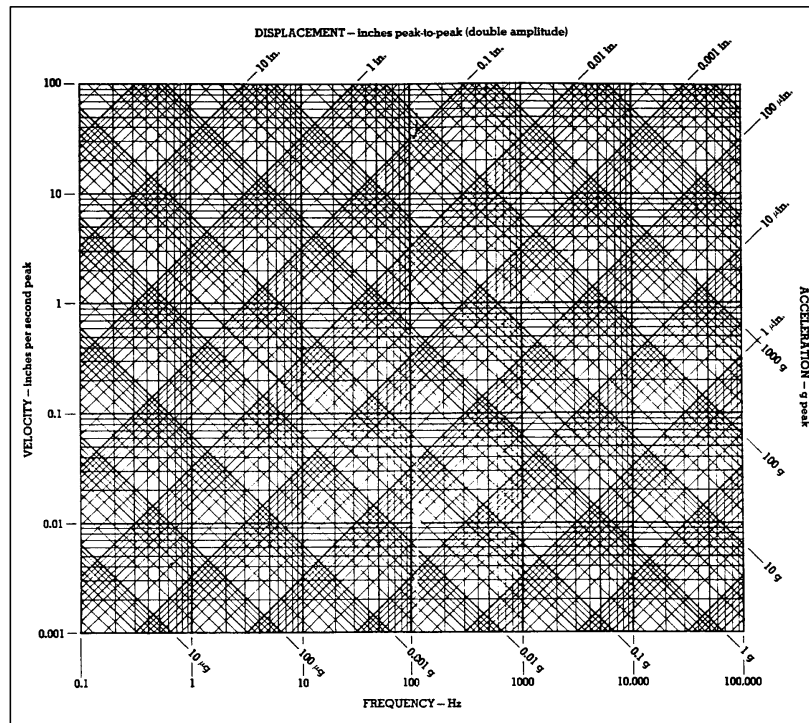


Figure 51 Vibration Nomograph for Sinusoidal Motion

The usefulness of this in flight testing is that it allows the determination of maximum displacement and velocity at an accelerometer response location if it appears to be excited by a single-degree-of-freedom undamped sinusoid. A case in point may be a vertical tail vibrating from side to side as the result of a vortex impinging on it during high angle-of-attack flight. The response of an accelerometer mounted at the tip of the surface would probably show a nearly repeatable peak acceleration at one dominant frequency. If the load (i.e., stress) in the tail is of concern but it has not been instrumented to provide this data, deriving the peak displacement will provide at least one indicator of how great a load is acting on the structure.

4.4.2 Complex Modes

The discussion so far has assumed only proportional damping is playing a role and it was modeled as viscous damping. This also implies that the phase at any point is either zero or 180 degrees. The result is a '**real mode**' in which the shape is that of a standing wave. In truth, other damping and nonlinearities produce more of a traveling wave in which the phase can be other than zero or 180 degrees, and all points do not reach maximum deflection at the same time. This is termed a **complex mode**. Where the damping is light, as in aircraft structures, the proportional damping assumption will generally yield adequate approximations to the modal parameters for practical purposes.

4.4.3 Beating

When two waveforms with nearly identical frequencies are summed, a result like that shown in Figure 52 occurs. This effect becomes difficult to perceive if the lower frequency is less than about 85 percent of the higher frequency. In real mechanical systems this 'beating' may even be audible as a warbling tone. The effect is important to understand because it indicates an approaching resonance condition with the large amplitudes that result. The frequency of the beat response shown by the dotted line in the figure (indicated by the period shown) is just the difference of the two original waveform frequencies.

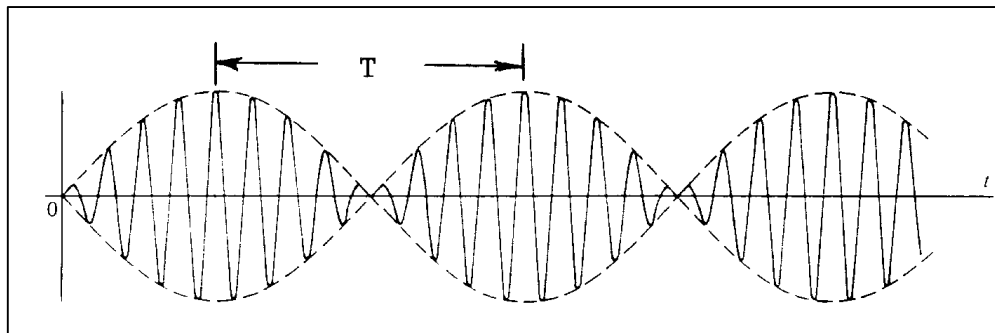


Figure 52 The Beating Phenomena

4.4.4 Harmonics

Often encountered are frequencies which are an integer multiple of some initial frequency (the **fundamental**). These integer multiples are called harmonics or **overtones**. The fundamental is the first harmonic, the first integral multiple the second harmonic, and so on. When a structure is observed to respond at fixed frequency intervals, twice some fundamental, three times, four times, and so on, harmonics should be suspected.

4.4.5 Jump Phenomenon

Figure 53 illustrates a curious effect that, while rare, is not unknown in the real world of nonlinear, damped systems. The figure shows that it is possible for the system to have more than one response amplitude at the same frequency.

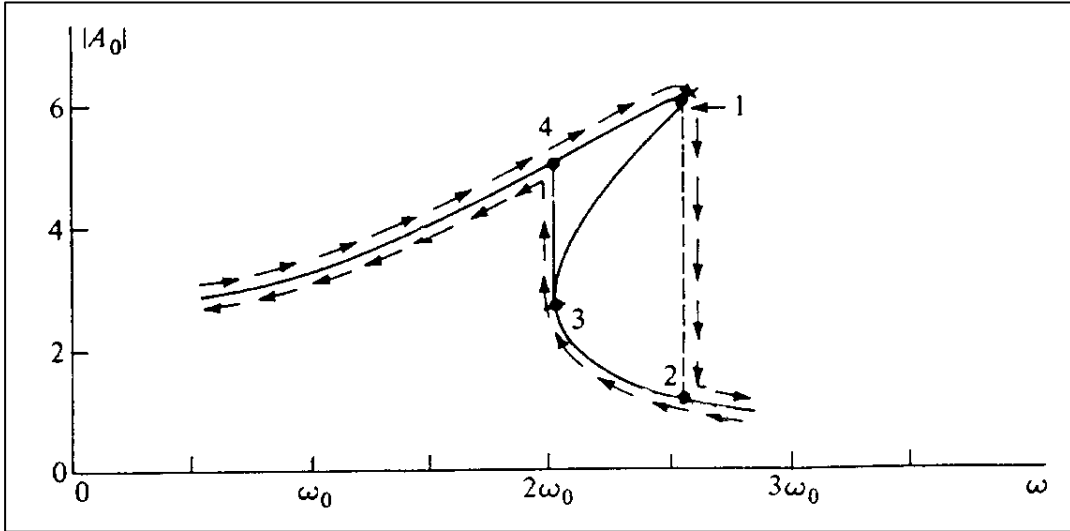


Figure 53 The Jump Phenomena

As the frequency is increased, the amplitude approaches point 1 and ‘jumps’ to point 2 for higher frequencies. If this effect were observed in a laboratory setup, there would be a sudden drop in displacement amplitude (for example) with little change in frequency. When decreasing frequency to point 3, the response would suddenly jump up to the point 4 amplitude. The area between point 1 and 3 is never traversed and is considered unstable. This phenomenon is very important in ground vibration tests and is the basis of nonlinearity checks (Section 7.9).

4.5 Modal Analysis

4.5.1 Multidegree of Freedom Systems

A real structure with many parts can be modeled with each part represented by a single mass attached to adjoining masses with springs and dampers. Even a simple beam with distributed mass and material properties can be broken down into such discrete elements. Each of these elemental masses can move relative to all the others but not without influencing the others. The motion of the masses are then said to be **coupled**. This relative motion requires a degree of freedom for each mass if the motion of the entire system is to be expressed mathematically. An example of such a multidegree of freedom system is shown in Figure 54. As before, the system is still being simplified considerably to keep the mathematics from getting out of hand.

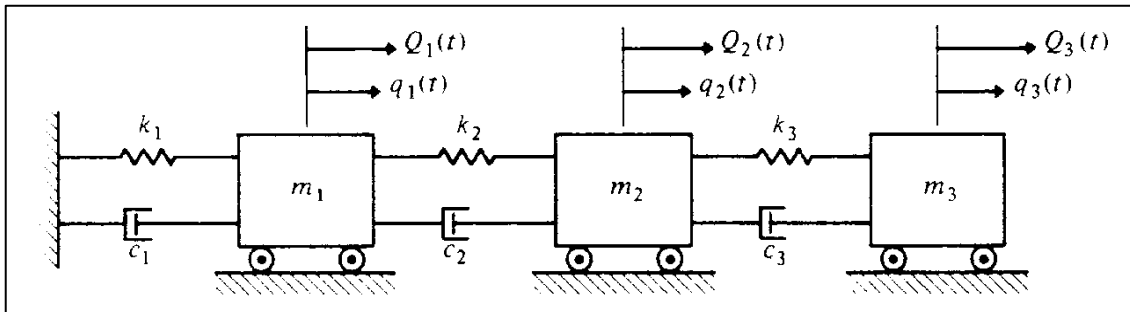


Figure 54 Example of a Multidegree of Freedom System

An equation of motion can be written for each of the masses in Figure 54 using the approach outlined in Sections 4.2 and 4.3. For the three masses, each excited by a separate force, the following series of equations can be formulated.

$$\left. \begin{aligned} Q_1 &= m_1 \ddot{q}_1 + (c_1 + c_2) \dot{q}_1 - c_2 \dot{q}_2 + (k_1 + k_2) q_1 - k_2 q_2 \\ Q_2 &= m_2 \ddot{q}_2 - c_2 \dot{q}_1 + (c_2 + c_3) \dot{q}_2 - c_3 \dot{q}_3 - k_2 q_1 + (k_2 + k_3) q_2 - k_3 q_3 \\ Q_3 &= m_3 \ddot{q}_3 - c_3 \dot{q}_2 + c_3 \dot{q}_3 - k_3 q_2 + k_3 q_3 \end{aligned} \right\} \quad (59)$$

where:

Q = the applied force, and

q = the coordinate of the model component related to the real structure.

The coefficients of these equations can be collected into three matrices; the **inertia** or **mass matrix** $[m]$, the **damping matrix** $[c]$, and the **stiffness matrix** $[k]$, as shown in equations 60 through 62.

$$[m] = \begin{bmatrix} m_1 & 0 & 0 \\ 0 & m_2 & 0 \\ 0 & 0 & m_3 \end{bmatrix} \quad (60)$$

$$[c] = \begin{bmatrix} c_1 + c_2 & -c_2 & 0 \\ -c_2 & c_2 + c_3 & -c_3 \\ 0 & -c_3 & c_3 \end{bmatrix} \quad (61)$$

$$[k] = \begin{bmatrix} k_1 + k_2 & -k_2 & 0 \\ -k_2 & k_2 + k_3 & -k_3 \\ 0 & -k_3 & k_3 \end{bmatrix} \quad (62)$$

The system's equation of motion can now be written as:

$$\{Q(t)\} = [m]\{\ddot{q}(t)\} + [c]\{\dot{q}(t)\} + [k]\{q(t)\} \quad (63)$$

where the **generalized coordinate** array $\{q(t)\}$ and the force array $\{Q(t)\}$ are:

$$\{q(t)\} = \begin{Bmatrix} q_1(t) \\ q_2(t) \\ q_3(t) \end{Bmatrix} \quad (64)$$

$$\{Q(t)\} = \begin{Bmatrix} Q_1(t) \\ Q_2(t) \\ Q_3(t) \end{Bmatrix} \quad (65)$$

The stiffness matrix can be considered as an **influence coefficient** matrix. That is, any element k_{ij} expresses the force needed at coordinate q_i for a unit displacement at q_j , with all other displacements equal to zero. The inverse of the stiffness matrix is called the **flexibility matrix**.

$$[a] = [k]^{-1} \quad (66)$$

Any a_{ij} expresses the displacement needed at coordinate q_i for a unit force at q_j .

4.5.2 Coordinate Transformation and Solution

If an expression that provides only the motion of one mode of the coupled system (one of the natural frequencies) is sought, it will be necessary to decouple the equations. This is done by changing the coordinate system to another in which equation 63 will be naturally decoupled, with each of the coefficient matrices diagonalized. The coordinates can be transformed to the new coordinates, $\eta_j(t)$ by use of a square transformation matrix $[u]$.

$$\{q(t)\} = [u]\{\eta(t)\} \quad (67)$$

with derivatives:

$$\{\dot{q}(t)\} = [u]\{\dot{\eta}(t)\} \quad (68)$$

$$\{\ddot{q}(t)\} = [u]\{\ddot{\eta}(t)\} \quad (69)$$

When these equations are applied to the equation of motion, the coefficient matrices will be postmultiplied by the transformation matrix. Both sides of the equation can also be multiplied by the transpose of the transformation matrix at the same time without loss of generality. This is equivalent to premultiplying the coefficient matrices, or

$$[M] = [u]^T [m] [u] \quad (70)$$

and likewise for the damping and stiffness matrices. Also,

$$\{N(t)\} = [u]^T \{Q(t)\} \quad (71)$$

is the generalized forces associated with the new generalized coordinates. The transformation matrix that makes the coefficient matrices diagonal (decoupled) is termed the **modal matrix** and the coordinates $\eta_j(t)$ are called the **natural** or **principal coordinates**. Such a transformation matrix is said to be **orthogonal**. The resulting coefficient matrices are now **modal mass** (M), **modal stiffness** (K), and **modal damping** (C) **matrices**.

If the transformation matrix had the effect of reducing the mass matrix to the identity matrix, that is:

$$[U]^T [m] [U] = [I] = \begin{bmatrix} 1 & 0 & 0 \\ 0 & 1 & 0 \\ 0 & 0 & 1 \end{bmatrix} \quad (72)$$

then the transformation is orthogonal. It is this relationship that is used to solve for the actual values of the elements of the transformation matrix. For such a transformation the final matrix equation of motion has the form:

$$\{N\} = [I]\{\ddot{\eta}\} + [C]\{\dot{\eta}\} + [K]\{\eta\} \quad (73)$$

or, since the equations are now decoupled and the matrices are diagonalized, only one equation at a time need be referenced. The equations would have the general form of:

$$N_r = \ddot{\eta}_r + 2\zeta_r\omega_r\dot{\eta}_r + \omega_r^2\eta_r \quad (74)$$

where:

$r = 1, 2, 3 \dots$ for each mode or resonant frequency, one equation for each.

This implies that the elements on the main diagonal of the orthogonal modal damping matrix are of the form $2\zeta_r\omega_r$ and the elements on the diagonal of the orthogonal stiffness matrix are ω_r^2 . The natural frequencies and damping coefficient of each mode can now be easily derived. But what modes are they?

Examine the modal matrix again. It has some important properties. The columns of the matrix are the mode shapes of the system. An example of a mode shape for a 5 degrees of freedom system is:

$$\begin{Bmatrix} 0.02 \\ 0.12 \\ 0.79 \\ 1.33 \\ 2.67 \end{Bmatrix}$$

The values in the column are not unique, only their amplitude relative to each other, or between columns, is unique. Therefore, the vector can be presented in a normalized form.

$$\begin{Bmatrix} 0.01 \\ 0.04 \\ 0.30 \\ 0.50 \\ 1.00 \end{Bmatrix}$$

For a simple cantilever beam, each of these numbers correspond to a point on the beam at which an imaginary concentrated mass was centered for the purpose of the analysis. The numbers give the magnitude of the displacement at each of the masses as shown in Figure 55 for the resonant frequency or mode. The first mode shown in the figure is called first bending. Other cantilever beam modes are also shown. Each will have its own unique resonant frequency. Such **mode shapes** or **normal modes (natural modes or characteristic modes)** are typically displayed in an exaggerated form so that the shape can easily be identified. Where the displaced shape crosses the undisturbed centerline indicating zero displacement (although rotation occurs there) is termed a **node** or **antiresonance**. Where the shape is at a maximum displacement is termed an **antinode** or **resonance** point. Note that the number of nodes corresponds to the order of the mode, that is third bending has three nodes (including the fixed end).

This development has been necessarily abbreviated and simplified for the purpose of illustration. Such a development would normally include a discussion of the undamped and unforced case which is solved as an **eigenvalue** problem, with the eigenvalues supplying the natural frequencies and the **eigenvectors** the mode shapes. There are other techniques in which the analyst makes a careful guess at the mode shape and then solves for the associated frequency. The method may involve an iteration process for convergence to the correct solution. These are the **Matrix Iteration** and **Rayleigh Quotient** methods. The methods may use the **dynamical matrix** as:

$$[D] = [m]/[k] = [m][a] \quad (75)$$

Energy methods can also be applied to multidegree of freedom systems. Modal analysis today is commonly done with finite element analysis, as described in Section 3.2.3.

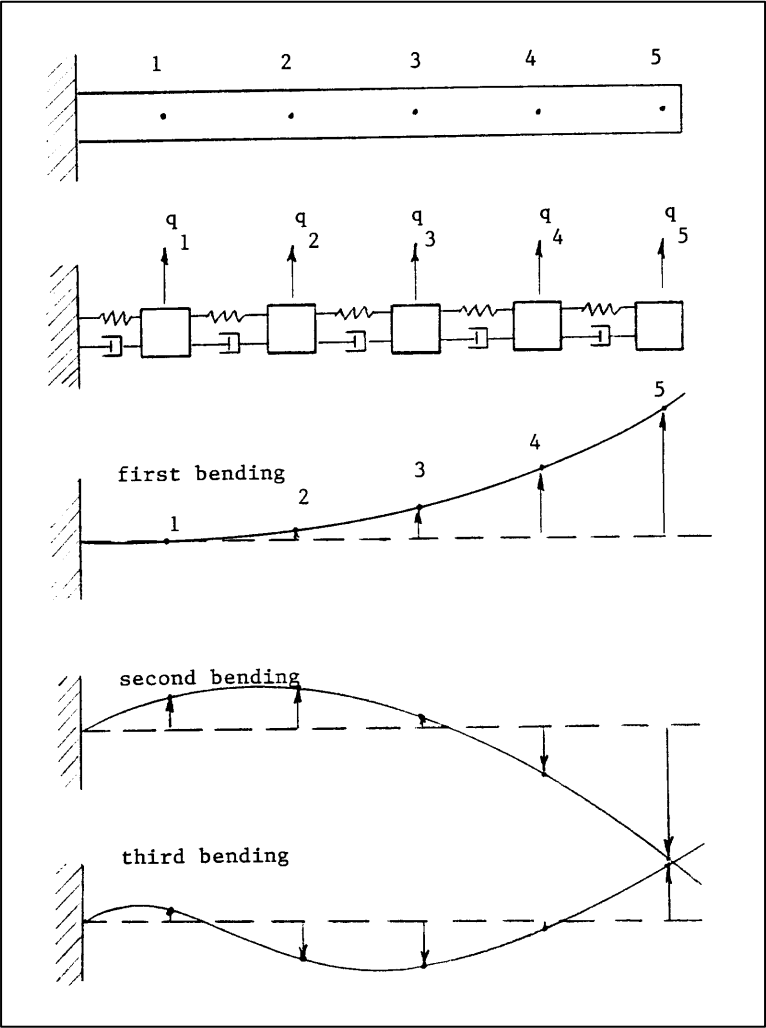
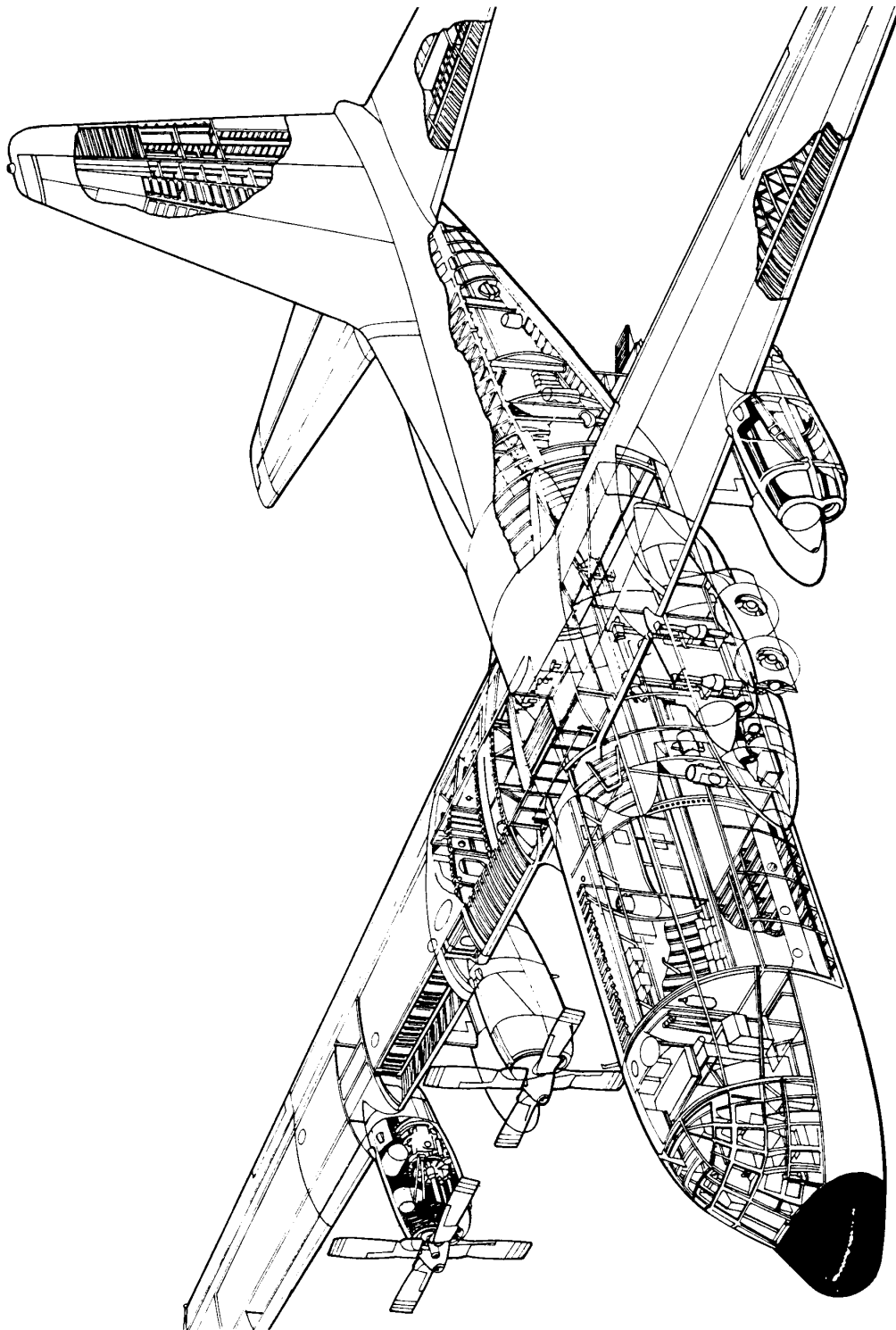


Figure 55 Beam Bending Problem with Mode Shape

SECTION 4 REFERENCES

1. Hartog, J.P. Den, *Mechanical Vibrations*, Dover Publications, New York, New York, 1984.
2. Jacobsen, Ludik S. and Ayre, Robert S., *Engineering Vibrations*, McGraw-Hill Book Company, New York, New York, 1958.
3. Meirovitch, Leonard, *Elements of Vibration Analysis*, McGraw-Hill Book Company, New York, New York, 1986.
4. Meirovitch, Leonard, *Analytical Methods in Vibrations*, Macmillan Publishing Company, New York, New York, 1967.
5. Myklestad, N.O., *Vibration Analysis*, McGraw-Hill Book Company, New York, New York, 1944.
6. Lang, George F., *Understanding Vibration Measurements*, Application Note 9, Rockland Scientific Corporation, Rockleigh, New Jersey, December 1978.
7. *The Fundamentals of Modal Testing*, Application Note 243-3, Hewlett-Packard Company, Palo Alto, California, 1986.



Lockheed C-130H Cutaway

5.0 LOADS

5.1 Introduction

This chapter will introduce the concept of airloads and will outline the basic airloads testing methods as well as review many of the more intractable problems and limitations of those methods. Frequently, the airloads issues which arise in development flight testing are the most significant from cost, schedule, and program performance aspects. And yet, the limitations of airloads testing methodology have often been little understood by the program managers and flight test leaders. It is important that all parties to the testing be familiar with these issues and how they are being addressed. The implications of the test plan and the compromises that have been made during the planning process must also be understood and accepted by all involved in the test conduct. This chapter will hopefully provide the necessary insights to make that understanding possible.

5.2 Types of Loads

Aircraft are carefully designed for light weight but great strength. This requires that the forces or loads applied to the aircraft structure be well known in terms of both amplitude and orientation as operating conditions change. The vehicle is subjected to an almost infinite variety of such loads acting on or distributed throughout the structure. These include:

- a. **Airloads** - forces resulting from external pressure gradients created by passage through the air
- b. **Maneuver Loads** - airloads produced through aircraft maneuvering
- c. **Inertia Loads** - the dead weight of structural and nonstructural mass (fuel, payload, engines), can increase with acceleration
- d. **Dynamic Loads** - additional airloads resulting from elastic oscillations of the structure
- e. **Reaction Loads** - static loads such as from resting on landing gear, towing, jacking, and hoisting
- f. **Live Loads** - thrust, arrestment, store separation, gun fire, etc.
- g. **Environmental Loads** - cabin pressurization, thermal gradients, etc.

The loads can be further categorized as:

- h. **External Loads** - requiring prediction of the aerodynamic forces, landing impact, taxi reactions.
- i. **Internal Loads** - requiring evaluation of load paths and stresses within the structure resulting from external loads, and reactions from such things as engine thrust transmitted to the airframe

The design process predicts the external forces imparted by the aerodynamic pressure gradients, dead weight of the structure, and inertial forces. The loads predictions use the shape of the airframe, its flight characteristics, and flight conditions derived from the mission definition. The resulting external loads predictions are then used to design the internal structure of the airframe, usually via a finite element model (see Section 3.2.3), to withstand the predicted loads. The magnitude of these loads can be surprisingly high, making the design process particularly challenging because aircraft are designed for light weight but great strength. It then becomes imperative to apply modeled loads to the structure on the ground and to measure the external airloads through flight testing to verify that the aircraft can perform its assigned tasks without structural failure and with adequate safety margin.

5.2.1 Maneuver Loads

Flight maneuvers in any of the three aircraft axes (see Section 2.3.1) can produce structural loads. The **vertical (normal) axis** is the most common for maneuvering. The load in this axis, termed the **normal load**, is produced by lift force and inertia (vertical accelerations). An example of normal load is shown in Figure 56 for an aircraft in a level (constant altitude) turn. The **normal load factor (n_z)** is defined as the lift force (L) divided by the gross weight (W) of the aircraft, and can be related to the bank angle (ϕ) shown in Figure 56.

$$n_z = 1/\cos\phi = L/W \quad (76)$$

The maximum load factor achievable at any airspeed and weight would occur at the maximum lift for that speed. This would be, using the equation 13,

$$L_{\max} = C_{L,\max}qS \quad (77)$$

A similar equation can be written for lift equal to the gross weight except that the airspeed would be at the stall speed. Combining such an equation with 77 gives an expression for the maximum load factor in terms of velocity, or

$$n_{\max} = (V/V_s)^2 \quad (78)$$

where:

V_s = stall speed.

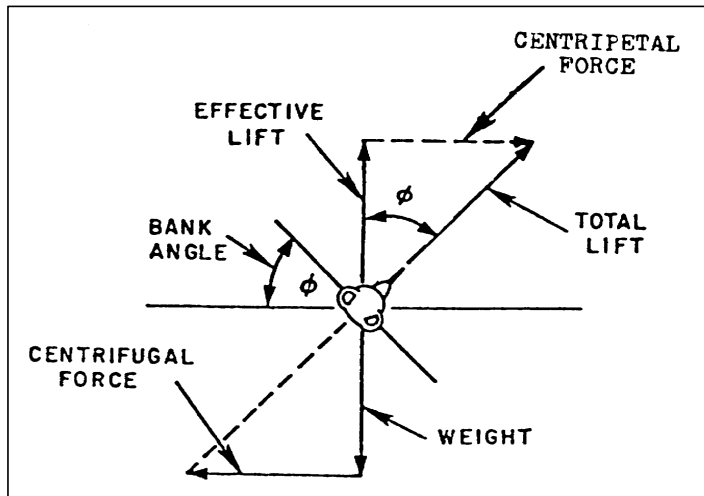


Figure 56 Forces Acting on an Aircraft in a Level Turn

The maximum or **limit load factor** is generally driven by mission requirements. Fighter, attack, and trainer aircraft generally require a -3.0 to 7.0 or 9.0 g normal acceleration while large transport or long-range patrol aircraft require about a -1.0 to 3.0 g. **Asymmetric normal loads** are produced by aircraft roll or asymmetric store configurations and can be important for the loads at the wing attachment, the fuselage structure, the vertical tail(s) as well as store pylons and attachments.

Using the concepts introduced in Sections 4.0 and 6.0, loads within the structure itself can be calculated using the following equation:

$$A\ddot{q} + (D + VB)\dot{q} + (E + V^2C)q = RU \quad (79)$$

where:

- q = generalized coordinate vector,
- A = structural inertia matrix,
- D = structural damping matrix,
- E = structural stiffness matrix,
- B = aerodynamic damping matrix,
- C = aerodynamic stiffness matrix,
- R = input force coefficient matrix,
- U = input scalar, and
- V = true airspeed.

For modern military aircraft the input force coefficient matrix could be a function of flight control system gains which can change automatically. These loads are usually expressed as bending moment, torque, and shear at a number of locations on the airframe (wing stations, for example).

It is important to understand that maximum normal load factor is not directly analogous to structural limit load or ultimate stress (see Section 3.2.2). For example, a maximum acceleration turn will not likely produce the maximum vertical tail bending load or any number of other critical loads. Load factor is used because it is so easily measured and displayed. It has immediate meaning to pilots because they frequently maneuver in the vertical axis and feel this load more directly. Some aircraft have an **Overload Warning System (OWS)** which automatically warns the pilot when the aircraft is near its normal load limit (a cockpit tone or verbal message), and even a g-limiter system that prevents the pilot from commanding more load than is recommended. **Side loads** generated in yaw maneuvers (Figure 57) are generally limited by control deflection limitations (full rudder deflection) to avoid overloads to the vertical tail, gear doors, etc. All of these limits vary as a function of aircraft external configuration and weight.

Because of the criticality of normal load factor, flight manuals normally contain a **V-n** (or **V-g**) **diagram** like that shown in Figure 58. There are four major maneuver conditions used in constructing this diagram. The first of these is positive high angle of attack (PHAA), or the condition related to the lowest airspeed at which the limit positive load factor can be attained. At lower airspeeds the wing stalls prior to the limit load factor. This condition is associated with the maximum compressive stresses on the forward upper wing root and maximum tensile stresses at the lower aft wing root, and represents the speed at which the pilot may command the tightest turn (highest load factor and smallest radius). The PHAA condition is labeled as A in the figure and is referred to as the '**corner**' point or **maneuver speed**. The next important condition for designing the V-n diagram is for negative high angle of attack (NHAA), or the lowest airspeed at which the maximum negative

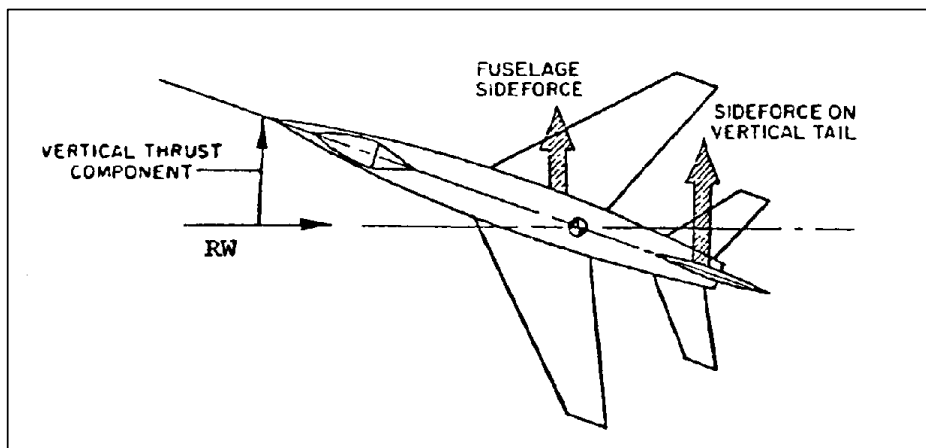


Figure 57 Forces Acting in a 90-Degree Roll Attitude

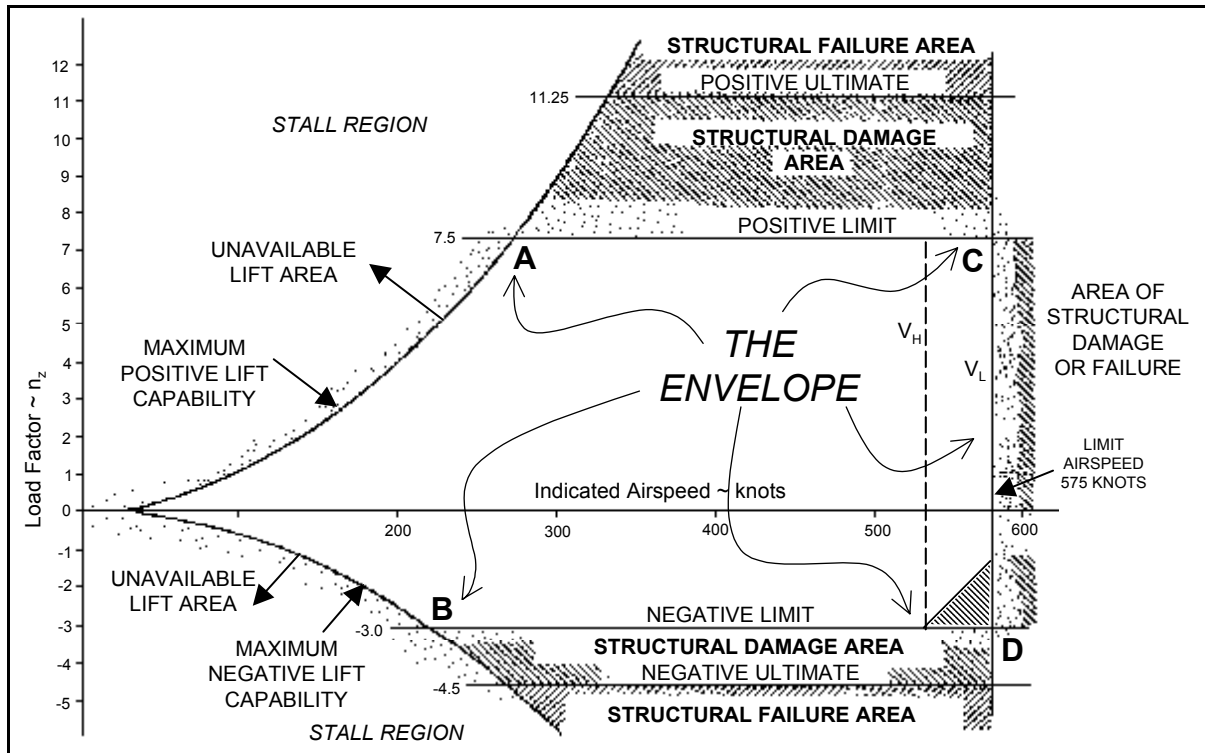


Figure 58 Significance of the V-n Diagram

angle of attack (AOA) is achieved without stalling and shown as B in Figure 58. The NHAA is associated with the maximum balancing tail upload, but the wing also sees the maximum compressive stresses in the lower forward wing root and highest tensile stresses in the upper aft root. Positive low angle of attack ([PLAA], labeled as C) is associated with the smallest AOA at which limit load factor can be achieved. This occurs at the maximum permissible dive speed. In this case the maximum compressive stresses are experienced at the aft upper wing root and maximum tensile stresses at the lower forward wing root. Similarly, negative low angle of attack ([NLAA], D) corresponds to the highest airspeed at which the maximum negative AOA can be achieved. Maximum compressive stresses are experienced at the aft bottom wing root and maximum tensile stresses at the top forward root.

Because NLAA is seldom used in practice and the weight penalty to meet the condition structurally can be quite high, the lower right corner of the V-n diagram is frequently cut off. The result is a **maximum level flight speed (V_H)** above which the maximum negative load factor is restricted to a lower value (See Figure 58). Other adjustment to the limits may be made to avoid phenomenon such as high-speed buffet engine compressor stall, tail blanking, etc.

Figure 59 shows how some of the maximum load conditions relate to the V-n (N_z for the figure) for one particular aircraft. Often more than one such diagram is given, one for each aircraft configuration such as heavy weight (fuel and stores), landing configuration (gear and flaps extended), various altitudes, etc. (Figure 60). The maximum allowable loads for an asymmetric maneuver are typically 80 percent of those for a symmetric maneuver (Figure 61) because of the additional load created during the roll, and are typically lower still with external stores.

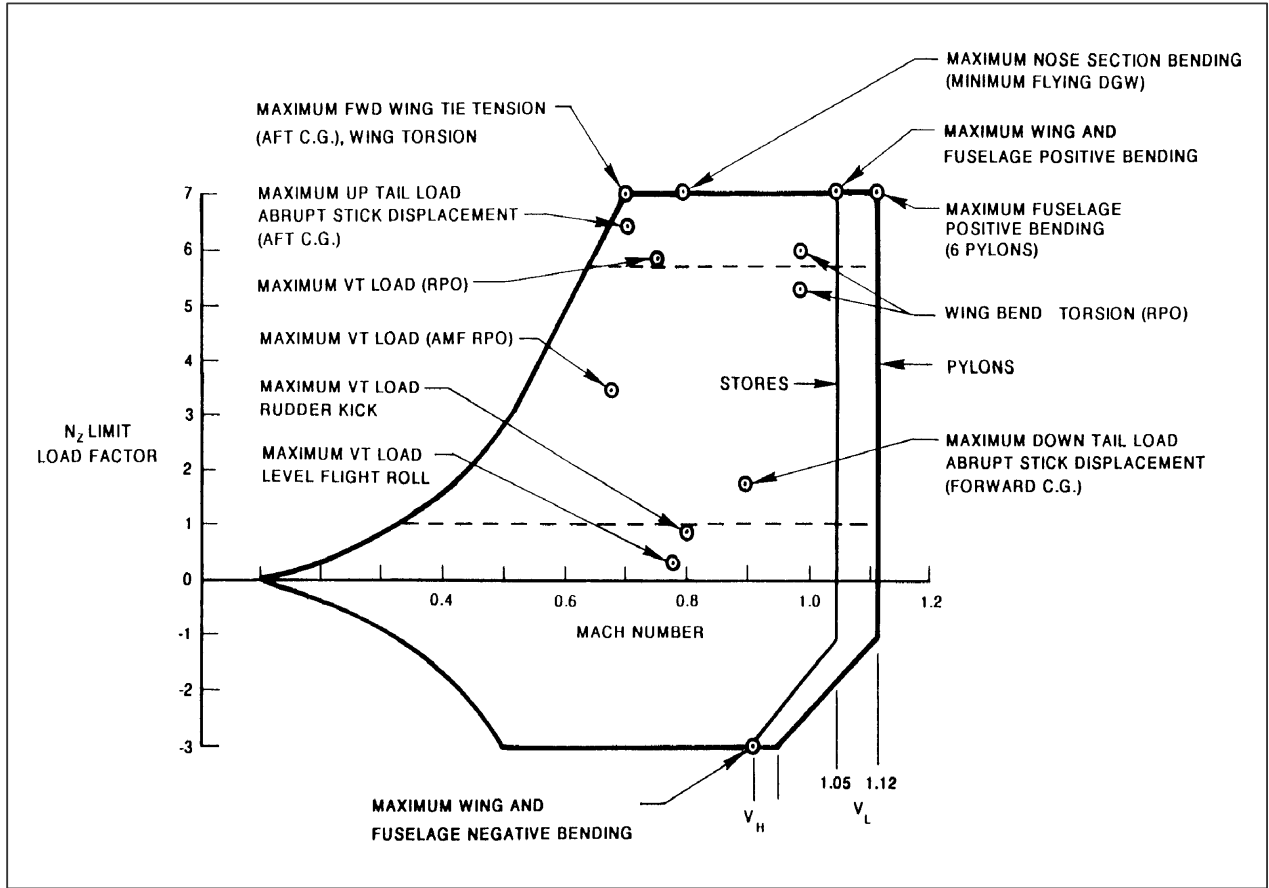


Figure 59 Example Maximum Loads Related to V-n Plot (Fighter-Bomber)

The **limit airspeed** (V_L), also known as the ‘**red line**’ **airspeed**, may be defined by an airload limitation, flight controllability limitation, flutter speed (Section 6.0), an aircraft system restriction (dynamic pressure on a ram scoop, for example), or simply as the maximum airspeed required by the aircraft’s mission. The maximum level flight speed (V_H) becomes the normal maximum permissible airspeed, with V_L then usually defined by some emergency upset dive recovery criteria (common for airliners).

Pilots sense maneuver loads as inertia forces acting on their bodies. However, for the aircraft structure the concern is for the actual loads to which it is subjected. The lift forces to keep a 20,000-pound airplane in straight-and-level flight are much greater than those required to keep the same airplane weighing 10,000 pounds at the same condition, all else remaining the same. (Note that the mass added to the wings helps relieve wing loads since the inertia effect acts counter to the lift upload. However, it becomes critical for ground taxi conditions.) If the pilots of these aircraft both perform a maneuver with a 4.0-g load factor the heavier plane is still being subjected to a greater overall load because of the larger initial lift, although the pilots of both machines feel only the 4.0-g normal load factor. Thus, the maximum load factor is proportionally lower as gross weight increases (Figure 61). Because of this, flight manual limit load factors and flight test conditions are frequently given as $n_z W$. Another important measure of this is **wing loading** or W/S (weight over wing area). An airplane with high wing loading is generally much less maneuverable (to avoid over-g of the structure) than an airplane with lower wing loading. Again, asymmetric loads are frequently the most critical conditions.

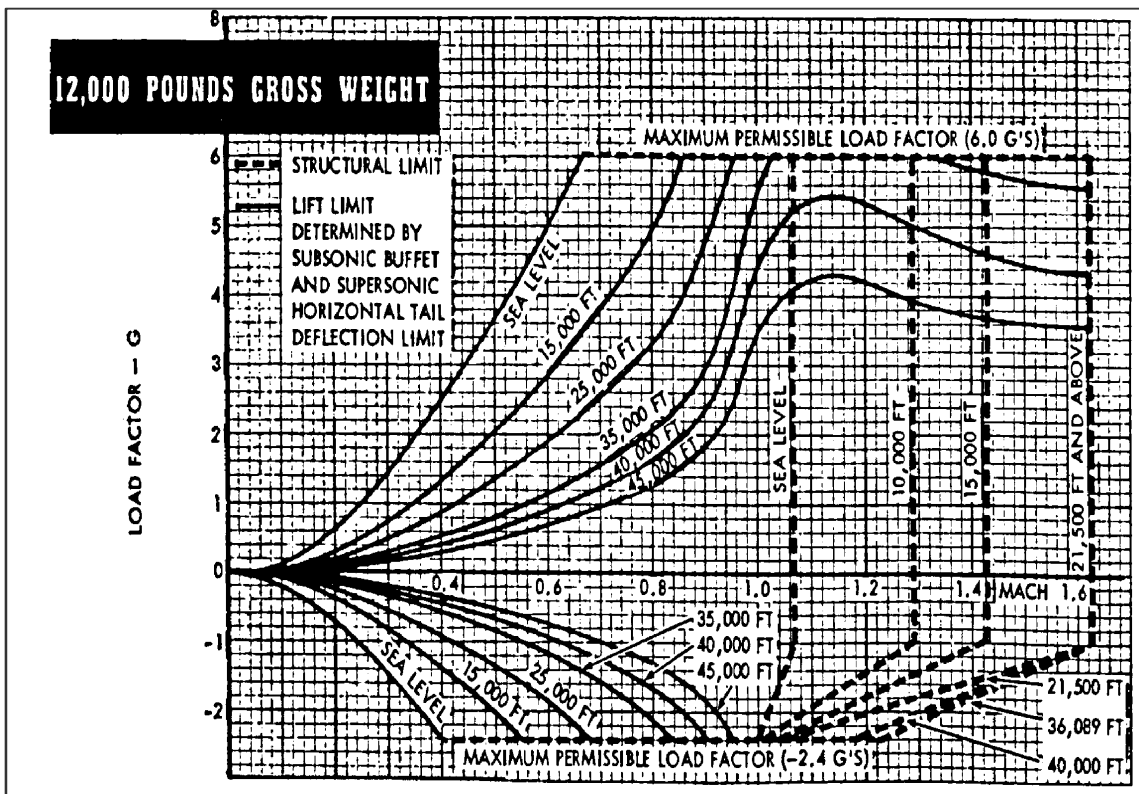
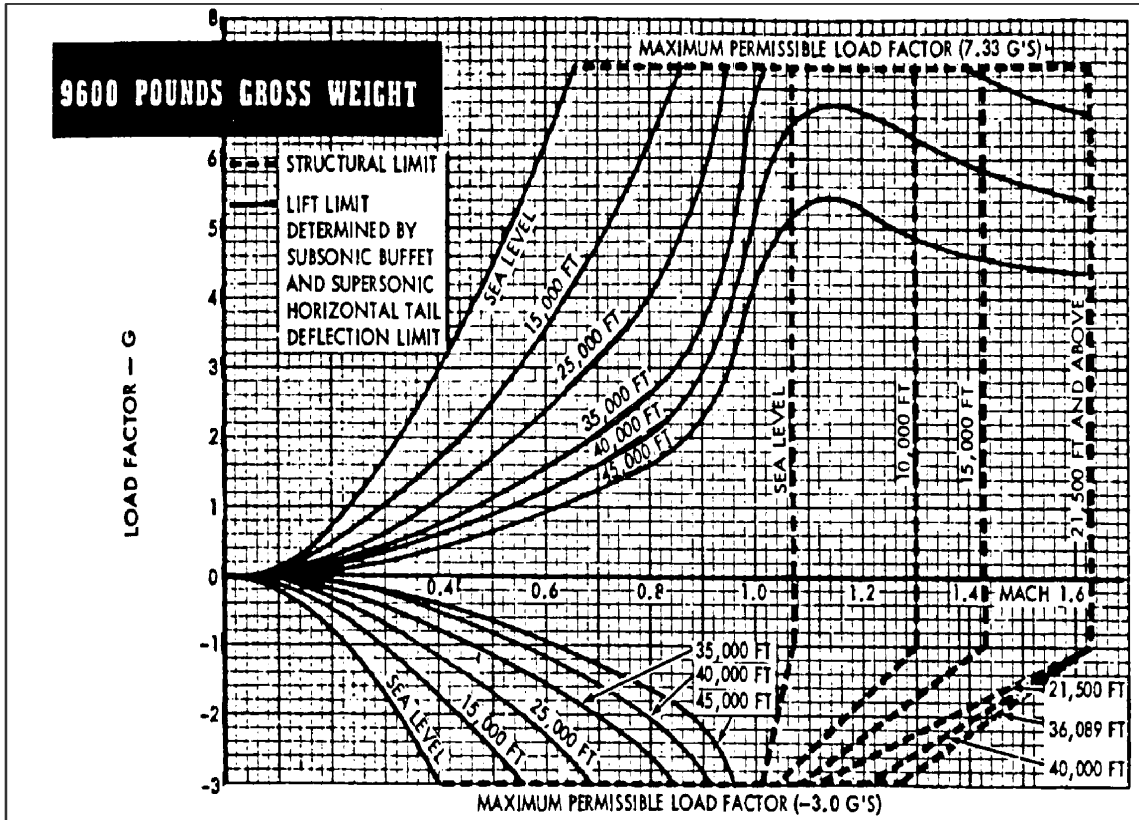
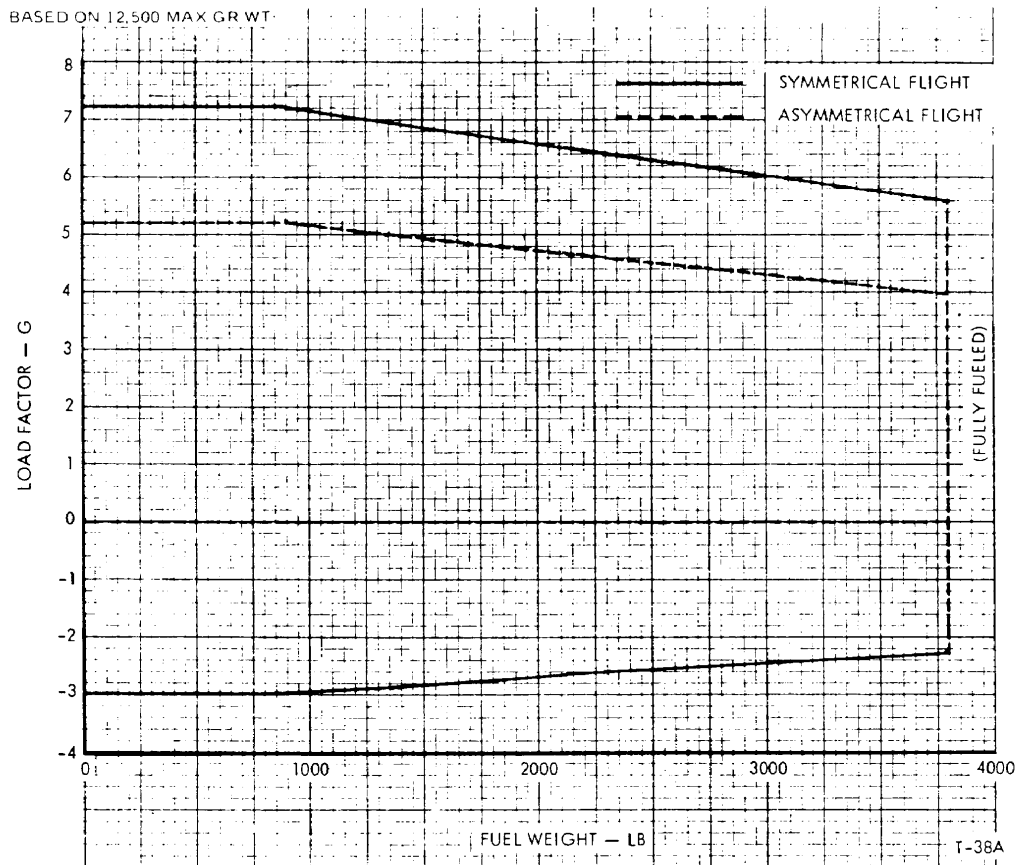


Figure 60 Example V-g Diagrams - T-38A Aircraft (Symmetric)



LOAD FACTOR LIMITATIONS

Do not exceed the following

SYMMETRICAL FLIGHT

Load Factor (G's)	Weight of Fuel Remaining (Pounds)
-2.3 to +5.6	3800
-2.6 to +6.4	2300
-3.0 to +7.33	900 or less

ASYMMETRICAL FLIGHT

Load Factor (G's)	Weight of Fuel Remaining (Pounds)
0 to +4.0	3800
0 to +4.6	2300
0 to +5.22	900 or less

Figure 61 Example Load Factor Limits Chart - T-38A Aircraft

The distributed airload on a control surface can be observed as a **hinge moment** - the amplitude of the airload acting on the surface multiplied by the distance from the centroid of the load (center of pressure) to the hinge line. The force produced by the actuator(s), or the pilot's muscles for reversible control systems, must be capable of overcoming this moment in order to move the surface. The measurement of hinge moments is then important in determining whether the loads analysis for the control surfaces has been performed correctly, the surface and attachment fittings adequately designed, and the proper actuators chosen.

5.3 Loads Ground Testing

A static loads ground test is conducted on an aircraft and separate components during the development stage of the project, prior to flight testing. The static loads test is performed to ensure that the aircraft is structurally adequate to withstand the anticipated stresses along with a safety margin. Because of this, the test structure must be as close to the final production configuration as possible. The characteristics of the structure (moduli, stress-strain relationship, fatigue, etc.) can also be explored during the test.

The initial portion of the static test loads the aircraft to 100 percent of the maximum loads expected to occur in normal operations, as dictated by mission requirements, and defined as the **design limit load (DLL)**. Up to these loads the structure must return to its undeformed shape after the load is relieved. Beyond 100 percent DLL and up to 150 percent DLL the structure is allowed to yield; that is take on a permanent deformation or set. This means that the elastic limit of the material has been exceeded. Only beyond 150 percent DLL (the **design ultimate load**) is the structure allowed to actually fracture, or break. This 50-percent pad on actual failure of the structure is called the **factor of safety** ([FOS], see Section 3.2.3) and allows the aircraft to be landed safely after an overload which does not exceed the design ultimate load. Any load-bearing capability beyond 150 percent DLL is defined as a **margin of safety**, as defined in equation 22. The test article may be taken to failure in important components like the wing to clearly define any additional margin.

Traditionally, only the control surfaces have been tested to 100 percent DLL prior to first flight of a prototype aircraft and flight up to 80 percent DLL. However, the 100 percent '**proof**' loads portion of the overall airframe in static tests are usually completed prior to airloads testing. Actual airloads flight testing to 80 percent DLL provides data to improve the mathematical airloads model, seeking to match the flight-measured loads. New airloads predictions are then generated for further ground and flight tests. Static tests to 150 percent DLL (**ultimate loads** testing) follow, and are usually necessary prior to flight beyond 80 percent DLL. These ultimate load ground tests may be waived for some portions of the airframe if structural adequacy can be demonstrated by comparison to similar structures or a substantial margin has been demonstrated by major subassembly tests. Flight to 100 percent airloads is performed to provide additional validation data while also demonstrating the maximum flight conditions. The 100-percent testing may reveal the need for additional ultimate loads static tests where the applied static loads were shown to be too conservative. Portions of the static test airframe may then be taken to failure to demonstrate any existing margin of safety. Mathematical models of the structural response are then improved by incorporating the results of these ground tests.

For loads ground testing, the airframe is usually mounted in a rigid test jig and the loads applied with hydraulic rams. This is also done to calibrate the airloads instrumentation, as detailed in Section 10.2.3. Similar tests using cyclically applied loads may be conducted to verify **fatigue** life predictions. Such tests may run through typical mission loading profiles on an accelerated schedule over months or years. For a pressurized structure, static pressure tests are also required. Tests to 133 percent of the maximum pressurization level must be demonstrated prior to the first flight with pressurization. **Durability** tests to twice the airframe life, fatigue and **damage tolerance** tests (the structure should be able to carry essential loads through several load paths to provide redundancy in the event of battle damage) are also routinely performed with detailed post-test inspections.

5.4 Airloads Flight Testing

As implied in the previous section, the principal objective of airloads flight testing is to validate the mathematical models used in the design of the aircraft by checking the loads or strains at several vital points on the airframe. The loads are expressed in terms of bending moment, torque, and shear at a number of stations on the wing, tail surfaces, fuselage, and pylons, plus control surface hinge moments. Flight loads test data may also be compared with analytical results to validate fatigue trends and service life predictions. It is impractical to verify the strength of every component of the plane and, from a safety point of view, is unnecessary. Less critical components are suitably checked during static loads testing and routine inspections.

The airloads testing also provides a controlled and safe buildup to the **flight operating limits (FOLs)** to demonstrate that the aircraft can withstand these conditions without failure. This demonstration of the structural

integrity through flight to maneuver limits (normal load factor, maximum rates, abrupt control inputs, etc.) is not always accepted as one of the objectives of an airloads test program. However, experience has shown that flight to FOLs is extremely valuable in revealing design deficiencies and obtaining operator 'buy-in' with the test results.

The tests are normally performed in two steps; to 80 percent of DLL (following acceptance of the design loads analysis) and then to 100 percent DLL (following ultimate loads static tests and verification of flight loads analysis with 80 percent flight test results). Both the 80 and 100 percent steps involve considerable buildup in airspeed, altitude, gross weight, center of gravity (see Section 2.3.2), control surface deflection and load factor. Progression along constant dynamic pressure (q) lines rather than a constant altitude is common practice. Tests at 100 percent may not be as thorough as those at 80 percent, although the buildup should be thorough, and are sometimes called 'demonstrations' because of this. It may not even be possible to produce 100-percent limit loads in some structural components within the allowable flight envelope and maneuver restrictions.

Traditionally, the airloads have neither been measured nor monitored during initial flight testing where loads are restricted to 80 percent DLL. The 80-percent restrictions are imposed through maneuver, flight condition, and configuration limitations which the airloads computations predict will ensure less than 80 percent DLL airloads. The initial 80-percent limit defines a flight envelope wherein other disciplines can conduct tests without the need to monitor airloads data at the same time. Loads flight testing will typically consist of flight to many loading conditions to provide the loads analyst plenty of data to correlate with the mathematical model. The test points are defined as specific flight conditions (altitude, airspeed, gross weight, center of gravity, etc.), aircraft configuration (flaps down, gear up, etc.), combined with a maneuver. The maneuvers are performed in one or a combination of axes with a buildup in an appropriate maneuver parameter (g , sideslip angle, aileron deflection, input abruptness, etc.). As with the ground tests, the aircraft must be as close to the final production configuration as possible.

Airloads must be monitored real time for tests between 80 and 100 percent DLL to ensure against an overload. They are also generally monitored during 80 percent buildup tests to obtain data to verify loads predictions prior to going above 100 percent DLL. Loads can then be extrapolated as the buildup progresses in order to clear the pilot to the next test point. Frequent comparisons with predicted load trends are also done in an effort to anticipate potential overload conditions. A poor match to predictions during the 80-percent buildup may require changes to the math model to more closely match test results and new predictions for 100 percent generated before flight testing is allowed to proceed. The airloads on highly-loaded stations (termed **critical structure**) are displayed opposite the corresponding limit load to permit the maneuver to be terminated if the limits are approached or exceeded.

These limit loads are derived from the maximum operating conditions used to design the aircraft, such as those plotted on the envelope shown in Figure 59. Since these design points are defined for discrete conditions, with individual values of the load parameters, the limit of one parameter cannot be defined without the limit of another (for example, a bending load in a swept wing will necessarily be accompanied by some value of torsion). Thus, for individual airframe stations, a crossplot or interaction diagram of these relationships can be drawn. An example of this relationship is shown in Figure 62, with the vertices of the limit load envelope corresponding to the individual maximum design conditions. The limit boundary is then simply the lines joining these few design points. For real-time use, the plot may display how the load varies during the maneuver (as shown in the Figure 62) or as a discrete point for the peak load experienced during the maneuver. Because these cross-plots are not generally axially symmetric, it is important to make sure the monitored loads have the correct sign conventions.

During the Airbus 330 and 340 flight testing measured airloads were compared with predicted loads real time and displayed as a time history of the two responses. The predicted airloads were previously computed for a range of influence factors (gross weight, airspeed, load factor, control surface deflection, etc.) and stored in look-up tables. This allowed interpolation of loads from measured influence factors at any instant of time (updated at 16 times per second, in the Airbus example) during an in-flight maneuver. A quantitative judgment of the predicted airloads versus measured values could then be made. Significant departure of flight test data from predicted trends would be cause to pause testing until the cause could be determined. Some quantitative measure of satisfactory match should be determined for this method to be truly useful. Also, techniques for

warning of imminent overload is still essential. In the Airbus program this approach was only used for pseudosteady loads induced by normal load factor in a simple longitudinal maneuver. However, the method may have broader application in the future as computing power allows actual airloads computations, using an equation such as 79, to be performed fast enough for comparison with measured loads and display in a control room.

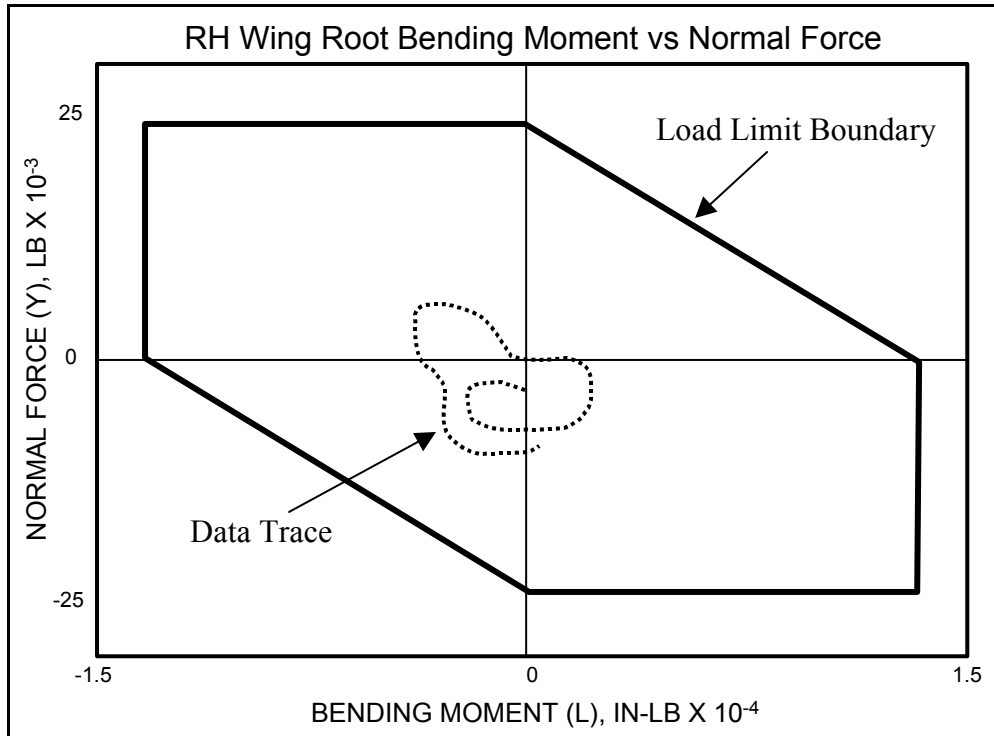


Figure 62 Example Loads Cross-Plot

When using the normal load factor in solutions or plots, it is common practice to correct it to some standard or design gross weight. This is done as shown in the following equation:

$$\text{corrected } n_z = (\text{test } n_z)(W_t / W_s) \quad (80)$$

where:

W_t = test day weight

W_s = standard weight.

It is widely accepted that a component which has been oversized to 187 percent DLL may fly to 100 percent DLL without loads instrumentation on the component and without ground loads tests. Otherwise, flight to 100 percent DLL is normally permitted only with proper instrumentation and monitoring. The 187 percent DLL criteria is generally reserved for modifications to existing air vehicles which have already undergone considerable loads testing.

The advent of the fly-by-wire aircraft (see Section 2.3.3) has added a new twist to flight loads testing. Critical loads distributions and load protection may be closely tied to electronic flight control system (EFCS) behavior. Thus, various EFCS modes may need to be tested to evaluate the structural implications. Changes to the EFCS software can change the airloads during maneuvers and may require subsequent loads retesting.

5.4.1 Maneuvers

Understanding some basic relationships of flight conditions with critical loads are helpful in planning a flight loads test. Maximum wing shear and bending moments are usually experienced at a light wing condition (no internal fuel or external stores) and maximum load factors. The highest torsion will likely be seen during maneuvers with leading or trailing edge high lift control surface deflected. The addition of stores, particularly those at the wingtip, and large fuselage protuberances can markedly alter the wing loads. The maximum fuselage shears and bending moments are typically found during maneuvers in each axis, such as vertical maneuvers and sideslips. Elevated aft fuselage torsion is most often experienced during rolling maneuvers. Large horizontal tail loads will occur during maximum stab or elevator deflections coupled with a pitch maneuver, usually at high airspeeds. Rolling and yawing maneuvers with large sideslip angles create high vertical tail loads. Maximum torsion in the vertical tail will be seen with the addition of large rudder deflections during the maneuver.

In addition to the maneuvers described below, any special missions such as aerial refueling, jinking, or missile breaks may also be performed if unusual loads are anticipated. Stalls and spins can produce special load conditions (particularly buffet) that may require testing.

An airloads flight should begin with a series of lightly loaded maneuvers intended to check the functioning of instrumentation, telemetry, and control room displays. During this **phase check**, the control room personnel should verify display scaling, ensure that the loads look reasonable in magnitude and direction (phase), and verify that critical instrumentation is functioning. Aircraft trim is generally set to zero for airloads maneuvers.

MIL-A-8871A (Reference 10) and MIL-A-8861A (Reference 6) describes each maneuver in detail, with precise guidance for accomplishment, and specifies the minimum number of test conditions for each. This document, plus past test plans and reports, should be consulted when formulating the tests for individual projects. The type of aircraft being tested and its mission will dictate much of the testing which will be required. Since the loads analyst on the design team will be the principal user of the airloads data, this individual should play prominently in the choice of tests.

5.4.1.1 Symmetric Maneuvers

a. *Steady and abrupt **pullups** (also known as normal symmetric pullups) to positive load factor with and without abrupt checking* - The maneuver is intended to produce high positive vertical symmetrical bending moments and shears in the wing, horizontal stabilizer and aft fuselage. Certain deployed control surface configurations (flaps, slats, spoilers, etc.) can also create high negative torques in the wing. This maneuver is very susceptible to pilot technique and has the potential to produce hazards associated with unusually high noseup attitudes. It may be desirable to begin the maneuver from a nose low attitude, at 1.0 g, to allow sufficient time to reach the target load factor without an excessive nose high attitude resulting. If the stick aft stop is reached before the target load factor, it may be possible to achieve the end point by pausing the stick at the stop and allowing inertia to carry the aircraft to the target load factor. In conditions where the aircraft is control performance limited, it may be possible to obtain additional pitch authority by adjusting the pitch trim prior to the maneuver. For some aircraft, the target normal load factor can only be maintained for a fraction of a second. The maneuver should not be continued beyond moderate airframe buffet as the loads data will most likely be worthless.

b. *Steady and abrupt **pushovers** to negative load factor with and without abrupt checking* - This maneuver is usually intended to produce high negative vertical symmetrical bending moments and shears in the wing, horizontal tail and aft fuselage. High positive symmetrical torques can be created in the wing and horizontal tail in some deployed control surface configurations. The comments relative to the symmetric *pullup* also apply here. Continuous attempts at *pullups* or pushovers, individually or in combination, have been called **rollercoaster maneuvers** for obvious reasons.

c. *Abrupt symmetric pullup to positive load factor with abrupt recovery* - This maneuver is intended to produce high positive vertical symmetric bending moments and shears in the horizontal stabilizer and aft fuselage. High negative symmetrical torques in the horizontal tail can also be created. Peak elevator hinge moments usually result as well. The rate of stick input is frequently as critical as the load factor in achieving the desired test conditions, and the loads analyst may need to provide some target rate or a buildup sequence for the pilot. Too rapid a stick snatch may produce an overload. During the recovery, the stick is not pushed beyond neutral. This can be critical, with much greater loads resulting if the stick does go beyond neutral. This is because the stabilizer will be highly loaded by virtue of being at high AOA and elevator trailing edge up displacement adds substantially to these loads. Too much elevator can drive these loads beyond 100 percent DLL. To fully recover the airplane, it may be possible to pause at neutral to allow the airloads to peak before again pushing the stick forward.

d. *Abrupt symmetric pushover to negative load factor with abrupt recovery* - This maneuver is intended to produce high negative vertical symmetric bending moments and shears, plus high symmetrical torques, in the horizontal stabilizer and aft fuselage. Peak elevator hinge moments usually result as well. High horizontal tail loads would result from a combination of elevator position and elevated AOA. The same precautions mentioned above apply for this maneuver.

e. *Windup turn ([WUT], turning maneuver of increasing normal load) to positive load factor* - This maneuver permits a gradual buildup in normal load and sustained target normal load factor without unusual attitudes. A descent may be necessary to maintain the target airspeed and for this reason it is often called a **wind-down turn**. The descent should be planned such that the target load factor is achieved within a predetermined band about the desired altitude. The WUT permits more control over the g onset rate with less likelihood of an over-g than with the steady *pullup*. Prolonged turns present the possibility that the test aircraft will pass through its own wake. This can produce a sudden spike in vertical load factor which, if it occurs at the wrong instant, can result in an over-g or confuse post-test analysis.

5.4.1.2 Asymmetric Maneuvers

a. *Uncoordinated aileron rolls to various angles of bank* - The rolls are intended to produce high asymmetrical bending moments, shears and torques on the wing. Peak aileron or flaperon hinge moments can also result. The buildup parameter is usually stick displacement, such as half lateral stick or three-quarters lateral stick, although a bank angle limit may also be specified. The peak load normally occurs at the instant the stick is reversed to reverse the roll. No rudder inputs are made and longitudinal stick inputs are usually restricted to that required to maintain 1.0-g flight. However, flight control systems may act to coordinate the roll even without pilot input and this is usually considered acceptable. The maneuver is performed in both directions to measure complementary loads in opposite wings.

b. *Elevated-g Roll* - Trim the aircraft at the desired positive or negative 1.0-g level flight condition. Initiate a 90 deg bank turn, applying longitudinal stick force to increase or decrease g to the desired level and increasing thrust as required to prevent excessive energy loss. While maintaining longitudinal control force, roll the aircraft using full lateral stick input. Check the roll by either applying full opposite lateral stick followed by a return to neutral or returning lateral stick to neutral stopping the aircraft at the desired bank angle change. Control inputs may be made normally or abruptly, as specified. Release the longitudinal control force following the termination of the roll. The maneuver may be performed either coordinated (with rudder) or uncoordinated (feet on the floor to preclude any inadvertent rudder inputs).

c. *Rolling Pullout (RPO)* - Trim the aircraft at the desired positive 1.0-g level flight condition. Execute a roll by applying a full lateral stick input. After a bank angle change between 90 and 270 deg, apply full longitudinal stick force and hold as required to achieve the desired load factor. Check the roll by applying full opposite lateral stick while simultaneously returning the longitudinal stick to neutral. Control inputs may be made normally or abruptly, as specified. The maneuver may be performed either coordinated or uncoordinated.

d. *Rudder kicks and abrupt rudder reversals* - This maneuver is intended to produce high lateral loads in the vertical tail and fuselage, to include lateral bending moment, shear and torque. Peak rudder hinge moments

also result. It is initiated in straight-and-level flight with a rudder pedal kick in the specified direction at an abrupt rate of input. Input rate may need to be specified and practiced. The pedal displacement is held until a steady angle of sideslip is attained. Lateral stick is used as necessary to keep the wings level. The rudder is then abruptly returned to neutral. Peak loads occur at the moment of initial input, at rudder reversal, and at the final recovery to neutral. A buildup in pedal displacement is commonly used for a corresponding buildup in load. The maneuver is usually performed in both directions.

e. *Asymmetrical power* - This maneuver is typically used with transports, tankers or bombers with engines nacelles on the wings. It is intended to produce high lateral loads in the vertical tail and fuselage, to include bending moment, shear and torque. It is initiated from straight-and-level flight with the throttles set at thrust for level flight. Buildups are usually in which engine is chopped - first an inboard, then an outboard, and then both engines (assuming four engines) on one wing. The rudder pedals are held at the neutral position until the maximum angle of sideslip is attained and steady. An abrupt rudder input is then made to bring the sideslip to zero. The abruptness of the rudder input is also frequently used as a buildup parameter. The maneuver is performed in both directions. Stick displacement is allowed as necessary to keep the wings level.

5.4.1.3 Ground Maneuvers

Some aircraft will experience high load conditions during landing or taxi, requiring that these be tested. High sink rate landings (Section 5.5.1.1) can impart strong down-loads in the structure. Derotation, with a sharp nose gear touchdown, will generate fuselage bending loads. Taxiing over runway undulations or a step (usually a short drop off a shallow ramp placed on the taxi surface) can induce high wing bending loads. Undulations and aircraft taxi speed are usually selected to produce varying inertia loads matching the fundamental bending mode frequency of the wing (Section 4.5.2) for the internal fuel state. Staggered undulations or steps will induce asymmetrical responses.

5.4.2 Instrumentation

A prototype or greatly modified aircraft will be heavily instrumented and may have hundreds of loads parameters that require examination as the loads buildup is underway. Accelerometers, force transducers and **pressure taps** (for pressure surveys) are occasionally used in loads tests. However, the most common transducer used is the **strain gage**.

It is wise to include a few accelerometers, placed at the aircraft's extremities, in the airloads instrumentation suite. Besides providing an outstanding indication of turbulence and buffet levels, these transducers can provide some indication of the load the structure may have been subjected to should the strain gages have failed or the loads equations found to be unusable. An acceleration amplitude at a specific frequency can be translated into a displacement (see Section 4.4.1), or strain, for associated components. A load likely to produce such a strain can then be determined using the mathematical model. This is at best a tertiary relationship, but can provide some insight into the potential that an overload has occurred when nothing else remains. It should not be considered a substitute for the traditional strain gage technique.

5.4.2.1 Strain Gages

The nature of the load the gage will measure (torsion, bending, shear, etc.) will dictate the orientation and calibration of the gages (Section 10.2). Instrumentation is arranged to measure the bending, torsion and shear loads in the primary load bearing structure plus secondary members as necessary. A typical transducer arrangement is shown in Figure 63. Strain gage instrumentation is 'calibrated' by applying known static loads (Section 10.2.3). Often more than one gage is used to determine a load measurement because of a complex load path. Each applied load is then correlated with the output of relevant gages and an equation is derived to define this relationship. Several equations using various combinations of gages can be derived for any one load parameter at an airframe station. Each equation should be supplied with an associated average error for several similar calibration loads, or identical loads applied and removed a number of times.

MIL-A-8871 specified a minimum strain gage installation for flight tests:

“Wing load distribution measurements by the strain gage method (one wing) shall include at least four stations for spanwise bending moment, shear, and torsion to cover the wing root, two midspan, and wingtip region(s) on small-to-medium-size airplanes (semispan along quarter-chord line, 50 feet or less); and at least six stations for spanwise bending moment, shear, and torsion measurements to cover the wing root, four midspan, and wingtip region(s) on medium-to-large-size airplanes (semispan along quarter-chord line greater than 50 feet). Unless otherwise agreed, spanwise distribution shall be obtained on the right wing. In such instances, however, instrumentation shall be provided for obtaining at least the total loads (bending moment, shear, and torsion) on the opposite wing to facilitate the determination of unsymmetrical loads. Tail loads measurement by the strain gage method shall include at least the total loads (bending moment, shear, and torsion) at the root of each vertical and horizontal surface. Vertical and side bending moments and shears shall be measured for at least one forward fuselage station and one aft fuselage station. For certain aircraft, additional strain gages may be required as agreed upon between the contractor and procuring activity.”

A data sample rate of about 50 samples per second (sps) is normally adequate for flight loads testing. An exception may be made for things like gear dynamic loads and gust loads test where 200 to 400 sps may be necessary because of the rapidly changing load. The sign convention for the forces and moments can change between projects and contractor, so the convention must be agreed upon immediately.

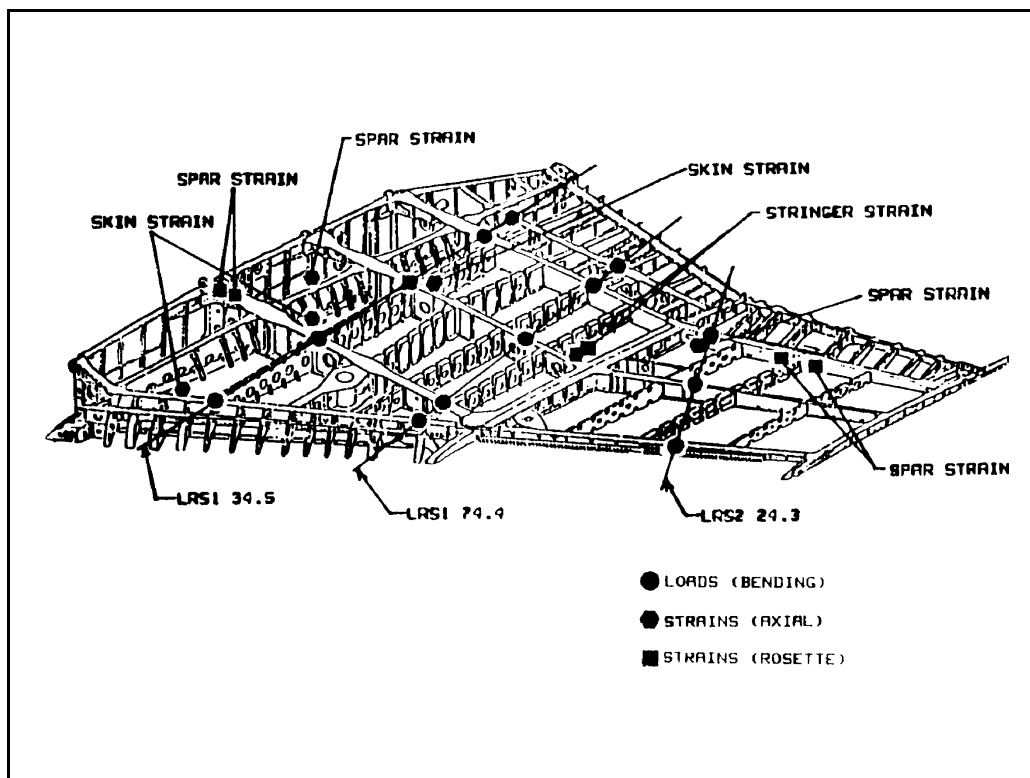


Figure 63 Example Loads Strain Gage Installation - F-15 Wing

Strain gages have a number of inherent limitations. The most basic of these is that they do not measure airloads directly, but only as a derived value through the strain of the structure under load and use of a mathematical relationship. The airframe static calibration loads used in deriving the equation are typically

limited to a few symmetrical or asymmetrical distributions of the load across the structure. Any real airload which does not conform to these pure distributions can result in strains and load paths for which the calibration equations are not valid. An apparent overload under such conditions can be neither confirmed nor refuted, and may be greater than indicated. Such circumstances usually result in obviously incorrect loads. Other unexpected loads can occur through unintended control surface motion driven by the electronic flight control systems - for example; asymmetrical spoiler motion during a roll which may not be exactly repeatable - or during dynamic loading conditions in which the structure is undergoing unsymmetrical aeroelastic oscillations such as might be induced by buffet or wake impingement. Every effort must be made to anticipate such occurrences and plan accordingly to avoid them.

Strain gage readings for identical strain conditions typically drift over the course of a flight. It is important to perform pre-flight and postflight checks of the loads to identify any substantial drift. Any drift beyond the equation error should be traced to its source (for example; localized strains due to cabin pressurization effects) and corrected, or the drift becomes a new level of recognized uncertainty in the measurements. The loss of entire load parameters (e.g., wing station 90.5 bending moment) are not uncommon. The test team must be willing and able to stop testing when the number of lost parameters has exceeded practical or safe limits. Strain gage bridges must be temperature compensated (Section 10.2.2) or considerable drift will result.

Strain gages can be easily damaged and are frequently inaccessible. They cannot simply be replaced without repeating a portion of the airloads calibration - at least not without introducing some unknown and potentially large error into the airloads measurements. A recalibration is seldom practical after flight testing has begun. This can sometimes be avoided by adding redundant gages beside the primary transducer, and including these in the calibration. Substituting gages during testing would then require only a small wiring change.

Many development teams include uncalibrated gages in the flight test airframe for the sole purpose of measuring strains in critical components or areas of particular interest to the stress analysts. Correlation of these stresses with the finite element and airloads models of the structure for specific flight conditions may provide some insight into the magnitude of an overload or judgment about load proximity to the material's elastic limit. This method is valuable if nothing else is available, if the strain gages have not been calibrated, or if data on only a few structural members are required to validate a modification. The uncertainty involved with this method is frequently great or ill-defined, and does not possess adequate safety measures for routine test application. It would almost certainly be inappropriate for a prototype aircraft.

The speed and volume of computational solutions now possible, and the ability to sample and process tremendous quantities of transducer data, may make it possible to perform airloads flight testing using stresses instead of derived airload measurements. This would allow real-time comparisons of measured stresses with yield stress envelopes. The method would reduce the uncertainty about how close a load is to the real load-bearing capability of the structure, eliminating the greatest worry associated with overloads.

5.4.2.2 Pressure Sensors

If an airloads parameter which has been lost simply must be measured, and installation and recalibration of new strain gages is impractical, the use of pressure transducers is an alternative. It will generally be impractical to disassemble the structure to install pressure taps as on a wind tunnel model, but bonding tiny piezoelectric transducers (Section 10.5) to the external surface of the structure may be possible. The compromise is that the sensors and associated wiring will necessarily disrupt the airflow and can thus alter the resulting derived airloads. However, current transducers, wiring and application techniques allow these to be fairly thin - as little as 1 millimeter. The measured pressures are compared with those predicted for the flight conditions and adjustments to the math model made to create a match. The assumption is that if the pressure gradients have been modeled accurately, the airloads should also be correct.

Measuring a pressure distribution actually provides a more direct measure of the airloads and avoids the time and expense of a loads calibration. Also, with the transducers applied externally, a dedicated airloads test aircraft is not necessary, although the tests should be performed as soon after application as practical. The data also has applications beyond the airloads analysis as it can reveal flow separation points, vortex impingement

areas, etc. While some transducer and wiring losses can be expected, these can be replaced with ease, unlike strain gages. Tests performed on the British Aerospace EAP aircraft showed the practicality of perform pressure survey airloads testing on a large scale (References 13 and 14). The EAP experience demonstrated a 16 Hz response time for the instrumentation which should be acceptable for most maneuvers and aircraft. Some test programs (including EAP) have used pressures exclusively for their airloads testing.

5.4.3 Inspections

All airload flights should be followed by a visual inspection of the airframe structure. This typically consists of a visual examination in and around the aircraft for any obvious abnormalities. The test team should ensure that the maintenance personnel have an approved checklist for this inspection and that everyone is familiar with its procedures (see the sample at the end of this chapter). When an overload or other unusual event occurs during a flight, the test engineers should direct that the inspection be concentrated on the affected area of the aircraft. The airloads analysts can evaluate the severity of any overload and recommend critically loaded areas of the airframe for particularly detailed examination, perhaps requiring partial disassembly. Some components may need to be removed for such nondestructive inspections (NDIs) as x-ray and dye penetration tests (see Section 3.5). Other nonvisual NDI techniques such as eddy current tests can be performed with the components in place.

The usual in-and-around inspection is naturally very limited and may not detect a failure which has occurred. For a complete airloads program it is simply impractical to perform a teardown inspection following every flight, or even every overload. Also, a detailed inspection of an area cannot examine every surface and component because much of the structure is simply inaccessible for visual inspection. The areas subjected to close examination may not have received any close inspection since manufacture. It is therefore possible that any failures found may not be attributable to an overload or test incident. The failure may have occurred many flights previously, or even during manufacture. It is simply impossible to know the state of every element of the airframe prior to an airloads test sortie so that this uncertainty can be eliminated.

5.4.4 Avoiding Overloads

5.4.4.1 Flight to 80-Percent Airloads

As discussed previously, flight to 80 percent DLL may be performed by any of the test aircraft without airloads instrumentation and before the static loads testing. One of the first discoveries during the actual 80 percent and survey airloads testing may be that the flight limitations intended to keep the loads under 80 percent DLL has failed to do so, and the load restriction has been repeatedly exceeded on previous flights. Remember that the flight limitations at that time are based on a mathematical model that has not been correlated with actual flight data. Also, airloads need not be monitored real time for the 80-percent airloads flight tests, nor necessarily examined between flights. This creates the possibility of an exceedence during one of these airloads missions which may not be identified until later. A test team may wish to reduce these risks by performing airloads testing early in the program and conduct the 80-percent portion using the more cautious procedures of the 100-percent portion. This is generally the best practice whenever possible.

5.4.4.2 Flight to 100-Percent Airloads

Some of the 100-percent test points may be beyond the normal operating limits of the aircraft and are unlikely to occur except for a few emergency situations in the life of the fleet. Some test points may involve more risk than seems justified for the value of the data. When military specifications or any other standards are used, a blind adherence to their test requirements is unwise. Each mandated test should be examined for its applicability to the aircraft and its mission. Unusual test requirements involving exceptional risk should be reviewed for their value. Some tests may be simply unwise to attempt. However, the implications of deleting a test must be clearly understood.

Flight tests which have the objective of achieving 100 percent DLL on some portion of the airframe for the first time have the potential for exceeding that limit. For a comprehensive 100 percent loads program, an

overload may be inevitable. While every effort must be taken to prevent an overload, no guarantees that an overload will not occur can be reasonably given. Before the testing begins the test engineers must ensure that everyone involved in test conduct and decision-making understand the risk and accept that an overload during testing should not necessarily precipitate a crisis. A carefully structured flight test program with an instrumented airframe, real-time monitoring of airloads, specially trained aircrew and control room personnel, and a safety chase airplane, are the best circumstances if an overload is to occur. Besides the 50-percent factor of safety on any structural failure, most aircraft structures have an actual load-bearing capability that exceeds the design ultimate load limit (illustrated in Figure 64) and material yielding just beyond 100 percent DLL is rare. If the program cannot tolerate an overload, for whatever reason, then flight to 100 percent DLL should not be attempted.

A basic limitation of 100-percent testing is that usually not all of the loads parameters can be monitored real time. Instead, monitoring is limited to those stations and parameters most likely to experience a high load, as indicated by the analysis. This means that an overload may go unnoticed during the flight and not be seen until data is analyzed postflight. All data should be reviewed between flights. An alternative is to have a computer calculate the airloads which are not monitored and to compare those with the limitations automatically during the test. The computer can then be programmed to alert the test personnel of an overload or a potential for an overload.

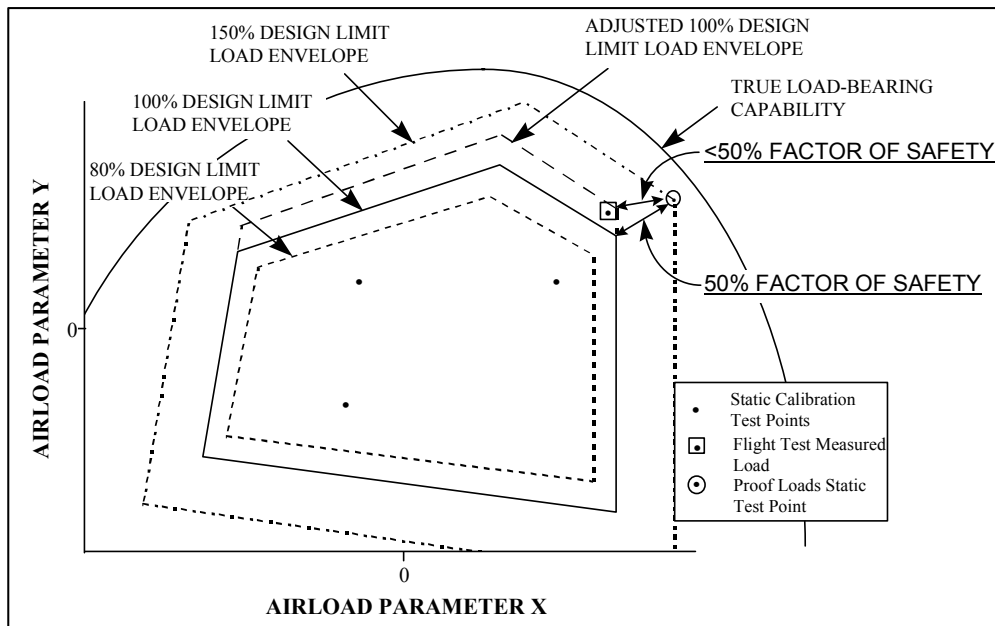


Figure 64 Illustration of Airloads Envelope Safety Margins

While every precaution can be taken to avoid an overload, the factors which can contribute to such an occurrence cannot be controlled absolutely. The test team can gain insight into these factors to help plan tests with the least likelihood of inadvertently exceeding 100 percent DLL. These factors include buildup tolerance, pilot input tolerance, flight characteristics, and airloads resolution. Each of these will be addressed.

5.4.4.3 Testing Tolerances

5.4.4.3.1 Airload Resolution Tolerance

Many airload tests are performed without real-time comparison with the individual load predictions. As long as the airloads are within an allowable limit (80 or 100 percent) envelope, they are considered acceptable for tests conducted in this manner. However, the hazards associated with prototype testing to 100 percent DLL,

and the tighter load tolerances to which aircraft are being designed today, make this approach generally unacceptable for initial expansion to these conditions. Also, 100-percent airload tests probably have the greatest prediction and measurement uncertainty of any hazardous aircraft trials.

The test team should ensure that the airloads analyst identifies the airload measurement stations most likely to experience a load in excess of 80 percent DLL, and particularly those expected to see 100 percent during individual endpoint maneuvers. Estimates of the highest predicted loads must be provided along with the analysis uncertainty. Any engineering prediction should be accompanied by an error analysis on which to base this uncertainty. This can be very difficult to derive for airloads predictions because they can include data from wind tunnel testing, aerodynamic coefficients provided by other elements of the design team, empirical factors with no clear history, and many other unclear elements. However, the test engineers must insist on some supportable determination of analytical uncertainty. This must then be compared with the airloads measurement uncertainty which should have been supplied with the airloads equations. An additional testing uncertainty may be added to these errors to account for failure to produce in flight the exact conditions called for by the analyst. The analyst can conduct a simple parametric study - varying airspeed, altitude, gross weight, primary maneuver parameter, etc. - that can provide data on which to base this number, or it can be based on experience. The greater of the analysis or calibration errors (not being dependent), with the addition of the flight test error, provides the basic airload resolution tolerance for each parameter. The test team may decide to add another increment of allowable deviation from predictions as determined from experience or other considerations.

For airloads being displayed on an interaction plot like Figure 65, the errors described above for each parameter are considered simultaneously. This can be depicted as an ellipse around the predicted load (a circle if the two errors are identical), as shown in the figure. The full y-axis or x-axis error determines the maximum vertical or horizontal dimension of the ellipse, respectively. A higher load produces a larger ellipse in at least one axis (on a linear plot) because, for example, 5 percent of a large load is greater than 5 percent of a small load. This can result in a larger error ellipse at the edge of the load envelope, as shown in the figure. Any measured airload, which falls outside this ellipse, would indicate that the analysis failed to predict the loads with sufficient accuracy to support hazardous flight testing. Testing should cease until the analyst can correct the math model and match measured loads within the acceptable tolerance. For this consideration, an over-predicted load would carry as much weight as an underprediction, unless the analyst can demonstrate that the deficiency in the airloads model will consistently overpredict the loads.

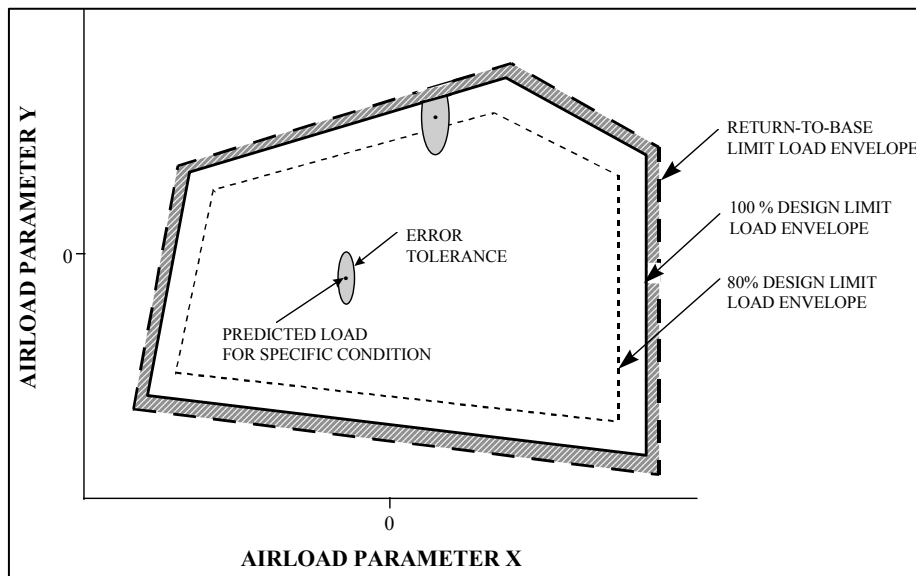


Figure 65 Definitions of Airloads Flight Test Measurement Limits

5.4.4.3.2 Data Resolution

Because real-time data for airloads tests greater than 80 percent DLL must be compared with the limit load interaction envelopes, the data is typically displayed on cross-plotting machines or television screens. It then becomes critical that the airloads data be sampled and displayed at rates adequate to reveal the highest load experienced within an acceptable resolution. (This discussion assumes that the displayed data is digitized, not analog.) If the test aircraft is capable of very rapid maneuvers, airload onset rates will be high and the display update rate will need to be greater than for a less maneuverable aircraft. While the airloads analysis can provide some insight in this regard, data collected during the 80 percent DLL portion of the testing will help to demonstrate the potential load onset rates anticipated during 100-percent maneuvers. Such consideration becomes especially critical when structural dynamic modes generate oscillatory load responses. Control room personnel must be alert for ‘choppy’ or discontinuous data traces which indicate too low an update rate. Section 12.2 provides insight into the selection of a suitable sample or display rate, but a good rule of thumb is that it be at least twice the highest frequency likely to contribute to an oscillatory load.

Possible unsteady loads must also be factored into the selection of data update rate. The unsteady loads most likely to be encountered result from buffeting induced by flow separation or wake from one part of the airframe impinging on another part. These are unlikely to exceed a few cycles per second, but have the potential for exciting a fundamental elastic mode of response of the structure which allows an amplified response and greater induced loads. The data display rate should be no less than five times the highest fundamental modal frequency likely to be excited (for example, horizontal antisymmetrical first torsion) to provide sufficient amplitude resolution to determine whether an overload has occurred. It may still be necessary to use interpolation to determine the peak load. Many unusual circumstances - such as aeroelastic or aeroservoelastic instabilities - can produce much higher frequency responses of the structure, but it will generally be impractical to account for these rare incidences. In these cases, the loads analyst may be able to provide insight into the loads to which the structure was subjected by examining the lower frequency data which were collected and the raw stresses that were measured.

5.4.4.3.3 Buildup Tolerance

Airload buildup maneuvers are normally designed with reasonable steps of increasing amplitude in the primary maneuver parameter for the test point (g, bank angle, rudder deflection, etc.). These are usually tailored to allow a few buildups to the endpoint condition. For example, a buildup to 3 g by abrupt symmetrical *pullup* may involve three steps: 2.4 g (repeat of the 80-percent test point); 2.7 g; and 3.0 g. If the 0.3-g cuts are considered too aggressive, it may be reduced to 0.2-g increments. A 0.1-g increment may be considered too tight a tolerance for the pilots to achieve in an abrupt maneuver and unnecessarily lengthening the testing. This typical approach to test point planning may not be sufficient to avoid an overload.

There is a possibility that the airloads may not increase proportionally with the buildup parameter, but may have a steeper gradient. This implies that the loads measured during the buildup points may give a false impression of how near to the limit load was the load measured on the previous test point, and how great a load will result during the next maneuver. In such circumstances, the seemingly over-conservative 0.1-g tolerance of the example may be itself inadequate to provide necessary warning of an overload. Using another maneuver which allows a more controllable and continuous increase in airloads can provide adequate overload warning (e.g., substituting a WUT for a steady *pullup*) may be wise in such cases. However, there may be no suitable substitute maneuvers which can provide any additional warning while also meeting the requirements of the test. The 80-percent data and the loads analyst may be able to provide some indication of load onset gradient, or it may be implied by the maneuver rates revealed during simulator practice sessions, but the problem remains a basic limitation of airloads flight testing. Only careful pre-test planning, and sound testing discipline in flight can help to reduce the risk of an overload in these circumstances.

5.4.4.3.4 Pilot Input Tolerance

As suggested in the previous paragraph, test planning must take into consideration the limit of pilot input tolerance. Beyond a certain point it is simply unreasonable to ask a pilot to make a finer input consistently. These inputs may be such things as stick or yoke displacement, pedal force, attitude capture, g capture, etc. The inputs usually must be made smoothly but rapidly and with no adjustment to the input after it is initially made. They are frequently atypical of most other test maneuvers and the pilot may have little or no experience with them. For airloads testing, it is unwise to simply accept a pilot's word that he or she can perform the input without difficulty. The best way to identify the limits on pilot tolerance is to practice the maneuvers in flight or in a pilot-in-the-loop simulator with provisions for monitoring the response. The minimum pilot input tolerance is by definition the minimum buildup tolerance. Should this minimum not provide a airload buildup with adequate warning of an overload then an alternative maneuver may be necessary, the test point should be limited, or the point dropped altogether as too hazardous.

The use of simulators to judge pilot input tolerance also provides the opportunity for pilots to practice difficult or hazardous maneuvers and to refine their control inputs. Serious consideration should be given to making this a mandatory pre-flight requirement. It is also wise to restrict the airload pilots to a small, select cadre who fly the maneuvers frequently enough to gain experience and progress along a learning curve. Certainly, it is unwise to resume a buildup interrupted on a previous flight using a different pilot. The buildup should be repeated to provide the current pilot the opportunity to adjust control inputs using the results of these maneuvers before attempting the 100-percent endpoint condition. Pilot confidence and assertions alone should not dominate considerations, only demonstrated abilities.

Recent test programs have had the flight control computer modified to fly stability and control test maneuvers which required close tolerances beyond the capability of most pilots. This same sort of approach can allow airloads maneuvers to be flown by the computer where the pilot tolerance is inadequate to prevent an overload.

5.4.4.3.5 Flight Characteristics

The airloads expansion will likely be performed in concert with the flight dynamics (flying qualities and flight controls) envelope expansion. This means that the airloads testing may be conducted at flight and maneuvers conditions not previously experienced. The possibility exists that previously unsuspected flight characteristics will be revealed which can effect the airloads. These characteristics may include such things as control authority limitations, unexpected EFCS actions, unexpected dynamic stability characteristics, buffet, etc. While all possible characteristics cannot be predicted or anticipated, simulations can provide insight into what can be expected during the airloads maneuvers.

The 100-percent endpoint maneuvers may be the most aggressive maneuvers attempted during a flight test program, and there is no excuse not to 'fly' these in a simulator before attempting them in flight. The resulting aircraft attitudes, rates, control surface responses, and flight control system actions should be monitored and the implications of these data considered. For example, tracking such relationships as stick displacement per g during a simulated normal load factor buildup may provide warning that the buildup gradient is too steep to prevent an overload. There are many other possible adverse influences. Will control system gains make precise control in some axes difficult at certain flight conditions? Will the EFCS or other limiter systems make an uncommanded input to recover the aircraft or coordinate the maneuver which can input additional or unsymmetrical airloads? Will various EFCS modes produce different responses during the airload maneuvers? Can the endpoint even be achieved given these responses and the limitations of control inputs and aircraft performance or rates? Limiter systems may be bypassed for the purpose of flight testing, but only after careful review of possible consequences. This same sort of awareness of flight dynamic influences should be carried to the control room. This means monitoring and considering flight dynamics data as well as the airloads data.

5.4.4.3.6 Overload Limits

Because an overload cannot be entirely prevented, the test team may wish to identify an overload limit beyond which the mission must be terminated and the aircraft returned for immediate inspection and detailed data review. The identification of the overload limit should be based on such factors as the overall error in the test, predicted margins of safety for the highly-loaded structure, experience, or other considerations. This 'return-to-base' (RTB) load limit is depicted in Figure 64. The test team may also decide to identify a marginally higher 'stop everything' or 'no confidence' overload limit beyond which the entire airloads analysis and testing approach should be reviewed thoroughly and necessary corrections made before resuming the test. An even higher overload limit can be chosen as the point at which the affected structure is no longer considered airworthy, regardless of inspections, and must be replaced.

5.4.4.4 Concurrent Testing

As already mentioned, the airloads expansion is frequently performed in concert with the flight dynamics envelope expansion. It is entirely likely that at some point the flight dynamics expansion cannot continue without airloads clearance beyond 80 percent DLL. Likewise, the airloads expansion may need to wait for the flight dynamics team to clear the aircraft for flight into an unexplored region of the flight envelope or control authority. Every effort should be made to identify these areas of mutual dependency to avoid 'busted' limits. A detailed plan for concurrent expansion must be prepared. Even with such a plan, it is wise to have members of each team attend the pre-flight briefing for nonconcurrent missions to ensure that test points have not crept into the flight cards which will bust a limit. Likewise, having members of each discipline in the control room will help avoid or identify busted limits by monitoring test maneuvers.

5.4.4.4.1 Following Overloads

There are four actions which can be taken following a 100 percent DLL overload.

- a. *The overload is considered 'minor' and unlikely to occur in fleet operations. No action is taken.*

This decision must be made only after detailed discussions between the designers, the eventual operators of the aircraft, and the test team. Test maneuvers are generally very artificial and the high loads may be isolated to a very narrow portion of the flight envelope. However, it is difficult to conclude that the load will never be experienced in service. Tactical aircraft can be subjected to many circumstances the designers never dreamed were possible, particularly in combat. Another line of reasoning is that if an overload is possible, it *will* happen at some point in the life of the design. Today, as carefree flight controls are sought, any instance where a pilot can overload the structure through inattention must be carefully reviewed before it is accepted. A decision to take no action may be considered reasonable, but it is prudent to instruct depot engineers to track airframe usage (perhaps by examining collected flight data recorder information) and to re-examine the decision after some period of fleet operation. Repeated occurrences of the overload means a reduction in the factor of safety for the affected structure (which may or may not have been demonstrated during ultimate loads static testing) and possible reduction in the fatigue life of the airframe. If the aircraft has limiter features which can preclude the overload, they may need to be revised to reduce their threshold levels.

- b. *The maneuver limits of the aircraft are revised to preclude the occurrence of the overload in fleet operations.*

A decision to restrict the aircraft must be made only with the concurrence of the eventual operator of the aircraft, particularly if the limitation will impact operations. Unless mechanical or electronic limiter systems are installed or adjusted, the decision will still leave the potential for a pilot to overload the aircraft through inattention, and the testers should document this fact.

- c. *The affected load envelopes may be expanded to encompass the measured airloads after examining the loads relative to the actual load-bearing capability of the structure.*

This measure should be of particular concern to the test engineers. Unless further ultimate loads testing is performed, the expanded envelopes are likely to cut into the demonstrated 50-percent FOS. The expansion of a portion of an envelope and the reduction in demonstrated FOS is illustrated in Figure 64. Even should the resources still be in place to repeat a portion of the ultimate loads testing, this will almost certainly be found programmatically unacceptable (cost, schedule, appearance of deficiency, etc.). The analysts and designers may present many arguments for why the expansion does not push the new, undemonstrated, design ultimate load beyond the actual load-bearing capability of the structure (Figure 64). Although the loads model has been shown to be deficient, they may explain that the data which have been collected, particularly any raw stresses which can be compared with finite element models and stresses measured on the static loads article during ultimate loads static testing, are sufficient for their extrapolation. However, this process of cutting into the demonstrated FOS runs counter to the fundamental intent of the airloads testing philosophy and should be done only rarely. As pointed out earlier, and shown in Figure 64, there are only a few design ultimate loads conditions actually tested. These few points are supposed to demonstrate in as nearly an indisputable manner as possible that the structure is capable of bearing the design limit loads while providing a basic factor of safety.

These envelope expansion measures should be performed only rarely. If the need for this sort of adjustment arises several times during the test program, the basic validity of the airloads analysis should be questioned and a halt to testing considered. The test team may wish to establish a limit on such envelope expansion before testing begins.

- d. *The structure is revised to accommodate the higher load and reestablish the necessary factor of safety.*

This action can seldom be accommodated today. The cost of redesign, generating new drawings, and revising the production line and assembly procedures are usually prohibitive. However, when it is done, it has the implications discussed next.

5.4.5 Regression Testing

5.4.5.1 Following Structural Changes

The ability to alter the performance and flying qualities of aircraft through flight control system software changes has greatly reduced the prevalence of aircraft structural redesign during prototype flight testing - at least for the primary load-bearing structure. However, this may still occur, and even changes in secondary structure can produce significant changes in airloads if they affect the flow field. As with any complex system, it is difficult for any one individual or analysis to predict all possible interactions of system components or influences. Thus, in holding to the principle that the test aircraft should be production representative, any change should prompt a repeat of all or a portion of the airloads testing. Since it is seldom practical to repeat all of the airloads tests, only a portion or none may be deemed necessary after considering the nature of the modification.

Any structural change should prompt several considerations by the airloads test engineers. First, the addition of material to a portion of an instrumented structure will change its elastic response. Since the strain gage method of measuring airloads assumes that the structure will deform the same under airloads as it did during the static calibration, this change may invalidate some of the calibration equations. While the designers and analysts may give assurances that the change in elasticity coefficients are immeasurably small, the best action is to recalibrate the affected instrumentation. Repeating all or a portion of the static calibration will probably be impractical. The next best check is to re-fly airloads tests which have already been conducted and to compare measured loads. If the two measurements differ by more than the prediction or measurement tolerances then the affected measurements should be considered invalid. It may be possible to adjust the loads equations for the effect, but this would require considerably more repeated test points to validate. A less desirable alternative is to derive a calibration using the new gage responses and the data from the test points performed prior to the modification. This method will result in equations with indeterminate error, and should be considered a last resort. The invalidated measurements may simply have to be abandoned.

A second consideration after a structural change is that the revised structure is unlikely to have been subjected to the ultimate loads static test. While assurances will probably be given that the revised structure has not suffered any degradation in load-bearing capacity, changes in load paths may load other portions of the structure beyond expected levels. Each change must be evaluated for possible regression testing - both ground and flight.

5.4.5.2 Following Software Changes

There appears to be a general lack of appreciation of how much the flight controls impact aircraft airloads. Changes in pilot input gains, stability axes gains (particularly for coupled axes), and control surface deflection scheduling/deflection rates can alter the external loads. Electronic flight controls may also have selectable modes (power approach, air-to-ground tracking, etc.) which will generally require consideration of repeating all or portions of the airloads flight testing in a number of these modes. While analysis alone can provide insight into how great the effect of flight control software changes may be, the same basic concerns described for structural changes apply.

Current aircraft designs are highly integrated and software-intensive. Software can easily exceed a million lines of code with so many functional elements that no one individual can envision all the implications of any one change. The controls engineers may provide assurance that a change will not affect the airloads, but the most seemingly innocuous software changes can have profound and unforeseen influences. Incidences in flight testing have usually been those which the test team was told “simply can’t happen.” Flight control changes should be subjected to the full regimen of software checks, hardware-in-the-loop and pilot-in-the-loop simulations, and ground resonance testing (see Section 8.4). The loads analyst must reflect the changes in the airloads model and confirm the influences. Prototype flight testing usually involves several changes to the flight control software, and it is admittedly impractical to repeat this full regimen each time. However, each change should prompt a review of the potential impact and an assessment made about which portion of these tests should be repeated. Some regression flight loads testing may be necessary. Flight testing is the best way to determine whether there is an impact to the airloads, and may be the least costly and time-consuming method of doing so. The need for this regression testing must be accepted by the test team and program managers before any airloads testing is undertaken, and perhaps a subset of airloads test points identified for this purpose. Certainly, any change that has the potential for affecting an airloads alleviation system should prompt serious consideration of regression testing.

5.4.6 Gust Loads

Clear air turbulence, thermals, and wake turbulence impose both vertical and horizontal airflow velocity vectors to the existing vectors (changing effective AOA), adding incremental air loads to those already acting on the vehicle. These incremental loads are typically brief, and possibly periodic in nature, and are referred to as gusts. Vertical loads from gusts are the most common and produce the largest increase in loads on a structure in flight. They do this by increasing the effective AOA of the wing, thus increasing the lift on the wing and the overall wing load. Aircraft frequently have an associated **thunderstorm** or **turbulence penetration speed** to protect against overloads due to gusts.

The increase in load factor from the gust (using nomenclature from Section 2.0) is:

$$\Delta n = 0.115m\sqrt{\sigma}V_e(KU)/(W/S) \quad (81)$$

where:

- Δn = increase in load factor due to vertical gust,
- m = slope of C_L vs AOA curve,
- σ = density ratio at flight altitude,
- V_e = equivalent airspeed (knots),
- KU = effective gust velocity (fps), and
- W/S = wing loading (psf).

The gust velocity can be visualized as a sine wave of velocity vectors, oriented both axially and transverse to the flight path of the aircraft. Gusts can also be characterized by a wave length, with the maximum amplitude of the wave being the maximum velocity of the gust. An aircraft traversing the wave very quickly will feel a sharper gust than an aircraft of the same weight which traverses the same gust at a slower velocity. The aircraft is never subjected to the entire maximum gust velocity (U) instantaneously. The actual gust velocity is multiplied by a gust alleviation factor (K). A typical value of K is 0.6 except for very sharp gusts (see MIL-A-8861A [Reference 6] for other values of K). The maximum value of U that is likely to be experienced at sea level in a storm-free weather system is 30 fps. A gust velocity of 50 fps may be expected in a thunderstorm penetration scenario.

A heavy aircraft will experience a relatively small increase in load factor and the pilot will not feel the turbulence as well as the pilot of a lighter aircraft. However, recall that the limit load factor is reduced as weight is increased. In fact, the limit load factor goes down faster than the gust imposed load factor (Figure 66). Therefore, heavily loaded aircraft can be more easily damaged by gust loads because of the limit load factor being exceeded, all without high g loadings being experienced by the pilot. Hence, transports and heavy bombers are the most common subjects for gust loads testing. MIL-A-8861A (Reference 6) provides detailed design criteria for gusts.

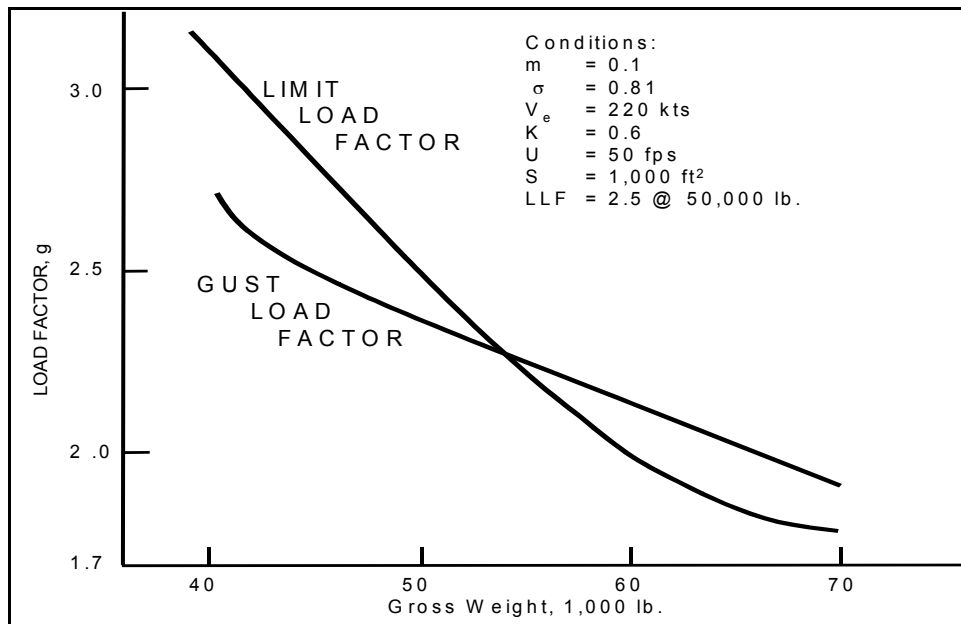


Figure 66 Comparison of Design Limit Load and Gust Load Factor with Weight

Each aircraft may have unique critical load conditions or areas susceptible to gust loading. Examples are engine pylons in lateral shear, vertical stabilizers and fuselages in lateral shear, bending, torsion, and wings in vertical bending and vertical shear. These structures would be instrumented in the same manner as that for other loads tests.

5.4.6.1 Gust Loads Flight Tests

There are two basic approaches to the flight testing of aircraft for gust loads. The first is to fly the aircraft at as low a gross weight as possible so that the structural inertia is very small. The gusts will produce the greatest possible structural deformation and facilitate measurement while the risk of an overload is reduced. The loads measured are then added to those expected or measured for the greatest loading conditions to ensure that the limit loads will not be exceeded. The second method is to fly the aircraft at incrementally heavier gross weight conditions, perhaps close to those predicted as the worst-case loadings, and actually demonstrate that the loads with gusts will not exceed limits. A combination of the two approaches is probably best. Real gusts of significant velocity may be difficult to find at high altitudes and are most likely to occur at low altitudes above

ridges or mountains, particularly in strong surface winds. Horizontal gusts are difficult to find except with this latter method. However, safety of flight considerations may effect how low an aircraft can be flown over turbulence-producing terrain. Gusts may be difficult to locate, requiring several flights in search of rough air.

The velocity of the gust in its various components can be measured with static ports on the aircraft or on a static pressure '**gust probe**' ahead of the nose. More than one probe may be needed on the very large aircraft because, for example, the gust at one wingtip may be different from that at the other wingtip, or the nose versus the tail. Using the RMS (root mean squared) value of the accelerations at the cg of the aircraft, integrated for velocities, can also be used as a measure of the gust velocity. MIL SPECS require that the frequency content of the gust be measured. This generally means that the bending of a gust probe and the elastic behavior of the airframe must be subtracted out of gust measurements by analytical means. The velocity of a gust is normally determined as a RMS value of a series of gusts encountered in a region of turbulent air.

A true gust velocity of 2 fps is generally considered to be the minimum necessary to produce measurable loads on transport aircraft with 1 to 3 minutes of data required to be averaged for power spectral density ([PSD], Section 11.3.3) analysis. However, any gust level that produces sufficient measurable response is acceptable. The structural response and gust input can be examined in a coherence plot (Section 11.3.7) to determine whether there is sufficient resolution of the loads resulting from the gust for evaluation. Good coherence would demonstrate that the data is suitable for comparison with analytical predictions. Historically, the coherence has been poor and gust load testing has been a problematical undertaking at best.

A third gust loads test method is to simulate gust loads by inducing abrupt loads into the airframe. The inputs can be made manually or electronically via the flight control surfaces or via some modal excitation device (Section 6.6.1). These data can then be correlated with analytical predictions to validate the gust loads model used to certify gust loads design adequacy. The assumption is that if the analyst is able to match the test loads with predictive models then the gust loads analysis is likely correct. This method offers the benefit of knowing precisely what the forcing function is (assuming an instrumented airframe) in addition to the structural response.

5.4.7 Load Alleviation Systems

The advent of fast, inexpensive, and reliable electrical flight control systems has permitted the introduction of **active control systems (ACS)** into flight vehicles (Section 8.0). This has in turn, allowed the incorporation of overload warning or prevention systems and automatic load alleviation systems into aircraft, particularly large transport and bomber types. The payoffs in such systems are protection against pilot inattention, weight savings and an increase in the fatigue life of the structure, increased aerodynamic efficiency, and improved ride quality. The result may be a structure that can withstand loads that it would otherwise not be able to sustain without an expensive and heavy 'beef-up.' These systems require testing to optimize their functions.

The purpose of load alleviation systems are to change the aerodynamic load distribution on the structure by use of the available control surfaces to create more favorable airloads. This can be done to reduce maneuver loads (**maneuver load control [MLC]**) or to reduce gust loads. The L-1011 airliner incorporates the latter system. Gusts loads are sensed by instrumentation and the MLC is triggered when the loads exceed a preset level. The ailerons are then automatically biased to move the center of lift on the wing inboard, thus lessening the wing bending loads (Figure 67). The B-1 bomber uses small, movable nose vanes to automatically suppress a 3 Hz forward fuselage oscillation that is distracting to the aircrew and would otherwise increase crew fatigue in low-altitude operations.

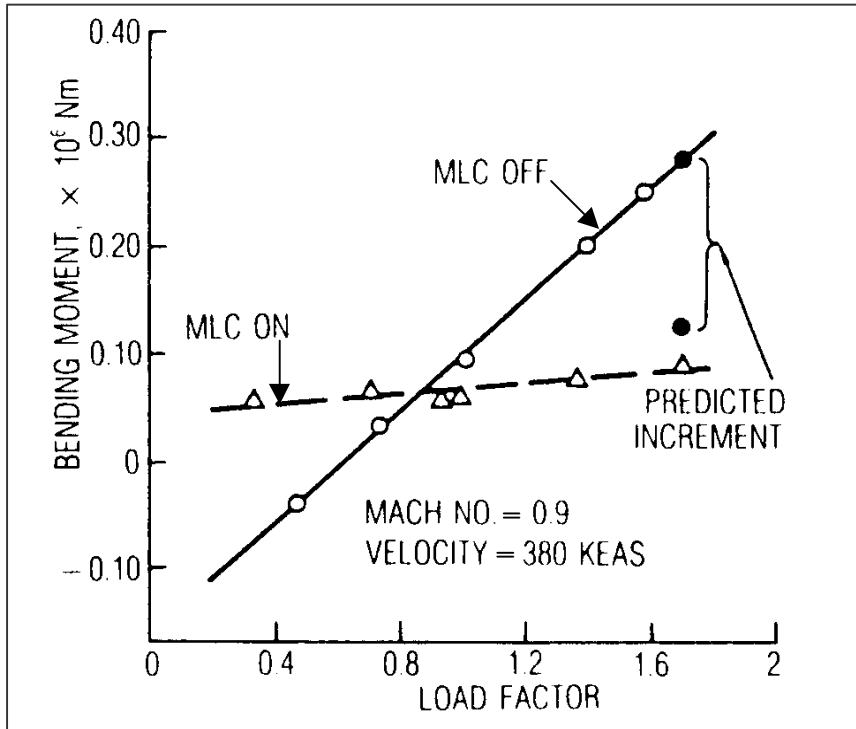


Figure 67 Maneuver Load Control Results for L-1011 (71 Percent of Semispan)

5.5 Landing Gear

5.5.1 Landing Gear Loads

Examples of gear loads of interest are vertical load, axial load, side load, drag load, drag moment, drag brace load, wheel spin-up and spring-back loads. The latter two develop during the landing impact itself. The landing gear landing vertical load factor is

$$N_{LG} = N_S X_S [V_S^2 / (2g) - N_T K_T X_T^2 / (2W) + (1 - L/W)(X_T + X_S)] \quad (82)$$

where:

- N_S = strut efficiency,
- X_S = strut stroke (ft),
- V_S = sink rate (ft/sec),
- N_T = nonlinear tire deflection factor,
- K_T = tire spring constant (lbs/ft),
- X_T = tire deflection under load (ft),
- W = gross weight,
- L = wing lift (lbs), and
- g = acceleration due to gravity (ft/sec²).

The last two terms in the equation and the strut efficiency can be neglected for quick formulations.

5.5.1.1 Landing Gear Loads Testing

During the aircraft development phase the gear will be tested to the design maximum sink rate impact either separately or mounted on the aircraft. This can be done by dropping the entire aircraft from an appropriate height (required for carrier-based naval aircraft), or the gear alone may be mounted in a rig and subjected to different loads varying in frequency, force level, and waveform. These data are then used along with an analytical model to develop load envelopes for each component of the gear.

Landing and taxi tests are necessary to produce and measure gear loads, providing data to verify that the gear has been adequately designed to meet service requirements without exceeding design limit loads. This testing takes the form of landings at different sink rates and attitudes, and taxi tests under various conditions. Experience has shown that most pilots have difficulty landing at specific sink rates (usually because of ground effect influence as the aircraft approaches the surface) within the tolerance required to avoid gear overloads. Thus, it may be unwise to attempt a landing at the 100-percent vertical load sink rate. Two- and three-point attitude braking rolls, unsymmetrical braking, reverse braking (backing condition with reverse thrust), turns, and towing are specifically required to be demonstrated. As with any loads test, an appropriate buildup is mandatory. Aircraft gross weight is a significant factor in gear loads and a weight build-up is reasonable. The taxi tests can become quite complex and will be covered in greater detail.

Strain gages are the preferred form of instrumentation for gear loads. MIL-A-8871A (Reference 10) states that:

“... the landing gear and backup structure shall be sufficiently instrumented with strain gages to measure vertical, drag, side, and torsion loads. Gear structure can vary greatly between aircraft types, but the resolution of vertical, side, and drag (longitudinal) loads are still the common results sought regardless of the design.”

For the taxi tests, the aircraft may be taxied over surfaces of varying roughness. This roughness can be simulated on a runway by securing elevated articles (e.g., 2 by 4 wood) or by creating uniform ‘ruts’ or **spalls** in the surface. Tests over various configurations of 1-cosine function bumps and dips (Figure 68) as well as 1- or 2-inch steps are also mandated. In the past these functions have been simulated by AM-2 runway repair mats or stacked plywood. A specific series of these concrete 1-cosine and step functions are in place in the Edwards AFB lakebed for such tests. The results of such tests are compared with the analytical model as well as ensuring that measured loads are within the design limits. The height and wavelength of the 1-cosine function may be selected to create the worst-case excitation of rigid and flexible modes at selected taxi velocities, or a number of more benign configurations tested to verify the analysis. If the match is adequate then the model will be accepted to clear the worst-case condition if it predicts loads within limits.

Miscellaneous loading conditions produced during towing, turning, and pivoting may also need to be tested. In addition, loads produced by hard landings (high rate of descent), high touchdown ground speed, gear side loads (landing in a crab), gear spring back, wheel spin up, and rough fields may also require testing to verify analyses.

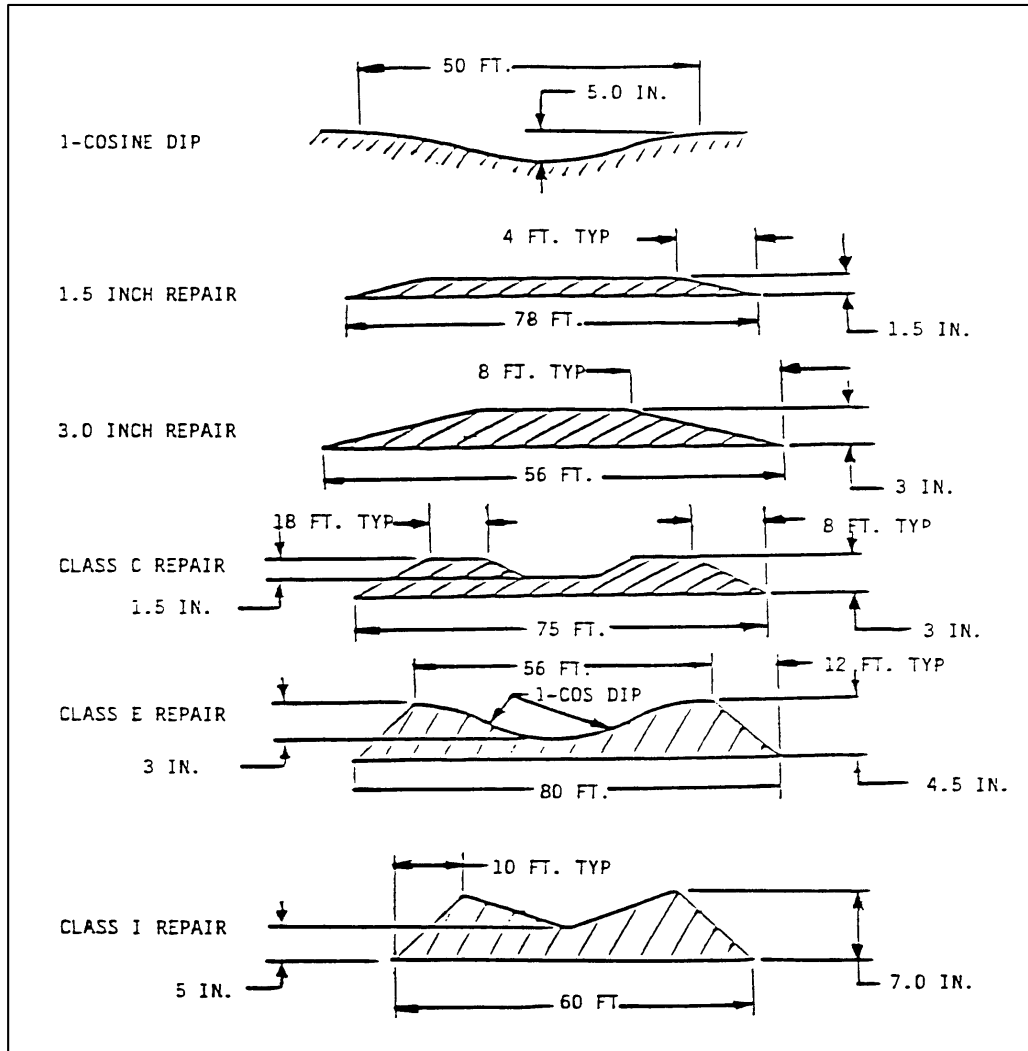


Figure 68 Typical Runway Repair Landing Gear Testing Profiles

Soft surfaces will create higher gear drag loads than a hard, concrete or asphalt surface. For aircraft intended to be operated on soft fields, gear testing at various surface densities is necessary. **California Bearing Ratio (CBR)** is the accepted measure of surface density. A CBR of about 32 is equivalent to concrete, with softer surfaces having progressively lower values.

Landing gear tests may be done at gross weights, taxi speeds and braking forces up to the maximum. Various center of gravity positions may be run to place the aircraft at different ground attitudes and static gear load states. Tire heating generated by brake rotor radiant heat and simple friction with the ground surface can create the hazard of tire bursting. A hydraulic leak can result in this inflammable fluid contacting the hot surfaces and igniting. These dangers require that brake and tire temperatures be monitored during these tests as well as taxi distance. These measurements are cross-referenced against flight manual brake energy and taxi distance charts. Most wheels incorporate 'fuse plugs.' These are soft metal plugs that melt down to relieve tire pressure when they reach a specified temperature. A flat tire is much easier and safer to deal with than a burst tire. Most modern aircraft brakes also incorporate an antiskid system which automatically relieves brake pressure if a sudden drop in wheel speed, indicative of a potential skid, is sensed. A skidding tire abrades rapidly and a rupture is likely.

The antiskid also creates the potential for an instability known as **gear walk**. This is created by an elastic fore-aft deformation of the gear structure creating a false wheel speed change indication. In applying or relieving brake pressure in response to the speed indication the antiskid may actually promote further elastic response and false indications. Thus, a sustained fore-aft gear oscillation can be created that can produce dangerously high bending loads in the strut. The A-10 aircraft suffered from gear walk during development testing. The solution is generally a change in brake hydraulic valve orifice or changes to the anti-skid digital control system. The normal brake testing should reveal the instability.

Arrestment tests are also routinely performed for those aircraft with tailhooks to ensure that it and associated structure has been adequately designed. Similarly, **barrier tests** that involve rolling the aircraft into a restraining net will also require contributions from the loads test engineer.

5.5.2 Landing Gear Shimmy

Shimmy is the undamped oscillation of landing gear during ground operations. Shimmy oscillations can produce severe vibration in the aircraft and result in overload failures in the gear assembly or other parts of the aircraft subjected to high inertia loads. The oscillations are typically dominated by torsional deformation, coupled with one or more other dynamic modes of the landing gear system or airframe structure backing-up the gear. Shimmy is normally experienced in an asymmetrical gear (such as a single-wheel fighter aircraft nose gear). It is excited by lateral force on the wheel such as induced by a sharp steering command, an abrupt brake input (main gear), or sudden unevenness (rut or obstruction) of the taxi surface. Factors which play into the problem are the tire and backup structure elastic characteristics, gear structural stiffness, the rotational inertia of the wheel, the distance of the wheel rotational center from the pivot point (the 'trail'), the steering angle (if relevant), lateral strut deflection, unfavorable gear system mass distribution, gear system freeplay, and the airframe motion. All these factors imply a complex system of springs, dampers and freeplay in multiple axes.

The initial taxi trials of prototype aircraft are carefully performed to ensure that no free-rolling landing gear dynamic instabilities occur which could cause a structural failure and hazard to the aircrew. The free-rolling (no external excitation or braking) structural damping of the landing gear was required by MIL SPECS to be greater or equal to 0.12-G total system damping. The shimmy testing summary for the C-17A detailed in Reference 1 is very instructive. Vibrations from tire imbalance (explained later), steering feedback and gear walk should not be confused with shimmy.

5.5.2.1 Landing Gear Shimmy Testing

Where possible, shimmy tests should proceed first flight of a prototype aircraft. For aircraft designed to operate on a variety of surfaces, the surface yielding the lowest additional torsional resistance should be used for the shimmy testing. The antiskid system should be active for the tests to evaluate any potential for the system to play in an instability, and because this is the normal operating state for the aircraft. Tires should be new and all servicing (tire pressure, shock strut pressure, lubrication servicing, bolt torques, etc.) should be nominal. Shimmy tests are performed by making abrupt brake and steering inputs while taxiing or by rolling the aircraft over discrete obstructions, such as a 2 by 4 piece of wood, typically oriented at 45 degrees to the path of the machine. The intention is to make a sharp torsional input to the gear. Tests are performed at ever increasing speeds. Testing on an unobstructed surface may be acceptable for aircraft with no off-field operation (landing on dirt). Rudder pedal and brake pulses should be used in this case. Data sample rates should be selected for the dynamics anticipated, as described in Section 5.4.4.3.2. If shimmy is excited, an immediate deceleration is necessary. Applying brakes may aggravate the shimmy, but is normally advisable in order to slow the aircraft rapidly. The shimmy may not cease immediately, even after decelerating slower than the shimmy onset speed. Shimmy testing and data analysis are much like that for flutter testing (Section 6.0).

Because of the many variables introduced by a landing impact - such as shock strut stroking, truck rotation, spring back, and tire deflection - landings are not a suitable excitation source. A true free decay of the gear dynamics can not be obtained from landings. However, landings may introduce more energy into torsional modes than taxi test methods. Gear dynamics should be monitored during landings until confident that these inputs will not excite shimmy.

The common solution to shimmy is the rebalancing of the gear to alter the modal frequencies. This is usually done by adding a ballast weight to the appropriate place on the gear. A redesign of the gear to redistribute mass and revise component stiffness' can also be done, but is seldom practical. An alternative method, used when redesign is impractical or a quick solution is required, involves the addition of a damper to the system which has been tailored to the shimmy frequency. Shimmy dampers are usually viscous oil dashpots, porting fluid between sides of a piston through a metered orifice (determining the damped frequency) as the piston strokes with the torsional displacement of the gear truck or wheel assembly.

Wheel oscillations may be observed during ground operations, especially during takeoff and landing roll, when the wheels are out of balance or the tires out-of-round (flat spots or other uneven wear). These dynamics may produce moderate airframe vibration when the wheel oscillations excite a natural mode of response in the gear of aircraft structure. The **wheel-driven dynamics** can be differentiated from shimmy by examining the frequencies associated with the oscillations. If the predominant mode is the same as the frequency of the tire rotation (a function of tire diameter) then wheel-driven dynamics should be suspected.

Inspector: _____ Date: _____ Time: _____

Structure: _____ Aircraft: _____ Flight: _____

IN-AND-AROUND STRUCTURAL INSPECTION

INSPECT OR PHOTOGRAPH THE SUBJECT AREA PRIOR TO FLIGHT
TO ALLOW IDENTIFICATION OF DIFFERENCES FOLLOWING LANDING

1. Perform the normal postflight securing of the aircraft without disturbing obviously-damaged structure. Follow special procedures requested by Structures Engineer(s) (such as leaving flaps down, etc.).
2. Visually check for abnormal misalignment of landing gear doors, access panels, lap and butt joints, antennas, pylons, engine nacelles, external stores, etc.
3. Check for missing parts (antennas, access covers, probes, etc.).
4. Look for paint abrasions that may have been caused by relative motion of parts (external stores, engine pylons, panels, etc.).
5. Check for bare metal or primer showing around rivets, lap or butt joints, screws, etc.
6. Check for popped rivets, missing screws, nonsecured fasteners, etc.
7. Check for elongated rivet, screw, and bolt holes.
8. Check for wrinkled skin, composite delaminations, and obviously bent parts.
9. Check for cracks in skin, primary and secondary structure, around fasteners, etc.
10. Check for proper fastener torque, where applicable, and note discrepancies.
11. Arrange for photography of any damage found. Store any damaged components which are found such that the fracture surface is protected.

* Open access panels and check inside structure if damage is suspected.
A flashlight and mirror may be necessary.

COMMENTS:

SECTION 5 REFERENCES

1. Norton, William J., Captain, USAF, *C-17A Landing Gear Dynamic Stability Testing*, AFFTC-TR-93-03, AFFTC, Edwards AFB, CA, May 1993 and Norton, William J., Captain, USAF, C-17A Landing Gear Shimmy Testing, Proceedings of the 24th Annual Symposium of the Society of Flight Test Engineers, July 1993, page 6-39 to 6-53.
2. Norton, William J., Major, USAF and John C. Wilson, *C-17A Airloads Flight Testing*, AFFTC-TR-94-18, AFFTC, Edwards AFB, CA, July 1995 and Norton, William J., Major, USAF and Melroy, Pamela C., Major, USAF, C-17A Airloads Flight Testing, Proceedings of the 38th Annual Society of Experimental Test Pilots Symposium, August 1994.
3. Dole, C.E., *Fundamentals of Aircraft Material Factors*, University of Southern California, Los Angeles, California, 1987.
4. Hurt, H.H., Jr., *Aerodynamics for Naval Aviators*, NAVWEPS 00-80T-80, U.S. Navy, January 1965.
5. Military Specification Airplane Strength and Rigidity - General Specification, MIL-A-8860.
6. Military Specification Airplane Strength and Rigidity - Flight Loads, MIL-A-8861A.
7. Military Specification Airplane Strength and Rigidity - Landplane Landing and Ground Handling Loads, MIL-A-8862.
8. Military Specification Airplane Strength and Rigidity - Miscellaneous Loads, MIL-A-8865.
9. Military Specification Airplane Strength and Rigidity Ground Tests, MIL-A-8867.
10. Military Specification Airplane Strength and Rigidity - Flight and Ground Operations Tests, MIL-A-8871A.
11. Aircraft Structures, General Specifications for, AFGS-87221A, United States Department of Defense, Washington D.C., 8 June 1990.
12. Moreland, William J., "The Story of Shimmy," in *Journal of the Aeronautical Sciences*, Vol 21, No. 21, December 1954.
13. Watson, A.J., "Development and Flight Testing of a Surface Pressure Measurement Installation on the EAP Demonstrator Aircraft," AGARD Conference Proceedings 519.
14. Smith, T.D., "A Pressure Plotting Technique for Flight Loads Measurement," British Aerospace Public Limited Company.

6.0 FLUTTER

6.1 Introduction

New engineers are encouraged to read some of the theoretical flutter material in References 1 through 16. A little theoretical knowledge will help in interfacing with flutter analysts, many of whom have a solid analytical background as well as practical experience in the subject.

It is important to understand that flutter prediction is far from an exact science. The mechanisms responsible for structural damping are still not entirely understood or fully predictable. There are many means of flight testing for flutter and interpretation of the results. Flutter is never entirely eliminated, simply delayed to airspeeds beyond the normal flight envelope of the aircraft. Flutter is little understood except by a relatively small number of analysts and flight test engineers. This tends to produce frustration and incaution in some test project participants. The pilot(s) and program management personnel must understand that flutter testing cannot be done by the ‘seat of the pants’ but requires careful buildup with concurrent analysis.

6.2 Description

Aeroelasticity is the complex interaction of unsteady aerodynamics, structural elasticity, and airframe inertia. Flutter is an aeroelastic instability usually producing a divergent oscillation of an aircraft structure or component. Therefore, it is a phenomenon seen only by those structures subjected to an unsteady fluid stream and treated as a nonrigid body, thus differing from the traditional treatment of aircraft dynamics. Flutter susceptibility generally increases with airspeed and is aggravated by thin, very flexible structures. With the ever lighter, complex, less stiff structures and higher speeds of modern aircraft, flutter continues to be a matter of great concern. Many problems would be nonexistent if aircraft were built to the highest rigidity that materials and construction techniques could allow, but the weight penalty would be prohibitive.

The effects of an unstable oscillation in an aircraft structure is seen as a **flutter mechanism**, a complex interaction of forces and moments, structural dampings, and structural stiffnesses. The change in the intensity and the distribution of airloads with associated structural deformation and restoring motion can result in a cyclic phenomena. Small perturbations about the steady-state flight attitude and small elastic structural deformations create the unsteady flow. Load factor, AOA, and the nonlinear lift curve slope (see Section 2.2.5) have also played in flutter mechanisms. As flutter begins, it is an oscillation of increasing amplitude with each successive cycle. If the oscillation is allowed to persist, the flutter will continue until some structural restraint is reached or until catastrophic structural failure occurs. Figure 69 shows how all the forces affecting a flight vehicle interact to form the aeroelastic and aeroservoelastic (Section 8.0) problem. Each effect will be dealt with to some degree in this handbook.

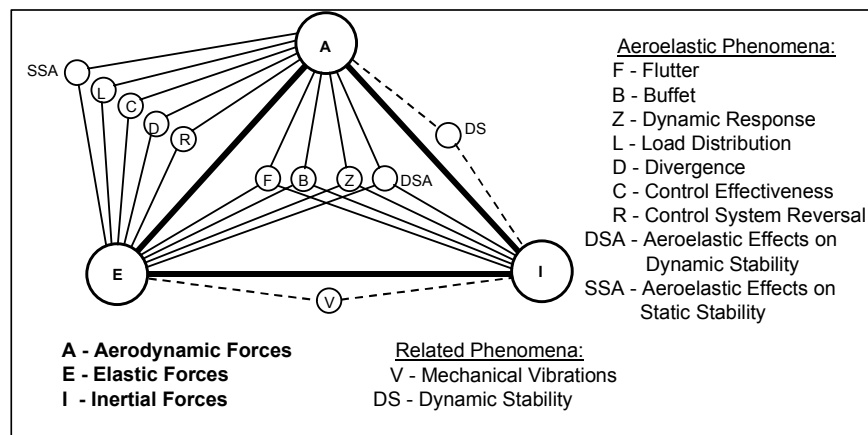


Figure 69 Collar's Aeroelastic Triangle of Forces

In the case of a multiple DOF system, the flutter mechanism is a **coalescence** of two or more natural vibration modes of the structure (see Section 4.0). The phase angles and frequencies of the individual modes shift in a manner that allows the coupling; a change from no net work of the system to positive net work. Even with coupled modes, the structural displacements reach their maxima or minima simultaneously. A coalescence of two modes is called **binary flutter**. If 3 degrees of freedom (DOFs) contribute to a flutter state, then it is termed **ternary flutter**. Four and five modes coupling is called **quaternary** and **quinary flutter**, respectively. However, flutter of more than 2 DOFs is rare. Flutter resulting from the coupling of a structural mode(s) and an aircraft rigid body mode (aircraft pitch, roll, yaw, and **plunge** or vertical translation) is termed **body freedom flutter**.

Assuming that the inertia and stiffness of the structure does not change in flight (neglecting heating effects and short term fuel burn), the overall system damping will change with a change in the magnitude and frequency of the aerodynamic forces. The natural frequency of all modes will change as the aerodynamic forces change (increased flow velocity, for example) with the frequencies contributing to the flutter mechanism approaching each other and the phase (see Section 4.3.2) shifting toward an unstable state. The damping of one of the modes moves towards zero. When the two modes finally coalesce to form the '**flutter mode**' the resulting mode shape will be a combination of both individual modes. The energy from each mode will now contribute to an increase in the net work done by the system.

Normal aluminum aircraft structures have about 2 percent of **inherent structural damping** (ζ , see Section 4.2). Composite aircraft structures have about 1-percent inherent damping. Just the mass of the air and the 'centering tendency' of a high velocity air stream will tend to damp aircraft structural oscillations. This is known as **aerodynamic damping**. The frequency content of unsteady aerodynamics will result in an oscillatory forcing function which may act positively (i.e., add to the system damping) or negatively (subtract from the damping) depending upon modal interaction. The net value of structural damping and aerodynamic damping is called the '**aeroelastic**' or **total (system) damping**. Total system damping generally tends to increase with an increase in airspeed until damping in a '**critical mode**,' or the mode with the lowest flutter speed, begins to decrease rapidly. At this point the critical mode begins to extract energy from the airflow and total system damping starts to decrease.

At the **flutter speed**, the damping of the mode is zero and the oscillation is just able to sustain itself without diverging (amplitude unchanging). Just a small addition of energy to the system by an increase in speed or a small disturbance can trigger the oscillation to diverge. When a flutter mechanism is active within a structure, overall system damping is negative. The aerodynamic damping has completely negated the structural damping and begins to add energy to the system. The amplitude of the cycles begins to increase over time rather than decrease as in the case of positive damping. This situation is termed **divergent flutter** and will eventually cause the structural limits of the component experiencing the flutter to be exceeded. The oscillations are very likely to damage the structure, possibly within only two or three cycles. Because of this, flutter is extremely dangerous. Once it starts, the motion is self-sustaining and requires no additional external forces.

Because control surfaces are specifically designed to rotate, they can be easily excited by aerodynamic forces or other structural motion. This makes them very important components to consider in flutter prediction and during flight testing. The rotation frequency of the control surface is of paramount concern. For surfaces moved by actuators, the rotation frequency is primarily contributed by the stiffness of this equipment. For surfaces moved by cables or push rods, the mass distribution of the surface will largely determine the rotation frequency. This can be altered as necessary by changing the balance weight. This is a concentrated mass placed ahead of the hinge line. **Mass balancing** is necessary every time there is a change to the surface, such as repairs or repainting. Balance weights are almost universally used even on surfaces driven by actuators to ensure against flutter should the actuator pressure decay due to a hydraulic failure.

Standard practice requires analysis to demonstrate, and flight test to verify as much as possible, that the flight vehicle is free of flutter or other aeroelastic instabilities to 1.15 V_L , or a 15-percent margin on the design limit flight speed (V_L). This provides a safety buffer on the normal aircraft red line in the event of overspeed. The damping (G) of any critical flutter mode or other significant dynamic response must be at least 0.03 at V_L . Some configurations may require a reduced flight envelope for flutter-free operation.

6.2.1 Flutter Examples

A few examples of flutter mechanisms are useful to illustrate real flutter events and to assist in identifying mechanisms that may be encountered during future tests. The reader may benefit from reviewing the following examples after reading this entire chapter to better appreciate the implications of these events.

Example 1 - A good example of binary flutter is the coupling between wing bending (also called **flexure**) and wing torsion; the classical **bending-torsion flutter**. If wing bending and torsion are in phase, that is, the surface reaches the maximum upward bending at the same time that it reaches the maximum leading edge down twist, and vice versa for downward deflection and leading edge up twist, there is no net work done by the system and it is stable. Seen another way, an upward translation of the wing produces a reduction in the effective AOA as does the nosedown twisting. These effects will naturally reduce further bending and torsion because of the loss in the lift force producing the deformation. However, if torsion lags the bending by 90 degrees, an unstable situation prevails. Now, an upward bending is accompanied by a positive increment in AOA due to twist that will increase the lift force and thus drive the wing to further deformation and yet further lift. The location of the wing center of gravity and its elastic axis have an important influence upon the likelihood of this flutter. The elastic axis is the spanwise line about which all torsion occurs and along which bending occurs perpendicularly.

Such a wing bending-torsion flutter occurred on the T-33 during testing with wingtip fuel tanks after the pilot took it upon himself to add some higher speed test points that were not planned. He managed to bring the aircraft back, but it was damaged beyond repair.

Example 2 - An often quoted example is the experience of the Handley-Page 0/400 bomber of World War I. In this case, a fuselage torsion mode coupled with asymmetric elevator rotation. Opposing rotation of the elevators, excited by the airflow under certain conditions, drove aft fuselage torsion. The fuselage twist in turn drove greater elevator rotation and an unstable condition resulted. The instability was seen as dramatic twisting of the aft fuselage and tail up to 15 degrees as the left and right elevator flapped violently about their hinge lines in opposing phase. The solution was to increase the elevator asymmetrical rotation frequency by joining the surfaces with a single torque tube (ever since a common practice for aircraft without differential stabilators). The increase in rotation frequency effectively eliminated the possibility of coupling with the fuselage mode within the normal flight envelope.

Example 3 - Another classical inertia coupling flutter case is that of **aileron rotation/wing bending**. The mechanism is not much different from Example 1. If the center of gravity (cg) of the aileron is aft of the axis of rotation or hinge line, then an upward motion of the wing will tend to produce a trailing edge down deflection of the aileron. Should the aileron rotation frequency occur at the same frequency as wing bending, an unstable condition is established and the wing or aileron may be driven to divergent oscillations. Trailing edge down rotation of an aileron produces an increase in lift on the wing for an upward bending moment on the wing. The opposite deflection occurs for downward bending of the wing but the effect is still unstable, tending to sustain or amplify the wing bending. The initial aileron rotation may be induced by rhythmic separation and reattachment of flow on the aft portion of the wing, producing an alternating high and low pressure on the control surface, but this is not required for the flutter mechanism. This is an example of how inertia effects can interact with unsteady airloads. This effect can also be seen in tab surfaces.

The most common solution to this problem is to increase the control surface rotational frequency by increasing the actuator stiffness, or by placing a mass ahead of the axis of rotation (mass balancing) to move the cg forward of the hinge line. Control surface **free-play (mechanical compliance)**, **backlash**, and general rigging can also play an important role in this flutter mechanism.

An example of this sort of flutter was seen during the T-46 flight testing when a substantial reduction in aileron mass balance was made to reduce drag. The flutter occurred at a previously cleared flight condition and with a simple lateral stick rap input. Oddly, the ailerons rotated symmetrically to couple with a symmetric wing bending mode. The symmetrical control surface rotation required some reversible control system (cables, pulleys, and backup structure) deformation. The flutter was nondestructive only because the rotation limit of the

ailerons was insufficient to drive the wing to great enough bending deformation. As it happened, this flutter had been predicted as a noncritical 'hump' mode, as explained later. The flutter commenced at 210 knots and did not cease until the aircraft had been slowed to 150 knots in 16 seconds. The wing experienced more than 50 g's acceleration at the wingtip with 9 inches of displacement. The tail experienced a 25-g acceleration.

High frequency, large amplitude control surface motion in a reversible control system resulting from flutter will result in violent stick motion that can be harmful to the pilot. Also, a **dynamic balance** to alleviate flutter may create objectionable static unbalance, requiring excessively large forces to displace the control. The use of mechanical dampers on the control surface may be dictated in such a case.

Example 4 - The frequent changes in the equipment contained in the large wing pods of the TR-1 and U-2R (the 'super pod'), often with antisymmetric loading, has resulted in occasional flutter events. These are associated with wing first torsion and sometimes in combination with aileron rotation. Such factors as speedbrake vibration, increased AOA, increased lift coefficient, increased normal load factor, transonic effects, aileron buzz (Section 6.4.2) and the normal biasing of the ailerons from the faired position to relieve gust loads, have all contributed to the problem. The flutter produced violent control surface motion up to 75 percent of full deflection, which displaced the cockpit control yoke with such force, that the pilot could not hold onto it. Considerable wing bending and torsion accompanied these oscillations while experiencing up to 18 g and some structural damage. Resolutions of the problem have included a limit to the speed envelope, load factor restrictions, and additional mass balancing of the ailerons. A 15-percent flutter margin does not exist at all points of the operating envelope for this aircraft.

Example 5 - The pitch or yaw of an engine nacelle or the motion of the wing on which the engine is mounted can excite a gyroscopic motion of the spinning propeller. This motion can diverge to produce **propeller whirl flutter** or the propeller motion can drive the wing to a flutter state. A variation of this was seen in the Lockheed Electra and led to many deaths until the cause was isolated. The subsequent investigation pointed to cracks in the engine mount or related structure altering the structural stiffness sufficiently to allow the engine to wobble. This changed the propeller disk incidence and the angle of forces acting on the wing. A coupling between wing and propeller motion then caused divergent flutter. The propeller disk was wobbling more than 35 degrees out-of-plane and the wing failed in bending/torsion after as much as 20 seconds of motion at about 3 Hz. The instability may have been excited by turbulence. The exact cause of the engine mount cracks was never conclusively determined. However, the main landing gear and engine mount assemblies were interconnected and landing impacts may have been the culprit. The Electra fleet suffered with a severe airspeed restriction until a redesign was made. This included changes to the engine mounts and cowlings to increase stiffness, and structural changes in the wings - all adding 1,400 pounds to the aircraft weight.

Example 6 - During initial flight testing of a small Israeli tactical transport called the Arava, flutter of the external wing strut was experienced. The strut failed, followed by the wing, and the aircraft and crew were lost. It was later determined that the nonaerodynamic design of the strut cross-section caused airflow which contributed to the instability.

The stiffness of an externally strutted wing is greatly dependent upon the strut. Should the attaching bolts between the strut and wing or strut and fuselage be inadequately torqued, stiffness can be compromised and flutter speed reduced. The same principle applies to other aircraft components, requiring that some bolt torques be checked periodically.

Example 7 - During early deployment of the KC-135 tanker the refueling boom began oscillating while in the trail position and separated from the aircraft. Fixes included a strengthening of the boom yoke and replacement of the cable stowing mechanism with a hydraulic system.

Example 8 - During initial flutter testing of the KC-135, a limited amplitude flutter was encountered in the vertical tail. In an effort to slow the aircraft, the pilot deployed the wing spoilers. However, the oscillations only grew in intensity. The peak-to-peak displacement of the vertical tail was 24 to 36 inches and was sustained for 46 seconds before the aircraft was finally slowed below the flutter onset speed. After considerable wind tunnel and flight testing with extensive analysis, a fix was finally arrived at. This included rudder and rudder tab

dampers, increased thickness of the front and rear spar caps, increased skin thickness in the two top panels between the front and rear spars, and increased rudder control cable tension.

In 1988 the E-6A TACAMO, a Navy derivative of the Boeing 707-320 aircraft—virtually the same airframe as the KC-135, experienced severe flutter in the vertical tail resulting in loss of the upper half of the fin and rudder. This occurred during sharp rudder inputs as part of the flutter clearance test. The next flight in 1989 resulted in nearly identical damage. The 320 vertical stabilizer had been altered for the E-6 application to reduce the cost of manufacture and this appeared to have recreated the instability experienced decades before in the KC-135 flight testing. While the problem was investigated, fleet aircraft were subject to an airspeed restriction to prevent any reoccurrence of the flutter. The final solution was to add a hydraulic flow restrictor to reduce pressure at the rudder hydraulic actuators by 75 percent above a certain airspeed. This prevented a control input of sufficient energy to induce the instability. Structural changes were also made to the fin to ensure a redundant path for structural loads.

Example 9 - The F-117A suffered a fin flutter during stores compatibility testing (Reference 16). The flutter testing had been performed twice using both manual inputs and electronic flight control system inputs through the control surfaces. The modal damping was difficult to extract from much of the data but the flight envelope was considered cleared. Between the flutter testing and the stores flight the area of the fins had been increased without a change to the interior box structure. This decreased the rotational frequency of the all-moving tail surfaces, allowing the first fin bending/torsion mode to couple with the first fuselage bending mode at 12 Hz. The flutter probably resulted from the fuselage bending producing a change in the angle-of-attack of the fin. The AOA change in turn, produced a pressure gradient across the fins which then bent and twisted in a manner that enhanced the fuselage bending, and the system became unstable. At limit speed, during a sideslip for the stores test, most of the left fin disintegrated in explosive flutter. The test conditions had been experienced a number of times without incident. The bearing friction in the fin rotation mechanism had also changed slightly during the flutter tests and tended to mask the critical nature of the mode.

To correct this serious problem, the ruddervator control axis was stiffened. Further testing was performed with the temporary installation of a low-friction bearing and a new oscillating mass exciter system. While the mode was stable, low damping was still observed in sideslips. Later, all-composite fins were used that further increased the flutter margin.

In a similar event, a Taiwan Indigenous Defensive Fighter (IDF) prototype crashed after experiencing horizontal stabilator flutter, killing the pilot. Subsequent analysis demonstrated that the tail lacked sufficient flutter margin in the low-altitude, high-speed flight regime. The stabilators later became all-composite and changes were made to the stab actuators and mounting hardware - most likely to alter the stiffness characteristics.

Example 10 - The addition of many external stores to the wing of an aircraft changes the mass distribution and airflow characteristics for the structure, requiring analysis and flight testing to ensure against flutter. However, sometimes the stores influence is more complex. In 1990 the empennage of a Tucano MK 51 was ripped from the aircraft and the plane crashed, killing the pilot. This occurred during high-speed dives in an effort to provide flutter clearance for a configuration with underwing stores. The cause of the flutter was traced to inadequate mass balancing of the rudder for a mode which included empennage motion resulting from the change in aircraft inertia with the wing stores.

Example 11 - An OV-10 aircraft, with its characteristic twin engine/tail boom configuration, was lost due to flutter in the early 1970's. The flutter included a tail boom mode which had not been accounted for in analysis or in the ground vibration tests (Section 7.0).

6.2.2 Flutter Suppression

The great advances in automatic flight controls has made flight possible in aircraft that are otherwise unflyable. In recent years this technology has also been used to alleviate gust loads, reduce crew and structural fatigue, and reduce troublesome vibrations by creating equal but opposite excitations. An example of this are the small movable vanes on the nose of the B-1B bomber. They serve to suppress a 3-Hz oscillation in the forward fuselage during low-altitude flight which interacts with the natural modes of the pilot's body and considerably reduces pilot tolerance and efficiency. Research has also been progressing in using active controls to suppress structural modes that might contribute to flutter or control surface divergence (Section 6.4.4). The concept has been proven in wind tunnel and experimental flight tests. The closest thing to a production application of this concept is active suppression of an objectionable 5 to 6 Hz heavy wing oscillation at low altitude for the F/A-18 with certain store loadings. The system uses the ailerons to damp the oscillations which are sensed by a lateral accelerometer beneath the pilot's ejection seat.

The easiest means of flutter suppression, if effective, is steady-state or oscillatory control deflections to counter sensed structural harmonics. A less practical but potentially more effective means is rapid mass redistribution within the structure. This has been used during flutter testing of an F-4 in Germany with masses on arms that swung out from the underwing fuel tanks. Research is underway into structures that actually change their stiffnesses upon demand by use of hydromechanical or electromechanical rams, or by applying a charge to a piezoelectric material distributed over the surface.

6.3 Flutter Prediction

The prediction of aircraft flutter is based upon well-developed structural and aerodynamic modeling methods combined with eigensolution matrix techniques. However, each component of such an analysis incorporates many simplifying assumptions (such as the small deflection assumption) in reduction of the myriad nonlinearities to make the solution more tractable and affordable. The study of unsteady aerodynamics and oscillating airfoils are still in its infancy and this also effects the validity of the predictions. The modeling of transonic aerodynamics is particularly limited and this presents a major stumbling block because of the large number of flutter mechanisms that occur in this regime. The prediction of separated flow characteristics is currently not possible at a practical level.

Static structural tests, **ground vibration test (GVT)**, wind tunnel results, and even flight test data are of help in refining the model to reflect the real vehicle. Flutter prediction remains something of a 'black art' in which engineering judgment and experience is more highly regarded than stacks of computer printout. Many flutter prediction codes exist (NASTRAN, FACES, UFAPS, to name a few), each having their own assumptions and solution techniques. The common assumptions are linear structures, small displacements, and a finite number of DOF (the semi-rigid case). Results are approximations only and generally cannot be counted on by themselves to clear a new or highly-modified aircraft. A safe envelope expansion flutter flight test is usually required.

Reference 11 provides some guidelines for the flutter prediction. One of the first steps is to perform an '**in-vacuo**' analysis, that is one in which the airflow is completely neglected. This is a static (zero airspeed) state with which GVT results (Section 7.0) may be compared. The mass of the static air is not considered since this is negligible. The more important analysis is done with the airflow effects included to act as an external forcing function. Supersonic and subsonic analyses are done separately because of the profound difference in modeling these flows. Transonic flow can be modeled by using some compressible flow assumptions with the subsonic analysis. The mathematical aerodynamics and structural models used in these analysis are later verified through wind tunnel and flight testing. Analysis including the effects of discrete failures such as a broken hinge, low actuator pressure, etc., should also be performed.

The analysis of the entire aircraft, or at least a substantial portion thereof, will be dealt with here. The basic 2 DOF wing analysis given in textbooks has little real value for accurate flutter prediction. Because of the tremendous increase in computer running time and cost as the number of DOFs are increased, components of the aircraft may be modeled separately with appropriate boundary conditions, but with the model for that

component greatly simplified when the entire aircraft model is simulated. Figure 70 shows a flutter structural model for the F/A-18 wing while the model for just one side of the F-15 STOL (Figure 71) has the structural components and control surfaces represented as just a series of beams.

The very basic flutter equation upon which all analysis is based is that defining the relationship between stiffness, mass and aerodynamic forces. In operator form this is:

$$\{M\} - \{A\} + \{K\} = Q \quad (83)$$

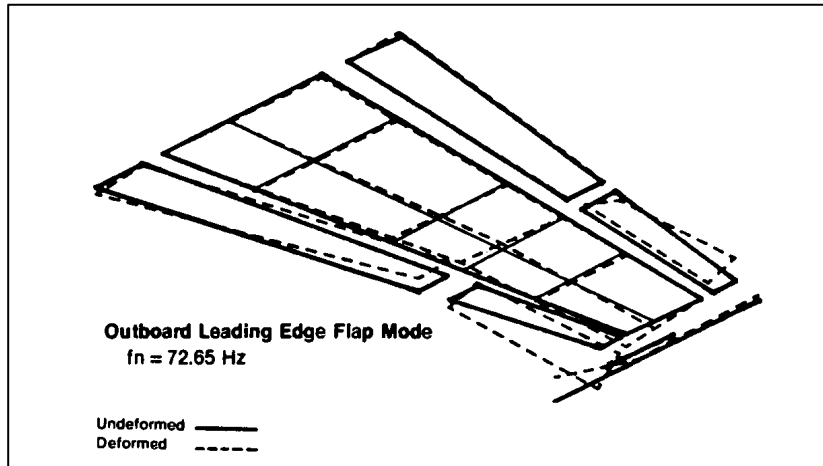


Figure 70 Example Wing Flutter Model and Deformed Shape - F/A-18 Wing

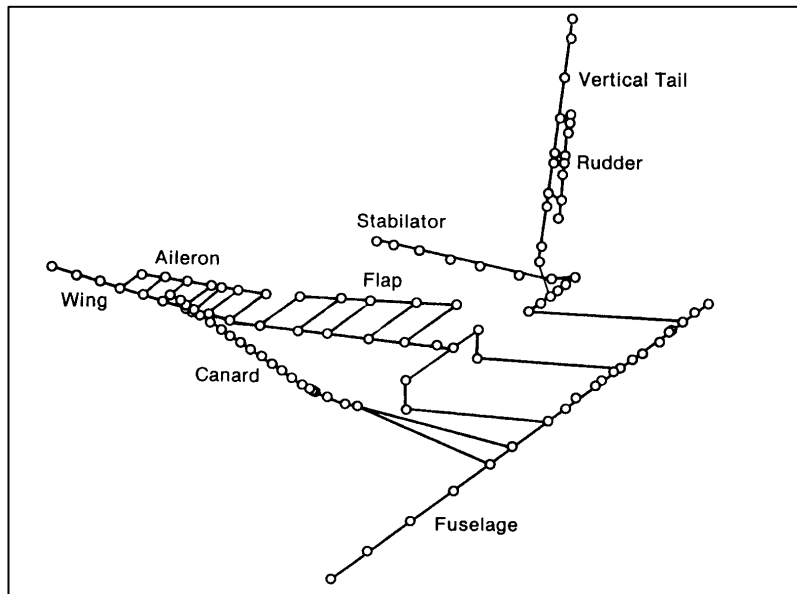


Figure 71 Example Aircraft Flutter Model - F-15 STOL

where:

- $\{M\}$ = the **mass operator**, including inertia, of the structure,
- $\{A\}$ = the **aerodynamics force operator**,
- $\{K\}$ = the **stiffness operator**, and
- Q = the **generalized forcing function**.

The forcing function may act through one or more of the operators. The mass of the air may or may not (the in-vacuo case) be included in the inertia operator. Creating appropriate forms of the operators can become very complex. A generalized modal matrix form (see Section 4.5.2) would be:

$$[M]\{\ddot{q}\} - [A]\{\dot{q}\} + [K]\{q\} = Q \quad (84)$$

where:

$\{q\}$ = the generalized coordinate vector.

Care must be taken to ensure that the matrices are compatible. The aerodynamics matrix defines the aerodynamic influences, the derivation of which is too complex to present in this handbook. It includes complex terms since it involves unsteady effects. The stiffness and mass matrices are usually produced by finite element modeling (see Section 3.2.3).

The solution as a matrix equation is typically accomplished by forming the **flutter determinant** and solving the resulting characteristic equation. That is, using the nonmodal stiffness, mass, and aero matrices:

$$|[k] + [m] - [a]| = 0 \quad (85)$$

Since the aero matrix is formulated for a single airspeed only, the solution is only valid at that airspeed. The eigenvalues of the flutter determinant will be complex, each representing a mode of deformation as defined by the eigenvectors. The real part of the eigenvalue will indicate whether the mode it represents is stable or unstable (see Section 4.3.1). A negative real part is stable, with the magnitude of the value indicating the amount of damping present. Conversely, a positive real part represents an instability and implies flutter. A zero real part implies a neutrally stable condition for which a zero imaginary part represents divergence and a nonzero flutter.

6.3.1 K-Method

For the K-method (sometimes known as the **American method** because it was created by the Air Material Command in 1942 when the only other such method was a British approach) the assumption of undamped, simple harmonic motion oscillations is made. In this case it is necessary to introduce an unknown **hysteretic damping** term, G (twice the damping factor introduced in Section 4.3.1 and based upon assumptions discussed in Section 11.3.4), to balance the imaginary aerodynamic damping terms and bring the system into neutral stability as the method demands. The damping term applied to the stiffness matrix is:

$$1 + iG \quad (86)$$

For sinusoidal motion, the generalized coordinates may be written as:

$$\{q\} = \{\bar{q}\}e^{\Omega t} \quad (87)$$

where:

Ω may contain damping.

If ω is the frequency of the undamped oscillations, then:

$$\Omega = I\omega \quad (88)$$

and equation 84 can now be cast in its most familiar form:

$$[-\omega^2[M] + [K] - [A]]\{\bar{q}\} = 0 \quad (89)$$

The aerodynamics matrix often uses a term known as **reduced frequency**, or:

$$k = \omega b / U \quad (90)$$

where:

b = a reference semi-chord of the wing, and
U = the freestream velocity.

Reduced velocity is the inverse of reduced frequency.

The equation to be solved in the K-method becomes:

$$\left[\frac{(1+iG)}{\omega^2} [K] - [M] - \frac{\rho b^2}{2k^2} [A] \right] \left\{ \bar{q} \right\} = 0 \quad (91)$$

where the multiplicative term on the stiffness matrix is taken as the eigenvalue, λ , to be solved for. A value for ρ (defining the altitude), and Mach number must be assumed for the calculation to proceed as the reduced frequency is varied. The important results are then obtained from the relationships:

$$\omega = 1 / \text{Re}(\lambda) \quad (92)$$

$$G = \omega^2 \text{Im}(\lambda) \quad (93)$$

and the corresponding velocity to produce the unstable state is derived from equation 90 using the reduced frequency from the aerodynamic computation and the derived ω . It is important to note that the sign of G, the total system damping, in this analysis is opposite to what one expects. A positive G will correspond to an unstable condition, and vice versa.

The principal advantage of the K-method is its lower analysis cost because of reduced computer time for a solution. Among its disadvantages is that the solution is only valid when G is equal to zero, and the aerodynamic model is for a purely steady-state oscillation.

Because of the assumption of zero damping, the prediction is only valid at the point of neutral stability. If the flutter velocity does not match that used in the aerodynamic calculations, then iterations must be performed until they do match. This is called a **matched point analysis** and may not always be done due to the large amount of computer time required. However, even when the flutter speed and analysis speed match, the rest of the frequencies and damping for all nonflutter modes are not true values but only guides to them. The predicted flutter speed should still only be used as a guide to the true speed. The number of eigenvalues produced depends upon the number of DOF modeled. Tracking the individual modes requires prior knowledge of corresponding frequencies (GVT results) and possibly examination of eigenvectors for mode shapes. Some programs include sophisticated algorithms that are able to track the modes automatically but may be confused when unrelated modes 'cross' at similar frequencies.

Typically, a velocity versus frequency (**V-f**) and velocity versus damping (**V-G**) or dynamic pressure (q) versus G plots are produced as a result of the flutter prediction (Figure 72a and 72b). Where two frequencies come together at an instability (crossing of the 0.0-G line in the V-G plot) the two modes are said to be coupling to produce the flutter. Recall that the K-method assumed that there was no system damping at all. Since we

know that a structure has some inherent damping, a 0.02- to 0.03-G crossing is usually taken as the flutter point. The velocity corresponding to such a crossing is used with the V-G and V-f plots to determine the flutter speed and frequency. The lowest such velocity, if several crossings exist, is the **critical flutter velocity**. The difference between this speed and the red line airspeed of the aircraft (assuming the former is higher than the latter) defines the **flutter margin**. The boundary of critical flutter modes may also be displayed on an airspeed-altitude (V-h) plot to allow a visualization of the areas of the envelope which may be most susceptible to flutter (Figure 73). This can be helpful during more routine flight test mission planning.

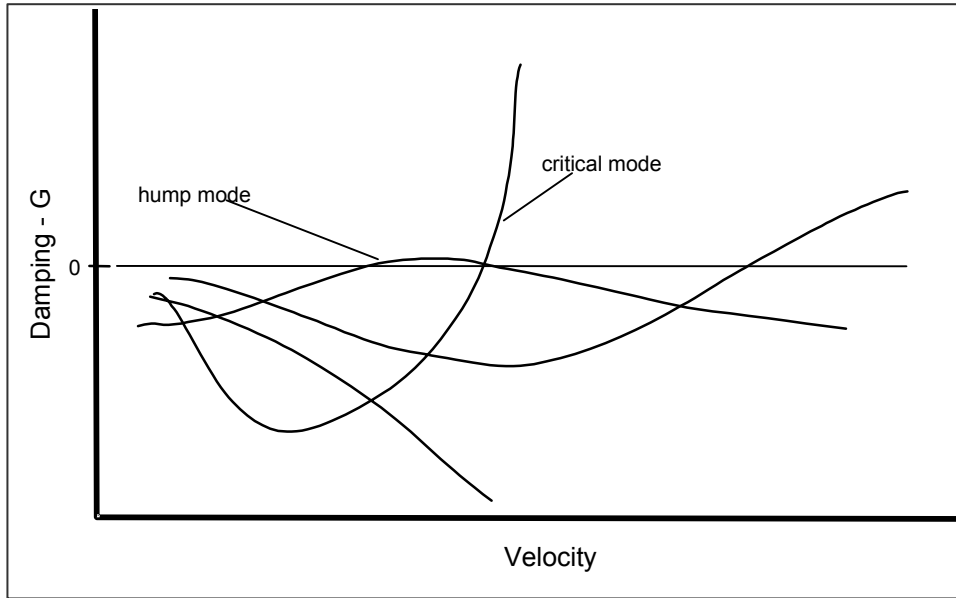


Figure 72a Example V-G Diagram

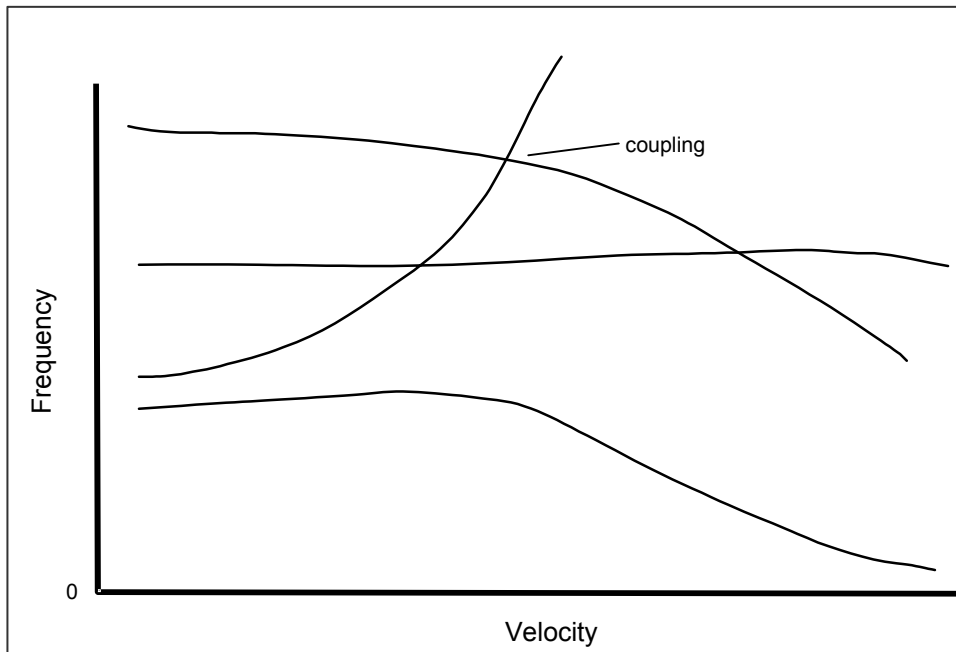


Figure 72b Example V-f Diagram

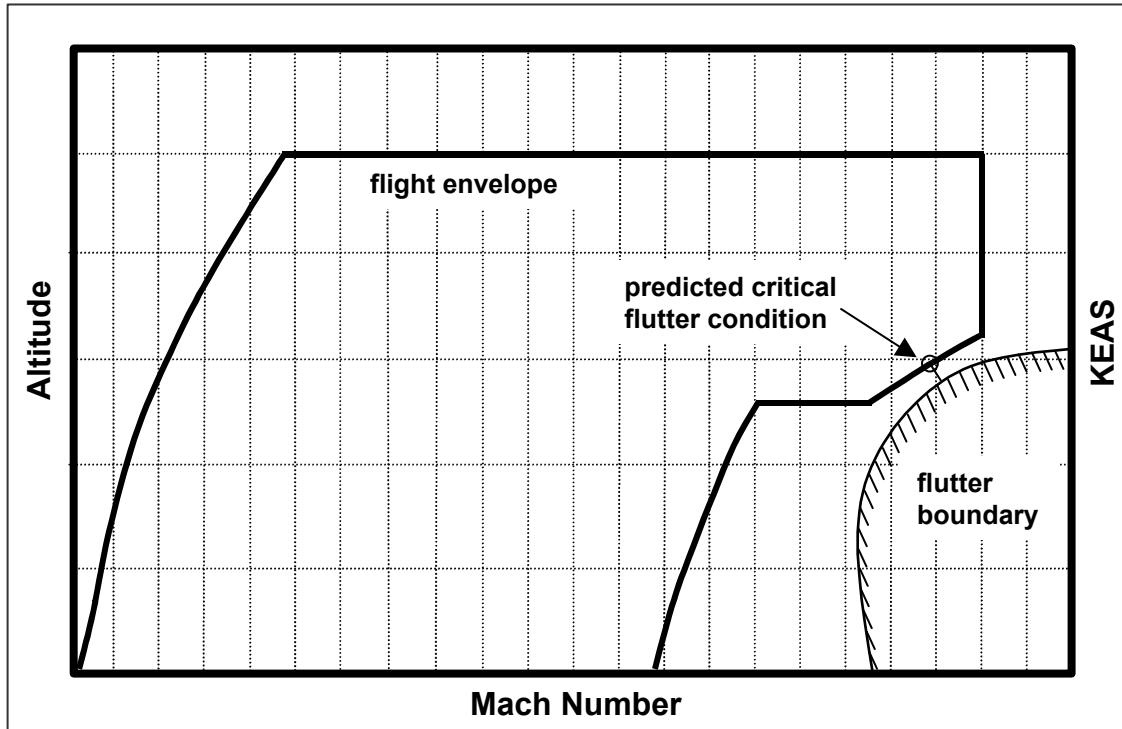


Figure 73 Example Flutter Boundary Analysis Result

The slope of a crossing of the 0.0-G line is also important. A very steep crossing implies **explosive flutter** or that which happens extremely quickly and with little warning because the damping drops very rapidly as the flutter speed is approached. A shallow crossing would provide more warning and may be recoverable once it begins. The airspeeds at which such shallow crossings occur should not be taken as precise. Small errors in the analysis that may raise or lower the modal line will result in relatively large changes in the flutter speed associated with the mode. Modes that cross shallowly and then recross to the stable side of the plot are called **'hump'** or **'dome' modes** (See Figure 72a) and may produce **limit cycle oscillation (LCO)** (Section 6.4.6) but is unlikely to produce explosive flutter. Hump modes are most common in store flutter and may be aggravated by elevated acceleration (g) loads.

6.3.2 PK-Method

The PK-method was created at the Royal Aircraft Establishment and is thus occasionally referred to as the **British method**. It assumes a response of the form e^{pt} prior to flutter where p can be either a real or a complex number:

$$p = \sigma + i\omega \quad (94)$$

The $-\omega^2$ of equation 89 is replaced by p^2 . The assumption that $p/(i\omega) = 1$ allows the imaginary part of the aerodynamic matrix to be multiplied by this ratio without effect and is called the aerodynamic damping. It may then be combined with the equivalent viscous structural damping to create the real **damping matrix** [B]. The real part of the aerodynamic matrix, termed the **aerodynamic stiffness**, is then combined with the structural stiffness matrix to form a [C] matrix. The resulting formulation is:

$$[[p^2[M] + p[B] + [C]] = 0 \quad (95)$$

The equation is solved for the eigenvalue p which will be of the complex form:

$$p = \omega(\gamma \pm i) \quad (96)$$

For small damping the artificial structural damping will be equal to

$$G = 2\gamma = 2\frac{\sigma}{\omega} \quad (97)$$

where:

γ = the estimated aerodynamic damping in the system.

Solutions are calculated by giving a value for ρ and Mach and varying velocity.

The advantages of the PK-method are that subcritical (less than the critical flutter speed) damping values are more realistic than with other methods, and it can solve for the flutter velocity directly. On the downside, the iterative processing method equates to high computer processing costs. The aerodynamic model is also quasi-transient.

6.3.3 P-Method

The P-method, an American modification of the PK-method, gives better subcritical trends for the more heavily damped modes by assuming damped harmonic functions for the generalized coordinates. For this approach, the Ω in equation 87 becomes:

$$\Omega = \omega(\nu + I) \quad (98)$$

where:

ν = the viscous damping coefficient.

Using the reduced frequency:

$$\Omega = Uk(\nu + I)/b \quad (99)$$

where:

$k(\nu + I)$ is called p .

The equation to be solved for this method is now:

$$[(Up/b)^2[M] + [K] - (\rho U^2/2)[A]]\{\bar{q}\} = 0 \quad (100)$$

The solution procedure is much the same as in the K-method except for the relationships:

$$\omega = (U/b)\text{Im}(p) \quad (101)$$

$$\nu = U\text{Re}(p)/(b\omega) \quad (102)$$

The P-method shares the same advantages as the PK-method, with the added benefit of having fully transient aerodynamics modeled. However, the transient aerodynamics models still tend to be immature, adding to the P-method disadvantages.

6.3.4 Other Methods

A variation of the K-method is the **KE-method**, which neglects viscous damping and eliminates eigenvectors from the output. While more limited than the standard K-method, it allows more modes to be followed more carefully without increasing the computer resources required.

Another flutter prediction method is to assume a mode shape that the structure may take on and use this in an energy analysis to arrive at the associated modal frequencies. This approach tends to be very involved and is still limited at this time.

In an effort to simplify the aerodynamic loads model, a quasi-steady or quasi-static assumption is made. This is generally considered valid when the reduced frequency is less than 1.0 ($k \ll 1$). That is, the airfoil is not in motion and the surrounding flow is in static equilibrium. Such an assumption generally produces large errors subsonically but may be acceptable at supersonic and particularly hypersonic airspeeds.

Aerodynamic and stiffness formulations are many and varied. The general dynamic equation formulation also shows some variations dependent upon application and the individual desires of the user. A great number of mathematical methods are common to simplify the matrix operations, such as converting the mass matrix to an identity matrix or diagonalizing other matrices. Some eigensolution techniques require the flutter mode to be assumed first. The degree of accuracy is also very broad and the results are subject to interpretation and the experience of the analyst. This presentation is, therefore, a general overview only of a field which is still growing. Detailed examples of flutter prediction can be found in some of the references provided at the end of the chapter.

6.4 Other Aeroelastic Phenomena

There are a number of other structural dynamic effects that must be dealt with, often in ways similar to flutter. Aeroservoelasticity and acoustics are dealt with separately in Sections 8.0 and 9.0, respectively.

6.4.1 Panel Flutter

An unsteady airload on the exterior skin of an aircraft can cause a periodic expansion and contraction of the membrane between supporting or stiffening members to produce a traveling or standing wave in the material. This single DOF flutter phenomena is most often seen on the forward fuselage. The B-1 bomber experienced annoying panel oscillations in this part of the structure. Frequencies on the order of 300 Hz are normally associated with panel flutter. Very high-speed aircraft can experience destructive panel flutter. It can be eliminated by increasing the stiffness of the surface by substitution of a thicker or stiffer material, or by addition of another stiffener inside the panel. The RF-4C experienced a vibration that began at a specific supersonic Mach number. It was isolated to a fuselage door that was 'oil canning' because a stiffener had somehow been left out in manufacturing. The fix was obvious.

6.4.2 Buzz

Flutter can occur as a single DOF mode. This type of flutter is called 'buzz' and can involve only small amplitude oscillations without the potential for destructive flutter or very large and dangerous motion. It is caused by phase lags associated with boundary layer or shock wave effects and interactions which result in the loss of aerodynamic damping. Separated flow over the control surface, perhaps caused by a shock, or the position of the shock on the surface itself are common causes for surface rotation buzz. Inlet buzz in supersonic aircraft is caused by the oscillation of a shock wave within the inlet. Panel flutter can be considered a special case of buzz but limited to membranes between supporting structure. Even if it is of limited amplitude, buzz is undesirable because of its tendency to distract the pilot and the potential for structural fatigue or over-stress.

There are a number of solutions to the buzz problem that do not require serious redesign. One approach is to change the flow over the surface. Delay of flow separation by use of vortex generators (see Section 2.2.5) are common. For control surfaces, increasing the elastic hinge stiffness (often objectionable to the pilot and controls

engineers) and decreasing the surface inertia have helped to increase the buzz onset speed. Rate dampers (damping only high velocity motion) have also been used in such cases.

6.4.3 Stall Flutter

Another rare single DOF flutter phenomena (typically wing torsion) is that induced by cyclical flow separation and reattachment on the wing at stall. A large change in lift forces occur in such a situation and create a powerful oscillating forcing function. Again, a change in the flow separation and reattachment characteristics can solve this problem.

6.4.4 Divergence

Divergence of an aerodynamic surface is a nonoscillatory instability in which high velocity and deformation of the structure create aerodynamic forces which tend to increase the deformation further. While aerodynamic forces increase with airspeed, structural restoring forces are constant. Therefore, a speed may exist in which the two forces are in balance. Beyond this speed, divergence is possible and will likely produce catastrophic failure of the structure. This airspeed is referred to as the divergence speed. The extremely light structures found in World War I aeroplanes, (e.g., the Fokker D-8), and the very thin wings on early supersonic aircraft were particularly susceptible to this phenomenon, and failure of wings in operation was not unknown.

The swept wing is characterized by a coupling between structural bending and twisting. The upward bending of an aft-swept wing results in a reduction in AOA in the streamwise direction producing a negative increment of lift. This negative lift effectively opposes further nose up twist of the structure. Divergence of an aft-swept wing is, therefore, unlikely because of the stabilizing influence of the wing torsion. The opposite is true for forward-swept wings wherein noseup twisting occurs with bending; a destabilizing influence. Only moderate amounts of aft sweep are sufficient to raise the divergence speed to the extent that divergence becomes practically impossible. Forward sweep of even small amounts can produce divergence at relatively low airspeeds. Divergence is not eliminated, only delayed by design to speeds beyond the craft's airspeed envelope. The X-29's forward-swept wing would diverge if the aircraft is just 15 percent beyond its design limit speed. Even this margin could only be achieved by careful tailoring of the bending and torsion response of the wing through the use of composite laminate construction (see Section 3.3).

If inertia effects in equation 85 are disregarded, a determinant suitable for divergence speed calculations results. For this steady formulation, the unsteady aerodynamic operator may be used with evaluation at a frequency of zero. The solution of the characteristic equation then yields a series of eigenvalues, the largest of which corresponds to the inverse of the divergence dynamic pressure. Divergence, a nonoscillatory phenomenon, can be considered as flutter at zero frequency.

6.4.5 Control Reversal

Lateral control reversal refers to an aeroelastic phenomena whereby wing deformation reduces the effectiveness of a roll control device to zero. The trailing edge down deflection of an aft-mounted aileron or flaperon induces a leading edge down twisting moment on the wing due to an aft shift of the center of pressure on the wing. This causes a reduction in the effective AOA of the wing-aileron combination and reduces the rolling moment normally expected of a rigid wing with deflected control surface. The torsional deformation will typically increase for control surfaces placed farther out on the semi-span, although rolling moment would also usually be expected to increase as the surface is moved outboard. This twisting moment increases with airspeed until reversal speed is reached where rolling moment from the control deflection is reduced to zero. Beyond this speed, aileron deflection will produce rolling moments opposite to the normal control sense.

Reversal is aggravated by aft wing sweep which normally increases wing torsional structural deformation under load. Early models of the B-52 suffered degraded aileron effectiveness at high speeds because of this effect, which led to the addition of spoilers (usually placed at the elastic axis) on later models of the aircraft. The F/A-18A had unacceptably poor roll performance, requiring a change in the composite wings for a more favorable torsional stiffness, extension of the aileron span inboard, and change in the use of differential flaps

and stabilators for additional roll authority. Rotating wingtips for roll control, with the rotation axis approximately at the elastic axis, is a seldom used solution to reversal. The term used to evaluate the control reversal effect is $Pb/2V$ (roll rate times wing mean semi-chord divided by twice the velocity) called the **helix angle** or **roll effectiveness**. When this term becomes negative, roll reversal occurs.

6.4.6 Limit Cycle Oscillation

Another flutter phenomena occurs when the aerodynamic damping exactly cancels the structural damping. This is called **LCO** and is characterized by sustained sinusoidal structural oscillations that neither increase nor decrease in amplitude over time (Reference 14). Limit cycle oscillation has also been called **limit cycle flutter (LCF)** in some sources, but is not flutter by a strict definition. So far LCO has defied accurate prediction and wind tunnel study due to nonlinearities. Leading edge control devices and increasing load factor, or AOA, have been associated with LCO. The amplitude of the oscillation will generally increase with airspeed. Where a control surface rotation is involved, the constraints on divergence may be simply the rotation angle stops of the surface. Limit cycle oscillations will continue indefinitely until a change in airspeed, altitude, or some disturbance initiates a change in aerodynamic damping. Since the change in flight conditions required to go from a slightly positively damped vibration to a negatively damped one are very small, LCO is not observed during most aircraft testing. Limit cycle oscillation has most often been observed during carriage of heavy underwing stores, most notably on the F-16, F-111, and the F/A-18, and so has been also called heavy store oscillation (HSO).

Limit cycle oscillation has been both resistant to a divergent response and highly susceptible to it. In any case, and as with any neutrally stable condition, it should not be taken lightly. At the very least, the oscillation can promote fatigue (particularly if control surface rotation is involved), will be uncomfortable to the aircrew, and possibly affect the efficiency of onboard systems. During flight testing, a ‘knock it off’ condition during LCO has been defined as a certain structural deflection limit (such as wingtip displacement) associated with a potential overload state. Since such deflection is seldom measured directly, the LCO frequency and peak acceleration is used as a measure of the displacement (see Section 4.4.1). A limit on peak acceleration for a given frequency ensures that excessive deformation does not occur.

6.4.7 Buffet

Buffet is the transient vibration of structural components induced by flow separation from portions of the airframe upstream of it, another aircraft ahead, or random air turbulence. As these impulses are generally random, loads effects are the usual concern. An example of this is horizontal tail buffet from wing flow separation at angles of attack approaching stall. Such empennage buffet was experienced during the initial flight testing of a Douglas dive bomber of World War II vintage when the large dive flaps ahead of the tail on the wings were deployed. The buffet produced severe structural deformation and was cured by perforating the flaps with a pattern of large holes. Another example of buffet is a 300-g low-amplitude response of the F-18 stabilators resulting from impingement of vortices shed from the aircraft’s leading edge extensions (LEXs) at high angles of attack. This response produced cracks in the honeycomb core of the stabs and even leading edge balance weight separation. The solution was the substitution of a stronger core and the addition of more composite plies to stiffen the structure and permit the removal of the balance weight altogether. Similarly, cracking in the vertical tails of the F-15 was caused by impingement of vortices shed off of the forebody during high AOA maneuvering.

6.4.8 Mechanical Vibration

This vibration is induced by internal sources, most commonly the engines. High frequency engine dynamics can couple with airframe modes to produce annoying vibrations or, over long exposure, metal fatigue. An example of this are the engine vibrations that occurred during the early flights of the British TSR-2 prototype. A low-pressure compressor shaft failure induced by a cooling airflow instability had the unfortunate tendency to cause the engine to explode above 97 percent power. This mandated that the pilots maintain this setting or lower. An out-of-tolerance reheat fuel pump also caused high-amplitude vibrations. At 87- to 96-percent power this vibration was near the resonant frequency of the pilot’s eye balls and caused his vision to washout.

6.4.9 Dynamic Response

This area is concerned principally with the loads induced by transient response of a structure due to such inputs as gusts, landing impacts, or taxi operations. An example occurred during the testing of the F-16XL when a flaperon torque spindle failed while the surface was under load. As the freely rotating flaperon oscillated, seeking freestream deflection, it set up a vibration in the wing that was amplified at the tip. The rapid, high-g deflections at the wingtip caused the tip missile and launcher to separate from the jet.

6.4.10 Aerothermoelasticity

As metal is heated, its modulus of elasticity (see Section 3.2.2) decreases. The magnitude of this decrease increases the higher the temperature becomes. The friction of the air upon the outer surface of an aircraft can produce extremely high temperatures at high Mach numbers (Figure 74). In this regime, the reduction in the stiffness due to aerodynamic heating can significantly reduce the natural frequencies of the structure and lower its resistance to static and inertia loads associated with vibration (Reference 4). These factors may act to allow a modal coupling that would otherwise not appear. Such an event was found during development of the X-15 hypersonic rocket-powered research aircraft. In a certain load and heating state the torsional rigidity of the stabilators were reduced to the point of permitting serious buckling problems. Changes to cure the problem resulted in a 21 percent weight increase in the surfaces.

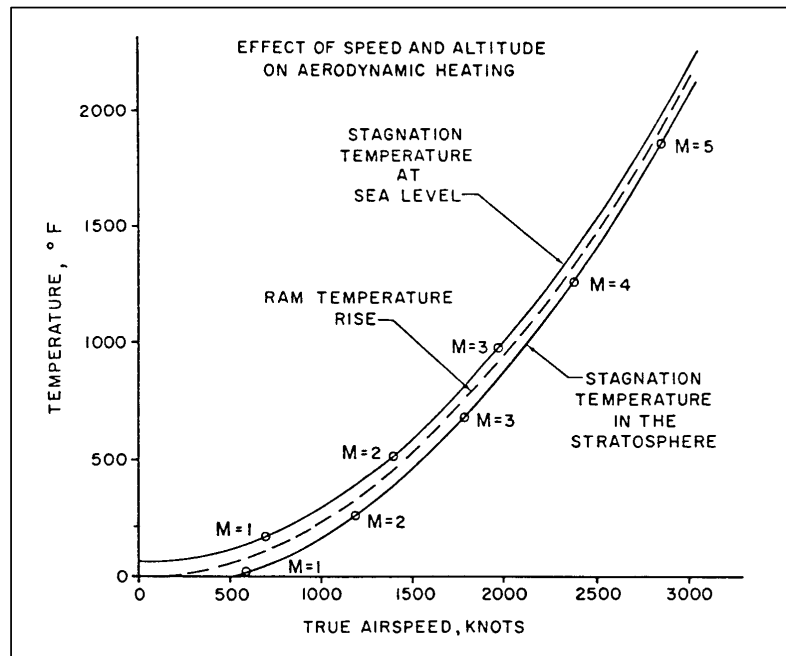


Figure 74 Stagnation Temperatures

6.5 Preliminary Ground Tests

Because mathematical modeling of the aerodynamics and structural properties of an aircraft are so subject to uncertainties, many ground tests are done with models and the full scale article prior to the beginning of flight testing. The results of such tests are used to improve the computer models and refine the estimates used in planning the flight test. This provides testers with more understanding about the aircraft prior to flight and reduces overall risk. The entire development flow is shown in Figure 75.

6.5.1 Wind Tunnel Tests

An important preliminary test conducted prior to flutter flight test of an aircraft is a wind tunnel flutter program. In the wind tunnel, an elastically and mass distribution-scaled model of the aircraft is subjected to an airstream that has also been scaled to the same dimension (i.e., reduced frequency number) as the aircraft. Only a partial model (e.g., tail surfaces removed) may be used in an effort to isolate effects. The scale model of the entire aircraft may be ‘flown’ either free or on bungees at speeds corresponding to the envelope of the real aircraft, and the flutter mechanisms verified as much as possible. It is common for the scale airspeed (occasionally produced with a gas other than air) to be taken beyond the normal envelope to verify the flutter margin. Definitely checking for the critical mode by observing the flutter (hopefully without destroying the model) is also done. Testing and data reduction methods are much the same as for full scale flight tests. General tunnel turbulence, upwind oscillating vanes, and external inputs (tapping the surface with a rod) are common excitation means. Mass, stiffness and shape changes can be made relatively easily and the effects tested on the model before being incorporated in the actual design. The wind tunnel data is always subject to errors involved in accurately modeling the aircraft and the airflow. Corrections to the wind tunnel data for tunnel effects and compressibility are typically performed, to include blockage effects (velocity errors).

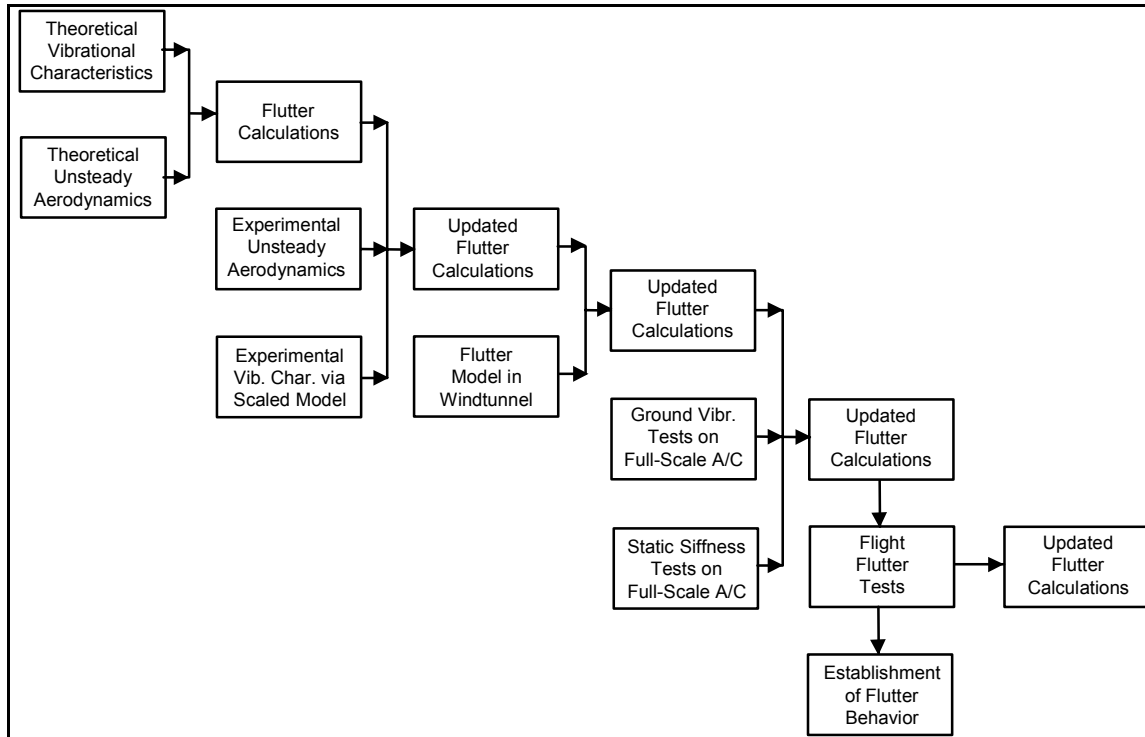


Figure 75 Diagram of Flutter Investigation During Development

6.5.2 Ground Vibration Tests

One of the typical essential preliminary tests conducted on an aircraft is the **ground vibration test (GVT)**. This test may be performed at an early stage on the wind tunnel model discussed in the previous section to ensure that it adequately replicates the desired stiffnesses. A full-scale GVT is mandatory for new designs and for any substantial changes to an existing aircraft. This test is used to verify and update the flutter model as well as provide a means of identifying modes from frequencies found in flight test data. Details of the GVT are contained in the next chapter.

6.6 Flutter Flight Tests

Flutter flight tests of aircraft are performed to verify the existence of the flutter margin of safety estimated by analysis. Flight near the estimated flutter speed entails a risk of accidentally encountering the flutter sooner than anticipated, with the potential for a catastrophic structural failure. For this reason, the flight envelope is cleared for flutter in an incremental fashion from a considerably lower subcritical airspeed. The frequency and damping of the vehicle's response to an excitation are measured at successively increasing increments of airspeed. The frequencies permit an identification of the modes of the response by comparison with ground test and analytical data. If sufficient instrumentation is installed, actual mode shapes can be determined to supplement the frequencies in performing modal identification. This is done by comparing phase and magnitude of responses from the transducers across the structure. The damping provides a quantitative measure of how near each airspeed point is to flutter.

The structural response is typically measured with accelerometers or strain gages (Section 10.0). Pressure transducers and velocity sensors have also been used. Anything which shows the dynamic response of the structure from which frequency and damping can be determined may be suitable. Strain gages have the advantage of naturally filtering high frequencies which may not be of interest, and therefore can provide 'cleaner' data than accelerometers. However, this also may make them unsuitable for adequately resolving modes greater than 10 Hz and cannot be used at extremities of surfaces where the strain goes to zero. They will also not show rigid body aircraft dynamics (pitch acceleration, for example) which the accelerometers will tend to show. Likewise, accelerometers cannot be used at the root or base of a surface where no acceleration occurs. A combination of accelerometers and strain gages has usually offered the best flutter instrumentation in the past.

6.6.1 Excitation

Several methods have been used to excite the aircraft structure to permit the individual response modes to be observed and their frequencies and dampings obtained. Some methods are more suitable than others for certain frequency ranges, nature of the modes sought to be excited, and amplitude or amount of energy to be put into the modes. Experience will also help in selecting the best method to use. Whatever the method used, it is important that the excitation be applied as close to the surface of interest as possible. For example, an impulse at the tip of the wing may not have much chance of sufficiently exciting a high frequency horizontal tail mode for adequate analysis. The position of the excitation source relative to the node lines of the significant modes (see Section 4.5.2) is also critical. Applying an impulse directly to the wing elastic axis has no chance of producing any torsional displacement. But, an impulse off of the elastic axis will produce both torsional and bending excitations. An impulse close to the node line will not produce as much displacement as the same amplitude of impulse farther from the node line by virtue of the longer moment arm.

6.6.1.1 Pulse

Pulses, or raps, are sudden control impulses made to produce sudden control surface movements that can excite up to 10-Hz modes very well, and occasionally to 30 Hz not so well. The objective is to produce an impulse that closely approximates a '**step**' **input** since such an input ideally contains the highest frequency content possible. Therefore, the sharper the input, the better the data. Longitudinal stick raps, lateral stick raps, and rudder kicks are the most common pulses used. The choice of pulse direction depends upon the modes sought to be excited.

For pulse excitation, the pilot will stabilize the aircraft on condition and make the rap. The stick pulse can be made by striking the stick with the palm of the hand or with a mallet. For irreversible control systems above a certain level of input abruptness, the flight control system or control surface actuator may attenuate the input and give no additional frequency content. Only trial inputs at a benign flight condition will demonstrate the best input to expect. Aircraft with automatic flight controls can be programmed to make these pulses without pilot intervention.

Sometimes, a rapid stick movement, with the stick held in the usual manner, (a '**singlet**') is sufficient excitation. More energy may be generated by a '**doublet**,' which is two such inputs in rapid succession in opposite directions. But, the singlet and doublet can only be done at a low frequency compatible with human limitations - about 4 Hz for stick inputs and less for rudder pedal inputs. A **control oscillation** is a variation of the doublet but with some specified time between the two inputs. An example may be a 1-inch aft stick deflection, hold for 3 seconds, and a return to neutral. A time to produce the control input, a 'ramp-up' time such as 1 second for the 1-inch stick deflection, may be specified to ensure that the mode is adequately excited. The oscillation is tailored to excite a specific mode, such as a 3-Hz fuselage first vertical bending mode for an elevator input.

The pilot may deflect the control surface and then fly 'hands-off' to allow the aircraft oscillations to naturally damp out ('**stick-free**' pulse), or the pilot may arrest the stick as it returns to the neutral position ('**stick-fixed**' pulse), depending upon which technique yields the best response from the aircraft. A variation is to hold the stick as the rap is made. For a large aircraft a rap may not produce enough control deflection for sufficient excitation. In this case a rapid, full-deflection displacement of the control followed by a release is useful.

It may be desirable to make several raps and to average either the time histories or fast Fourier transformations ([FFTs], Section 11.3.1) of the raps together to remove noise and other corrupting influences. The principal deficiencies of the pulse technique are the nonselectivity of the frequencies to be excited and the generally poor energy content above about 10 Hz.

6.6.1.2 Sweep

This is the most attractive and preferred excitation means but is also one of the most complex and expensive to implement. Sweep data and burst data (Section 6.6.1.3) requires the use of an excitation system to 'shake' the aircraft or individual surfaces in flight. Frequencies as high as 65 Hz have been successfully excited by this method. A mechanical 'exciter' system added to the aircraft or the vehicle's own control surfaces are generally used to make the sweeps. The frequency response characteristics of the exciter system or control surface actuators will determine the modal frequencies, which can be excited. Hydraulic or electric actuators generally show an attenuation of response amplitude beyond 30 Hz. This method of excitation requires some time and thus, may be unsuitable if the test condition can only be obtained briefly, such as in a dive. Several different types of sweep exciters have been used.

B-1 flight testing included use of a '**wand**' at the wing and tail extremities (Figure 76). The wand consists of a mass placed at the end of a pivoted arm attached to the tip of the structure. The oscillation of the mass about the pivot point produces a periodic structural response by virtue of the inertial displacement of the mass on the arm. Other such inertia exciters use out-of-balance rotating masses. One drawback to this technique is the disturbance in the airflow if the wand extends beyond the surface of the aircraft. Another disadvantage is that larger masses are needed to excite lower frequencies, and the overall system weight may become prohibitive or alter the modal characteristics of the structure to which they are attached.

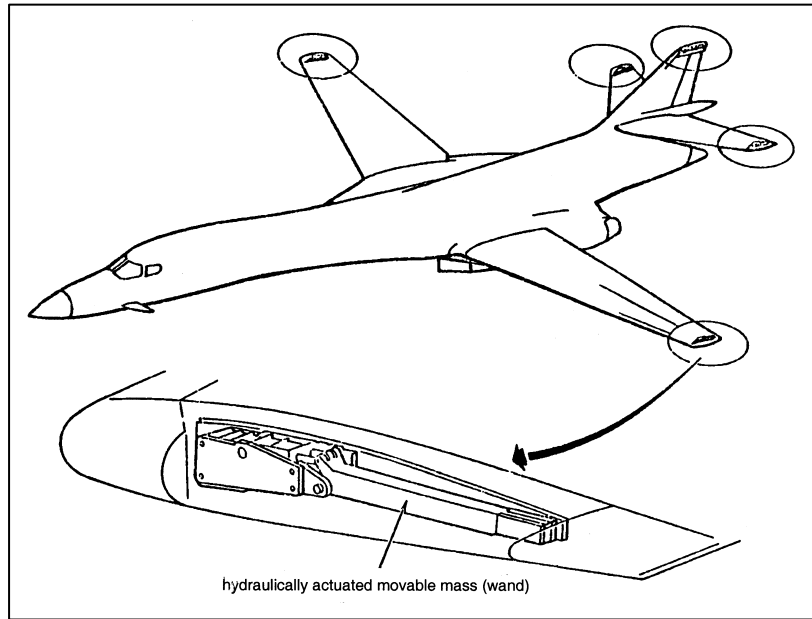


Figure 76 Wand Flutter Exciter System

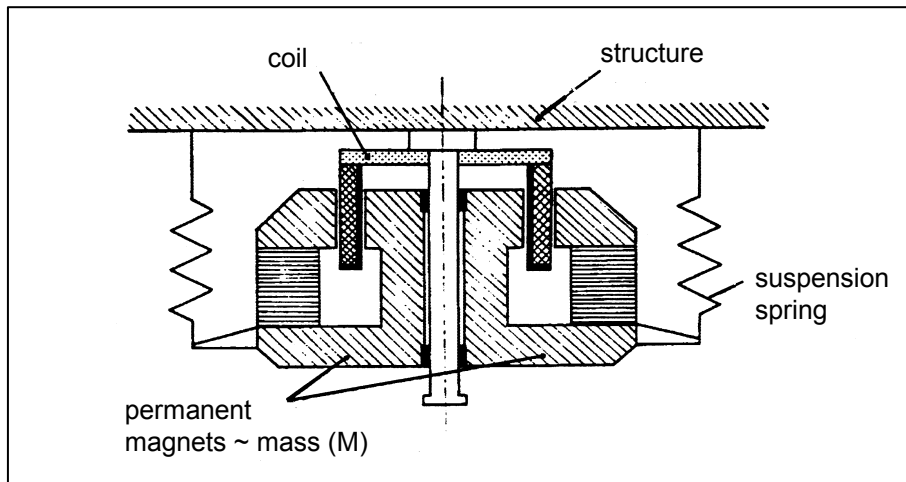


Figure 77 Electrodynamic Exciter

The French have done quite a bit of work with electrodynamic exciters. Akin to electrodynamic shakers used in GVTs (Section 7.6), a mass is suspended within the structure by springs. The mass incorporates coils that are in close proximity to coils attached to the structure (Figure 77). By sending an alternating current through the coils, the mass can be made to move within the electromagnetic field with the frequency of the movement proportional to the electrical signal. Although successfully used on many European projects such as the Transall and Concorde, the advantages and disadvantages are much the same as those for the other systems discussed here, with the added difficulty of access once the units are enclosed within the aircraft structure. Also, greater moving mass is required to adequately excite lower frequency modes.

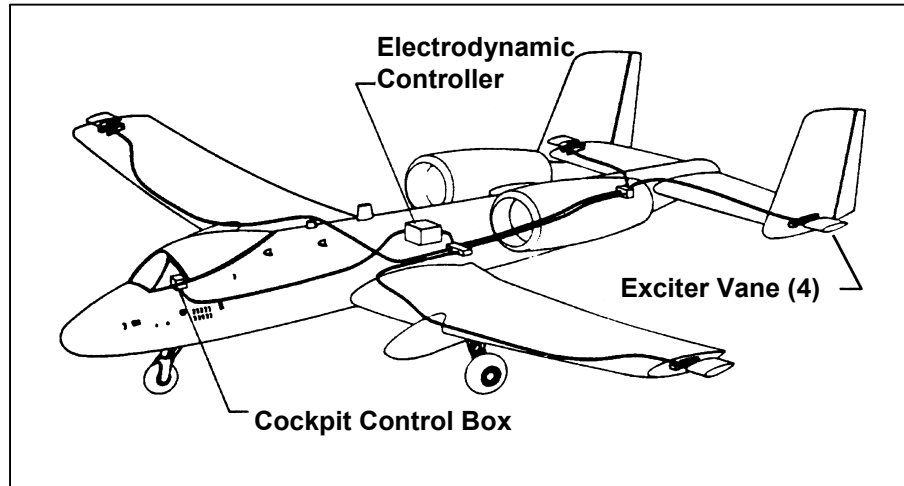


Figure 78 Vane or Flutteron Exciter

Oscillating vanes, or ‘flutterons,’ mounted on wings and tails have been used many times, namely the T-46, A-10, and C-17 test programs (Figure 78), as well as several recent airliner tests. The vanes create a varying aerodynamic force that acts on the aircraft structure. Several sizes and masses of vanes may need to be available as the speed and dynamic pressure at different points in the envelope alter the effectiveness of the inputs. The great advantage of this system is that it can easily excite low-frequency modes and higher frequencies are only limited by the frequency response of the vane actuator. Below 3 Hz the input may not be sufficient to adequately excite the structure under test. A disadvantage is the change to the mass distribution of the surface upon which the system is attached and the disturbance to the normal airflow that its presence and operation engenders. Interfaces with the normal aircraft electrical and hydraulic systems may be costly. Also, when commanded to stop, the vanes may ‘wind down’ and input forces at undesirable frequencies. An abrupt stop may also be detrimental since it would impart an impulse load with broad frequency content. The stopping characteristics of the vane system should be examined during test preparation.

A variation on the oscillating vane is a rotating slotted tube. This system produces oscillating airloads on the tube but does not add significant weight or disturb the airflow as much as a vane. It was used quite successfully on NASA’s testing of the F-16XL.

For ‘fly-by-wire’ aircraft, using the flight control system as an excitation means has the attraction of requiring no additional hardware to that of the basic aircraft. The oscillatory signal to the control surface actuator(s) is produced by a special function of the flight control computer, or injected into the loop by a separate unit. The pilot is generally provided the means of varying the sweep rate, end frequencies, and amplitudes of the inputs. Random inputs by this means are also possible. There is difficulty in exciting high-frequency modes because the attenuation or rate-limiting characteristics of the actuator will limit the displacement or level of excitation in this part of the spectrum. This method has been used with great success on the various F-16 test programs and the B-2 bomber.

When sweep data is collected, the excitation system is run through one or more frequency sweeps at a predetermined rate. Common rates are linear, such as 1 decade per minute (Section 9.3), or a logarithmic variation. The proximity of modes and the potential for noise problems may effect the selection of sweep rate. Sweep data is normally analyzed on a computer to determine frequencies to use for a burst-and-decay method or to stand on its own. This method is analogous to conducting a GVT in flight, measuring a forced response of the structure. Its greatest advantage is to directly apply energy into modes that may otherwise be very difficult to excite with sufficient energy by other means.

As with GVT excitation (Section 7.8.3.1), sweeps have a tendency to increase the noise from local nonlinearities. A sweep performed too quickly will also tend to make the modes appear to have a slightly greater frequency and damping value than they really do. If there is no transient response evident following termination of the excitation, the response is termed ‘**deadbeat**.’

6.6.1.3 Burst-and-Decay Data

Burst-and-decay data are collected by running the excitation system at a specific frequency and then shutting it off to allow the structure of the airplane to damp itself out. This is typically done at the frequency that will excite the critical modes(s) to specifically check the damping of these responses. Generally, only a few cycles are necessary before stopping to allow the decay. For a mechanical excitation system, the winddown characteristics - that is its ability to cease movement when commanded without overshoots - becomes important to clean decay data.

6.6.1.4 Pyrotechnic

The so-called ‘**bonker**’ is a very small pyrotechnic charge that is typically placed externally near the trailing edge of a control surface and detonated electrically. The tiny explosion produces a sharp pulse excitation that comes very close to simulating the ideal step input. A series of such charges may be placed along the surface trailing edge so that many such impulses may be produced on a single flight. The disadvantage of the method is the limited number of excitations that can be produced in a flight and the disturbance of the normal airflow created by the presence of the charges and their wiring. The bonker has seen wide use in Europe on such programs as the Airbus, Jaguar, and Tornado.

6.6.1.5 Air Turbulence

Random air turbulence can be used as a source of excitation. Even if not felt by the pilot, there is always some energy content to an air mass. Generally, low altitudes have a greater magnitude of this excitation. The area around Edwards AFB is ideal for this technique in that deserts have many rising columns of air and high winds that, when flowing over mountains, produce a good deal of instability in the air. Weather fronts also produce turbulent air. This technique, while attractive from a cost standpoint, must be used with prudence. There is generally very little energy to be obtained in the spectrum above about 20 to 30 Hz and some structures will not respond to turbulence as well as others because of differences in wing loading (Reference 13). Also, some turbulence is not ‘random,’ but has dominant frequencies.

The normal procedure is to have the aircraft stabilize on condition and collect response data for some predetermined time period, as much as 2 minutes. The resulting data (the response of the aircraft to the random inputs) is collected on the computer and analyzed (Section 11.0) to determine the frequencies and dampings of the observed modes. A ‘near real-time’ computer analysis is required for point-to-point clearance if dampings must be tracked. The approach to an instability may sometimes be seen by a ‘burst,’ a brief period of lowly damped, higher amplitude response, or by Lissajous figure indications (Section 11.2.6). This is referred to as **incipient flutter**.

Another approach using turbulence is to measure the gusts using a ‘gust probe.’ This may be very sensitive alpha (AOA) and beta (sideslip) vanes on a nose boom, or pressure sensors at the tip oriented to allow measurement of vertical and lateral gust components. An accelerometer or strain gage may be mounted on the boom to allow rigid body aircraft and boom dynamics to be removed. The result is a measure of the input forcing function, with the resultant aircraft structural dynamics measured in the usual way. Knowing the input and output allows a transfer function (Section 11.3.6) to be formed. This provides a powerful means of predicting modal response at other points in the flight envelope.

Deployment of speedbrakes, landing gear, flaps or other device on the aircraft that will produce a great deal of buffet vibration, and even flying in the wake of another aircraft, have also been used for turbulence excitation. Such techniques are likely to introduce a dominant response representing the primary vibration frequency of the device (vortex shedding rate off of the speedbrake, for example) that may mask true structural responses.

6.6.2 Procedures

In the normal conduct of a flutter test, a buildup procedure is used, whereby less critical points are flown prior to more critical ones. This technique allows the engineers to determine damping trends as dynamic pressure and Mach number are increased. These two parameters are normally treated separately. Because high Mach numbers are generally only possible at high altitude, and high q 's are obtained at low altitudes, there is usually a considerable altitude difference between the two test conditions. If the critical mode(s) are suspected to be altitude critical then a buildup in altitude may also be necessary. In any event, a minimum safe altitude for the testing should be established. If q is determined to be more critical than Mach (as is commonly the case), the Mach points may be flown first, although jumping between the two conditions in the course of the testing for the purposes of a concurrent buildup in both parameters is not unknown (Figure 79). Because q is so often the determining factor in flutter susceptibility, equivalent airspeed is generally used for velocity references during flutter flight testing. Testing across the transonic range is important because of the significant aerodynamic changes which occur there. Having the pilot maintain precise airspeed control and using corrected airspeed readings (calibrated airspeed to match a target equivalent airspeed, see Section 2.2.2) is essential to avoid overspeeding a test point and creating a potentially hazardous situation. A careful airspeed calibration must precede or be conducted concurrent with the flutter program. However, the error in the damping and frequency values determined from flutter data is generally great enough to make any data corrections in airspeed and altitude for Pitot-static errors superfluous.

Many aircraft airspeed-altitude envelopes have an inflection point at the high-speed end (the 'knee' of the curve). This is normally a good mid-altitude to perform another buildup combining Mach and q effects. The buildup at this altitude would required prior Mach and q clearances at high and low altitudes. An example of envelope clearance flutter test points is shown in Figure 79. A separate, perhaps more abbreviated, buildup to the point in the airspeed-altitude envelope where the lowest damping of a critical flutter mode is predicted may also be advisable.

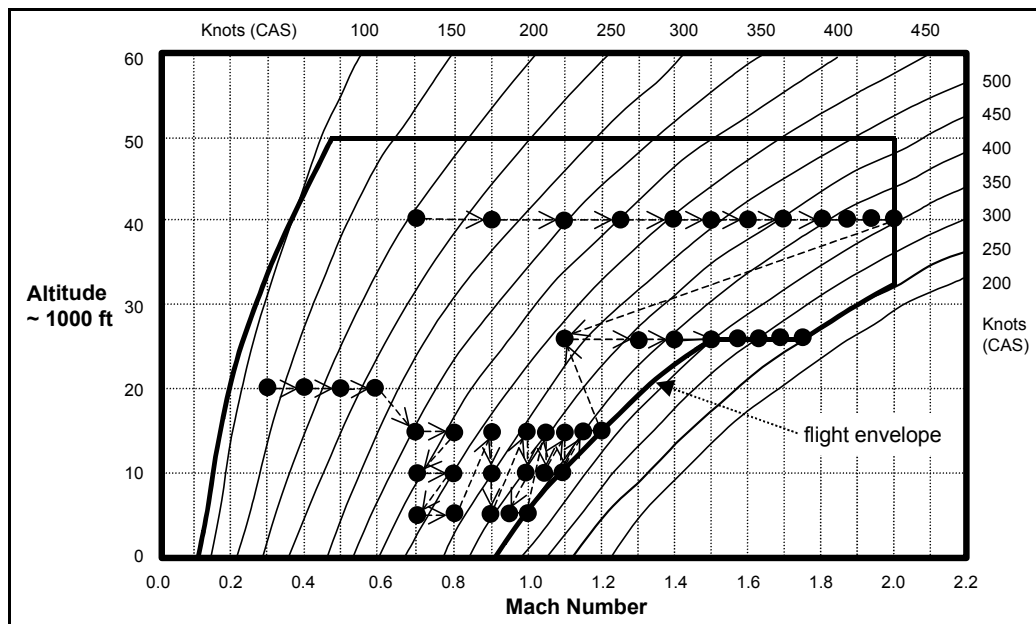


Figure 79 Flutter Expansion Example

Generally, the buildup will consist of points of ever-increasing airspeed. The airspeed increments between points will depend upon the proximity to the predicted flutter boundary and the confidence in the flutter prediction. Smaller steps are required when close to a flutter condition or where a rapid decrease in damping is observed. Naturally, some practical airspeed must be selected to begin the buildup since the aircraft must takeoff and climb to the test altitude, as indicated in Figure 79. The choice of this airspeed must be based upon a conservative review of the predicted flutter modes and flutter margin. A reasonable tolerance on airspeed and altitude must be established and published in the test plan. Naturally, no overspeed at the aircraft maximum airspeed is permissible. The test conductor must remain flexible and be prepared to take smaller airspeed steps than the test cards dictate if low damping is observed. This decision can be facilitated by real-time analysis of the data, either on the strip chart, computer, or both, prior to each successive test point. For the purpose of other testing, the aircraft is restricted to the envelope that has been cleared by flutter testing. This is necessarily much less than the ultimate flight envelope of the aircraft, but will slowly be expanded to this objective as testing proceeds.

The maneuvers used in flutter testing depend upon the type of data to be collected. If sweep, burst-and-decay, or random data is acquired, the aircraft will stabilize on condition (i.e., fly a constant airspeed and altitude) for the time required. Sometimes, when dive test points have to be flown, the aircraft will reach a target airspeed, and the random, burst-and-decay, or sweep data will be taken between a band of altitudes to prevent significant changes in the air density (i.e., dynamic pressure). In some test programs, an airspeed schedule is flown to ensure that the aircraft flies along a given flight profile and does not overshoot its target airspeed, q , or Mach. This is usually done when the test conductor wishes to verify flutter free flight along the redline airspeed curve after clearing to this speed at discrete altitudes. Instead of flying many stabilized points at many different altitudes, the plane is dived along this 'line' and brief excitations made to verify that no lowly damped responses are seen. The whole line can be cleared in one test maneuver. This technique is good for demonstration purposes but is not advised if useful damping values are sought. It should only be done after the test team is reasonably confident that flutter will not occur along the line, because the dive does not allow as quick a recovery from a flutter event as a straight-and-level condition.

If personnel at the ground telemetry station or the pilot(s) sees flutter beginning, immediate action must be taken to save the aircraft and possibly the aircrew. The command 'Terminate, Terminate, Terminate,' or similar words like 'Abort' and 'Stop' are transmitted to the pilot(s). The flutter engineer(s) monitoring the aircraft response should have a direct radio link to the aircraft to reduce the reaction time needed to have someone else communicate a termination command. The immediate cockpit action must be to pull the engine power back to slow the aircraft from the critical speed as quickly as possible. Deploying speedbrakes (airbrake) or similar devices may also be advisable, but caution is required as some speedbrake locations may aggravate flutter. Commanding a slight nose-high attitude will also assist in slowing the aircraft. This last maneuver is not advised when store loadings are involved since g-loading has been known to aggravate store flutter. A normal load factor limit should be specified in the test cards. If a loaded maneuver is in progress, unloading and returning to straight-and-level flight is required. For aircraft with podded engines, a throttle chop to slow down may impart moments to the wing structure which may be undesirable. These considerations point to a need to analyze the consequences of recovery procedures with regard to the most likely flutter mode(s). Mechanical excitation systems should be immediately arrested if in action. It is important that the pilot(s) have direct means of stopping the exciter, usually with a switch on the control column or throttle. The structural oscillations may not immediately die out when 'backing off' the test condition.

A safety chase aircraft is almost always mandatory for flutter testing (Section 13.0). Because flutter testing is typically labeled as medium risk, and usually high risk, only minimum flight crew is permitted. The airspeed system should have been calibrated so that a confidence of 2 to 3 knots, at most, in the airspeed readings exists. The aircrew should be cautioned against over-speeding the test points. Such testing is normally conducted in clear air without turbulence (unless used as an excitation source) since it may corrupt the data and add to analysis difficulties. Since the fuel mass in wing and fuselage tanks can significantly effect modal responses, analyzing and testing the aircraft at various fuel states may be advisable. In such cases, tolerances on fuel quantities in the tanks may need to be dictated.

Since the impulse caused by the sudden release of stores may also excite flutter, apart from the loads aspect, this should also be considered in analysis and perhaps flight tested. It is also usually advisable to perform flutter testing with any stability and control augmentation system in both the ON and OFF (if possible) states in the event that these systems are adding damping which is hiding a potential flutter response. Consistent and proper servicing of the aircraft is important to avoid shifts in modal frequencies and dampings. The torquing of bolts holding major components on the airframe, such as external stores, can be an important factor in stiffnesses. Wear of such components as hinges and bearings can change rotational frequencies. For example, the X-29 had a rubber-like fairing to fill the gap between each canard and the fuselage. During the course of flutter testing this fairing slowly abraded and caused a decrease in the canard rotational frequency. However, some test teams intentionally introduce hysteresis into control surface hinges (so-called 'sloppy bolts') to duplicate an extreme wear condition.

Fuel slosh can be a source of oscillatory inertia input to the aircraft that may, at first, be overlooked. The internal fuel mass at each fuel state will have a natural slosh frequency in the longitudinal and lateral axes. Longitudinal sloshing is usually the issue with fuselage tanks. When cyclical fuel sloshing occurs in tanks located at outboard wing stations, particularly of large transport aircraft, an antisymmetrical wing bending may result or the lateral response can be sensed and fed back through the electronic flight controls (Section 8.1). An unexpected response during flutter testing may also be attributable to fuel slosh, and engineers should be familiar with the predicted slosh frequencies. Sloshing can be minimized through the use of segmented fuel tanks or baffles, but a concern may remain at some specific conditions requiring the collection of flight test data. Analysis should yield the fuel state, flight conditions and axes of maneuver that have the greatest potential for fuel slosh. Should the analysis suggest that the resulting inertia input is an aeroelastic concern, these conditions can then be tested in flight. A manual maneuver (longitudinal or lateral doublet and the required frequency) is usually performed to induce the sloshing so that the resulting dynamics can be measured.

6.7 Data Reduction

The methods used to analyze flutter test data are discussed in Section 11.0. The results of data analysis are typically airspeed (V , M , or q) versus frequency (V - f) and airspeed versus damping (V - G) showing the modes being tracked. Clearly, some prior knowledge of modal frequencies is required to identify modes from the flight test data unless sufficient instrumentation has been installed to allow actual mode shapes to be determined (rarely the case). If some measure of the structural input is available, then more detailed systems analysis is possible using transfer functions (Section 11.3.6).

Data is used to establish a safe flight envelope for the aircraft based upon extrapolation of the damping trends to the case of zero damping (onset of flutter) and application of the 15-percent safety margin in airspeed below the predicted 'flutter airspeed.' Usually, the aircraft is not tested at damping values less than 2-percent damping or 0.02 G (although 0.03 G is specified by MIL-A-008870). During stores testing of the F-16, damping as low as 0.01 G was permitted because of a frequently encountered LCO (0.0 G, see Section 6.4.6). Other lowly damped responses, such as engine nacelle rocking, may be acceptable once understood and with ample evidence that they display no propensity to diverge.

The extent of the analysis of real-time data is at the discretion of the flutter test director. In some cases, an experienced test director may be able to determine the damping by 'eye-balling' the strip chart, or time history display, traces without extensive analysis. This would be especially true for aircraft, which have already undergone considerable flutter testing, such as a fighter-bomber subjected to many external store clearance tests. Some aircraft or modes are more easily excited than others and strip chart traces alone may be adequate for a point-to-point clearance. In other cases, particularly where more than one mode is present, more detailed analysis, perhaps involving computers, is required. Real-time analysis or even display of every flutter parameter may not be technically or practically feasible. The flutter engineer must apply his or her best judgment as to the most critical parameters. If time history shows damping of 0.05 G or less, or when more than one mode is present, more detailed computer-based (either time- or frequency-domain) analysis is advisable.

If it is important to track damping of critical modes (both predicted and those found to have decreasing damping) for point-to-point flight clearance, then a ‘real-time’ analysis will be required before clearing the pilot to accelerate to the next test condition or a more critical configuration. The dominant mode appearing in the data is not necessarily the most important mode to watch. A mode that is not easily excited or seen may still have low damping and is waiting to make life interesting. Typically only one of the two participating modes will show the rapid drop in damping as flutter is approached, so it is important that the frequency shifts and damping of many modes be tracked. Detailed analysis between flights should always be done using all available data to track frequency and damping of significant modes with the best precision available in an effort to predict flutter onset from the trends.

Modal frequencies and dampings can be extracted from the data using any number of the methods discussed in Section 11.0. By using an exciter system, it is possible to obtain an input function for transfer function and particularly coherence plots (Section 11.3.7). However, it is important to remember that the exciter signal or output is not the true or even the only forcing function acting on the aircraft. The changes to the airflow on the aircraft or the impulsive inertia change is the true structural input. Turbulence, general aerodynamic forces, and miscellaneous pilot and systems inputs will still be present as uncorrelated signals. These will impact the quality of the plots and may lead to erroneous conclusions.

A method for extrapolation of flutter test data by employing a 2 DOF math model to predict the flutter onset (Reference 10) has shown promise. This has the advantage of using actual test data to provide a measure of the flutter margin from the last test condition flown. Although employing many limiting assumptions, these flutter margin calculations provide the flight test engineer with another tool for safe flutter clearance.

6.8 Store Flutter Testing

The addition of external stores on the aircraft and the many download variations have a tendency to reduce flutter speeds. The modes that participate in a store flutter event are generally low-order wing modes. Stores testing is generally restricted to the subsonic range due to aircraft limitations. Flutter speed tends to increase with asymmetric loads and modes become more difficult to excite in such configurations. When doing a symmetric stores loading test, it is important that the loads are as truly symmetric as possible—that is, everything on one side of the airplane weighs the same as everything on the other side. This should be verified by careful mass properties tracking of stores, racks, and pylons. Fuel distribution should also be watched carefully. The aircraft-to-pylon, pylon-to-rack/launcher, and rack/launcher-to-store interfaces greatly increase the nonlinearities which can create analysis difficulties. Care should be taken to reduce these ‘rattles’ as much as possible. It is critical that such attachment fittings as rack sway brace bolts be torqued down similarly and to maintenance specifications. Since the flutter speed of external store loading configurations are occasionally influenced by acceleration loads, such maneuvers as ‘windup turns’ (see Section 5.4.1.1) may be used to produce these accelerations.

Exciters have been incorporated directly into the stores or pylon/racks/launchers. This helps to ensure that the store is adequately excited without having to be concerned with amplitude or frequency attenuation through the intervening structure between the exciter and the store. A vertical and lateral accelerometer at the tip of the store, perhaps at the front and rear, and maybe on the pylon, are very common instrumentation installations (Figure 80).

Serious store oscillation or flutter problems can be remedied in whole or in part by the addition of isolators between the various components, or between the airplane and the store components. These usually take the form of dashpots to change critical frequencies, such as missile launcher pitch, and reduce the potential for adverse coupling. Slight changes in the store location can produce beneficial mass redistribution or move the store out of an adverse flow field.

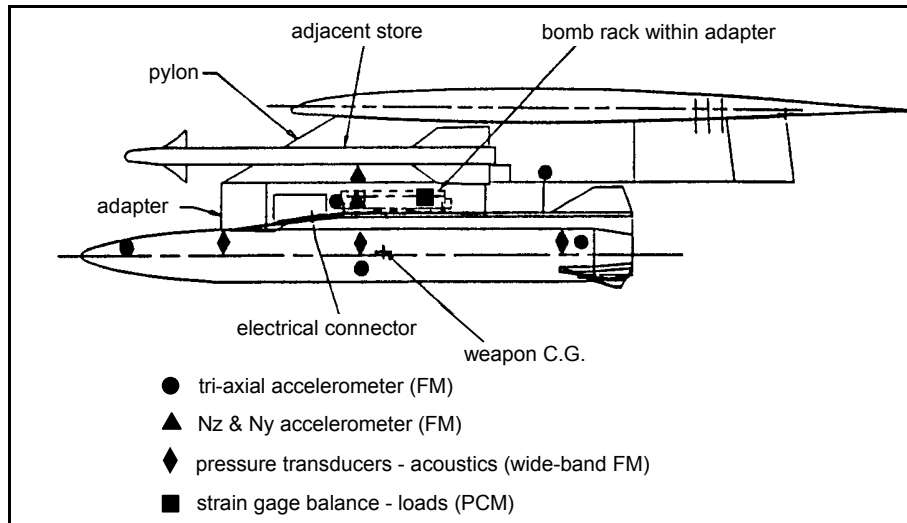


Figure 80 Example Store Flutter Instrumentation Installation

6.9 Rules of Thumb

Certain facts derived from practical experience in the last 80 years of flutter flight testing are worth recording.

a. Elevated AOA seldom aggravates flutter except where vortex shedding may act as an unsteady forcing function.

b. An increase in distributed structural mass will tend to decrease natural frequencies while an increase in stiffness will tend to increase natural frequencies. Adding mass ahead of a surface's center of gravity will tend to lower torsional or rotational frequencies.

c. In manned aircraft, modal frequencies up to 60 Hz, but occasionally as high as 100 Hz, are of concern in flutter prediction depending upon the design. Flutter testing seldom addresses frequencies above 30 Hz unless modes beyond this are considered critical. Damping values on the order of 0.01 to 0.30 G are to be expected.

d. Control surface flutter modes may be altitude-dependent, but few other types of flutter have displayed such a tendency.

e. As the number of control surfaces increase, the higher the order of the modes that may participate in a flutter event. Generally, only a few modes above the fundamental modes are important as these lower-order modes are more efficient at extracting energy from the airflow. However, for the F/A-18, with two leading edge and two trailing edge control surfaces, modes as high as the 25th in ascension of frequency needed to be considered.

f. In general for wings, when torsional rigidity alone is increased, flutter speed also increases. However, when bending rigidity alone is varied, only a small difference in the flutter speed is seen. The minimum flutter speed will usually occur when the flexural rigidity becomes so large that the frequency of the uncoupled oscillation is equal to that of the uncoupled torsional oscillation. Further increase in this rigidity increases the flutter velocity.

g. Control surface backlash or free-play should be kept to less than 0.25 degree to assist in avoiding buzz.

h. Most structural modes can be expected to show an increase in frequency as airspeed is increased because of aerodynamic 'stiffening.'

i. Asymmetrical mass distribution (fuel, external stores) tends to be stabilizing, increasing the flutter speed.

SECTION 6 REFERENCES

1. Bisplinghoff, R.L., Ashley, H. and Halfman, R.L., *Aeroelasticity*, Addison-Wesley Publishing Company, Menlo Park, California, 1955.
2. Bisplinghoff, R.L. and Ashley, H., *Principles of Aeroelasticity*, Dover Publications, New York, New York, 1975.
3. Fung, Y.C., *An Introduction to the Theory of Elasticity*, Dover Publications, New York, New York, 1969.
4. Garrick, I.E., A Survey of Aerothermoelasticity, *Aerospace Engineering*, AIAA, Washington D.C., Vol. 22, No. 1, January 1963, pp. 140-147.
5. Jones, W.P., ed., *Manual on Aeroelasticity*, AGARD Vol. V, London, England, 1960.
6. Rodden, W.P. and Harder, R.L., *Aeroelastic Addition to NASTRAN*, NASA Contractor Report 3094, 1979.
7. Sanford, M.C., Irving, A. and Gary, D.L., *Development and Demonstration of a Flutter-Suppression System Using Active Controls*, NASA TR R-450, December 1975.
8. Van Nunen, J.W.G. and Piazzoli, G., *Aeroelastic Flight Test Techniques and Instrumentation*, AGARD-AG-160, Vol. 9, AGARD, London, England, February 1979.
9. Weisshaar, T.A., *Aeroelastic Tailoring of Aircraft Subject to Body Freedom Flutter*, AFWAL-TR-83-3123, AFWAL, Wright-Patterson AFB, Ohio, November 1983.
10. Zimmerman, Norman H., *Prediction of Flutter Onset Speed Based On Flight Testing at Sub-Critical Speeds*, in AIAA/AFFTC/NASA-FRC Conference on Testing of Manned Flight Systems, 4-6 December 1963.
11. *Military Standard Airplane Strength and Rigidity, Flutter, Divergence and Other Aeroelastic Instabilities*, MIL-A-008870.
12. *Aeroelasticity, Chapter 12, Flying Qualities Theory and Flight Test Techniques*, USAF Test Pilot School, Edwards AFB, California.
13. Norton, William J., Captain, USAF, *Random Air Turbulence as a Flutter Test Excitation Source*, Society of Flight Test Engineers 20th Annual Symposium Proceedings, September 1989.
14. Norton, William J., Captain, USAF, *Limit Cycle Oscillation and Flight Flutter Testing*, *Society of Flight Test Engineers 21st Annual Symposium Proceedings*, August 1990.
15. Scanlan, R.H. and Rosenbaum, R., *Introduction to the Study of Aircraft Vibration and Flutter*, Dover Publications, New York, New York, 1968.
16. Farley, Harold C., Jr., and Abrams, Richard, *F-117A Flight Test Program, Thirty-Sixth Symposium Proceedings*, Society of Experimental Test Pilots, 1990.
17. Flomenhoft, H.I., *The Revolution in Structural Dynamics*, Dynaflo Press, Palm Beach Gardens, Florida, 1997.

7.0 GROUND VIBRATION TESTS

7.1 Introduction

The concept of the ground vibration test ([GVT], sometimes referred to as a **ground vibration survey**) was first introduced in Section 6.5.2 as a critical ground test preceding a flight flutter test program. The purpose is to determine the true frequency, mode shapes and zero-velocity damping of the most important structural modes of vibration. The results can then be used to update mathematical models that are used to predict the flutter susceptibility of the aircraft, and to assist in identifying the modes in flight test data. The GVT is very complex, with many factors which can effect the validity of the resulting data. The reader will need to refer to Sections 4.0, 11.0, and 12.0 for explanations of dynamics terms, data presentation formats, and signal processing techniques while reading this chapter. Because the GVT is so complex, it is difficult to fully explain all aspects of it in a short chapter. Readers are strongly encouraged to observe or participate in a GVT when possible. Reading GVT reports can also provide useful insights.

7.2 Overview

A basic illustration of the typical GVT is in order before delving into details. The aircraft or aircraft component should be structurally as close to the final production configuration as is practical. The **rigid body responses** of the airplane (that is, those obeying Newton's laws of motion) must be isolated and their frequencies reduced below the lowest structural mode so they do not obscure the elastic responses that are sought. These rigid body modes are roll, pitch, yaw, and translation about or along the three axes (see Section 2.3.1). In most cases the GVT will be conducted with the aircraft on its landing gear, and the plane will have unique rigid body reactions in this condition. Special measures can be taken to '**suspend**' the plane to reduce the rigid body frequencies. The idea is to reduce the influence of boundary conditions to simulate the in-flight **free-free condition**.

Structural responses are most often sensed with accelerometers (Section 10.3) attached to the surface of the airplane. Usually, only one or two axes of motion are of interest at any location, but tri-axial accelerometers are still frequently used. The tips of aero surfaces (wings, horizontal and vertical tails, control surfaces), fuselage extremities, engine nacelles, and pylon or stores are the typical positions for the accelerometers. The test may involve dozens of transducers and associated wires which require careful organization to avoid confusion and safety hazards. When the excitation to the test article has begun, it is important to allow time for the transient portion of the forced response (see Section 4.3.2) to die away to the steady-state condition before taking data. The structural response over a broad frequency band is usually followed by a **survey** at a single frequency. The survey entails moving a '**roving**' **accelerometer** to pre-selected positions on the structure so that responses at positions other than the few fixed accelerometer locations can be obtained and the entire mode shape clearly seen and positively identified. Animated mode shapes can be displayed on a computer screen for this purpose. There are some mathematical analysis techniques that do not require a survey.

The excitation of the aircraft structure is most often produced by **electrodynamic shakers**. These are essentially electric motors which cause a center **armature** to translate up and down as a function of the applied current. The armature of the shaker is attached to the structure of the aircraft by a **sting**. The surface on which the shaker is placed will respond to the shaker dynamics and can generate rigid body shaker motion that will produce confusing results. Therefore, measures to suspend the shaker may need to be taken to reduce or increase its rigid body frequencies so they are not within the frequency band of the test subject which is of interest. There are many types of shaker inputs that can be used for different results, and more than one shaker may be used at the same time.

7.3 Underlying Assumptions

The GVT rests on three basic assumptions; stationarity, linearity, and reciprocity. The first of these assumptions is that the responses will not change over time. This principle of **stationarity** means that, all else remaining the same, the test can be done at any time of the day and on any day of the week and the results will be the same. Since wind can rock and buffet the airplane during the test, causing extraneous and unaccounted inputs, the test should be done indoors and in an area without strong air currents. Since temperature changes can alter the structural response through thermal expansion, the temperature at the test location should be regulated to within a range of about 10 degrees Fahrenheit. Fuel leaks, hydraulic leaks, people climbing on the machine, and other such controllable factors can also affect the results by violating the stationarity assumption.

For consistent results, it is important that the structural response is not appreciably nonlinear with input force. **Linearity** demands that the test be conducted in the force region in which the response is linear with increasing force levels. **Linearity** checks are discussed in Section 7.9. However, by its nature, an aircraft structure is nonlinear because of the thousands of fasteners and numerous joints.

Even if the excitation is made at only a single point, the structural response will typically be recorded from several other locations simultaneously. This is permitted by the principle of **structural reciprocity**. **Maxwell's Reciprocity Theorem** states, "for real structures, the motion at one point in the structure due to a force at another point is equal to the motion at the second point due to the same force applied at the first point." Thus, certain symmetry is to be expected. Outputs and inputs can be swapped with the same results, meaning that the associated frequency response functions ([FRFs], Section 11.3) would be identical. Reciprocity can be checked by comparing FRF plots from two stations with the excitation applied at each in turn. Significant differences such as frequency and phase shifts for the same modes, poor modal resolution, or missing modes, indicate that nonlinearities and nonstationarity are adversely affecting the data.

Another essential assumption is that a typical mode can be excited at any point in the structure (except where the mode shape has zero displacement at the node line described in Section 4.5.2). The modal parameters are global and can be estimated from FRFs taken anywhere on the structure. It is still wise to take redundant measurements to ensure that the various experimental errors that can crop up are not adversely influencing the results.

7.4 Preparation

A GVT is one of the most complex and expensive aircraft ground tests that can be performed. It is also one in which the data is most subject to undesirable influences and subjective interpretation. There are any number of problems which can render the test results questionable or useless. It is essential that the test be done properly the first time. Careful test preparation will help to keep irate supervisors and analysts at bay. A detailed test plan is essential if wasted time, high costs, and disputed results are to be avoided. The GVT is typically preceded by a detailed mathematical analysis of the test subject. This will provide insight into the frequencies of the most significant modes of vibration. This helps in focusing the GVT team's attention on the most important modes and in identifying the modes which are found. It is possible to do a GVT without this analysis, but it will likely require much more time than would otherwise be the case.

7.4.1 Aircraft Configuration

As mentioned earlier, the test article should structurally be as close to the final production configuration as possible. Incidental components like certain instruments, avionics boxes, electrical lines, antennas, etc., need not be in place for the GVT if they do not significantly affect structural response or the inertia of the test item. In fact, many such components will respond at their own resonant frequencies which are of little interest to the structural dynamicist. These responses may be detected by the test sensors and show up as noise or misleading signals in the data. Such noise is referred to as **nonlinearities**. Tests of individual components (control surfaces, for example) can be done separately as a matter of convenience. This allows their responses to be accounted for more readily during the complete aircraft test where high modal density can make mode separation and identification difficult.

The objective is to get the aircraft into as close to a flight configuration as practical. Physically, this means access doors, canopies, and panels should be closed. Systems-wise, this means that at the aircraft hydraulics (or at least the hydraulic system controlling the control surfaces) should be powered. The hydraulic or electrical control surface actuators must be powered to provide representative in-flight reaction stiffnesses, although unpowered controls may be tested as a check of failure conditions. A problem here is that hydraulic power ground carts may not be able to supply the required flow rate required to represent in-flight conditions (actuator stiffness) without flow fluctuation. Electronic flight controls are seldom required for the GVT but are used in the similar ground resonance test (GRT, Section 8.4). Controls should be correctly rigged with the proper balance weights. Powering some of the electronic systems may also be necessary. It may be necessary to temporarily defeat some fail-safe devices to achieve this simulated flight condition.

If the aircraft is capable of carrying external tanks and stores, it is advisable to test the response of the structure and these external components as well as the 'clean' configuration. Fuel distribution within the aircraft may significantly affect the modal characteristics and so should be considered when selecting test configurations. It is usually wise to test at several fuel loading configurations. The associated hazard of having a fueled aircraft within a hangar or other shelter may require the substitution of some inert fluid (as long as the density is nearly the same as fuel) or moving the test to an outside location.

Engine vendors often require that the engines aboard the test aircraft be rotated periodically in the course of the test to prevent flat spots from developing on bearings. The rotation can be done with compressed air blown through the engine or by some other means.

7.4.2 Reducing Nonlinearities

The problem of nonlinearity noise was introduced in the last section. Reducing these nonlinearities will help to ensure clean and representative frequency response data. When attempting to curve fit a linear math model to the data from a necessarily nonlinear structure, reducing the nonlinearities is critical for a faithful match and good approximations to the modal characteristics extracted from that model. It may be desired to evaluate the amount of nonlinearity in a structure. In this case reducing nonlinearities, particularly by some of the excitation or analysis techniques discussed later, is not necessarily desirable.

The easiest means of reducing such nonlinearities is to remove the component causing the rattle. However, this is not always desirable or practical. The distributed mass of such articles within an airplane structure can make up a significant mass of the structure and removing them can change the modal response. Normal maintenance servicing (tightening nuts, adding washers) may eliminate the source of the problem. Unimportant components such as gear doors, spoilers, etc., can be pinned or tied off against one end of its freeplay band as long as it does not artificially increase stiffness elsewhere in the structure, which will affect the validity of the GVT results.

7.4.2.1 Preloads

Freeplay in the flight controls or other movable aircraft components can produce the annoying nonlinearities that corrupt response data. Attempts to remove this freeplay by normal rigging and maintenance efforts is not always successful. An additional method to remove the freeplay is to preload the surface. This may consist of nothing more than taping the component off to keep it from rattling. Large components such as a control surface may require such measures as hanging a mass from the trailing edge to artificially increase the inertia of the component and hold it against one end of the freeplay displacement range. The amount of mass used depends on how effective the preload is in reducing the problem. But, again, care should be taken to ensure that such added mass is a very small percentage of the overall mass of the structural component. A soft spring must be placed between the hanging mass and the structure to reduce the dynamics associated with the preload. Sometimes a bungee of a suitable spring constant is simply connected to the control surface and the floor, a wall, or whatever is stiff and convenient. Of course, preloads on control surfaces cannot be used when the surface rotation frequency is being sought. In general, preloads should be avoided when possible because of the change in stiffness and mass distribution that they introduce to the structure. Another method of preload in combination with the shaker is discussed in Section 7.6.3.

Another sort of preload that can be helpful are those used to reduce the influence of structural members in order to isolate some other component. An example may be to pre-load a wing so that shaking on the aileron will excite only aileron modes within the frequency range of interest. This can be done by placing heavy bags of shot on top of the wing, placing jacks under the wing pressing against the bottom surface, placing a sling under the wing and pulled from above, or a combination of these. These will artificially stiffen the wing and greatly increase its resonant frequencies beyond those of the aileron.

7.5 Aircraft Suspension

In most cases, the GVT will have to be conducted with the aircraft resting on its landing gear. If the gear is attached at the fuselage this is generally acceptable as long as fuselage modes are not critical. However, if the gear is attached at the wing, the modal responses measured on the gear may be so dissimilar to an in-flight condition that an on-gear GVT would be unacceptable.

A form of soft suspension can be placed beneath the tires to help replicate in-flight modal conditions. The suspension system will have resonance's that are of no interest, and the gear struts and tires will have similar reactions which must be reduced or eliminated. The plane will also have the usual rigid body pitch, roll, yaw, and translation modes while on its gear, or suspended which must also be recognized or reduced so that they are not confused with actual structural dynamics. The landing gear modes are easier to reduce to this level than a series of jacks holding the aircraft up so that the gear can be retracted. For this reason, conducting a GVT with the plane on jacks is seldom practical. It may be possible for the small planes to be hung via **bungees** so that the gear can be raised. For this method, the cantilever response of the crane holding the aircraft up must be considered as well as that of the bungee. In any case, the undesired rigid body responses must be accounted for and reduced to about one-third of the first aircraft flexible mode frequency. The first step in a GVT should be to actually check the aircraft rigid body frequencies to ensure that they are low enough so as not to influence the data being sought.

For the on-gear condition, the gear struts can be depressurized and the tires partially deflated. Placing the plane on specially prepared pads with adjustable reaction frequencies (usually a pneumatic flotation system) is the most desirable solution. Another method has been to place the strut axles in bungee slings. Bungees can be obtained with various stiffnesses and even combined in parallel for the desired characteristics. The length of the bungee(s) and the mass of the airplane will determine the pendulum frequency of the suspension. **Slip plates** riding on a film of oil placed beneath the tires have also been used successfully to reduce the lateral rigid body mode.

If only a component of an aircraft is being tested then it must be supported in a fixture with rigid body modes that will not affect the reading of true structural dynamics of the test subject. The fixture is usually very rigid by nature, so the easiest means of ensuring that its dynamics do not influence the test results is to make sure that it is stiff enough to have its lowest flexible frequency above the highest frequency of interest for the test subject. The frequencies of the fixture must be checked the same way those of the entire airplane are checked. For control surfaces, actuator and hinge stiffnesses, either real or simulated, must be provided.

7.6 Electrodynamic Shakers

Structures such as space satellites may be excited as a unit by placing it on a **vibration table** for a **base excitation**. This approach may also be employed in laboratory tests of such items as ejection seats, avionics boxes, etc. This, however, is seldom practical for an aircraft or major aircraft structural components, and the venerable shaker is most commonly used.

7.6.1 Characteristics

The size or weight of the shaker is a direct function of the frequency range in which it can respond and the mass of structure it can effectively displace or excite. Shakers vary in size from units that fit in the palm of the hand, to monsters weighing hundreds of pounds used to shake buildings. Apart from the mass, there are many other characteristics that are important to consider when choosing a shaker for a test. An essential piece of equipment used with the shaker, which is not discussed, is the power amplifier that boosts the excitation signal

to the level necessary to produce the desired force amplitude, which then powers the shaker. A schematic of a typical GVT equipment arrangement is provided in Figure 81.

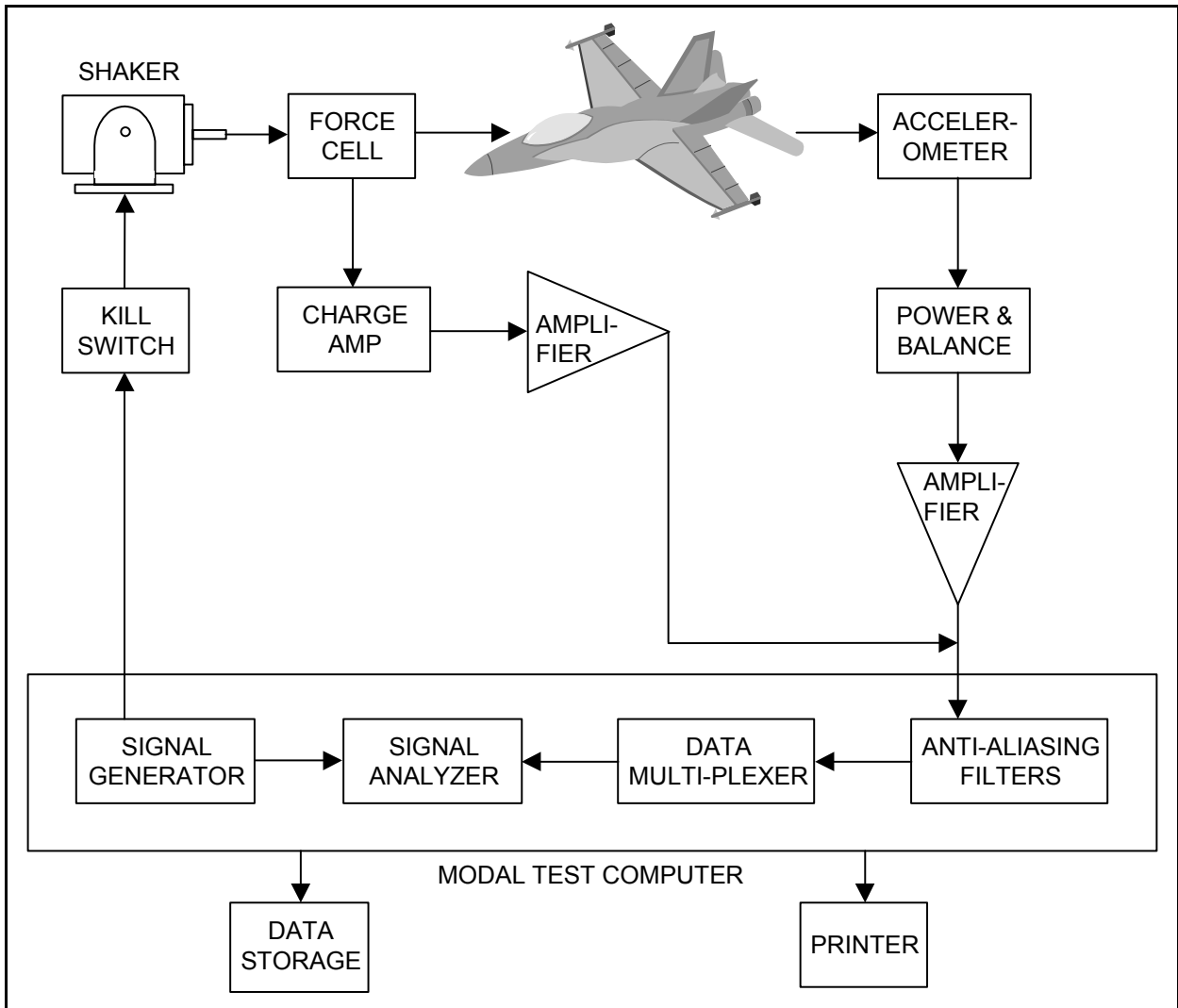


Figure 81 Schematic of Typical Ground Vibration Test Equipment Arrangement

7.6.1.1 Physical Features

The electrodynamic shaker is essentially an electric motor with the center armature translating axially instead of rotating. Hydraulic shakers have been used for very large structures, but they are seldom useful for aircraft GVTs. The frequency and amplitude of armature displacement are a function of the input current to the shaker. The mass of the armature will then determine the actual magnitude of the force produced. The applied current and motion of the armature can create detrimental heating that typically requires a **blower** to be attached to the unit for cooling.

7.6.1.2 Selection

A reasonable requirement in shaker selection is that the output force actually displaces the structure to which it is attached. If the structural inertia is greater than the force, then the shaker may simply displace itself instead of the test subject, or the armature will simply resist displacement. Another vital limitation is that the

armature mass be a small fraction of the structural mass. With the armature/sting attached to the structure, it essentially becomes part of the structure and contributes its mass. This is referred to as **effective mass** and will unavoidably alter the response characteristics which are sought. One method for getting a handle on this effect is to add mass to the armature, twice the armature/sting mass for example, and observe the amount of the shift in frequencies that result.

If you wish to stop the shaker abruptly in order to allow the structure to damp out naturally, the ability of the armature to stop with few overshoots, akin to a spring response, will be an important consideration. Actually, this 'spring' characteristic is always present when the shaker is operating. Because of the inertia and spring characteristics of the armature, the output of a load cell placed between the shaker attachment and the test subject should be used when the input force is needed (for a transfer function, for example) and not the signal sent to the shaker. Another consideration, although one that is seldom a problem, is the stroke of the armature while attached to the structure. Large displacements could produce significant rigid body motion that will feed into other shakers that may be operating simultaneously, or the structure may even be overloaded and damaged.

Shakers are most often rated by their electrical load, weight, and maximum force displacement. Actually, these are all related in ways far too complicated to elaborate on here. Suffice it to say that a 50-pound shaker can produce a larger force than a 20-pound shaker. The 50-pound shaker will give much better low-frequency inputs by virtue of its armature mass, but will be unable to produce appreciable displacements at high frequency for the same reason. It is sometimes possible to add weights to the top of the armature to increase its mass. For low-frequency inputs, relatively large strokes are necessary to get measurable excitations, so checking the maximum stroke capability of the unit is recommended. At higher frequencies, large strokes are less likely, and eventually become impossible anyway, due to the inability of the shaker to respond fast enough (**attenuation**). A typical 50-pound shaker used in aircraft GVTs will usually be useful to around 2,000 Hertz (Hz).

7.6.2 Suspension

As with the reduction of the aircraft rigid body modes, the reaction of the shaker and whatever surface the shaker is placed on must be considered and adjusted when necessary to beyond the frequency range to be investigated. At least the rigid body dynamics of the shaker will then be effectively decoupled from those of the test article. Placing the shaker directly on a concrete floor is best because such a floor can be considered to have infinite stiffness when compared with an aircraft structure. So, the response of the floor transmitted to the structure through the shaker case and armature will be of such high frequencies and low amplitudes that it will not influence the structure to any appreciable degree. However, it is often necessary to place a shaker on a stand to get it close to a portion of the aircraft, such as a vertical tail. In this case the reaction of a comparatively flimsy maintenance stand can produce dynamics which will feed into the aircraft structure in the same way as pure armature displacement. For this reason, shaker stands tend to be very heavy steel constructs. A careful choice of stand and recognizing the frequencies in which the stand influence will be felt (a minor GVT of the stand may be necessary) can all help to reduce this problem. A special suspension system can be used for the shaker the same as for the aircraft.

Occasionally, it is necessary to hang the shaker from a crane in order to excite a particularly inaccessible part of the plane (high vertical tail, for example). The shaker should be attached to the crane by a bungee or other damping system to reduce the vertical displacement frequency that is a characteristic of the crane arm bending and suspension cable stretching. Pendulum motion, however, is a frequent problem. This frequency should be identified by calculation or by running the shaker through a frequency sweep and observing where the pendulum motion occurs. The pendulum frequency can be reduced simply by altering the cable length between the crane arm to the shaker or by adding mass to the shaker unit. The latter method will also help to assure that the structure is displaced by the armature and not the shaker case.

7.6.3 Attachment to the Structure

It is theoretically possible to extract all of the necessary modes from an aircraft using a single exciter location, a wingtip for example. In practice, though, a structure as complex as an aircraft requires several

locations to be used to get enough energy into the modes to clearly distinguish them and to obtain useful modal parameters. For example, a shaker input on one wingtip may be inadequate in exciting the opposite wing via the carry-through structure to give suitable resolution to all the modes of interest. Such locations as the wingtips, horizontal tail tip, vertical tail tip, fuselage extremities, control surface trailing edge, pylons, engine nacelles, and external store extremities are the most common excitation points. It will be obvious whether a vertical, lateral or longitudinal excitation is best, especially when mathematical analysis has already provided an initial prediction of the modes of interest. Multishaker techniques would use similar input locations; just several used simultaneously.

If the modes are not being excited adequately, the attachment point may be near the elastic axis or node line of the motion (imaginary line about which deformation takes place). Moving the input point a few inches may cure this problem. At a wingtip, for example, the shaker input should be made near the leading or trailing edge of the structural box beam or spars to ensure that both bending and torsion modes are excited.

The shaker armature is typically attached to the structure through a sting (also known as a **quill** or **thruster**). This is typically a steel or aluminum shaft of appropriate length which has a fairly high compression and tension stiffness to ensure that its natural frequencies are of no concern. The sting will likely incorporate a thin steel rod. The rod acts as a **structural** or **mechanical fuse** such that it will fail at a specified tension or off-axis load during input to the structure. This is a safety measure to ensure against damage to the article under test or shakers which cannot abide off-axis loads. The thin member also allows some needed lateral flexibility since the structural displacements are usually more of a rotation than a pure translation. Another technique of attachment requires an armature with a hole that passes directly through its center. A piano wire attached to the structure passes through this hole. The free end of the wire is attached to a bungee or some other elastic anchor that permits the test item to be preloaded (see Section 7.4.2.1). The armature and wire are then attached together so that when the shaker is activated they will move together. This approach allows a preload without additional equipment, reduces effective mass, and incorporates the functions of a structural fuse without additional components.

The sting should be aligned with the axis of motion to be excited, but need not be aligned with more than 'eyeball' precision. Slight misalignments will only mean that some of the input force is going into more than one axes of motion, and this is usually tolerable to a small degree. Having some input energy expended in bending of the thruster is also tolerable. It is sometimes practical to maintain a preload in tension on the thruster to ensure against these bending moment errors.

A load cell is typically placed between the shaker and the thruster to permit monitoring of the input force. This is done both to ensure against overloading the test subject and for linearity measurements, as explained later. It is important that the load cell input axis be precisely aligned with the armature axis for a valid input function to be measured if transfer functions using this signal are planned. Placing an accelerometer at this same point (often called the **reference accelerometer**, as is any other fixed accelerometer) permits a **driving point measurement** to be taken. Other measurements are termed **cross point measurements**. The distinctions between the two are shown in Figures 82 and 83. In the imaginary plot of the driving point response, all of the resonant peaks fall on the same side of the zero axes. Response data taken at the driving point will have distinct **antiresonances** or **nodes** between every resonance, minimum value valleys, when plotted with a logarithmic amplitude scale. The phase is also seen to lead as the magnitude enters an antiresonance and then lags through a resonance. All of the modes are necessarily in phase with each other and the imaginary resonant peaks need not all lie on one side of the zero axes. This is not necessarily true at the cross points, as shown in Figure 83. Clear antiresonances will not appear between two modes that are not in phase.

The end of the sting can be attached to the structure by means similar to the attachment of the accelerometers. Section 10.3.4's discussion of accelerometer attachment is generally applicable to thruster attachment. Attachment can be by screwing into an existing screw hole in the structure or a specially prepared hole, gluing, or attachment to a pad held on by bee's wax. A vacuum pad can also be used to hold the sting to the structure. This allows easy moving of the attachment, but a vacuum source must be available, with the airhoses and pumps add additional complexity to an already cumbersome experimental setup.

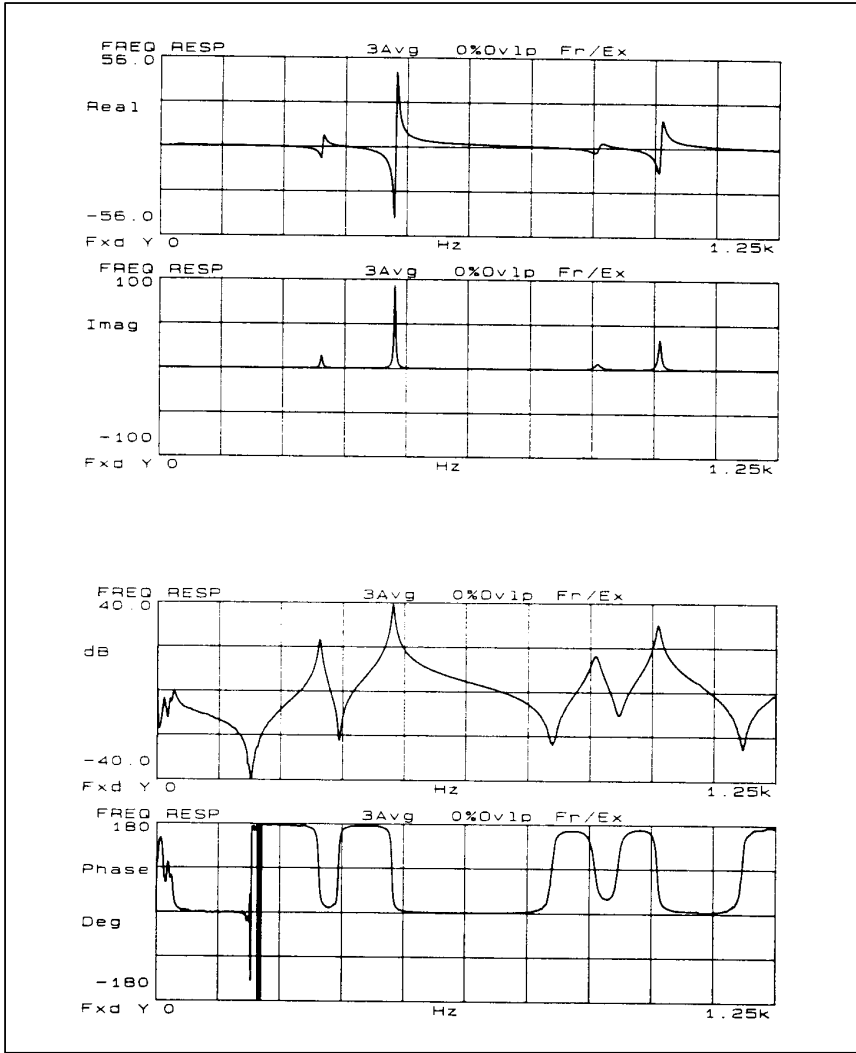


Figure 82 Characteristics of a Driving Point Measurement

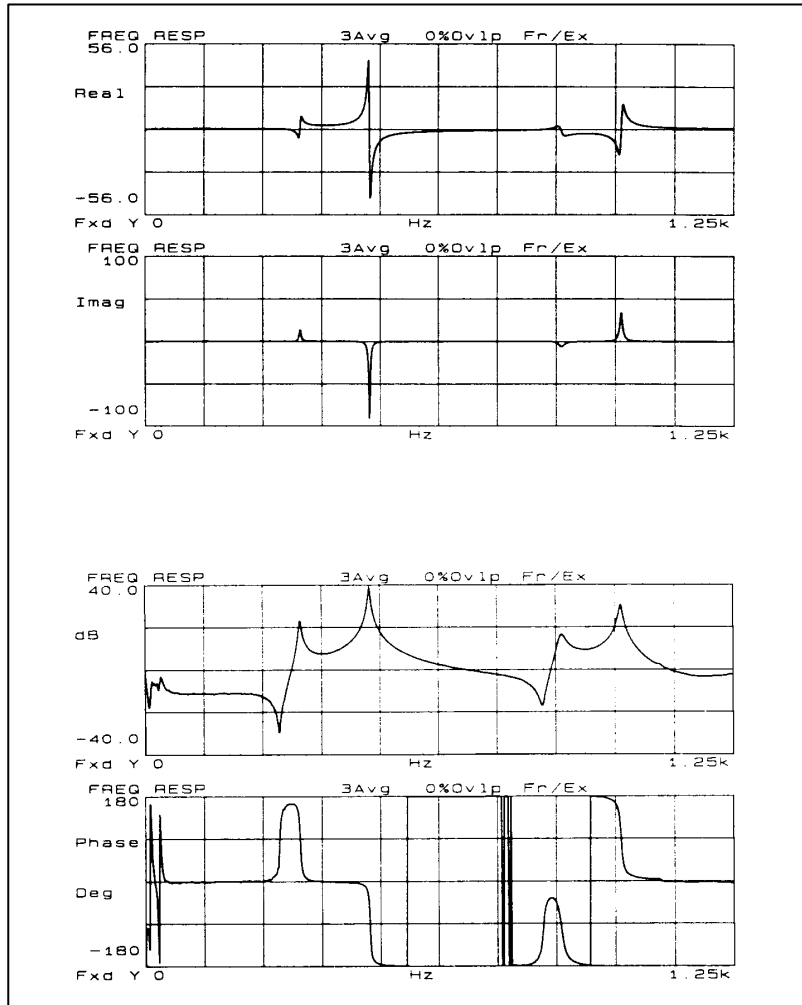


Figure 83 Characteristics of a Cross-Point Measurement

7.6.4 Impedance Mismatch

The signal amplifier and the electrodynamic shaker do not pass an electrical signal completely unaltered. Both will have their own individual capacitance, resistance, and inductance. This **electrical impedance** between the two units should be matched or the excitation signal sent via a cable to a shaker will not be seen by the structure exactly as produced by the signal generator. The electrical impedance of the shaker is a function of the amplitude of the armature displacement. The force level throughout the bandwidth of the signal will be altered. It is possible that the excitation at a critical frequency will be changed to such a low input level that the structure will not be adequately excited. This problem may go completely unnoticed, with the misleading results having serious consequences during later flutter analysis and flight testing.

The mass and spring-like characteristics of the shaker are a form of **mechanical impedance** that can alter the test results in ways that may be difficult to define quantitatively. The shaker force tends to drop off at resonance because the structure is resisting less. This makes the force measurement more susceptible to noise.

If an impedance mismatch problem is suspected during the course of the test, then a trial and error substitution of cables, amplifiers and shakers are the usual remedy. Simply moving the shaker to a location where the mechanical impedance has less effect can also improve the situation. A more rational approach is to

characterize the impedance of the system before testing to avoid a mismatch. Changes to the setup can then be made or the input signal can be tailored to ensure that the structure is excited as desired.

7.7 Transducer Installation

The actual mechanics of accelerometer installation is covered in Section 10.3.4. The selection of accelerometer location is very important for accurate data that can be readily correlated with an analytical model. The reference accelerometers should be placed in what are called ‘**hot spots**,’ where a large response for all anticipated modes can be expected. This would certainly include where the force is being applied. Placing an accelerometer at the root of the wing would be of very limited value because of the very small motion that would actually occur there. A location at the midchord of the wing may be very close to the elastic axis where little motion also occurs. The sensors should be aligned with some structural axes of the test subject. For an entire plane, this would probably be either parallel to or perpendicular to the floor, and parallel to and perpendicular to the aircraft centerline. To achieve this on curved surfaces, the sensors will need to be placed on specially formed blocks fastened to the surface which transitions from the curve to a flat, aligned area. The alignment should be done with care, but location marking using a yard stick referenced to normal panel lines of the airplane will usually be adequate.

Sensor locations relative to the modes of interest are important. For example, to positively identify a wing torsion mode with reference accelerometers alone or without referring to analysis results, it is necessary to place a transducer at the leading edge and another near at the trailing edge of the surface. Determination of whether a mode is antisymmetric or symmetric will require transducers on both sides of the aircraft centerline. Accelerometer responses from one side of the plane can be added or subtracted from the response at the mirror image location on the opposite side of the plane, or from the leading and trailing edges of a surface, to positively differentiate symmetric and antisymmetric modes, or bending and torsion modes.

One important precaution is to ensure that transducer cables are not free to flap about excessively or strike the structure during excitation as this can produce distorted signals. It may be necessary to tie the cables off to a stand placed next to the plane to reduce flapping.

7.8 Excitation Techniques

While the electrodynamic shaker is the most commonly used excitation source for aircraft GVTs, there are many signal forms available to drive the shaker. The driving signals should be selected after considering the nature of the structure and the desired data resolution. Certain inputs may fall out of favor occasionally or particular equipment may not be able to produce some of the forms discussed here. However, no single method of excitation or data/signal processing is superior in every application. Pros and cons of the various methods are summarized in Table 2. It is important for the engineer to have some familiarity with the typical inputs that have been used over the last 25 years. Keep them all in mind as alternatives when unique problems crop up.

7.8.1 Operating Inputs

It is occasionally possible to use the aircraft itself or its ambient environment to excite the structure. These so-called operating or **self-operating inputs** might include programming the automatic flight control system to command rudder motion, the inertia of which will excite modes in the vertical tail and aft fuselage. A manual control input is seldom controlled enough to provide the force levels and frequency content necessary. Simply running the engine(s) might provide sufficient excitation for usable modal data. This approach is typically more trouble than it’s worth, and has found few adherents. The force levels tend to be very small, have dominant characteristic frequencies, and produce poor data. But, for some test articles this is the only practical excitation.

Table 2
COMPARISON OF GROUND VIBRATION TEST EXCITATION FORMS

			Periodic			Transient		
	Sine Steady State	True Random	Pseudo Random	Random	Fast Sine	Impact	Burst Sine	Burst Random
Minimize Leakage	NO	NO	YES	YES	YES	YES	YES	YES
Signal to Noise Ratio	YES HIGH	FAIR	FAIR	FAIR	HIGH	LOW	HIGH	FAIR
RMS to Peak Ratio	HIGH	FAIR	FAIR	FAIR	HIGH	LOW	HIGH	FAIR
Test Measurement Time	VERY LONG	GOOD	VERY GOOD	FAIR	FAIR	VERY GOOD	VERY GOOD	VERY GOOD
Controlled Frequency Content	YES	YES	YES	YES	YES	NO	YES	YES
Controlled Amplitude Content	YES	NO	YES	NO	YES	NO	YES	NO
Remove Distortions	NO	YES	NO	YES	NO	NO	NO	YES
Characterizes Nonlinearity	YES	NO	NO	NO	YES	NO	YES	NO

7.8.2 Transient

Also known as **impulse testing**, this method of excitation is based upon producing individual transient responses of the structure by a sharp, almost-step input which has high frequency content. It can then be repeated as necessary. The major disadvantage of the method is the difficulty in precisely controlling the content of the input.

7.8.2.1 Impact

This approach consists of striking the structure, usually with a special hammer, to produce the transient excitation. The method gives a fairly constant force over a broad band of frequencies. This allows many excitations to be made over the test article in a very brief time, allowing a modal survey (explained later) to be completed very quickly without shakers. Very large hammers are available for large structures but these are impractical for aircraft use because of potential damage to the airframe. The hammer typically has a force transducer or load cell at the head to measure the impulse. The hammer and transducer must be calibrated as a unit.

The frequency content of the impact is inversely proportional to the width of the pulse and the weight of the hammer, and directly proportional to the hardness of the hammer tip. Several types of impact head weights and tip materials (rubber, phenolic, and steel) are available to provide some control over the impact form and duration. A harder tip will excite higher frequency modes whereas a softer one will more effectively excite low-frequency modes (Figure 84). The technique would require a very soft head if frequencies below 20 Hz are sought. In general, a wider force impulse will excite lower frequency modes. The force of the impact is dependent upon the velocity and weight of the hammer (Figure 85). Most impact hammers have additional weights that can be added. However, if the weight of the hammer becomes too great, it will be difficult to avoid multiple impacts for a single blow that will produce poor data.

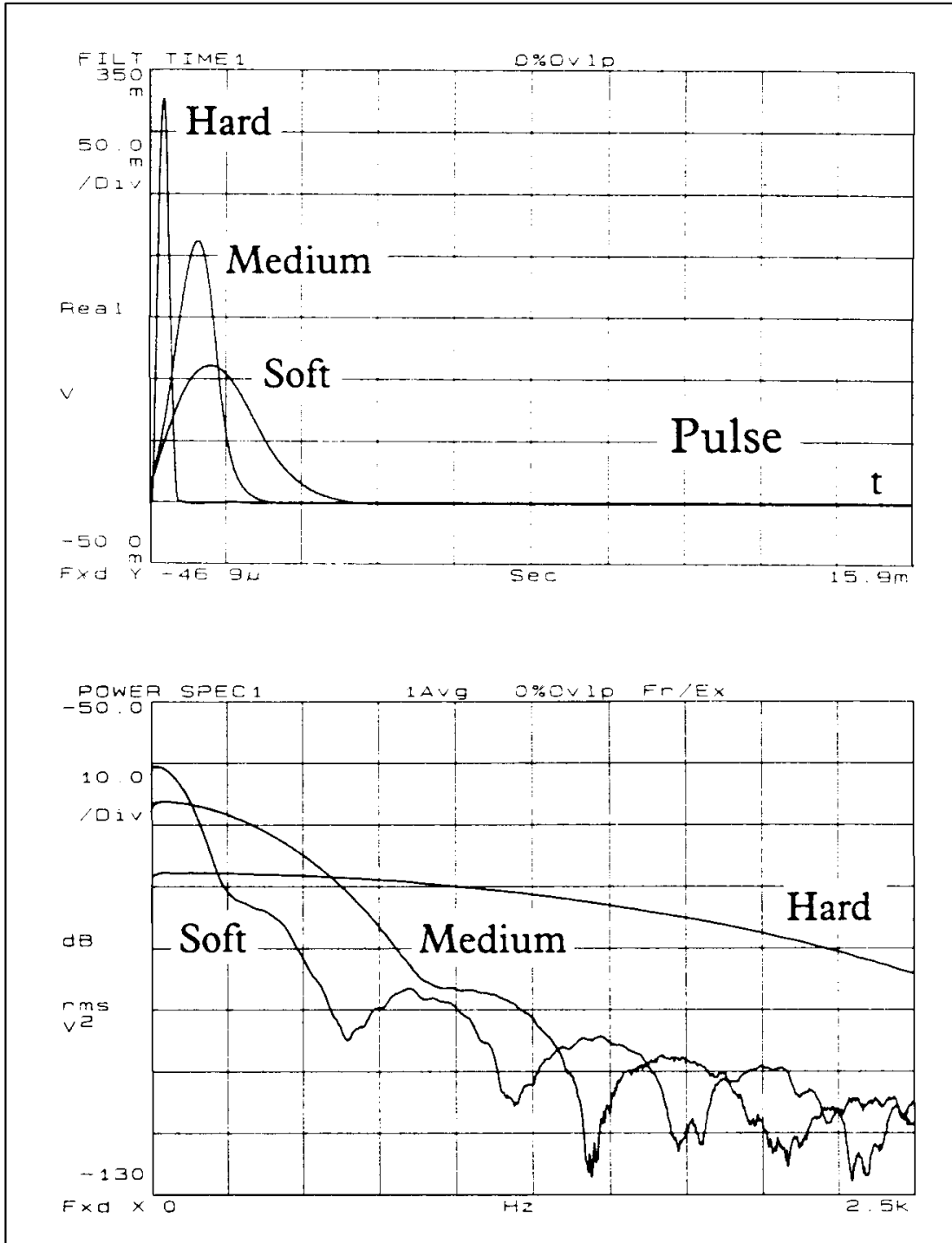


Figure 84 Influence of Impact Hammer Tips

The impact technique offers a particularly easy way of extracting the mode shapes. The response at all selected point on the structure is recorded for an impact at each of these points individually. The magnitude of the imaginary component of the inertance (acceleration/force, see Section 4.4.1) for each response at each

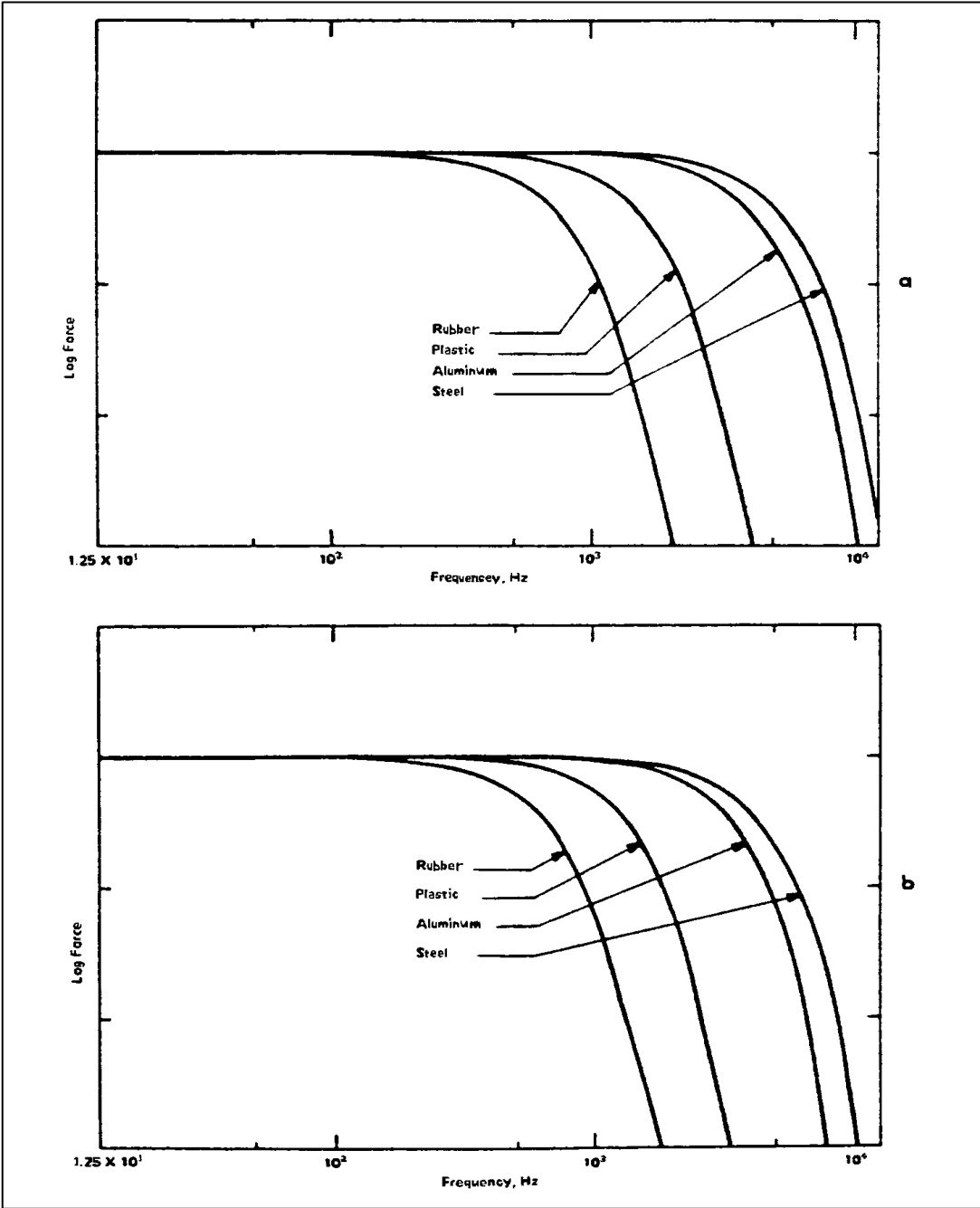


Figure 85 Influence of Impact Hammer Weight and Force (Hammer b with More Weight than Hammer a)

resonant frequency is then determined. For a cantilever beam with four impact/response points (point 1 near the free end, point 4 near the fixed end), the results might look like:

Impact Point	Mode			
	<u>1</u>	<u>2</u>	<u>3</u>	<u>4</u>
1	7.93	15.10	19.50	17.00
2	6.25	-7.31	-28.60	-45.00
3	3.68	-17.50	5.81	32.40
4	1.37	-16.00	32.50	-20.10

where each successive mode has a higher frequency. Each of the columns are then the mode shape for the mode whose frequency is obtained as described in Section 4.5.2. The columns are typically normalized by dividing through by the largest value in the column. By examining the results, it can be seen that mode 1 is the first cantilever beam bending mode, the second mode the second bending mode, and so on.

The impact method is applicable only for very light structures and, because the impact excites many nonlinearities, it is only suitable for relatively linear structures. Checking the coherence of the data (Section 11.3.7) will assist in determining the quality of the results. The method has a low signal-to-noise ratio ([S/N], Section 12.3.5) and so should only be used in a low-noise environment and with equipment possessing a large measurement dynamic range. At best, the frequency response functions (FRFs) are ‘noisy’ and require the averaging of the results of several raps to be useful. Also, since the response of a lightly damped structure may not decay to zero within the sample window, leakage problems are possible (Section 12.3.3). Another principal drawback of impact testing is that the input form is largely unpredictable. It is also difficult to get enough energy into complex structures to excite all of the important modes.

Since most data acquisition systems require sensitivity gain to be set to the anticipated level of the input and response signals, success is therefore, very much dependent upon the technique of the person handling the hammer. It sometimes takes several tries to achieve the right impact without overloading the acquisition system. Hitting too hard also excites nonlinearities. Trial data should be taken in an effort to set the sensitivities properly and train the person swinging the hammer.

7.8.2.2 Step Relaxation

Another form of transient testing, the step relaxation method entails preloading the structure to the desired force level with a high tension but lightweight cable or wire. A step input is produced when the cable is suddenly severed or released to allow the structure to relax to its unloaded state. Because of the sound caused by releasing the restraint, this method is often referred to as a ‘**twang**’ test. This step input produces the transient response. The method is capable of putting considerable energy into the low-frequency end of the spectrum, but is a slow method and can have a complex test setup.

7.8.3 Sine Waveforms

The sine waveforms as a GVT excitation is the oldest and most widely used input. Its principal points of praise are the very good signal-to-noise ratio, less influence from nonlinearities, the ability to visually see the resonances, the good resolution at high frequencies, and the ease of understanding and implementing the method. Its primary problem is the length of time the test takes when compared with the random techniques.

7.8.3.1 Sine Sweep

The sine sweep is often the first part of a GVT, followed by sine dwells at the frequencies identified from the results of the sweep. The sweep involves exciting the structure with a sine waveform that increases in frequency from a set lower limit to a set upper limit that includes the frequency range of interest for the structure under test. The sweep can be done linearly, exponentially, or any other sweep rate method the user can conceive. The sweep is usually logarithmic, increasing in rate with frequency because enough cycles must occur

in the vicinity of a frequency for sufficient energy to be transmitted to the structure. Obviously, more cycles occur in a brief time at high frequencies than at low frequencies. As the input frequency coincides with the normal modes of the test subject, a large amplitude response will result. At least theoretically, all of the modes can be identified from the resulting frequency response function.

As mentioned, the problem with this method is that the sweep must be conducted very slowly to meet the assumption of quasi steady-state conditions. Such a sweep over 50 Hertz could require as much as 15 to 20 minutes. If the sweep is conducted too quickly, shifts in resonant peaks and erroneous damping and amplitude data will result (Figure 86). Even when the sweep is done slowly, the data may only be used as a guide for a sine dwell test or other methods. A common practice is to conduct a sweep with increasing frequency and then repeat it with decreasing frequency. The former will tend to shift resonances to higher frequencies and the latter to lower frequencies. By examining the two resulting FRFs, a more precise estimate of the true resonant frequencies will generally lie between the two slightly separated peaks for each resonance from the two plots. Time averaging of reverse sweeps (Section 12.4.2) can also help in eliminating the shift problem. Transfer function type FRFs do not suffer from the shift at all.

Multiple input tests using a swept sine signal is not uncommon. For example, exciting wing modes with a shaker on each wing using a symmetric or an antisymmetric excitation will provide a much more easily analyzed response than for a single shaker on one wing. It may, in fact, be the only way to get data clean enough to correlate with mathematical analysis results.

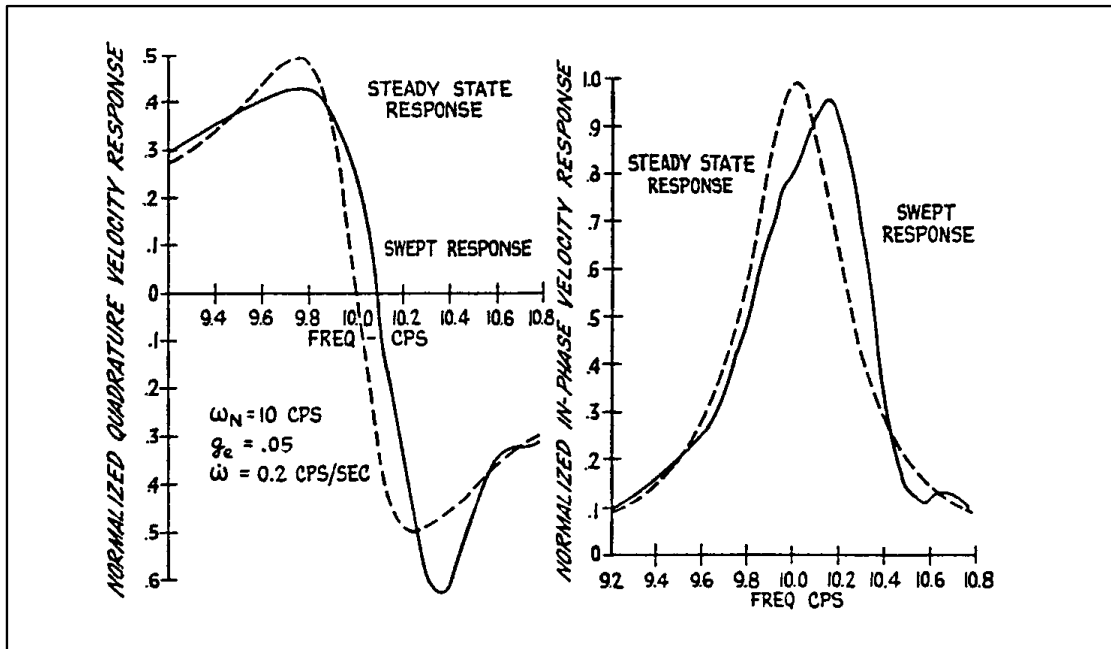


Figure 86 Effect of Sine Sweep Rate on Data

7.8.3.2 Sine Dwell

The ability to apply a steady sinusoidal input to a structure at a constant frequency can permit a careful physical and visual study of the resulting motion. If the mode is properly 'tuned,' the motion at various points throughout the structure will be either in phase or out of phase. This tuning operation consists of slight frequency adjustments and changes to the input force until the response meets the criteria for a **normal mode** (acceleration 90 degrees out of phase with the force, no beating in the decay, etc.). Lissajous figures (Section 11.2.6) or CO/QUAD displays (Section 11.3.8) are used to judge when the mode has been tuned or the quality of the best tuning which can be achieved. Another criterion that might be used is that the measured shaker force drops at resonance because the structure is not resisting the motion as much.

Shakers may have to be repositioned if difficulty is encountered in the tuning. If a mode is not truly symmetric or antisymmetric but shows a disproportionate displacement from one side to another (for example, the wingtip on one side displacing twice as much as the other tip while still in phase), then equal shaker force from two symmetrically placed shakers will not produce a perfectly in-phase response. Instead, the force amplitudes are tailored proportionally to the displacement of the mode shapes at the shaker input locations. This type of response is termed an **asymmetric mode**, and this method of tuning is called the **proportional force method** of shaker excitation. Single input sine dwell mode tuning might be used during a random test where there are very close modes or where nonlinearities complicate the analysis, but setups are common.

7.8.3.3 Chirp

The chirp, or **fast sine dwell**, is a brief logarithmic sweep that begins and ends within the sampling window to reduce leakage effects. The sweep can be repeated as many times as necessary and the results averaged. A series of small chirps can be performed to cover the entire spectrum desired. The result is a reduction in excitation time compared to a slow sweep. As with other sine methods, it is not possible to eliminate all nonlinear distortions. A similar method is the **stepped sine** technique which utilizes brief, discrete sine sweeps at many frequencies necessary to cover the desired spectrum.

7.8.4 Random

The use of random signals as GVT excitation sources has become very popular in recent years because of digital processing and the great reduction in testing time it often allows. However, there are many cautions in the following paragraphs that must be considered when using this approach. Also, because random methods can tend to obscure the nonlinear behavior, a nonconservative overestimation of damping is likely to result.

7.8.4.1 Pure Random

The pure random signal is not periodic in any manner, so it never repeats (Figure 87). A signal generator is typically set up to concentrate the energy of the signal within a bandwidth of interest with a flat spectrum (same level throughout the band). Because of the nature of the pure random signal, there is no chance that the input or the response will be periodic within the sampling window; therefore, a weighting function must be used to reduce the possibility of leakage (Sections 12.3.3 and 12.4.1).

The greatest advantage of pure random is that each succeeding sample of data can be ensemble averaged together to remove noise and nonlinearities (Section 12.4.2), and this is frequently essential to produce useful data. The signal also produces the best linear approximation of a nonlinear system for curve fitting purposes. If the signal is produced by an analog signal generator (often the case for pure random) it may not be possible to tailor the signal to the impedance mismatch of the system. This can prove a major disadvantage of this excitation input.

7.8.4.2 Pseudorandom

The pseudorandom signal has equal, repeated periods of the same random signal and thus, leakage effects are reduced if the period of the signal is the same as the sample period. A reasonably good measurement can also be obtained with just one sample. Because all desired frequencies are being excited during each signal period, the energy input at any one frequency is fairly small. This produces a comparatively low S/N. Unlike the pure random, ensemble averaging will not remove structural nonlinearities and distortions, appearing as spikes in the plots, since these will be exactly repeated during each period of the excitation. This constitutes a major disadvantage of using the pseudorandom signal.

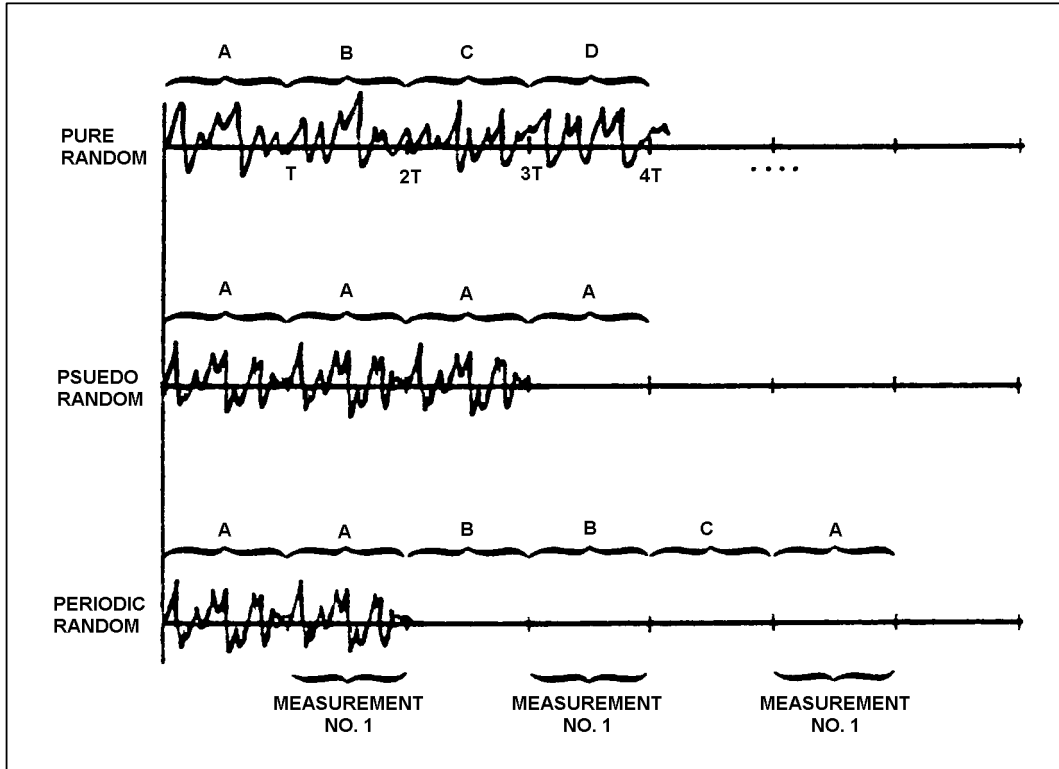


Figure 87 Characteristics of Various Random Signal Types

7.8.4.3 Periodic Random

This waveform combines the best features of the pure and pseudorandom signals without the disadvantages. A certain random signal is repeated a few times and then another random signal is repeated for a few periods, and so on (see Figure 87). For each signal, the transient response of the signal is allowed to die out before the structural response is sampled. Ensemble averaging can then be done as with pure random, and the signals will be periodic within the sample window as with pseudorandom. It is also a good input for modeling a nonlinear system in curve fitting approaches. The disadvantage is that a test by this method will generally take two to three times as long as with the other random inputs.

7.8.4.4 Burst Random

This signal uses one of the random forms discussed previously, but provides the input in a burst that begins and ends within the sample window to reduce leakage effects. The time between the end of the input and the end of data sampling permits time for the transient structural response to die out, or to be artificially set to zero, in the data sample. The input is then repeated at discrete intervals. The approach is claimed to provide better modal resolution and S/N.

7.9 Linearity Check

The concept of structural linearity was presented in Section 7.3. For the purposes of the GVT, the concern is with the extent of nonlinearity that would produce shifts in modal frequencies at progressively higher input force levels. At a certain input force level, slippage in joints and other events that might produce changes in frequency response can occur and cause a change in modal response. It is then necessary to test below this force level. Of course, at very high force levels the structure may be damaged and cause a considerable change in response.

The linearity check is performed by simply measuring the response of each transducer for each frequency dwell. The measurement is taken at a series of ever-increasing force levels to the highest level anticipated to be used in the test. A comparison of responses at each level for each transducer will reveal any nonlinearity effects as great changes in the responses. Generally, the highest practical force within the linear region is used to ensure adequate excitation of all modes. The influence of nonlinearities on damping can also be checked in the same manner.

7.10 Surveys

If the testing involves a dwell on a tuned mode (discrete sine dwell), it is possible to verify the modal identification or mode shape by conducting a survey across the surface. The mode tuning process itself will help to separate true normal modes from ‘local’ or false modes (a rattle, a substructure mode, etc.) and other misleading signal analysis errors. The survey entails moving an accelerometer around to different locations on the test article and recording the amplitude and phase of the signal. A sketch or computer generated diagram of the amplitude vectors with the appropriate phases on a drawing of the test subject will provide a visualization of the mode shape. Node lines can be quickly located in this manner if data is simply examined on an oscilloscope or other device. Otherwise, the node line is interpolated from the resulting mode shape display or printout. Many points will have to be surveyed before the entire mode shape can be defined. By making the survey at pre-selected points on the surface, generally a grid pattern (Figure 88), it is possible to locate nodes by interpolating to a zero response or sign change by using the trends identified in the survey.

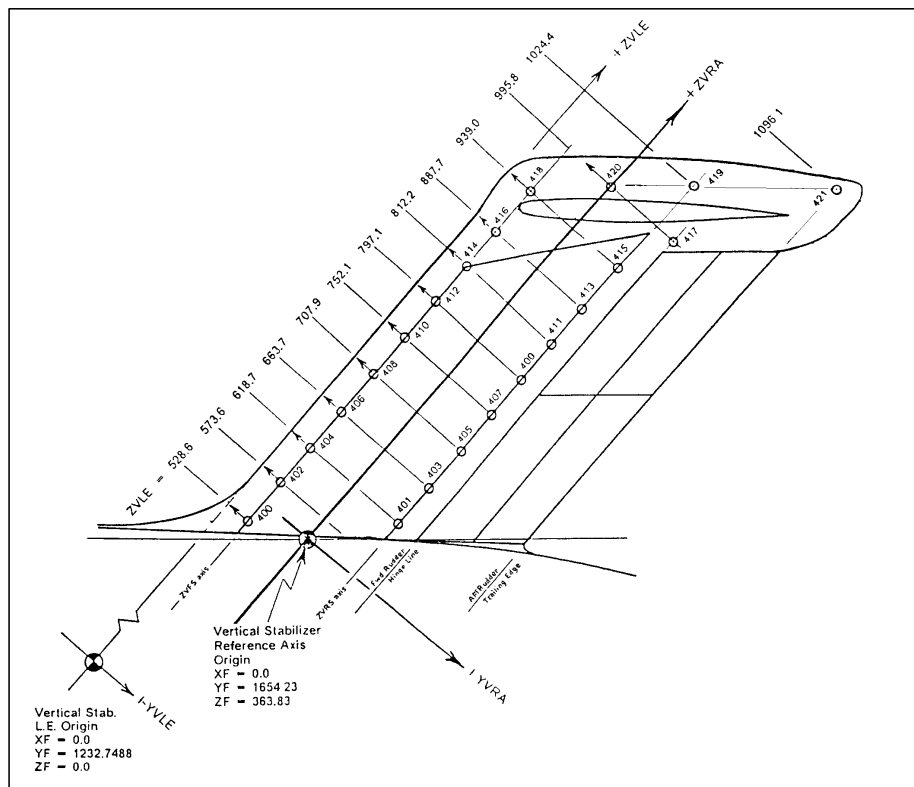


Figure 88 Example of a Ground Vibration Test Survey Grid

During the survey, the roving accelerometer can be temporarily attached to the surface (double-sided tape, bee’s wax, etc.) or placed against the surface using a ‘wand.’ The wand is a pole (sometimes quite long if it has to reach to the top of a vertical stabilizer) with the transducer mounted near the end. The end must have a soft spring to which the transducer mounts to isolate the wand modes from the response. For this to happen, the

spring, often just a light aluminum band screwed to the wand, must have a natural frequency much lower than that of the dwell frequency.

Tests such as multipoint random (Section 7.11.1) do not allow a survey such as is done with sine dwell. Instead, transducers must be placed at each of the points that would otherwise have been surveyed, and all of the response data are collected at once. This can amount to well over a hundred accelerometers for an entire airplane test, and provides a challenging organization problem. The wires from each of the transducers must be carefully coordinated, and the floor quickly becomes a sea of ‘spaghetti.’ While the price of accelerometers has decreased markedly in recent years, this may still be an expensive undertaking. A large number of signal conditioners, filters and analog-to-digital converters (Section 10.0) may also be required with their attendant expense. However, if successfully done, a great savings in time (also associated with test cost) can be realized.

7.11 Modal Results

7.11.1 Multipoint Data

Digital test equipment and mathematical techniques now allow the use of several exciters operating simultaneously and with the response of many sensors on the structure being recorded at once. Multipoint excitation analysis can be highly dependent on computer curve fitting methods to extract the modal data. To check that the inputs are not correlated at any frequency (not sharing identical inputs), forming a **partial coherence** (Section 11.3.7) between each pair of inputs will help in evaluating this. Low coherence would indicate little correlation. **Multiple coherence** between an output and some or all of the inputs would help in gaining confidence in the modes shown in the FRFs and to see how much nonlinearity and leakage effects are present. Values close to unity are considered reliable data.

Knowing each input signal from the load cells at the shakers, and each response from the accelerometers placed on the surface, it is possible to form input autopower spectrums of all of the inputs in the matrix $[G_{xx}]$ and the cross-power spectrums between all inputs and all outputs, $[G_{xy}]$ (Section 11.3.2). A transfer function $[H]$ between one and the other, expressed as:

$$[G_{xy}] = [H][G_{xx}] \quad (103)$$

will provide the frequency response functions needed to obtain the required modal parameters. This matrix can be solved for by the expression:

$$[H] = [G_{xy}][G_{xx}]^{-1} \quad (104)$$

Of course, some important matrix properties are necessary to ensure that the autospectrum matrix can be inverted. Most of these rest on the requirement that the inputs be uncorrelated at any frequency. There are other mathematical means of solving Equation 103 without an inversion, however, the FRF matrix will look like:

$$[H] = \begin{bmatrix} H_{11} & H_{12} & H_{13} & \dots & H_{1n} \\ H_{21} & H_{22} & H_{23} & \cdot & \cdot \\ H_{31} & H_{32} & H_{33} & \cdot & \cdot \\ \cdot & \cdot & \cdot & \cdot & \cdot \\ \cdot & \cdot & \cdot & \cdot & \cdot \\ \cdot & \cdot & \cdot & \cdot & \cdot \\ H_{n1} & \cdot & \cdot & \cdot & H_{nn} \end{bmatrix} \quad (105)$$

Reciprocity has already dictated that:

$$H_{ij} = H_{ji} \quad (106)$$

so there is some redundancy in the off-diagonal measurements. The diagonal terms (driving point measurements) are unique and so essential. Any single row or column contains sufficient information to derive a complete set of modal parameters for all of the modes, at least theoretically.

The curve fitting (also called **parameter extraction, estimation, or identification**) routines for modal parameter extraction used by many of the microcomputer software packages for obtaining the modal data, sometimes combining time domain and frequency domain analysis such as **Poly Reference** or **Ibrahim Time Domain**, involve theories and mathematics far too lengthy and complicated to delve into here. The vast majority of the methods are based on linear models, so nonlinearities will only increase the error in the results. Highly damped or closely spaced modes may not be suitably modeled, if at all. The reader is referred to some of the modal analysis texts shown at the end of this chapter for detailed presentations. Most analysis methods, particularly those that employ minicomputers, cannot deal with nonlinear results and so a best estimate curve fit is used; therefore, results cannot be considered to be absolutely faithful.

Adding frequency response functions from symmetric locations on the aircraft will enhance symmetric modes and assist in differentiating them from antisymmetric ones. The subtraction of the FRFs would conversely enhance antisymmetric modes. This approach is particularly valid for dual-input excitations, for example on opposite wings. However, it is necessary that the responses be measured simultaneously.

7.11.2 Mode Visualization

As a modal survey is conducted, the response at each survey point (velocity and phase, for example) can be read off of a voltmeter, oscilloscope, or other device. This data can then be manually plotted for a visualization of the mode shape. Current data analysis systems will often have the means of extracting the mode shapes from the modal data. The success of the calculations depend directly upon the number of response transducers placed across the test subject. For example, visualizing third wing bending with any measure of certainty with only a tip accelerometer is unlikely. At least fore and aft vertical accelerometers locations at the tip and two inboard wing stations will probably be required if such data is desired. The computer may then be able to display the shapes graphically, either statically or as an animated model. The analysis techniques involve considerable smoothing and curve fitting, so the results are not going to be precise.

One very old but still useful method for visualizing mode shapes is by spreading a thin layer of sand on the object under test (if this is practical). During the excitation the **sand pattern** particles will migrate to the node lines as these areas are moving the least. The resulting pattern will permit a relatively easy determination of the node lines and thus, the actual mode. The drawback is the fury of the aircraft maintenance people who find sand in the workings of their machine and the requirement that the surface be level.

Figure 89 shows typical mode shape results. Tables 3 through 5 give frequency data obtained from a wide variety of aircraft types. These may be used as a guide for planning future GVTs.

7.11.3 Orthogonality Check

Another confidence check of the applicability of the data is the orthogonality check. If measured mode shapes are going to be associated with a finite element model of the structure (see Section 3.2.3), it will probably need to be adjusted to match the lumped mass modeling of the analysis. Unless the GVT survey points exactly match the lumped mass model locations, the mode shape will have to be adjusted to match the modeled points while still providing essentially the same shape. After this has been done, the following operation is performed:

$$[\Phi]^T [M] [\Phi] \quad (107)$$

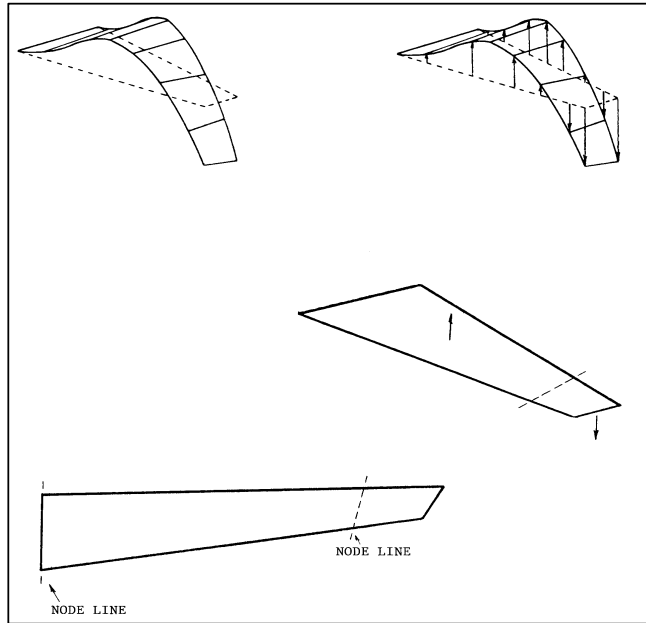


Figure 89 Example Wing Second Bending Mode Shape Presentations

Table 3
EXAMPLE C-17A MODES

Type	Frequency (Hz)	Mode Identification
Symmetric	1.70	Inboard Engine Nacelle Yaw
	2.17	Wing First Bending
	2.56	Inboard Engine Nacelle Pitch
	3.72	Vertical Tail Pitch
	4.51	Inboard Engine Nacelle Roll
	5.62	Horizontal Tail Bending
	6.18	Wing Second Bending
	6.93	Wing Fore/Aft Bending
	9.45	Fuselage Vertical Bending
	10.16	Wing Torsion
Antisymmetric	1.64	Vertical Tail Lateral Bending
	1.77	Inboard Engine Nacelle Yaw
	2.23	Vertical Tail Torsion
	3.13	Inboard Engine Pitch
	3.67	Aft Fuselage Lateral Bending
	4.19	Horizontal Tail Bending
	4.51	Inboard Engine Nacelle Roll
	4.84	Wing Second Bending
	7.94	Wing Third Bending
	8.44	Wing Fore/Aft Bending
9.99	Wing Torsion	

(For Illustration Purposes Only)

Table 4
EXAMPLE AFTI F-111 MODES

Type	Frequency (Hz)	Mode Identification
Symmetric	3.79	Wing First Bending
	5.13	Wing Chordwise Deformation
	13.29	Stabilizer Bending
	14.09	Wingtip Torsion
	15.63	Stabilizer Pitch
	26.64	Wing Second Torsion
Antisymmetric	5.13	Wing Chordwise Deformation
	6.81	Wing First Bending
	15.06	Stabilizer Bending
	26.97	Wing Second Torsion
Fuselage	7.91	First Vertical Bending
	9.33	Lateral Bending
	17.02	Torsion
	21.77	Second Vertical Bending
Vertical Tail	12.38	Left Wing Torsion

(For Illustration Purposes Only)

Table 5
EXAMPLE T-46 MODES

Type	Frequency (Hz)	Mode Identification
Rigid Body	2.12	Yaw
	4.43	Pitch
	5.31	Roll
	6.35	Plunge
Symmetric	8.33	Wing First Bending
	9.80	Horizontal Tail Bending
	21.86	Rudder Rotation
	26.17	Vertical Fin Lateral Bending
	26.77	Vertical Fin Fore/Aft Bending
	30.33	Wing Second Torsion
	44.27	Wing Torsion
Antisymmetric	12.59	Horizontal Tail Torsion
	14.59	Wing First Bending
	20.76	Vertical Fin Lateral Bending
	23.82	Rudder Rotation
	44.63	Wing First Torsion
Fuselage	7.42	Aft Torsion
	19.71	Lateral Bending
	27.27	First Vertical Bending
	31.94	Vertical Bending/Torsion
Miscellaneous	48.99	Aileron Tab Rotation

(For Illustration Purposes Only)

where $[\Phi]$ in Equation 107 is the adjusted mode shape matrix in which columns are the eigenvectors and $[M]$ is the modal mass matrix (see Section 4.5.1). The result is near diagonalization of the resulting matrix with values close to 1 on the diagonal and values close to zero in the off-diagonal terms. Perfect orthogonality would have exactly ones and zeros. Experimental reality dictates that the data will not produce exact unity or null values, so 10 percent of these targets are accepted as good orthogonality, and the data can be confidently correlated with the finite element model. Poor orthogonality might indicate that some of the inputs were correlated, the modes were not mapped with fine enough resolution (insufficient survey points), or 'false' modes are included in the eigenvector matrix. A **cross-orthogonality** can be performed where the GVT eigenvector matrix is augmented with the eigenvector matrix from a previous test or from analysis.

SECTION 7 REFERENCES

1. Ewins, D.J., *Modal Testing: Theory and Practice*, John Wiley & Sons, New York, New York, 1984.
2. Lang, George F., *Understanding Vibration Measurements*, Application Note 9, Rockland Scientific Corporation, Rockleigh, New Jersey, December 1978.
3. Stroud, Richard C., "Excitation, Measurement, and Analysis Methods for Modal Testing", in *Sound and Vibration*, August 1987.
4. *The Fundamentals of Modal Testing*, Application Note 243-3, Hewlett-Packard Company, Palo Alto, California, 1986.
5. Lenzi, David C. and Cogburn, Lowell T., *AFTI/F-111 Mission Adaptive Wing Ground Vibration Test*, AFFTC-TR-85-1, AFFTC, Edwards AFB, California, February 1985.
6. Ramsey, Kenneth A., "Effective Measurements for Structural Dynamics Testing," *Sound and Vibration*, November 1975, pp. 24-35.
7. Halvorsen, William G. and Brown, David L., "Impulse Technique for Structural Frequency Response Testing," *Sound and Vibration*, November 1977, pp. 8-21.
8. Brown, D., Carbon, G and Ramsey, K., Survey of Excitation Techniques Applicable to the Testing of Automobile Structures, in *International Automobile Engineering Congress and Exposition*, held by Society of Automotive Engineers, Detroit, Michigan, February 28 to March 4, 1977.
9. Lally, Robert W., "Testing the Behavior of Structures," *Test*. August/September 1978.
10. Allemang, R.J., Rost, R.W. and Brown D.L., *Multiple Input Estimation of Frequency Response Functions: Excitation Considerations*, 83-DET-73, The American Society of Mechanical Engineers.
11. Stahle, Clyde V., Modal Test Methods and Applications, in *The Journal of Environmental Sciences*, January/February 1978.

8.0 AEROSERVOELASTICITY

8.1 Introduction

The sensors for measuring flight parameters such as aircraft motion (normal and lateral accelerations, pitch, roll and yaw rate, etc.) are mounted in the aircraft. Since the aircraft structure is not infinitely stiff, these sensors will also measure acceleration and angular velocities resulting from structural deformation such as fuselage bending and torsion. Control surface rotation and elastic modes will also be picked up via surface position sensors. General structural motion can cause what are perceived as uncommanded aircraft motion or control surface deflections. The signals produced by the sensors will then be fed into the electronic flight control system (EFCS) computer which will, in turn, command control surface deflections (for fly-by-wire aircraft or automatic flight control systems) to counter what are perceived to be aircraft rigid body motions or erroneous control surface positions. If the phase lag from the sensor to the control surface is 180 degrees and the system gain is high enough, a sustained surface motion can result. These sorts of feedback are called **structural feedback** or **structural coupling**. It is possible for structural feedback to produce large neutrally damped or even divergent oscillations of the control surfaces, resulting in overall system instability and the possibility of structural failure. Even if control surface motion is not divergent, the response can be at a frequency and amplitude that promotes general aeroelastic flutter. This class of problems is addressed in the field of **aeroservoelasticity** or **ASE**.

High loop gain (explained later) is a principal factor in ASE difficulties. Design features that lead to such high gains are high dynamic pressure, relaxed static stability (see Section 2.3.3), leading edge control devices, and forward-swept wings. In general, any condition where high control system gain is matched with low structural frequencies can aggravate ASE instabilities.

An example of structural coupling occurred during ground tests of the F-15 STOL aircraft. With the control system engaged and the angle-of-attack (AOA) probes sitting above 15 degrees, a divergent asymmetric rotation of the stabilators (stabs) was observed. At high AOA, the system was designed to move the stabs asymmetrically to counter high yaw rates that tend to develop due to asymmetric vortex shedding off of the nose. This stab motion excited a first asymmetric stab-bending mode that was felt through the structure at the yaw rate sensor. This response was fed back through the system and resulted in additional stab rotation to counter what the system interpreted as an oscillatory yawing motion of the aircraft. The larger stab motions only enforced the bending response, thus leading to the divergent rotations. The fix was a digital filter to attenuate the bending frequency to the point that it no longer adversely affected the control system.

The effects of structural coupling of the kind just described can be reduced by placing the sensors at ideal locations or ‘**sweet spots**’ within the structure. These are generally locations with the least motion overall, but may also be where particular structural modes are least likely to create feedback problems. Figure 90 shows how a fuselage second longitudinal bending mode has two points of least angular motion and one practical point of least linear motion. The point of least angular motion (the antinode of the motion) is ideal for a gyro sensor, and the point of least linear motion (at the node) is ideal for an accelerometer. Note that the same is not true for the first bending mode, but in this case it is less likely to contribute to a feedback problem. Low order modes generally contain the most energy and sensors are usually placed to minimize influence from them. Figure 91 shows how the best location was found for the F-15 STOL using this criteria, although practical limitations on the placement must also be considered. All of this was accounted for during the design of the X-29 aircraft but problems were encountered when an ‘oil canning’ effect (panel oscillation) of the bulkhead to which the sensor package was mounted produced adverse feedback.

More typical today, the structural signal is simply filtered at the frequency of concern. Because of the bandwidth of flight control sensors and the low energy of high frequency structural modes, structural coupling will usually involve fundamental or other low order modes. Analysis and testing, therefore, concentrates on these modes. However, it is difficult to filter out low frequency responses like fuselage first and second bending while maintaining adequate gain and phase margins (Section 8.2.3.2) and acceptable handling qualities.

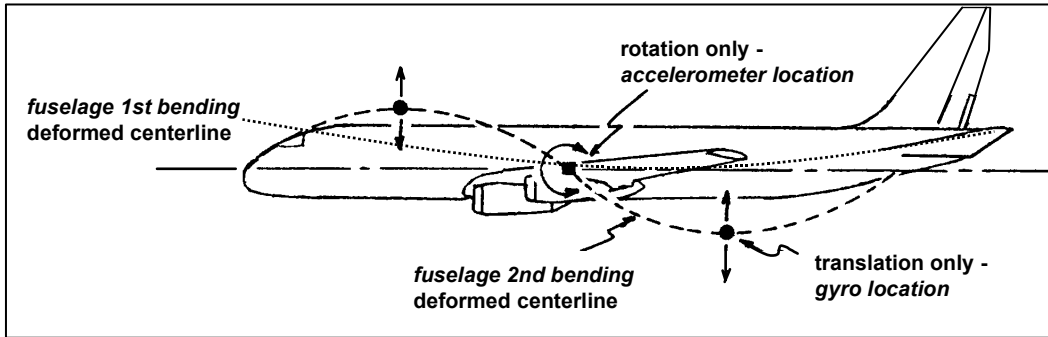


Figure 90 Example Sensor Placement Considerations

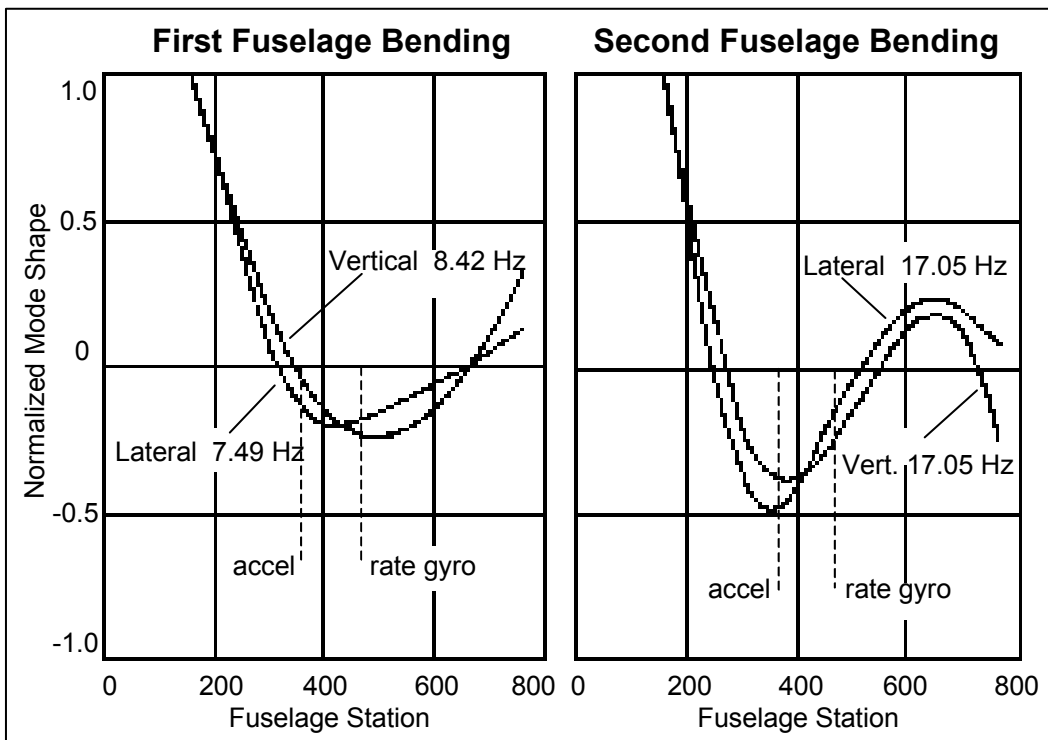


Figure 91 Example Determination of Sensor Locations

8.1.1 Pilot-In-The-Loop Oscillations

Another example of an elastic structure causing control problems was the oscillations of heavy stores on the wings of the F-111 fighter-bomber. An antisymmetric store pitching occurred near the edge of the envelope which, due to the high inertia of the stores, actually caused the airplane to roll. The motion was at a low enough frequency for the pilot to 'get in the loop,' or accentuate the motion when trying to stop it. Even when the pilot tried to hold the stick centered, the rolling accelerations caused his body to sway from side to side and lateral stick inputs were still made. Releasing the stick was no good because the pendulum mode of the stick was nearly the same as the rolling motion and the stick simply oscillated stop to stop. The only way to recover was to slow down.

The situation in which a pilot may couple with the aircraft elastic motion, acting through the flight control system is illustrated in Figure 92. This figure illustrates the first vertical bending mode of the YA-12A (SR-71 predecessor). The elastic response can produce pilot cues or aircraft rigid body motion which can be enhanced when the pilot attempts to damp the oscillations, and a pilot-induced oscillation (PIO, see Section 2.3.4) results. In addition to the hazards of PIO (dangerous attitudes and airloads), the addition of the aeroelastic element can also mean dangerous structural dynamics.

Several scenarios producing pilot-in-the-loop structural instabilities are possible. Aeroelastic structural deformations can produce accelerations or attitude changes at the pilot station which results in PIO when the pilot intentionally attempts to counter these dynamics. Also, aeroelastic structural deformation can produce an aircraft rigid body response which results in PIO when the pilot intentionally attempts to counter these dynamics. In another case, aeroelastic oscillations or mechanical vibrations can produce accelerations at the pilot station which the pilot unintentionally couples with, sustaining or enhancing the dynamics. The latter case has been called pilot-augmented oscillation (PAO). All of the factors contributing to pilot-in-the-loop instabilities are shown in Figure 93.

The lower order structural modes generally contain the most energy, produce the greatest structural deflection, and are the most likely to be within the active bandwidth of the flight control laws and the pilot responsiveness. Since the practical limit of a manual pilot input bandwidth is about 3 Hz, the structural modes contributing to an aeroelastic PIO would typically be restricted to this level as well. However, there have been examples of PIO in which the pilot response and the PIO resonance did not share the same frequency. Because PAO is an unintended input created by a physical vibration of the pilot-stick or pilot-throttle system, frequencies above 3 Hz can come into play in such instabilities. Accelerations as low as 0.01 g can be sensed by pilots and so contribute to coupling. Control system physical as well as virtual dynamics can also aggravate these instabilities. The excited and sensed elastic mode may alter the gain and phase characteristics of the control system such as to allow a PIO to develop at a frequency different from the elastic mode's frequency.

For the case of the YF-12A example shown in Figure 92, the aircraft experienced a small amplitude oscillation during aerial refueling. When the pilot attempted to damp the oscillation manually, he excited the fuselage first longitudinal bending mode. This mode produced even greater motion at the pilot station and a mild aeroelastic PIO resulted. An example of an unintentional coupling was experienced on the C-17A aircraft during flight testing. A abrupt application of lateral stick excited the 2.2-Hz antisymmetrical wing bending mode. The wing bending and twisting, combined with engine nacelle pitching, produced an oscillatory roll rate superimposed on the steady-state roll response. This ratcheting motion was felt as a lateral acceleration at the pilot station. The pilot then unintentionally fed the oscillation as the motion shook the arm-stick combination (a limb-bobweight influence), generating aileron inputs.

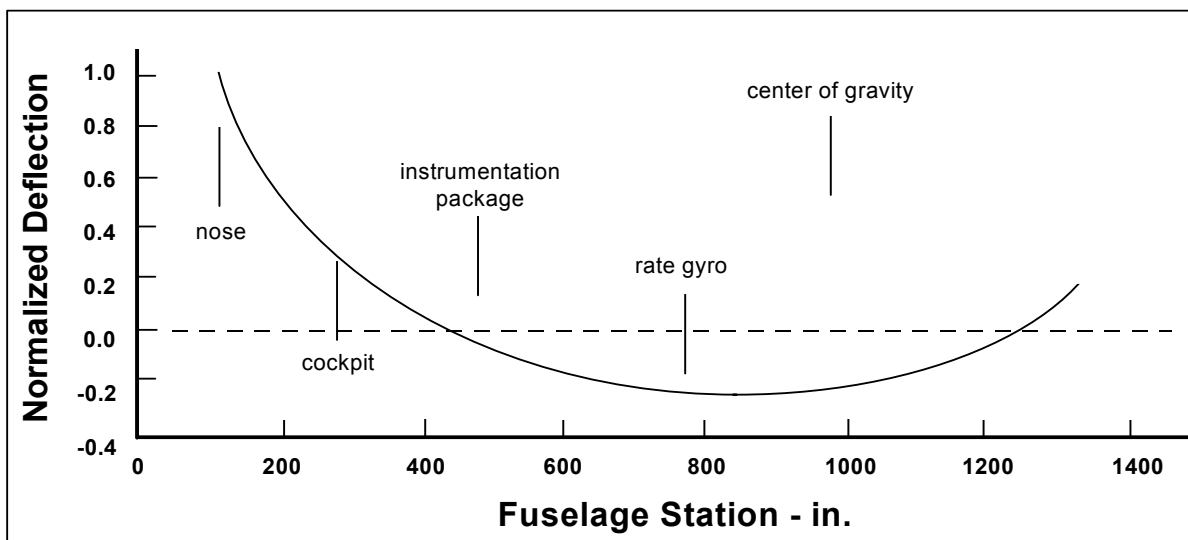


Figure 92 Example Fuselage First Vertical Bending Mode Shape

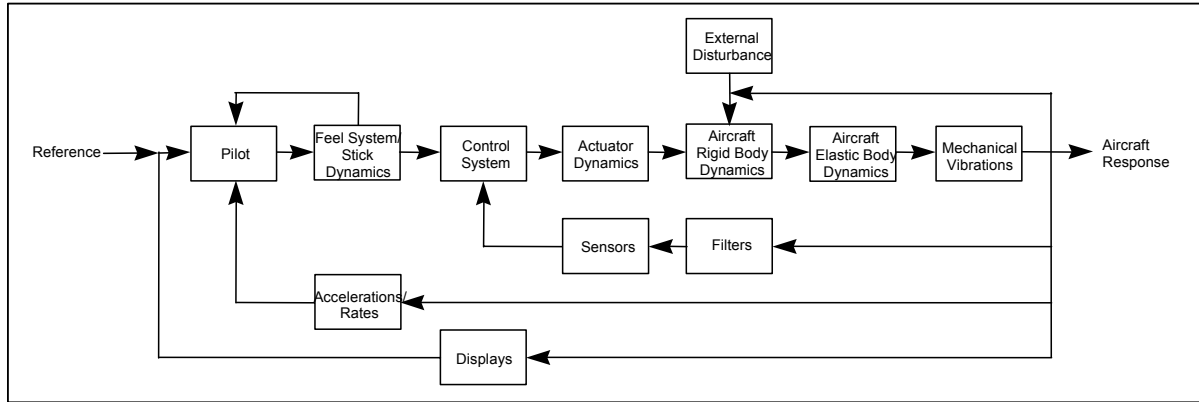


Figure 93 Aeroservoelastic System Diagram

8.2 Control Theory

The structures engineer must have a background in the basics of control theory to understand the stability and control engineers' language and their diagrams. This section is taken principally from Reference 1 which may serve as a good starting point for more detailed information. A course in linear control theory is the best way to go. The Reference section lists some other worthy texts that may provide answers to questions and explanations of advanced analysis techniques.

8.2.1 Basic Concepts

A system can be described as a series of operations working together to perform a specific function. A simple block diagram of this is shown in Figure 94. This is termed an **open-loop** system as opposed to a closed-loop system. The **closed-loop** system modifies the response of the system by **feedback** of one or more responses of the system (Figure 95), making the ultimate control action dependent upon the output. Open-loop system control action is independent of the output. **Multiple-input, multiple-output (MIMO)** systems will be of primary concern here versus **single-input, single-output (SISO)** systems. An example of a MIMO system, a simplified aircraft lateral-directional control system, is shown in Figure 96.

The arrows in Figures 94 and 95 indicate the direction of flow of the indicated signal. Signals may be added or subtracted at a summing point (as shown). Other points are simple takeoff points where a signal goes to two or more points in the system. Boxes may indicate a **plant**, that is parts of the system that use or modify the incoming signals. Plants can also be considered a transfer function (Section 11.3.6) and are normally modeled as mathematical equations. Other boxes are system elements that may represent a transducer that transforms the signal to an appropriate form. The disturbance is some undesirable input signal such as electrical system noise or atmospheric turbulence. System diagrams can be reduced with block diagram algebra as shown in Figure 97.

It is generally oscillatory structural responses that are a primary ASE concern, with **time-variant systems** being more susceptible than **time-invariant systems**. The former is of primary concern here. The range of frequencies over which the system will satisfactorily respond is termed the **bandwidth**. An **unstable system** is one that will tend toward an output of ever-increasing amplitude at a certain input condition.

Initial system conditions often play a significant role in system performance and must be taken into account. Certain definitions with regard to the system response to a **step input (indicial response)** may arise. A **time (transport) delay** is the time between when the input is made and when the system begins to respond. The time for the system to reach 67 percent of its final value (excluding any time delay) is termed **rise time**, and the time to arrive within 2 to 5 percent of the final value is **settling time**. These terms have importance for real systems that do not respond to indicial inputs ideally; that is, the response must reach a steady-state value in a finite time and then return to its initial state in some finite time after the input is terminated. System **error** refers

to the difference between the desired output and the actual output. One of the principal purposes of feedback is to minimize this error and to stabilize the system. The sensitivity of the system to the disturbances or other inputs may also need to be considered.

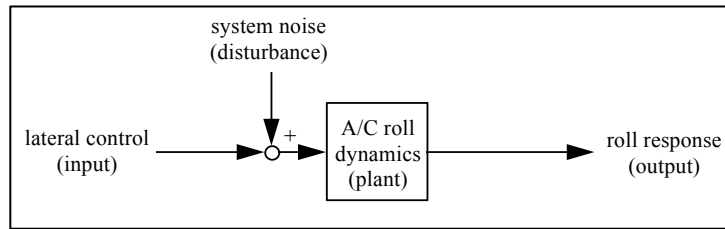


Figure 94 Open-Loop System Diagram

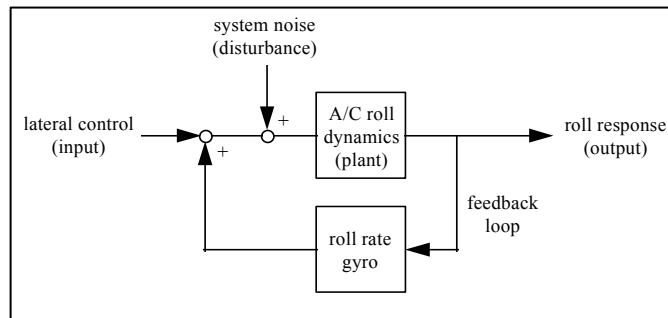


Figure 95 Closed-Loop System Diagram

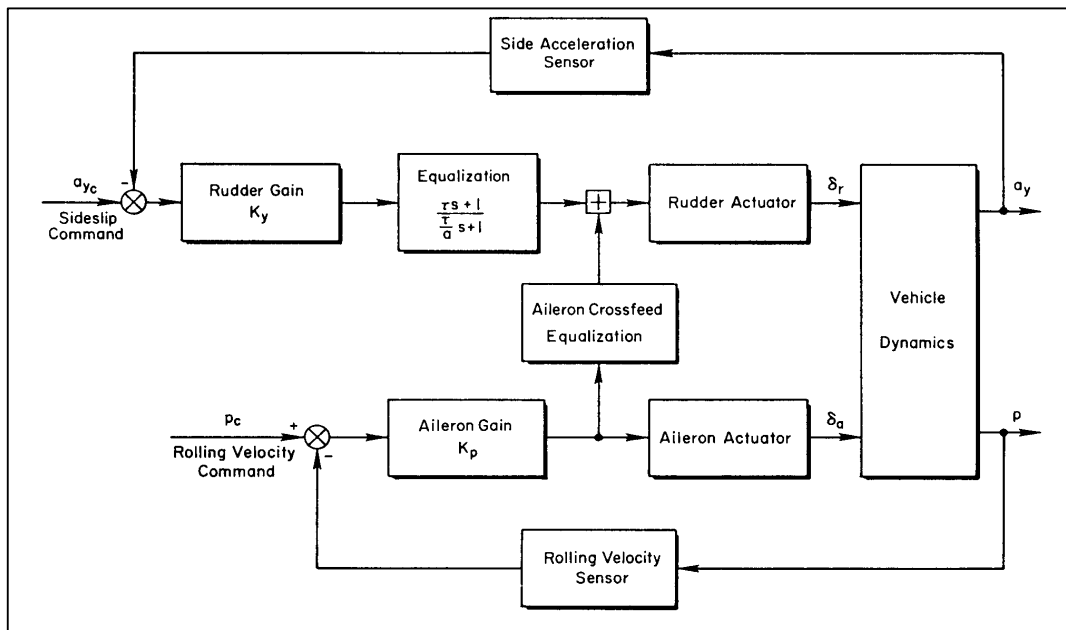


Figure 96 Example Multiple Input/Multiple Output System - Aircraft Lateral-Directional Control System

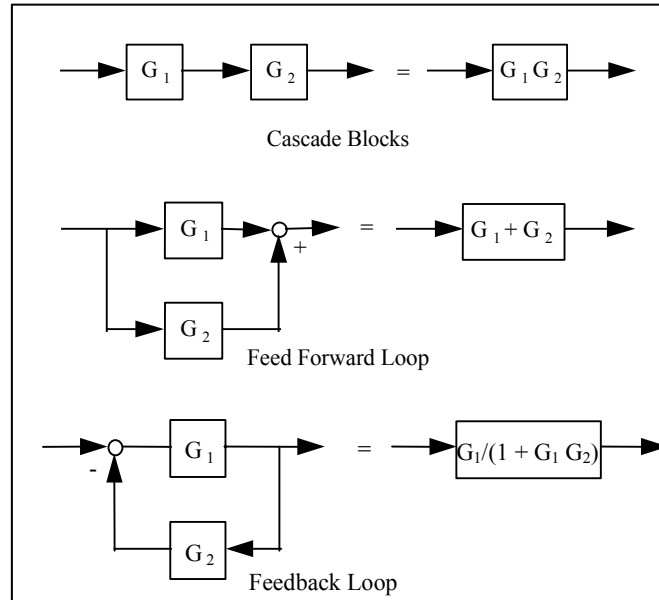


Figure 97 Block Diagram Algebra

Most systems, particularly aircraft systems, are nonlinear and the mathematical modeling equations may be complex, of high order, and involve differentials and integrals to adequately describe the system linearly. The rapid solution of these equations, often by specialized methods, are very computer intensive and constitute a significant area of control theory.

System **gain** is the weighting given to an individual feedback or input to the system. Changing of gains is a simple means of modifying system performance. For example, using Figure 95, the output of the roll rate gyro may be boosted to increase its weighting with respect to the pilot's lateral input. The system may also include **filtering** elements so that only certain parts of the signal are passed. For example, a filter downstream of the roll rate gyro in Figure 95 may be used to pass only low frequency output so that higher frequency structural responses (**structural filtering**) are not passed.

8.2.2 Compensation

The EFCS may be programmed to change the basic control laws at different flight conditions for suitable flying qualities as the aircraft dynamics and aerodynamics change throughout the flight envelope. This is known as **compensation**. The simplest compensation is variation of basic gains, but this is not always successful. The response of a system can also be modified by introducing basic control elements into either the forward or feedback loops, or both. This is known as **dynamic compensation**. Three types of dynamic compensation will be introduced here; lead, lag, and lag-lead compensation. The effects of compensation will be shown graphically in Section 8.2.3. In a block diagram, it would be represented by a mathematical formulation in an element block.

Lead takes its name from its phase-lead characteristic. It results in an increase of system bandwidth. It also permits an increase in system gain without adversely affecting **transient performance** (unforced response following termination of the input). Depending upon how it is implemented, lead compensation may provide better performance through smaller system error. The phase-lag characteristic of a **lag** compensator attenuates high frequency response resulting in a reduction in bandwidth and slowing of system response. System error may tend to increase with lag compensation. **Lag-lead** incorporates many of the advantages of the two previous compensations without excessive bandwidth change.

8.2.3 Representations

Four principal system response representations—root-locus, Bode, Nyquist, and polar form—will be introduced along with general interpretation and how the effects of compensation can be seen. They will be discussed further in Section 11.3.6 with regard to how they are used in structural dynamics analysis. The Nichols form is seldom used in ASE analysis and will not be covered in this handbook.

8.2.3.1 Root-Locus

The first requirement in producing a root-locus plot is an equation describing the system in **s-plane form** by use of **pole-zero** or fractional form and the Laplace transform. This is a transfer function, representing the system plant, with a **numerator (zero) polynomial** divided by the denominator or **characteristic polynomial**. How this is done is beyond the scope of this text, but an example of such a transfer function is as follows:

$$F(s) = \frac{2(s+1)(s-2)}{(s+3)(s^2+2s+2)} \quad (108)$$

where:

the numerator 2 = the gain.

The second order term in the denominator must be factored for plotting. Each of the expressions in parenthesis will then yield a root of the system. The roots in the numerator are termed **zeros** of the system (plotted with a small circle) and those in the denominator are called **poles** (plotted with a small x). The complex roots will have the form:

$$s = \sigma \pm \omega j \quad (109)$$

where:

j represents an imaginary number, and is plotted in the s-plane in a pole-zero plot as shown in Figure 98 for the system of Equation 108.

The stability of a system can be determined from the root-locus. The presence of a pole in the **right half-plane (RHP)** of the plot implies an instability or divergent response. A system with open-loop poles or zeros in the RHP is referred to as a **nonminimum phase system**. Otherwise, it is a **minimum phase system**.

Compensation can correct instabilities as well as alter the dynamics of the system. If the gain(s) change then the system will have different roots. Plotting the roots as a function of varying gain will show the movement of the poles and zeros with the change in gain (or compensation) and the best gain for the desired system response can be determined. An example of this is shown in Figure 99 for Equation 108. Such a plot may indicate an unstable or nearly unstable condition at some gain. In general, poles will tend to converge to the zeros or go to infinity. The position of the poles and zeroes in the s-plane are significant to system characteristics. Section 11.3.10 discusses how some of these characteristics can be extracted from the root-locus.

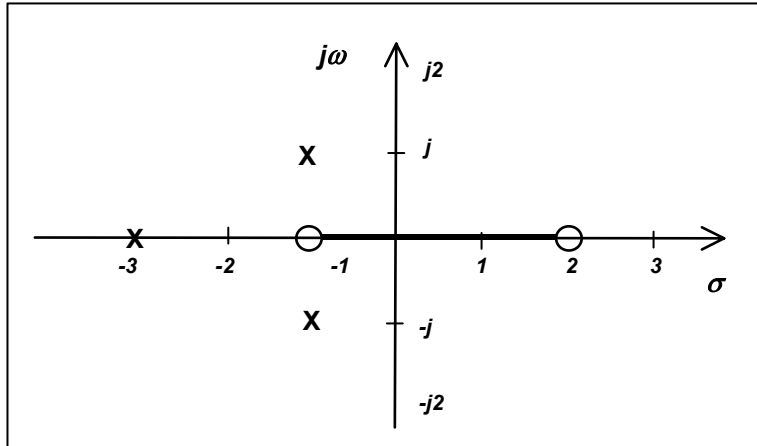


Figure 98 Typical Pole-Zero Plot

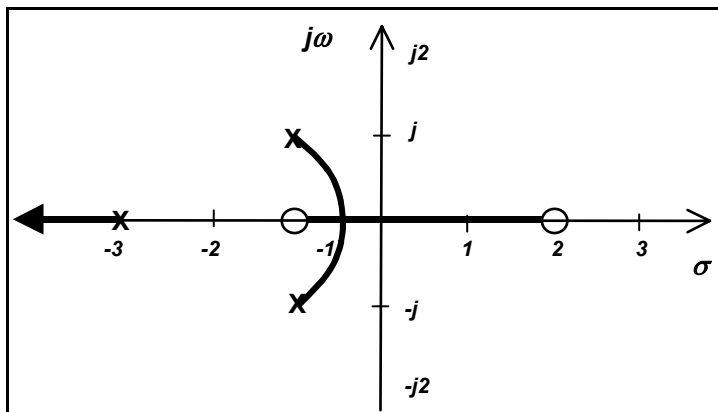


Figure 99 Root-Locus Plot of Figure 98

Lead compensation will be equivalent to applying a term like that shown in Equation 110 to the Laplace equation of the system, where b is greater than a .

$$\frac{s + a}{s + b} \quad (110)$$

Lag uses a term like Equation 111, where b is again greater than a .

$$\frac{a(s + b)}{b(s + a)} \quad (111)$$

Lag-lead would look like:

$$\frac{(s + a)(s + b)}{(s + c)(s + d)} \quad (112)$$

where:

c is greater than a and b is greater than d . The requirement for $ab = cd$ is often imposed for mechanization considerations.

8.2.3.2 Bode

Like the root-locus, Bode plots require the transfer function to be cast in what's called the Bode form. An example of this is shown in Equation 113.

$$G(j) = \frac{j^{\omega/2} + (\omega/2)^2}{j\omega(1 + j\omega/0.5)(1 + j\omega/4)} \quad (113)$$

The means of separating the magnitude and phase from this equation and the plotting of each element is beyond the scope of this handbook. Converting the magnitude to **decibels** (dB) is done as shown in Equation 114.

$$(\text{mag})\text{dB} = 20\log_{10}(\text{mag}) \quad (114)$$

The resulting plot for Equation 113 will look like Figure 100, with a logarithmic frequency scale. The magnitude and **phase** (in degrees, sometimes referred to as **phase angle**) are sometimes plotted on top of each other with the respective axes on opposite sides of the plot, as shown.

Figure 101 shows how the gain margin and phase margin are determined from a Bode plot of the open-loop system. These two parameters are a measure of the closed-loop system stability. **Gain margin** is defined as the maximum gain which can be added to the system without producing an instability. This is the gain at the frequency where the phase angle is at the **phase crossover**, or -180 degrees. The **phase margin** (ϕ_{pm}) is defined as 180 degrees plus the phase angle corresponding to a magnitude of 1.0 (unity gain) or 0 dB. For a minimum-phase system, it represents the amount of phase shift that is possible without causing instability, and which must be positive for a stable system. The larger the ϕ_{pm} , the more stable the system.

Simple gain compensation will result in moving the magnitude plot up or down on the dB scale and will not effect the phase plot. Lead compensation will lower the overall magnitude plot in the low frequency regime and raise the phase curve in the low to middle frequency range. In general, it has the effect of increasing the gain or phase margins, or both, or to increase the bandwidth. Lead compensation has the form:

$$P(j\omega) = [(a/b)(1 + j\omega/a)]/(1 + j\omega/b) \quad (115)$$

where:

a is less than b.

The lag compensator would have the form:

$$P(j\omega) = (1 + j\omega/b)/(1 + j\omega/a) \quad (116)$$

and has the effects discussed in Section 8.2.2.

The lag-lead compensator has the form:

$$P(j\omega) = \frac{(1 + j\omega/a)(1 + j\omega/b)}{(1 + j\omega/c)(1 + j\omega/d)} \quad (117)$$

with properties also presented earlier.

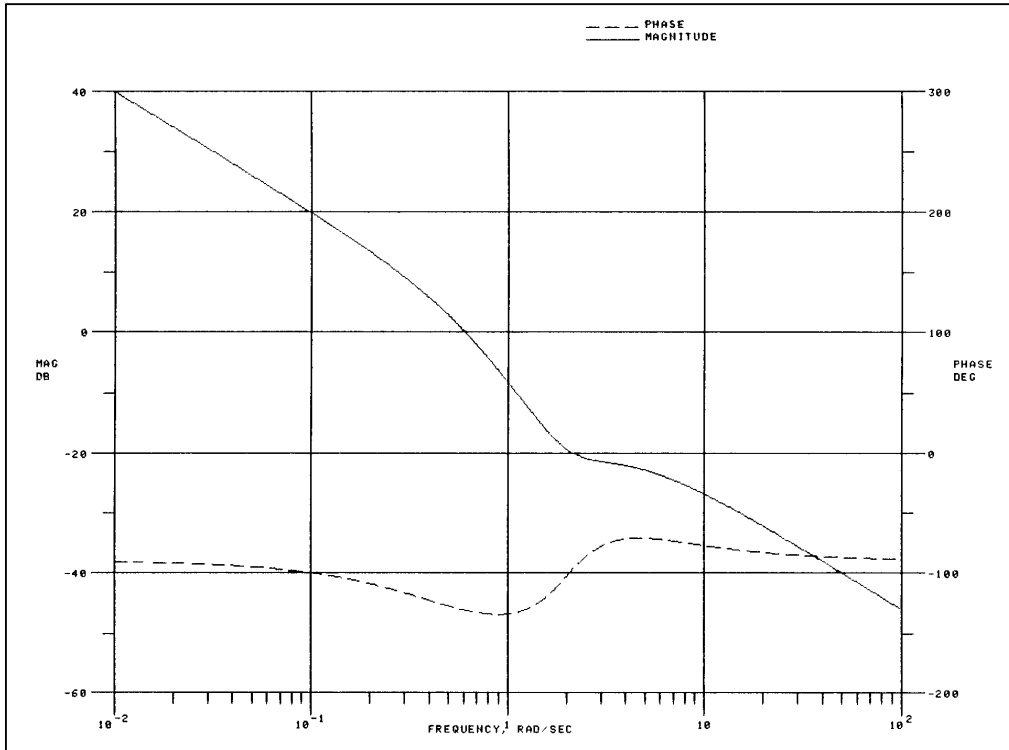


Figure 100 Bode Plot for Equation 113

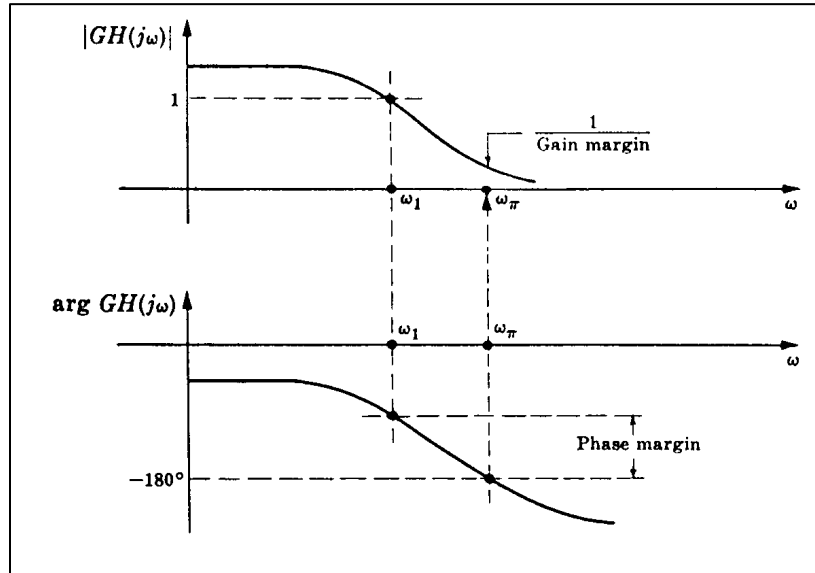


Figure 101 Determining Phase and Gain Margin from a Bode Plot

8.2.3.3 Nyquist and Polar

The polar plot is an s-plane presentation in which $j\omega$ is substituted for s in the expression for $P(s)$. The plot can be shown in three possible coordinate systems:

Polar Coordinates:

$$P(j\omega) = |P(j\omega)| \angle \varphi(\omega) \quad (118)$$

Euler Coordinates:

$$P(j\omega) = |P(j\omega)| [\cos \varphi(\omega) + j \sin \varphi(\omega)] \quad (119)$$

Rectangular Coordinates:

$$P(j\omega) = \text{Re}P(j\omega) + j\text{Im}P(j\omega) \quad (120)$$

Gain margin is found from the polar plot as shown in Figure 102 and:

$$1/|GH(j\omega_{\pi})| \quad (121)$$

where GH is the open-loop transfer function, and the crossing of the negative real axis is termed the **phase crossover frequency**. The same figure shows how the phase margin is found, where the **gain crossover frequency** is associated with the point where the unit circle intersects the curve. There is a graphical means of determining the resonant frequencies and damping from the same plot but, as this has been supplanted by much more accurate and simpler techniques, it will not be covered.

The Nyquist plot is a polar plot of the open-loop transfer function, which provides a graphical means of determining the exact stability of a closed-loop system. The plot is done in the s-plane (see Section 8.2.3.1) which consists of $\text{Re}P(s)$ and $\text{Im}P(s)$ axes, these being the real and imaginary parts of $P(s)$, the coupled function, respectively. System stability is determined by using the **Nyquist Stability Criterion**. This states that the number of clockwise encirclements by the plot of the point $(-1,0)$ must be less than or equal to zero (counterclockwise encirclements are taken as positive) for stability, where the direction of the encirclement is determined by increasing frequency. This process is shown and discussed further in Section 11.3.9.

8.3 Analysis

The dynamics of the aircraft (equations of motion) are modeled by control theory methods and run in simulations long before the aircraft ever flies. The simulations play a large role in the overall aircraft design to meet the customer requirements, particularly the flight computer software design. This aspect of the design process becomes very critical for 'fly-by-wire' aircraft. An attempt is made to predict structural dynamics at this conceptual design stage so that these may be incorporated into the simulation as elements of the transfer functions representing the aircraft dynamics. This is the earliest stage at which structural filters or sensor locations are considered. The analysis will follow the flow indicated in Figure 103. There are separate programs available to check for aeroservoelastic instabilities in the models. Ground vibration tests (GVT), ground resonance tests ([GRT], Section 8.4), and early flight results may cause changes as required to reduce detrimental structural feedback. The structures flight test engineer must be familiar with all of this work and participate to the largest extent possible to ensure that structural effects are considered in the control design, all necessary testing is completed, and potentially dangerous feedback is accounted for.

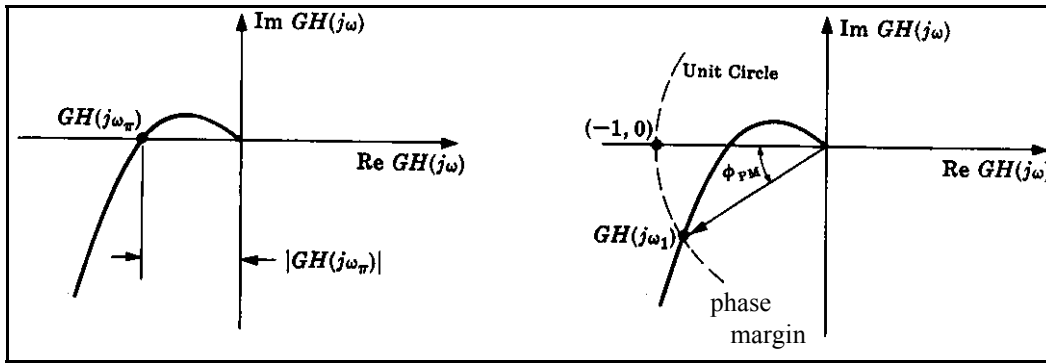


Figure 102 Determining Phase and Gain Margin from a Polar Plot

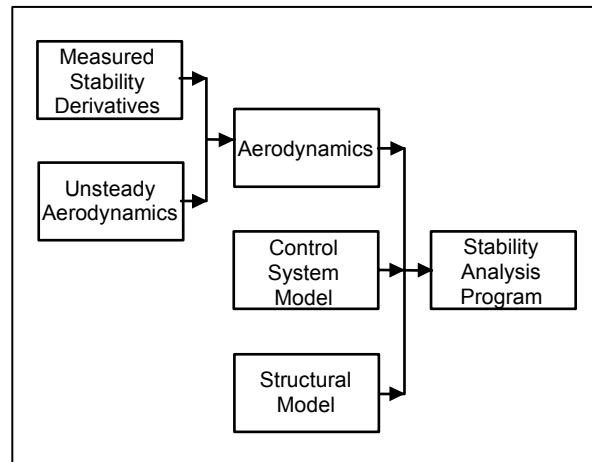


Figure 103 Aeroservoelastic Analysis Flow Diagram

8.4 Ground Tests

Aeroservoelasticity ground tests should be preceded by stability tests of the control system alone using aircraft hardware. This may be done as a bench test or using an **ironbird**. The ironbird has control surface actuators and representative surface masses, to ensure that there is no confusion as to the source of instabilities.

MIL-F-87242 states that:

“Prior to first flight the following minimum testing will be performed.”

- Gain margin tests to demonstrate the zero airspeed 6 dB stability margin requirements for feedback systems depending on aerodynamics for loop closure and to demonstrate stability margins for nonaerodynamic loops. Primary and secondary structure shall be excited, with special attention given to areas where feedback sensors are located with loop gains increased to verify the zero airspeed requirements. For redundant and multiple-loop systems, the stability requirements in degraded configurations should also be demonstrated. (These tests are performed in conjunction with structural testing. They are designed to determine if structural mode frequencies are propagating into the EFCS and, if so, if there is proper compensation.)

- Ground vibration tests with active controls using soft suspension system to simulate free-free condition. Flight control sensor outputs and open-loop frequency response data should be recorded for correlation with analytical results in predicting servoelastic and aeroservoelastic stability.
- Taxi tests with increasing speed and all feedback loops closed to examine servoelastic stability above zero airspeed. Flight control sensor outputs and control surface deflections should be recorded.”

The static structural coupling ground test described in the passage is called a **GRT** (also known as a **structural mode interaction [SMI]**, **structural coupling** or **structural resonance test**). It is not a true ASE test since the aerodynamics are not simulated. This testing should not be confused with **limit cycle tests** in which the aircraft rigid body motions are simulated using the aircraft’s equations of motion and fed into the EFCS for general system stability checks.

There are two types of structural coupling tests: open-loop frequency response and closed-loop gain margin tests. The objective of these tests is to determine the gain margin plus the sensor and overall system susceptibility to structural coupling.

In an open-loop frequency response test, each feedback loop of the system is opened separately and a signal (swept sinusoid being common) is injected at the ‘downstream’ side of the break. For Figure 96, this would be between the rolling velocity (roll rate) sensor and the command input summing point, or between the side (lateral) acceleration sensor and the sideslip (lateral acceleration) command summing point. The output is monitored at the ‘upstream’ side of the break, or the end toward the lateral acceleration or rolling velocity sensor in Figure 96. The sine sweep signals (linear or logarithmic) may be produced by a ground unit or as a special function of the flight control computer. Tests with a constant input at both large and small amplitudes should be conducted in case of nonlinear response behavior. The open-loop frequency response is obtained using a dynamic analyzer. Open-loop frequency response plots are made for several different input amplitudes to observe the system’s input amplitude sensitivity. The amplitudes and the phase angle of the input and output signals are plotted (transfer function) as a Bode plot. The same open-loop frequency response results would be obtained using either a swept sine input or a random noise input of equivalent intensity over an equivalent frequency range for a purely linear system.

In any linear system the frequency response is not a function of input amplitude. However, in real systems numerous nonlinearities are present. These can be such factors as break-out forces, hysteresis, nonlinear response, or rate limiting of actuators. An intentionally designed nonlinearity is scheduled gain changes in the control laws. The effect of these nonlinearities on system stability can be observed by obtaining the frequency response for several different input amplitudes. Most often, the greatest structural coupling has been found to occur at relatively small amplitudes. Therefore, the amplitudes chosen for use in the frequency response usually represent only a small percentage of that which is possible.

Closed-loop tests involve structural excitations to directly test for structural feedback. The EFCS may be used to excite the structure through control surface rotations using the swept sine signals or similar functions described above. The signal can be sent directly to the control actuators themselves for a purely structural input. Manually induced stick raps and rudder kicks may also be used in this portion of the testing. The closed-loop gain margin test is performed by inserting a variable gain at an appropriate location in the EFCS. The loop gain is increased until a condition of lightly damped or undamped response occurs. The frequency and gain for this condition are recorded and their correspondence with data from the open-loop tests checked. Since normal practice requires a 6-dB gain margin, or twice the nominal gain, without instabilities (see Table 6 for precise gain and phase margin requirements), a simple demonstration of this without actually going to instability is generally sufficient. However, it is best to find the actual gain to produce instability in the event that gains are altered in the course of flight testing; a common occurrence.

Table 6
GAIN AND PHASE MARGIN REQUIREMENTS

Airspeed Modes Frequency (Hz)	below $V_{o_{min}}$	$V_{o_{max}}$ to $V_{o_{min}}$	Limit Airspeed (V_L)	$1.15 V_L$
$f_M < 0.06$	GM = 6dB (no phase require- ment below $V_{o_{min}}$)	GM = ± 4.5 PM = ± 30	GM = ± 3.0 PM = ± 20	GM = 0 PM = 0 (stable at nominal phase & gain)
$0.06 \leq f_M < \text{first aero-elastic mode}$		GM = ± 6.0 PM = ± 45	GM = ± 4.5 PM = ± 30	
$f_M < \text{first aeroelastic mode}$		GM = ± 8.0 PM = ± 60	GM = ± 6.0 PM = ± 45	

where: $V_{o_{min}}$ = minimum operational airspeed
 $V_{o_{max}}$ = maximum operational airspeed

These tests should be performed in all the different control modes, including degraded modes or failure scenarios. It will probably be necessary to create the conditions of flight artificially with a pneumatic ground test unit attached to Pitot-static sensors. Hydraulic power and electrical power to the aircraft will also be required. Every effort should be made to ensure that the hydraulic flow rate is not less than that normally supplied by the aircraft pumps or the control surface responses and actuator stiffnesses will not be faithfully duplicated. The test is often performed with the aircraft in the same arrangement as for a GVT (see Section 7.0) such as suspension and sensors. In fact, the GVT and GRT are often done back-to-back since much of the test and analysis equipment is common to the two tests. The use of electrodynamic shakers to excite the structure is not advised because the shaker armature does not move very far and will also resist control surface motion commanded by the EFCS. This can result in a shaker thruster being driven through a surface.

Tests at different aircraft configurations (stores, fuel, wing sweep, etc.) may be necessary. It is also important that the control laws and structure be as close to the final production form as possible for the test to be valid. If significant changes are made to these in the course of flight testing, it may be necessary to repeat portions or all of the test. It is also critical that a single emergency cut-off switch be available to open all feedbacks and kill the artificial input signal in the event of a divergent control surface oscillation that may damage the aircraft.

Prior to the first flight, the aircraft should undergo taxi tests to greater and greater speeds. This will test system responses to actual operational mechanical inputs (taxiing over the ramp tar strips, engine vibrations, etc.) and observe the effect of automatic gain changes as the airspeed increases.

8.5 Flight Tests

Aeroservoelasticity flight testing is a cross between flutter (see Section 6.0) and basic flight controls (flying qualities) testing. Some of the instrumentation is similar to that used for flutter testing; strain gages or accelerometers for structural response and displacement transducers for control surface motion. These serve to warn the test engineers of any undesirable response due to structural feedback. And, some of the maneuvers are the same as for flying qualities testing.

Testing should begin with the gains at half that found to produce an instability in the GRT or the nominal gain, whichever is lowest. The gain can then be incrementally increased in flight to the nominal condition. This naturally requires a means of changing the gains in flight - a feature usually only available on prototype or research aircraft. A means of rapidly opening the feedbacks loops (or at least reducing the gains to nominal values if the aircraft is unstable without feedback), as in the GRT, is essential for safe recovery in the event of an instability. In the event of a pilot-in-the-loop instability, a recovery would normally include slowing down and having the pilot

either freeze the controls or taking the pilot out of the loop completely by releasing the controls. Transfer function plots of surface motion and other aircraft responses (rates and attitudes) can be produced point-to-point or flight-to-flight to determine phase and gain margins and for comparison with model and simulator results. These plots will assist in identifying any unusual characteristics that may contribute to or are directly attributable to structural feedback.

This flight testing is usually conducted in association with the flying qualities engineers. The reader is referred to texts on stability and control test methods such as Reference 2 and 7. During the envelope expansion buildup, the test engineers should watch for any sign of lightly damped control surface or stick motion, a lightly damped rigid body oscillation of the aircraft, or any significant deviation from predicted response as seen on real-time transfer function plots (usually gain and phase margins) or in postflight analysis. Using a flutter test exciter system (see Section 6.6.1), stick raps, doublets, control sweeps made by the pilot, similar inputs made as a function of the flight control computer, or other stability and control test maneuvers are helpful in exciting the structure and generating any potential feedback. Test instrumentation will be a mix of those used in flutter testing and those used by the stability and control engineers. Testing in certain degraded flight control system modes (**failure modes**) is important because this may affect certain feedback and coupling characteristics.

The fundamental handling qualities test methods are also suitable for revealing aeroelastic pilot-in-the-loop oscillation susceptibility. These methods normally consist of performing high gain handling qualities during tracking (HQDT) tasks such as air-to-air gun tracking. Other basic stability and control tests such as abrupt *pullups* and pushovers with an attitude capture on return to steady level flight, and abrupt sideslips, have a higher potential for exciting structural elastic modes which could contribute to a PIO event. However, such maneuvers are seldom performed during HQDT. The sharp manual control inputs common in flight flutter testing will produce the highest manually-induced elastic response and, although not normally concurrent with a high gain pilot task, might uncover any inherent aeroelastic/pilot resonance. An opportune gust or the inertia effects of store release also have the potential for producing the elastic response that results in an instability. Therefore, the normal envelope expansion testing consist of concurrent structural dynamic and flying qualities testing in the normal buildup fashion with basic tasks performed as early in the test program as reasonable. The early look at operationally realistic mission tasks may also provide insight in this regard.

Pilot-induced oscillation (PIO) or PAO susceptibility may be strongly dependent on individual pilot sensitivities and reactions. Therefore, a single unsatisfactory finding among a sampling of pilots, indicating poor handling qualities, should not be dismissed as anomalous. The damping of the basic rigid body modes of the aircraft should be tracked during the buildup and care taken when approaching low damping. The frequencies of structural modes should be tracked in concert with the rigid body modes during an envelope expansion buildup to provide warning of the potential for the coupling of these modes. Pilot inputs should be monitored for signs of PIO or PAO. This requires the close association of the flying qualities and structural dynamics test engineers. Testing should, of course, include failure cases with stability augmentation system turned off (where practical), reversion to mechanical systems, and other such conditions to ensure PIO-free control in these states. Such systems have the potential for artificially damping an elastic mode when active, so an aeroelastic pilot-in-the-loop oscillation may develop when they are deselected.

8.5.1 Notch Filter

Should an undesirable system or aircraft response, or the potential for one, be uncovered, the easiest remedy without disturbing beneficial flying qualities is the application of a notch filter. Shown in Figure 104, this is either an analog filter or a digital algorithm which seeks to attenuate a signal (output of the roll rate gyro, for example) at a specific frequency to a level that will no longer produce the detrimental system response. The results of the use of such a filter are shown in Figure 105. As with any changes to the flight controls, a subsequent flight test is to verify the corrective change and to ensure that other detrimental effects have not resulted (instabilities or undesirable flying qualities). The control system should be designed with structural filters from the beginning using predicted modal responses for the airframe and control surfaces, and these may need to be changed during the course of testing. The data update rate of the EFCS also serves as a form of self-filtering. An update rate of 30 samples per second should effectively ensure that modes above 30 Hz will not be a problem. However, aliasing (Section 12.3.2) may cause responses within the sample range from higher frequency modes unless good anti-aliasing filters are used.

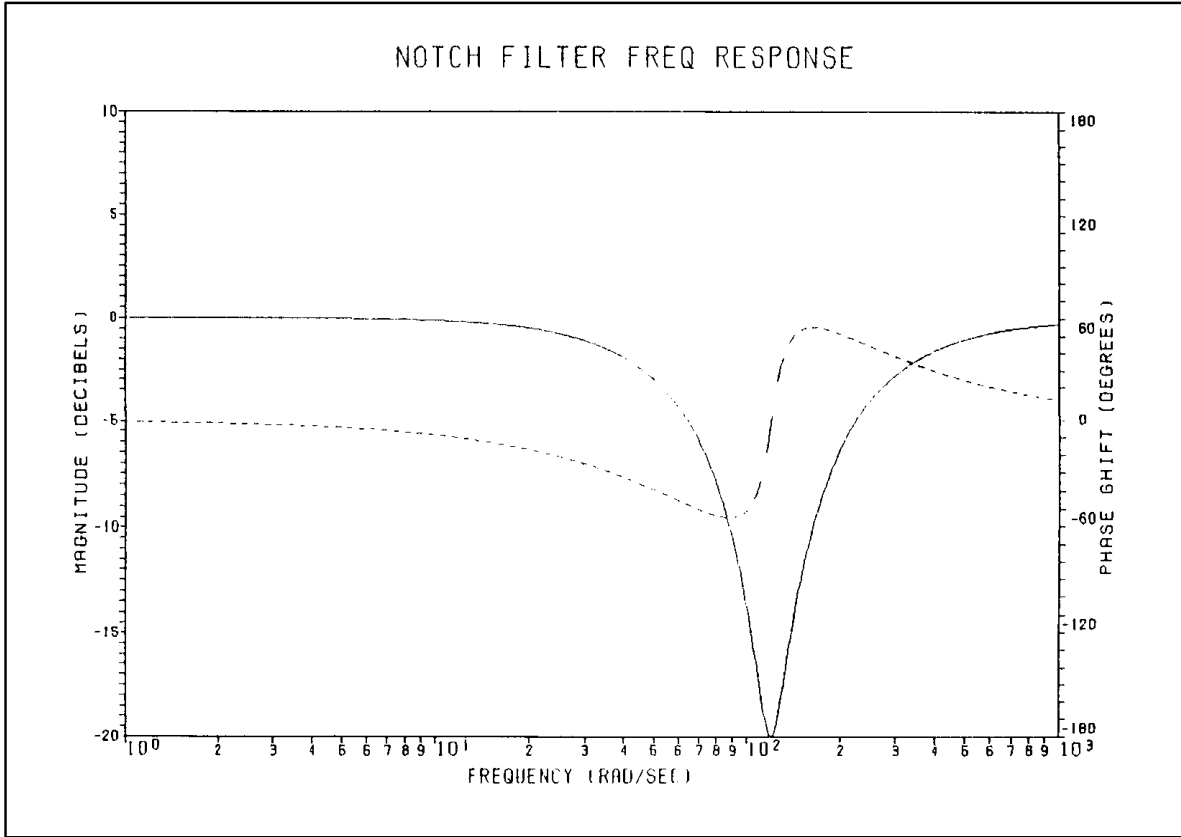


Figure 104 Example Notch Filter

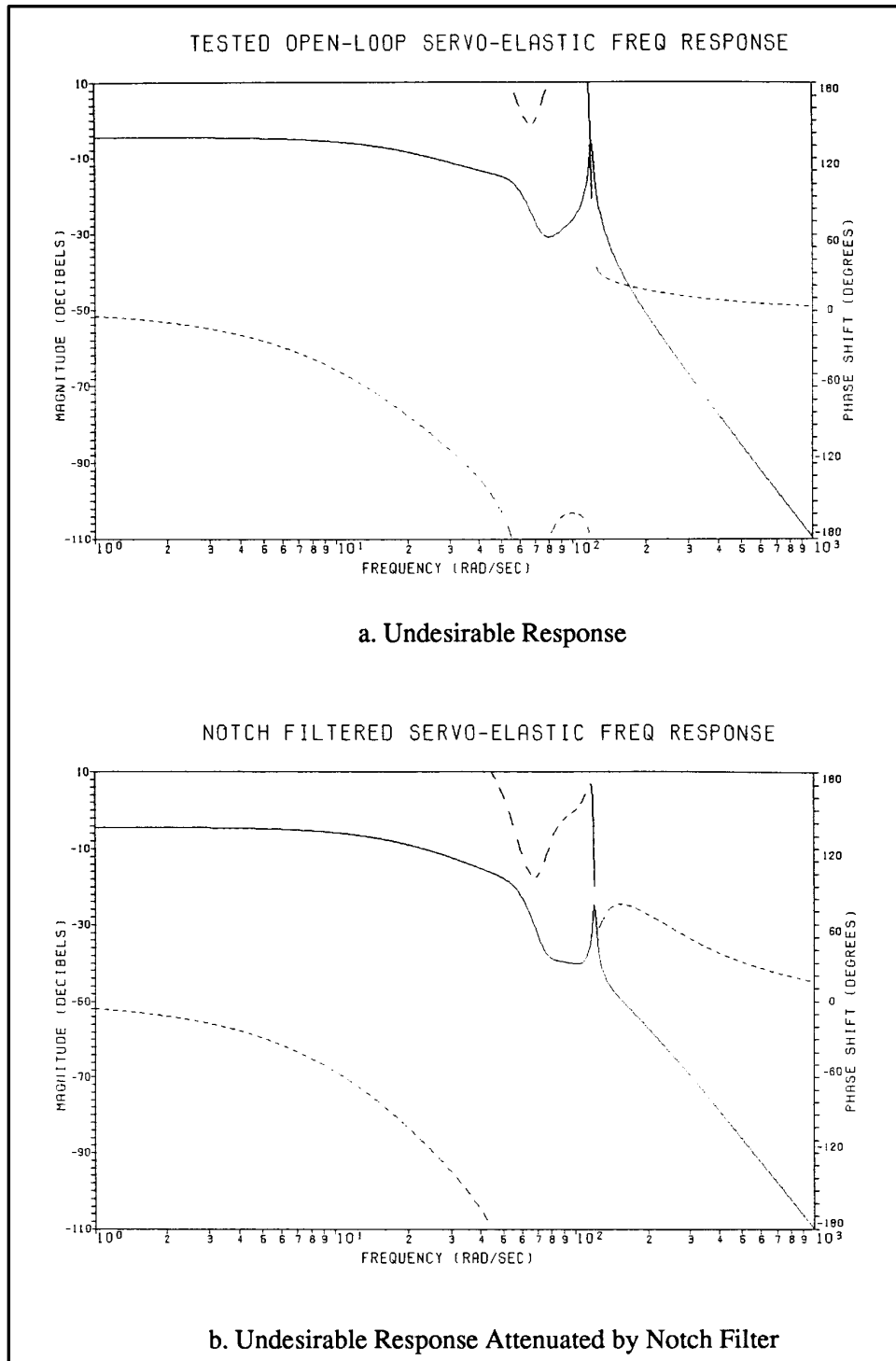


Figure 105 Effects of Notch Filter

SECTION 8 REFERENCES

1. DiStefano, Joseph J., III, Stubberud, Allen R. and Williams, Ivan J., *Theory and Problems of Feedback and Control Systems*, Schaum's Outline Series, McGraw-Hill Book Company, New York, New York, 1967.
2. Nagy, Christopher J., *A New Method for Test and Analysis of Dynamic Stability and Control*, AFFTC-TD-75-4, Edwards AFB, California, May 1976.
3. D'Azzo, J.J. and Houpis, C.H., *Linear Control System Analysis and Design*, McGraw-Hill Book Company, New York, New York, 1981.
4. McRuer, D., Ashkenas, I. and Graham D., *Aircraft Dynamics and Automatic Control*, Princeton University Press, Princeton, New Jersey, 1973.
5. Reid, J.G., *Linear System Fundamentals, Continuous and Discrete Classic and Modern*, McGraw-Hill Book Company, New York, New York, 1983.
6. Franklin, G.F., Powell, J.D. and Emani-Naeini, A., *Feedback Control of Dynamic Systems*, Addison-Wesley Publishing Company, Menlo Park, California, 1986.
7. Flying Qualities, Theory and Flight Test Techniques, USAF Test Pilot School, Edwards AFB, California.
8. "Flight Control System - Design, Installation and Test of Pilot Aircraft, General Specification for," MIL-F-9490D.
9. Kirsten, Paul W., "Flight Control System Structural Resonance and Limit Cycle Oscillation," in AGARD Conference Proceedings No. 233, *Flight Test Techniques*.
10. Norton, William J., Major, USAF, "Aeroelastic Pilot-in-the-Loop Oscillations," in AGARD AR-335 *Flight Vehicle Integration Panel Workshop on Pilot Induced Oscillations*, February 1995, Proceedings of the NATO Advisory Group for Aeronautical Research & Development (AGARD) Flight Vehicle Integration Panel Workshop on Pilot-Induced Oscillations, May 1994.
11. Norton, William J., Captain, USAF, "Aeroelastic Pilot-Induced Oscillation," in Proceedings of the 23rd Annual Society of Flight Test Engineers Symposium, August 1992.

9.0 VIBRO-ACOUSTICS

9.1 Introduction

The operation of onboard equipment and the influence of aerodynamic forces create a broad spectrum of vibration sources that can affect an airplane in many different ways. The study of a portion of these influences have been called vibro-acoustics, **aero-acoustics**, or noise and vibration (N&V). Nearly every flight test discipline has to concern itself with this subject to one extent or another. The vibration environment to which an avionics box is subjected is very critical to its reliability and sometimes its ability to function properly. Early KC-135 testing revealed a coupling between the fuselage vertical bending mode and the autopilot shock mount frequency that caused the autopilot to command sharp pitch oscillations so violent as to yank the control yoke from the pilot's grasp. While such a problem would not normally be within the purview of the structures engineers, their understanding of structural interactions and frequency response analysis techniques tends to draw them into these other areas of testing.

The acoustics source of the vibration problem will be given dominant attention in this chapter. Sound is but a vibration in the atmosphere or a series of traveling pressure waves. This vibration is transmitted to a structure immersed in the air. High noise levels from boundary layers, separated or turbulent flow (see Section 2.2.5), aircraft maneuvering, engine operation and other onboard equipment can excite high frequency resonances in an aircraft structure that may cause local overloads or lead to fatigue (known as **sonic fatigue**) of components and the general airframe (see Section 3.4.5). Frequencies up to 60 Hz (cycles per second) in the range of the more powerful airframe natural frequencies, and high amplitude excitations in this range can induce severe damage. Frequencies on the order of thousands of cycles per second can also contribute to fatigue in aircraft structures, as well as degrading electronic components and other equipment. Vibro-acoustic problems can be relieved by changing the structure to alter the natural frequencies and strength, applying a passive damping material, or by active suppression (applying an equal but opposite excitation).

An example of the problems noise can cause is the severe aft fuselage skin cracks found early in the life of the KC-135A tankers. These aircraft used water injected into the turbojet engine exhaust for increased mass flow in heavy weight takeoffs. The water injection created a tremendous amount of noise that fatigued the aircraft structure aft of the engines. The solution was to add many external metal hoop bands around the aft fuselage. Much later in the service life of the KC-135A, a proposal was made to place a thin polymer layer on the inside skin of the aft fuselage to act as a passive damper to reduce vibration levels and extend the fatigue life even further.

Externally mounted guided weapons are particularly susceptible to frequencies up to 200 Hz with wakes (often oscillatory) from other stores, unstable shock waves, excessively turbulent flow, and vibrations from aircraft internal components creating an environment the weapon developers may not have anticipated. An example of this sort of problem is the case of a shallow weapons bay with a length-to-depth ratio of 4.5:1 (such as used for a semi-submerged store). At transonic speeds this cavity can experience pressures generated by unstable shock waves equivalent to being 3 feet behind an F-15 in full afterburner. An example of external store acoustics problems are those on the F-15. Testing of the Advanced Medium Range Air-to-Air Missile (AMRAAM) was greatly troubled by failures attributable to a bad vibro-acoustics environment induced by airflow spillage from the inlets during throttle transients.

The study of acoustics is largely concerned with human factors; the effects of noise on the performance and health of people. This is not of interest for this handbook and will not be discussed. The measurement of **sound intensity** also constitutes to a sizable portion of the acoustics field. This is the accurate measurement of the noise in an area closely surrounding the source of the sound. The intent is to determine the best means of reducing the intensity and sound level in the areas subjected to the sound. Since the noise we are concerned with in flight testing is seldom present except during flight and for which only aerodynamic changes to the aircraft will produce sound intensity changes, intensity measurements are impractical and will also be excluded from the handbook.

9.2 General Vibration

Much of the avionics and other internal components will have undergone laboratory shock and vibration tests, using shaker tables (see Section 7.6) to specification limits of g's as a function of axis and duration (Reference 7). Flight testing is still necessary because there is no certainty that these tests have adequately replicated the true in-flight conditions. General shock and vibration environmental testing uses much the same instrumentation and analysis techniques as flutter testing (see Section 6.0). The specification limits to which the results are compared are presented similarly to that discussed in Section 9.5.3. The basic approach is to determine critical locations (such as an autopilot computer mounted in an avionics compartment) and instrument each location with a tri-axial accelerometer (Section 10.3). Data is collected at representative flight conditions (taxi, max-power takeoff, low-level cruise, aerial refueling, etc.) with 30 seconds to a few minutes dwell on each condition. Results are typically presented as a power spectral density (PSD) or other frequency response function (Section 11.3) with averaging used to smooth the data.

Avionics boxes, mechanical subsystems, and other components can be partially shielded from adverse vibration, within certain ranges and levels, using **isolator mounts**. These normally take the form of a dashpot, spring column, or rubber pad with stiffness designed to damp a specific frequency range and amplitude of response.

9.3 Fundamentals of Sound

If sound is thought of as a pressure wave, an associated wavelength and frequency can be surmised. **Wavelength** can be defined as:

$$\lambda = (\text{speed of sound})/\text{frequency} \quad (122)$$

where:

the speed of sound in air at 21 degrees Celsius is 344 meters per second.

This is shown graphically in Figure 106. Humans can hear sounds from 20 to 20,000 Hz, above which is termed **ultrasound** and below it is **infrasound**. Sounds outside this human hearing range can still adversely effect aircraft structures.

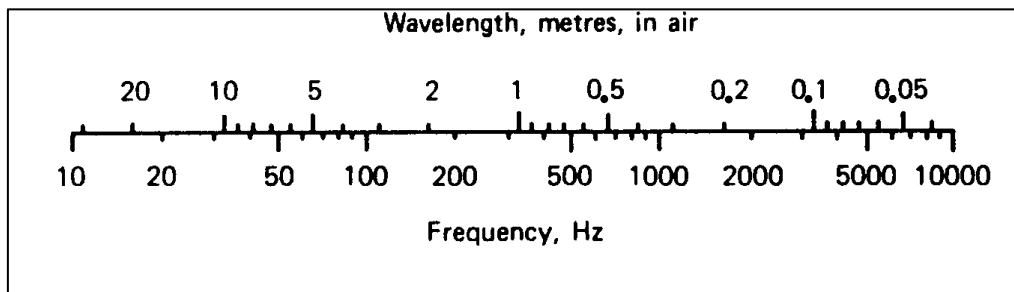


Figure 106 Wavelength Versus Frequency of Sound in Air

For a pressure wave in the atmosphere (or any medium), it makes sense to define 'sound pressure' as a dynamic variation in atmospheric pressure. This can be used to provide a definition of sound amplitude, what is call **sound pressure level (SPL)**, or:

$$L_p = 20 \log_{10} (p/p_o) \quad \text{in decibels (dB)} \quad (123)$$

where:

p = the root mean squared (RMS) value of sound pressure in Pascals (Pa), and
 p_o = a reference value of pressure (for 0 dB), or 20 μ Pa for air.

The RMS value is used, from a set of instantaneous values, because it is directly related to the energy content of the sound. The convenience of expressing the result in units of dBs is that it compresses a wide range of amplitudes to a small set of numbers, accentuates peaks, and allows percent changes in dB to be read directly. The most significant thing to remember about dBs is that it is a logarithmic function (see Equation 114). This means that a doubling of dB values does not correspond to a doubling of the measured pressure, but an increase in the pressure ratio of 1.26 ($2\text{dB} = 1.26$ increase in p/p_0).

It is often convenient to deal with just parts of the frequency spectrum. These can be identified as octave or decade bands. An **octave** is a band with the upper frequency exactly twice the lower frequency. It is common in acoustics to work with **third octaves** (highest frequency 1.26 times the lower, or a ratio of $2^{1/3}$). The most recognized octave bands and the center frequencies of each band are shown in Table 7. You can see that the upper bands encompass much more of the spectrum than the lower bands. A **decade** is a band in which the upper frequency is 10 times the lower frequency (such as 3 to 30 Hz). Like the octave, higher decade bands contain much more of the spectrum.

Noise can be classified in three ways. **Random noise**, of most interest in the aircraft structures discipline, has an instantaneous amplitude that cannot be specified at any instant of time, but can only be defined statistically by an amplitude distribution function. **White noise**, often used in ground tests or simulations, is broad band noise with constant energy per unit of frequency. Finally, **pink noise** is also broad band but with an energy content which is inversely proportional to frequency (-3 dB per octave or -10 dB per decade).

9.4 Measurement of Sound

The SPL cannot be reliably measured close to the object emitting the sound because different parts of the object may emit sounds at different amplitudes. A suitable distance is defined as greater than the wavelength of the lowest frequency emitted or twice the greatest dimension of the object, whichever is greater. To meet this criteria, it is necessary to get beyond the **near field** and into a region where the sound has assumed an even distribution. This latter region is called the **far field** (Figure 107). In the far field the sound level will decrease -6 dB as the distance from the source is doubled. This is due to the **inverse square law** or the spherical spreading of the pressure waves and their associated dissipation of energy. Figure 108 shows the effects of the inverse square law and the natural sound absorption capability of air in attenuating the sound level. If the noise source is within an enclosure, the sound waves can be reflected from the walls and confuse level readings (the **semireverberant field**). For the applications addressed in this handbook, it is assumed that the measurements are always in the **far field** for ground tests, or directly on the aircraft for in-flight measurements.

The presence of a transducer (pressure sensor or microphone), its supporting mount and wiring, and any associated recording and analysis apparatus can influence the SPL reading. Depending upon the type of transducer used (Section 10.6), its orientation may also be critical. However, for our applications, the transducer is typically mounted within the aircraft structure flush with the external surface and all supporting equipment is inside the aircraft.

For human factors applications, the SPL measurement is often multiplied by different factors for different parts of the spectrum so that the levels can be more easily associated with the varying sensitivity of the human ear. The most popular such correction is the **A weighting**. For structures applications no weightings should be used.

When more than one sound source is present, it may be desirable to know the total SPL with both emitting after making separate measurements, or to find the level of one source knowing only the level of the other source and the combined level with both emitting. It is not proper to simply add and subtract SPLs because of the logarithmic dB scale. Instead, the two plots in Figures 109 and 110 are used. For two separate SPL readings from two sources, Figure 109 with the difference of the two readings (L_1 & L_2) should be used to get the additional level (L_+) to be added to the higher of the two measurements for the combined peak level (L_T). Similarly, with the total SPL (L_{STN}) and a level for one (L_N) of the two sources, using Figure 110 with the difference of the two readings will yield the level (L_-) to be subtracted from the total for the SPL of the unknown source.

Table 7
OCTAVE AND THIRD-OCTAVE PASSBANDS

Band Number	Nominal Center Frequency (Hz)	Third-Octave Passband (Hz)	Octave Passband (Hz)
1	1.25	1.12 to 1.41	
2	1.60	1.41 to 1.78	
3	2	1.78 to 2.24	1.12 to 2.82
4	2.50	2.24 to 2.82	
5	3.15	2.82 to 3.55	
6	4	3.55 to 4.47	2.82 to 5.62
7	5	4.47 to 5.62	
8	6.3	5.62 to 7.08	
9	8	7.08 to 8.91	5.62 to 11.20
10	10	8.91 to 11.20	
11	12.50	11.20 to 14.10	
12	16	14.10 to 17.80	11.20 to 22.40
13	20	17.80 to 22.40	
14	25	22.40 to 28.2	
15	31.50	28.20 to 35.50	22.40 to 44.70
16	40	35.50 to 44.70	
17	50	44.70 to 56.20	
18	63	56.20 to 70.80	44.70 to 89.10
19	80	70.80 to 89.10	
20	100	89.10 to 112	
21	125	112 to 141	89.10 to 178
22	160	141 to 178	
23	200	178 to 224	
24	250	224 to 282	178 to 355
25	315	282 to 355	
26	400	355 to 447	
27	500	447 to 562	355 to 708
28	630	562 to 708	
29	800	708 to 891	
30	1,000	891 to 1,120	708 to 1,410
31	1,250	1,120 to 1,410	
32	1,600	1,410 to 1,780	
33	2,000	1,780 to 2,240	1,410 to 2,820
34	2,500	2,240 to 2,820	
35	3,150	2,820 to 3,550	
36	4,000	3,550 to 4,470	2,820 to 5,620
37	5,000	4,470 to 5,620	
38	6,300	5,620 to 7,080	
39	8,000	7,080 to 8,910	5,620 to 11,200
40	10,000	8,910 to 11,200	
41	12,500	11,200 to 14,100	
42	16,000	14,100 to 17,800	11,200 to 22,400
43	20,000	17,800 to 22,400	

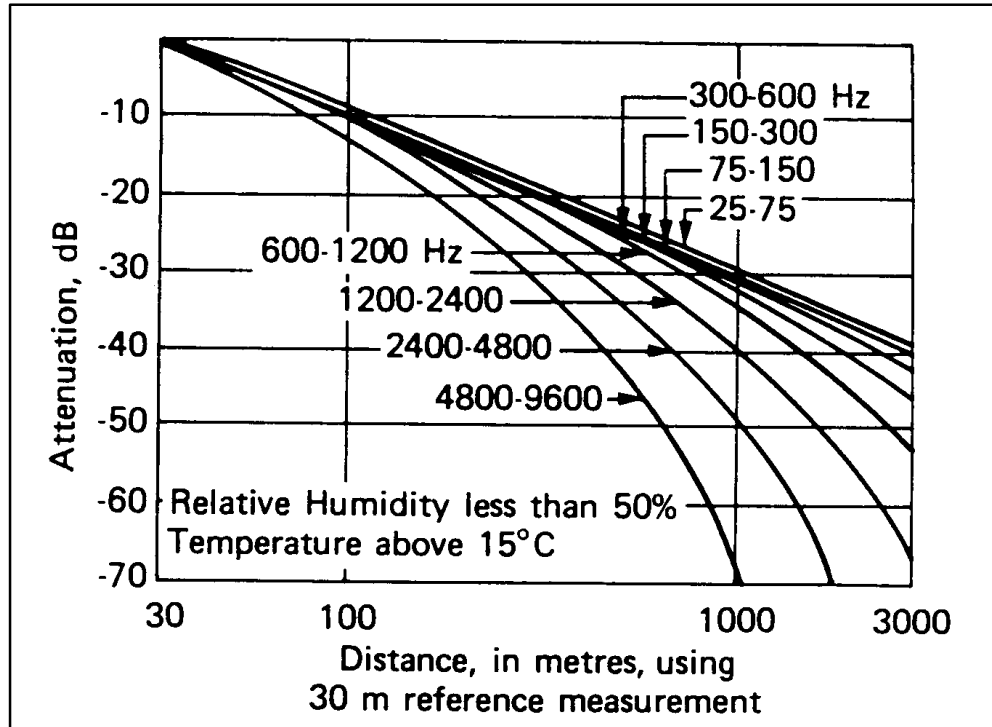


Figure 107 Sound Fields

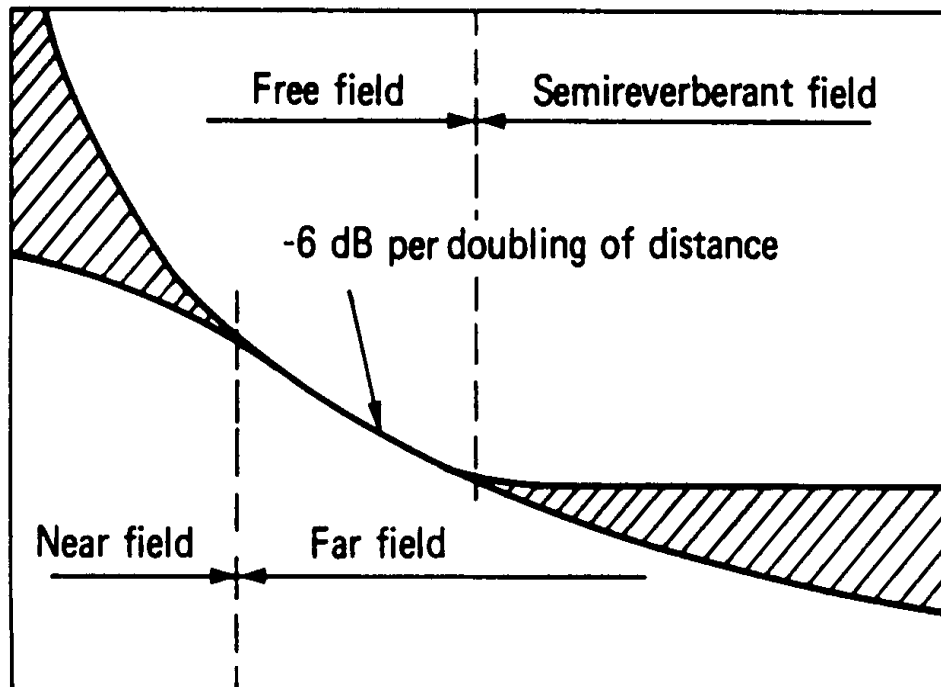


Figure 108 Sound Attenuation in Air

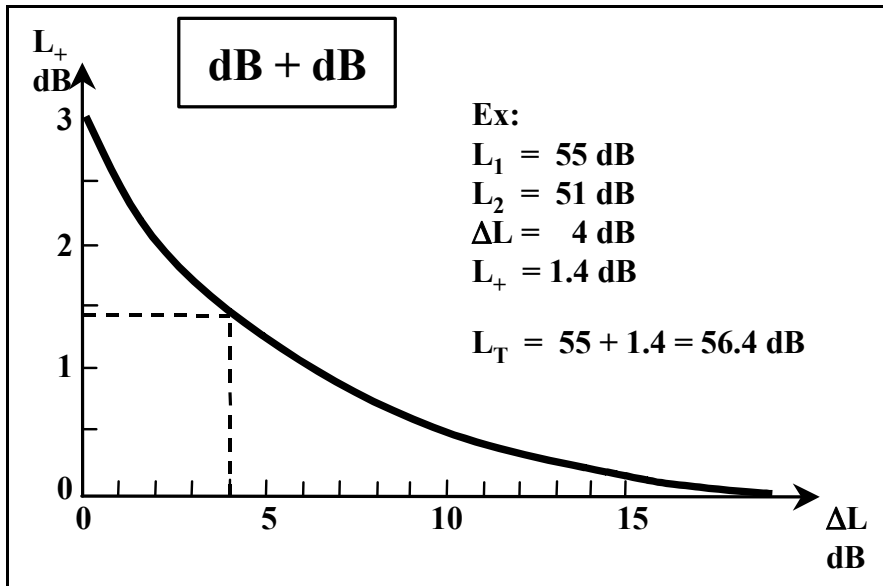


Figure 109 Summing Sound Pressure Levels

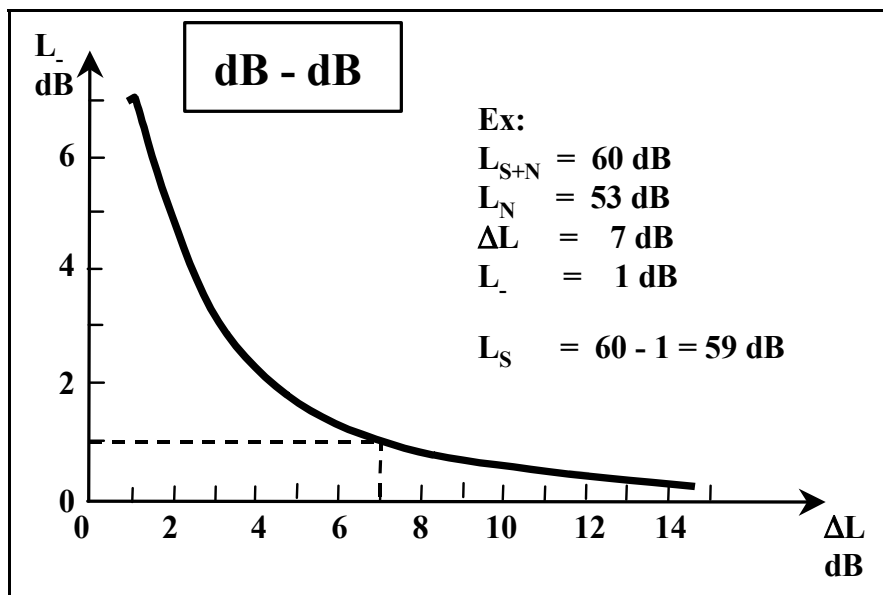


Figure 110 Subtracting Sound Pressure Levels

Although SPL is most often measured with RMS values, it may also be given as a peak value. Only RMS values can be added and subtracted as discussed above. Because experimentally measured environmental noise, particularly that from flight testing, can vary greatly in amplitude at any given frequency over a period of time, using peak values can be very misleading. Of more interest is some average SPL that the structure will be subjected to over the long term. It is most often desirable to see the SPLs as a function of frequency, but it is also occasionally necessary to obtain a single value defining a broad band level. Assuming that the response of the sensing and analysis equipment is 'flat' throughout the frequency range of interest, it is possible to produce this broad band result called the **overall sound pressure level (OASPL)**. This is a time-averaged integration of

the levels throughout the spectrum and is essentially an integration of all the power under the SPL curve. It represents the total power of the signal. For example:

$$\text{OASPL} = 10 \log_{10}(\sum 10^{\text{SPL}/10}) \quad (124)$$

where:

SPL = each octave, third octave, or individual spectral line sound pressure values, whichever is desired, composing the entire spectrum to be analyzed.

Because the sound level often varies over a time period in a random fashion, sampling must occur for a long enough time to be certain that the RMS value will be suitably close to the true average. This creates an element of uncertainty in the dB readings as shown in Figure 111. The conclusion is that at least 10 seconds should be allowed for a reading, and perhaps as great as 30 seconds or more in flight testing.

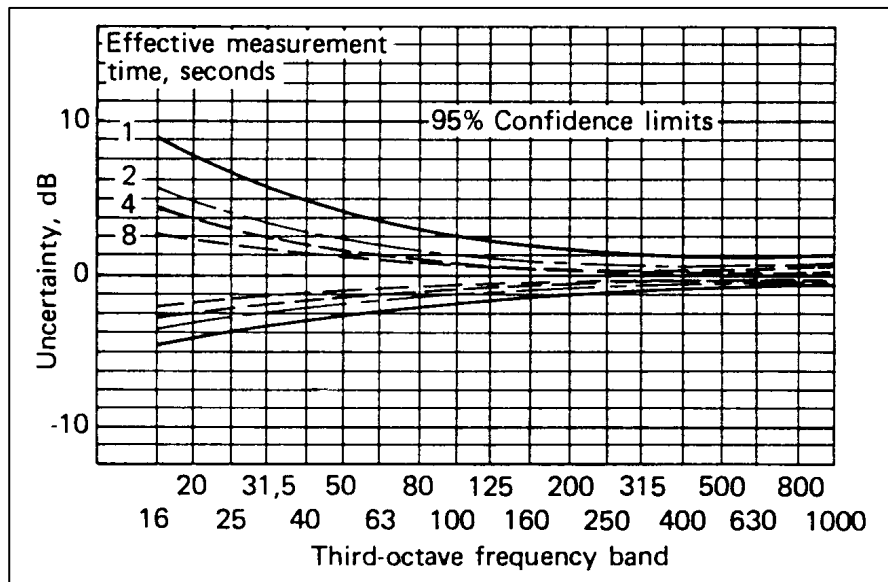


Figure 111 Effect of Measurement Time on Sound Pressure Level Results

It is occasionally useful to determine a sound power, measured as **sound power level**, or the total sound energy radiated by a source per unit of time. That is:

$$L_w = 10 \log (P/P_0) \text{ in dBs} \quad (125)$$

where:

P = the RMS of the sound power in watts (W), and
 P₀ = a reference value of 1 pW.

Some additional terms may also present themselves from time to time. **Power spectrum level** is the level of power contained in a band 1 Hz wide, referenced to some given reference level. The **sound exposure level (SEL)** is a constant sound level acting for 1 second with the same acoustic energy as another, nonconstant level sound. The **equivalent continuous sound level (L_{eq})** is similar to SEL but can be for any given time period.

9.5 Flight Tests

Several years ago, an airworthiness flight test was conducted on a heavily modified C-135 aircraft. The modification included several deep fairings added to the underside of the fuselage. These produced violent turbulence and vortex shedding that caused cracks to appear on the belly of the aircraft aft of the fairings and also broke an antenna off in flight. The antenna subsequently impacted the plane and punched a hole. In order to determine exactly how long most of the belly skin and underlying structure could survive in this environment, it was necessary to do an acoustics flight test to find the exact pressure levels on the belly as a function of frequency and to compare this with empirical data for the fatigue life of the material.

Vibro-acoustic data is collected as a matter of course in areas of high susceptibility, determined through analysis, during the early development flight test effort. Problems like the KC-135 sonic fatigue cracking discussed in Section 9.1 is the most common reason for doing vibro-acoustics testing. The intention is to define the environment to which a piece of equipment will be subjected and to match this against its specifications or lab test levels. Apart from simply measuring the sound levels, loads and accelerations of the test subject are typically the most important data to come out of such tests. However, it is often questionable whether the excitations are due strictly to acoustics, are transmitted by the airframe from internal components, or are just general structural dynamics. This can become important if a decision is made to try altering these inputs instead of simply isolating the victim system.

9.5.1 Preliminary Ground Tests

The in-flight acoustic environment can be replicated, to some degree, using a sound chamber. While seldom practical for an entire airframe, components and stores can greatly benefit from such ground testing. The test is tailored to the customer's specification under which the item was developed and built. Acoustic and vibration MIL SPECS for aircraft and aircraft equipment have been specifically written to reflect historical and projected levels. They are stated in terms of frequency, pressure levels, accelerations, and duration of exposure for certain phases of operation and flight. It is common to subject the test object to white noise in which the energy content decreases linearly or exponentially as frequency increases. This simulates a decrease seen in actual conditions. Typically, the article must survive up to 162 dB OASPL for a brief period before it is considered safe to fly. Fatigue of metal aircraft structure becomes a concern at levels above 140 dB OASPL. For the example of a shallow weapons cavity at transonic speeds discussed in Section 9.1, the SPL experienced was 170 dB. It is always wise to ensure that chamber tests have been performed and to review the results versus the specifications.

During flight testing of a missile externally mounted on a carrier aircraft, many problems with cracks, popped rivets, delaminations, and the like occurred on the store and adjacent structure of the aircraft. Acoustic measurements showed that levels greater than 165 dB were being experienced. The missile was returned for chamber tests to 167 dB (an increase of over 20 percent in the external pressures) during which many more failures occurred. A **progressive wave chamber** had been used, although MIL-STD-810C (Reference 7) called for the more common **reverberant chamber** test, and it was later shown that the test produced much higher loads than those recorded in flight at similar SPLs. It is also possible that chamber simulations will produce lower load conditions than those experienced in flight. It is always necessary to fly an instrumented article and inspect it for failures to be certain that its design is adequate.

9.5.2 Test Concepts

Sound pressure level is measured either with a microphone or a pressure transducer (Sections 10.5 and 10.6). Calibrations of the microphones before the test, and possibly after, is important. The transducer must be mounted flush with the surface of the article (aircraft skin) or suspended in the region of interest. If it is mounted so that a cavity exists between the face of the transducer and the surface, the cavity will act as an organ pipe, greatly amplifying any sound with a wavelength matching the cavity dimensions.

Tests should be conducted at representative operational ground and flight conditions. This may include different aircraft engine power settings, taxi conditions, takeoff and climbout, cruise at a variety of altitudes and

airspeeds (particularly at the edges of the normal operating envelope and with afterburner), in various flight configurations like weapons or cargo bay doors open, landing gear, flaps or spoilers extended, approach and landing, etc. Even a sudden reduction in power, a throttle 'chop,' can be a problem. The inlet air spillage from a chop can impact stores downstream, as was found on the F-15. It is essential that an adequate dwell time on condition for sufficient data collection be allowed, at least 30 seconds to 1 minute. Transducers should be scattered around the area of interest so that sound level contours (also known as **isobel contours**) can be traced out (Figure 112). Also, since vibro-acoustics data is typically of such low signal levels, it is important to define the noise level of signal processing and recording equipment to determine the percentage of the response attributable to this noise.

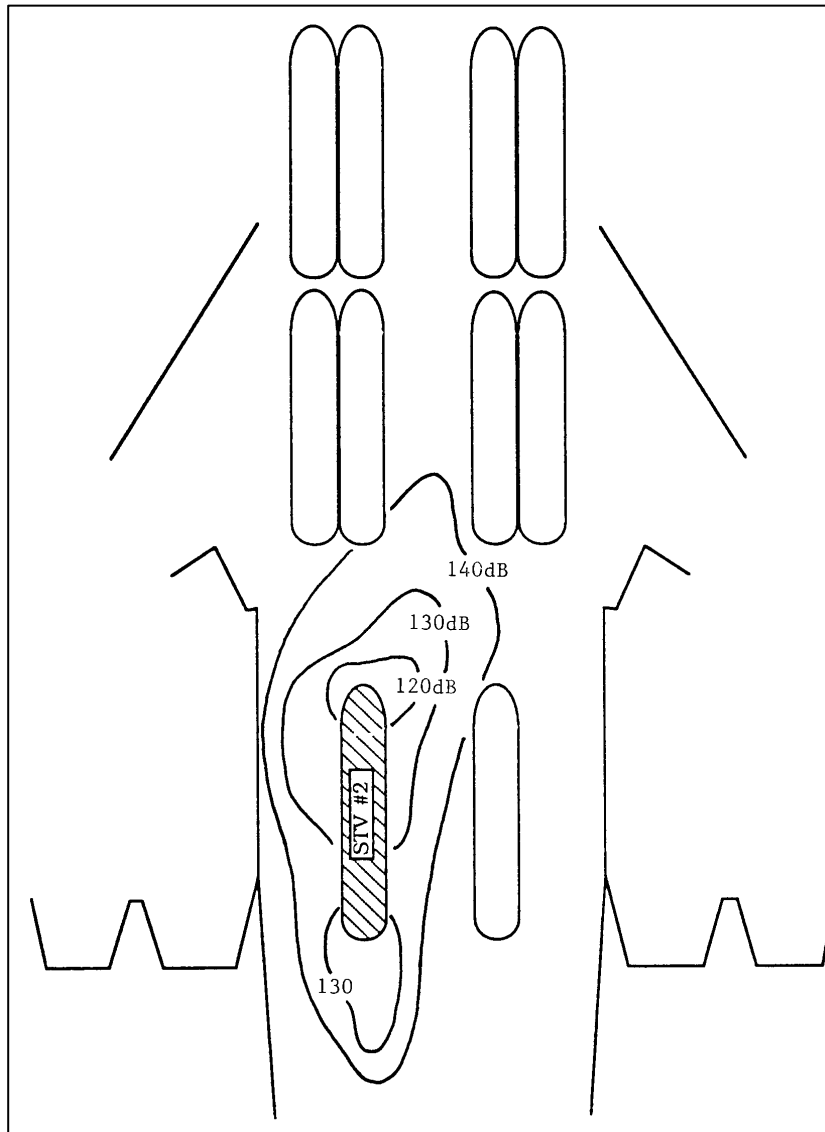


Figure 112 Example Sound Contour Pattern
(B-1B Underbelly with Missile Shapes Installed) (for illustrative purposes only)

9.5.3 Data Analysis

As with the analysis of other frequency-type data discussed in this handbook, it is most helpful to present the SPL as a function of frequency. This can be done by performing a Fourier transformation (Section 11.3.1). To conform with standard acoustics practice, the analysis is most often shown as third octaves. In a sound level meter or dedicated acoustics-type signal analyzer, no transformation takes place. Instead, third-octave filters specifically designed to the conventional center frequencies shown in Table 7 and attenuation standards will selectively analyze the entire spectrum in pieces as shown in Figure 113. The SPLs for each third octave can then be presented on a frequency scale as shown in Figure 114. This can be termed a **spectrogram** as opposed to a true Fourier transformation. Of course, the results of a Fourier transformation can also be presented in such a form, if desired. They can be shown as a 'stair step,' as in Figure 114, or by simply connecting the levels at the center frequencies by straight lines for a 'sawtooth' type pattern.

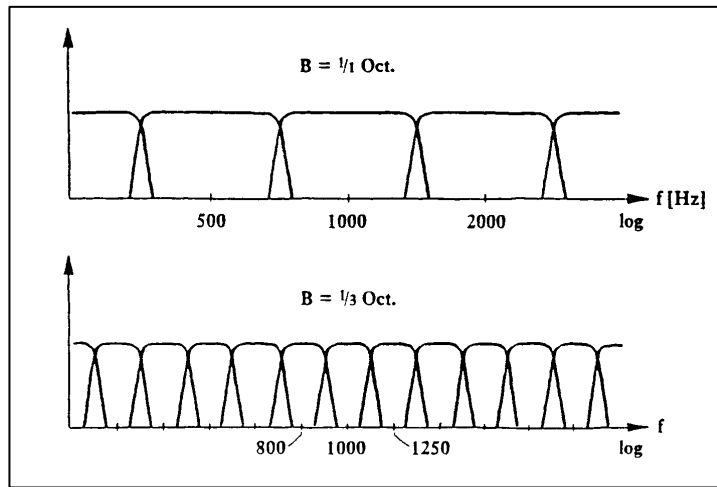


Figure 113 Illustration of Octave and Third-Octave Segmentation of Frequency Spectrum

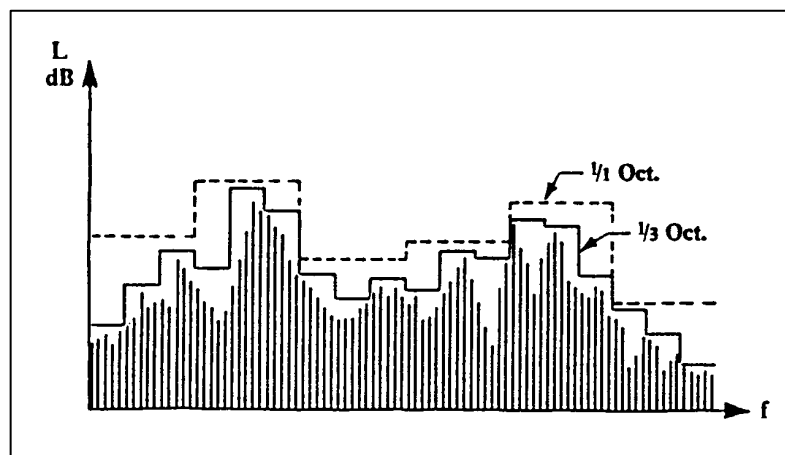


Figure 114 Illustration of Octave and Third-Octave Sound Pressure Level Versus a Fourier Transform Presentation

The test data should be shown versus the specification limits. An example of this is shown in Figure 115, in which the 'sawtooth' presentation is used. Note that the plot should indicate both the reference atmospheric pressure used in the analysis as well as the test condition (configuration, transducer location, dynamic pressure, etc.). In this case the SPL limits have been exceeded at several points in the spectrum. It must then be decided what has caused these high levels and the easiest ways to reduce them if they are considered critical.

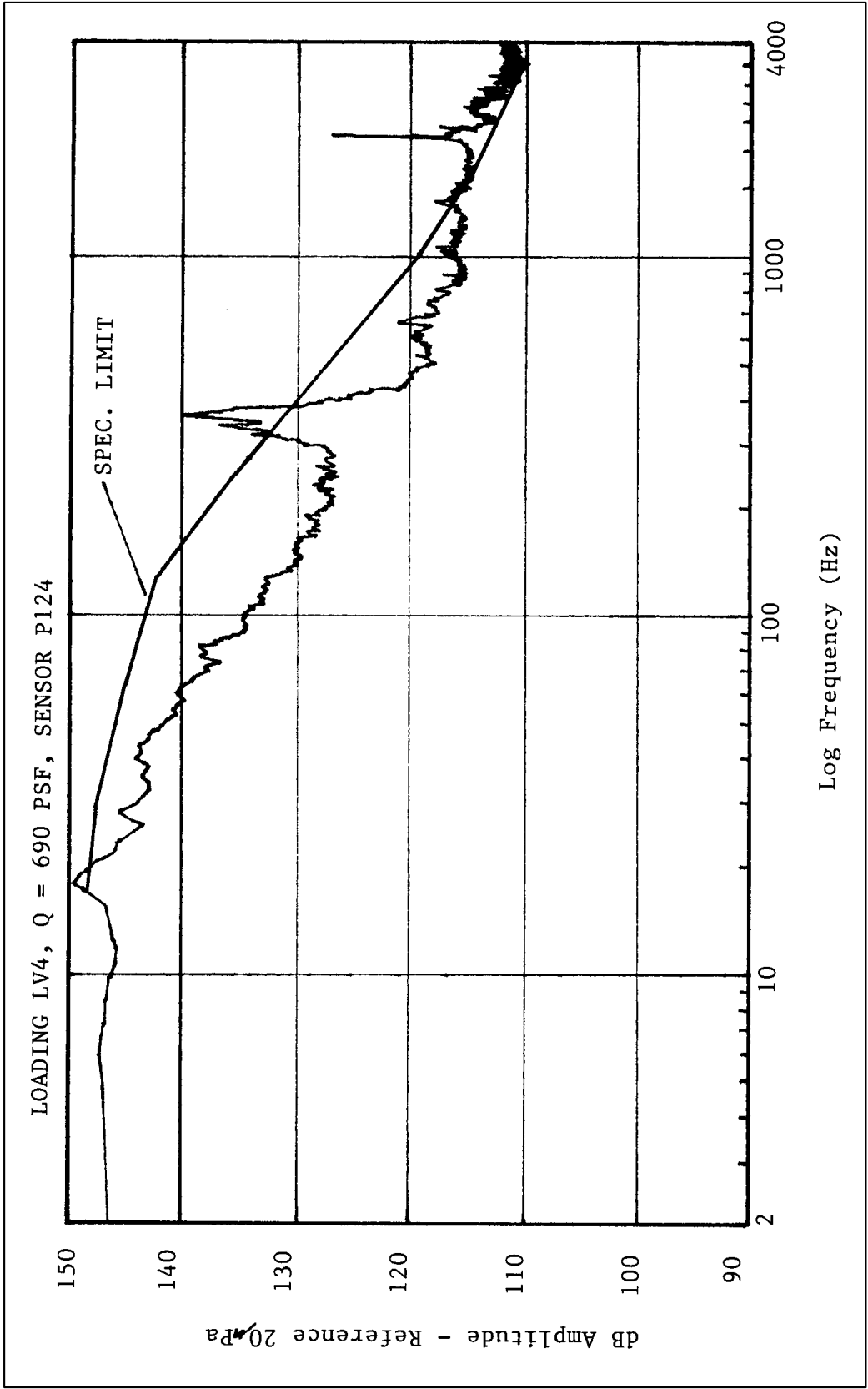
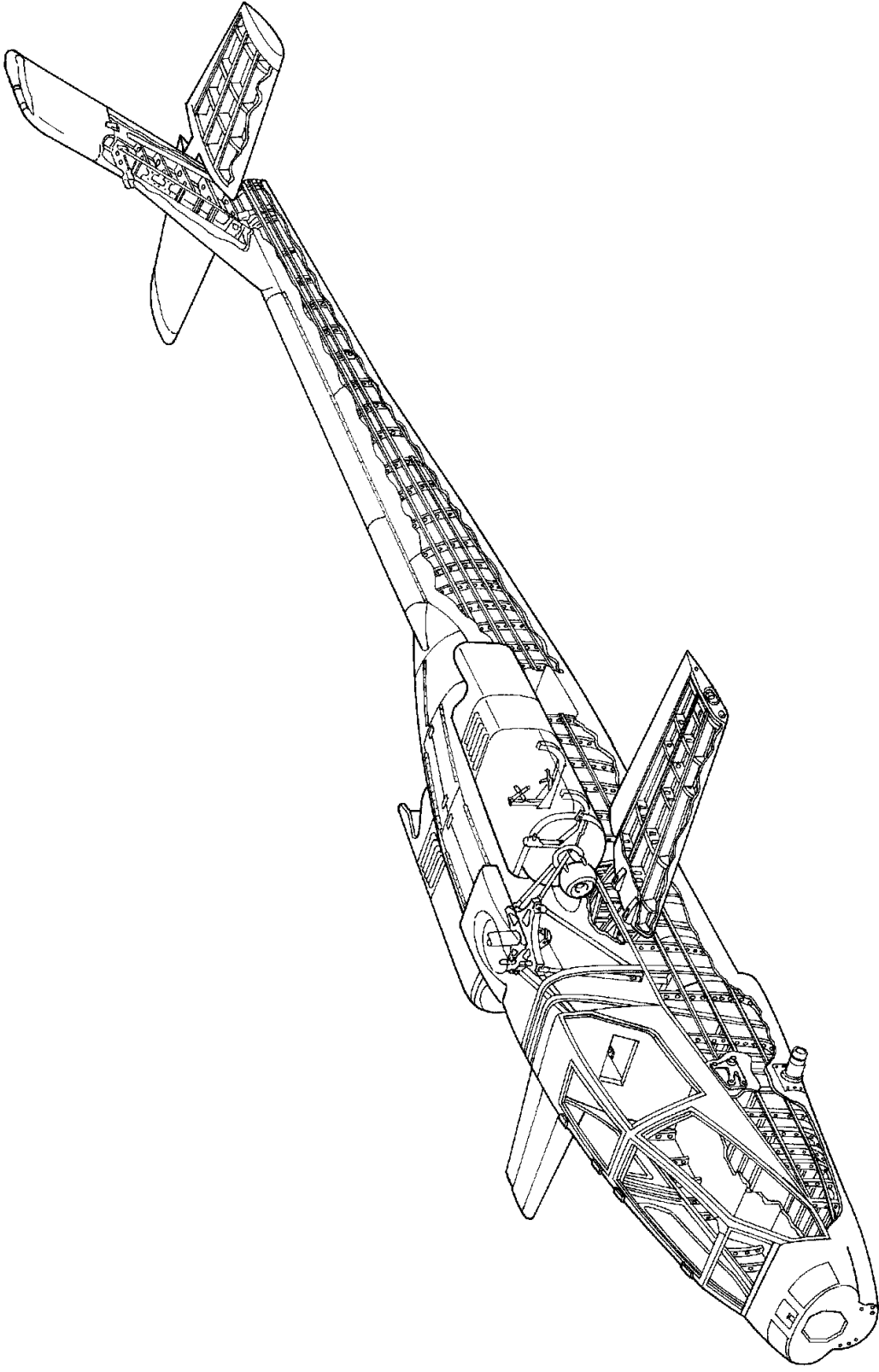


Figure 115 Example of Sound Pressure Level Test Data Versus Specification Level

SECTION 9 REFERENCES

1. *Measuring Sound*, (Pamphlet), Bruel & Kjaer, Naerum, Denmark, September 1984.
2. Pocket Handbook, Noise, Vibration, Light, Thermal Comfort, Bruel & Kjaer, Naerum, Denmark, 1986.
3. Peterson, Arnold P.G. and Gross, Ervin E., Jr., *Handbook of Noise Measurement*, GenRag Incorporated, Concord, Massachusetts, 1978.
4. Hunter, Joseph L., *Acoustics*, Prentice-Hall Incorporated, Englewood Cliffs, New Jersey, 1957.
5. Beranek, Leo L., *Acoustic Measurements*, John Wiley & Sons, New York, New York, 1956.
6. Graf, Phil A. and Drake, Michael L. *Elimination of KC-135A Aft Fuselage Acoustic Fatigue Failures*, UDR-TR-85-22, University of Dayton Research Institute, 31 January 1985.
7. Military Standard Environmental Test Methods, MIL-STD-810C.
8. Low-Drag Weapon Carriage in *Interavia Aerospace Review*, January 1990, pp. 12-13.
9. Frost, W.G., Tucker, P.B. and Wayman, G.R., Captive Carriage Vibration of Air-to-Air Missiles on Fighter Aircraft, *The Journal of Environmental Sciences*, September/October 1978.



McDonnell-Douglas AH-64A Apache Structure

10.0 INSTRUMENTATION

10.1 Introduction

While structures flight test engineers are seldom responsible for the actual installation of test instrumentation in an aircraft, or the assembly of the entire instrumentation system for recording and transmission of data, they often select the transducers, choose their location, and specify required accuracies. To perform this task effectively, it is essential that the engineer be conversant in the various transducers available and understand what happens to the data from the point at which it is sensed until it is displayed in **engineering units (EUs)** for analysis. This requires at least a broad understanding of instrumentation and telemetry systems so that the structures and test range people can talk to each other with reasonable certainty of being understood. Such understanding is essential when working with those who do the instrumentation design and installation, and when resolving problems which crop up during testing. This chapter, as with all others in this handbook, just touch the surface of this subject, and the reader is strongly encouraged to do supplemental reading as interest or project requirements dictate.

Flight test aircraft (also known as **testbeds**) are often prototype vehicles heavily instrumented with thousands of individual measurements (also known as **measurands**). Much of this instrumentation is installed at the time of construction and may not be readily accessible, if at all. The associated system equipment is identifiable by the insignia orange color used on all test system boxes and wiring. An effort is made to allow instrumentation systems to be reconfigurable to meet the requirements of the most current flight test objectives. Such systems are very complex and the associated technology is constantly being improved. However, the structures engineer should get to know the responsible systems engineer and become familiar with the capabilities and limitations of the instrumentation package on the test aircraft.

In aircraft modified for a flight test project, the modifications necessary to conduct the test as well as instrumentation installation, should take place prior to or during the test approval cycle. The structures engineers on the project should review the '**project history**,' the list of the instrumentation parameters that will be available as part of the instrumentation data stream that is recorded on board and perhaps telemetered to the ground. The engineer should ensure that all parameters essential to meeting the specific test objectives are being used and are within the proper data ranges. Most projects will have an instrumentation engineer assigned who is a good source for such information.

During the test planning phase, a list of **technical Go/No-Go** parameters are decided upon by the engineers. Lack of these parameters would make performing the test maneuvers pointless in meeting the test objectives during the flight. Those measurands that are necessary to ensure that the test is conducted in a safe manner are known as **safety-of-flight (SOF)** Go/No-Go parameters. They are measurements which are felt to be essential for monitoring on the ground or in flight when dealing with a test aircraft or equipment of uncertain characteristics. Safety of flight parameters must be verified as functioning before the flight is launched. The flight will be terminated immediately should one of these critical measurands fail during the flight. A variation on the technical and SOF measurands is the **safety-of-test (SOT)** parameter which must be functioning to safely perform a certain type of test, although the plane may fly otherwise. It is always wise to provide backups to critical measurands for redundancy. Failure of a technical Go/No-Go or the SOT measurand need not result in test termination if other test points can be performed for which the lost parameters are not necessary.

10.2 Strain Gages

Strain gages are the common means of measuring strain from which stress can be derived (see Section 3.2) to ensure that the limit stress of the material is not being exceeded. They can also be used to measure loads, as will be explained later. They can be employed in a static loading situation or in a dynamic application where their response can be used to measure the oscillatory motion of a structure. The strain gage employs the principle that the electrical resistance in a metal element will change with a change in length. Thus, the change in resistance of such an element bonded to a test specimen in such a way that it will experience the same deformation as the specimen under a load will be a measure of the strain within the specimen. The change in resistance is extremely small, requiring sensitive equipment to monitor. In fact, the change in resistance is so

small as to be on the order of that produced by temperature or shunting due to moisture, and so requires great care in transducer installation and use. It is clear that the strain gage is very simple in concept and design, but some further information is needed to use them properly.

10.2.1 Selection

The most common gages used in aircraft flight testing are small foil gages. These consist of a thin metal foil photo-etched to the desired pattern and bonded to a nonconductive but durable backing. The patterns are optimized for particular applications but usually look like that shown in Figure 116 (greatly enlarged). It allows any strain to be experienced by the greatest portion of the foil conductor. The gage shown in Figure 116 is designed to measure strain only along its longest axis, as shown by the arrows (not part of the gage). This is a **uniaxial gage** and is suitable for components in which the stress is expected to be uniaxial, or for which only the stress along the axis of the gage is of interest. The **bi-axial strain gages** have two uniaxial elements at 90 degrees to each other (Figure 117a) which can be aligned with known **principal stress** directions (the direction of the maximum and minimum stresses) or any direction of choice. For an application in which the principal stress directions are not known and multi-axial stresses are expected, a **rosette** strain gage can be used (Figure 117b). The rosette typically has three uniaxial gage elements oriented at either 120 (delta type) or 45 degrees (rectangular type, Figure 117d) from each other. For pressure vessels, the **spiral gage** (Figure 117c) can be used. There are many other gage patterns available in many different sizes, and most manufacturers will prepare a pattern to customer specifications.

Apart from gage pattern, gage size, resistance and temperature limits must also be considered. Special gages are manufactured for high temperature applications. A large gage will be easier to install and may be necessary for high-stress situations where the strains expected could exceed the capability of a small gage (cause the gage to exceed its elastic limit and possibly break). However, a large gage will usually not be as sensitive as a small gage. Typical unstrained resistances are 120, 350, and 1,000 ohms. Matching the gage material to the test article material (aluminum gage to aluminum test specimen, brass to brass, etc.) is important to avoid problems with incompatible thermal expansion characteristics.

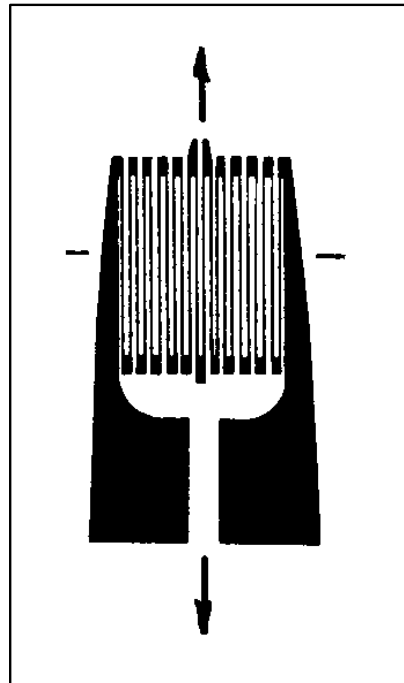


Figure 116 Typical Uniaxial Strain Gage Configuration

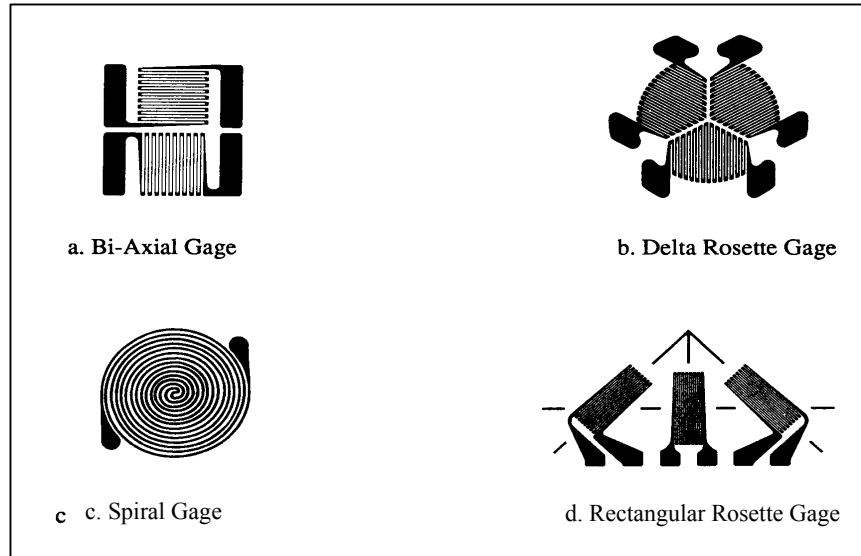


Figure 117 Other Common Strain Gage Configurations

10.2.2 Measurement

Each strain gage or batch of gages will have a **gage factor** (K) determined by the manufacturer prior to packaging. The gage factor permits a conversion of resistance change to strain as expressed by:

$$K = (\Delta R / R) / e \quad (126)$$

where:

- ΔR = the change in resistance,
- R = the specified gage resistance (unstrained), and
- e = the strain experienced.

Thus, strain can be derived from the equation and converted to stress as shown in Equation 20. Of course, a negative value of ΔR indicates compression. It can be seen with some thought, a strain gage with a higher gage factor and resistance would be more desirable than one with lower values. For the bi-axial gage already oriented with the principal axes, each leg is analyzed as a uniaxial gage using Equation 126 for the principal strains. The associated stresses are then:

$$\sigma_{\max} = E(e_{\max} + \nu e_{\min}) / (1 - \nu^2) \quad (127)$$

$$\sigma_{\min} = E(e_{\min} + \nu e_{\max}) / (1 - \nu^2) \quad (128)$$

where:

- e_{\max} and e_{\min} (a negative value) = the measured principal strains in the appropriate legs of the bi-axial gage,
- E = the Young's modulus of the material (see Section 3.2.2), and
- ν = the Poisson's ratio of the material (see Section 3.2.2).

For the rectangular rosette gage, the principal strains and stresses are derived as:

$$e_{\max,\min} = 0.5(e_a + e_c) \pm 0.5\sqrt{(e_a - e_c)^2 + (2e_b - e_a - e_c)^2} \quad (129)$$

$$\sigma_{\max,\min} = E/2[(e_a + e_c)/(1-\nu)] \pm \sqrt{(e_a - e_c)^2 + (2e_b - e_a - e_c)^2} / (1+\nu) \quad (130)$$

where:

e 's denote the strains in each of the three legs of the rosette, and \pm is used for the maximum or minimum.

For the delta rosette:

$$e_{\max,\min} = (e_a + e_b + e_c)/3 \pm \sqrt{[e_a - (e_a + e_b + e_c)/3]^2 + (e_c - e_b)^2} / 3 \quad (131)$$

$$\sigma_{\max,\min} = E\{(e_a + e_b + e_c)/[3(1-\nu)] \pm \sqrt{[e_a - (e_a + e_b + e_c)/3]^2 + (e_c - e_b)^2} / 3 / (1+\nu)\} \quad (132)$$

Because the change in resistance in a strain gage under load is so small, a **Wheatstone bridge** is used to convert the resistance change to a voltage, amplify the signal, and provide compensation for temperature changes. The typical elements of this dc circuit are shown in Figure 118. The **temperature compensating gage (dummy gage)** should be identical to the active gage and bonded to a sample of identical but unstressed material and subjected to the same ambient conditions. The circuit will then automatically subtract out the stresses due to temperature variation. The adjustable resistor allows for balancing of the bridge or the zeroing out of any **residual strain** reading in an unloaded state. Using the nomenclature for resistances from Figure 118:

$$A/B = D/C \quad (133)$$

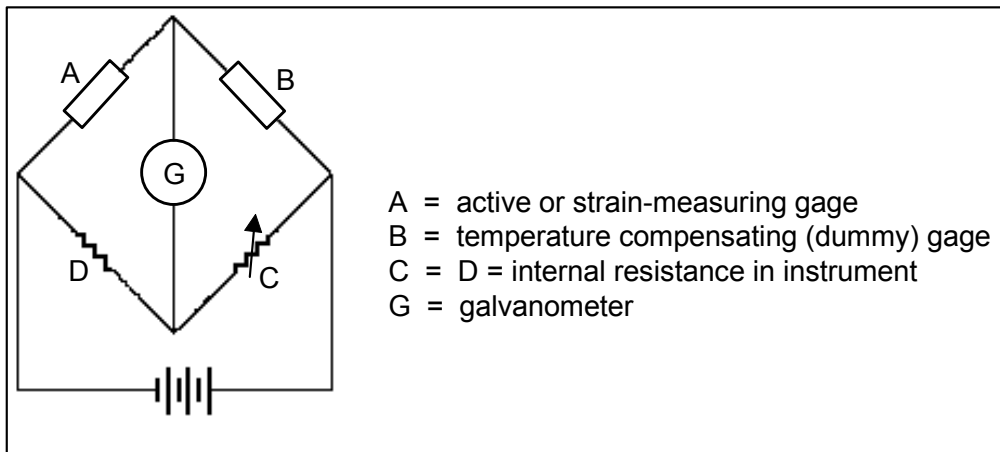


Figure 118 Typical Wheatstone Bridge Circuit

In a loaded situation the bridge will be unbalanced. For static tests it is good practice to record the zero-load strains both before and after the loading to account for 'drift.' The bridge used in flight testing will typically lack the galvanometer (strain meter). Some people make a point of using gages from the same package for a bridge to reduce differences introduced by manufacturing tolerances.

In the laboratory, a purpose-built **strain meter** (rather than a simple volt meter) can be used into which the gage factors can be set, no-load zero offset readings can be nulled, and multiple gages can be read. In flight testing this is not available, and the analysis is usually done by computer using recorded gage outputs.

10.2.3 Calibration

Strain gages are often used to measure loads. A load applied at a specific spot on a structure will always give the same stress/strain at another specific spot, all else remaining the same. By measuring gage output for incrementally increased loads, the strain gage can be ‘calibrated’ so that strains read in flight can be used to determine the loads at that condition. Shears, bending moments, and torques are the load components that are typically measured by the strain gages in such tests. This is a fairly straightforward thing when dealing with a uniaxial load in a simple component like a beam. However, measuring loads in a complex structure like a wing, with distributed and varying loads, required a much more involved setup and calibration.

For loads measurement applications, the strain gages should be applied where the stresses will be adequate to obtain good sensitivity, but away from areas of local stress concentrations. Ideally, the gages intended for measurement of a particular type of load should be located where that load is dominant. In practice this is seldom a clear-cut decision. For wing applications, the gages intended for shear measurements should be placed on the shear web of the spars, the bending moment gages on the spar caps or the skin, and torque gages on the structure’s torque boxes (Figure 119). Care must be taken not to place the gage at an area of potential stress concentrations (such as weld joints, cutouts, sharp corners, edges of doubler plates, attachment fittings, severe buckling areas, etc.) which could produce confusing readings. It is a common practice to use redundant gages in these areas, such as either side of the shear web, top and bottom of the spar caps, etc. Analogous areas should be used for structures other than a wing. Generally, as many as three to five gages (bridges) are used to derive a single force component. This is done for the sake of accuracy and to ensure that the strains in all primary relevant areas of the structure are accounted for. The output of more than one gage is then used to derive the desired loads. This makes the calibration a very involved process.

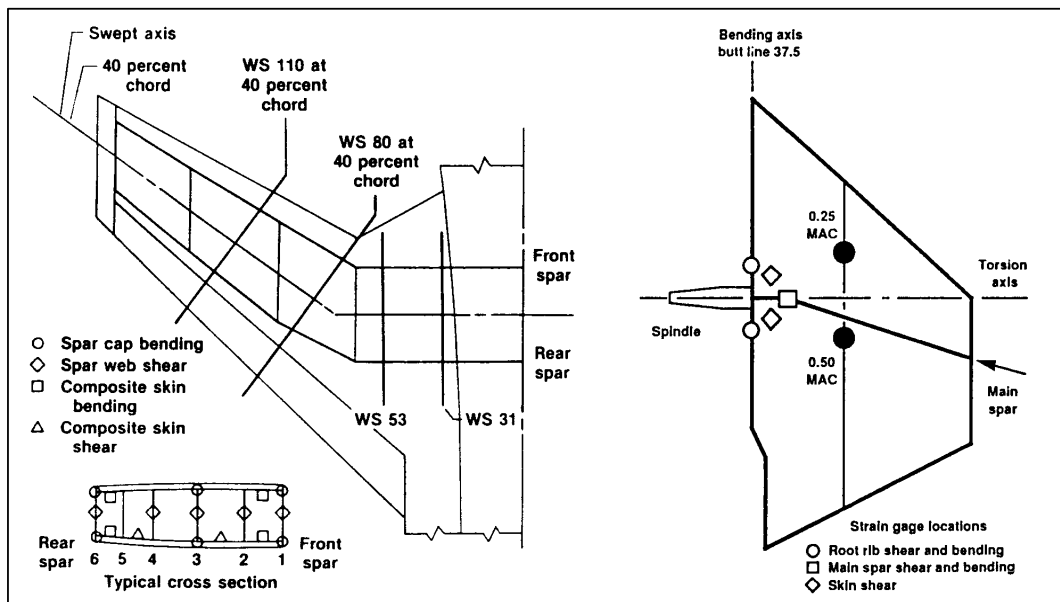


Figure 119 Example Strain Gage Installation Loads Measurements - X-29 Wing and Canard

Reference 7 provides a very detailed discussion of how a strain gage **loads calibration** is performed, with a complete derivation of equations and discussion of assumptions. The calibration uses the **principle of superposition**. That is, the strain at a particular location due to loads applied simultaneously at several points on the structure is the algebraic sum of the strains due to the same loads applied individually. The individually applied calibration load can then be used to derive an equation for determining the distributed load on the structure. The calibration measurements would be used to fill the strain matrix of the following equation for shear (V), and likewise for torque (T) and moment (M).

$$\begin{Bmatrix} V_1 \\ V_2 \\ \cdot \\ \cdot \\ V_i \end{Bmatrix} = \begin{bmatrix} u_{11} & u_{12} & \dots & u_{1j} \\ u_{21} & u_{22} & \dots & u_{2j} \\ \cdot & \cdot & \cdot & \cdot \\ \cdot & \cdot & \cdot & \cdot \\ u_{i1} & u_{i2} & \dots & u_{ij} \end{bmatrix} \begin{Bmatrix} C_{11} \\ C_{12} \\ \cdot \\ \cdot \\ C_{1j} \end{Bmatrix} \quad (134)$$

where:

u = nondimensional bridge outputs.

An i number of shear loads are applied at various chordwise positions on the structure and the measured strains on j bridges recorded for each loading. What is sought is a single expression that would permit shear to be solved for, having only the strain outputs from the bridges. That is:

$$V = C_{11}u_1 + C_{12}u_2 + \dots + C_{1j}u_j \quad (135)$$

and similarly for torques and moments. Equation 134 gives j unknowns and i equations which can be solved simultaneously for the coefficients C , as long as i is greater than j . The same process is done with torque and bending moment loadings and the coefficients for the analogous equations to 135 solved. It is common to calculate the errors to be expected if the equations are solved with one or more of the original gages nonfunctional. The application of precise calibration loads generally requires fixtures, jigs, calibrated pneumatic or hydraulic load rams, and the like which makes the process a major laboratory test when an entire airframe is involved. It is possible to provide a low-level loads calibration using just onboard fuel and weapons to load the structure, although it is not a recommended procedure.

Another method for calibrating the gages installed in an aircraft structure is to associate readings measured at specified flight conditions with loads analytically predicted or historically seen for that flight condition. A finite element model of the aircraft can provide predicted loads at the strain gage locations for exactly specified flight conditions like altitude, airspeed, and maneuver. The measured stresses at these actual conditions in flight will then be a measure of the loads which are assumed to be the same as those predicted mathematically or seen previously (perhaps on another aircraft of the same model). The problem with this method is that predictions are just that, and will vary from the actual loads by some unknown percentage. The ability of the pilot to fly the conditions precisely will also add some uncertainty to the calibrations. The method should not be used on a prototype airframe or one that has been substantially modified. A precise ground loads test approach is still considered the best calibration method, albeit expensive and time consuming. It is much more practical to apply the minimalist approach to more simple components, such as actuators or support members. In such cases it may be advisable to use up to eight gages per bridge for linearity and to render the output as much a unique function of the load as possible.

10.2.4 Installation

The bonding of the strain gage to the surface of the test item is extremely important for accurate strain readings. The surface should be carefully prepared before cementing the gage. This is done by removing any paint or other coatings, lightly sanding and polishing the bare material, followed by a thorough cleaning. Several cements are suitable, some dictated by the test environment. The gage must be protected against damage during the cementing, and excessive cement and trapped air bubbles must be avoided. Alignment marks typically must be made so that the gage is properly aligned (often of paramount importance) but these must not be under the gage itself. This entire process takes much practice for a proper gage application.

The gage will usually have tiny wires from the small solder pads on the gage itself to bigger pads where larger, more durable wires can be soldered. These larger wires must be secured so that they cannot be pulled

out, and then a stress-relieving loop added as an extra precaution (Figure 120). The wiring should be shielded to reduce contamination of the signal by the surrounding electromagnetic environment. The gage is protected against moisture with a coat of varnish or other substance that will dry to a hard surface. In flight testing, the gage and wires immediately adjacent are 'potted' or covered with a thick, durable coating of a rubber-like compound. This is particularly important for gages mounted external to the aircraft. Even with these measures the strain gage is very easily damaged or the wires pulled loose. For this reason it is a common practice to mount redundant or backup gages for each primary gage. For a structure with many gages installed, just about any of the calibrated gages can be used to measure the strain for which another gage is primarily installed, although the measurement will not be as efficient.

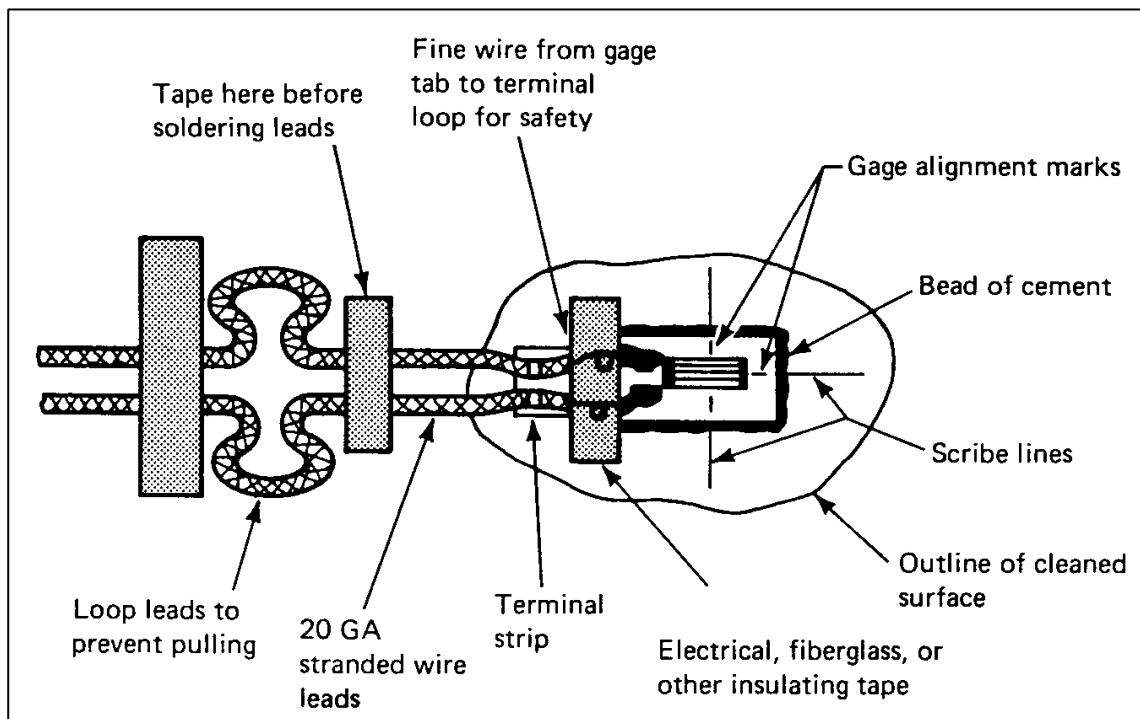


Figure 120 Example Strain Gage Installation

10.3 Accelerometers

The piezoelectric accelerometer is now the widely accepted means of measuring structural accelerations. These transducers are available in very small sizes with outstanding frequency range, resolution, and linearity, and are extremely durable. The piezoelectric device contains a piezomaterial element that generates a small electrostatic charge when compressed, or stressed by force or acceleration. Since the charge is proportional to the applied force it can be used as a measure of that force. The orientation of the element will determine whether the generated charge (measured as picoCoulombs [pC]) is positive or negative.

The basic structure of the piezoelectric accelerometer is shown in Figure 121. The piezomaterial is highly preloaded between the case or sleeve and a seismic mass. The inertia of the mass will act as the force transmitted to the piezomaterial. The greater this mass the greater will be the sensitivity of the transducer. A **triaxial accelerometer** is simply three accelerometers assembled as a single unit with each sensor precisely oriented to three mutually orthogonal axes. The 'triax' is very useful for testing vibration environments at an internal location and greatly reduces installation difficulties where three axes accelerations must be obtained. For the more 'dirty' installations, a carefully machined block with three mounting points for accelerometers in the mutually orthogonal pattern has the advantage of quick installation, and lower initial expense and maintenance of a triax. Accelerometer packaging has continued to be reduced until some are less than half a gram in weight.

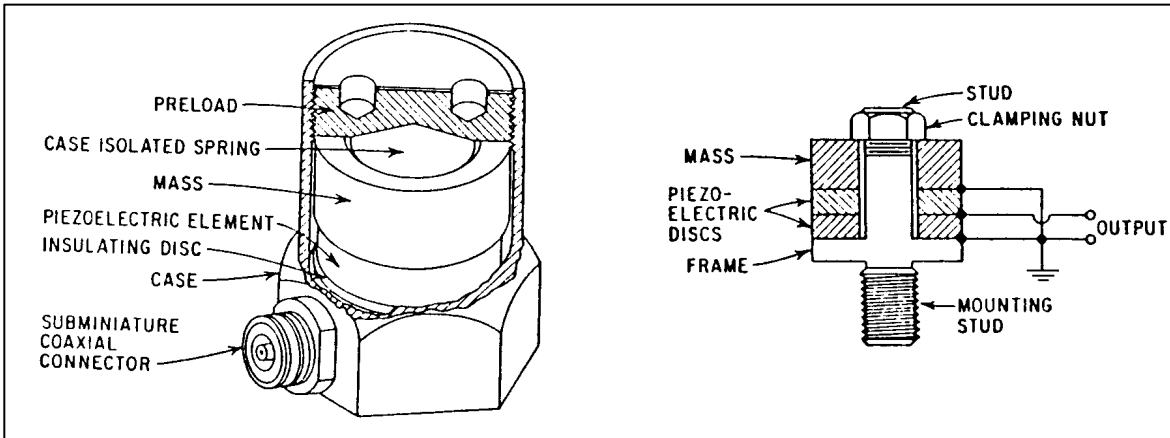


Figure 121 Common Piezoelectric Accelerometer Components

The **piezoresistive accelerometer** is based on an element analogous to a strain gage, the output of which is a function of the acceleration. This device has high accuracy but has many other limitations that has reduced its usefulness over the past decade or so. The **servo accelerometer** is also a very specialized device beyond the limited scope of this text.

10.3.1 Selection

The three basic types of accelerometer designs are illustrated in Figure 122. The choice of **compression accelerometers**, **upright**, or **inverted** will depend upon mounting application or restraints. The upright design is most frequently used because the case is more shallow and the coaxial cable from the transducer can be secured to the mounting surface to reduce the risk of damage. The inverted design sees use in ground vibration tests (see Section 7.0). The **shear mode transducer** is also of shallow design and may have a through-the-case mounting screw method.

Frequency range and resolution are the most important criteria for accelerometer selection, although most accelerometers today are good for a wide range of applications. Transducers that respond to very high frequencies are usually good down to only around 3 to 5 Hz at the low end. More generally, they should not be trusted below about 20 percent of the natural frequency of the transducer itself. For good resolution at very low frequencies, an accelerometer with a larger seismic mass must be used which in turn makes it unsuitable for high frequency applications. The user should assure that the linearity of the response and the frequency resolution is adequate for the entire frequency range of interest. The natural frequency of the transducer itself must be beyond the frequency range of interest, and this is generally the case for aircraft use. **Sensitivity** (mv/g), where g is the acceleration due to gravity, should also be considered to ensure that the anticipated acceleration level can be faithfully transduced by the device. Lastly, the mass of the transducer must not add significantly to the mass of the structure and change its modal characteristics. One method which has been used to check this is by comparing the response of the structure with the accelerometer and then with a second accelerometer placed on top of the first. Adverse changes in frequencies and amplitudes will indicate that the first device alone is probably adding too much mass. The device and associated wiring must also be capable of withstanding the in-flight environment and be properly shielded against unwanted outside electromagnetic signals.

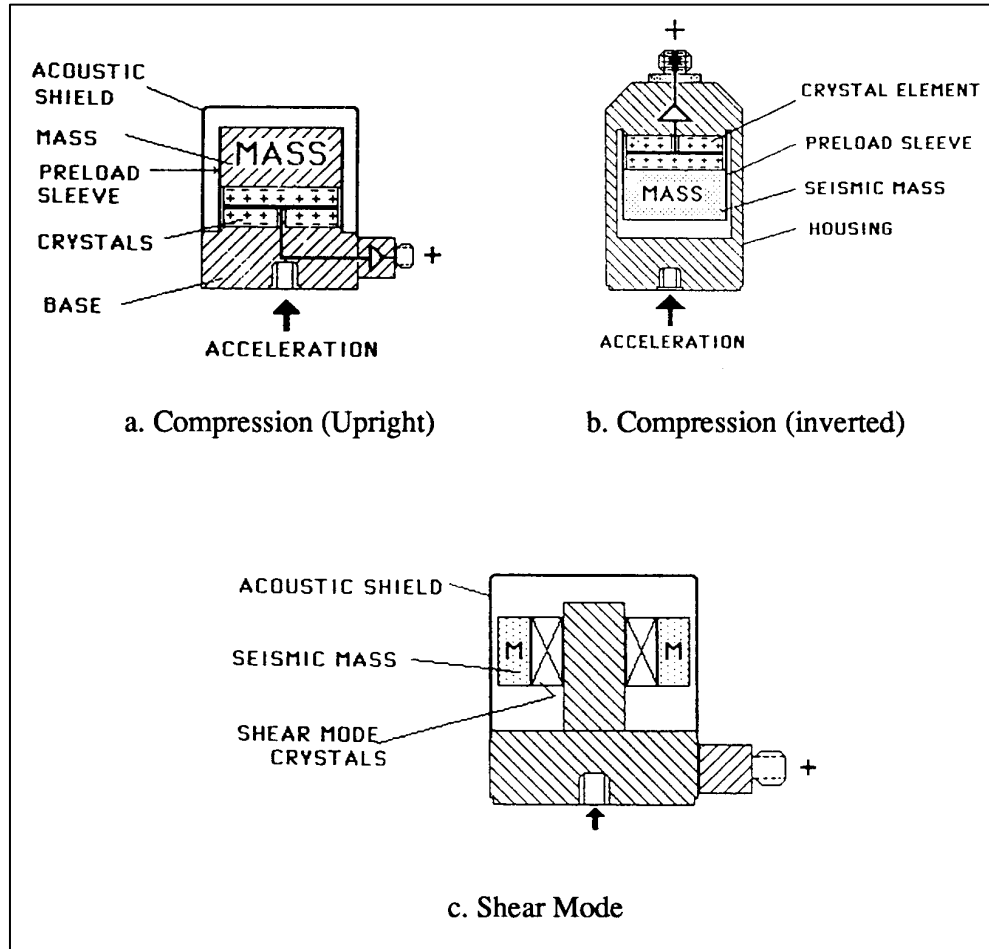


Figure 122 Three Common Accelerometer Configurations

10.3.2 Measurement

Because the high impedance charge output of the piezodevice is so small, it is necessary to pass the signal through a signal conditioner to make it suitable for read-out instruments or recording. The conditioner may also filter, digitize, or provide other signal processing functions (Section 12.0). This will typically be a **charge amplifier** for flight test applications in which a charge mode type of transducer is used. A **voltage mode transducer** incorporates an impedance converter within the transducer itself to maximize the signal-to-noise ratio and eliminate the capacitance of the coaxial cable so that only a power source is required.

The transducer **scale factor** allows the measured signal to be associated with an acceleration as determined during the calibration of the device. The scale factor is provided with each unit and must be set in the charge amplifier sensitivity setting for correct readings. This will be in units of pC/g or mv/g.

10.3.3 Calibration

Accelerometers must be periodically recalibrated. The high frequency response in particular tends to deteriorate with age. The typical calibration is usually performed using a special laboratory calibration accelerometer which is carefully preserved just for this purpose and is in turn, precisely calibrated against a universally accepted standard. Most users send their accelerometers to the manufacturer for calibration. However, as the price of the accelerometers normally used for aircraft structures applications continue to fall, it is now more practical to discard the device rather than accept the time and expense of a recalibration.

10.3.4 Installation

There are many methods for mounting accelerometers with varying ease and suitability depending upon applications. The transducer will be supplied with a small threaded mounting stud and matching hole in the case of the unit. If it is practical to prepare a threaded mounting point in the structure to be tested then the stud mount can be used. This is probably the most suitable approach and allows the transducer to be easily installed and removed. Placing a thin film of silicon grease at the cleaned interface of the transducer and structure will improve coupling and frequency response. Care must be taken not to over-torque the device during installation as it can introduce measurement errors. In aircraft ground vibration test applications in which many devices need to be mounted or moved around, the stud mount is usually impractical.

Where the stud mount is not practical but a permanent installation is required, a variety of cements can be used. Dental cement is frequently used as it dries to a very hard surface (high natural frequency) and has a very high bonding strength. Whatever is used, it is important that the glue film not be excessive. The cement may tend to shift the transducer resonance to a lower frequency and this should be considered to ensure that it is still beyond the frequency range of interest. For installations in which the transducer is expected to be moved around or is a temporary installation, beeswax or tape can be used. The wax must be softened with a hot air hand blower, and again, an excessive amount must be avoided. Double-backed duct tape is the easiest application method. Wax and tape are less desirable from a resonance perspective but are usually adequate for aircraft ground tests. They are generally unsuitable for the flight environment. If high frequency vibrations are to be measured then these methods should be avoided. Small and inexpensive mounting blocks have appeared in which the transducer can be simply slid in and out. Many of these can be quickly cemented to the structure for a ground test and eliminate the uncertainties of other temporary installation methods. Magnetic transducer mounts are widely suspect and are usually impractical for aircraft use anyway.

For all mounting techniques, it is important that the base of the device be flush with the structure to be tested, or at least not edge-mounted. This may require that a specially fabricated shim be installed so that the base is flat against the mount and properly aligned with the desired acceleration axis (Figure 123). It is important that the shim's natural frequency be much greater than the frequency range of interest. A metal or phenolic material is commonly used. There are a number of special purpose jigs and other tools to ensure that the accelerometer is properly aligned with the desired axis. Depending upon the nature of the test and the required accuracy of the data, some amount of rotation of the transducer off of the selected axis may be acceptable.

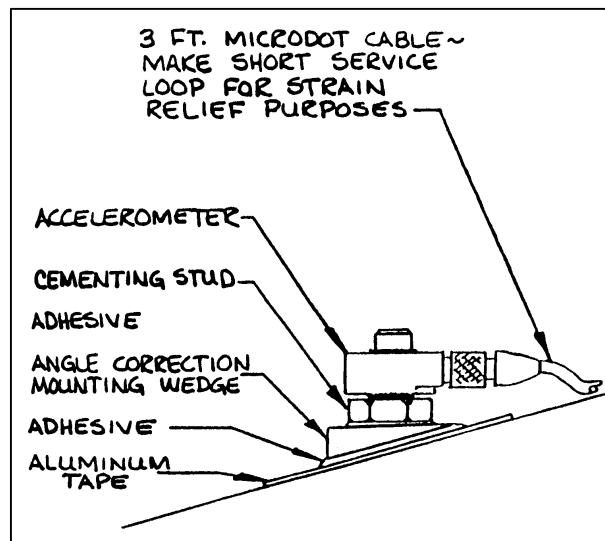


Figure 123 Example of Shim-Mounted Accelerometer

The coaxial cable from the accelerometer must be taped or glued down to prevent it from flopping around from structural motion. This flopping introduces noise into the signal, can cause it to work loose from the transducer, and can wear the cable to failure. A small stress-relieving loop in the cable near the transducer is a good idea to avoid failures from an over-stressed cable during surface motion. If the cable-to-transducer connection is likely to be subjected to moisture, like rain or condensation, then it should be sealed. Care in shielding and grounding will help to ensure that the local electromagnetic environment does not corrupt the accelerometer signal. An annoying limitation of the accelerometer is that there is no easy way to check the integrity of the transducer while in place on the test article, apart from striking the adjacent structure or jumping up and down on the aircraft.

10.4 Force Transducers

The typical mechanical force transducer or **load cell** used today is nearly identical to the accelerometer. The standard configuration of the piezoelectric force sensor is illustrated in Figure 124. When a precise measure of the force and its frequency content is necessary for use in a frequency response plot (Section 11.0) then this sort of force transducer should be chosen over a calibrated strain gage.

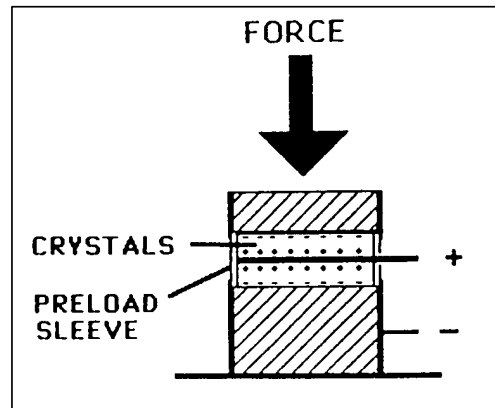


Figure 124 Force Transducer Components

Some standard piezoelectric force sensor designs are shown in Figure 125. The **compression-tension-impact** model is most often seen incorporated into the impact hammer used for vibration testing (see Section 7.8.2.1), while the **force link** may be used in a ground vibration test - placed between the shaker and the structure under test (see Section 7.6.3). The **quartz force ring** has little application in aircraft tests. All the discussions of the operation, measurement, calibration, and installation for the accelerometer also apply to the force sensor. Sensitivity (mV/lb) should be considered in the same way as with the accelerometer. Expected loads must fall within the linear response range of the transducer. The shock rating should be compared with the anticipated accelerations and the operating environment. When used during a ground vibration test or similar application, the natural frequencies of the device must be considered, the same as for an accelerometer.

10.5 Pressure Sensors

The pressure sensors typically used in structures testing to measure acoustic pressures (see Section 9.0) are piezoelectric devices (Figure 126) and the piezoresistive device incorporating tiny strain gage bridges (Figure 127). It can be seen that the piezoelectric type is much like the force sensor except for the diaphragm across the top. The diameter of the diaphragm and the number of piezoelements determines the sensor's sensitivity. The piezoresistive devices can come in extremely tiny sizes, as small as 0.03 inches in diameter. The flat-package configuration typically used in flight test applications is shown in the figure. This transducer is often mistakenly referred to by the brand name of **Kulite**. The flat-package form is easily cemented to the surface of a structure. The cylindrical type typically require that a hole be drilled in the structure and the device cemented in from the back so that the diaphragm is flush with the surface - a much more involved operation.

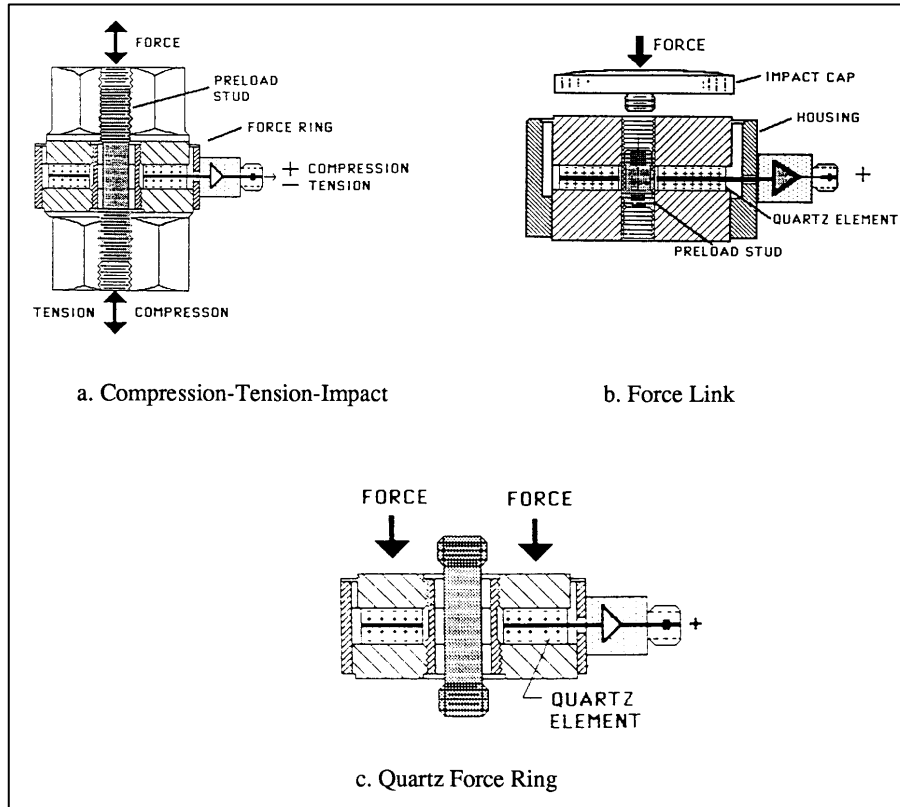


Figure 125 Common Force Transducer Configurations

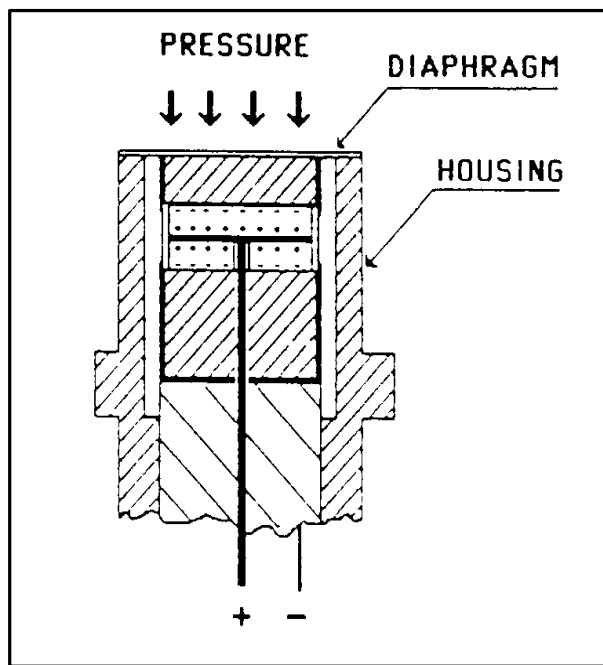


Figure 126 Pressure Transducer Components

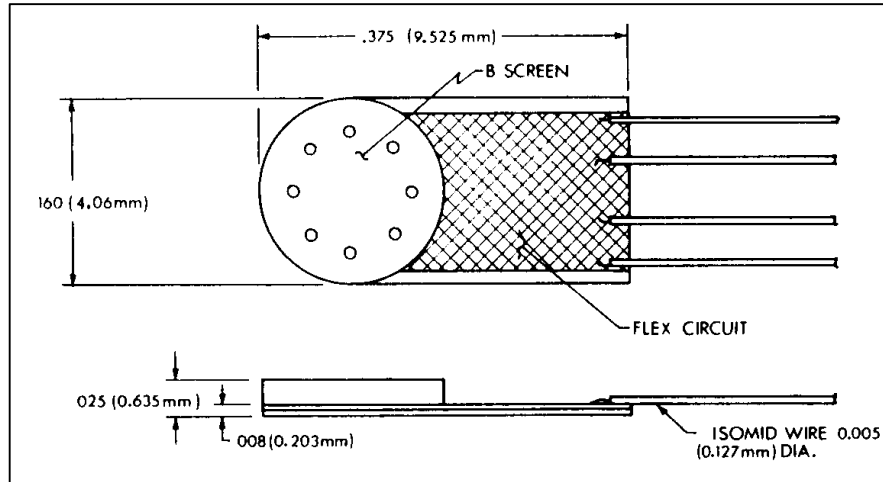


Figure 127 Typical Small Piezoelectric Pressure Transducer

10.6 Microphones

Microphones are also pressure sensing devices, but incorporate many more features than the simple piezoelectric sensor which makes them superior in frequency response. Because of this, such microphones are sometimes called **dynamic pressure transducers (DTPs)**. However, they need repeated calibration, are less durable, and are generally larger than the piezopressure sensors.

Figure 128 shows typical measuring microphones which incorporate a diaphragm and a perforated plate as a damper. The **ceramic microphone** uses a ceramic piezoelectric element to generate the measurement signal. The **condenser microphone** uses the variation in electrical capacitance between the diaphragm and a backplate to generate the signal when a polarizing voltage is applied. This type of microphone is less suitable for very low frequency sound measurements. Since the sensor will be oscillating with the structure, this will be sensed as an incoming pressure wave which is not a true environmental input. To correct for this, an accelerometer is incorporated into the microphone to automatically cancel the portion of the signal produced by sensor motion. Most such devices are omnidirectional so that only pressure waves perpendicular to the face will be faithfully measured.

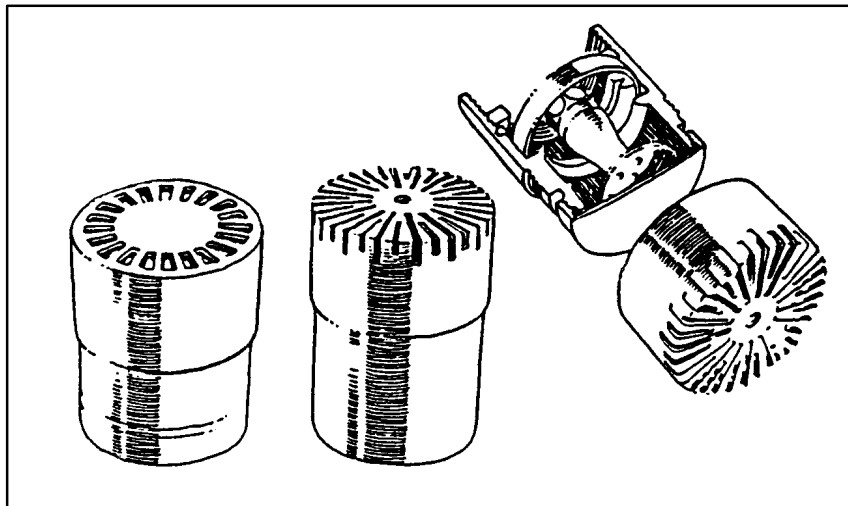


Figure 128 Common Measurement Microphones and Components

It is important that the face of the microphone be flush with the surface of the structure under test. If a cavity exists between the surface and the face of the instrument, an organ pipe sort of arrangement is created. Any pressure front with a wave length identical to the dimensions of this cavity will be artificially amplified and provide erroneous readings. The device can extend beyond a surface if a precise measurement on the surface is not necessary, such as in measuring the general sound pressure levels in a weapon bay or avionics compartment. Calibration is usually performed with a precision sound generating device that fits over the face of the transducer. Such things can be purchased and the calibration done by the user. Most of the other sensor considerations already discussed are applicable to the microphone.

10.7 Other Common Transducers

There are many other instrumentation transducers that the flight test engineer may come across which have little application to structures testing. However, there are a few which require a short introduction as they occasionally have a small role to play in loads and flutter tests.

10.7.1 Temperature Sensors

The very small voltage, proportional to temperature, produced at the junction of two dissimilar metals provides a simple but effective means of measuring temperatures on a surface. This may be important where high temperatures can cause a reduction in the modulus of the material and a loss of strength. These **thermocouple** devices are easy to install, are inexpensive, and may be nonlinear. It is important with these devices to avoid dissimilar metals in cable runs and plugs. Another simple method of obtaining temperature information is with a **resistance device (RTD)**. These consist of a single material element as opposed to the two materials in the thermocouple. Even more basic is the **'temp tab.'** This is a small self-adhesive strip with temperature-reactive chemical dots. Tabs can be selected for the general temperature range anticipated. The dots (marked for a narrow temperature range) discolor when exposed to the matching temperature environment.

10.7.2 Displacement Transducers

The displacement of a control surface or other structure may need to be monitored to detect any tendency to divergent oscillations caused by flutter or structural feedback. This is frequently done with a rotary or linear displacement transducer. The typical position transducers used are potentiometers, **linear variable differential transformer (LVDT)**, and strain gage bending beams. One form of this is the **'string pot'** which uses a string between the moving part and the transducer fixed to a nonmoving member. These are essentially potentiometers that have a rotating component attached to a brush contact. The motion of the contact causes a change in output voltage. By calibrating the displacement of the object under test against this voltage, a relationship can be determined. Actually, a position transducer can be any electromechanical device which produces an electrical output proportional to some physical variable, and need not be a string pot configuration. Another common form of position transducer is the strain gage bending beam, the output of which is also calibrated to the displacement of the object to which it is attached. The position transducer function has also been performed by lasers and photocells. As with other transducers, the position transducer typically requires signal conditioning for power and signal amplification (Section 10.8). The transducer may not be at the moving surface itself but buried within the control system, perhaps at a pulley or bellcrank.

10.7.3 Time Code Generators

It is seldom necessary to time sync structures test data. However, knowing the time at which an event occurred is often required for locating related data on a magnetic tape or to associate the data with other events which occurred on the aircraft. The time is produced by a digital time code generator (**TCG**). During the flight, 'range' time will be displayed digitally in the control room. This is the same time that will be recorded on tape and to which the aircraft TCG will be synced. The display is produced by a time code generator that can either count the time itself or repeat the time recorded on tape during a playback of the flight's data. The time can be altered by controls on the face of the instrument. Range time is generally set to an international standard and processed using a recognized format, generally inter-range instrumentation group-B (**IRIG-B**).

Range time may be traced out at the edges of strip chart recorder pages using a **binary** numbering system called **slow code**. This system uses ones and zeros (on and off) to represent whether a digit is active or not. The progression of digits is with each succeeding digit twice the value of the preceding digit, beginning at 1 (1, 2, 4, 8, 16, etc.). Groups of digits then form a number. Figure 129 is an example of slow code. Reading the digit groups from left to right; the U denotes units, T denotes tens, and H denotes hundreds representing the 191st day, 14th hour, 8th minute, 32nd second at the right hand reference mark.

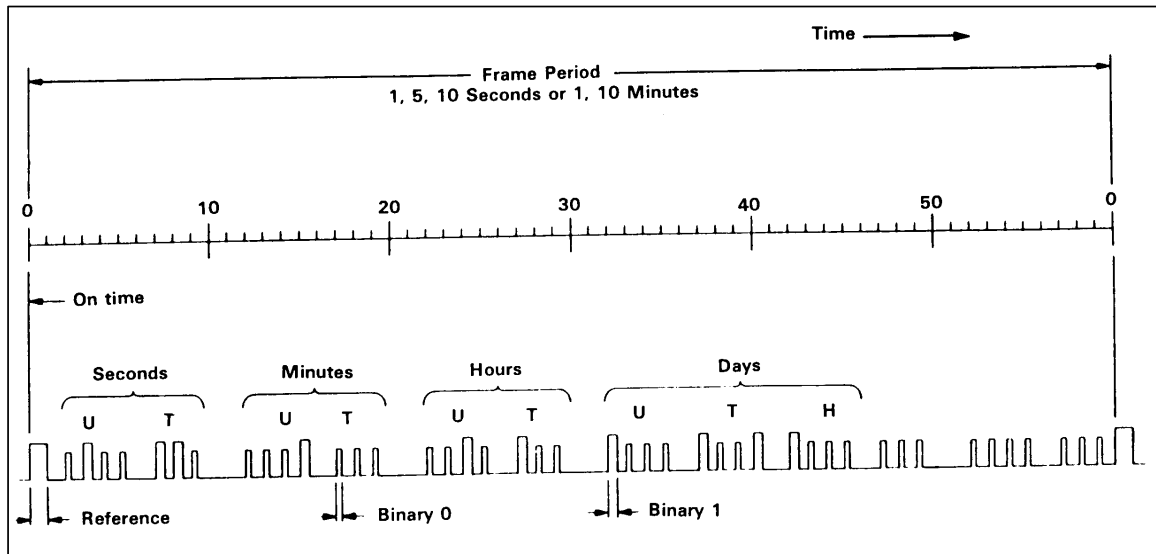


Figure 129 Example Strip Chart Recorder Slow Code Trace

10.7.4 Discretets

Some data need be no more than on/off information, such as the weight-on-wheels switch on or off. The test engineers may be provided with an **event switch** that allows them to mark an event, like the beginning of a test maneuver. Such data are called discretets and are handled as a binary, a 1 for on and a 0 for off.

10.8 Instrumentation Systems

The basic components of the typical instrumentation system are shown in Figure 130. The system allows multiple transducer signals to be compiled in an efficient manner for recording, transmission, and later display for analysis. The signals must first be processed by the **signal conditioner**. This instrument may provide power or excitation to the transducer, completion networks such as Wheatstone bridge components for strain gages, provisions for calibration signals prior to flight, amplification of the signals, and any necessary filtering. All data comes out as voltage levels, usually 0 to 5 V dc. These signals are then coded, to allow them to be distinguished from one another, in a manner unique to the type of system being used. The **multiplexer**, or **mux**, mixes these signals so that multiple transducer signals can be combined sequentially into just a few magnetic tape tracks or radio transmission channels. A **demultiplexer** allows the individual signals to be recovered later for display.

The radio transmission of data is termed **telemetry**. Tape recording of data aboard the aircraft as well as on the ground at the receiver station allows redundancy in the event that something happens to one of the systems during the flight, or a tape is lost or damaged after the flight. The aircraft tape is generally the best source of data for later analysis because it would not have noise introduced by the radio transmission and reception process, or actual **loss of signal** which produce **dropouts**. Dropouts are erroneous data usually identified by an excursion of the data to **band edge** - either the upper or lower limits of the transducer output. The typical tape used store data on 14 or 28 tracks (physical locations on the tape width), that is 14 or 28 channels of multiplexed data which may contain hundreds of measurands each.

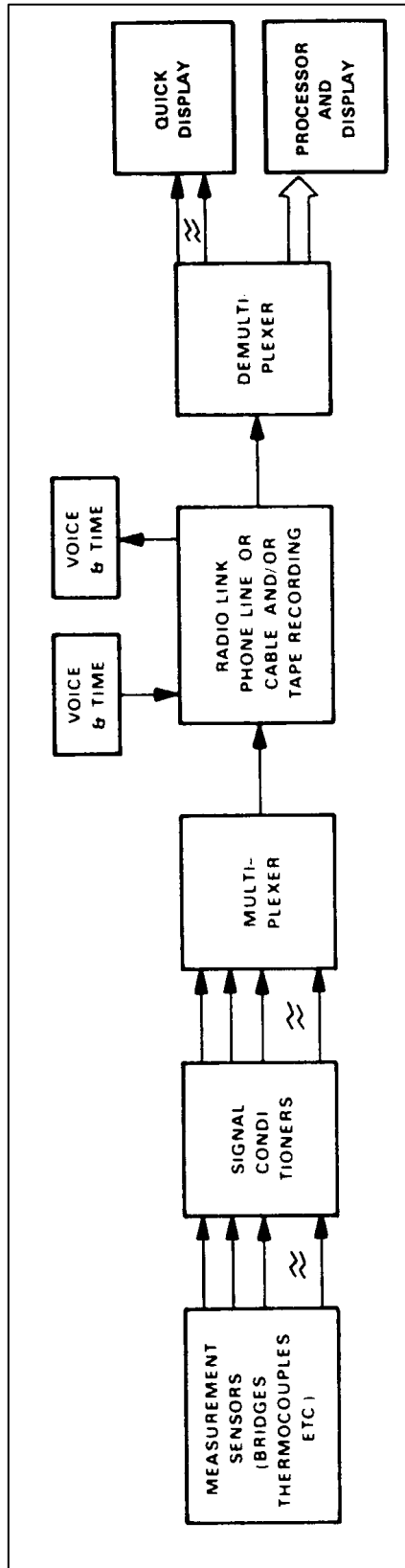


Figure 130 Typical Instrumentation System Configuration

Aircraft tapes can be run at different speeds (measured in inches per second [ips]) with the fastest speed giving generally better data resolution. However, the faster the tape is run the quicker it will be exhausted and the less that can be accomplished on the flight. To save tape, the aircrew is often instructed to turn the tape on before a specific test maneuver and then off again after the event. This means that the tape is not running for the entire flight which typically has only 50 percent of the time devoted to actual test accomplishment.

Data can be displayed in an unprocessed form such as on a **strip chart recorder (SCR)**; a scrolling paper plotter with usually eight parameters to a page. The minimum and maximum input voltage signal correspond to some minimum and some maximum equivalent engineering units for the measurand, and this is what is displayed on the SCR - a simple linear conversion. A variation on the SCR is the **visicorder** which uses a scanning light to trace out high frequency data on light-sensitive paper. The visicorder should be considered when high frequency responses must be observed as the SCR begins to attenuate a response at about 60 Hz. More and more data is now being presented on television screens in either a digital (tabular or 'tab') or plotted format. Data may need to be subjected to second-generation processing such as the combining of parameters or transformation to the frequency domain (section 11.3) prior to display to be truly useful to the engineer. Dedicated processing systems are used to perform these functions.

There are two basic types of instrumentation systems commonly used; the **FM (frequency division multiplex)**, and the **PCM (pulse code modulation)** systems. The basic nature of these systems will now be discussed.

10.8.1 Frequency Division Multiplex Systems

The FM systems are analog instrumentation techniques and are typically used where a high frequency response is required without concern about aliasing (Section 12.3.2), such as for flutter measurands. Each transducer signal modulates a separate **subcarrier oscillator (SCO)** or **voltage control oscillator (VCO)** whose output frequency shifts in relation to the voltage from the associated transducer. This process is known as frequency-division multiplexing. **Discriminators** later filter for each distinct frequency in order to recover the individual transducer data for display (Figure 131).

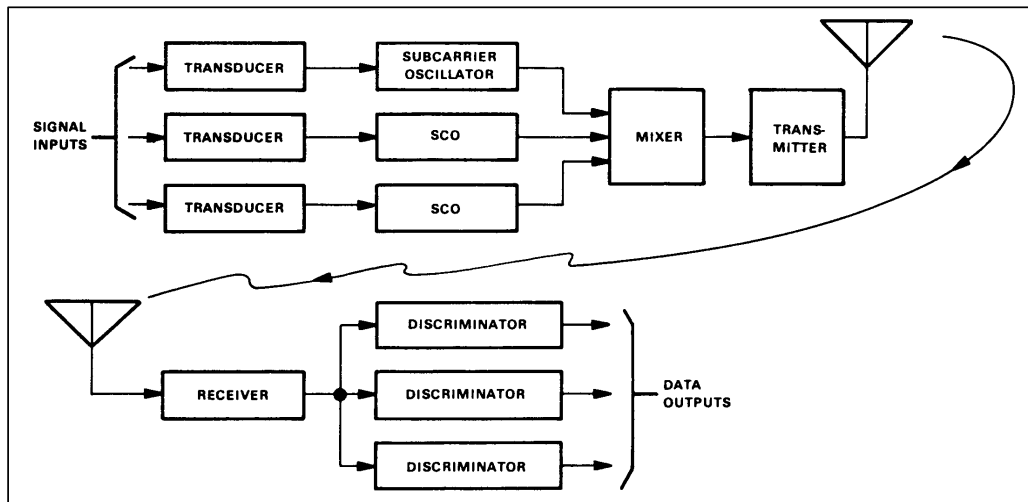


Figure 131 Basic Frequency Division Multiplex System Components

10.8.2 Pulse Code Modulation Systems

The basic components of a PCM system are illustrated in Figure 132. This is a digital technique in which the data is converted to binary format (see Section 10.7.3) and encoded into a digital signal during the mixing process. This encoding may use the amplitude of the analog signal to determine the binary representation as Figure 133 illustrates. Some typical terms used in this digital processing is the **bit** (binary digit, a single pulse or absence of pulse), and a **word** (a group of bits representing a single sample of information from a single channel). The number of bits comprising any word is a measure of the data resolution. A 10-bit system would have 1,024 binary numbers possible to represent amplitudes between the band edges. Increasing the bits/word from 10 to 12 will produce an increase in data resolution.

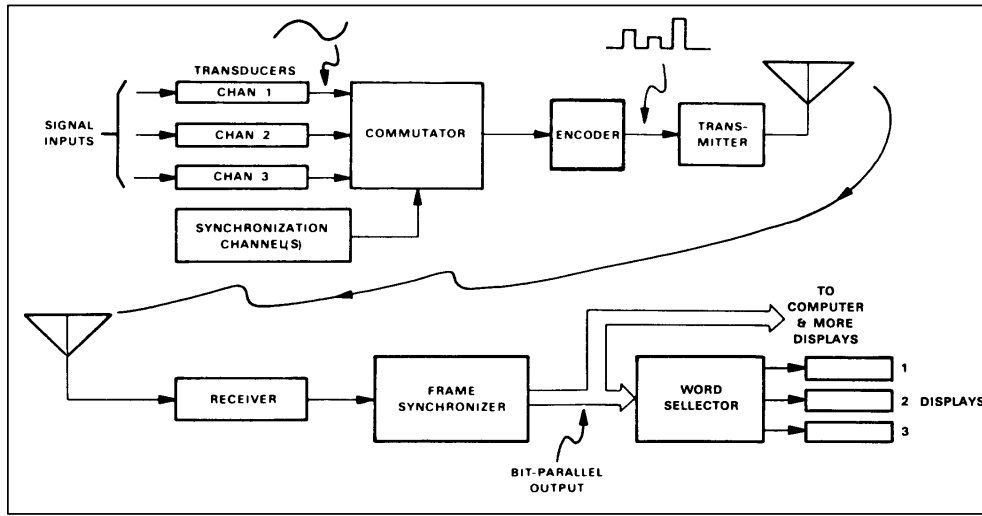


Figure 132 Basic Pulse Code Modulation System Components

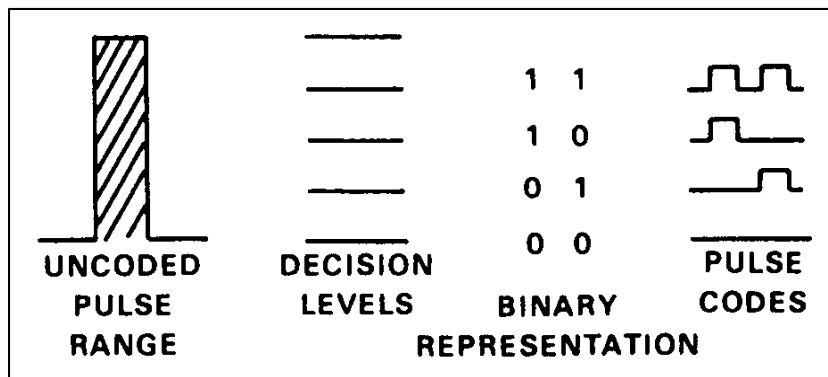


Figure 133 Example of Pulse Code Modulation Encoding

Pulse code modulation uses time-division multiplexing, or sampling of each parameter in turn at a specific sample rate. This sampling can be performed mechanically with a **syncro** in the **commutator** as suggested by Figure 134. A **decommutator** reverses the process so that the signal can be analyzed as individual data channels. More commonly today, a digital encoding routine is used to mix the data signals and later to separate them out again. The sampling rate is usually set at about five times the highest frequency of interest for fidelity. A **frame** refers to a block of data from the signal produced by a single syncro revolution, or one complete sampling cycle with a word from each channel. Today, the frame length, or words per syncro, is programmable.

The encoding of the commutator output into a digital form involves the use of a **analog-to-digital converter (ADC)**. The actual transducer outputs are analog signals which must be interpreted and coded into a digital format. Pulse code modulation systems usually have a lower signal-to-noise ratio than FM systems. It also lends itself more easily to the current digital signal processing methods.

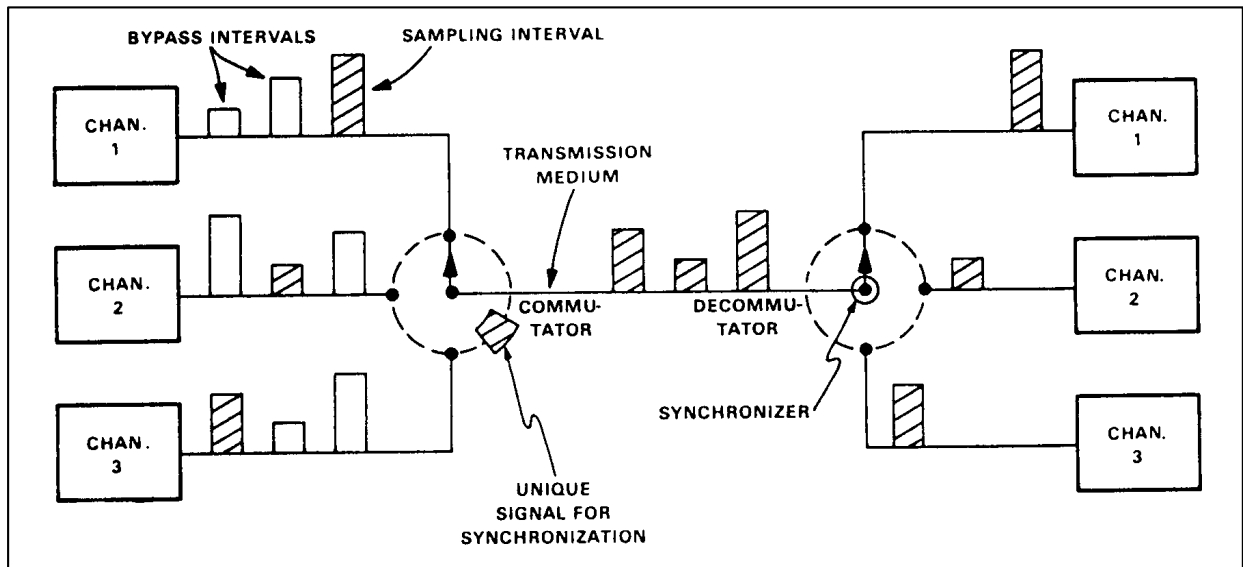


Figure 134 Illustration of Commutator Function

SECTION 10 REFERENCES

1. KcKinley, Joe, *Fundamentals of Stress Analysis*, Matrix Publishers, 1979.
2. Petterson, Arnold P.G. and Bross, Erwin E., Jr., *Handbook of Noise Measurement*, GenRad Incorporated, Concord, Massachusetts, 1978.
3. Davis, Harmer E., Troxell, George E. and Wiskocil, Clement T., *The Testing and Inspection of Engineering Materials*, McGraw-Hill Book Company, New York, New York, 1955.
4. Stiltz, Harry L., *Aerospace Telemetry*, Prentice-Hall Incorporated, Englewood Cliffs, New Jersey, 1961.
5. Strock, O.J., *Telemetry Computer Systems, An Introduction*, Instrument Society of America, 1983.
6. Doebelin, Earnest O., *Measurement Systems: Application and Design*, McGraw-Hill Book Company, New York, New York, 1983.
7. Skopinski, T.H., Aiken, William S., Jr. and Huston, Wilbur B, Calibration of Strain Gage Installations in Aircraft Structures for the Measurement of Flight Loads, NACA Report 1178, 1954.
8. Sims, Robert, McCrosson, Paul, Ryan, Robert and Rivera, Joe, X-29A Aircraft Structural Loads Flight Testing, *Society of Flight Test Engineers 20th Annual Symposium Proceedings*, 18 to 21 September 1989.

11.0 FREQUENCY RESPONSE DATA ANALYSIS

11.1 Introduction

Test data must be presented in a format that permits complete and relatively simple analysis. The dynamic response of a structure can be displayed in the time or the frequency domain. The response can also be expressed as an equation of motion. This latter method is seldom employed with aircraft structural data, either from flight or ground tests, because the complexity of the structure and the presence of nonlinearities and other noise makes the extraction of the necessary parameters from the test data extremely difficult, at best. The sought after modal parameters are typically extracted from plots, known collectively as **frequency response functions (FRFs)** in the frequency domain.

The principal objective of frequency response test data analysis is the determination of the frequency, amplitude, and damping of the response modes observed and a measure of the reliability of the results. The frequency may be used in correlating the test results with predictions in order to identify the modes of response. The damping allows an evaluation of how close the dynamic mode is to instability.

11.2 Time Domain

The analysis of a single degree of freedom (SDOF), **unforced response (transient impulse response)** in the time domain is relatively easy and so will be presented first. Figure 135 shows a typical time-history trace for a damped system of this type. The dotted line in the figure describes the classical exponential damping decay envelope. The response may be displacement, velocity, or acceleration. Analysis of such a response should follow the removal of any average **zero-offset** of the response, the so-called **dc component**. This operation is **dc suppression**. Some typical definitions related to the figure (see also Section 4.0) are the **damping rate** (σ), the **damping ratio** or **damping coefficient** (ζ) which is the actual damping divided by critical damping, the **period** (T) or time between successive pulses, the **natural frequency** (ω_n), the **damped natural frequency** (ω_d), the **residue** (R) which is indicative of a mode's strength, and the **structural damping** (G). Common relationships between these terms are:

$$\sigma = \zeta\omega \quad (136)$$

$$T = 2\pi/\omega_d \quad (137)$$

$$G = 2\zeta \quad (138)$$

$$\omega = 1/T \quad (139)$$

When the damping is extracted from flight test data, both structural damping and aerodynamic damping is measured. This is then called the **total system damping**, also denoted with a G .

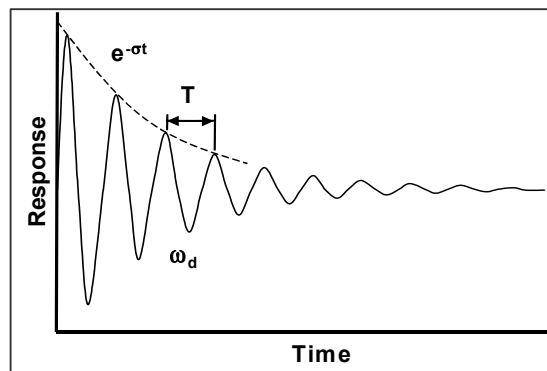


Figure 135 Damped Impulse Response Time History

11.2.1 Logarithmic Decrement Method

By counting a fixed number of cycles on the time history and determining the amplitude of the initial and final cycle used, the damping can be determined using the following equation. This is the log decrement (**log dec**) method.

$$G = \ln(A_o/A_N)/(\pi N) \quad (140)$$

where:

- N = the number of cycles used in the analysis,
- A_o = the amplitude of the first cycles used, and
- A_N = the amplitude of the final cycle used.

This equation can be quickly applied to a response like that in Figure 135 which is representative of those often produced real-time on strip chart recorders with a single mode dominating the damped impulse response to some excitation. A trace of real structural response flight test data will seldom be as 'clean' as that shown in the figure. As long as a single mode is clearly dominant, drawing a line with a french curve fit to the general decay will allow a log dec analysis by pulling the points from the drawn line adjacent to the trace peaks. When the decay trace contains small amounts of other spectral components (more than one mode) which will adversely affect the results of a log dec calculation, **log decrement averaging** can be used. This involves separate calculations starting at each successive half-cycle peak until all of the peaks have been used. The results are then averaged to yield a better damping value than may have been possible otherwise.

An even quicker way to simply approximate the damping is to determine the number of cycles to the cycle that is nearest to one-half the amplitude (N_½) of the first cycle used. Equation 140 then becomes:

$$G = 0.22/N_{\frac{1}{2}} \quad (141)$$

11.2.2 Logarithmic (Peak) Amplitude Method

The **log amplitude**, or **peak amplitude**, method provides a means of 'curve fitting' a damping to test data that does not display a clean exponential damping envelope. The method entails plotting natural logarithms of the half-cycle amplitudes versus the associated half-cycle number (Figure 136). By using the slope of the best straight line fit to the data points, Equation 142 can be used to determine the damping.

$$G = -2(\text{slope})/\pi \quad (142)$$

Although not accomplished quickly, and cumbersome for use in a mission control room, this method is superior to the log dec technique because it uses all of the available data, not just two peaks.

11.2.3 Multiple Degrees-of-Freedom Responses

The analysis techniques presented in Sections 11.2.1 and 11.2.2 are useful only with time histories that have SDOF responses or ones that are almost entirely dominated by a single mode. Figure 137 is an example of a response that has more than one mode present. Clearly the log decrement or log amplitude methods cannot be used. The solution to this problem is to curve fit the best equation of motion to this response. The coefficients of the equation will provide the frequency response parameters sought.

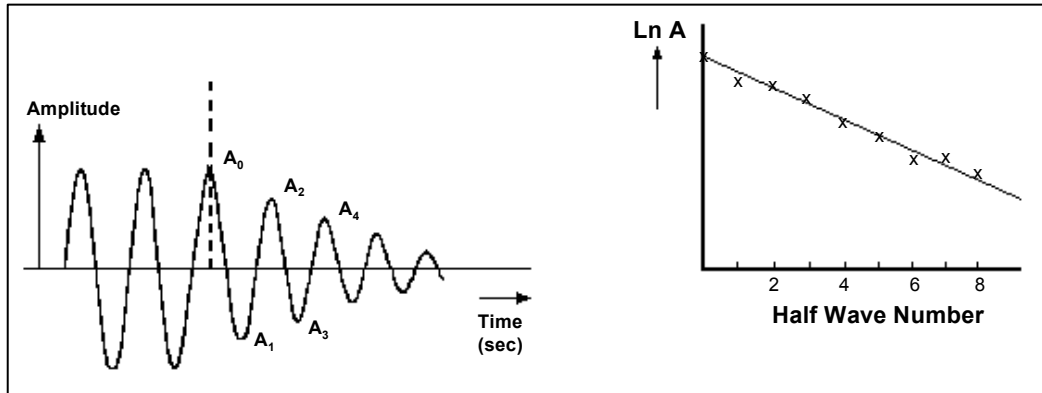


Figure 136 Log Amplitude Plot

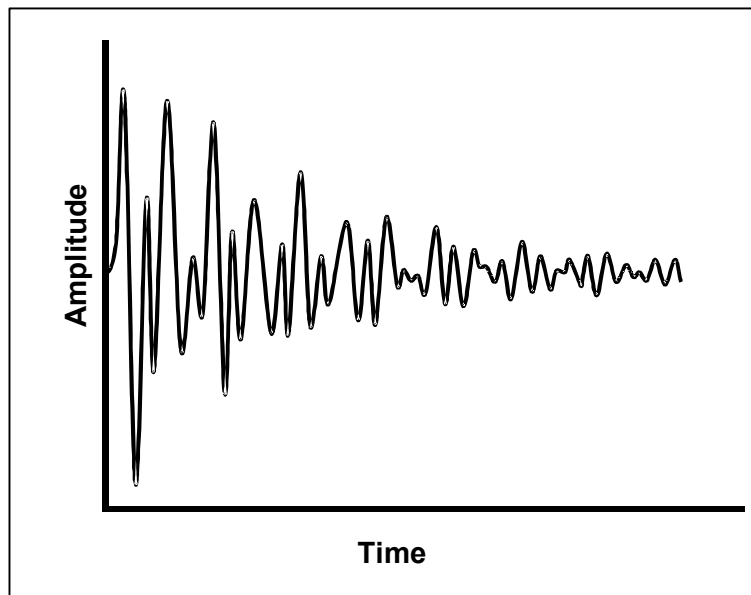


Figure 137 Multiple Degrees of Freedom Impulse Response Function

One form of the equation to be fitted to data of any number of degrees of freedom is a sum of sinusoids, or:

$$y(t) = C + \sum_{n=1}^N A_n e^{-\zeta_n f_n t} \sin(f_n t + \phi_n) \quad (143)$$

where:

- A_n = the amplitude of mode n in $y(t)$ units,
- C = the **zero offset** correction in $y(t)$ units,
- t = time in seconds,
- $y(t)$ = the value of the transient at t ,
- N = the maximum mode number,
- ϕ_n = the **phase angle** of mode n in radians,
- f_n = the natural frequency of mode n in radians/second, and
- ζ_n = the damping ratio of mode n .

There are a number of successful ways of arriving at the equation's coefficients that will result in the best representation of the experimental data. One of the easiest approaches is the **least squares curve fit** method. Put simply, this technique requires an initial guess at the coefficients. The difference between the calculated response and the measured response is used to correct the initial coefficients and another calculation and comparison is made. This iteration process is continued until the square of the difference between the two has been reduced to a pre-selected level. The resulting waveform and measured response are usually compared visually. The coefficient of the former yield the best estimate of the modal properties. This approach is also call **Prony Analysis**.

11.2.4 Random Decrement Method

The structural response time history produced by frequent random excitations would normally display no discernible individual modes from which damping and frequency can be determined (Figure 138). To extract such data, a time-history data crossing of a selected trigger level serves to represent an impulse excitation for subsequent structural response (the transient response due to an initial displacement). A percentage of the root mean squared (RMS) value of the entire output signal is often used as the trigger level. The triggering may be with a positive slope crossing of the trigger level, a negative slope crossing, or both. A **signature length** of data is taken at each subsequent crossing of the trigger level and each is averaged with the previous signature(s).

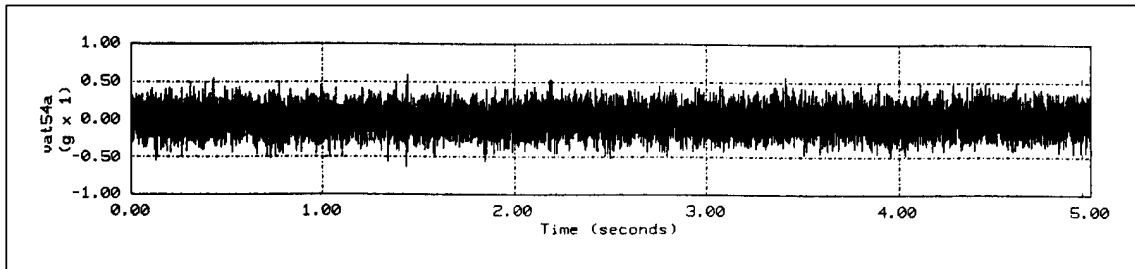


Figure 138 Random Excitation Response Time History

Assuming linear superposition (see Section 10.2.3), sufficient **ensemble averages** will permit the signature to converge to the structural response due to a single excitation with extraneous noise averaged out (Section 12.4.2). The final signature will then be in the form of a single or sum of damped sinusoidal functions. The quality of the signature and any subsequent analysis will increase with the number of averages used. This, then, is the essence of the random decrement or **Randomdec** method. The resulting signature can be used to find the desired modal parameters by the methods described in this section. Using frequency domain analysis on a Randomdec signature is not advised because of the additional error which would be introduced to data that has already been greatly manipulated.

The time-history slices representing the decaying response to an intentional structural input, such as used in the burst-and-decay test method (see Section 6.6.1.3), can also be averaged in a process called **Pseudo Randomdec**. Again, a trigger level needs to be established so that the ensembles all represent decayed responses. Care must also be taken to ensure that the identical signature lengths do not include anything but the decay and random spectral elements. This may require zeros (Section 12.4.5) or a constant offset value to be inserted for undesirable data toward the end of some signatures.

11.2.5 Correlation Functions

Correlation functions provide another means of extracting useful modal parameters from random vibration data, or data with random noise superimposed on the signal. Correlations are produced by an averaging technique that will produce the structural response in the same way as that with the Randomdec method. True random noise averages out.

Put simply, correlation functions are produced by multiplying two time histories point-by-point, repeating the process after shifting one of the histories by a time increment, and finally averaging all of the products. An **auto-correlation** results from using the same time history twice in this process (input or output response). **Cross-correlations** result from using two different histories, typically the input and the output responses. Since flight test data will seldom have the input signal recorded (or even completely known), attention will first focus upon the auto-correlation of the output waveform.

The auto-correlation algorithm for a continuous output function, $x(t)$, is:

$$R_{xx}(\tau) = \lim_{T \rightarrow \infty} (1/T) \int_{-T/2}^{T/2} x(t)x(t + \tau) dt \quad (144)$$

Since digitized test data is a discrete, noncontinuous data stream, Equation 144 needs to be expressed as a summation or in a discrete form, such as:

$$R_{xx}(\tau) = R_{xx}(mT) = [1/(P - m)] \sum_{K=1}^{P-m} (x_K y_{K+m}) \quad (145)$$

$$m = 0, 1, 2, 3, \dots, M$$

where:

- P = the total number of data points,
- m = the correlation shift or 'lag' number,
- M = the maximum number of time shifts to be performed, and
- T = the sampling period (inverse of the data sampling rate).

Plotting the result of this calculation gives a waveform like that in Figure 139(b). Since this waveform is symmetric about zero, the left side of the plot is generally neglected. The auto-correlation would then look like Figure 135 and can be analyzed by the techniques discussed previously. The amplitude of the resulting waveform is the square of the true amplitude, so the square root of the value of the auto-correlation should be taken before further processing. The correlation function can also be produced by plotting the sums of the time-lag products against the time shift or lag number. This number can be converted to time by the expression:

$$\Delta t = (\text{lag number}) / (\text{sample rate}) \quad (146)$$

The algorithm for the cross-correlation (where $y(t)$ is the input signal or any other response signal) is:

$$R_{xy}(\tau) = \int_{-\infty}^{\infty} x(t)y(t + \tau) dt \quad (147)$$

or

$$R_{xy}(mT) = [1/(P - m)] \sum_{K=1}^{P-m} x_K y_{K+m} \quad (148)$$

$$m = 0, 1, 2, 3, \dots, M$$

and

$$R_{yx}(mT) = [1/(P-m)] \sum_{k=1}^{P-m} y_k x_{k+m} \quad (149)$$

$$m = 0, 1, 2, 3, \dots, M$$

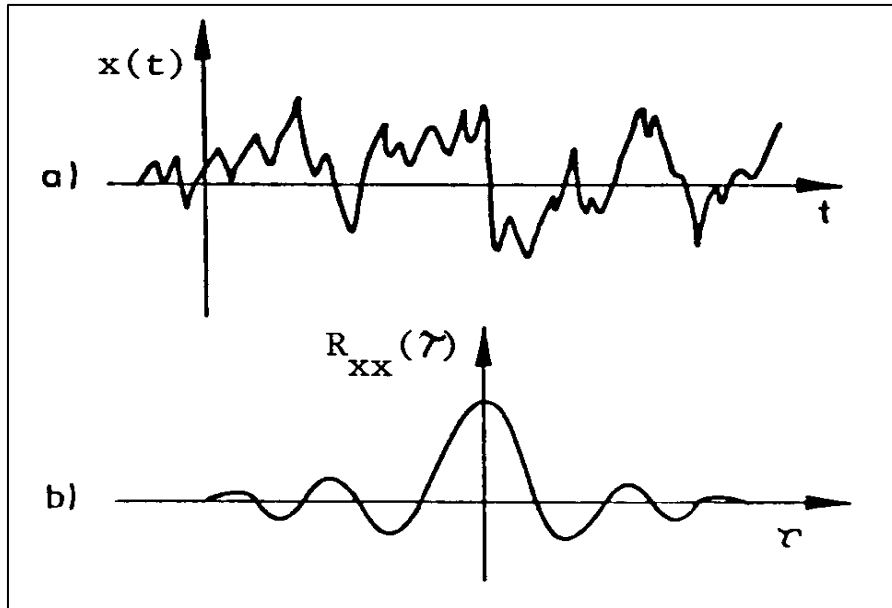


Figure 139 (a) Original Random Response Time History (Single Degree of Freedom)
 (b) Associated Auto-correlation Function

By itself, the cross-correlation function can identify periodic functions which are common in the two time histories and time delays between the two signals, while the auto-correlation tends to identify a sinusoidal or periodic function within a noisy time response.

Time domain correlation functions are seldom used by themselves because they are so subject to signal processing-induced errors and noise. They are, however, often used in producing power spectral densities (Section 11.3.3) and transfer functions (Section 11.3.6) with which better analysis can be performed.

11.2.6 Lissajous Figures

A useful means of displaying two undamped sinusoidal waveforms in a manner that permits determination of relative frequency, amplitude and phasing is a cross-plotting, or ‘beating,’ of the two signals (not to be confused with the ‘beating’ described in Section 4.4.3). The resulting display is formed as shown in Figure 140 and is called a Lissajous figure. They are commonly displayed on oscilloscopes in laboratory investigations.

Relative phase is determined as shown in the Figure 140 or by employing the following equation:

$$\text{phase}(\phi) = \sin^{-1}(y_{\text{intercept}} / y_{\text{max amplitude}}) \quad (150)$$

Relative frequencies are determined visually as shown in Figure 141. The relative amplitudes are determined by examining the gain settings on the display instrument for each channel necessary to produce a symmetric figure.

Some figures used to manually ‘tune’ modes are shown in Figure 142. In a ground vibration test ([GVT], see Section 7.0), for example, a resonance occurs when the structural acceleration response is 90 degrees out of

phase with the excitation force. This can be determined by beating the excitation force signal against the signal from the response transducer, and slowly increasing the forcing frequency until a Lissajous figure like Figure 142(c) is obtained. If a flutter mechanism in an aircraft wing is bending coupling with torsion with a 90-degree phase difference, then flutter susceptibility increases as the Lissajous resulting from the beating of a bending and a torsion response expands from a line to a circle. This can be used during a flutter flight test, although setting of instrument gains often proves difficult in such circumstances. Collapsing to a line from a circle is possible by integrating one of the signals.

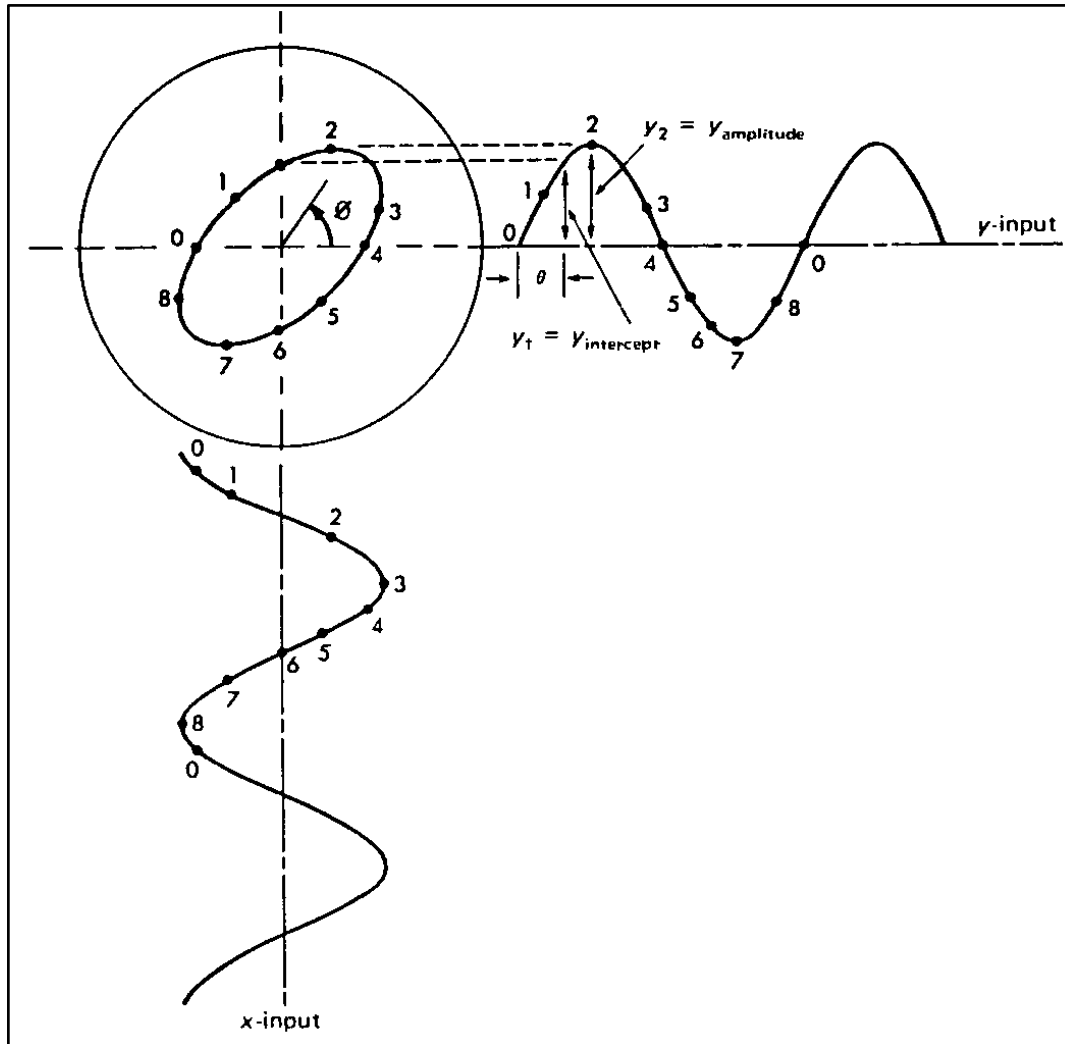


Figure 140 Sample Lissajous Construction

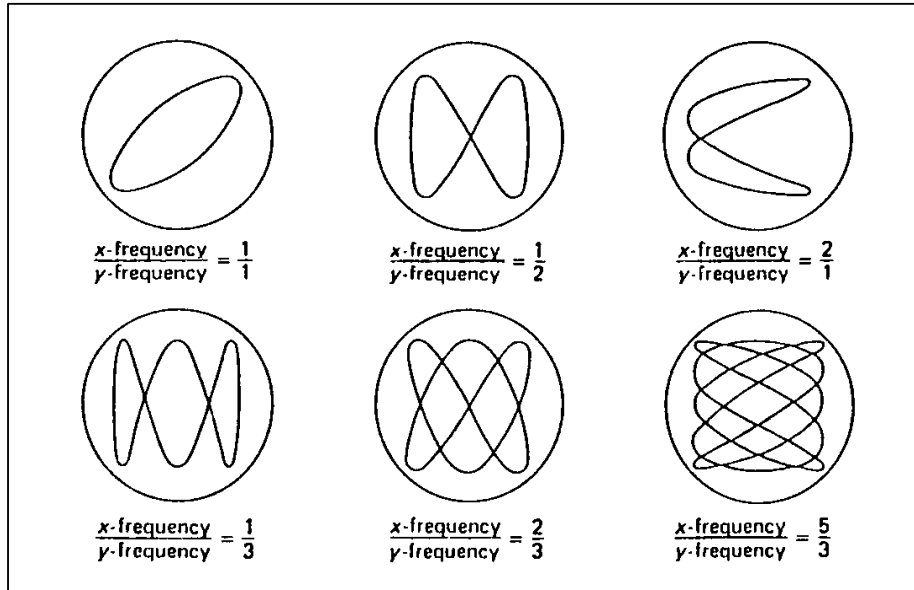


Figure 141 Lissajous Displays for Sinusoidal Inputs at Various Frequency Ratios

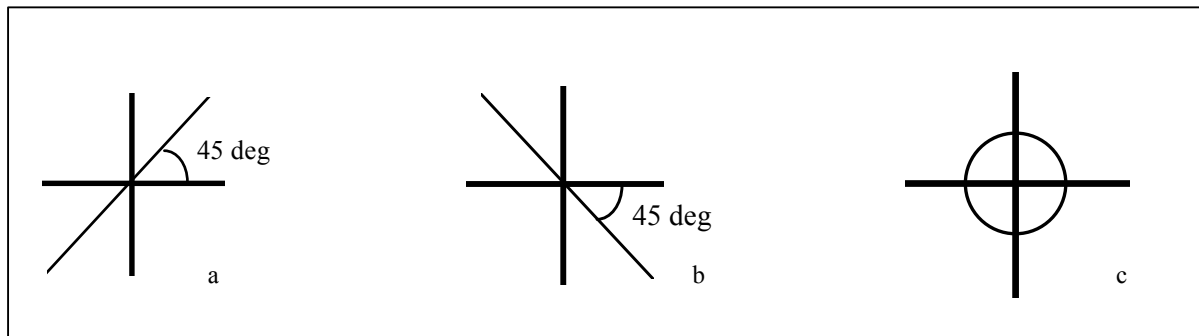


Figure 142 Important Lissajous Figures (Same Frequency and Amplitude for Both Signals)
 (a) Line, Positive 45-degree Slope, In Phase
 (b) Line, Negative 45-degree Slope, 180 degrees Out of Phase
 (c) Circle, 90 degrees Out of Phase

11.3 Frequency Domain

Frequency domain modal analysis of test data provides many advantages over time domain analysis. Multiple degrees of freedom (MDOF) systems can be analyzed with ease and the relative dominance of modes readily observed. Many forms of data presentation are available, some more suitable for a particular application than others. Manipulation of the data to improve resolution and remove errors introduced by the acquisition method or noise is done easily, with many techniques available (Section 12.0).

11.3.1 Fourier Transformations

When the input frequency to a system is known at every instant of time, it is possible to measure frequency response functions directly. Since this is seldom the case, the heart of the frequency domain methods is the ability to transform data from the time domain. This must be done by numerical methods since continuous functions for defining the frequency response are seldom available from tests. The most widely used means for performing this transformation is the Fourier transformation.

Engineers are usually introduced to the Fourier transformation in the series form in which a complex waveform is represented by a series of sine and cosine functions. That is:

$$f(t) = A_0/2 + \sum_{k=1}^{\infty} [A_k \cos(k\omega_0 t) + B_k \sin(k\omega_0 t)] \quad (151)$$

where:

$$A_0 = 2/T \int_0^T f(t) dt \quad (152)$$

$$A_k = 2/T \int_0^T f(t) \cos(k\omega_0 t) dt \quad (153)$$

$$B_k = 2/T \int_0^T f(t) \sin(k\omega_0 t) dt \quad (154)$$

where:

- $f(t)$ = a periodic function,
- ω_0 = the fundamental frequency of the function, and
- T = the period of $f(t)$.

Representation in the frequency domain requires the identities

$$\text{dc component amplitude} = A_0/2 \quad (155)$$

$$\text{Amplitude at any frequency} = \sqrt{A_n^2 + B_n^2} \quad (156)$$

The B_n component is actually an imaginary term and A_n the real term. For plotting purposes, the transformed result is generally multiplied by its complex conjugate, or

$$\text{Amplitude} = \text{Re}^2 + \text{Im}^2 \quad (157)$$

This results in the units of the measured values plotted as squared terms (e.g., g^2). This is essentially an **autospectrum** rather than a simple transform, and looks like Figure 143 in which the discrete calculated amplitudes are plotted at each frequency as **spectral lines**. A pure autospectrum would possess both positive and negative values; one the mirror image of the other. Because the data sought can be obtained from just a single side of the spectrum, the positive side is usually the only one plotted. The contribution of the negative side can be accounted for by multiplying the displayed side by 2. If the amplitude of the dynamic response in the frequency domain is important, in environmental vibration tests for example (see Section 9.0), it is absolutely essential to know whether or not the spectrum has been multiplied by 2.

The transformation of a single sine wave component would appear as a single spectral line at the associated frequency. Referring to Figure 143, the spectral lines on either side of the resonant (peak) line are due to the

nonlinearities of real structures or signal processing considerations (Section 12.0). The **dc component** (borrowed from electrical applications) is generally removed by displaying only the spectrum to the right of its line or by subtracting the average of the time domain data (zero offset) prior to transformation. This is done because the magnitude of this component is generally much greater than the rest of the response, and scaling makes analysis of the relatively smaller magnitudes in the rest of the spectrum difficult. The dc component is also normally of no interest.

The principal difficulty in implementing an algorithm such as equation 151 in practice is the unlimited frequency range specified and the requirement to evaluate integrals of the unknown continuous expression for $f(t)$. These problems can be circumvented by numerical integration techniques which essentially sums the area under the time history of $f(t)$. Thus,

$$A_o = \frac{2}{N} \sum_{K=0}^{N-1} f(k\Delta t) \quad (158)$$

$$A_n = \frac{2}{N} \sum_{K=0}^{N-1} f(k\Delta t) \cos(n\omega_o Kt) \quad (159)$$

$$B_n = \frac{2}{N} \sum_{K=0}^{N-1} f(k\Delta t) \sin(n\omega_o Kt) \quad (160)$$

where:

$$T = N\Delta t \quad (161)$$

and Δt is the time between data points (N total). This permits the transformation of discrete data and is called the **discrete Fourier transformation (DFT)**.

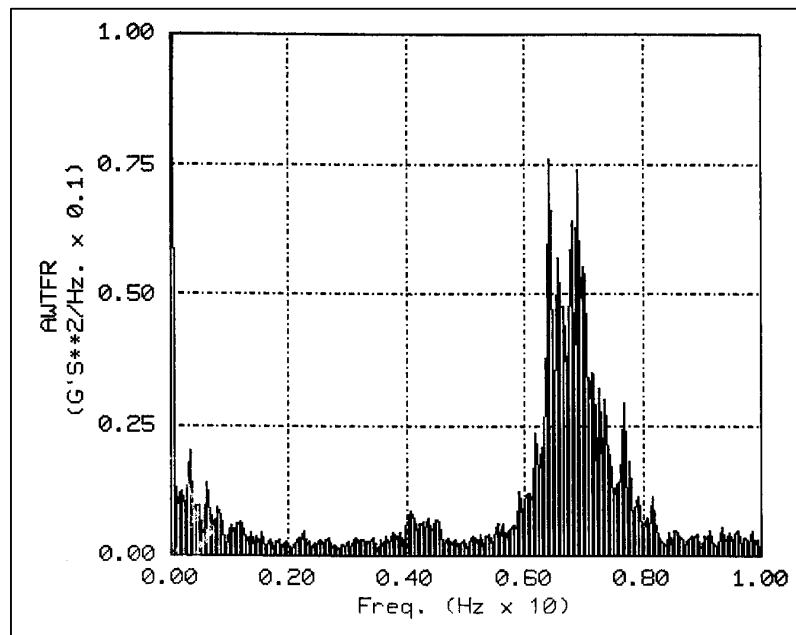


Figure 143 Typical Fourier Transformation Results

For computer applications, a more tractable form of the transformation is:

$$F(\omega) = \int_{-\infty}^{\infty} f(t)e^{-i\omega t} dt \quad (162)$$

which, for an input signal (x) or an output signal (y) shall be denoted as:

$$S_x(\omega) = F[x(t)] \quad (163)$$

$$S_y(\omega) = F[y(t)] \quad (164)$$

In a DFT format (Reference 5) the expression is:

$$X_n = \frac{1}{N} \sum_{k=0}^{N-1} x_k \omega_N^{kn} \quad (165)$$

where:

- N = the number of data points,
- X_n = the array of complex transformed values,
- x_k = the time domain data points (complex), and
- X_0 = the dc term.

Also,

$$\omega_N = e^{-2\pi i/N} \quad (166)$$

The associated **inverse Fourier transformation (IFT)** to return to the time domain is:

$$x_n = \sum_{k=0}^{N-1} X_k \omega_N^{-kn} \quad (167)$$

A pure IFT will reproduce the original time history unless DFT averaging, widening, and other data smoothing work has been employed (Section 12.0). An IFT of such a DFT from random data will appear as an impulse response rather than the initial time history. This and the fact that random noise is eliminated in the averaging process will improve a time domain analysis of the resulting IFT. An example of an IFT from processed data is presented in Figure 147, as discussed in Section 11.3.4.

Since test data is almost always nonimaginary, employing a special case form of Equation 165 can increase computational speed. That is:

$$x_{N-n} = \frac{1}{N} \sum_{k=0}^{N-1} x_k \omega_N^{kn} \quad (168)$$

By employing mathematical reductions and recognizing certain symmetries in the computations, the number of operations by the computer can be significantly reduced. These methods produce the **fast Fourier transformation (FFT)**.

11.3.2 Autospectrums

Autospectrums were first introduced in the last section. Correlations in the frequency domain are done in an analogous manner to those in the time domain (see Section 11.2.5) with the averaging of FFT outputs (or **instantaneous spectra**) of two channels; inputs only, or a combination. This produces the autospectrums or **autopower spectrums**. It can also be generated by taking a DFT of the auto-correlation function, or:

$$G_{xx}(\omega) = F[R_{xx}(\tau)] \quad (169)$$

$$G_{xy}(\omega) = F[R_{xy}(\tau)] \quad (170)$$

where the equation 170 formulation is called the **cross-power spectrum**. However, the autospectrums are more frequently derived in the manner described in the previous section, or:

$$G_{xx}(\omega) = S_x(\omega)S_x(\omega)^* \quad (171)$$

$$G_{yx}(\omega) = S_y(\omega)S_x(\omega)^* \quad (172)$$

where:

the asterisks denote the complex conjugate.

S_y and S_x denote the Fourier transforms of the response and the input signals, respectively. Note that:

$$G_{yx}(\omega) = G_{xy}(\omega) \quad (173)$$

which is true for similar functions.

The autospectrums provide essentially the same information as the time domain correlations. Additionally, the autospectrum can be used to determine the power or energy content as a function of frequency. The cross spectrum is a measure of the power shared between two signals but can also be used to analyze the phase relationship between the signals.

11.3.3 Power Spectral Density

As a means of normalizing peaks in the autospectrum plot, the amplitude can be divided by its frequency resolution ($[\Delta f]$, Section 12.2.1) to produce a power spectral density (PSD) plot (Φ). For example:

$$\Phi_{xx}(\omega) = G_{xx}(\omega)/\Delta f \quad (174)$$

A useful expression for Δf can be found in Section 12.2.1. When the amplitude is plotted on a log scale this operation has the effect of amplifying peaks while reducing the level of noise, leakage, and other undesirable signal processing consequences (Section 12.0). The amplification process increases the accuracy and ease of the damping calculations. The units of the magnitude axis are now the square of the response divided by frequency (i.e., g^2/ω or g^2 sec). The resulting plot is called a PSD. These plots are widely employed in modal analysis and provide a means of maintaining consistency within the field. The name is derived from the electrical engineering field and the earlier electrical methods for producing the PSD.

There are alternative ways to produce the PSD. In a general formulation,

$$\Phi_{xx}(\omega) = (1/2\pi) \int_{-\infty}^{\infty} R_{xx}(\tau) e^{-i\omega\tau} d\tau \quad (175)$$

$$\Phi_{xx}(\omega) = \text{Re}\{F\{R_{xx}(mT)\}\} \quad (176)$$

That is:

$$\Phi_{xx}(\omega) = T \left[R_{xx}(0) + 2 \sum_{m=1}^{M-1} R_{xx}(mT) \cos m\omega T + R_{xx}(mT) \cos M\omega T \right] \quad (177)$$

A similar formulation can be made for the output.

A **cross-spectral density (CSD)** can also be defined as:

$$\Phi_{xy}(\omega) = (1/2\pi) \int_{-\infty}^{\infty} R_{xy}(\tau) e^{-i\omega\tau} d\tau \quad (178)$$

Note that $\Phi_{xy}(\omega) = \Phi_{yx}^*(\omega)$.

11.3.4 Half-Power Method

The most common technique for determining the damping of a mode in the frequency domain is by use of the half-power method. This approach is based upon the following approximation for the damping of a single structural mode.

$$G \approx (\Delta\omega / \omega_o) \sqrt{|A_{\max}|^2 / |A|^2 - 1} \quad (179)$$

where:

$|A_{\max}|$ = the maximum response amplitude at ω_o , and
 $|A|$ = the response at some ω where:

$$\omega = \omega_o + \Delta\omega / 2 \quad (180)$$

and where ($\Delta\omega \ll \omega_o$). For $|A| / |A_{\max}| = 1 / \sqrt{2}$ (or 0.707), then

$$G \approx \Delta\omega / \omega_o \quad (181)$$

The half-power method applied to a plot such as the imaginary portion of the frequency response (Section 11.3.8) will use this criteria as shown in Figure 144 where:

$$\sigma = \zeta_r \omega_d \quad (182)$$

The residue is a measure of a mode's energy content and is defined as:

$$R \approx 2 |A_{\max}| \sigma_r \quad (183)$$

Also, a **quality factor** can be defined as:

$$Q = \omega_o / \Delta\omega \quad (184)$$

When the magnitude of a response plot is squared, as in an autospectrum or a PSD (see Section 11.3.3), then one-half of the resonance is used instead of 0.707 (Figure 145). If the plot is further modified by showing the magnitude on a log scale, then the $\Delta\omega$ is found as before, depending on whether the amplitude was initially squared or not. Data can be plotted using $20\log(\text{magnitude ratio})$, where the ratio is determined by dividing by some convenient reference magnitude, or just $\log(\text{magnitude})$ for a transfer function (Section 11.3.6). This results in units of decibels (dBs). Now -3 dB down would be the required amplitude for the analysis (Figure 146) if the original amplitude was not squared, and -6 dB (half the power) is used when the original magnitude was squared.

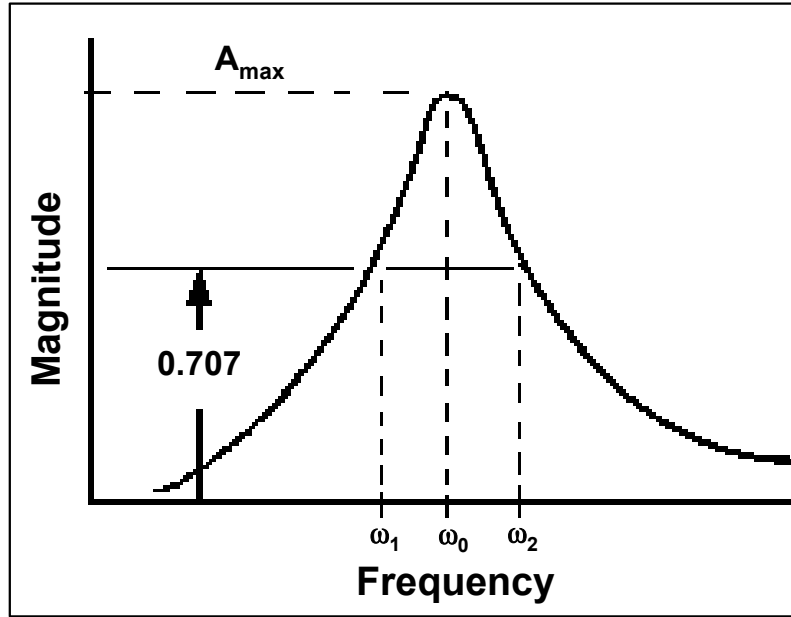


Figure 144 Half-Power Damping from a Nonsquared Frequency Response Function

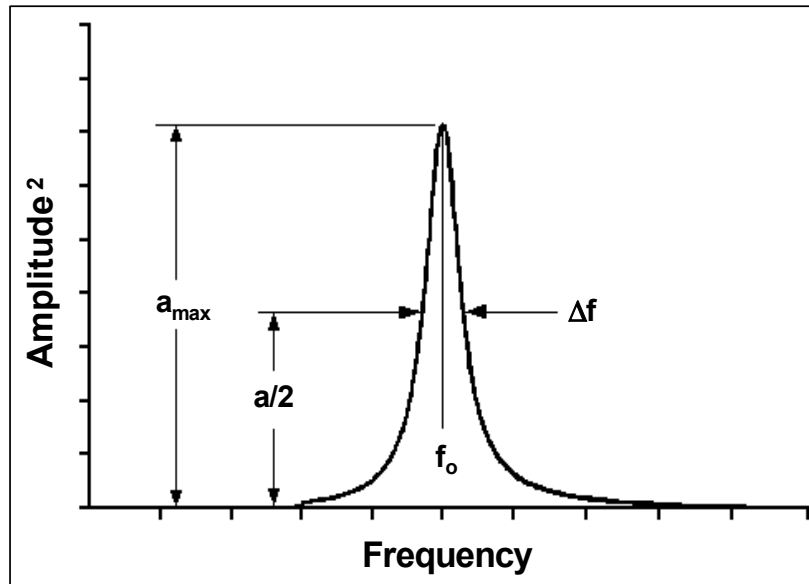


Figure 145 Half-Power Method from a Squared Frequency Response Function

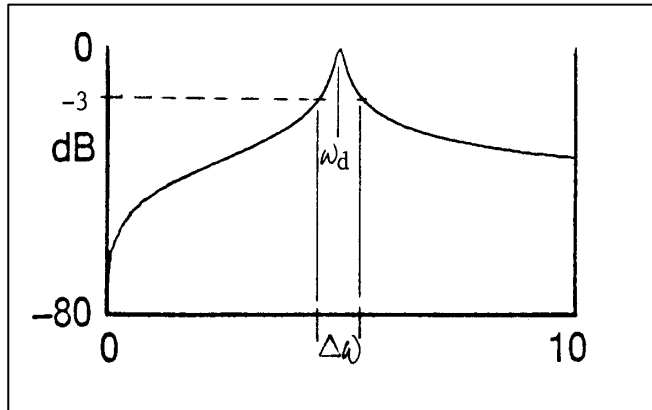


Figure 146 Half Power Applied to Decibel Scale (Nonsquared Frequency Response Function)

The half-power method assumes that only one mode is influencing the results; the mode being analyzed. This will almost certainly not be the case unless the single response is greatly dominant. The fidelity of the damping result is a function of how pure the mode appears or how close other modes are to the one being analyzed. It may be necessary to extrapolate the skirts of the mode in order to do a half-power analysis where close modes have clearly expanded the skirt. This sort of analysis of one mode at a time versus a curve fit of the entire FRF is termed **peak picking**.

Figure 147 shows an analysis performed using several of the techniques discussed so far, and using some automated processing techniques. The portion of the original PSD (Figure 147[a]) of interest is isolated (Figure 147[b]) using a narrow band pass window function (Section 12.4.1) forcing the response to zero within the window. An IFT of Figure 147(b) produces an auto-correlation function which may be seen as the single decay shown in the figure, or as a series of beating-type responses typical of close modes and analogous to a transient response. The first damped response, if several beat responses are present, is the dominant mode; it is the damping of this that is usually of most interest. The mode is marked with a line at the peak of the response or beginning of the decay portion ('M' at zero, in this case) and a line to mark the lowest response level at the end of the decayed portion ('C' for cutoff, in the figure). An exponential window (Section 12.4.1.5) is used to force the time domain decay to zero. The choice of the E line shown in the figure dictates the shape of the exponential envelope superimposed on the decay and forces the response to 2 percent of the response at M at the selected point. The closer the E is to the cutoff, the sharper the decay will be. All of this serves to isolate and smooth a single mode, or several if such is included in the IFT cutoff. The PSD of the selected mode is shown in Figure 147(d). The peak of the resulting smoothed mode is chosen, the half-power line is automatically calculated and drawn on the plot, and the x-axis values of the skirt crossings are marked. While this approach may be the only means of extracting useful damping data from poorly excited response data with close modes, it is about the limit of the processing advised without losing confidence in the resulting damping and frequency values.

11.3.5 Other Common Presentations

The dynamic response relationships introduced in Section 4.4.1 provide important information when plotted in the frequency domain. Figure 148 provides examples of these functions. The **compliance**, **mobility** and **inertance** plots identify resonance as maximum value 'spikes,' while the **apparent stiffness**, **impedance** and **apparent mass** identify resonances at the minimum 'valleys,' **antiresonances** or **nodes** (see Section 4.5.2). The apparent mass (inverse of inertance) displayed as logarithmic amplitude is simply the mirror image of the inertance plots so that they are analyzed in an inverse manner (valleys being resonances, etc.). Note that the phase shifts 180 degrees at resonance for inertance and 90 degrees for compliance and mobility. This fact is used to separate 'true' modes from 'false' modes (spikes produced by structural nonlinearities or signal processing errors). Note that at resonance the real component of inertance has a value of zero, and the imaginary component has a local minimum (negative spike).

Figure 148 also illustrates for inertance how a logarithmic amplitude (dB) allows more detail in low energy modes while a linear display allows resonances to be seen more easily. This is generally true for most frequency domain plots.

These relationships provide another way of extracting modal parameters. Using compliance (displacement divided by force, or x/f), the following relationship can be defined as:

$$G = \frac{|x/f|(f_0)}{|x/f|(0)} \quad (185)$$

where:

$x/f(f_0)$ = the amplitude of the compliance at the resonant frequency, and
 $|x/f|(0)$ = the static compliance or the magnitude at zero frequency.

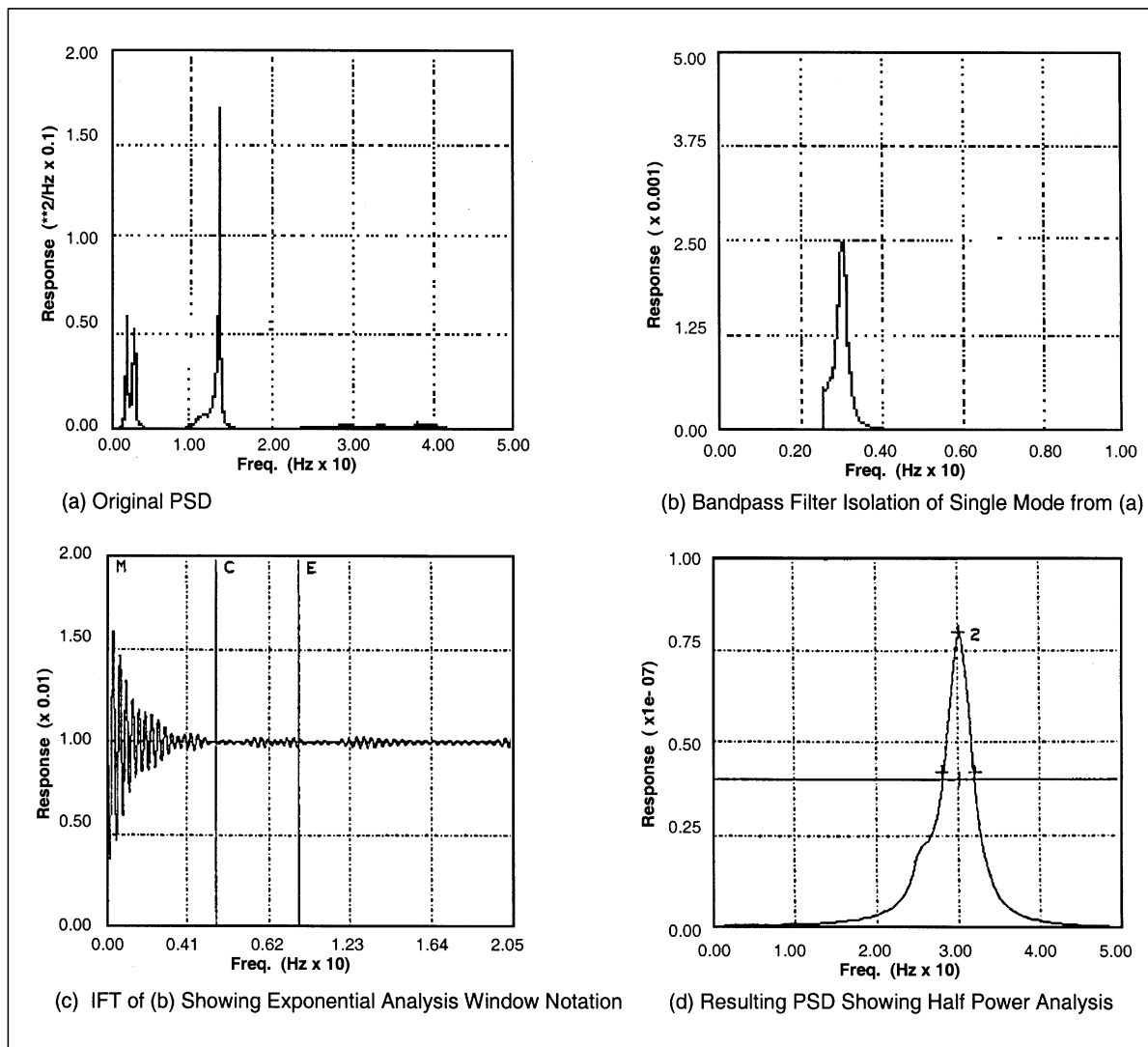


Figure 147 Half-Power Method Using an Inverse Fourier Transformation for Smoothing

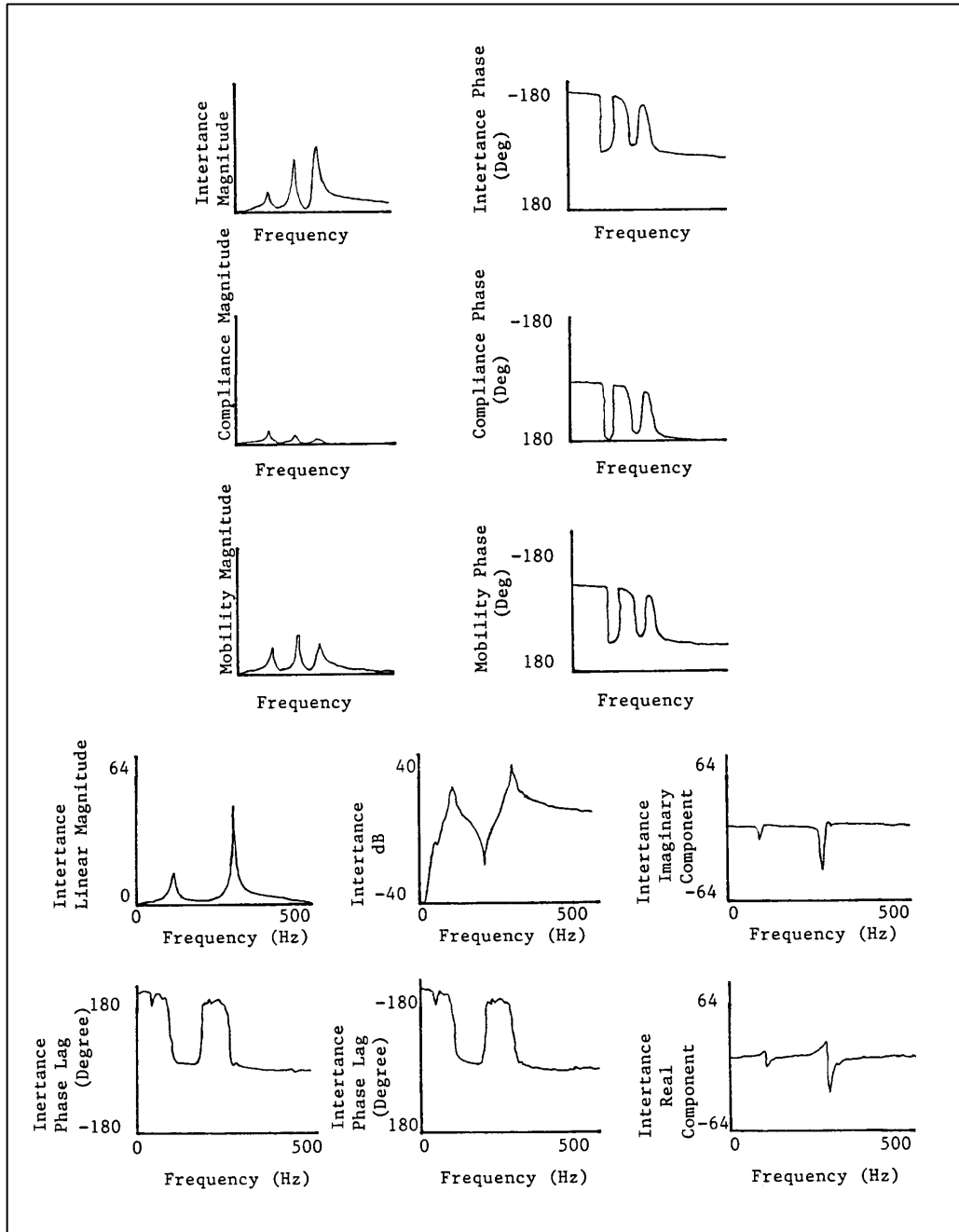


Figure 148 Common Data Presentations

Figure 149 shows how stiffness and mass can be obtained from the displacement, velocity, and acceleration plots. For frequencies much less than the resonant frequency, the slopes of the curves (called the **stiffness line**) are proportional to the stiffness (k), as shown. These slopes are 0, 1, and 2 for displacement, velocity and acceleration, respectively. For frequencies much greater than the resonant frequency, the slopes of the curves are proportional to the mass (termed the **mass line**), as shown, where the slopes are -2, -1, and 0 for displacement, velocity and acceleration, respectively. All of this naturally assumes that the data is clean and only one mode is affecting the response at the frequency of interest.

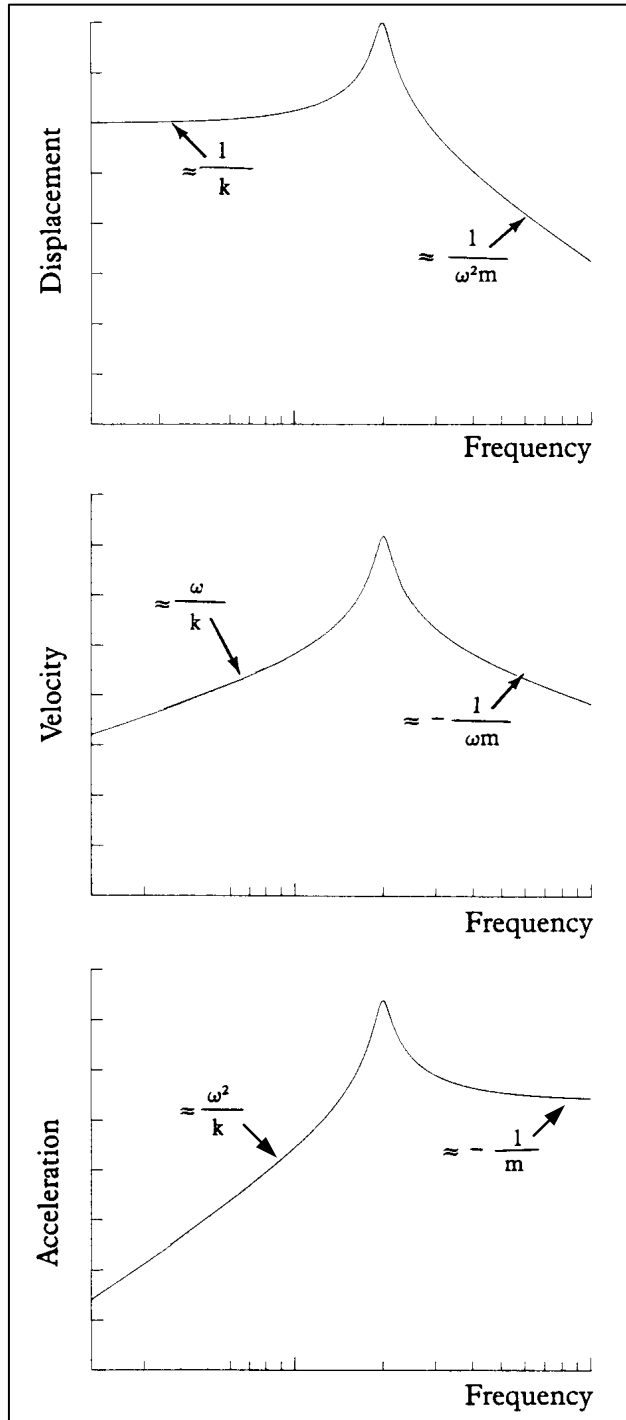


Figure 149 Modal Parameters from Simple Response Plots

11.3.6 Transfer Functions

A transfer function is a mathematical model of a system (the structure, in our case) that transforms the input excitation into the output response, as shown by Figure 150.

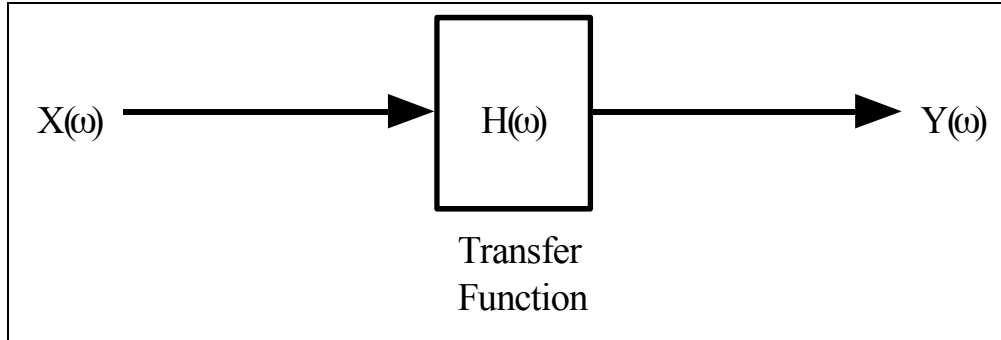


Figure 150 Diagram of Transfer Function Operation

It can be defined as:

$$H(\omega) = Y(\omega)/X(\omega) \quad (186)$$

or, using the notation from Section 11.3.2 as:

$$H(\omega) = G_{xy}(\omega)/G_{xx}(\omega) \quad (187)$$

Similarly, in the Laplace domain (Section 11.3.10),

$$H(s) = Y(s)/X(s) \quad (188)$$

Or, using power spectral densities,

$$H(\omega) = \Phi_{xy}(\omega)/\Phi_{xx}(\omega) \quad (189)$$

and

$$|H(\omega)|^2 = \Phi_{yy}(\omega)/\Phi_{xx}(\omega) \quad (190)$$

This last equation allows us to eliminate the input power spectral density if the input can be assumed to be sufficiently flat in the frequency range of interest (such as free air turbulence excitation). That is,

$$|H(\omega)|^2 = \Phi_{yy}(\omega)(\text{const } \omega) \quad (191)$$

The power of the transfer function rests in its ability to predict the response to any input, if it can be so defined, by reforming equation 186 as:

$$Y(\omega) = H(\omega)X(\omega) \quad (192)$$

This section deals principally with modal parameters derived more or less manually from response plots. However, there are many transfer function curve-fitting routines that can be used to extract the parameters, which provide the modal data. These are very mathematically intensive and too lengthy to detail here. A few curve-fitting routines allow some correction for modal contributions from responses outside the frequency range

being analyzed. These are called the **residuals**. Curve fitting in the frequency domain has the advantage of being able to fit only those portions of the spectrum of interest and thus, eliminate those areas with noise or signal processing problems and obtain a better fit. Curve fitting in the time domain has the advantage of using data that has not been subjected to extensive processing that can introduce errors. The reader is encouraged to read the many papers that discuss FRF curve fitting.

11.3.7 Coherence Function

The coherence function can be formed using the power spectral densities (see Section 11.3.3) or the autospectrums (see Section 11.3.2), as shown in equations 193 and 194, respectively.

$$v_{xy}(\omega) = |\Phi_{xy}(\omega)|^2 / [\Phi_{xx}(\omega)\Phi_{yy}(\omega)] \quad (193)$$

$$v_{xy}(\omega) = |G_{xy}(\omega)|^2 / [G_{xx}(\omega)G_{yy}(\omega)] \quad (194)$$

The coherence function is used when both the input and response functions are known, most often when attempting to form a transfer function (previous section). The coherence between single input and single output signals has been called **ordinary coherence**.

The ordinary coherence function will always be between 0.0 and 1.0, as shown in Figure 151, and shows the amount of response due to the input alone, and how much is due to noise or parasitic excitation and leakage (Section 12.3.3). At 1.0 the response is due entirely to the input (perfect correlation), with no noise present. Conversely, at 0.0 there is no correlation at all. A value of greater than 0.7 is considered acceptable and modal parameters extracted from the FRFs at corresponding frequencies should be reliable. A value of less than 0.7 is considered unacceptable and the test should be repeated with different excitations or the data analyzed again in an effort to reduce noise and processing errors.

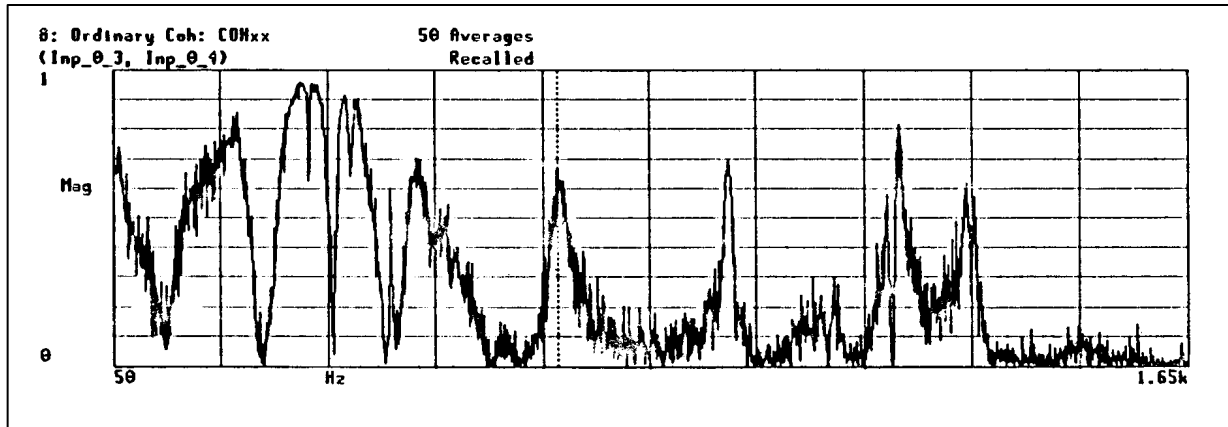


Figure 151 Example of Ordinary Coherence Function

When more than one input and output are involved, other coherence functions can be defined. **Partial coherence** is essentially an ordinary coherence function but with one or both of the signals ‘conditioned’ by removing the potential contributions from other influences, such as from other forcing functions. It is most often used to determine whether another input is correlated in any way with the input of interest and thus, influencing the output signal. In the case of a coherence between two inputs, a low value of coherence would indicate little or no correlation. A **multiple coherence** is done between a single output and all known input signals. This allows an evaluation of how much unknown or undesirable inputs are influencing the response. A multiple coherence would involve a matrix of input cross spectrums (G_{xx}) in which each element is a cross spectrum of an input ‘I’ with an input ‘j,’ one for each or $G_{xx}(i,j)$. This matrix is then augmented with an array of output-input cross spectrums, $[G_{yx}]$ to produce:

$$[G_{yxx}(i)] = \begin{bmatrix} G_{yy}(i,i) & G_{yx}(i,1) & G_{yx}(i,2) & G_{yx}(i,3) & \dots \\ G_{yx}(1,i) & G_{xx}(1,1) & G_{xx}(1,2) & G_{xx}(1,3) & \dots \\ G_{yx}(2,i) & G_{xx}(2,1) & G_{xx}(2,2) & G_{xx}(2,3) & \dots \\ G_{yx}(3,i) & G_{xx}(3,1) & G_{xx}(3,2) & G_{xx}(3,3) & \dots \\ \dots & \dots & \dots & \dots & \dots \end{bmatrix} \quad (195)$$

In a multiple coherence for output i , $v_M(i)$ can now be determined by using the determinant of this matrix and the matrix of input cross spectrums.

$$v_M = \frac{1 - \text{DET}[G_{yxx}(i)]}{G_{yy}(i,i)\text{DET}[G_{xx}]} \quad (196)$$

11.3.8 CO/QUAD Method

Another way of analyzing frequency domain data is by examining the real and imaginary parts of the frequency response. These are shown in Figure 152 for a single mode, and other forms have already been presented in Figure 148. Notice that at resonance the mobility has only real amplitude while the compliance and inertance has only imaginary amplitude. The real part of the response is in phase or **coincident (CO)** with the forcing function, and the imaginary part is out of phase with the response (**quadrature [QUAD]**). The imaginary part is especially helpful in distinguishing close modes as single peaks result for each and will likely have opposite signs. The peak of the QUAD will occur at the resonance frequency, the same as the CO zero or axis crossover.

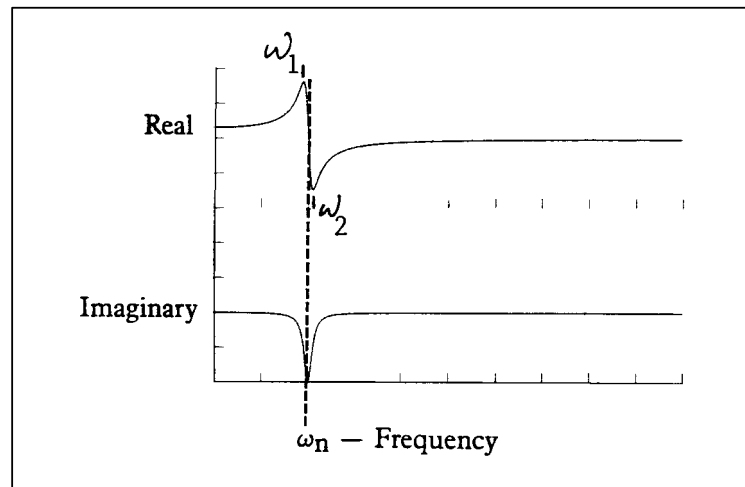


Figure 152 CO/QUAD Elements

The peak of the CO can be used to find the damping by using the real portions of the compliance and inertance (imaginary for mobility) as indicated in Figure 153 and with the following equation:

$$G = [(f_a / f_b)^2 - 1] / [(f_a / f_b)^2 + 1] \quad (197)$$

Damping derived from the QUAD was presented in Section 11.3.4.

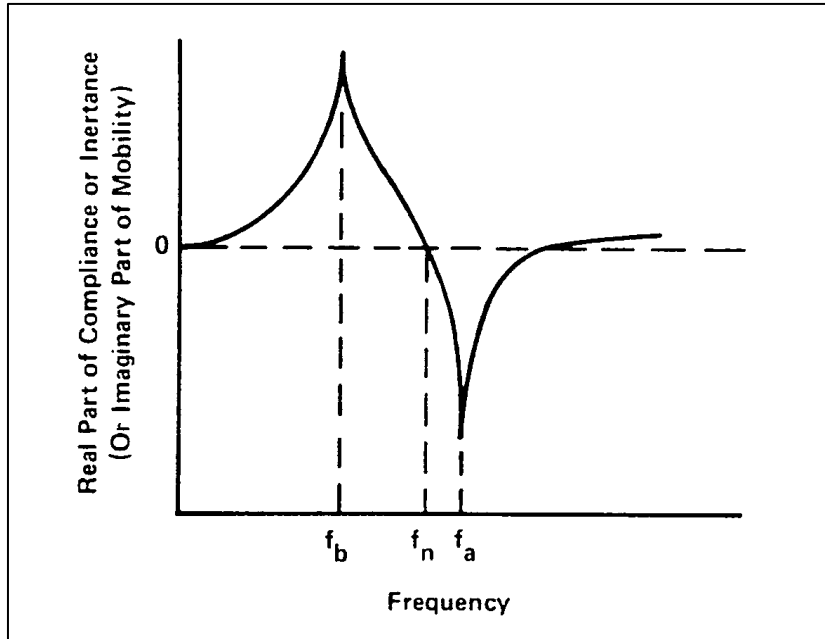


Figure 153 Determining Damping from Real or Imaginary Response

11.3.9 Nyquist Plots and Circle Fit

If the two curves of Figure 152 are plotted against each other then a plot like Figure 154 will result for a SDOF. Plots for acceleration, velocity (mobility) or displacement (compliance) would be identical, but for a 90-degree rotation of the trace each time. When examining the imaginary and real axes alone in the Argand plane, a circle is seen. This is called a Nyquist, or Polar plot, and can also be produced by plotting magnitudes at the corresponding phase angles, as in Figure 155. The circle is easily plotted by employing the simple geometric identities

$$\text{Re} = \text{mag}(\cos \varphi) \quad (198)$$

$$\text{Im} = \text{mag}(\sin \varphi) \quad (199)$$

At a phase angle of 90 degrees the amplitude is at maximum with the real component zero. This condition corresponds to resonance, so the frequency of this point is the resonant frequency. Larger diameters represent lower damping than small diameter circles.

Real data for a MDOF system would appear more like Figure 156(a). The distortion and offset of the circle are the effects of coupling between off-resonant modes (vector OA in Figure 156[b]) or the presence of nonlinear restoring and damping forces. The peak response is found as shown in Figure 156(b) and the damping by equation 200. Using the notation of Figure 156(b):

$$\zeta = 2(\omega_C - \omega_D) / \omega_0$$

(200)

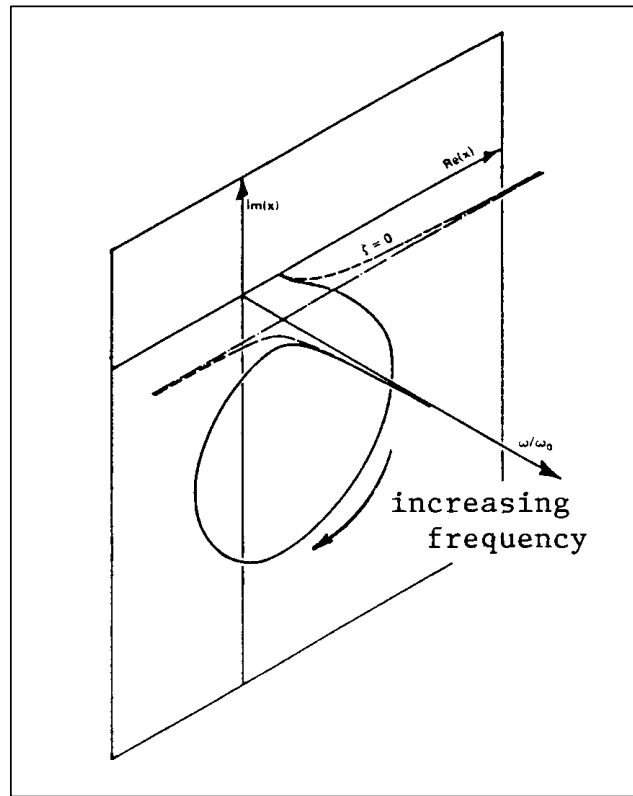


Figure 154 Three-Axis Frequency Response Plot

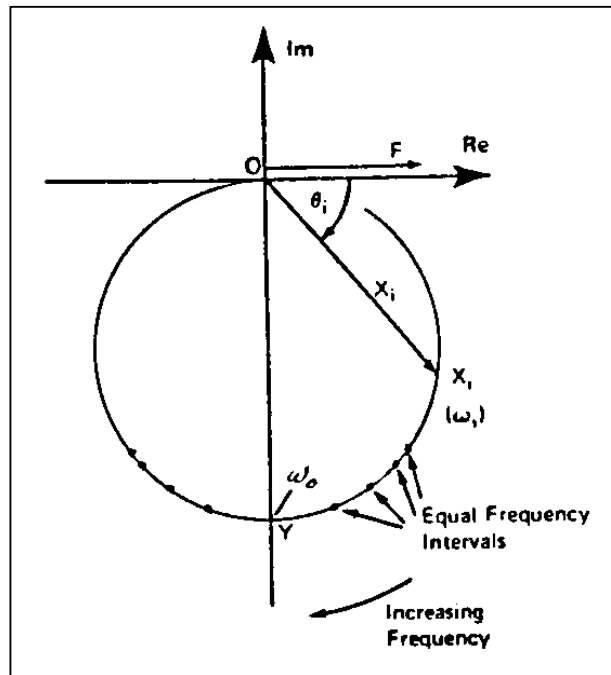


Figure 155 Single Degree of Freedom Nyquist Plot

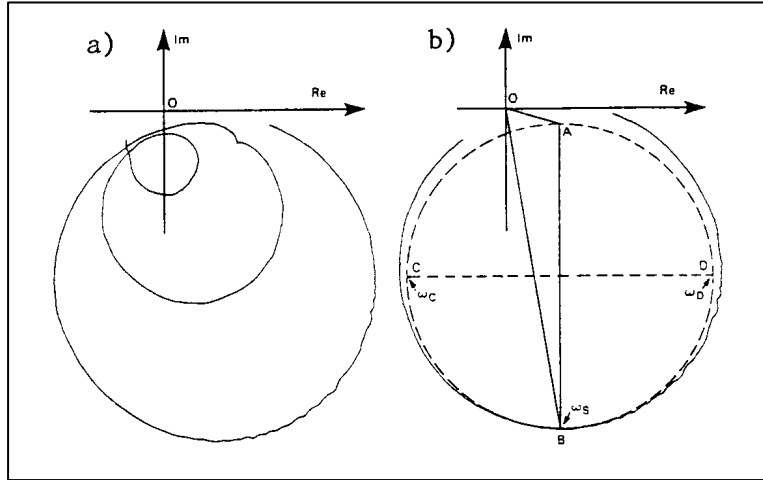


Figure 156 Nyquist Plot Analysis

11.3.10 Laplace (S-Plane) Transformation

Analysis is occasionally done in the s-domain where s is the Laplace variable defined as:

$$s = \sigma \pm j\omega \quad (201)$$

or,

$$s = \zeta\omega_n \pm i\omega_n\sqrt{1-\zeta^2} \quad (202)$$

and is plotted in Figure 157(a) and 157(b) where only negative values of σ (damping axis) is shown. Note in the figure that the dashed line is the frequency response function and the surface represents the transfer function.

For a continuous function, the Laplace transformation is defined as:

$$x(s) = \mathcal{L}x(t) = \int_0^{\infty} e^{-st} x(t) dt \quad (203)$$

The transformation of a transfer function can be cast in partial fraction form in which the roots of the denominator terms are called poles and the roots of the numerator terms are zeros. For example;

$$H(s) = \frac{2(s+1)(s-2)}{(s+3)(s+1+j)(s+1-j)} \quad (204)$$

For the purpose here only the poles are of interest and these are the peaks of Figure 157. The poles and zeros can be shown as in Figure 158 in which a root-locus analysis can be performed on the s-plane. Only the following identities are needed:

$$\zeta = \cos \beta = \sigma / \omega_n \quad (205)$$

and ω_n is equal to the distance from the origin to the pole, or

$$\omega_n = \sigma / \cos \beta = \omega_d / \sin \beta \quad (206)$$

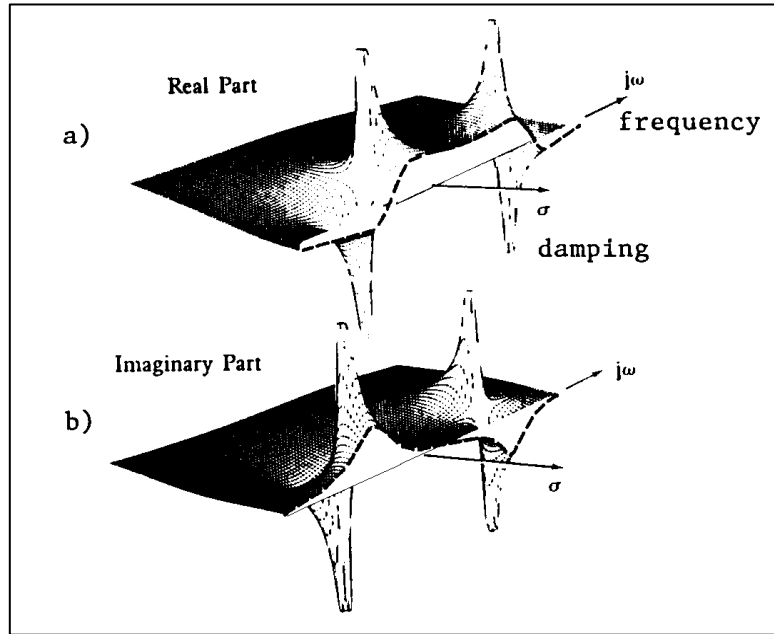


Figure 157 S-Plane Representations (Single Degree of Freedom)

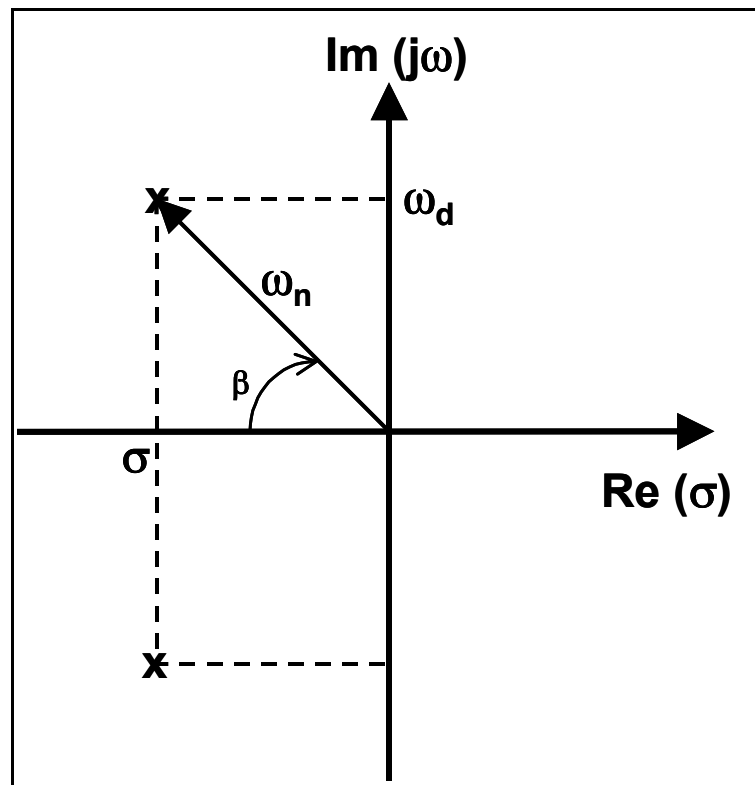


Figure 158 Example S-Plane (Root-Locus) Analysis (Single Degree of Freedom)

Some modal analysis techniques (particularly those that utilize transfer functions) operate on frequency response data as a Laplace transform by assuming that the structural damping is negligible and setting $\sigma = 0$ in equation 201. This leaves amplitude versus frequency, as we have dealt with in previous portions of this section.

11.3.11 Bode Plots

The real and imaginary parts of the frequency response, like that of the s-plane definition (Figure 158), can be replotted as magnitude and phase, where phase (ϕ) is

$$\phi = \tan^{-1} [\text{Im}(\omega) / \text{Re}(\omega)] \quad (207)$$

and magnitude is

$$A(\omega)^2 = \text{Re}(\omega)^2 + \text{Im}(\omega)^2 \quad (208)$$

The result would appear as a Bode plot (Figure 159). As with Figure 157, the dashed line is the frequency response function and the surface represents the transfer function.

It is more typical to examine the positive axis alone as well as define the amplitude as a decibel (dB) value to accentuate peaks, as explained in Section 11.3.4. The result is shown in Figure 160.

The Bode plot has many important uses in control theory (see Section 8.0). For purely structural purposes it is useful in identifying true resonant peaks in what is often called a **transmissibility plot** (or **T-plot**). The magnitude plot may show many peaks, but a true resonant peak must occur at ± 90 degrees of phase. It is then an easy matter to cross-reference peaks in the magnitude plot to phase at the same frequency to verify resonance. This is particularly useful in examining the results of a frequency sweep during a ground vibration test (see Section 7.8.3.1).

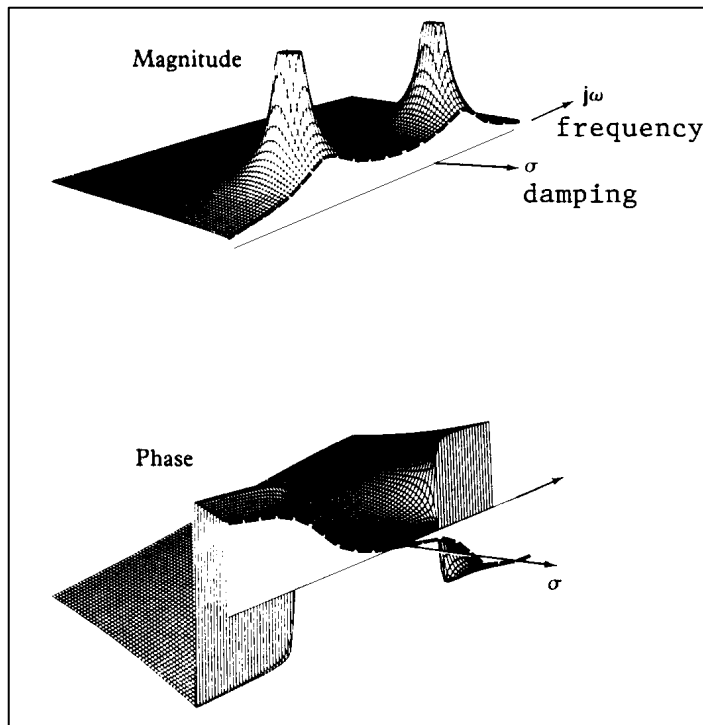


Figure 159 Magnitude and Phase Diagrams

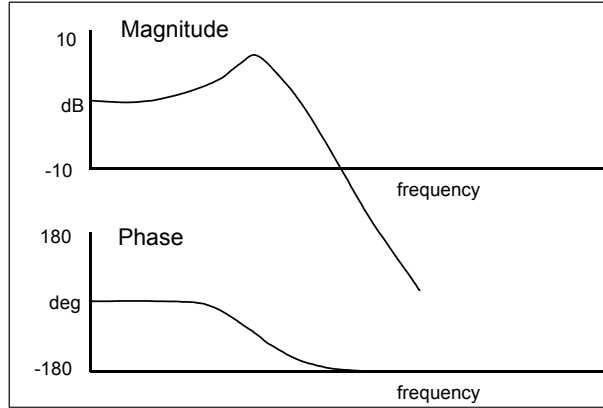


Figure 160 Single Degree of Freedom Bode Plot

11.3.12 Z-Plane Transformation

For test data analysis the Laplace transformation defined by equation 203 is impractical since a continuous function defining the frequency response is seldom available. The z-transform provides a discrete technique which is analogous to the s-plane. It is defined as:

$$X(z) = \sum_{n=-\infty}^{\infty} x(n)z^{-n} \quad (209)$$

or the limits $n = 0$ to ∞ for a one-sided transformation. The inverse is:

$$X(n) = [1/(2\pi j)] \int_C X(z)z^{n-1} dz \quad (210)$$

where:

$$Z = e^{sT} \quad (211)$$

and where T is the sampling rate for the data. Clearly then, z has the characteristics of a sampled Laplace transformation.

The z-plane will look like Figure 161 where lines of constant σ in the s-plane map into circles of radius $e^{\sigma T}$, and lines of constant ω become radial rays at an angle ωT , and a constant ζ becomes a logarithmic spiral. For system analysis, the consideration of roots falling within the unit circle is important for stability (Reference 3).

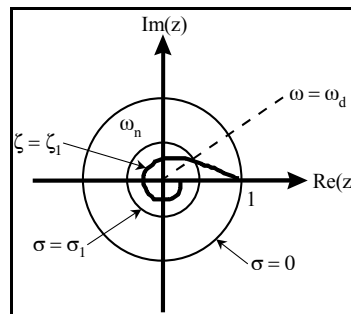


Figure 161 Example Z-Plane

SECTION 11 REFERENCES

1. *The Fundamentals of Modal Testing*, Application Note 243- 3, Hewlett-Packard Company, 1986.
2. *Flutter Testing Techniques*, NASA SP-415, October 1975.
3. *Linear Control Theory, Analysis and Design*, J.J. D'Azo and C.H. Houpis, McGraw-Hill Book Co., 1981.
4. *Feedback and Control Systems*, Schaum's Outline, J.J. DiStefano, A.R. Stubberud and I.J. Williams, McGraw-Hill, 1967.
5. *MASSCOMP Array Processor Programming Manual*, John Sundman, Massachusetts Computer Corporation, 1985.
6. *Modal Testing: Theory and Practice*, D.J. Ewins, John Wiley and Sons Inc., 1984.
7. *Digital Time Series Analysis*, R.K. Otnes and L. Enochson, John Wiley and Sons, 1972.
8. *Understanding Vibration Measurements*, George F. Lang, Application Note 9, Rockland Scientific Corp., December 1978.
9. *Advanced Engineering Mathematics*, C. Ray Wylie, McGraw- Hill Book Company, New York, 1975.

12.0 SIGNAL PROCESSING

12.1 Introduction

Structures testing most often uses digitized data. This refers to the time sampling of an analog, continuous voltage signal and recorded as binary numbers representing the signal's amplitude. The binary numbers are sequentially recorded for time reference. The digitizing process can create errors or present limitations that must be understood in order to ascertain the validity of the data. Any data signal must be processed in some manner for presentation, and this can lead to errors and general corruption. Some processing methods permit the data to be corrected and 'smoothed' for easier analysis. This chapter will highlight some of the more common concepts and processing techniques currently employed in instrumentation data manipulation.

All of the information in this chapter is in simplified, summary form. Whole books have been written on this subject. For detailed work in this area, many worthy sources are noted at the end of the section.

12.2 Resolution

It is important to determine the required resolution of critical parameters during the planning for a test, and then verify that the data conforms to these requirements. The required frequency and damping resolutions should determine sampling and digitization parameters, not the other way around.

12.2.1 Frequency Resolution

For a digitized **block** or **frame** of time history, data will consist of a **block size (N)** of equally spaced samples. In most cases, this block is a base 2 number like 1,024. When a Fourier transformation is performed, this number will be halved because at each frequency, amplitude and phase information is present. A plot of amplitude alone from a block of 1,024 points will have only 512 spectral lines (see Section 11.3.1). The **bandwidth (BW)** is then represented by this N/2 data block. The **sampling rate (SR)** must be at least twice the maximum frequency that can be resolved, per **Shannon's Sampling Theorem**. That is:

$$f_{\max} = SR/2 \quad (212)$$

or

$$f_{\max} = (N/2)/T \quad (213)$$

where:

T = the period of the time record.

In practice, the sampling rate is typically five or more times the maximum frequency of interest for the purpose of practical frequency resolution to support modal analysis. Figure 162 illustrates how at least five data points are necessary to identify a mode (full cycle) with any certainty in the time domain as well as in the frequency domain (modal peak).

Rayleigh's Criterion states that the lowest frequency resolution, or the minimum resolvable frequency obtainable, is inversely proportional to the sample period

$$f_{\min} = \Delta f = 1/T \quad (214)$$

or, using other identities associated with a frequency domain analysis

$$\Delta f = SR/N \quad (215)$$

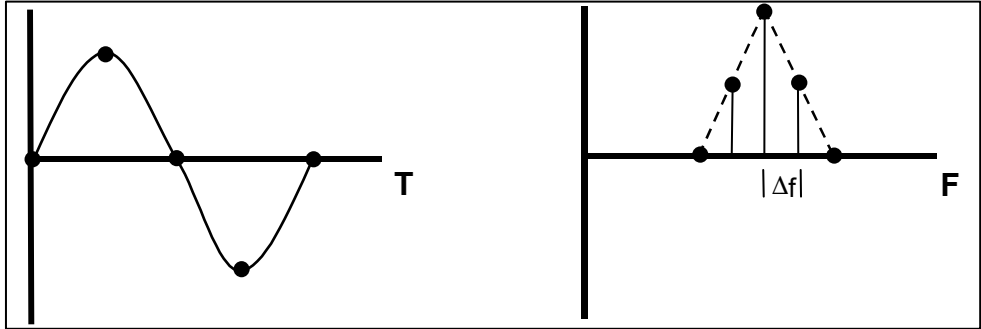


Figure 162 Points Required to Define a Mode

For a **baseband analysis**, that is one in which the lower frequency of the bandwidth is zero, the BW would become f_{\max} and the maximum frequency resolution obtainable would be:

$$\Delta f = BW/(N/2) \quad (216)$$

So, to analyze up to the maximum desired frequency requires that the SR increase. However, this is detrimental to frequency resolution in the frequency domain unless N is not also increased.

12.2.2 Damping Resolution

The analysis of damping with the half-power method (see Section 11.3.4) has a practical minimum damping that can be resolved. The worst-case half-power analysis using the best positioning of the spectral lines is shown in Figure 163. From this it can be concluded that:

$$G_{\min} = \Delta f / f \quad (217)$$

where:

- f = the center frequency,
- G = total system damping (see Section 6.3.1)

or using relationships that have already been established.

$$G_{\min} = SR / fN \quad (218)$$

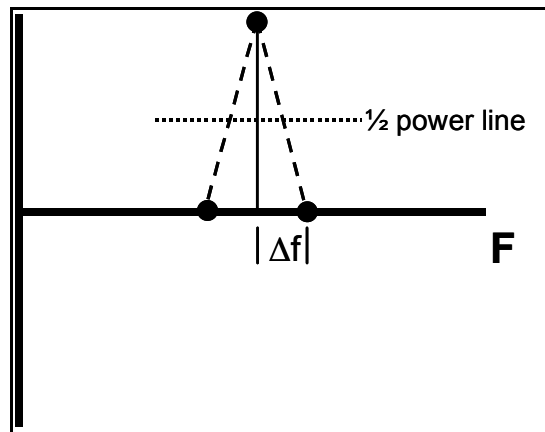


Figure 163 Illustration of Minimum Damping Resolution

So, an increase in N alone will increase damping resolution, but an increase in SR will decrease resolution. Also, lower frequencies will have lower damping resolution than higher frequencies for the same processing parameters. Although the theoretical G_{min} can be obtained with only three spectral lines included in the **spectral lobe**, as shown in Figure 163, experience has shown that at least five spectral lines (like Figure 164) with at least three at or above the half-power line (see Section 11.3.4) are necessary in the lobe to get a reliable estimation of damping. So, twice the G_{min} of equation 218 should probably be used in reality.

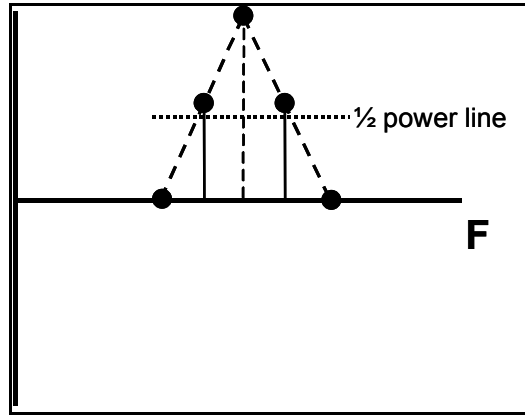


Figure 164 Illustration of Minimum Spectral Lines Required per Spectral Lobe to Achieve Reasonable Damping Values

12.2.3 Amplitude Resolution

If the frequency of a response is not a multiple of Δf , then a spectral line representing the mode will fall between two lines which are actually produced in the frequency domain plot, as suggested by Figure 164. The amplitude would only be partially represented by the two adjacent spectral lines. Only an increase in frequency resolution can reduce this problem. Section 12.3.1 discusses an error source that can further reduce amplitude resolution.

12.3 Error

A total data error of 5 percent is considered good for flight test data. A smart test engineer will attempt to quantize the accuracy of data by considering resolution, errors, and effects of processing. This section will provide some basis for assessing the quality of the data in the presence of the multiple errors produced in flight testing.

12.3.1 Quantization

The resolution of a signal amplitude represented by a binary word depends upon how many bits are used (see Section 10.8.2). A 12-bit word would have greater amplitude resolution than a 10-bit word. This is a fundamental limitation of the analog-to-digital converter (ADC) equipment and establishes one element of the error band for the data. The actual error is:

$$E = \pm 0.5(U_r / 2^M) \quad (219)$$

where:

U_r = the maximum range for the engineering unit that is encompassed by the signal voltage range, and
 M = the number of bits in the binary word.

So, if the maximum range is 100 g with a word of 10 bits, the quantization error is 0.05 g.

12.3.2 Aliasing

If frequency components greater than one-half of the sampling frequency (the **Nyquist** or ‘**folding**’ frequency, f_N) are recorded (recall **Shannon’s Sampling Theorem**), a significant frequency or amplitude error is possible. A frequency higher than signal f_N may be misinterpreted as a lower frequency or even as zero frequency because of the relationship between the sampling rate and the period of the signal. Figure 165 shows that for a mode at exactly the sampling frequency, f_s , a false response is shown at zero hertz in the frequency domain. Sampling at higher frequencies has the potential for misrepresenting a waveform as a lower frequency as the bottom plot in Figure 165 indicates. Aliasing is then a folding back of higher frequency components into the frequency range of interest. The practical result is an apparent response at less than the true frequency of a mode beyond the Nyquist frequency, thus allowing a misinterpretation of the data. Figure 166 shows a way of determining the potential aliased sources for a suspect response. The response at $2/3f_N$ could be folded down from the crossings of the diagonal lines, or $4/3f_N$, $8/3f_N$, $10/3f_N$, etc. Examining ground vibration or modal analysis data for a mode at these frequencies can provide insight into the source of a suspicious response.

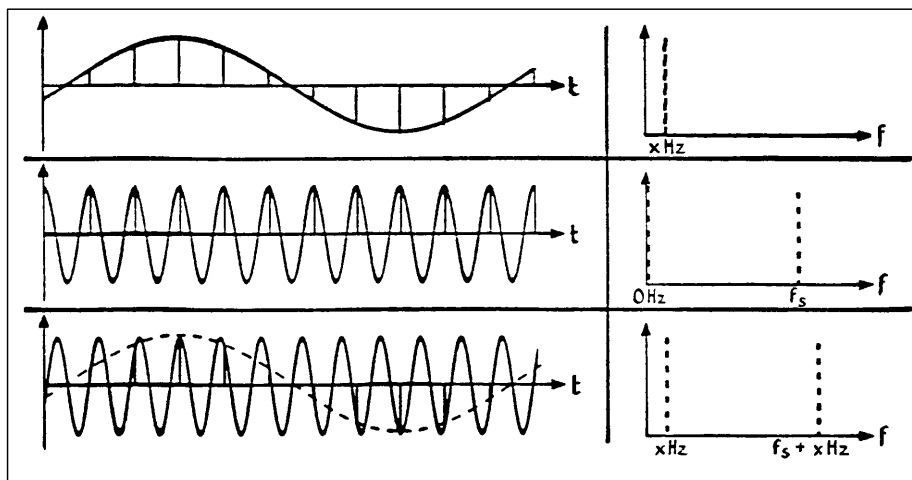


Figure 165 Examples of Aliasing Error

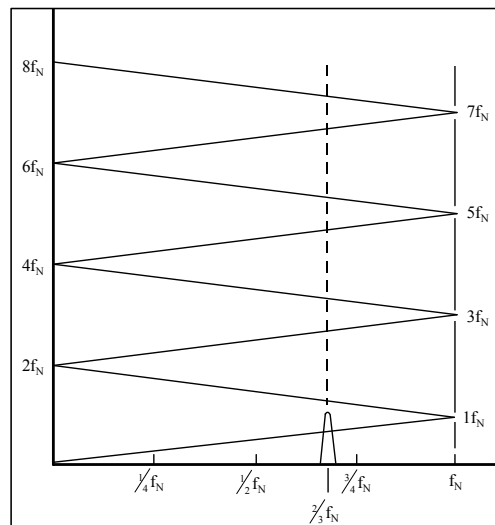


Figure 166 Aliasing Fold-Down Chart

The simplest solution to the aliasing problem is to use an analog filter (low pass, Section 12.4.8) to remove all of the frequency content above one-half the sampling rate prior to the ADC. If the ADC is on board the test vehicle, the filter will also have to be on the vehicle. Because filters have practical limitations on their ability to completely attenuate signals above the Nyquist frequency, the sample rate is generally set at greater than twice the filter cutoff frequency (Section 12.4.8). A factor of 1.28 times the highest frequency of interest has been used successfully in the past.

12.3.3 Leakage

The assumptions entailed in the fast Fourier transformation (FFT, see Section 11.3.1) include the requirement for the analog signal to be periodic and with a period equal to that of the time sample. Essentially, the sample must be periodic within the **window** being transformed and continuous throughout time. This is because the FFT must operate on a finite portion of the signal in a discrete fashion. For a signal that is not periodic within the frame, the FFT will be based upon a distorted waveform, as shown in Figure 167. The result is a smearing of modal energy that is referred to as **leakage** in the frequency domain, and **wrap around** in the time domain. Energy from the nonperiodic parts of the signal (the theoretical single mode spectral line) will 'leak' into the periodic parts of the spectrum (adjacent spectral lines) or, described another way, the response leaks out of the current data sample into the next.

Leakage is most readily seen as the expanding of the 'skirt' on either side of the mode's peak, as shown in Figure 168, instead of a 'clean' peak. This will produce an over-estimation of the damping. Amplitudes will also be truncated. Leakage is also seen as large dips in a coherence plot (see Section 11.3.7) in the vicinity of the modal peaks. Besides producing falsely high damping values, small signals close to the primary mode may be masked within the exaggerated skirt. One approach to reducing this error is to increase the frequency resolution. But, this is not always practical. Another method is **windowing**, covered in Section 12.4.1.

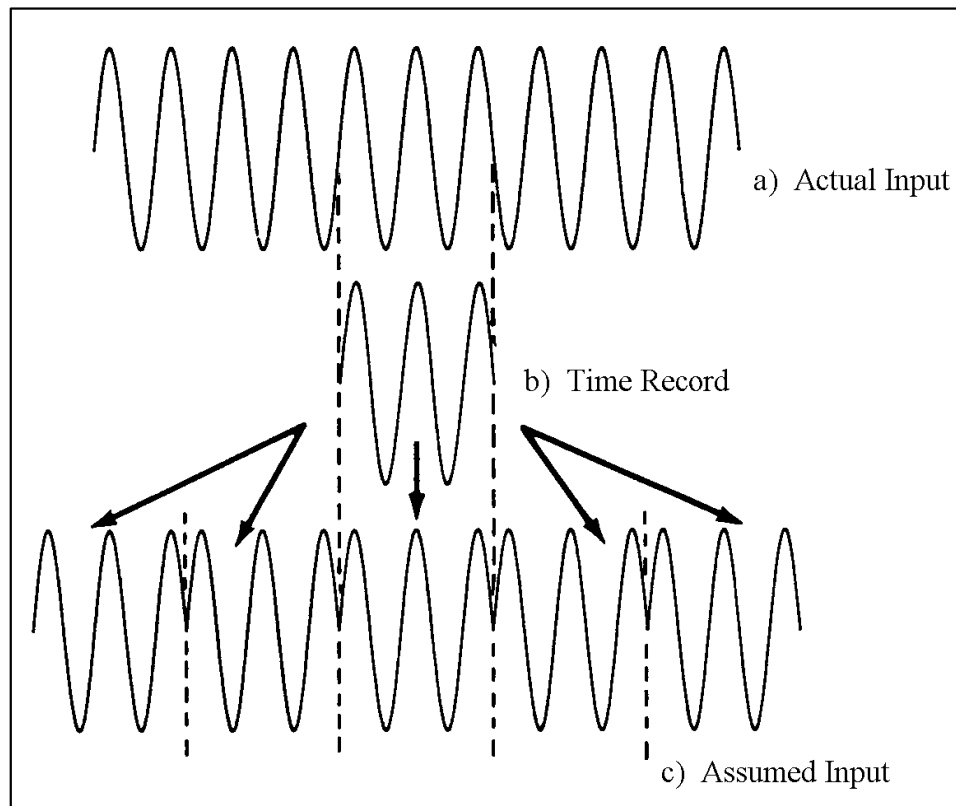


Figure 167 Distorted Waveform Producing Leakage

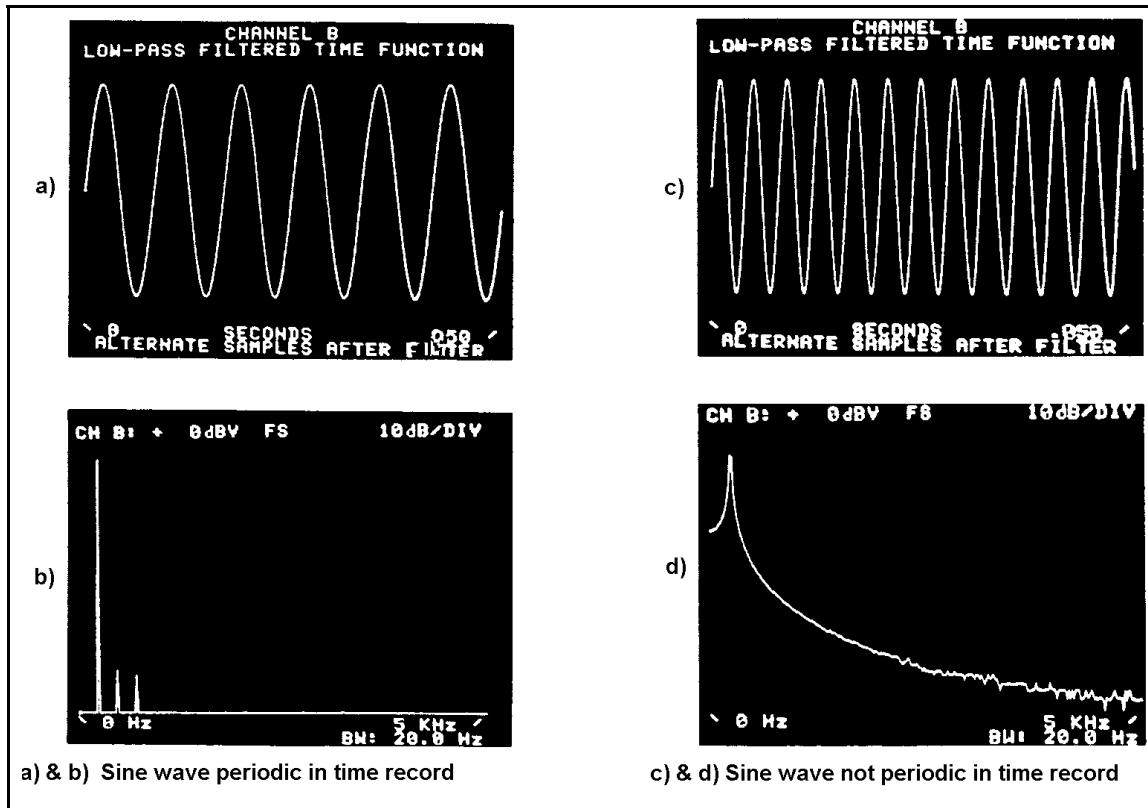


Figure 168 Illustration of Leakage Error

12.3.4 Ranging

The sensitivity of recording on analysis equipment should be set so that the anticipated signal level is about half the setting chosen. This is termed **half-ranging** and helps to ensure that the data is not **under-ranged** or **over-ranged**. Over-ranging or **over-loading** can lead to **clipping** of the data where the maximum values measured are simply not recorded and are cutoff at the maximum sensitivity level. Under-ranging can produce noisy data with poor frequency response results because the full dynamic range of the equipment is not utilized.

12.3.5 Other Sources of Error

There are many other sources of error that may need to be tracked if there is a concern about accuracy in readings. The transducers themselves will have measurement tolerances and drift which provide the first source of error to be accounted for.

Bit dropout refers to the failure of one bit in the ADC to be set. This is usually easily identified as a discrete band edge excursion of the data (see also Section 10.8). Dropouts are particularly troublesome when transforming data to the frequency domain. Such a sharp data excursion is interpreted as an impulse response with infinite frequency content and will result in broadband noise being superimposed on the frequency response plots. Most automated analysis routines will provide a means of identifying a signal level beyond which the data is considered to be a dropout. This level must usually be set only after visually inspecting the data. Dropouts are then set to zero, to the value of an adjacent data point, or some user-selected value.

The ADC reference voltage may also drift during the sample periods, introducing error. **Aperture error**, or **clock jitter**, may result in the measured value not being assigned to the correct time segment. **Digitizer error** may cause a random setting of a bit. This is commonly seen as a narrow band of clipped noise apparently

superimposed on the signal. One very common source of error or noise is the electrical noise occurring at harmonics of the power transmission frequency, usually 60 cycles.

An ever-present noise that contaminates structures flight test data is due to unknown excitations, the nonstationary nature of the flight environment, and necessary restrictions on the length of the test points. The myriad sources of line noise, transmission noise, and structural nonlinearities (rattles) will produce a low level clutter that will generally be at an average level called the **noise floor**. If the **signal-to-noise (S/N)** ratio is fairly low, then it may be difficult to clearly discern the important data and analyze it properly. When this happens, more fundamental measures must be taken such as boosting the signal, reducing the transmission range, shielding instrumentation cables and sensors, and attempting to locate and eliminate component rattles in the test article. Since the sensitivity of an ADC is frequently set in advance of a test, it is possible that an important signal is below the noise floor of the processor or so high as to be clipped (as described in the previous section). The sharp change in the response produced by clipping will also produce a broadband noise in the frequency domain as does dropouts. An overload of the ADC may take several sampling increments to recover. This is usually evident as an apparent **loss of signal (LOS)**.

A Fourier transform may produce a relatively large amplitude response at 0 Hz. This is the **dc component** described in Section 11.3.1; a **zero offset** of the data in the time domain. Its amplitude may well cause more important responses to be scaled so small that they would be difficult to analyze. For this reason the dc response is generally filtered prior to plotting. This can be done simply by subtracting the mean value of the entire data sample from each point in the sample.

12.4 Processing Techniques

The methods discussed in this section are used to smooth data, removing errors to facilitate data analysis. Caution must be taken to ensure that the consequences of employing a particular technique are known. A general warning is in order against using more than two processing methods on any single block of data. The data may look better but the results may be getting farther from the true parameter values being sought. Time and funds permitting, the same data should be processed separately using more than one technique and the results compared.

12.4.1 Windowing

Multiplying the analog signal by a weighting function to force the response signal to become periodic within the window for the reduction of leakage (see Section 12.3.3), or to reduce discontinuities at the boundaries of the sample, is known as windowing. The result is an improvement in the frequency domain of amplitude and frequency resolution accuracy, and makes damping analysis easier. There are a number of different window functions, each with their own special applications. Windowing the data also creates problems and limitations that must be considered. Only the most common windows are discussed.

12.4.1.1 Hanning Window

This window is a bell-shaped curve (Figure 169) that is typically used with undamped or slowly decaying signals. Its mathematical form is:

$$w(t) = [1 - \cos(2\Delta t / N)] / 2 \quad (220)$$

The result is to force the signal to zero at the window boundaries and retain the true amplitude only at the center. In the frequency domain, this window causes an artificial increase in the damping(s) because it tends to slightly reduce the amplitude of a resonant peak while also spreading out the skirt a little. The worse this error can get is $0.5\Delta f/f$, however the error decreases as the frequency resolution increases. A true analytical correction for this artificial damping is beyond the scope of this text, but an adequate frequency resolution should reduce the error to a negligible level. The Hanning window gives very good frequency resolution but generally poor amplitude accuracy. Applying this window to a signal that is already periodic in the sampling window will unnecessarily distort the signal and produce misleading data.

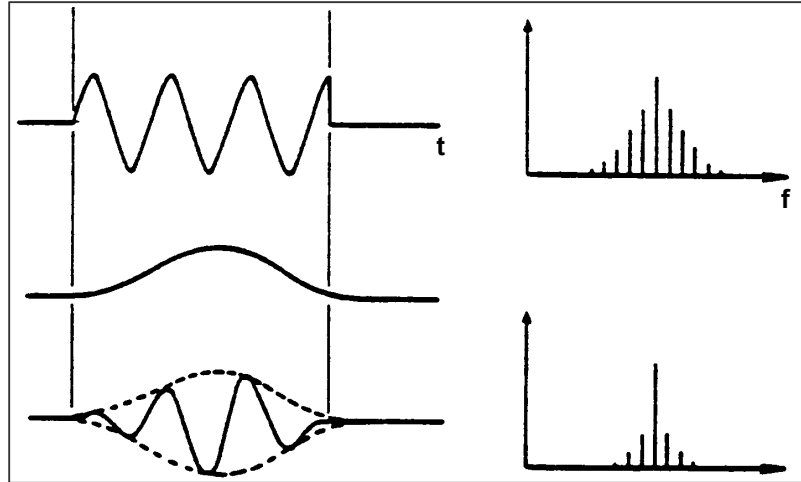


Figure 169 Application of Hanning Window

There are a number of other window function similar to the Hanning window but with slightly different mathematical forms. Among these are the **Hamming Window**, the **Kaiser-Bessel Window**, and the **Blackman Window**. The unique characteristics and benefits of these specialized functions are beyond the scope of this text.

12.4.1.2 Flat Top Window

Examining the Hanning window in the frequency domain (Figure 170), it can be seen that the passband shape (essentially a filter) has a relatively sharp peak. As already mentioned, this will tend to produce large amplitude errors except very close to the peak. It can be seen in the figure that the flat top window has a flatter peak and so will produce less amplitude error for a broader range of frequencies. However, the skirts are wider and this reduces the ability to resolve small spectral components. Therefore, the flat top window gives very good amplitude accuracy at the expense of frequency resolution. This window (Figure 171) is generally applied to an input signal.

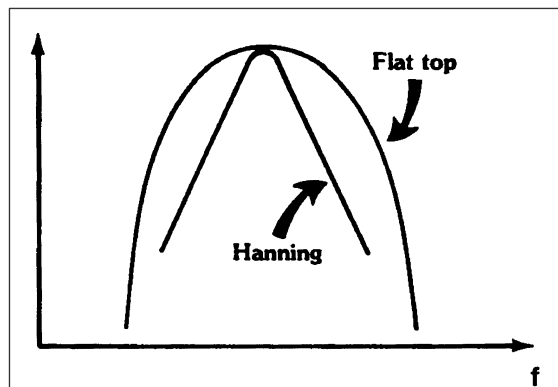


Figure 170 Comparison of Hanning and Flat Top Windows

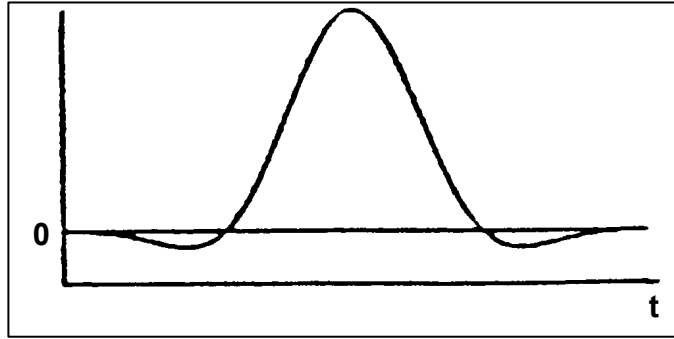


Figure 171 Flat Top Window

12.4.1.3 Uniform Window

As shown in Figure 172, this window gives equal weighting to all portions of the signal. So, the uniform window, also known as the **rectangle** and **boxcar** window, actually contributes nothing. It is analogous to isolating a sampling frame. It is generally used only with **self-windowing signals** (impulse, shock response, sine burst, chirps, and noise burst inputs (see Section 7.8), which are already periodic within the sample when the analysis routine demands that some window function be defined.

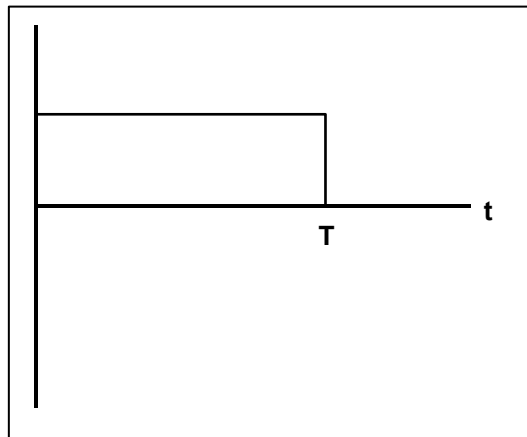


Figure 172 Uniform Window

12.4.1.4 Force Window

This window is primarily used with data obtained during impact testing (see Section 7.8.2.1) and is shown in Figure 173. The force window modifies the input or force signal from the impacted transducer to ensure that it begins at unity and eliminates any unwanted signal (noise) before and after the input. Since the force window is essentially a bandpass filter, it will not have the perfectly square form shown in Figure 173, but will have some slope associated with the rise and decay (Section 12.4.8). Using the force window with a stationary signal like a continuous sine wave will result in large errors.

A variation of the force window is one that is similar to the uniform window but does not extend all the way to the beginning and end of the block. The effect is to eliminate a small portion of the initial and trailing portion of the block to reduce leakage effects. While this is usually only employed with data that is not adversely effected by the loss of this data (such as with turbulence excitation), occasionally the window is applied to a doubled block consisting of the initial sampled block appended to itself. Thus, the middle of the new block includes the beginning and end of the initial block, and so this data is not lost.

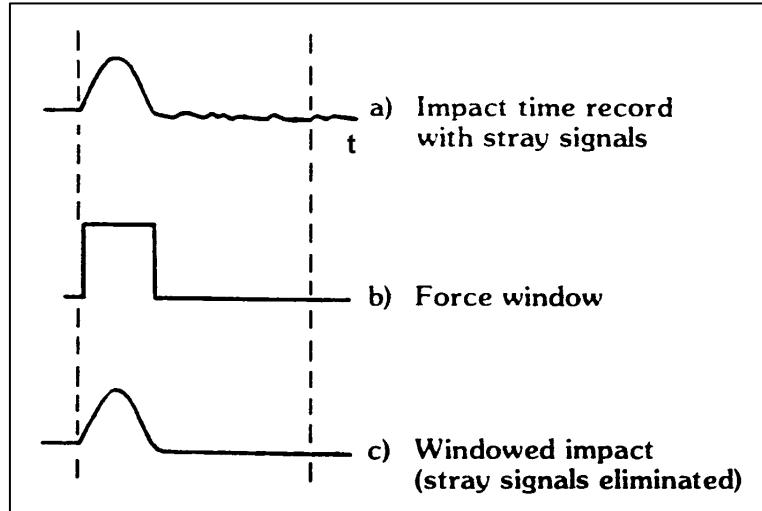


Figure 173 Application of Force Window

12.4.1.5 Exponential Window

This algorithm has the form:

$$x = Ae^{-\alpha t} \quad (221)$$

where:

α = the damping coefficient of the exponential curve to be used.

The window modifies a decaying response to ensure a smooth decay to zero within the window, as shown in Figure 174. The time needed to reduce the amplitude by $1/e$, the time constant, should be about a quarter of the window length. The damping represented by the exponential window function is added to that of the signal, and so will result in an apparent increase in damping of the convoluted waveform. This additional damping must be subtracted for correct values. Problems are likely to arise if the added damping is significantly greater than the actual structural damping. The tendency to increase the damping can also result in the inability to discern closely spaced modes in the frequency domain. The setting of any 'noise tail' on the response to zero by application of the window will also be beneficial.

The exponential window can be used as a smoothing function even when applied to multiple degree of freedom time-history data. A frequency response plot from such smoothed data will be much easier to analyze. It is essential that the dc (zero offset) component be removed before applying this window. As with the force window, using the exponential with a continuous signal will produce large errors.

12.4.2 Ensemble Averaging

The averaging of time domain or frequency domain responses will tend to reduce the influence of nonlinearities, noise, and distortion effects. This ensemble averaging is permitted as long as the nature of the input excitation does not vary. An example of this is the use with random excitation such as discussed in Section 11.2.4. The number of averages required or desired is strongly dependent upon the excitation and the test subject.

When the data fails to fill a data block, it is still possible to use this data for the purposes of averaging. The rest of the block can be filled with values equal to the value of the last data point, or by taking the appropriate

number of data points from the previous block. If the original data makes up less than half of the new block, the data is typically discarded.

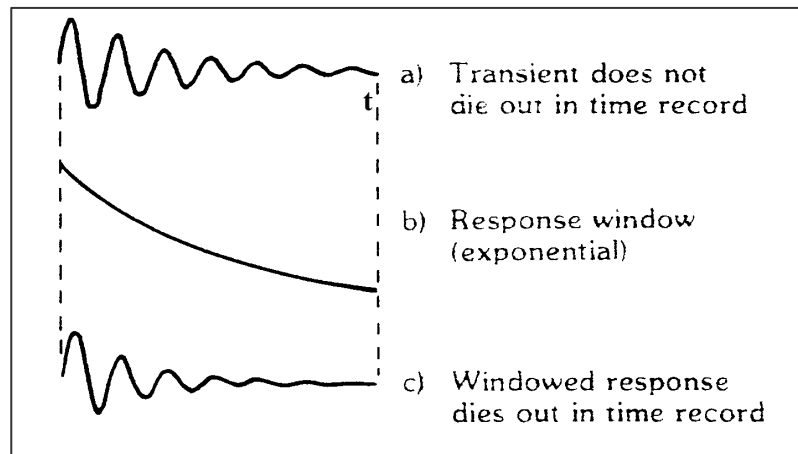


Figure 174 Application of Exponential Window

12.4.2.1 Root Mean Squared Averaging

A root mean squared (RMS) average (also known as **power averaging**) will only give a better estimate of the true signal plus the noise. Naturally, as with any averaging technique, the more averages that are taken the more accurate the final result. However, some practical limit can usually be established after which further averaging has no apparent effect.

12.4.2.2 Linear Averaging

Linear averaging requires that a time domain trigger be used to start the sampling period. The **triggering** will usually be chosen as some signal level well above the noise floor. It ensures that the periodic part of the signal will always be the same in each time record while the noise will not, thus allowing the noise to average out.

12.4.2.3 Overlap Averaging

Instead of simply averaging consecutive data blocks, it is possible to use part of the last block in the next average. This overlapping of blocks allows many more averages from a given data sample and, when averaging with either of the techniques described in the previous two sections, produces a much better final result to facilitate analysis (Figure 175). The triggering described in Section 12.4.2.2 will likely result in an overlap, although perhaps not with a uniform shift delta. A uniform percentage of previous blocks to be used in the averaging can be specified, although usually making up less than half of the new block.

12.4.3 Adding and Subtracting Spectra

Spectrums can be produced for a single response and for a sum or difference of responses. This latter method may be useful in discerning close structural modes or to increase the resolution of like modes. For example, if the response signals from transducers located in like positions on the opposite wings are added, then antisymmetric modes would not appear in the spectra because their opposite phases at identical frequencies would cause them to cancel out. Conversely, symmetric modes would show an increase in magnitude. Subtracting the same signals would enforce antisymmetric modes but cause symmetric modes to cancel out. This simplifies both identifying the modes with respect to their phase as well as separating the symmetric and antisymmetric modes that are often inseparable by other means.

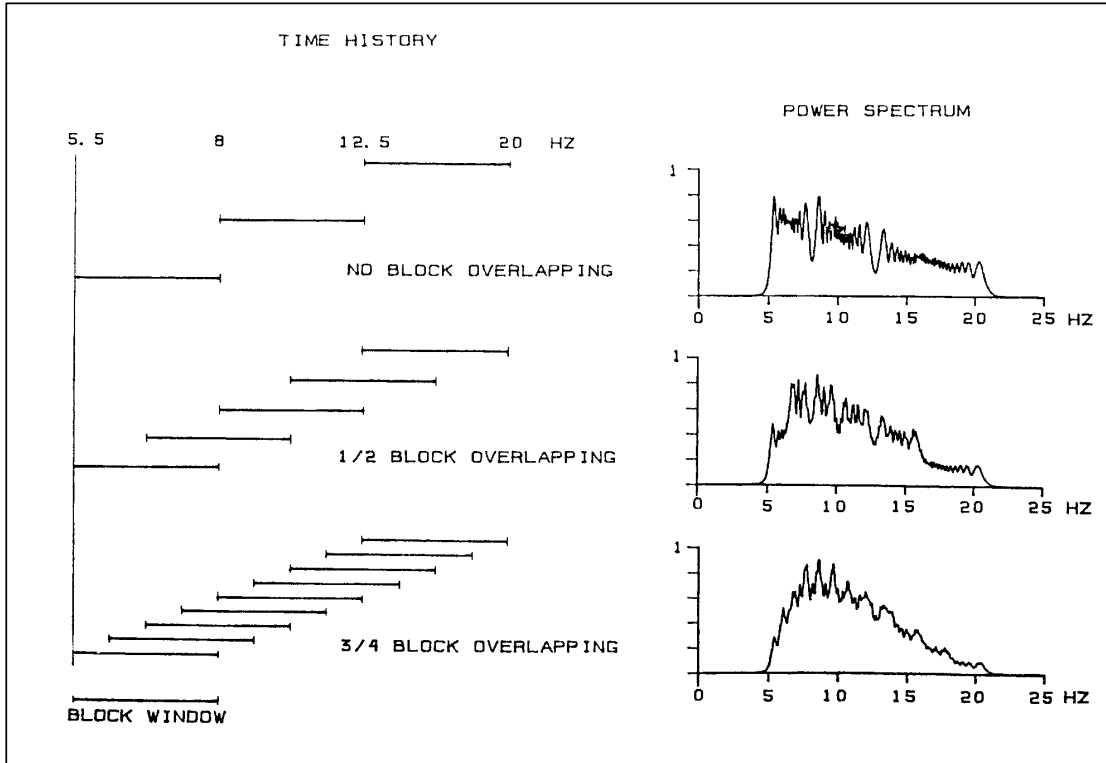


Figure 175 Illustration of Overlap Averaging and Result

12.4.4 Zoom Transform

If an FFT of 0 to 60 Hz has been done with a data block of 1,024 points, this would yield a frequency resolution of 0.12 Hz (see Section 12.2.1). The subject under test may be such that there is great modal density (close modes) in one part of this bandwidth that cannot be adequately discerned with this resolution. Simply increasing the block size to increase the resolution is not always practical from a computer capacity or a time perspective. In this case, it is desirable to 'zoom' in on the dense region and perform the transformation again with the consequently increased frequency resolution (Figure 176). If 1,024 lines are used for a 10- to 15-Hz bandwidth, now the resolution is 0.01 Hz. The measurement must be taken again to obtain more points in the region of interest.

This zoom procedure has also been called band selectable Fourier analysis (BSFA) or simply band selectable analysis (BSA) and is only useful when the data can be acquired again with the new bandwidth. Recorded data has generally already been sampled and digitized for a specific block size. In these cases, only a magnification of the desired region is possible with no increase in resolution. An added benefit of zooming is the reduction of leakage effects and broadband (white or impulsive) signal components. Data acquisition time may also increase.

12.4.5 Zero Insertion

Inserting zero amplitude data points at the end of the time domain data block allows an increase in the block size (sampling period) without increasing the sample rate and without sampling the data again. This has the effect of increasing the frequency resolution and the damping resolution (more points in the frequency domain, see Section 12.2) without affecting the validity of the frequency domain data. Doubling the block size with zero insertion will double the frequency and damping resolution. Inserting the zeros in the frequency domain to artificially increase the block size and then transforming back to the time domain has the effect of increasing the sample rate (time resolution, more points in the time domain) which reduces the frequency and

damping resolution. It is important that the insertion be made at a point where the real data is approximately zero itself. Otherwise, the sharp discontinuity in the data will be seen as a broadband noise superimposed on the frequency response plot.

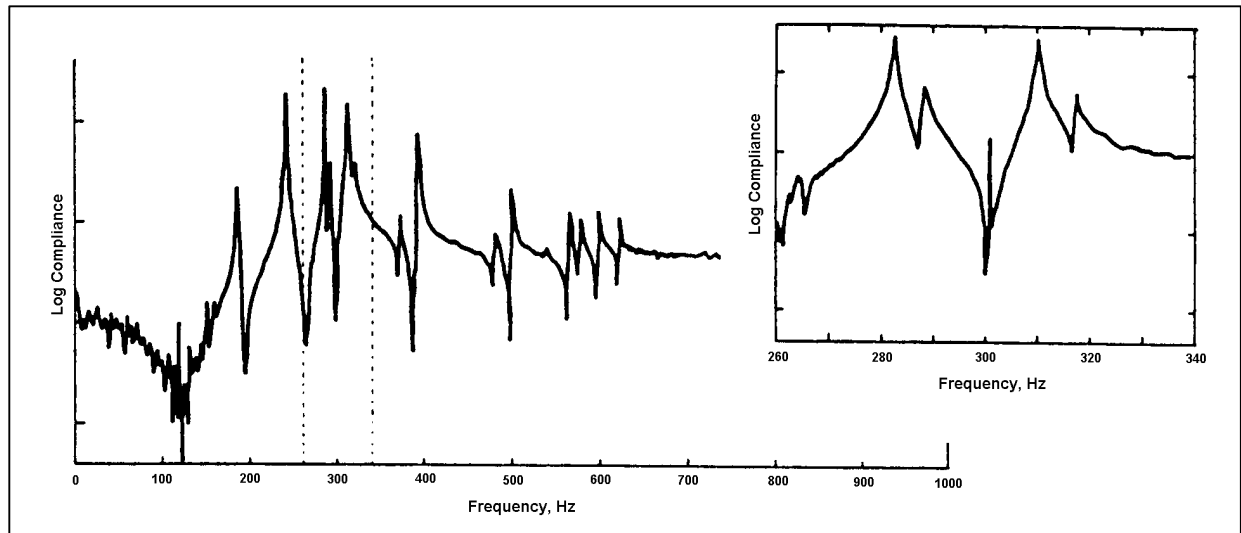


Figure 176 Example of Zoom Transform Application

12.4.6 Decimation

This is the elimination of a set number of equally distributed time domain data points from the data record. An example would be removing every other point, or effectively reducing a block from 1,024 to 512. For this example, it has the effect of halving the sample rate which consequently reduces the maximum frequency that can be resolved. However, it also results in a smaller frequency resolution and an improvement in the damping resolution in the frequency domain (see Section 12.2). An essential precaution is to apply an anti-aliasing filter at about half the new sample rate before decimating.

12.4.7 Cutoff

Similar to the force window, cutoff is simply setting the data points within the time domain block beyond a designated cutoff point to zero. It is used where a signal of interest has clearly ceased (the structure has damped out, for example) and only noise remains. Otherwise, a sharp discontinuity in the data will result with the consequences discussed in the Section 12.4.5 if the cutoff is not set at a point where the data is naturally zero. Removing this noise will provide a much improved frequency domain plot or improve a time domain curve fit.

12.4.8 Filtering

Filters are either analog or digital devices or processes that only allow a specified frequency range of signals to pass. A **high-pass filter** passes signals above a certain level and **low-pass filters** only pass signals below a certain frequency. In combination, these are called **bandpass filters**. Filters permit undesired parts of a signal to be eliminated to prevent errors, to eliminate noise, or to permit a more practical scaling of the presented data.

Design limitations do not permit the realization of perfect filters where the signal drops to zero instantly at the desired frequency. Instead, there is a decay of the signal, called **rolloff**. This rolloff will begin before the frequency set as the cutoff to ensure that the signal is significantly attenuated at the required frequency. If a true signal amplitude is required up to the cutoff then the filter should be set slightly higher than this frequency. How quickly the rolloff occurs varies from one type of filter to the next, and may be very important to a certain

application. A rapid rolloff, or sharp 'skirts,' are generally desired. Digital filters will usually provide better characteristics than analog filters, but the latter are often necessary for such uses as anti-aliasing filtering which is done prior to digitization.

Figure 177 illustrates several of the terms commonly used when discussing filters used in structures tests. Here, B is the **cutoff frequency** and R is the **rejection frequency**. Other characteristics that must be considered in the choice of filters are **ripple** power (small oscillation in the passband), **sidelobe** power (caused by amplitude modulation), and noise bandwidth. Filters are rated by dB/octave to indicate how quickly they rolloff. For example; one may wish the amplitude to be reduced by one-half in one octave, or 3 dB/octave. A digital filter can be set to pass whatever frequency range is required by the application. For analog filters, a series or bank of narrow bandpass filters are needed if a broad spectrum is to be covered selectively (Figure 178). Another type of filter passes just a narrow band but can be swept across a broad spectrum as an alternate way of providing a frequency domain plot without an actual transformation. This is called a **tracking filter**. Examples of how filters are used are presented elsewhere in this section.

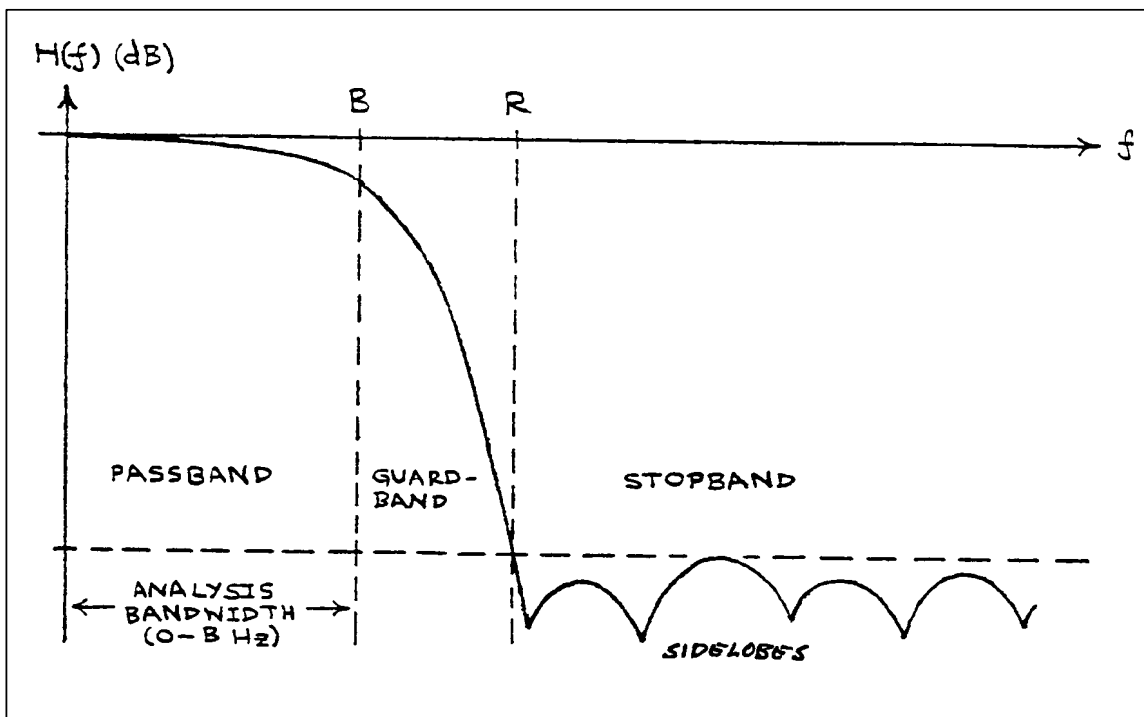


Figure 177 Filter Characteristics

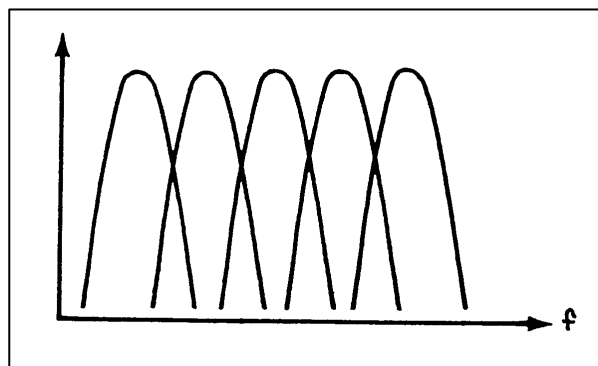


Figure 178 A Bank of Hanning Passbands

Filters may be used to remove all spectral components but for the region of interest in a frequency response plot, such as around one mode or a group of modes. The result can then be transformed back to the time domain (IFT, see Section 11.3.1), smoothed with a window such as an exponential window, and transformed back to the frequency domain for final analysis. This is shown in Figure 147. Another example is isolating a mode(s) in the frequency domain, transform to the time domain for smoothing or analysis, and then subtract this mode(s) from the initial data. This eliminates all contributions from this mode(s) that may be overshadowing higher frequency but lower energy modes. Such a process allows these other modes to be more easily extracted and analyzed.

One problem with filters, which is annoying in frequency response analysis, is called '**ringing**.' This appears as a damped sinusoidal response resulting from an electronic resonance within the filter device. Ringing has been observed to be excited by specific frequencies unique to each filter.

SECTION 12 REFERENCES

1. Otnes, Robert K. and Enockson, Loren, *Digital Time Series Analysis*, John Wiley & Sons, New York, New York, 1972.
2. Haidl, G. and Steininger M., *Excitation and Analysis Techniques for Flight Flutter Tests*, AGARD Report No. 672, AGARD, London, England, January 1979.
3. Rabiner, Lawrence R. and Gold, Bernard, *Theory and Application of Digital Signal Processing*, Prentice-Hall Incorporated, Englewood Cliffs, New Jersey, 1975.
4. *The Fundamentals of Signal Analysis*, Application Note 243, Hewlett-Packard Company, Palo Alto, California, 1985.

13.0 FLIGHT TESTING AT THE AIR FORCE FLIGHT TEST CENTER

13.1 Introduction

In order to conduct and support flutter, loads, aeroservoelastic, vibration, and acoustics testing, the Air Force Flight Test Center (AFFTC) relies upon the aircraft structures test engineers of the 412th Test Wing (TW) for engineering expertise in airframe structures technology. The Test Wing ensures the availability of a lead structures engineer and any number of additional engineers needed to support an individual test. This structures team should be involved early in the test planning phase. Responsibilities regarding the conduct of the test and the reporting of results are set in this phase. The charter of the team requires that its engineers ensure the safe, efficient, and effective conduct of all structures tests, whether conducted by a government contractor, the Air Force, another service, or as a joint effort, if any AFFTC resources are to be employed. In the case of certifying aircraft modifications or store configurations, the structures engineers will:

- a. Ensure that the proper decision regarding the need for flight testing has been made,
- b. Will sign off on those tests where additional flight testing is not required; and
- c. Will interface with other organizations tasked with making such decisions.

The flight testing of modern aircraft is a lengthy and expensive process that requires careful planning and teamwork to achieve optimum results as efficiently as possible. This chapter will outline the process by which this is done at the AFFTC. While often slow and frustrating, and certainly far from perfect, this process has evolved over decades of experience to ensure smart and safe flight testing. General flight test practices can be learned in short courses taught by various institutions across the United States. Those individuals without flight test experience are strongly encouraged to acquire such training as soon as possible and to work under an experienced flight test engineer for some time. This chapter will not substitute for such training and experience.

13.2 Responsible Organizations

The 412 TW is an organization within the AFFTC, which is in turn an organization within Air Force Materiel Command (AFMC)—a major command of the USAF. The mission of the AFFTC is to conduct and support tests of manned and unmanned aerospace vehicles. As a part of this responsibility, flutter and loads testing normally occurs prior to other tests on a new airframe. Since flutter can have such drastic consequences, the intent is to avoid flutter while performing other less hazardous tests. Other structures tests are performed after these fundamental envelope expansion tests are substantially completed. When substantial modifications are made to an airframe already in service, or if new configurations of external stores are to be flown, the AFFTC may have the responsibility for testing these modifications or configurations and to verify their safety, compliance with requirements, and suitability for operation.

Normally, all new aircraft or missiles will be tested for flutter, loads, and other aeroelastic phenomena. Whether the testing is done by the manufacturer with Air Force support, or by the either alone, is normally decided by the **system program office (SPO)** or **joint program office (JPO)** with responsibility for managing the program as a whole. An advanced development program office (ADPO) occasionally manages research programs. These organizations, normally based at Wright-Patterson AFB, Ohio, for projects involving Air Force aircraft, has the ultimate acquisition and development authority over the project. The program office pays the bills. The AFFTC is responsible to them for flight test activities. However, the AFFTC has veto authority over any decisions involving aircraft that will be tested using AFFTC resources (the range, aircrew, etc.). Therefore, if the program office decides to test a new configuration for performance, handling, etc., the AFFTC must verify ('sign off') that the aircraft is safe to fly with or without additional structures testing in the new configuration. Specifically for stores, the Air Force Development Test Center (AFDTC) at Eglin AFB, Florida, will also play a leading role in this decision.

The organization, which will act as the lead agency for the conduct of the test, is termed the **responsible test organization (RTO)**. The Test Wing may establish a **combined test force (CTF)** that consists of both USAF and contractor personnel working jointly toward program success.

13.3 Aircraft Modifications

The structures engineer may be asked to prepare or review documentation for aircraft modifications (mods). The documentation package helps to ensure that all relevant analysis has been satisfactorily completed. Temporary modifications for the purpose of a development test effort are termed '**Class II**' and extremely superficial modifications are '**Class III**' mods. A **Class I** mod involves a permanent change to the aircraft fleet. Documentation should include drawings plus a statics and dynamics analysis. The analysis should include the flight environment stated in military specifications, particularly MIL-A-8861 and MIL-A-8870.

Any change to a military aircraft requires a considerable amount of documentation and coordination for approval. The electrical load, electromagnetic compatibility, and weight-and-balance impact must be reviewed and documented. Each mod must be reviewed and approved by the Deputy Commander for Maintenance (DCM) prior to installation and after installation through a process called the **Configuration Control Board (CCB)**. Complex installations involving many aircraft systems may require ground testing to ensure proper and safe functioning prior to flight. Dedicated flight tests may also be mandatory. The Class II modification office under the DCM is a vital source of information and assistance in this area.

Most changes in electrical equipment on an aircraft, including instrumentation changes, require an **electromagnetic compatibility/electromagnetic interference (EMC/EMI)** ground testing. This is to verify that the normal aircraft electrical systems do not adversely effect the new equipment, and that the new equipment does not effect the pre-existing equipment. An EMC/EMI problem can be analogous to turning on a newly installed car radio and finding that the windshield wipers automatically begin to operate at the same time.

13.3.1 Analysis

Modifications or onboard equipment designed at the AFFTC are occasionally analyzed for the effects of flight loads by the structures team using dedicated computer software. Dynamics analysis and flutter analysis can also be done by the AFFTC but this has become rare in recent years because of the prohibitive time and manpower this requires. Generally, the team does not attempt to analyze the effects of the modification on the aircraft support structure since this would require detailed mathematical models of the aircraft which are seldom available to the government. If this is deemed necessary, then the original manufacturer or an independent contractor is generally hired to do the analysis, with an Air Force review.

13.3.2 Flight Tests

Flight tests of aircraft modifications will follow the general pattern of those outlined in this handbook. Testing will be reduced to concentrate on the mod and its effects on the rest of the aircraft. Load paths, stress concentrations, mass redistributions, and downstream airflow effects should be considered in making this assessment. Instrumentation will concentrate on the modified structure but must include some measurands on the flight vehicle as a whole to see the effects of the mod throughout the machine. Testing may be waived entirely depending on the nature of the mod and whether similar mods have been flown previously on a similar structure at similar flight conditions.

The modified structure and added articles (stores, pallets, etc.) must be specifically designed to withstand the load spectrum for taxi, landing, in-flight gusts, and maneuvering (both symmetric and asymmetric) scenarios. Any cuts in the airframe pressure vessel must be thoroughly documented and analyzed. It is strongly advised that the test engineer contact the engineers at the responsible aircraft depot and consult with them about material problem in the areas intended to be modified, or at the normal load and maneuver conditions intended for the flight test. Certain inspections may be necessary to ensure that the aircraft structure is sound (particularly for an old aircraft) before testing is allowed to proceed. Flight testing normally consists of testing the aircraft to

the flight manual limits of normal load (positive and negative), roll rate, and steady-heading sideslips. Strain gage instrumentation is advisable but not always necessary.

A flutter analysis is usually required for significant changes to structural stiffness or mass distribution. A flutter speed of at least 115 percent of redline airspeed is mandatory unless a restricted flight envelope is accepted. Flight testing can consist of as little as approaching the red-line dynamic pressure and Mach conditions while performing control raps. Control surface positions and wing/empennage tip accelerations should be monitored and a damping evaluation performed.

External protuberances can have a profound effect on internal noise, airframe buffet, airflow over critical surfaces, structural fatigue life, aircraft stability and control, plus stall speed and poststall characteristics. Wind tunnel tests are common in assessing potential trouble areas. Tufting is advisable for initial flight testing to help visualize airflow disturbances. For serious situations, it may be necessary to add acoustic instrumentation and pressure taps to assist in analysis. Common handling quality and approach to stall tests should also be performed.

13.4 Test Planning

13.4.1 Preliminary Planning

It is best if the flight test engineer can be part of the initial design reviews prior to prototype construction or the test airframe modification. This provides the opportunity to understand the design philosophy and the analysis techniques used. Flight test experience gives the flight test engineer (FTE) insights that the design engineer may not have, and FTE comments can be very helpful in avoiding difficulties later in the flight test phase. These design reviews are normally conducted at the manufacturer's plant, and are termed the **Preliminary Design Review (PDR)** and the **Critical Design Review (CDR)**. Following the CDR, changes in the design become very difficult to initiate, such as additional instrumentation in the prototype, so that it becomes urgent for a structures FTE to be present at this important review.

The Program Office will conduct periodic reviews of the test plans, both by mail and in meetings. These meetings are generally called a **Test Plan Working Group (TPWG)** or a **Technical Interchange Meeting (TIM)**, and the structures FTE should attend those meetings touching on the structures field. This ensures that relevant issues are given the proper attention. The engineer must consider whether the plan is actually executable, will provide the necessary data to meet the test objectives, and can be conducted with available resources (time, money, personnel, equipment, etc.). A broad picture of all the testing in the program (generally large projects), identification of the responsible test organizations (RTOs), and required test resources will be described in the **Test and Evaluation Master Plan (TEMP)**. This document is prepared with inputs from all agencies involved with the project and will be changed during the course of the program as required. When coming onto an already established project, becoming familiar with the TEMP should be an early priority.

13.4.2 The Test Plan

The test matrix and instrumentation requirements are all included in the test plan. This document also contains procedures for conducting the test, **flight test techniques (FTTs)**, flight maneuvers, plus personnel, equipment, and data requirements. The contents of this document are spelled out in AFFTC-TIH-93-01, *Air Force Flight Test Center Test Plan Preparation Guide* (Reference 1). The first portion of the test plan is the Test Objectives section which details the purpose(s) of the test. All of the subsequent sections contain information on procedures and requirements that will be necessary to accomplish the test. The test planning process is outlined in AFFTCI 99-1, *Test and Evaluation - Test Plans* (Reference 2).

The test engineer is advised to read plans from prior projects to become familiar with test planning and the test plan format. The test plan should contain information on the number of personnel needed to conduct the test, their identity, and roles they will play. As a minimum, a strip chart operator for each critical strip chart or screen, a computer operator, a test director, and an aircraft controller are required. All support equipment and aircraft modifications needed to support the test are also detailed in sections of those names. Finally, the amount

and types of data (the Data Requirements section of the test plan) to be analyzed, the methods used to analyze it, and the responsible organizations are discussed. The safety of flight and safety of test parameters must be identified.

The test plan may specify a control room layout that details locations of strip charts or monitors, personnel, and the data analysis computers. Each CTF is required by AFFTCI 99-5, *Test Control and Conduct* (Reference 3) to develop an **operating instruction (OI)** for control room procedures. The control room layout is designed to allow sufficient space for all strip chart and computer operators, and also to provide the structures test director access to all critical data sources.

13.4.3 The Review Cycle

Once the test plan has been prepared, a **Technical Review Board (TRB)** is convened. The purpose of the TRB is to critique the test plan to ensure that the test objectives can be met following the procedures outlined, that the procedures can be accomplished, and all technical preparation requirements have been adequately addressed.

Normally, when a structures-type test plan is reviewed, the Flight Dynamics Division Chief acts as board chairman. The Structures Branch chief (or assigned representative) is a board member as well as a Flying Qualities Branch representative. A pilot from the appropriate squadron or with requisite experience is required to determine whether the maneuvers and test points called for are within the capability of the aircraft. This is the minimum board membership.

Members of the CTF, if applicable, that attend the TRB often include the CTF **Unit Test Safety Officer (UTSO)**, the lead airframe engineer, the structures engineers working on the project, and a higher level CTF manager to represent the CTF director. Sometimes the **Test Safety Office** representative may be invited to attend the TRB in order to obtain background information in preparation for the coming **Safety Review Board (SRB)**, and to recommend possible changes to make the SRB go more smoothly. The contractor and Program Office involved may also send a structures engineer to the TRB.

The SRB follows the TRB. One of the principal tasks of the SRB is to assign a **risk level**. The risk assessment is either a low, medium, or high (hazardous) risk, based upon the maneuvers involved, the predicted behavior of the aircraft, and the proximity of test points to the edges of the flight envelope. The risk assessment will often be increased based upon the confidence (or lack of confidence) in the analytical model and ground tests results. Each hazard requires detailed examination and explanation of minimizing procedures in **Test Hazard Analysis (THA)** sheets, AFFTC Form 5028A, which become part of the safety package that results from the SRB. The AFFTC Test Safety Office has files of past THAs which will be useful to those preparing safety review packages. The general safety approach (minimum altitudes, chase aircraft, abort criteria, etc.) is outlined in the AFFTC Form 5028, Test Project Safety Review, and amended when necessitated by subsequent test plan changes which also becomes part of the safety review package. The principal purpose of the SRB is to assess a risk level, but the board may recommend changes to the test plan to minimize the risk. A very detailed outline of safety issues is contained in AFFTCI 91-5, AFFTC Test Safety Review Process (Reference 4).

For a flutter test, the structures and flight controls representatives from the TRB normally function as SRB members as well as the Test Safety Office representative (chairman) and a pilot representative. Lead structures engineers, the squadron UTSO, and contractor engineers normally attend as well, but they are not board members. For tests of sufficient simplicity, the TRB and SRB is sometimes done through informal coordination, with no formal meetings convened.

After the SRB, for high-risk tests, the Commander of the AFFTC is briefed regarding the program objectives and the risk assessment. The Test Safety Officer, CTF UTSO, lead structures engineer, or project pilot may together or one alone conduct the briefing. Contractor engineers may attend the briefings to the Commander if it is believed that they will have something to contribute. The path from test plan writing to TRB to SRB to the Commander's briefing is normally termed the 'test approval cycle.'

13.4.4 Final Preparations

During, or immediately following the test approval cycle, the CTF Deputy Commander for Operations (DO) will begin to schedule resources to support the test, with the 'leg work' actually done by the responsible engineers. These resources will normally include a control room to conduct the test, needed strip charts and monitors, the data analysis computer, the aircraft and stores (if any), and any other support equipment needed. If a CTF is not involved, the structures engineer may need to perform these tasks.

When all of the data has been gathered to the satisfaction of the engineers involved, the program will be terminated and the aircraft, stores, and any other equipment needed for the test will be released for use on other programs.

13.5 Conduct of the Test

AFFTCI 99-5 (Reference 3) contains a detailed guide to flight test conduct, but a brief overview is in order.

13.5.1 Preflight Briefing

Preflight briefings should be conducted to review the operating limitations, safety considerations (the AFFTC Form 5028 and any 5028b's) and, most importantly, the '**flight cards.**' These are the cards that guide the team through the test mission. In the preflight briefing, the pilot should completely understand the maneuvers to be flown and the test point progression. The '**chase**' pilot, a pilot who will follow the test aircraft in the safety chase aircraft to assist in an emergency (loose or detached aircraft components during test, etc.), will be fully briefed either during the preflight briefing or immediately thereafter.

13.5.2 Control Room Operations

As already mentioned, each CTF will prepare an OI defining all control room setups and procedures. A mock room setup should be conducted for training and to prove out all procedures. All strip charts, monitors, computers, chairs, tables, headsets, etc., that will be used in the test should be in place to verify that a workable arrangement has been designed. Actually playing some data through the system to verify that the data recording and display systems are properly setup is essential.

During or following the mock setup, a ground check of the telemetry (TM) is made to ensure the operational status of all instrumentation devices, the TM system, antennas, TM encoders, decoders (for encrypted data), etc. All transducers should read their proper steady-state values. The ranges for parameters on the strip charts should be checked and any changes made to allow easier readability and to allow accurate display of data. An **end-to-end check** of the system may reveal unexpected results like missing or corrupted data, incorrect computations or displays, improper sample rates, etc.

Prior to the test, strip chart operators, data monitors, and computer operators should be trained in the proper use of the equipment. They must be briefed on the purpose of the test, test conduct, and their roles during the test. Responsible engineers will verify that any project computer software functions properly, and they will create directories, files, paper charts for recording run numbers, etc. prior to the test.

Control room operations should be well-defined and orderly to prevent confusion during the flight. The OI or test cards will detail the roles of all test personnel, the criteria for test termination, and the procedures in the event of an emergency. All personnel involved directly with the test should be briefed on the contents of the instructions and given a copy to use as a reference.

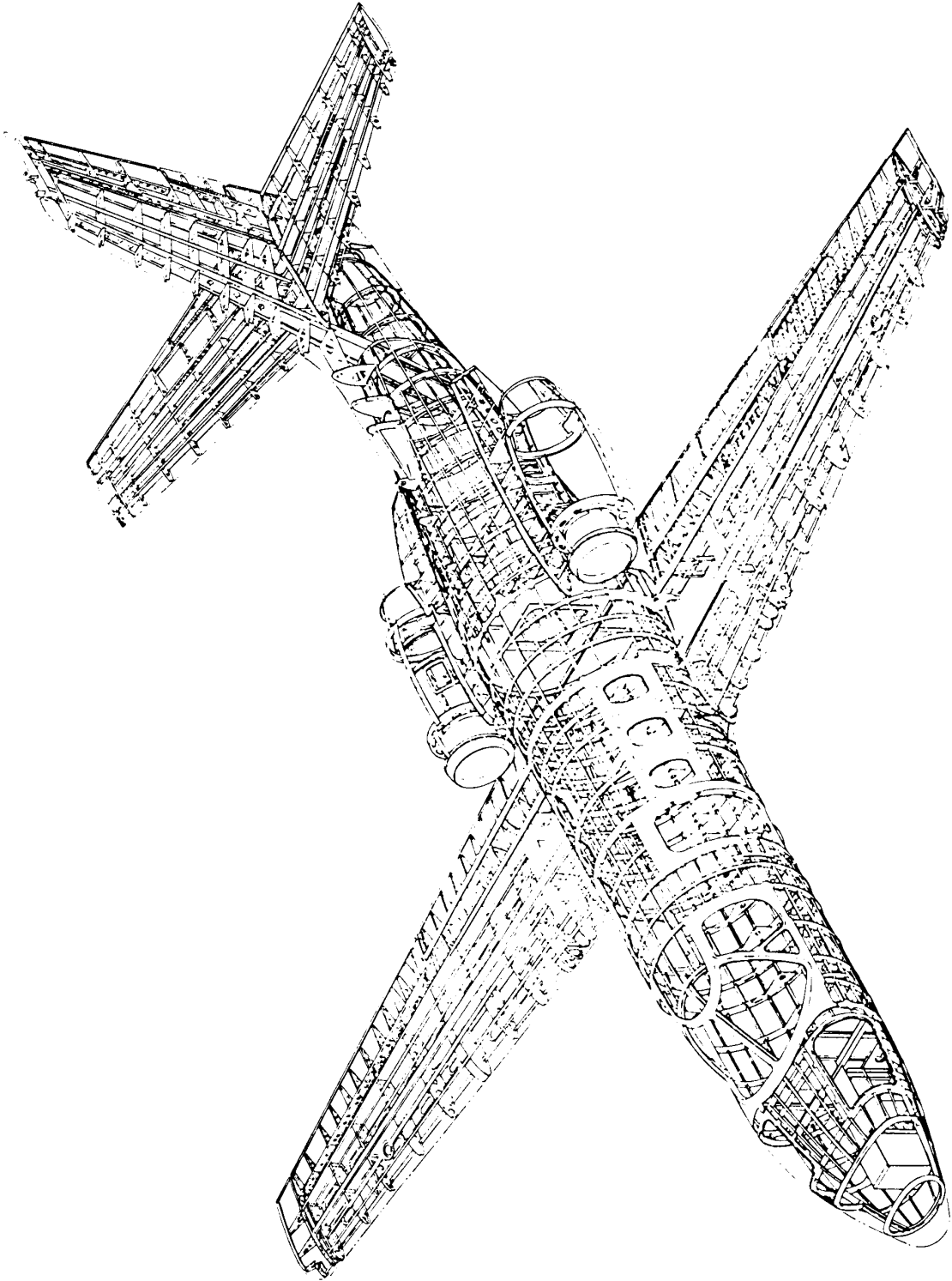
13.6 Test Reports

Most structures programs will result in the production of a technical report; preparation of which may be the responsibility of the Air Force lead structures engineer, the contractor, or both working as a team. The technical report will contain details of the aircraft configuration, test instrumentation, test conduct, results, and conclusions based upon those results. Lower level efforts or preliminary results may be reported in a technical letter report or a **preliminary report of results (PRR or 'PR squared')**. The format for all AFFTC reports is contained in AFFTC-TIH-97-01, *Writing AFFTC Technical Reports* (Reference 5).

Following any structures project, **Lessons Learned** summaries may be submitted by the lead engineer and approved by the Structures Branch chief. The Lessons Learned papers should contain information about new techniques used to conduct the tests, old techniques that did not work, or possibly suggestions for better and safer techniques. Problems encountered with particular data analysis methods should be discussed, and solutions presented. These Lessons Learned papers are designed to be read by lead engineers on other programs to benefit from the mistakes or suggestions of others.

SECTION 13 REFERENCES

1. AFFTC-TIH-93-01, *Air Force Flight Test Center Test Plan Preparation Guide*, AFFTC, Edwards AFB, California, May 1994, revised February 1999.
2. AFFTCI 99-1, *Test and Evaluation - Test Plans*, AFFTC, Edwards AFB, California, 10 November 1998.
3. AFFTCI 99-5, *Test Control and Conduct*, AFFTC, Edwards AFB, California, 26 May 1998.
4. AFFTCI 91-5, *AFFTC Test Safety Review Process*, AFFTC, Edwards AFB, California, 12 July 1999.
5. AFFTC-TIH-97-01, *Writing AFFTC Technical Reports*, revision 4, AFFTC, Edwards AFB, California, October 1997.



Cessna Citation Structure

LIST OF ABBREVIATIONS, ACRONYMS, AND SYMBOLS

(Acronym definitions with a superscript number refer to the section number in which the definition is referenced.)

<u>Abbreviation</u>	<u>Definition</u>	<u>Unit</u>
A	aspect ratio ¹ ; cross-sectional area ³ ; amplitude ⁴ ; aerodynamic operator ⁶ ; one leg of Wheatstone bridge ¹⁰ ; constant ¹¹	---
AMRAAM	advanced medium range air-to-air missile	---
ACS	active control system	---
ADC	analog-to-digital converter	---
ADPO	Advanced Development System Office	---
AFDTC	Air Force Development Test Center	---
AFFTC	Air Force Flight Test Center	---
AFMC	Air Force Materiel Command	---
AOA	angle of attack	---
APU	auxiliary power unit	---
AR	aerial refueling	---
ASE	aeroservoelasticity	---
a	speed of sound ² ; constant, flexibility matrix ⁴ ; nonmodal aerodynamics ⁶	ft per sec ²
ac	alternating current	---
B	damping matrix ⁶ ; one leg of Wheatstone bridge ¹⁰ ; constant ¹¹	---
BL	butt line	---
BSA	band selectable analysis	---
BSFA	band selectable Fourier analysis	---
BW	bandwidth	---
b	wing span ¹ ; constant ⁴ ; reference semi-chord ⁶	---
C	Centigrade or Celsius ² ; stiffness matrix ⁶ ; one leg of Wheatstone bridge, coefficient ¹⁰ ; zero offset, constant ¹¹	---
CAS	calibrated airspeed	kt
CBR	California Bearing Ratio	---
CCB	configuration control board	---
CDR	critical design review	---
CFD	computational fluid dynamics	---
CO	coincident part	---
CSD	cross spectral density	---
CTF	combined test force	---
C _D	drag coefficient	dimensionless

LIST OF ABBREVIATIONS, ACRONYMS, AND SYMBOLS (Continued)

<u>Acronym</u>	<u>Definition</u>	<u>Unit</u>
C _L	lift coefficient	dimensionless
C _l	roll moment coefficient	dimensionless
c	constant, coefficient of viscous damping	---
cg	center of gravity	pct MAC
c.p.	center of pressure	---
c _r	critical damping coefficient;	---
D	total drag ² ; one leg of Wheatstone bridge ¹⁰	---
DCM	Deputy Commander for Maintenance	---
DET	determinant	---
DFT	discrete Fourier transformation	---
DLL	design limit load	---
DO	Deputy Commander for Operations	---
DOF	degree of freedom	---
DTP	dynamic pressure transducer	---
d	constant	---
dB	decibel	---
dc	direct current	---
dt	derivative with respect to time	---
E	Young's Modulus ³ ; quantization error ¹²	---
EAS	equivalent airspeed	kt
ECS	environmental control system	---
EFCS	electronic flight control system	---
EGT	exhaust gas temperature	deg
EMC	electromagnetic compatibility	---
EMI	electromagnetic interference	---
EPR	engine pressure ratio	---
EU	engineering unit(s)	---
EW	electronic warfare	---
e	strain; exponential constant	---
F	force ⁴ ; function ⁸ ; Fourier transformation ¹¹	---
FEM	finite element modeling	---
FFT	fast Fourier transformation	---
FITT	inter-turbine temperature	---
FM	frequency division multiplex	---

LIST OF ABBREVIATIONS, ACRONYMS, AND SYMBOLS (Continued)

<u>Acronym</u>	<u>Definition</u>	<u>Unit</u>
FOL	flight operating limit	---
FOS	factor of safety	---
FRF	frequency response function	---
FS	fuselage station	---
FTE	flight test engineer	---
FTT	flight test technique	---
f	frequency	Hz
fps	feet per second	---
ft	feet	---
f(t)	periodic function	---
f _{max}	frequency maximum	---
G	Shear Modulus ³ ; total system damping, hysteric damping, inherent structural damping ⁶ ; Bode form function ⁸	---
GH	open-loop transfer function	---
GRT	ground resonance test	---
GVT	ground vibration test	---
G _{min}	total system damping minimum	---
G _{xx}	input autopower spectrum	---
G _{xy}	cross-power spectrum	---
g	acceleration due to gravity	32.2 fps ²
H	transfer function ⁷ ; hundreds digit ¹⁰	---
HSI	horizontal situation indicator	---
HQDT	handling qualities during tracking	---
HSO	heavy store oscillation	---
HUD	head-up display	---
Hg	mercury	---
Hz	hertz	---
I	cross-sectional area moment of inertia, identity	---
IAS	indicated airspeed	kt
IDF	Indigenous Defensive Fighter	---
IFF	identification friend or foe	---
IFT	inverse Fourier transformation	---
Im	imaginary part	---
INS	inertial navigation system	---

LIST OF ABBREVIATIONS, ACRONYMS, AND SYMBOLS (Continued)

<u>Acronym</u>	<u>Definition</u>	<u>Unit</u>
IRIG	Inter-Range Instrumentation Group	---
ITT	inter-turbine temperature	deg
i	imaginary number ⁴ ; complex number ⁶	---
in	inch(es)	---
ips	inches per second	---
J	cross-sectional polar moment of inertia	---
JPO	Joint Program Office	---
j	imaginary number	---
K	gust alleviation factor ⁵ ; stiffness operator ⁶ ; gage factor ¹⁰ ; counter, maximum value ¹¹	---
KCAS	knots calibrated airspeed	---
KIAS	knots indicated airspeed	---
k	spring constant ⁴ ; nonmodal stiffness, reduced frequency ⁶ ; counter ¹¹	---
L	rolling moment ² ; length ³ ; lift force ⁵ ; level ⁹	in-lb
LCF	limit cycle flutter	---
LCO	limit cycle oscillation	---
LEX	leading edge extension	---
LOS	loss of signal	---
LVDT	linear variable differential transformer	---
M	flight of freestream Mach number, pitching moment ² ; applied torque, generalized mass ⁴ ; mass operator ⁶ ; modal mass ⁷ ; moment, mass ¹⁰ ; maximum number of time shifts ¹¹ ; number of bits in a binary word ¹²	dimensionless
MAC	mean aerodynamic chord	---
MDOF	multiple degrees of freedom	---
MIMO	multiple input, multiple output	---
MLC	maneuver load control	---
MPD	multipurpose display	---
m	Mass ⁴ ; slope of C_L versus AOA curve ⁵ ; nonmodal mass ⁶ ; correlation shift or lag number ¹¹	slug
mag	Magnitude	---
mm	Millimeter	---
mux	Multiplexer	---
mv	Millivolts	---
N	yawing moment ² ; number of loading cycles ³ ; generalized force ⁴ ; vertical load factor, efficiency factor ⁵ ; block size ¹²	in-lb

LIST OF ABBREVIATIONS, ACRONYMS, AND SYMBOLS (Continued)

<u>Acronym</u>	<u>Definition</u>	<u>Unit</u>
NDI	nondestructive inspection	---
NHAA	negative high angle of attack	---
NLAA	negative low angle of attack	---
NPR	nozzle pressure ratio	---
N_1	low-pressure core rotational speed	---
N_2	high-pressure core rotational speed	---
n	mode number	---
n_z	normal load factor	g
OASPL	overall sound pressure level	---
OI	operating instruction	---
OWS	overload warning system	---
P	pressure ² ; loads ³ ; roll rate ⁶ ; function ⁸ ; RMS sound power ⁹ ; total number of data points ¹¹	---
Pa	Pascal	---
PCM	pulse code modulation	---
PDR	preliminary design review	---
PHAA	positive high angle of attack	---
PIO	pilot-induced oscillation	---
PLAA	positive low angle of attack	---
PRR	preliminary report of results	---
PSD	power spectral density	---
P_T	total pressure	lb per ft ²
p	complex operator ⁶ ; RMS sound pressure, pico ⁹	---
pC	pico Coulomb	---
psi	pounds per square inch	---
Q	Force ⁴ ; generalized forcing function ⁶	---
QUAD	quadrature part	---
q	dynamic pressure ² ; coordinate ⁴	lb per ft ²
R	gas constant, Rankine ² ; resistance ¹⁰ ; residual ¹¹	---
Re	real part	---
RAT	ram air turbine	---
RHP	right half-plane	---
RMS	root mean squared	---
RPO	rolling pullout	---

LIST OF ABBREVIATIONS, ACRONYMS, AND SYMBOLS (Continued)

<u>Acronym</u>	<u>Definition</u>	<u>Unit</u>
RTB	return to base	---
RTD	resistance device	---
RTO	responsible test organization	---
Re	real part	---
R _{xx}	auto-correlation	---
R _{xy}	cross-correlation	---
rad	radian	---
S	wing area ¹ ; applied stress ³	ft ²
SCO	subcarrier oscillator	---
SCR	strip chart recorder	---
SDOF	single degree of freedom	---
SEL	sound exposure level	---
SISO	single input, single output	---
SMI	structural mode interaction	---
S/N	signal-to-noise ratio	---
SOF	safety of flight	---
SOT	safety of test	---
SPL	sound pressure level	dB
SPO	System Program Office	---
SR	sample rate	---
SRB	Safety Review Board	---
S _x	Fourier transformation of input	---
s	roots ⁴ ; landing gear stroke ⁵ ; Laplace variable ⁸	---
sec	second(s)	---
sps	samples per second	---
T	period of oscillation ⁴ ; torque, tens digit ¹⁰ ; period of time record ¹²	---
TAS	true airspeed	---
TCG	time code generator	---
TEMP	Test and Evaluation Master Plan	---
THA	test hazard analysis	---
TIM	test interchange meeting	---
TM	telemetry	---
TPS	test pilot school	---
TPWG	Test Plan Working Group	---

LIST OF ABBREVIATIONS, ACRONYMS, AND SYMBOLS (Continued)

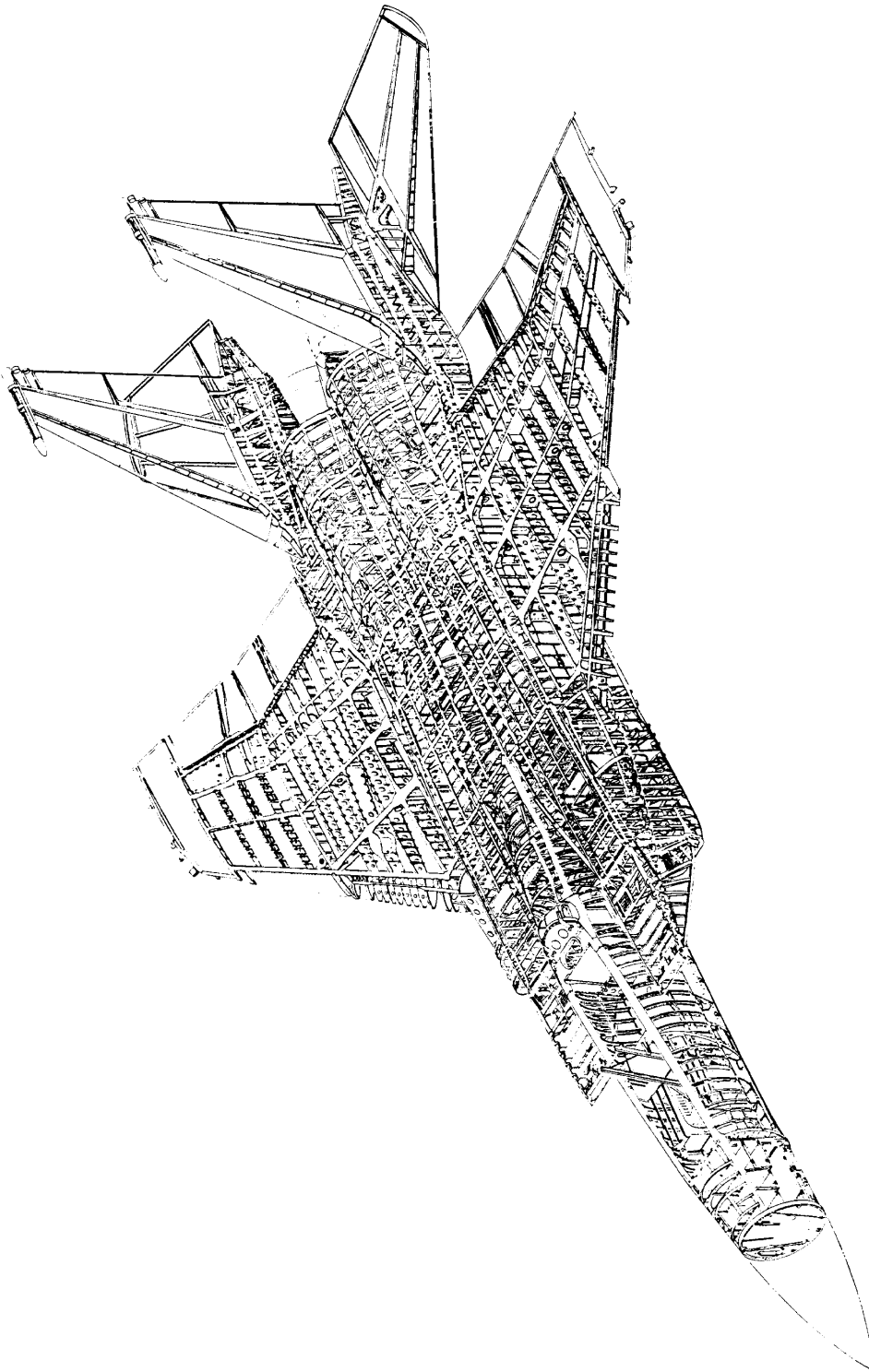
<u>Acronym</u>	<u>Definition</u>	<u>Unit</u>
TRB	Technical Review Board	---
t	absolute temperature; time	deg
U	gust velocity ⁵ ; freestream velocity ⁶ ; shear, units digit ¹⁰ ; engineering unit quantity ¹²	---
UTSO	Unit Test Safety Office	---
u	transformation matrix ⁴ ; nondimensional Wheatstone bridge output ¹⁰	---
V	velocity true airspeed ⁵ ; shear ¹⁰	ft per sec
VCO	voltage control oscillator	---
V d	volts direct current	---
VG	vortex generator	---
W	gross weight ⁵ ; watt ⁹	lb/watts
WL	water line	---
WS	wing station	---
WUT	windup turn	---
w	weighting function	---
X	longitudinal axis ² ; deflection ⁵ ; output function ¹¹	---
x	displacement ⁴ ; function ¹²	---
Y	lateral axis ² ; input function ¹²	---
Z	altitude, vertical axis	---
ρ	air density	slug per ft ³
α	angle of attack ² ; damping coefficient ¹²	deg
ϕ	bank angle	deg
σ	density ratio ² ; stress ³ ; operator, aerodynamic damping ⁶ ; complex variable coefficient ⁸ ; damping rate ¹¹	dimensionless
λ	eigenvalue ⁶ ; wave length ⁹	---
ω	frequency	Hz
Δ	increment of change	---
∞	infinity	dimensionless
Φ	mode shape ⁷ ; power spectral density plot ¹¹	---
Φ_{xx}	input power spectral density	---
Φ_{xy}	cross spectral density	---
Ω	operator	---
∂	partial derivative	---

LIST OF ABBREVIATIONS, ACRONYMS, AND SYMBOLS (Continued)

<u>Acronym</u>	<u>Definition</u>	<u>Unit</u>
ϕ	phase	---
φ	phase angle	---
μ	Poisson's Ratio ³ ; micro ⁹	---
δ	pressure ratio ² ; deflection at point of application ⁴	dimensionless
γ	shear strain ³ ; operator ⁶	---
β	sideslip angle	deg
Σ	Sum	---
θ	temperature ratio ² ; angular displacement ⁴	dimensionless
τ	time constant ⁴ ; integration variable function of time ¹¹	---
η	transformed coordinate	---
ν	viscous damping coefficient ⁶ ; Poisson's Ratio ¹⁰ ; coherence ¹¹	---
ζ	viscous damping factor ⁴ ; damping ratio, damping coefficient ¹¹	---
π	Pi	---
K	modal stiffness	---
M	modal mass	---
C	modal damping	---
<u>Subscripts</u>		
A	structural inertia matrix	---
a	one leg of rosette	---
B	aerodynamic damping matrix	---
b	one leg of rosette	---
C	aerodynamic stiffness matrix	---
c	one leg of rosette	---
D	structural damping matrix	---
d	damper, damped	---
E	structural stiffness matrix	---
e	equivalent condition	---
eq	equivalent	---
H	maximum level of flight	---
i	matrix column counter ⁴ ; matrix row counter ⁷	---
j	matrix row counter ⁴ ; matrix column counter ⁷	---
k	counter	---
L	limit	---

LIST OF ABBREVIATIONS, ACRONYMS, AND SYMBOLS (Concluded)

<u>Subscripts</u>	<u>Definition</u>	<u>Unit</u>
LG	landing gear	---
l	tension	---
M	mode ⁸ ; multiple ¹¹	---
m	mass	---
max	maximum	---
min	minimum	---
N	with respect to Nth cycle ¹¹ ; Nyquist ¹²	---
n	natural	---
o	reference value at 0 dB ⁹ ; with respect to first mode or cycle ¹¹	---
p	peak ⁴ ; pressure ⁹	---
pm	phase margin	---
q	generalized coordinate vector	---
R	input force coefficient matrix	---
r	mode or DOF counter; range	---
S	stall condition, sink, strut ⁵ ; sampling ¹²	---
s	standard day condition ² ; spring ⁴	---
st	static	---
T	total ² ; tire ⁵	---
t	true condition ² ; test condition ⁵	---
u	input scalar	---
V	true airspeed	---
w	compression ³ ; power ⁹	---
½	with respect to half amplitude cycle	---
<u>Superscripts</u>		
L	limit condition	---
-	generalized coordinate, harmonic motion	---
.	first derivative	---
..	second derivative	---
*	complex conjugate	---



McDonnell-Douglas F-15A Structure

INDEX

<u>A</u>	
Accelerance	56
Accelerometer	
Calibration	189, 191
Compression	188, 191
Frequency range	188
Installation	134, 190, 191
Measurement	191
Natural frequency	188
Reference	131, 134
Roving	125, 142
Scale factor	185
Selection	134, 188
Sensitivity	187
Servo	188
Shear mode	188
Tri-axial (triax)	125, 168, 187
Upright	188
Voltage mode	189
Accessory gearbox	11
Accumulator	11
Acoustic chamber tests	
Progressive wave chamber	174
Reverberant chamber	174
Active Control System (ACS)	89
Advanced Development Program Office (ADPO)	245
Adverse yaw	31, 32
Aerial refueling (AR)	13, 14, 75
Aero-acoustics	167
Aerodynamic	
Center (a.c.)	27, 30
Quasi-static	109
Quasi-steady	109
Stiffness	67, 107
Aeroelasticity	25, 27, 33, 97
Effects on stability & control	33,
Aeroservoelasticity (ASE)	149
Analysis	159, 160
Flight test	162
Ground test	161
Aerothermoelasticity	112
Afterburner	11, 15, 167, 175
Aileron	2, 4, 5, 31, 33, 73, 76, 89, 99
Roll	76
Airbrake	5, 11, 120
Aircraft	
Basics	1
Geometry	1
Airfoil	8, 24-28, 30, 102, 109
Airload (see Load)	
Airspeed	
Calibrated (CAS)	22, 119
Calibration	22, 119
Equivalent (EAS)	22, 87, 119
Indicated (IAS)	22
Indicator	15
Limit	69
Red line	69, 106
True (TAS)	22, 67
Aliasing	163, 197, 233, 234, 242, 243
Altimeter	15, 21
Altitude	
Density	21
Pressure	21
AM-2 runway repair mat	91
American method	104
Amplitude resolution	231
Analog-to-digital converter (ADC)	143, 199, 231,
Angle of attack (AOA)	26, 27, 29, 67, 68, 76,
87, 97, 99, 101	
Anhedral	2, 4
Animated mode shape	125
Antinode	61, 149
Antiresonance	61, 131, 215
Aperture error	235
Argand plane	222
Arrestment tests	93
Aspect ratio	2
Asymmetric mode	140
Atmosphere	19, 21 22, 39, 167, 168
Attitude indicator	15
Augmentor	11
Auto spectrum or auto power spectrum	143, 209-213, 220,
Autopilot	13, 32, 33, 167, 168
Auxiliary power unit (APU)	11
Avionics	5, 8, 11, 126, 128, 167, 168, 194
Averaging	
Ensemble	140, 141, 204, 239
Linear	240
Log Decrement	202
Overlap	240, 241
Power	240
Root Mean Squared (RMS)	89, 169, 172,
173, 240	
Axes	
Body fixed	30
Directional	29, 31, 32
Lateral	29, 31, 121
Longitudinal	29, 32
Normal	66
Vertical	29, 31, 66, 67

INDEX (Continued)

- | | |
|--|--|
| Axes | Pressure (c.p.) 27, 71, 110 |
| Yaw 29 | Centering tendency 98 |
| B | Chaff 15 |
| Backlash (see Freeplay) | Characteristic polynomial 155 |
| Band edge 195, 198, 235 | Charge amplifier 189 |
| Band Selectable Analysis (BSA) 241 | Chirp (see Sine input) |
| Band Selectable Fourier Analysis (BSFA) 241 | Chord, wing 1, 146 |
| Bandwidth 133, 140, 149, 151, 152, 154, 157, 229, 230, 241, 243 | Circuit breakers 11 |
| Barometric pressure 15, 19, 21 | Circulation 26, 28 |
| Barrier test 93 | Clipping error 235, 236 |
| Baseband analysis 230 | Clock jitter error 235 |
| Beating 57, 139, 206, 207, 215 | Closed-loop 161 |
| Bending 32, 33, 35, 46, 61, 62, 67, 72, 75-79, 88, 89, 93, 99-101, 110, 114, 115, 121, 123, 130, 131, 134, 138, 144, 145, 149, 151, 167, 181, 185, 186, 194, 207 | Test 161 |
| Bernoulli Equation 21, 26 | Coalescence 53, 98 |
| Binary numbers 198, 229 | Coherence 89, 122, 138, 143, 220, 221, 234 |
| Bit 116, 198, 231, 235 | Ordinary 220, 221 |
| Bleed air 11 | Multiple 143, 221 |
| Block 229, 233, 238, 239 | Partial 143, 221 |
| Diagram 152, 154 | Coincident (CO) 221 |
| Diagram algebra 152, 154 | Cold working 41 |
| Size 229, 241 | Combined Test Force (CTF) 247, 249, 250 |
| Blockage 113 | Combustion section 8 |
| Blower 129, 190 | Commutator 199 |
| Bode plot 157, 158, 161, 226, 227 | Compensation 154-157, 160, 184 |
| Bonker 118 | Dynamic 154 |
| Boom refueling 13 | Gain 157 |
| Boundary layer 26, 27, 109, 167 | Lag 154 |
| Turbulent 26 | Lead 154, 156 |
| British method 107 | Lead-lag 154 |
| Brittleness 43 | Compliance 215, 216, 221, 222, 246 |
| Buffet 68, 75, 77, 79, 83, 84, 111, 119, 126, 248 | Dynamic 56 |
| Bump and dip test 91 | Mechanical 99 |
| Burst 92, 115, 141, 238 | Composites 35, 40, 41 |
| Burst-and-decay 117, 118, 120, 204 | Compressible flow 102 |
| Butt line (BL) 5, 7 | Compression 28, 32, 35, 37, 40, 41, 131, 183, 188, 191 |
| Buzz 100, 109, 110 | Compressor 8, 11, 68, 111 |
| Bypass ratio 8 | Computational fluid dynamics (CFD) 28 |
| C | Concurrent testing 85 |
| California Bearing Ratio (CBR) 92 | Configuration Control Board (CCB) 247 |
| Camber 25, 26, 28 | Control |
| Canard 4, 5, 31, 121, 185 | Oscillation 115, 162 |
| Center of | Pulse 115 |
| Gravity (cg) 30, 73, 92, 99, 123 | Rap 99, 115 |
| | Reversal 33, 110, 111 |
| | Room 75, 81, 83, 85, 249, 250 |
| | Theory 152, 154, 159, 226, 228 |
| | Coordinates |
| | Generalized 59, 60, 104, 108 |
| | Natural 59, 60 |
| | Transformation 59, 60 |
| | CO/QUAD method 139, 221 |
| | Correlation function 205, 206, 212, 215 |

INDEX (Continued)

- | | |
|---|--|
| Auto-correlation | 205, 206, 212, 215 |
| Cross-correlation | 205, 206 |
| Frequency domain | 144, 201, 204, 208, 209,
211, 213, 215, 216, 219, 221, 229-
231, 233-237, 239, 241-244 |
| CO/QUAD method | |
| Time domain | 144, 201, 206, 208, 212, 215,
229, 234, 236, 239-242, 244 |
| Corrosion | 42 |
| Electrochemical | 42 |
| Coupling | 98-100, 105, 110, 112, 122, 149,
151, 161, 207, 222 |
| Cracking | 38, 41, 111, 174 |
| Creep | 41 |
| Critical | |
| Damping coefficient | 49 |
| Design Review (CDR) | 248 |
| Structure | 73 |
| Cross-orthogonality | 147 |
| Cross point measurement | 131 |
| Cross spectral density (CSD) | 213 |
| Cross spectrum or cross power
spectrum | 143, 212, 221 |
| Curve fitting | 140, 141, 143, 144, 202, 219, 220 |
| <u>D</u> | |
| Damage tolerance | 44, 72 |
| Damper | 33, 45, 46, 48, 49, 55, 94, 167,
Viscous 45, 46, 49, 57, 107-109 |
| Damping | 45, 53, 60, 98, 101, 104, 108 |
| Aerodynamic | 67, 98, 104, 107, 108, 111, 201 |
| Aeroelastic | 98 |
| Coefficient | 41, 61, 201, 239 |
| Coefficient of viscous | 45 |
| Coulomb | 46 |
| Critical | 49, 201 |
| Equivalent | 107 |
| Error | 119, 234, 236 |
| Hysteretic | 46, 104 |
| Inherent structural | 98 |
| Matrix | 59, 61, 107 |
| Negative | 32, 98, 111, 224 |
| Neutral | 32, 50, 149 |
| Positive | 32, 98, 111 |
| Proportional | 46, 57 |
| Rate | 110, 201 |
| Ratio | 49, 107, 201, 203 |
| Resolution | 229-231, 234, 241, 242 |
| Structural | 46, 67, 93, 97, 98, 107,
108, 111, 201, 225, 239 |
| Total system | 93, 98, 105, 201, 230 |
| Viscous | 45, 46, 49, 57, 107-109 |
| Data bus | 8 |
| Data error | 231 |
| dc | |
| Component | 201, 210, 236 |
| Off set (see Zero offset) Suppression | 201 |
| Deadbeat | 50, 118 |
| Decade | 117, 169, 188, 246 |
| Decibels(dB) | 157, 168, 213 |
| Decimation | 242 |
| Degree of freedom (DOF) | 45, 58 |
| Multiple | 54, 58, 62, 212, 239 |
| Single | 47, 201, 206, 223, 227 |
| Delamination | 41, 174 |
| Demultiplexer | 195 |
| Design | |
| Limit load (DLL) | 38, 72-74, 80-85 |
| Ultimate load | 38, 72, 81, 86 |
| Diffuser | 11 |
| Digitizer error | 235 |
| Dihedral | 2, 4 |
| Direct current (dc) | 184, (see also dc) |
| Discrete | 195, 205, 209, 210, 227, 234, 235 |
| Discriminator | 197 |
| Displacement transducer | 162, 194 |
| Divergence | 50, 102, 104, 110, 111, 124 |
| Divergent response | 32, 111, 155 |
| Dome mode | 107 |
| Dorsal | 4 |
| Doublet | |
| Aerodynamic | 28 |
| Input | 115 |
| Lattice method | 28 |
| Downwash | 26, 28 |
| Drag | 27 |
| Form | 27 |
| Induced | 27 |
| Interference | 28 |
| Parasite | 28 |
| Profile | 27 |
| Skin friction | 27 |
| Total | 28 |
| Wave | 28 |
| Driving point measurement | 131, 132, 144 |
| Dropouts | 195, 225, 236 |
| Ductility | 41, 43 |
| Durability | 43, 72 |
| Dutch roll mode | 33 |
| Dye penetration inspection | 42 |
| Dynamic | |
| Balance | 100 |
| Pressure (q) | 21, 22, 105, 110, 117, 119,
120, 149, 193, 248 |
| Pressure Transducer (DTP) | 193 |

INDEX (Continued)

Response 39, 98, 112, 114, 201, 209,
215
Dynamical matrix 61

E

Eddy current inspection 43, 80
Effective mass 130, 131
Eigensolution 102, 109
Eigenvalue 61, 104, 105, 108, 110
Eigenvector 61, 104, 105, 109, 147
Ejection seats 15, 128
Elastic
 Axis 99, 110, 111, 114, 131, 134
 Limit 38, 72, 79, 182
 Range 45
Elasticity 37, 43
 Modulus of 37, 112
Electrical bus 11
Electrodynamical exciter 116
Electrodynamical shaker 116, 125, 128, 129, 133,
134, 162
 Armature 125, 129-131, 134, 162
 Attachment to the structure 130
 Characteristics 128, 129
 Multishaker techniques 131
 Physical features 129
 Selection 129
 Sting 125, 130, 131
 Stroke 130
 Suspension 130
Electromagnetic compatibility/
electromagnetic interference (EMC/EMI) 247
Electronic Flight Control System
(EFCS) 74, 84, 149, 154, 160-163
Electronic warfare 15
Elevated-g roll 76
Elevator 4
Elevon 5
Empennage 4, 101, 111, 248
End-to-end check 250
Engine pressure ratio (EPR) 15
Engineering units (EU) 181, 197
Ensemble averaging (see Averaging)
Environmental control system (ECS) 8, 11
Euler coordinates 159
Event switch 195
Excitation
 Base 128
 Flutter test 97, 124, 163
 Parasitic 220
 Pyrotechnic 118
Exciter system 101, 115, 116, 124, 163

Exfoliation corrosion 42
Exhaust gas temperature (EGT) 15
External tanks 12, 127

F

FACES 102
Factor of safety 38, 39, 72, 81, 85, 86
Failure modes, 40, 163
flight control system 101, 114, 117, 134, 149, 151,
163, 166
Fan section, engine 8
Fast Fourier transformation (FFT) 211
Fatigue 41, 72, 85, 89, 102, 109, 111, 167, 174, 248
Fatigue
 Life 41, 72, 85, 89, 167, 174, 248
 Sonic 44, 167, 174
 Tests 72
Feedback 13, 93, 149, 152-154, 159-163, 194
Fillet 7
Filter 149, 154, 163, 197, 234, 242-244
 Bandpass 238, 242, 243
 Cutoff frequency 234, 243
 High pass 234
 Low pass 234
 Rejection frequency 243
 Ripple 243
 Ringing 244
 Roll off 243
 Sidelobe 243
 Skirts 243
 Structural 149
 Tracking 243
Finite element modeling (FEM) 39, 104
Flaking corrosion 42
Flap 2
Flaperon 31
Flexibility matrix 60
Flight
 Cards 85, 250
 Computer 8, 33, 159
 Data recorder 42, 85
 Mechanics 19, 29
 Operating limits (FOL) 72
Flight test techniques (FTT) 248
Flotation system 128
Flow
 Straighteners 26
 Visualization 22
Flutter 97, 149
 Aileron rotation/wing bending 99
 Bending-torsion 99
 Binary 98, 99

INDEX (Continued)

- | | | |
|---|-----------------------------|--|
| Hamilton's Principle | 54 | |
| Handling qualities during tracking (HQDT) | 163 | J |
| Harmonic | | |
| Excitation | 52 | Jump phenomenon |
| Function | 52, 108 | 57 |
| Harmonics | 57, 102, 236 | K |
| Head-up display (HUD) | 15 | |
| Helix angle | 111 | KCAS (calibrated air speed) |
| Hinge moment | 71, 72, 76 | 22 |
| Hooke's Law | 37, 38 | KE-method |
| Horizontal situation indicator (HSI) | 15 | 39 |
| Horizontal stabilizer | 4, 5, 75, 76 | K-method |
| Hot spots | 134 | 104, 105, 108, 109 |
| Humidity | 19 | Knots |
| Hump mode | 107 | 22 |
| Hydraulics | 5, 11, 127 | Kulite |
| Hypersonic | 24, 109, 112 | 191 |
| | I | L |
| Ibrahim Time Domain | 144 | Lag |
| Identification Friend-or-Foe (IFF) | 15 | 32, 149, 154, 157, 205 |
| Impact testing | 138, 238 | Lead |
| Impedance | 56, 189, 215 | 154 |
| Electrical | 133 | Lagrangian |
| Mechanical | 133 | 54 |
| Mismatch | 133, 140 | Landing gear |
| Incidence, wing | 2 | 5, 11, 100, 119, 125, 128, 175 |
| Indicial response | 152 | Load tests |
| Inertance | 56, 136, 215, 216, 221, 222 | 91 |
| Inertia | | Vertical load factor |
| Matrix | 59, 67 | 76, 90 |
| Moment of | 46 | Laminar flow |
| Polar moment of | 47 | 26, 27 |
| Inertial navigation system (INS) | 15 | Laplace |
| Influence coefficient matrix | 60 | 49, 54, 155, 156, 219 |
| In-homogeneous material | 39 | Laplace |
| Inlet | 8, 109 | Domain |
| Inspection | 42, 80 | 219, 224 |
| Instantaneous spectra | 212 | Transformation |
| Instrumentation systems | 181, 195, 197 | 156, 224, 227 |
| Intake | 8 | Variable |
| Intercom | 15 | 49, 224 |
| Interphone | 15 | Lateral-directional |
| Inter-turbine temperature (ITT) | 15 | Axes (see Axes) |
| In-vacuo analysis | 102 | Control system |
| Inverse square law | 169 | 152 |
| IRIG-B | 194 | Leakage error |
| Ironbird | 160 | 235, 238 |
| Isobel contours | 175 | Least squares curve fit |
| Isolator mounts | 168 | 204 |
| Isotropic material | 40 | Lessons learned |
| | | 251 |
| | | Lift |
| | | 25-28, 30, 31, 33, 42, 66, 69, 75, 87, |
| | | 89, 90, 97, 99, 100, 110 |
| | | Coefficient |
| | | 26 |
| | | Lifting line theory |
| | | 28 |
| | | Limb-bobweight influence |
| | | 151 |
| | | Limit Cycle Oscillation (LCO) |
| | | 107, 111, 121 |
| | | Limit Cycle Flutter (LCF) |
| | | 111 |
| | | Limit cycle test |
| | | 161 |
| | | Limit load factor |
| | | 66-69, 88 |
| | | Linear variable differential transformer |
| | | (LVDT) |
| | | 194 |
| | | Linearity check |
| | | 126, 141, 142 |
| | | Lissajous figures |
| | | 139, 206, 208 |
| | | Load |
| | | Airload |
| | | 65, 69, 71, 79-84, 109 |
| | | Alleviation system |
| | | 87, 89 |
| | | Asymmetric normal load |
| | | 66 |
| | | Calibration |
| | | 77, 78, 185, 186 |
| | | Cell |
| | | 130, 131, 135, 143, 191 |

INDEX (Continued)

Multiplexer (mux) 195
 Multiple-input, multiple-output (MIMO) 152
 Multipoint data 143
 Multifunction display (MFD) 15

N

Nacelle 5, 7, 8, 77, 95, 100, 121, 125, 131, 145, 151
 NASTRAN 39, 102
 Newton's Second Law of Motion 46
 Node 39, 61, 114, 126, 131, 142, 144
 Line 114, 126, 131, 142, 144
 Noise 115, 117, 118, 126, 127, 140, 152, 161, 167, 169, 174, 175, 179, 191, 195, 200, 201, 204, 205, 208, 211, 219
 Floor 236
 Pink 169
 Random 169, 205, 211
 White 169, 174
 Non-destructive inspection (NDI) 42
 Nonlinearities 57, 102, 111, 118, 122, 126, 127, 130, 140, 142, 144, 161, 201, 210, 215, 236, 239
 Normal
 Load correction 85
 Load factor 66, 67, 69, 73-76, 84, 100, 120
 Notch filter 163-165
 Nozzle 11-13, 15, 27
 Nozzle pressure ratio (NPR) 15
 Nyquist
 Plot 159, 222-224
 Stability Criterion 159

O

Octave 169, 176
 Octave
 Third-octave 169, 176
 Oil canning effect 149
 Open-loop 152, 153, 155, 157, 159, 161
 Test 161
 Operating inputs 134
 Operating Instruction (OI) 249
 Orthogonal 61, 187
 Transformation 60
 Orthogonality
 Check 144
 Cross-orthogonality 147
 Orthotropic material 40

Overall sound pressure level (see Sound)
 Overdamped 50
 Overload
 Limits 85
 Overload Warning System (OWS) 67
 Overtones 57
 Oxidation 42

P

Panels 4, 5, 28, 95, 101, 127
 Parameter
 Estimation 144
 Extraction 144
 Identification 144
 Peak
 Amplitude method 202
 Picking method 215
 Perfect Gas Law 19
 Phase
 Angle 52-55, 98, 157, 161, 203, 222
 Check 75
 Crossover 157, 159
 Crossover frequency 159
 In phase 53, 55, 99, 131, 139, 140, 208, 221
 Lag 109, 149
 Margin 149, 157, 159, 161-163
 Margin requirement 161, 162
 Shift 55, 126
 Phugoid mode 32
 Piezoelectric 79, 102, 187, 188, 191, 193
 Piezoresistive 188, 191
 Pilot-augmented oscillations (PAO) 151, 163
 Pilot-in-the-loop 84
 Instabilities 151
 Oscillations 150, 166
 Pilot induced oscillations (PIO) 32, 151, 163
 Piston theory 28
 Pitch 29, 30, 32, 75, 100, 114, 167
 Pitot-static boom 22
 Pitting corrosion 42
 PK-method 107, 108
 Planform, wing 1
 Plant 152, 155, 159, 248
 Plasticity 43
 Plunge 98, 146
 P-method 108
 Poisson's ratio 37, 183
 Polar
 Coordinates 159

INDEX (Continued)

Plot 159, 160, 222
 Pole 142, 155
 Pole-zero 155
 Plot 159
 Poly Reference 144
 Position error 22
 Power spectral density (PSD) 168, 212, 213, 215
 Pre-flight briefing 85
 Preliminary Design Review (PDR) 248
 Preliminary Report of Results (PRR) 251, 254
 Preload 127, 128, 131, 138, 187
 Pressure
 Distribution 8, 19, 22, 24, 28, 79
 Gradient 22, 26, 28, 65, 79, 101
 Sensor 79, 118, 169, 191, 198
 Taps 77, 79, 248
 Probe and drogue refueling 13, 14
 Project history 181
 Prony Analysis 204
 Proportional force method 140
 Propulsion 8
 Pseudo Randomdec method 204, 205
 Pullup 75, 76, 83, 163
 Pulse code modulation (PCM) 197-199
 Pushover 75, 76, 163

Q

Quadrature (QUAD) 139, 221, 222
 Quality factor 213
 Quantization error 231
 Quill 131

R

Radome 5
 Rayleigh's
 Criterion 229
 Quotient 61
 Random decrement (Randomdec) method 204
 Random input 54, 117, 118, 141
 Burst 141
 Periodic 141
 Random input
 Pseudorandom 140
 Pure 140
 Rate-of-climb indicator 15
 Ram air turbine (RAT) 11
 Ranging 235
 Half-ranging 235
 Over-ranging 235

Under-ranging 235
 Receiver, refueling 13
 Reciprocity 126, 144
 Rectangular coordinates 159
 Reduced
 Frequency 105, 108, 109, 113
 Velocity 105
 Regression testing 86, 87
 Relative wind 27, 29
 Reservoir, hydraulic 11
 Residue 11, 201, 213
 Residual 35, 184, 219
 Resilience 43
 Resistance device (RTD) 194
 Resonance 52, 54, 55, 57, 61, 87, 131, 138, 139, 151, 159, 161, 163, 166, 167, 190, 206, 213, 215, 216, 221, 222, 226, 244
 Response
 Forced 52, 117, 125
 Free 48
 Impulse 201-203, 211, 235
 Rigid body 125, 128, 151
 Steady-state 52
 Transient 52, 112, 118, 135, 138, 141, 204, 215
 Unforced 154, 201
 Responsible Test Organization (RTO) 248
 Right half-plane (RHP) 155
 Rigid body mode 32, 98, 125, 128, 130, 163
 Rise time 152
 Risk level 249
 Roll 2, 4, 29, 31-33, 66, 67, 76, 79, 110, 111, 125, 128, 146, 149, 150, 151, 154, 163, 248
 Effectiveness 111
 Rolling pullout 76
 Rollup 33
 Root-locus 155-157, 224, 225
 Roving 125, 142
 Rudder 4, 13, 31, 33, 67, 75-77, 83, 93, 100, 101, 114, 115, 134, 146, 161
 Kicks 76, 114, 161
 Reversals 76
 Ruddervator 4, 101
 Rust 42

S

Safety chase aircraft 120, 250
 Safety Review Board (SRB) 249

INDEX (Continued)

- Sample Rate (SR) 78, 93, 199, 205, 241, 242, 250
- Sand pattern 144
- Schlieren 22
- Self-operating input 134
- Separated flow 26, 102, 109
- Self-windowing signals 238
- Settling time 152
- Shaker (see Electrodynamic shaker)
- Shannon's Sampling Theorem 229, 233
- Shear 35, 37, 38, 47, 67, 72, 75-78, 88, 185, 186, 188, 190
 - Modulus 38, 47
- Shimmy
 - Landing gear 93, 96
 - Testing 93
- Shock wave 8, 22, 24, 25, 109, 167
 - Normal 24
 - Oblique 24
- Short period mode 32
- Sideslip 29, 31-33, 73, 75, 77, 101, 118, 161, 163, 248
- Signal conditioner 143, 189, 195
- Signal-to-noise ratio (S/N) 138, 189, 199
- Signature Length 204
- Sine input 161
 - Chirp 140
 - Dwell 138, 140, 142, 143, 168
 - Stepped sine 140
 - Sweep 138-140, 161
- Single-input, single-output (SISO) 152
- Singlet 115
- Sink 28, 77, 90, 91
- Sinusoidal motion 56, 104
- Skirt, modal 215, 236
- Slip plate 128,
- Slow code 195
- S-N diagram 41
- Sound 138, 148, 167-169, 172
 - Chamber tests (see Acoustic chamber tests)
 - Data analysis 176, 201
 - Equivalent continuous sound 173
 - Exposure level (SEL) 173
 - Far field 169
- Sound
 - Infrasound 168
 - Intensity 167
 - Level 168
 - Near field 169
 - Overall sound pressure level (OASPL) 172
 - Power level 173
 - Pressure 168
 - Pressure level (SPL) 168
- Semireverberant field 169
- Testing 83, 176
- Ultrasound 168
- Source 28, 35, 42, 79, 114, 118, 121, 127, 131, 134, 160, 167, 169, 173, 181, 189, 195, 231, 232, 234, 235, 246
- Spalls 91
- Span, wing 1
- Spectral
 - Lines 209, 210, 229-231, 234
 - Lobe 231
- Spectrogram 176
- Speed
 - Maximum level flight 68, 69
 - Of sound 22, 24, 168
- Speedbrake 5, 100, 119, 120
- Spin 32
- Spiral mode 33
- S-domain 224
- S-plane 155, 159, 224-227
- Spoiler 4
- Spring Constant 45-47, 90, 127
- Spring-mass-damper system 48, 55
- Stability 29, 30-34, 84, 87, 96, 104, 105, 121, 149, 152, 155, 157, 159-161, 163, 166, 227, 248, 264
 - Artificial 32
 - Axes 29, 87
 - And Control 29, 33, 34, 84, 121, 152, 163, 251
 - Dynamic 32, 84, 96, 166
 - Derivative 33
 - Longitudinal 30
 - Static 30, 32, 149
- Stabilator, stab 4, 31, 41, 99, 101, 111, 149
- Stable system 152, 157
- Stagnation point 22, 39
- Stall 26, 66, 110, 111, 248
 - Flutter 110
- Standard
 - Atmosphere 19-21
 - Day 19, 21
- Static pressure test 19, 21, 22, 24, 26, 89
- Stationarity 126
- Stator 8
- Steady-heading sideslip 31, 248
- Step input 118, 135, 138, 152
- Step relaxation input 138
- Stick
 - Fixed 32
 - Free 32
 - Stiffener 109

INDEX (Continued)

Stiffness	45-47, 53, 56, 59-61, 67, 93, 94, 97-107, 109, 110, 112, 113, 121, 123, 127, 128, 130, 132, 162, 168, 215, 217, 248	Filters	159, 163
Aerodynamic	67, 107	Fuse	131
Apparent	56, 215	Inspection	80, 85, 95
Dynamic	56	Mode Interaction (SMI) test	161
Line	217	Resonance test	161
Stop drill	41	Subcarrier oscillator (SCO)	197
Strake	7	Subsonic	8, 24, 102, 109, 122
Strain	35	Superposition, principle of	157
Hardening	41	Supersonic	8, 12, 22, 24, 28, 102, 109, 110
Meter	184	Sweep	
Principal	37	Excitation	115, 117, 118, 138
Residual	184	Wing	1, 110, 162
Strain gage	77-80, 86, 91, 114, 118, 162, 183, 185-188, 191, 194, 195, 200	Sweet spots	149
Bi-axial	182	Syncro	199
Calibration	185	System	
Drift	79, 184	Error	152, 154
Dummy	184	Minimum phase	155
Gage factor (K)	183	Non-minimum phase	155
Installation	185-187, 200	Program Office (SPO)	246
Measurement	78, 183, 185		
Rosette	182	<u>T</u>	
Selection	182	Tail	
Spiral	182	Aircraft	4
Temperature compensation	184	Hook	5
Uniaxial	182	Taper	2
Streamline	22, 24	Taper ratio	2
Strength	28, 40, 42-44, 72, 96, 124	Taxi	
Stress	35	Loads	65, 77
Analysis	38, 39, 200	Tests	91, 112, 161, 162
Axial	35	Technical Interchange Meeting (TIM)	248
Bending	35	Technical Review Board (TRB)	249
Compression	35	Telemetry	75, 120, 181, 200, 250
Concentration	35	Temperature, stagnation	112
Limit	38	Temp tabs	194
Principal	35	Tension load	37
Residual	35	Test And Evaluation Master Plan (TEMP)	248
Shear	37	Hazard Analysis (THA)	249
Tension	35	Plan	248
Torsion	35	Plan Working Group Meeting (TPWG)	248
Ultimate	38	Planning	248
Visualization	42	Report	251
String pot	194	Testbed	181
Strip theory	28	Thermal	
Stripchart recorder (SCR)	197	Expansion	39, 41, 126, 182
Structural		Stresses	39, 41
Coupling	149, 161	Thermocouple	194
Coupling test	161	Third-octave (see Octave)	
Structural		Thruster	131, 162
Feedback	149, 159, 161-163, 194	Thunderstorm penetration speed	87, 88
		Time	
		Code generator (TCG)	194
		Constant	49, 53, 239

INDEX (Continued)

- | | | | |
|------------------------------------|--|--|-----------------|
| Delay | 152 | | <u>V</u> |
| Time | | | |
| Domain analysis | 144, 208, 211 | | |
| Time-invariant systems | 152 | | |
| Time-variant systems | 152 | | |
| Torque (see torsion) | | | |
| Torsion | 32-35, 47, 73, 75, 77, 78, 83, 88, 91, 99, 101, 110, 131, 134, 207 | | |
| Toughness | 43 | | |
| T-plot (see transmissibility plot) | | | |
| Trailing cone | 22 | | |
| Transfer function | 118, 121, 122, 130, 131, 139, 143, 152, 155, 157, 159, 161, 163, 206, 213, 219, 220, 224-226 | | |
| Transformation matrix | 60 | | |
| Transient | | | |
| Performance | 154 | | |
| Response | 52, 112, 118, 135, 138, 141, 204, 215 | | |
| Transmissibility Plot | T-plot 226 | | |
| Transonic | 24, 28, 100, 102, 119, 167, 174 | | |
| Transponder | 15 | | |
| Transport delay | 152 | | |
| Triggering | 204, 240 | | |
| Trim | 31 | | |
| Tab | 4, 31 | | |
| T-tail | 4 | | |
| Tufts | 22 | | |
| Tuning of modes | 140, 142 | | |
| Turbine, section | 8 | | |
| Turbojet | 8 | | |
| Turbofan | 8 | | |
| Turboprop | 8 | | |
| Turbulence | 77, 87-89, 100, 111, 113, 118, 119, 120, 122, 124, 152, 174, 219, 238 | | |
| Penetration speed | 87 | | |
| Random | 111, 118 | | |
| Twang test | 138 | | |
| | <u>U</u> | | |
| UFAPS | 102 | | |
| Ultimate load | 38, 72, 73, 85-87 | | |
| Ultrasonic inspection | 42 | | |
| Undamped | 32, 49, 50, 51, 53, 56, 57, 61, 93, 104, 161, 206, 236 | | |
| Underdamped | 50 | | |
| Unit Test Safety Officer (UTSO) | 249 | | |
| Unstable system | 50, 152 | | |
| Unsteady flow | 27, 97 | | |
| Upwash | 26 | | |
| | | | |
| V-f plot | 105 | | |
| V-G plot | 105 | | |
| V-g diagram | 70, 106 | | |
| V-n diagram | 67, 68 | | |
| Ventral fin | 4 | | |
| Vertical tail | 31, 32, 57, 66, 67, 75-77, 100, 101, 111, 125, 130, 131, 134, 145, 146 | | |
| Vibration table | 128 | | |
| Vibro-acoustics | 167, 174, 175 | | |
| Viscous damping factor | 49 | | |
| Visicorder | 197 | | |
| Voltage control oscillator (VCO) | 197 | | |
| Vortex | 26-28, 57, 79, 109, 119, 123, 149, 174 | | |
| Generators (VG) | 27, 109 | | |
| Sheet | 28 | | |
| V-tail | 4 | | |
| | | | <u>W</u> |
| Wand | 115, 116, 142 | | |
| Washin | 2 | | |
| Washout | 2, 33, 111 | | |
| Water line (WL) | 5 | | |
| Wavelength | 91, 168, 169, 174 | | |
| Weight | 30 | | |
| And balance | 13, 30 | | |
| Empty | 30 | | |
| Gross | 30 | | |
| Weighting | 140, 154, 169, 236, 238 | | |
| Wheatstone bridge | 184, 195 | | |
| Wheel | | | |
| Spin-up | 90 | | |
| Wheel-driven dynamics | 94 | | |
| Wind tunnel test | 22, 82, 113, 248 | | |
| Wind-down turn | 76 | | |
| Wind-up turn | 76, 122 | | |
| Window, data | 237 | | |
| Windowing | 234, 237 | | |
| Bessel | 237 | | |
| Blackman | 237 | | |
| Windowing | | | |
| Boxcar | 238 | | |
| Exponential | 239 | | |
| Flat top | 237 | | |
| Force | 238 | | |
| Windowing | | | |
| Hamming | 237 | | |
| Hanning | 236, 237 | | |
| Rectangle | 238 | | |
| Uniform | 238 | | |

INDEX (Concluded)

Wing 1
 Loading 69
 Station (WS) 2, 79
Winglet 2
Work 7, 98, 99, 116, 159, 169, 191, 211, 229, 246
Work-hardening 41
Wrap around 234

X

X-ray inspection 80

Y

Yaw Damper 33
Yield 38, 41, 57, 72, 79, 81, 93, 110, 115,
 121, 155, 169, 202, 204, 241
Young's Modulus 37, 46, 183

Z

Zero
 Insertion 241
 Offset 184, 203, 210, 236, 239
 Polynomial 155
Zoom transformation 241
Z-plane transformation 227